THE GUT MICROBIOME IN HEALTH AND DISEASE

EDITED BY: Nathan W. Schmidt, Venkatakrishna Rao Jala, Michele Marie Kosiewicz and Pascale Alard

PUBLISHED IN: Frontiers in Cellular and Infection Microbiology

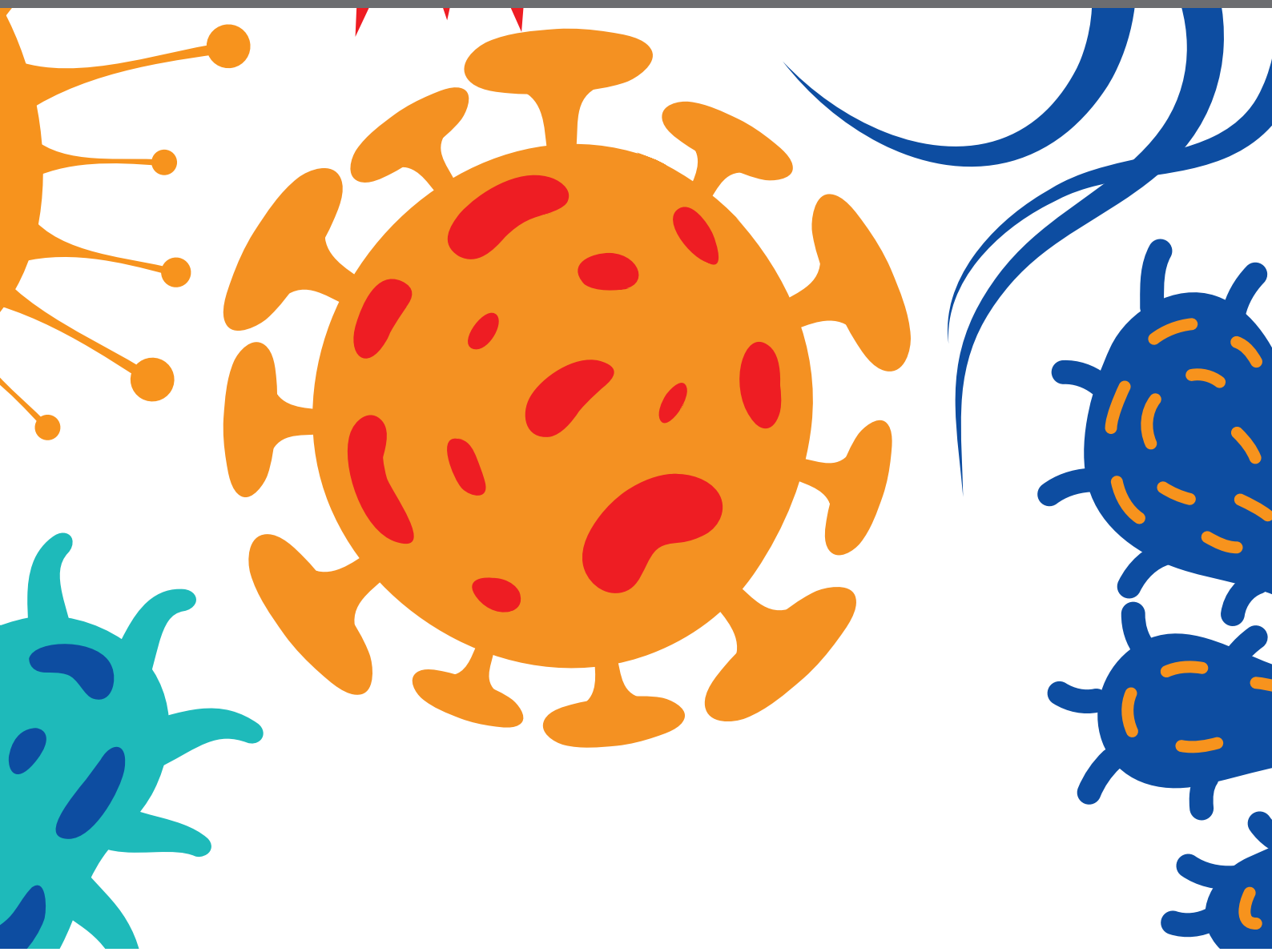

frontiers Research Topics

frontiers

Frontiers Copyright Statement

© Copyright 2007-2019 Frontiers Media SA. All rights reserved.

All content included on this site, such as text, graphics, logos, button icons, images, video/audio clips, downloads, data compilations and software, is the property of or is licensed to Frontiers Media SA ("Frontiers") or its licensees and/or subcontractors. The copyright in the text of individual articles is the property of their respective authors, subject to a license granted to Frontiers.

The compilation of articles constituting this e-book, wherever published, as well as the compilation of all other content on this site, is the exclusive property of Frontiers. For the conditions for downloading and copying of e-books from Frontiers' website, please see the Terms for Website Use. If purchasing Frontiers e-books from other websites or sources, the conditions of the website concerned apply.

Images and graphics not forming part of user-contributed materials may not be downloaded or copied without permission.

Individual articles may be downloaded and reproduced in accordance with the principles of the CC-BY licence subject to any copyright or other notices. They may not be re-sold as an e-book.

As author or other contributor you grant a CC-BY licence to others to reproduce your articles, including any graphics and third-party materials supplied by you, in accordance with the Conditions for Website Use and subject to any copyright notices which you include in connection with your articles and materials.

All copyright, and all rights therein, are protected by national and international copyright laws.

The above represents a summary only. For the full conditions see the Conditions for Authors and the Conditions for Website Use.

ISSN 1664-8714
ISBN 978-2-88963-003-5
DOI 10.3389/978-2-88963-003-5

About Frontiers

Frontiers is more than just an open-access publisher of scholarly articles: it is a pioneering approach to the world of academia, radically improving the way scholarly research is managed. The grand vision of Frontiers is a world where all people have an equal opportunity to seek, share and generate knowledge. Frontiers provides immediate and permanent online open access to all its publications, but this alone is not enough to realize our grand goals.

Frontiers Journal Series

The Frontiers Journal Series is a multi-tier and interdisciplinary set of open-access, online journals, promising a paradigm shift from the current review, selection and dissemination processes in academic publishing. All Frontiers journals are driven by researchers for researchers; therefore, they constitute a service to the scholarly community. At the same time, the Frontiers Journal Series operates on a revolutionary invention, the tiered publishing system, initially addressing specific communities of scholars, and gradually climbing up to broader public understanding, thus serving the interests of the lay society, too.

Dedication to Quality

Each Frontiers article is a landmark of the highest quality, thanks to genuinely collaborative interactions between authors and review editors, who include some of the world's best academicians. Research must be certified by peers before entering a stream of knowledge that may eventually reach the public - and shape society; therefore, Frontiers only applies the most rigorous and unbiased reviews.
Frontiers revolutionizes research publishing by freely delivering the most outstanding research, evaluated with no bias from both the academic and social point of view. By applying the most advanced information technologies, Frontiers is catapulting scholarly publishing into a new generation.

What are Frontiers Research Topics?

Frontiers Research Topics are very popular trademarks of the Frontiers Journals Series: they are collections of at least ten articles, all centered on a particular subject. With their unique mix of varied contributions from Original Research to Review Articles, Frontiers Research Topics unify the most influential researchers, the latest key findings and historical advances in a hot research area! Find out more on how to host your own Frontiers Research Topic or contribute to one as an author by contacting the Frontiers Editorial Office: researchtopics@frontiersin.org

THE GUT MICROBIOME IN HEALTH AND DISEASE

Topic Editors:
Nathan W. Schmidt, University of Louisville, United States
Venkatakrishna Rao Jala, University of Louisville, United States
Michele Marie Kosiewicz, University of Louisville, United States
Pascale Alard, University of Louisville, United States

Citation: Schmidt, N. W., Jala, V. R., Kosiewicz, M. M., Alard, P., eds. (2019). The Gut Microbiome in Health and Disease. Lausanne: Frontiers Media.
doi: 10.3389/978-2-88963-003-5

Table of Contents

frontiers in Cellular and Infection Microbiology

GENERAL COMMENTARY
published: 24 October 2018
doi: 10.3389/fcimb.2018.00374

Response: Commentary: Reducing Viability Bias in Analysis of Gut Microbiota in Preterm Infants at Risk of NEC and Sepsis

Gregory R. Young[1], Darren L. Smith[1], Nicholas D. Embleton[2], Janet Elizabeth Berrington[2], Edward C. Schwalbe[1], Stephen Paul Cummings[3], Christopher J. van der Gast[4] and Clare Lanyon[1]**

[1] Faculty of Health and Life Sciences, University of Northumbria, Newcastle upon Tyne, United Kingdom, [2] Newcastle Neonatal Service, Newcastle upon Tyne Hospitals NHS Foundation Trust, Newcastle upon Tyne, United Kingdom, [3] School of Science and Engineering, Teesside University, Middlesbrough, United Kingdom, [4] School of Healthcare Science, Manchester Metropolitan University, Manchester, United Kingdom

OPEN ACCESS

Edited by:
Pascale Alard, University of Louisville, United States

Reviewed by:
Bjoern O. Schroeder, University of Gothenburg, Sweden
Natalia Shulzhenko, Oregon State University, United States

***Correspondence:**
Gregory R. Young
gregory.young@northumbria.ac.uk
Clare Lanyon
clare.lanyon@northumbria.ac.uk

Specialty section:
This article was submitted to Microbiome in Health and Disease, a section of the journal Frontiers in Cellular and Infection Microbiology

Received: *28 June 2018*
Accepted: *05 October 2018*
Published: *24 October 2018*

Citation:
Young GR, Smith DL, Embleton ND, Berrington JE, Schwalbe EC, Cummings SP, van der Gast CJ and Lanyon C (2018) Response: Commentary: Reducing Viability Bias in Analysis of Gut Microbiota in Preterm Infants at Risk of NEC and Sepsis. Front. Cell. Infect. Microbiol. 8:374. doi: 10.3389/fcimb.2018.00374

Keywords: PMA, viability analyses, microbiota, methods—analytic, bias, clinical samples

A Commentary on

Commentary: Reducing Viability Bias in Analysis of Gut Microbiota in Preterm Infants at Risk of NEC and Sepsis
by Agustí, G., and Codony, F. (2018). Front. Cell. Infect. Microbiol. 8:212. doi: 10.3389/fcimb.2018.00212

We would like to thank Agustí and Codony (2018), for their interest in our recent manuscript (Young et al., 2017), and valuable comments. We agree that non-viable cell exclusion is an important consideration, worth making when conducting analyses of microbial communities via targeted DNA sequencing and amplification approaches. The technique is especially pertinent in environments where large volumes of non-viable bacteria are expected, such as in preterm infant stool, where multiple clinical interventions manifest deliberate bacterial killing.

Whilst we agree with the general principles with regards to sample collection and handling described by Agustí and Codony (2018) we maintain that these are not always possible in real-life, clinical patient samples. For example, as patient care is the primary concern in this cohort, sample collection is convenience based rather than experimentally dictated. This requires samples to be spontaneously collected and stored prior to processing. We concede this increases the likelihood of loss of anaerobic bacterial viability. We would, however point out that the study by Brusa et al. (1989), highlighted in the commentary defines viability purely as culturability. Studies (Contreras et al., 2011; Nocker et al., 2011) have reported loss of culturability occurs at lower stress levels than loss of membrane integrity. Thus, suggesting greater cellular stress may be required to deplete DNA signals from non-viable cells, as determined during PMA-based viability assays. Moreover, we highlight in our manuscript that PMA is a conservative parameter for loss of viability. We also propose that, in the specific cohort investigated, conservative non-viable determination is preferable to over-exaggerated determination or a complete absence of it. This is especially true when non-treated samples can be analyzed in parallel.

DNA retention on microtube surfaces and subsequent inclusion in the viable communities may well be an issue in PMA-based viability determination. In our study however, samples were not heat-killed at any point. This is in contrast to the study by Agustí et al. (2017), in which DNA binding to microtube walls may have occurred prior to PMA-treatment. Furthermore, the methods

described by ourselves outline transfer between sterile glass pots during initial sample collection and several microtubes and well plates from PMA-addition to incubation and photo-activation and, finally DNA isolation. We propose that these several steps are sufficient to reduce the impact of DNA retained on microtube surfaces on the assigned live DNA fraction.

In addition to the valuable comments made by Agustí and Codony (2018), where the target sequence is <300 bp we recommend combination of a nested-PCR approach, comprising initial long fragment pre-amplification, followed by subsequent target amplicon sequencing/quantification, first described by Luo et al. (2010). This increases the likelihood of encountering intercalated PMA during the DNA amplification process.

The use of PMA as a viability-dye is extremely useful in microbial community analysis. As a greater volume of literature becomes available regarding it's use, the technique will no doubt refine. From our experience with the technique, we propose several important considerations to be made when planning any study in which PMA-based non-viable cell exclusion is employed:

- Is the sample likely to contain substantial volumes of DNA originating from non-viable bacteria?
- Are the collection and storage methods likely to impact community viability?
- What is the composition of the sample? (Homogenisation may be required)
- What is the optimal concentration of PMA required to ensure non-viable cell DNA quenching?
- Is there potential for extra-cellular DNA carry-over in the methods? (specifically from DNA retained on plastics surfaces)
- What is my light-source for photoactivation (464 nm is excitation maxima of PMA therefore substantial emission at this wavelength is required)
- Can I employ a nested-PCR approach to maximize intercalated PMA impact?
- Can I afford to sequence the non-treated sample also? (Particularly useful in clinical environments to ID bacterial communities that may have been viable recently)
- Can I afford to supplement this technique with another to confirm presence/viability? (e.g., FISH, flow cytometry, selective culture)

We would further direct anyone interested to a comprehensive review of the technique by Fittipaldi et al. (2012).

AUTHOR CONTRIBUTIONS

GY wrote the response. All authors proofread and approved this commentary response.

REFERENCES

Agustí, G., and Codony, F. (2018). Commentary: Reducing viability bias in analysis of gut microbiota in preterm infants at risk of NEC and sepsis. *Front. Cell Infect. Microbiol.* 8:212. doi: 10.3389/fcimb.2018.00212

Agustí, G., Fittipaldi, M., and Codony, F. (2017). False-positive viability PCR results: an association with microtubes. *Curr. Microbiol.* 74, 377–380. doi: 10.1007/s00284-016-1189-3

Brusa, T., Canzi, E., Pacini, N., Zanchi, R., and Ferrari, A. (1989). Oxygen tolerance of anaerobic bacteria isolated from human feces. *Curr. Microbiol.* 19, 39–43.

Contreras, P. J., Urrutia, H., Sossa, K., and Nocker, A. (2011). Effect of PCR amplicon length on suppressing signals from membrane-compromised cells by propidium monoazide treatment. *J. Microbiol. Methods* 87, 89–95. doi: 10.1016/j.mimet.2011.07.016

Fittipaldi, M., Nocker, A., and Codony, F. (2012). Progress in understanding preferential detection of live cells using viability dyes in combination with DNA amplification. *J. Microbiol. Methods* 91, 276–289. doi: 10.1016/j.mimet.2012.08.007

Luo, J. F., Lin, W. T., and Guo, Y. (2010). Method to detect only viable cells in microbial ecology. *Appl. Microbiol. Biotechnol*. 86, 377–384. doi: 10.1007/s00253-009-2373-1

Nocker, A., Caspers, M., Esveld-Amanatidou, A., van der Vossen, J., Schuren, F., Montijn, R., et al. (2011). Multiparameter viability assay for stress profiling applied to the food pathogen Listeria monocytogenes F2365. *Appl. Environ. Microbiol.* 77, 6433–6440. doi: 10.1128/AEM.00142-11

Young, G. R., Smith, D. L., Embleton, N. D., Berrington, J. E., Schwalbe, E. C., Cummings, S. P., et al. (2017). Reducing Viability bias in analysis of gut microbiota in preterm infants at risk of NEC and sepsis. *Front. Cell Infect. Microbiol*. 7:237. doi: 10.3389/fcimb.2017.00237

Conflict of Interest Statement: The authors declare that the research was conducted in the absence of any commercial or financial relationships that could be construed as a potential conflict of interest.

Copyright © 2018 Young, Smith, Embleton, Berrington, Schwalbe, Cummings, van der Gast and Lanyon. This is an open-access article distributed under the terms of the Creative Commons Attribution License (CC BY). The use, distribution or reproduction in other forums is permitted, provided the original author(s) and the copyright owner(s) are credited and that the original publication in this journal is cited, in accordance with accepted academic practice. No use, distribution or reproduction is permitted which does not comply with these terms.

frontiers in Cellular and Infection Microbiology

ORIGINAL RESEARCH
published: 07 September 2018
doi: 10.3389/fcimb.2018.00281

Alterations in the Abundance and Co-occurrence of *Akkermansia muciniphila* and *Faecalibacterium prausnitzii* in the Colonic Mucosa of Inflammatory Bowel Disease Subjects

Mireia Lopez-Siles[1], *Núria Enrich-Capó*[1], *Xavier Aldeguer*[2], *Miriam Sabat-Mir*[3], *Sylvia H. Duncan*[4], *L. Jesús Garcia-Gil*[1]* *and Margarita Martinez-Medina*[1]

[1] *Laboratory of Molecular Microbiology, Biology Department, Universitat de Girona, Girona, Spain,* [2] *Department of Gastroenterology, Hospital Dr. Josep Trueta, Girona, Spain,* [3] *Department of Gastroenterology, Hospital Santa Caterina, Girona, Spain,* [4] *Microbiology Group, Rowett Institute of Nutrition and Health, Aberdeen, United Kingdom*

OPEN ACCESS

Edited by:
Venkatakrishna Rao Jala, University of Louisville, United States

Reviewed by:
Susan M. Bueno, Pontificia Universidad Católica de Chile, Chile
Valerio Iebba, Sapienza Università di Roma, Italy

***Correspondence:**
L. Jesús Garcia-Gil
jesus.garcia@udg.edu

Specialty section:
This article was submitted to Microbiome in Health and Disease, a section of the journal Frontiers in Cellular and Infection Microbiology

Received: *15 December 2017*
Accepted: *25 July 2018*
Published: *07 September 2018*

Citation:
Lopez-Siles M, Enrich-Capó N, Aldeguer X, Sabat-Mir M, Duncan SH, Garcia-Gil LJ and Martinez-Medina M (2018) Alterations in the Abundance and Co-occurrence of Akkermansia muciniphila and Faecalibacterium prausnitzii in the Colonic Mucosa of Inflammatory Bowel Disease Subjects. Front. Cell. Infect. Microbiol. 8:281. doi: 10.3389/fcimb.2018.00281

Akkermansia muciniphila and *Faecalibacterium prausnitzii,* cohabitants in the intestinal mucosa, are considered members of a healthy microbiota and reduction of both species occurs in several intestinal disorders, including inflammatory bowel disease. Little is known however about a possible link between the reduction in quantity of these species, and in which circumstances this may occur. This study aims to determine the abundances and co-occurrence of the two species in order to elucidate conditions that may compromise their presence in the gut. Loads of *A. muciniphila*, total *F. prausnitzii* and its two phylogroup (16S rRNA gene copies) were determined by quantitative polymerase chain reaction in colonic biopsies from 17 healthy controls (H), 23 patients with ulcerative colitis (UC), 31 patients with Crohn's disease (CD), 3 with irritable bowel syndrome (IBS) and 3 with colorectal cancer (CRC). Data were normalized to total bacterial 16S rRNA gene copies in the same sample. Prevalence, relative abundances and correlation analyses were performed according to type of disease and considering relevant clinical characteristics of patients such as IBD location, age of disease onset, CD behavior, current medication and activity status. Co-occurrence of both species was found in 29% of H, 65% of UC and 29% of CD. Lower levels of total *F. prausnitzii* and phylogroups were found in subjects with CD, compared with H subjects ($P \leq 0.044$). In contrast, no differences were found with the regard to *A. muciniphila* abundance across different disease states, but CD patients with disease onset below 16 years of age featured a marked depletion of this species. In CD patients, correlation between *A. muciniphila* and total *F. prausnitzii* ($\rho = 0.362$, $P = 0.045$) was observed, and particularly in those with non-stricturing, non-penetrating disease behavior and under moderate immunosuppressants therapy. Altogether, this study revealed that co-occurrence of both

species differs between disease status. In addition, IBD patients featured a reduction of *F. prausnitzii* but similar loads of *A. muciniphila* when compared to H subjects, with the exception of those with early onset CD. Depletion of *A. muciniphila* in this subgroup of subjects suggests that it could be a potential biomarker to assist in pediatric CD diagnosis.

Keywords: *Akkermansia muciniphila*, *Faecalibacterium prausnitzii*, Crohn's disease, ulcerative colitis, inflammatory bowel diseases

INTRODUCTION

Crohn's disease (CD) and ulcerative colitis (UC) are the two major types of idiopathic inflammatory bowel diseases (IBD) (Mendoza Hernández et al., 2007). Both are chronic inflammatory disorders of the gut. UC typically begins in the rectum and inflammation may extend continuously to involve the entire colon. In 20% of CD patients the disease affects the colon exclusively (Silverberg et al., 2005), but the most commonly involved areas are terminal ileum and the beginning of the colon. In CD any part of the gastrointestinal tract (from the oropharynx to the anus) may be affected in a patchy pattern (Mendoza Hernández et al., 2007). Other than location, differences in the mucosal lesions exist between these conditions. Inflammation in CD can be transmural reaching the serosa, whereas inflammation in UC patients is generally restricted to the mucosa.

The inner layer of the bowel wall is a niche of particular importance, because of the spatial proximity between epithelial cells and gut bacteria, and thus the study of human intestinal mucosa biopsies provides meaningful insights of host-bacterial interactions. Numerous studies have been prompted over the last decade aiming at deciphering the exact role of gut microbiota in IBD. Nowadays there is a wide variety of clinical and experimental studies revealing microbial implication in IBD (Sartor, 2006, 2008; Seksik et al., 2006; Manichanh et al., 2012). The most replicated finding by far has been disturbances in the intestinal microbiota composition balance, situation known as dysbiosis (Gophna et al., 2006; Manichanh et al., 2006; Martinez-Medina et al., 2006; Andoh et al., 2009; Willing et al., 2009; Sokol and Seksik, 2010; Joossens et al., 2011; Mondot et al., 2011; Machiels et al., 2013). In this state, dominating species, to whom a beneficial role to preserve gut homeostasis has been attributed, become underrepresented.

Akkermansia muciniphila inhabits mainly in the mucosa, and represents between 1 and 3% of the gut microbiota (Derrien et al., 2004, 2008). A decrease of this species has been demonstrated in feces and/or biopsies of several disorders including autism, obesity, type 2 diabetes, appendicitis, and IBD (Belzer and de Vos, 2012; Everard et al., 2013). Studies in mice models have shown that gut colonization by this species affects expression of genes involved in immune response-regulatory processes (Derrien et al., 2011) as well as in host's lipid metabolism (Lukovac et al., 2014), especially in the colon. It is of note that extracellular vesicles derived from this species have a protective function that ameliorates severity of induced colitis in mice, suggesting that it has an important role in the maintenance of intestinal homeostasis (Kang et al., 2013). *A. muciniphila* is essential for a healthy mucus layer in the human gut in terms of mucus production and thickness (Belzer and de Vos, 2012). This species is not only important for the host, but also for gut microbial community. Its specific capability to degrade mucus results in the release of oligosaccharides and the production of propionate and acetate (Derrien et al., 2004) as well as amino acids, important co-factors and vitamins (van Passel et al., 2011) that become available for other gut symbionts. However, significant co-occurrence of this species with other bacterial taxa present in the gut has not been revealed in feces (Lozupone et al., 2012).

In turn, *Faecalibacterium prausnitzii* is also an abundant intestinal microorganism with a feco-mucosal distribution, and whose relative abundance can represent between 2 and 15% of intestinal bacterial communities (Swidsinski et al., 2005; Baumgart et al., 2007; Flint et al., 2012). Several studies, of fecal and/or mucosal samples, have shown that *F. prausnitzii* prevalence and abundance are reduced under certain disorders such as celiac disease (Swidsinski et al., 2008; De Palma et al., 2009), obesity and type 2 diabetes (Furet et al., 2010; Graessler et al., 2012), appendicitis (Swidsinski et al., 2011), chronic diarrhea (Dörffel et al., 2012), irritable bowel syndrome (IBS) of alternating type (Rajilić-Stojanović et al., 2011), colorectal cancer (CRC) (Balamurugan et al., 2008; Lopez-Siles et al., 2016), and particularly in IBD (Sokol et al., 2008, 2009; Swidsinski et al., 2008; Willing et al., 2009; Machiels et al., 2013; Lopez-Siles et al., 2014). Low abundance of this species has been linked with active IBD (Sokol et al., 2009), and some complications such as a higher risk of post-operative recurrence (Sokol et al., 2008) or pouchitis (McLaughlin et al., 2010). Other than butyrate production (which can reduce intestinal mucosa inflammation and is the main energy source for the colonocytes), additional anti-inflammatory properties have been attributed to *F. prausnitzii* (Sokol et al., 2008; Miquel et al., 2013; Martín et al., 2014). Both, cell and supernatant fractions of this species, have been proven to reduce severity of acute (Sokol et al., 2008; Rossi et al., 2015), chronic (Martín et al., 2014) and low grade (Martín et al., 2015) inflammation in murine models. This has been attributed to an enhancement of intestinal barrier function related with the expression of certain tight junction proteins other than claudin (Carlsson et al., 2013). *F. prausnitzii* also influences gut physiology through the production of mucus O-glycans, and may help to maintain suitable proportions of different cell types of secretory linage in the intestinal epithelium, as evidenced in rodent studies (Wrzosek et al., 2013). To date, it remains unclear which conditions are likely to compromise this species in the

gut. Alterations in gut pH or bile salt concentration have been suggested (Lopez-Siles et al., 2012), but a break in the ecologic relations with other gut symbionts that support its presence in the gut may also contribute, but have been little studied. Co-occurrence network analysis of gut bacteria found in feces, showed that *F. prausnitzii* co-occurs with several members of the *C. coccoides* group and Bacteroidetes (Lozupone et al., 2012). As *F. prausnitzii* growth is stimulated by acetate (Duncan et al., 2002), its presence in the gut may also be favored by acetate producers like *A. muciniphila*. However, little is known about interaction between these two species.

This work is aimed at determining the variation of mucosa-associated *A. muciniphila* and *F. prausnitzii* between healthy control subjects (H) and patients suffering from IBD, in order to elucidate in which conditions imbalances of these species take place, and if both species are affected equally. Some IBS and CRC patients have been included for comparative purposes. Prevalence and abundance of mucosa-associated *A. muciniphila* and *F. prausnitzii* have been determined in colonic samples by quantitative polymerase chain reaction (qPCR). Data have been analyzed taking into account patients' most relevant clinical characteristics. Medication at sampling was also considered in order to determine if any of the current therapies are effective in restoring these species levels to those found in H. In addition, correlation analysis of their load has also been conducted to provide supporting evidence on the effect of one population over the other, or about whether or not they are influenced by similar gut factors.

MATERIALS AND METHODS

Patient Recruitment and Characteristics

The study population was a cohort consisting of Spanish volunteers including 54 IBD (31 CD and 23 UC), three IBS, three CRC patients and 17 H (**Table 1**). Subjects were gender matched for all the groups. Concerning age, CD patients were younger than those in the H group ($P = 0.002$), whereas CRC patients were significantly older than those with IBD ($P \leq 0.028$). Besides, at disease onset, CD patients were younger than UC (mean age ± SD; UC = 37.2 ± 13.3 years, CD = 28.0 ± 12.4 years; $P = 0.012$).

Subjects were recruited by the Gastroenterology Services of the Hospital Universitari Dr. Josep Trueta (Girona, Spain) and the Hospital Santa Caterina (Salt, Spain) between 2006 and 2010. To avoid bias between centers, patients with IBD were diagnosed according to standard clinical, pathological, and endoscopic criteria and categorized according to the Montreal classification (Silverberg et al., 2005). IBS patients were diagnosed according to Rome III criteria (available at http://www.romecriteria.org/criteria/). The diagnosis of CRC was established by colonoscopy and biopsy, and data correlated with high risk of developing this disease was recorded. Controls consisted of subjects who underwent colonoscopy for different reasons as rectorrhagia ($n = 8$), colorectal cancer familial history ($n = 3$), and abdominal pain ($n = 6$), and all featured normal colonoscopy. Clinically relevant data of all the patients was collected (**Table 1**). Percentage of active patients was higher in CD patients than in UC ($P = 0.036$). Individuals included in this study were >18 years old, did not have any other intestinal disease and were not pregnant. Antibiotic treatment within 2 months before colonoscopy was an exclusion criterion.

Ethics Statement

This work was approved by the Ethics Committee of Clinical Research of the Hospital Universitari Dr. Josep Trueta (Girona, Spain) and the Institut d'Assistència Sanitària of Girona (Salt, Spain) on 26th May 2006 (protocol code BACTECCU, Ref CEIC: 08/06) and 21st April 2009 (protocol code BACTODIAG, Ref CEIC: 10/08), respectively. All subjects gave written informed consent in accordance with the Declaration of Helsinki.

Sample Collection and DNA Extraction

Cleansing of the gastrointestinal tract using Casenglicol® was performed prior to colonoscopy, following manufacturer's guidelines. During routine endoscopy and following standard procedures, a biopsy (<25 mg) from non-affected tissue of the colon was taken for each subject. All biopsies were immediately placed in sterile tubes without any buffer. Following completion of the whole endoscopic procedure, all samples were stored at −80°C upon analysis.

To discard transient and loosely attached bacteria, biopsies were subjected to two mild ultrasound wash cycles, as reported previously (Martinez-Medina et al., 2006). Afterwards, DNA was extracted using the NucleoSpin® Tissue Kit (Macherey-Nagel GmbH & Co., Duren, Germany). The support protocol for Gram positive bacteria (consisting of pre-incubation during 1 h at 37°C with buffer T1 (20 mm Tris/HCl, 2 mM EDTA, 1% Triton X-100, pH 8) supplemented with 20 mg/ml lysozyme), and the RNAse treatment step were carried out. Genomic DNA was eluted with 10 mM Tris-HCl (pH 7.4) and stored at −80°C until use. DNA concentration and purity of the extracts were determined with a NanoDrop ND-100 spectrophotometer (NanoDrop Technologies, USA). The average purity and concentration of the DNA extracts was (mean ± SD) 1.794 ± 0.579 Abs260/280 ratio and 174.864 ± 131.829 ng/μl, respectively.

Quantification Standards for qPCR

Standard DNA templates from *F. prausnitzii* strain S3L/3 (phylogroup I), *F. prausnitzii* DSM 17677 (phylogroup II) and *A. muciniphila* (ATCCBAA-835) were prepared as genetic constructs after PCR amplification of the whole 16S rRNA as previously reported (Lane, 1991; Weisburg et al., 1991), and subsequent insertion of this gene into a pCR®4-TOPO® cloning plasmid (Invitrogen, CA, USA) following manufacturer's guidelines.

After purification with the NucleoSpin® Plasmid kit (Macherey-Nagel GmbH & Co., Duren, Germany), plasmids were linearized with *SpeI* and quantified using Qubit™ Quantitation Platform (Invitrogen, Carlsbad, USA). Initial target concentration was inferred taking into consideration the theoretical molecular weight (3.58×10^6 Da) and the size of recombinant plasmid (5421 pb).

TABLE 1 | Sample size and clinical characteristics of subjects.

	Healthy	Irritable bowel syndrome	Colorectal cancer	IBD		*P*-value[§]
				Ulcerative colitis	Crohn's disease	
n (patients)	17	3	3	23	31	
Age (mean years ± SD)	48.1 ± 15.8	35.0 ± 7.0	69.3 ± 16.0	40.5 ± 13.5	33.6 ± 12.2	**0.002****
Male (*n*, %)	10 (58.8%)	1 (33.3%)	3 (100%)	13 (56.5%)	20 (64.5%)	0.826[†]
Active (*n*, %)	na	na	na	3 (13.0%)	13 (41.9%)	**0.036**[†]
Previous surgery (*n*, %)	na	na	na	1 (4.3%)	6 (19.4%)	0.213[†]
Smokers (*n*, %)	0 (0%)	0 (0%)	0 (0%)	2 (8.7%)	5 (16.1%)	0.410[†]
Treatment (*n*, %)*						0.494[†]
No treatment	na	na	na	11 (47.8%)	10 (32.3%)	
Mesalazine	na	na	na	3 (13.0%)	3 (9.7%)	
Moderate immunosuppressant	na	na	na	4 (17.4%)	10 (32.3%)	
Anti-TNFα (infliximab, adalimumab)	na	na	na	3 (13.0%)	6 (19.4%)	
CD Montreal classification						
Age of diagnosis (*n*, %)*						**0.007**
<16 yeays (A1)	na	na	na	na	5 (16.1%)	
17–40 years (A2)	na	na	na	11 (47.8%)	21 (67.7%)	
>41 years (A3)	na	na	na	9 (39.1%)	3 (9.7%)	
Location (*N*, %)						na
Ileal-CD (L1)	na	na	na	na	13 (41.9%)	
Colonic-CD (L2)	na	na	na	na	7 (22.6%)	
Ileocolonic-CD (L3)	na	na	na	na	10 (32.3%)	
Behavior (*N*, %)*						na
Non-stricturing, non-penetrating (B1)	na	na	na	na	19 (61.3%)	
Stricturing (B2)	na	na	na	na	8 (25.8%)	
UC classification (*n*, %)*						na
Ulcerative proctitis (E1)	na	na	na	5 (21.7%)	na	
Distal UC (E2)	na	na	na	11 (47.8%)	na	
Extensive UC or ulcerative pancolitis (E3)	na	na	na	6 (26.1%)	na	

IBD, Inflammatory bowel disease; TNF, tumor necrosis factor; na, not applicable.

**Medical treatment at the time of sampling was available in 21/23 UC, and 29/31 CD patients; Age of disease onset was available for 20/23 UC patients, and 29/31 CD patients; Disease behavior at last follow-up before the time of sampling was available in 27/31 CD patients, and none had penetrating CD (B3); Maximal disease extent at the time of sampling was available in 22/23 UC and 30/31 CD patients.*

*[§]Groups were compared by appropriate statistical tests, and P-value ≤ 0.05 was considered significant, [†] χ^2 test, **ANOVA. Analyses statistically significant are highlighted in boldface.*

Standard curves were obtained from 10-fold serial dilutions of the titrated suspension of linearized plasmids. Strains used to construct each standard curve are indicated in **Table 2**. To prepare the standard curve, only dilutions within the linear dynamic range span of each reaction were used, as detailed in **Table 2**. Total bacteria 16S rRNA gene quantification was used to intercalibrate all the standard curves, in order to make sure that results obtained were comparable. Accordingly, plasmid preparations for *A. muciniphila* standard and phylogroups standards were run as unknown samples in a total bacterial qPCR. Specific intercalibration of total *F. prausnitzii* qPCR was not required as it uses the same standard curve template employed for total bacterial qPCR (**Table 2**). Quantification values obtained were compared to initial target concentration inferred from DNA concentration, and <10% variation was obtained.

qPCR Assays

Previously reported 16S rRNA gene-targeted primers and probes were used for total *F. prausnitzii* (Lopez-Siles et al., 2014), phylogroups (Lopez-Siles et al., 2016), *A. muciniphila* (Collado et al., 2007) and total bacterial (Furet et al., 2009) quantification through qPCR.

Amplification reactions were performed as described elsewhere (Collado et al., 2007; Furet et al., 2009; Lopez-Siles et al., 2014, 2016) with slight modifications detailed in **Table 2**. Briefly, quantifications were carried out in a total volume of 20 µl reactions containing: 1× TaqMan® Universal PCR Master Mix 2× or SYBR®Green PCR Master Mix 2× (Applied Biosystems, Foster City, CA, USA) as required, 300–900 nM of each primer and 250–300 nM of probe if necessary. Up to 50 ng of genomic DNA template was added in each reaction. All primers and probes used in this study as well as PCR conditions are detailed in **Table 2**. Total *F. prausnitzii*, and total bacteria primers and

TABLE 2 | 16S rRNA-targeted primers and probes used in this study.

Target	Primers and probe	Sequence (5′-3′)[a]	Final conc. (nM)	Strain used as standard	Standard curve*	qPCR conditions[c]					References
						Fluorescence reporting method	Cycles	Denat. T[a] (°C); *t* (s)	Annealing and extension T[a] (°C), *t* (s)	Melting curve[d]	
Total bacteria (Eubacteria)	F_Bact 1369	CGGTGAATACGTTCCCGG	300	*F. prausnitzii* DSM 17677	10^7-10^3; 89.0 ± 7.0	Hydrolysis probe	40	95; 30	60; 60	No	Furet et al., 2009
	R_Prok1492	TACGGCTACCTTGTTACGACTT	300								
	P_TM1389F	**FAM-CTTGTACACACCGCCCGTC-TAMRA**	**250**								
Akkermansia muciniphila	AM1-F	CAGCACGTGAAGGTGGGGAC	300	*A. muciniphila* ATCCBAA-835	2×10^2 - 2×10^7; 93.9 ± 4.2	SYBR Green	50	95; 15	65; 30 and 72; 32	Yes	Collado et al., 2007
	AM2-R	CCTTGCGGTTGGCTTCAGAT	300								
Faecalibacterium prausnitzii (total)	Fpra428F	TGTAAACTCCTGTTGTTGAGGAAGATAA	300	*F. prausnitzii* DSM 17677	10^7-10^3; 84.8 ± 3.2	Hydrolysis probe	40	95; 15	60; 60	No	Lopez-Siles et al., 2014
	Fpra583R	GCGCTCCCTTTACACCCA	300								
	Fpra493PR	**FAM-CAAGGAAGTGACGGCTAACTACGTGCCAG-TAMRA**	**250**								
IAC[b]	IAC F	TACGGATGAGGAGGACAAAGGA	300	DNA IAC	n.a.	Hydrolysis probe	40	95; 15	60; 60	No	Lopez-Siles et al., 2014
	IAC R	CACTTCGCTCTGATCCATTGG	300								
	IAC PR	**VIC®-CGCCGCTATGGGCATCGCA-TAMRA**	**250**								
F. prausnitzii (phylogroups)	Fpra 136F	CTCAAAGAGGGGGACAACAGTT	900	*F. prausnitzii* S3L/3 (phylogroup I) and DSM 17677 (phylogroup II)	10^6-10; 86.3 ± 6.1; 95.3 ± 11.9	Hydrolysis probe	40	95; 15	64; 60	No	Lopez-Siles et al., 2016
	Fpra 232R	GCCATCTCAAAGCGGATTG	900								
	PHG1 180PR	**6FAM-TAAGCCCACGACCCGGCATCG-BHQ1**	**300**								
	PHG2 180PR	**JOE-TAAGCCCACRGCTCGGCATC-BHQ1**	**300**								

**Range span (16S rRNA gene copies), Efficiency (mean ± standard deviation); n.a., not applicable.*

[a]Probe sequences are in bold. FAM™, 6-carboxyfluorescin; VIC®, 6-carboxyrhodamine; JOE, 4′,5′-dichloro-2′,7′-dimethoxy-5(6)-carboxyfluorescein; TAMRA™, tetramethylrhodamin; BHQ1, Black Hole Quencher1.

[b]IAC, internal amplification control; 10^3 copies of appropriate DNA template were added in each reaction. DNA IAC sequence (5′-3′), DNA IAC sequence: 5′-TACggATgAggAggACAAAggACgCCgCTATgggCATCgCACCAATggATCA gAgCgAAgTg-3′ (according to Lopez-Siles et al., 2014).

[c]An amperase treatment (50°C, 2 min) and an initial denaturing step (95°C, 10 min) were performed for all the reactions. For assays based on hydrolysis probes, annealing and extension steps were performed simultaneously.

[d]Melting curve consisted on 95°C 15 s, 60°C 1 min, 95°C 15 s, and 60°C 15 s (average temperature slope 0.58°C/s).

hydrolysis probes were purchased from Applied Biosystems (Foster City, CA, USA), whereas primers and hydrolysis probes for *F. prausnitzii* phylogroups and *A. muciniphila* were acquired from Biomers (Ulm, Germany). DNA of the internal amplification control (IAC) was synthesized by Bonsai technologies group (Alcobendas, Spain). All oligonucleotides were purified by HPLC. Plates and optical caps were provided by Applied Biosystems (Ref. 4323032 and Ref. 4306737, respectively).

Samples were run at least in duplicate in the same plate (**Table S1**), which was set up manually. For data analysis, the mean of the quantifications was used. Duplicates were considered valid if the standard deviation between quantification cycles (C_q) was <0.34 (i.e., a difference of <10% of the quantity was tolerated), and if not quantification was repeated. Quantification controls consisting of at least five reactions with a known number of target genes were performed to assess inter-run reproducibility. Inhibition was controlled on total *F. prausnitzii* quantification by adding 10^3 copies of an internal amplification control (IAC) template to each reaction. It was considered that there was no inhibition if the obtained C_q was <0.34 different from those obtained when quantifying the IAC alone for any of the replicates. In each run, a non-amplification control (NTC) which did not contain any DNA template (either bacterial or IAC) was also included. In all cases with hydrolysis probes, NTC resulted in undetectable C_q values whereas for SYBR Green assays NTC had C_q >35, and melting curve analysis confirmed no specific amplification.

A 7500 Real Time PCR system (Applied Biosystems, USA) was used to perform all qPCR. The thermal profile used for each assay is detailed in **Table 2**. In summary, it consisted of a first step at 50°C during 2 min for amperase treatment followed by a 95°C hold for 10 min to denature DNA and activate Ampli-Taq Gold polymerase; and a further 40–50 cycles consisting of a denaturation step at 95°C for 15 s, followed by an annealing and extension step at 60°C (or at 64°C for phylogroups quantification) for 1 min. When required, melting curve analysis was performed to assess whether or not fluorescence was due to specific amplification products. Data were collected and analyzed using the 7500 SDS system software version 1.4 (Applied Biosystems). Assays were performed under average PCR efficiencies of (mean ± SD) 89.9 ± 4.6% (**Figure S2**).

Data Normalization and Statistical Analysis

Regarding the qualitative analyses, absence of *F. prausnitzii*, its phylogroups or *A. muciniphila* was considered if no detection was obtained during the qPCR analysis, corresponding to samples that carried these bacteria below the detection limit (i.e., 106.6, 1.10, 2.39, and 374.09 16S rRNA genes per reaction for total *F. prausnitzii*, phylogroup I, phylogroup II, and *A. muciniphila*, respectively). Pearson's χ^2 test was used to compare the prevalence between groups of patients, by IBD disease location, age of disease onset and other clinically relevant data as activity, treatment and whether or not patients have had intestinal resection.

Referring to quantitative analyses, total *F. prausnitzii,* phylogroups and *A. muciniphila* 16S rRNA gene copy detected in each sample were normalized to the total bacterial 16S rRNA gene copies in the same sample. Data are given as the $\log_{10}$ of the ratio between 16S rRNA gene copies of the target microorganism and million of total bacterial 16S rRNA genes detected in the same sample. No further correction to adjust for differences in 16S rRNA gene operons in each species was performed, as no consensus has been achieved to date for *F. prausnitzii* according to *rrn*DB (Stoddard et al., 2015). For those samples with no detection of *F. prausnitzii*, phylogroup or *A. muciniphila*, the number of copies corresponding to their respective detection limit was used for calculations of relative abundances. Kruskal–Wallis non-parametric test was applied to assess differences in variables with more than two categories such as diagnostics, CD and UC disease location, age of disease onset, and current medication. Mann–Whitney *U* test was used to perform pairwise comparisons of subcategories of these variables, and FDR after multiple comparisons was assessed (**Table S2**). Mann–Whitney *U* test was also used to compare, variables with two categories such as activity (active CD and UC patients when CDAI > 150 (Best et al., 1976) and a Mayo score >3 (Pineton de Chambrun et al., 2010), respectively), and intestinal resection. In addition, ratios between 16S rRNA gene copies of either total *F. prausnitzii*, phylogroup I or phylogroup II and *A. muciniphila* were calculated and analyzed as detailed above. Spearman correlation coefficient and significance between total *F. prausnitzii,* or phylogroup quantities and *A. muciniphila* load was calculated. The same statistical method was used to analyze the correlation between the quantity of each bacterial group, and continuous clinical data such as time (in years) since disease onset. All the statistical analyses were performed using the SPSS 15.0 statistical package (LEAD Technologies, Inc.). Significance levels were established for $P \leq 0.05$.

RESULTS

Prevalence of Mucosa-Associated *A. muciniphila* and *F. prausnitzii*

To assess co-occurrence of both species, prevalence of *F. prausnitzii* (total or separating by phylogroups), and *A. muciniphila* as calculated from positive determinations over total samples, was analyzed by condition, by IBD location and also taking into account relevant clinical data (**Figure 1**). Four categories of patients were established based on: detecting only *F. prausnitzii*, detecting only *A. muciniphila*, detecting both species, or none of them. Most of the subjects carried both species or *F. prausnitzii* alone, whilst finding *A. muciniphila* alone was rare and in some cases, none of the two species was found suggesting that if present, they are below the detection limit of our assays.

When analysing the cohort by diagnostics (**Figure 1A**), only statistically significant differences in the proportions of each category were observed for the co-occurrence of *F. prausnitzii* phylogroup I and *A. muciniphila* ($P < 0.001$). As a particularity of CD, none of the two species was detected in 51.61% of subjects of this group, which was a higher proportion than in the other groups of subjects (ranging from 4.35% to 33.3%). In 64.71% of H subjects only one species (*F. prausnitzii* phylopgroup I) was

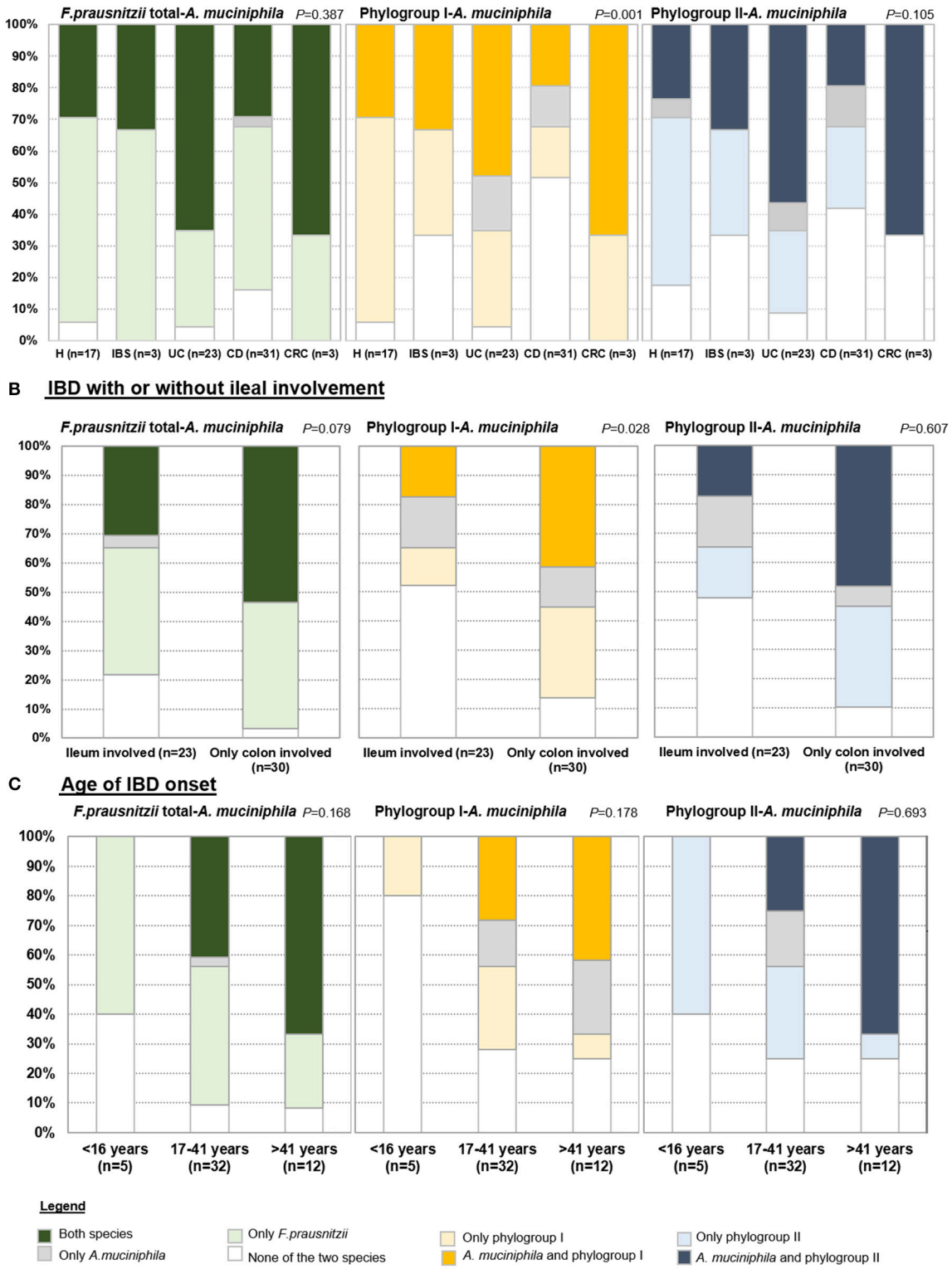

FIGURE 1 | Prevalence of total *F. prausnitzii,* phylogroups and *A. muciniphila* in **(A)** each group of patients, **(B)** in Inflammatory bowel disease (IBD) subjects according to whether or not ileum is affected, and **(C)** in IBD by age of disease onset. H, control subjects; IBS, irritable bowel syndrome; UC, ulcerative colitis; CD, Crohn's disease; CRC, colorectal cancer.

detected, while this category was present in between 16% and 34% in the other groups of subjects. *F. prausnitzii* phylogroup I and *A. muciniphila* were found in approximately 30% of H, 33.33% of IBS and 20% of CD subjects, whereas 47.82% of UC and 66.67% of CRC patients fall into this category. Similar trends were observed for *F. prausnitzii* phylogroup II and *A. muciniphila* co-occurence analysis ($P = 0.105$), whereas percentages of each category were more similar between groups of subjects when analyzed in conjunction prevalence of total *F. prausnitzii* and *A. muciniphila* ($P = 0.387$). Of note, all subjects with IBS or CRC had at least one of the two species.

When analysing the cohort by IBD disease location, no significant differences within UC and within CD subtypes were achieved (**Figure S1**). However, a trend toward different proportions was observed. Half of subjects with distal UC (E2) were characterized by presenting only *A. muciniphila*. All patients with UC and also those with C-CD carried at least one species, whereas lower prevalences were found in CD patients with ileal involvement. Particularly, none of the two species were detected in 10–31% of CD patients with ileal disease location, whereas in 23.1% of I-CD and 40% of IC-CD, both species co-occurred. As the frequencies observed in C-CD patients resembled in some cases those in UC, we analyzed IBD subjects by grouping those with (either I-CD or IC-CD) or without (i.e., C-CD or UC) ileum involved (**Figure 1B**). Interestingly, when analyzing co-occurrence of *F. prausnitzii* phylogroup I and *A. muciniphila* the percentage of subjects with none or only one species detected was over 80% in those with ileal disease whereas in approximately 40% of subjects with colonic disease both species were found ($P = 0.028$).

When analyzing prevalence taking into account clinical data of the patients, no significant differences were observed by activity, medication or intestinal resection neither in CD nor in UC. No differences were found within CD patients according to disease behavior. Interestingly, *A. muciniphila* was not detected in any of the CD patients diagnosed with disease onset below 16 years of age (**Figure 1C**). It remains to be stablished if this is a common issue with UC patients, as none with early disease onset was included in our cohort.

Abundances of Mucosa-Associated *A. muciniphila* and *F. prausnitzii*

A. muciniphila, total *F. prausnitzii* and its phylogroups load was compared amongst patients with different intestinal conditions (**Table 3**). Total *F. prausnitzii* was less abundant in CRC and IBD patients as compared to H subjects. However, statistically significant differences were achieved only for CRC ($P = 0.028$) and CD patients [$P = 0.021$, but not sustained after FDR assessment (**Table S2**)], probably because the reduction is lower for UC patients and the high variability between subjects. In CD patients, those with ileal involvement presented the lowest levels of this bacterium ($P = 0.050$), whereas IC-CD patients and C-CD were similar to UC (**Table 3**). Slight differences in average load were also found within UC patients although these differences were not statistically supported. Patients with ulcerative proctitis (E1) and extensive UC (E3) presented *F. prausnitzii* loads similar to H subjects, whereas those with E2 had abundances between CD patients and H subjects.

F. prausnitzii phylogroup I load was reduced in all groups of patients in comparison to H subjects. This reduction was particularly noticeable in CD and CRC patients ($P < 0.008$), while in UC and IBS patients, it was observed as well, but less apparent. When analyzing data by disease location, I-CD patients showed the most marked reduction of phylogroup I counts in comparison to other CD locations ($P = 0.025$). Values did not differ significantly in UC patients when analyzed by location. However, loads in E2 and E3 subjects resembled that of CD patients, while for E1 subjects, their profiles were closer to that observed in H subjects.

With respect to *F. prausnitzii* phylogroup II, its abundance was significantly reduced in CD patients when compared to UC subjects ($P = 0.015$) while similar loads were observed between all the other groups of subjects (**Table 3**). Although no differences by IBD location were found, loads tend to be lower in those with ileal involvement (either I-CD or IC-CD, $P = 0.069$).

Interestingly, *A. muciniphila* load was similar between all the groups of subjects and also no differences were observed between IBD locations ($P > 0.540$; **Table 3**). In all groups of subjects, total *F. prausnitzii* counts outnumbered *A. muciniphila*, but there was a high variability between subjects, even within each condition. No difference in the ratio of total *F. prausnitzii*: *A. muciniphila* was found by group of subjects, neither when analyzing by IBD subtypes according to disease location. In contrast, when calculating these ratios by *F. prausnitzii* phylogroups, significant differences were found between conditions (**Figure 2**). CD patients, featured lower phylogroup I:*A. muciniphila* ratios than H ($P = 0.031$), and also lower phylogroup II: *A. muciniphila* ratios compared to UC ($P = 0.017$). When analyzing IBD groups by disease location, no significant differences were observed, probably due to the high dispersion of data and to the fact that when separating by location the number of patients included within each category is reduced. Nonetheless, subjects with a larger disease extension, or with ileum involvement, tended to feature lower values of both ratios. These differences in ratios are due to differences in *F. prausnitzii* (or phylogroup) load, as *A. muciniphila* load was similar across all subjects.

A. muciniphila and *F. prausnitzii* Abundances in Relation to Patients Clinical and Treatment Data

No differences in *A. muciniphila,* counts were observed in either UC or CD patients according to activity status. Nevertheless, those patients with active UC featured the lowest load. *F. prausnitzii* and the abundance of the phylogroups did not differ between active and inactive UC patients (**Table 4**). CD patients with active disease feature lower levels of total *F. prausnitzii* and phylogroups in comparison to patients in remission, but differences did not achieve statistical significance either.

Resection in CD patients was not a determining factor for *A. muciniphila* loads, either (**Table 5**). Instead, *F. prausnitzii* abundance was lower in those CD patients that underwent intestinal resection, with significant statistical differences for

TABLE 3 | Abundances of mucosa-associated *F. prausnitzii*, its phylogroups and *A. muciniphila* in controls (H), irritable bowel syndrome (IBS), colorectal cancer (CRC), Ulcerative Colitis (UC), and Crohn's disease (CD) patients.

	***n* patients**	***F. prausnitzii**§**	**Phylogroup I*§**	**Phylogroup II*§**	***A. muciniphila***
H	**17**	**5.07 ± 0.70^{a}**	**3.00 ± 0.81^{a}**	**2.32 ± 1.69^{ab}**	**3.49 ± 0.81**
IBS	**3**	**5.50 ± 0.16^{ab}**	**2.16 ± 1.54^{ab}**	**2.00 ± 1.33^{ab}**	**3.63 ± 0.95**
CRC	**3**	**4.24 ± 0.34^{b}**	**1.12 ± 0.91^{bc}**	**2.06 ± 1.62^{ab}**	**2.84 ± 1.35**
UC	**23**	**4.82 ± 0.67^{ab}**	**2.16 ± 1.26^{ac}**	**2.79 ± 1.07^{a}**	**3.07 ± 1.14**
UC location					
Ulcerative proctitis (E1)	5	5.01 ± 0.20	3.07 ± 0.32	3.44 ± 0.51	2.77 ± 1.36
Distal UC (E2)	11	4.77 ± 0.61	2.41 ± 1.11	2.74 ± 0.99	3.13 ± 1.24
Extensive UC or ulcerative pancolitis (E3)	6	5.03 ± 0.76	1.18 ± 1.36	2.69 ± 1.23	3.11 ± 0.98
CD	**31**	**4.22 ± 1.31^{b}**	**1.13 ± 1.64^{b}**	**1.47 ± 1.37^{b}**	**3.19 ± 1.35**
CD location					
Ileal-CD (L1)	13	3.52 ± 1.33$^{\bullet}$	0.17 ± 1.10$^{\bullet}$	1.18 ± 1.55	2.87 ± 1.28
Colonic-CD (L2)	7	5.00 ± 0.93$^{\blacksquare}$	1.73 ± 1.94$^{\blacksquare}$	2.12 ± 1.36	3.33 ± 1.23
Ileocolonic-CD (L3)	10	4.47 ± 1.18$^{\bullet\blacksquare}$	1.87 ± 1.60$^{\blacksquare}$	1.28 ± 1.09	3.42 ± 1.61
p-value group of subjects		**0.024**	**0.002**	**0.015**	0.540
p-value UC location		0.568	0.110	0.432	0.961
p-value CD location		**0.050**	**0.025**	0.349	0.538

§*Mean log_{10} (16S rRNA gene copies/million bacterial 16S rRNA gene copies) ± standard deviations.*

**Statistics was calculated separately for each variable (column). Only for those analyses statistically significant (P-value in bold), pairwise comparisons were conducted, and groups of patients with similar abundances are indicated with the same superscript (a, b). Disease locations of UC and CD patients have been analyzed as independent groups. Similarly, patients' subtypes with similar abundances are indicated with the same superscript (•■). In both cases, groups not sharing superscript are those with statistically different median abundance values (P-value < 0.05).*

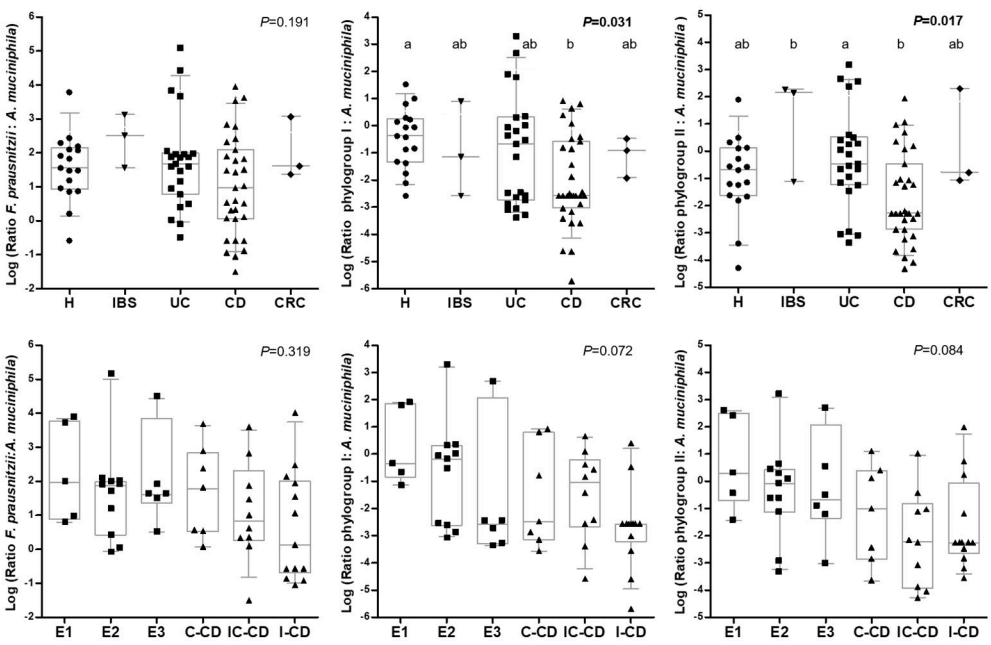

FIGURE 2 | Box and whiskers plot of the ratio total *F. prausnitzii*: *A. muciniphila*, *F. prausnitzii* phylogroup I: *A. muciniphila,* and *F. prausnitzii* phylogroup II: *A. muciniphila:* (from left to right) by group of subjects (up) and by Inflammatory Bowel Disease subtype (down). Data are represented as log_{10} of each ratio. The median is represented by the horizontal line in each box. Boxes cover the 25 and 75% quantiles, and bars show the 10 and 90% quantiles. Individual data are also shown. Homogeneous subgroups in each plot are indicated with the same superscript. H, control subjects; IBS, irritable bowel syndrome; UC, ulcerative colitis; CD, Croh's disease; CRC, colorectal cancer; E1, ulcerative proctitis; E2, ulcerative left-sided colitis; E3, ulcerative pancolitis; IC-CD, ileocolonic CD, I-CD, ileal CD; C-CD, colonic CD. *A. muciniphila*, 16S rRNA gene *Akkermansia muciniphila; F. prausnitzii*, 16S rRNA gene total *Faecalibacterium prausnitzii;* Phylogroup I, 16S rRNA gene *F. prausnitzii* phylogroup I; Phylogroup II, 16S rRNA gene *F. prausnitzii* phylogroup II.

TABLE 4 | *F. prausnitzii*, its phylogroups and *A. muciniphila* abundance in inflammatory bowel disease patients by disease activity status.

Diagnostics[§]	*n*	*F. prausnitzii**	*P*-value	Phylogroup I*	*P*-value	Phylogroup II*	*P*-value	*A. muciniphila**	*P*-value
UC									
Active	19	4.85 ± 0.71	0.464	2.12 ± 1.35	0.787	2.76 ± 1.11	0.523	3.04 ± 1.06	0.651
Inactive	3	4.61 ± 0.52		2.39 ± 0.97		3.18 ± 1.04		2.56 ± 1.29	
CD									
Active	18	4.10 ± 1.42	0.650	0.86 ± 1.45	0.373	1.36 ± 1.54	0.514	3.06 ± 1.28	0.514
Inactive	13	4.39 ± 1.19		1.52 ± 1.87		1.63 ± 1.15		3.36 ± 1.48	

Active CD and UC were defined when CDAI >150 (Best et al., 1976) and a Mayo score >3 (Pineton de Chambrun et al., 2010), respectively.
**Median (log_{10} 16S rRNA gene copies/million bacterial 16S rRNA gene copies) ± standard deviations.*
[§]UC, ulcerative colitis; CD, Crohn's disease.

TABLE 5 | *F. prausnitzii*, its phylogroups and *A. muciniphila* abundance in inflammatory bowel disease patients depending on whether or not they have had intestinal resection during the course of the disease.

Diagnostics[§]	*n*	*F. prausnitzii**	*P*-value	Phylogroup I*	*P*-value	Phylogroup II*	*P*-value	*A. muciniphila**	*P*-value
UC									
Non-resected	19	4.73 ± 0.68	na	1.97 ± 1.21	na	2.79 ± 1.01	0.544	3.05 ± 1.14	na
Resected	1	4.91		3.45		2.68		4.11	
CD									
Non-resected	21	4.46 ± 1.33	0.239	1.33 ± 1.84	0.842	1.85 ± 1.40	**0.018**	3.29 ± 1.44	0.476
Resected	6	3.89 ± 1.04		1.07 ± 1.33		0.59 ± 0.44		3.46 ± 0.45	

**Median (log_{10} 16S rRNA gene copies/million bacterial 16S rRNA gene copies) ± standard deviations; na, not applicable. Analyses statistically significant are highlighted in boldface.*
[§]UC, ulcerative colitis; CD, Crohn's disease.

phylogroup II. Precisely, resected subjects had 10 times less phylogroup II than those without intestinal surgery ($P = 0.018$) whereas the phylogroup I load was only slightly lower in resected than non-resected patients.

The *A. muciniphila* load was lower in CD patients who presented with the disease below 16 years of age (**Table 6**). This group of patients also featured very low quantities of *F. prausnitzii* phylogroup I although statistical significance was not achieved. No differences in these bacterial loads were observed between groups of UC patients with different age of disease onset. We also analyzed disease duration, but no statistically significant correlation was found between any of the bacterial loads and time of disease duration (data not shown).

Finally, data were analyzed by taking into account the medication of the patients at the time of sampling (**Table 7**). No differences in *A. muciniphila*, *F. prausnitzii* or in phylogroups abundances were observed between medications for any IBD. However, those UC patients that received anti-tumor necrosis factor had the lowest levels of *A. muciniphila*. In contrast, those CD patients receiving moderate immunosupressants had lower *F. prausnitzii* loads than patients without treatment or receiving therapies such as mesalazine or anti-tumor necrosis factor.

Correlation Between *A. muciniphila* and *F. prausnitzii* Abundances

Correlation between *A. muciniphila* and *F. prausnitzii* numbers was analyzed to provide supporting evidence for a direct/indirect effect of one population over the other or about a putative common factor affecting both species populations in a given condition (**Figure 3**).

No correlation between these two species was found in H or UC patients (**Figure S3**). Therefore, in these conditions, factors of the gut environment may be differentially impacting on each species. In contrast, positive correlation of both species load was observed in CD subjects (**Figure 3**). Analysis by phylogroups indicated that *A. muciniphila* quantity tended to positively correlate with phylogroup I in CD patients ($P = 0.060$), whereas no significant correlation was observed with phylogroup II (**Figure S3**).

Moreover, no significant correlation between the two species was observed, when splitting subjects by activity status or whether or not they have had intestinal resection. Of note, a positive correlation between *A. muciniphila* and *F. prausnitzii* (particularly phylogroup I) was observed in CD patients with non-stricturing, non-penetrating disease (B1) and in those under moderate immunosuppressants ($\rho \geq 0.539$, $P \leq 0.017$). In contrast, in UC patients with disease onset between 17 and 40 years of age, a negative correlation between *A. muciniphila* and *F. prausnitzii* phylogroup II was observed ($\rho = -0.673$, $P = 0.023$).

DISCUSSION

A. muciniphila and *F. prausnitzii* are two symbiotic and numerically abundant members of the gut microbiota, and both have been associated with dysbiosis in several disease conditions, including IBD. Their niche is close to the intestinal mucosa,

TABLE 6 | *F. prausnitzii*, its phylogroups and *A. muciniphila* abundances in inflammatory bowel disease patients by age of disease onset.

Diagnostics[§]	*n*	*F. prausnitzii**	*P*-value	Phylogroup I*	*P*-value	Phylogroup II*	*P*-value	*A. muciniphila**[#]	*P*-value
UC									
17–40 years (A2)	11	4.87 ± 0.47	0.676	2.52 ± 1.09	0.171	3.12 ± 0.88	0.305	2.93 ± 1.19	0.569
>41 years (A3)	9	4.64 ± 0.91		1.65 ± 1.42		2.58 ± 1.10		2.88 ± 1.07	
CD									
<16 years (A1)	5	3.62 ± 1.59		0.004 ± 0.44		1.65 ± 1.71		1.76 ± 0.73[a]	
17–40 years (A2)	21	4.26 ± 1.36	0.562	1.40 ± 1.87	0.112	1.30 ± 1.34	0.547	3.31 ± 1.16[b]	**0.030**
>41 years (A3)	3	4.67 ± 0.71		0.97 ± 0.48		2.26 ± 1.47		4.20 ± 2.15[b]	

*Median (log_{10} 16S rRNA gene copies/million bacterial 16S rRNA gene copies) ± standard deviations.
[§]UC, ulcerative colitis; CD, Crohn's disease.
[#]Statistics was calculated separately for each variable (column). Groups of patients with similar abundances of A. muciniphila are indicated with the same superscript (a, b) whereas groups not sharing superscript are those with statistically different median abundance values ($P < 0.05$). Analyses statistically significant are highlighted in boldface.

TABLE 7 | *F. prausnitzii*, its phylogroups and *A. muciniphila* abundances in inflammatory bowel disease by medication at sampling.

Diagnostics[§]	*n*	*F. prausnitzii**	*P*-value	Phylogroup I*	*P*-value	Phylogroup II*	*P*-value	*A. muciniphila*	*P*-value
UC									
No treatment	11	4.81 ± 0.72		1.94 ± 1.35		2.74 ± 1.13		3.10 ± 1.11	
Mesalazine	3	4.87 ± 0.40	0.783	2.30 ± 0.97	0.578	3.20 ± 1.01	0.639	3.53 ± 1.82	0.387
Mod. Immsup	4	4.95 ± 0.61		2.97 ± 0.33		3.18 ± 1.54		3.06 ± 0.51	
Anti-TNF	3	4.35 ± 0.96		1.53 ± 1.85		2.37 ± 1.03		2.10 ± 1.52	
CD									
No treatment	10	4.30 ± 1.51		1.04 ± 1.96		1.67 ± 1.61		2.69 ± 1.08	
Mesalazine	3	5.00 ± 0.41	0.537	1.30 ± 1.67	0.975	2.24 ± 1.89	0.719	3.90 ± 2.20	0.125
Mod. Immsup	10	3.84 ± 1.21		0.99 ± 1.50		1.15 ± 1.09		3.72 ± 0.97	
Anti-TNF	6	4.31 ± 1.68		1.42 ± 1.76		1.60 ± 1.42		2.72 ± 1.78	

*Median (log_{10} 16S rRNA gene copies/million bacterial 16S rRNA gene copies) ± standard deviations.
[§]UC, ulcerative colitis; CD, Crohn's disease; Mod. Immsup, moderate immunosuppresants; Anti-TNF, Anti-tumor necrosis factor.

and therefore it can be hypothesized that they may play a key role in cross-talk with the host. Both species are considered to have a part in a well-functioning gut and thus are considered as promising next generation probiotics (Neef and Sanz, 2013; Martín et al., 2017). In the present study we have analyzed the prevalence and abundance of mucosa associated *A. muciniphila*, total *F. prausnitzii* and phylogroup in H and IBD subjects, taking into account the diversity of disease locations and the clinical features of patients. Some IBS and CRC have been included as well, but only for illustrative purposes given the low number of patients engaged. The abundance of both species has been previously reported to be reduced in several intestinal disorders (Belzer and de Vos, 2012; Miquel et al., 2013), but here for the first time we correlate the load of both species. Through analysis of clinical data, we consider which particular conditions this underrepresentation is favored, and whether or not the imbalance of one species is linked to changes in the abundance of the other.

Our data show that the *A. muciniphila* load in the mucosa of H subjects is slightly higher (2.0- to 4.5-fold, respectively) than in IBD and CRC patients, but is not statistically significant. An increase in *A. muciniphila* abundance in CRC patients compared to controls has been previously found in stools (Weir et al., 2013) but not in mucosal biopsies (Mira-Pascual et al., 2015), and the analysis of our limited cohort is in line with this finding. Previous studies have reported a significant decrease of this species in IBD subjects (Png et al., 2010). Methodological differences may explain the inconsistency with our findings, as we exclusively focused on colonic samples. In biopsy samples, Png and collaborators observed a reduction of this species in IBD patients that ranged between 2.9- and 3.9-fold when compared to controls, which is similar to the reduction observed in our subjects. In that study (Png et al., 2010), differences were observed depending on whether or not the tissue was affected, with the depletion being more conspicuous in inflamed tissue, and without reaching significant differences between non-inflamed tissue of CD and controls, which is in line with our results as we used non-affected tissue. In addition, we have explored differences taking into account disease location, activity or intestinal resection, but no association between *A. muciniphila* load and these variables has been revealed. Intriguingly, CD patients who presented with disease below 16 years of age had a striking reduction of this species compared to those with disease onset at a later age. *A. muciniphila* has been reported to colonize the gut in early infancy, and loads in infants 1 year old are similar to that found in adults (Collado et al., 2007). Therefore, it seems likely that this depletion is not a general phenomenon that occurs in IBD or age-driven, but due to particular features of pediatric IBD that are sustained throughout the disease. In line with this, discrepancies between dysbiosis signatures in adult and

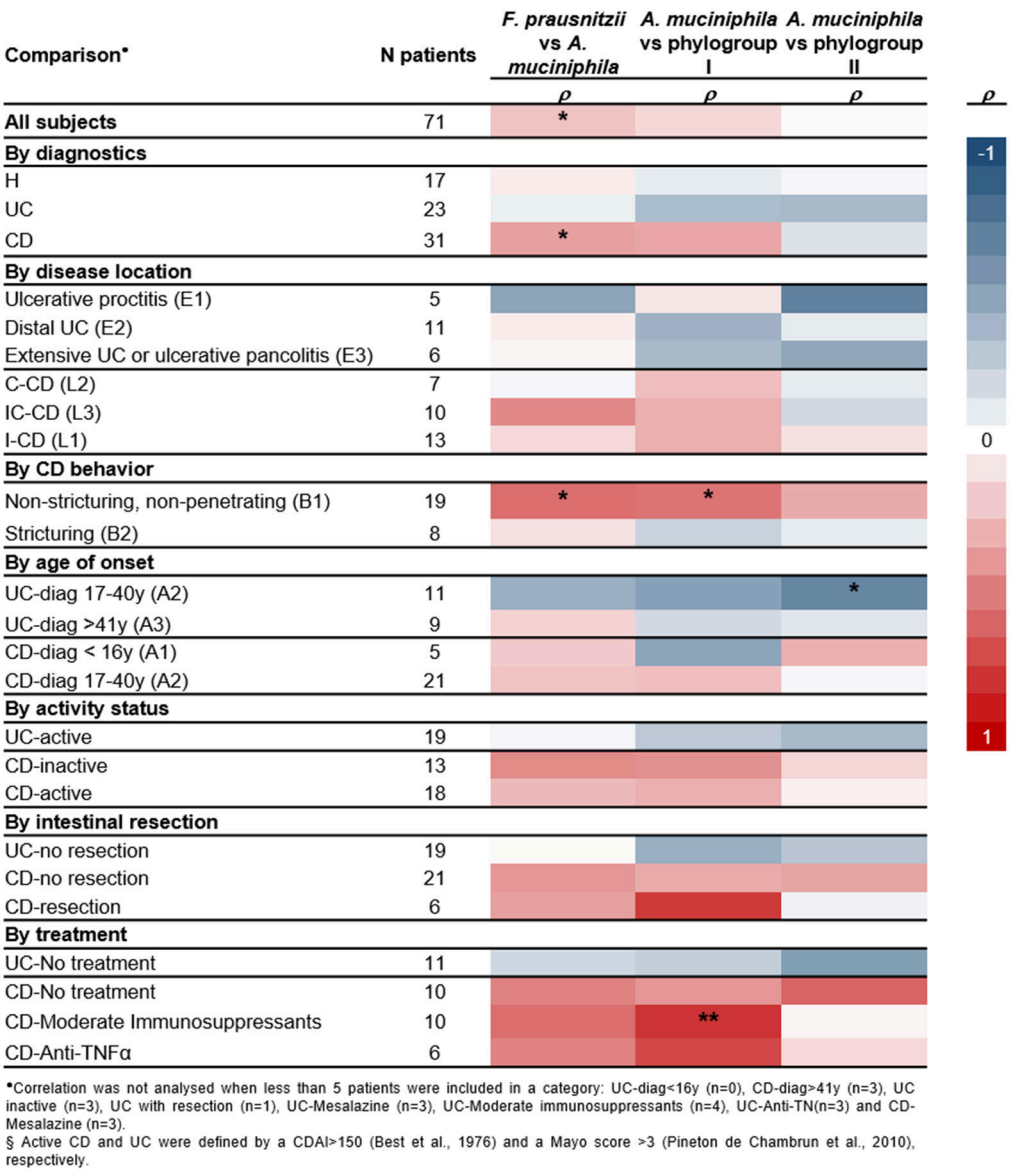

FIGURE 3 | Heatmap of spearman correlation cofficients between *A. muciniphila*, total *F. prausnitzii* and its phylogroups abundances, splitting up patients by diagnostics, inflammatory bowel disease subtypes, and main clinical characteristics. Significant correlations are indicated $^{*}P < 0.05$, $^{**}P < 0.01$.

infant IBD patients have been previously reported (Hansen et al., 2012) and it remains to be explored through prospective studies if early disease onset results in long term microbial signatures. Another future application of this finding could be to explore the usefulness of *A. muciniphila* depletion as a biomarker to assist in pediatric IBD diagnosis.

Regarding mucosa-associated *F. prausnitzii* loads we have observed a marked reduction in CRC and CD patients, especially in those with ileal involvement, affecting both phylogroups of this species. Although less prominent, UC patients also featured lower *F. prausnitzii* abundance than H subjects. Our study is in agreement with previous reports which found *F. prausnitzii* to be reduced in CRC and IBD adults (Swidsinski et al., 2005, 2008; Martinez-Medina et al., 2006; Frank et al., 2007; Sokol et al., 2008, 2009; Willing et al., 2009; McLaughlin et al., 2010; Vermeiren et al., 2012; Kabeerdoss et al., 2013; Machiels et al., 2013; Miquel et al., 2013; Lopez-Siles et al., 2014, 2016). Besides, lower abundance of both *F. prausnitzii* phylogroups has been previously reported concerning CD patients (Jia et al., 2010; Lopez-Siles et al., 2016), which is in line with our findings. Moreover, because we have observed differences between IBD subtypes, our results support the hypothesis that patients with ileal disease location constitute a differentiated pathological entity (Willing et al., 2009). We have corroborated that the reduction of *F. prausnitzii* numbers compared to H subjects takes place in both active and inactive IBD patients (Willing et al., 2009), with active CD patients featuring the lowest levels of phylogroup I. Also in agreement with previous studies

(Sokol et al., 2008) lower numbers of *F. prausnitzii* were detected in resected CD patients, but in our study, statistically significant differences were only achieved for phylogroup II, probably because the depletion was more striking. It remains unknown why there are shifts in particular subgroups of this species. To date, several articles convey the point that the genus *Faecalibacterium* hosts a complex diversity (Lopez-Siles et al., 2015; Benevides et al., 2017; Martín et al., 2017). This diversity has been shown mainly through phylogenetic methods, but phenotypical diversity also exists. Supporting this point, studies characterizing several strains of this species isolated from different origins have failed to find phenotypic traits that consistently distinguish members from one or other subtype (Lopez-Siles et al., 2012; Foditsch et al., 2014; Martín et al., 2017). However, the effect of host factors differentially influencing *F. prausnitzii* subpopulations has been poorly explored which may explain our results. Another hypothesis could be that subtypes of *F. prausnitzii* interact in a different manner with other members of the microbiome, which has also been scarcely studied to date.

We have explored co-occurrence and correlation between *A. muciniphila* and *F. prausnitzii* in H and IBD patients. We considered that both species may have a syntrophic relationship, thus we hypothesize that the depletion or enrichment of one would imply the same effect on the other. In particular, *A. muciniphila* mucolytic activity could release oligosaccharides, co-factors, vitamins, and short chain fatty acids, including acetate that juxtaposed species could use for growth. Indeed, *F. prausnitzii* has been proven to be able to use some oligosaccharides derived from mucus and its growth is stimulated by acetate and requires presence of vitamins in the medium (Duncan et al., 2002; Lopez-Siles et al., 2012). These compounds, can be provided by *A. muciniphila,* although not exclusively, and therefore establish cross-feeding interactions. A recent study based on co-culture experiments demonstrated this trophic interaction (Belzer et al., 2017). However, in most of the cases studied here, we did not find a correlation between *F. prausnitzii* and *A. muciniphila* abundances, and the two species co-occurred only in 41.5% of subjects engaged in the study. This may be because *F. prausnitzii* does not depend exclusively on by-products synthesized by *A. muciniphila*. In agreement with that, other studies have reported that *F. prausnitzii* can benefit from the presence of a variety of acetate-producing species (Wrzosek et al., 2013; Rios-Covian et al., 2015). It would be interesting to determine whether this species (or other mucus-inhabiting species) increase in patients in which *A. muciniphila* diminishes, and thus may be partially replacing its role concerning acetate production.

Nonetheless, we observed that positive correlation between the two species happens in CD patients, and particularly for those with B1 behavior or under immunosuppressant therapy. The fact that there is a positive correlation of the two species indicates that their abundance varies in a similar way in this particular condition. The most likely scenario is that in CD the two bacteria are similarly affected by host and gut environmental factors. To support this hypothesis, both species share the characteristic that their growth is severely compromised at pH < 5.5 (Derrien et al., 2004; Lopez-Siles et al., 2012) and in turn, acidic stools have been reported for IBD patients (Nugent et al., 2001; Barkas et al., 2013). Notably, in those cases of correlation between both species, only members of phylogroup I were involved. It would be interesting to perform co-culture studies with different *F. prausnitzii* strains, and monitor their growth under different conditions in order to determine more accurately their relationship.

In our cohort, *A. muciniphila* was not detected in 57.1% of all subjects but this seems to be related to the fact that this species has a lower relative abundance in the gut, rather than to a higher sensitivity to gut disease. In contrast, *A. muciniphila* was more frequently found in UC patients. This could be partially explained by the fact that a higher proportion of loose mucus has been found in UC patients (Antoni et al., 2014), which is the likely niche for *A. muciniphila*. Another hypothesis that can not be ruled out is that some factor of UC patients favors the presence of *A. muciniphila*. In our limited cohort, we have also observed higher prevalence of this species in CRC group compared to controls, which is in line with previous findings (Mira-Pascual et al., 2015). However, our data points out that this higher presence does not imply an increase in the abundance at the mucosal level. In contrast, almost 90% of subjects were *F. prausnitzii* carriers and thus the fact that it is a second-liner in the mucosa and the fact that this species can rely on other members of the gut microbiota for cross-feeding may explain its higher ubiquity and abundance compared to *A. muciniphila*.

Finally, our study revealed that CD patients are characterized by a low *F. prausnitzii*: *A. muciniphila*, ratio affecting both phylogroups. This indicates that compared to H and UC, these patients have an altered proportion of beneficial microorganisms in the mucosa. Although our study does not allow us to decipher if this imbalance is a cause or a consequence of the disease, it can be an aggravator because the two species have been linked to be key for mucus integrity (Derrien et al., 2004; Wrzosek et al., 2013) and gut homeostasis. A significant depletion of both species has also been reported in children with atopic disease (Candela et al., 2012), and therapeutic strategies to restore these species needs to be explored, particularly for disorders that have in common to feature chronic inflammation. In addition, two recent studies have linked the two species with response to immunotherapy treatment (Gopalakrishnan et al., 2017; Routy et al., 2017), thus pointing out another situation in which it is relevant to have these bacteria. Further studies to assess implications in IBD treatment response would be interesting, as immunomodulators are among the usual therapies prescribed to IBD patients. Finally, further confirmation of our results in a larger cohort would be required given that we have engaged a limited number of subjects, and thus it would provide robustness to those findings not sustained after FRD assessment.

CONCLUSIONS

IBD patients are characterized by a reduction of *F. prausnitzii* and a slight underrepresentation of *A. muciniphila* in the colonic mucosa, regardless of disease activity status. While differences in *F. prausnitzii* load have been observed for I-CD patients, early onset CD is characterized by a lack of *A. muciniphila*, but further prospective studies are required to assess if this feature is sustained long term. Positive correlation between the two

species was found in CD patients, and further studies are required to elucidate which common factors alter both populations in particular gut disorders.

AUTHOR CONTRIBUTIONS

XA, SD, LG-G, ML-S, and MM-M study concept and design. XA, NE-C, ML-S, and MS-M acquisition of data. ML-S and MM-M interpretation of data and statistical analysis. ML-S drafting the manuscript. XA, SD, NE-C, LG-G, MM-M, and MS-M critical revision of the manuscript for important intellectual content. LG-G and MM-M obtained funding. All authors have approved the final version of the manuscript and agree to be accountable for all aspects of the work, ensuring that questions related to the accuracy or integrity of any part of the work are appropriately investigated and resolved.

FUNDING

This work was funded by the Universitat de Girona projects MPCUdG2016-009 and GdRCompetUdG2017, and the Spanish Ministry of Education and Science through projects SAF2006-00414, SAF2010-15896 and SAF2013-43284-P, being the last co-funded by the European Regional Development. Dr. Sylvia H. Duncan acknowledges support from the Scottish Government Research and Environment Science and Analytical Services Division (RESAS).

ACKNOWLEDGMENTS

We appreciate the generosity of the patients who freely gave their time and samples to make this study possible, and the theater staff of all centers for their dedication and careful sample collection. Thanks are due to MD. David Busquets and Ms. Romà Surís for assistance with samples collection and analyses, respectively. We are thankful to Ms. Natàlia Adell for statistical help.

SUPPLEMENTARY MATERIAL

The Supplementary Material for this article can be found online at: https://www.frontiersin.org/articles/10.3389/fcimb.2018.00281/full#supplementary-material

REFERENCES

Andoh, A., Tsujikawa, T., Sasaki, M., Mitsuyama, K., Suzuki, Y., Matsui, T., et al. (2009). Faecal microbiota profile of Crohn's disease determined by terminal restriction fragment length polymorphism analysis. *Aliment. Pharmacol. Ther.* 29, 75–82. doi: 10.1111/j.1365-2036.2008.03860.x

Antoni, L., Nuding, S., Wehkamp, J., and Stange, E. F. (2014). Intestinal barrier in inflammatory bowel disease. *World J. Gastroenterol.* 20, 1165–1179. doi: 10.3748/wjg.v20.i5.1165

Balamurugan, R., Rajendiran, E., George, S., Samuel, G. V., and Ramakrishna, B. S. (2008). Real-time polymerase chain reaction quantification of specific butyrate-producing bacteria, *Desulfovibrio* and *Enterococcus faecalis* in the feces of patients with colorectal cancer. *J. Gastroenterol. Hepatol.* 23, 1298–1303. doi: 10.1111/j.1440-1746.2008.05490.x

Barkas, F., Liberopoulos, E., Kei, A., and Elisaf, M. (2013). Electrolyte and acid-base disorders in inflammatory bowel disease. *Ann. Gastroenterol.* 26, 23–28.

Baumgart, M., Dogan, B., Rishniw, M., Weitzman, G., Bosworth, B., Yantiss, R., et al. (2007). Culture independent analysis of ileal mucosa reveals a selective increase in invasive *Escherichia coli* of novel phylogeny relative to depletion of Clostridiales in Crohn's disease involving the ileum. *ISME J.* 1, 403–418. doi: 10.1038/ismej.2007.52

Belzer, C., Chia, L. W., Aalvink, S., Chamlagain, B., Piironen, V., Knol, J., et al. (2017). Microbial metabolic networks at the mucus layer lead to diet-independent butyrate and vitamin B_{12} production by intestinal symbionts. *MBio* 8:e00770–17. doi: 10.1128/mBio.00770-17

Belzer, C., and de Vos, W. M. (2012). Microbes inside—from diversity to function: the case of *Akkermansia*. *ISME J.* 6:1449. doi: 10.1038/ismej.2012.6

Benevides, L., Burman, S., Martin, R., Robert, V., Thomas, M., Miquel, S., et al. (2017). New Insights into the diversity of the genus *Faecalibacterium*. *Front. Microbiol.* 8:1790. doi: 10.3389/fmicb.2017.01790

Best, W. R., Becktel, J. M., Singleton, J. W., and Kern, F. Jr. (1976). Development of a Crohn's disease activity index. National Cooperative Crohn's disease study. *Gastroenterology* 70, 439–444. doi: 10.1016/S0016-5085(76)80163-1

Candela, M., Rampelli, S., Turroni, S., Severgnini, M., Consolandi, C., De Bellis, G., et al. (2012). Unbalance of intestinal microbiota in atopic children. *BMC Microbiol.* 12:95. doi: 10.1186/1471-2180-12-95

Carlsson, A. H., Yakymenko, O., Olivier, I., Håkansson, F., Postma, E., Keita, A. V., et al. (2013). *Faecalibacterium prausnitzii* supernatant improves intestinal barrier function in mice DSS colitis. *Scand. J. Gastroenterol.* 48, 1136–1144. doi: 10.3109/00365521.2013.828773

Collado, M. C., Derrien, M., Isolauri, E., de Vos, W. M., and Salminen, S. (2007). Intestinal integrity and *Akkermansia muciniphila*, a mucin-degrading member of the intestinal microbiota present in infants, adults, and the elderly. *Appl. Environ. Microbiol.* 73, 7767–7770. doi: 10.1128/AEM.01477-07

De Palma, G., Nadal, I., Collado, M. C., and Sanz, Y. (2009). Effects of a gluten-free diet on gut microbiota and immune function in healthy adult human subjects. *Br. J. Nutr.* 102, 1154–1160. doi: 10.1017/S0007114509371767

Derrien, M., Collado, M. C., Ben-Amor, K., Salminen, S., and de Vos, W. M. (2008). The mucin degrader *Akkermansia muciniphila* is an abundant resident of the human intestinal tract. *Appl. Environ. Microbiol.* 74, 1646–1648. doi: 10.1128/AEM.01226-07

Derrien, M., Van Baarlen, P., Hooiveld, G., Norin, E., Müller, M., and de Vos, W. M. (2011). Modulation of mucosal immune response, tolerance, and proliferation in mice colonized by the mucin-degrader *Akkermansia muciniphila*. *Front. Microbiol.* 2:166. doi: 10.3389/fmicb.2011.00166

Derrien, M., Vaughan, E. E., Plugge, C. M., and de Vos, W. M. (2004). *Akkermansia muciniphila* gen. nov., sp. nov., a human intestinal mucin-degrading bacterium. *Int. J. Syst. Evol. Microbiol.* 54, 1469–1476. doi: 10.1099/ijs.0.02873-054/5/1469

Dörffel, Y., Swidsinski, A., Loening-Baucke, V., Wiedenmann, B., and Pavel, M. (2012). Common biostructure of the colonic microbiota in neuroendocrine tumors and Crohn's disease and the effect of therapy. *Inflamm. Bowel Dis.* 18, 1663–1671. doi: 10.1002/ibd.21923

Duncan, S. H., Hold, G. L., Harmsen, H. J., Stewart, C. S., and Flint, H. J. (2002). Growth requirements and fermentation products of *Fusobacterium prausnitzii*, and a proposal to reclassify it as *Faecalibacterium prausnitzii* gen. nov., comb. nov. *Int. J. Syst. Evol. Microbiol.* 52, 2141–2146. doi: 10.1099/00207713-52-6-2141

Everard, A., Belzer, C., Geurts, L., Ouwerkerk, J. P., Druart, C., Bindels, L. B., et al. (2013). Cross-talk between *Akkermansia muciniphila* and intestinal epithelium controls diet-induced obesity. *Proc. Natl. Acad. Sci. U.S.A.* 110, 9066–9071. doi: 10.1073/pnas.1219451110

Flint, H. J., Scott, K. P., Louis, P., and Duncan, S. H. (2012). The role of the gut microbiota in nutrition and health. *Nat. Rev. Gastroenterol. Hepatol.* 9, 577–589. doi: 10.1038/nrgastro.2012.156

Foditsch, C., Santos, T. M., Teixeira, A. G., Pereira, R. V., Dias, J. M., Gaeta, N., et al. (2014). Isolation and characterization of *Faecalibacterium prausnitzii* from calves and piglets. *PLoS ONE* 9:e116465. doi: 10.1371/journal.pone.0116465

Frank, D. N., St Amand, A. L., Feldman, R. A., Boedeker, E. C., Harpaz, N., and Pace, N. R. (2007). Molecular-phylogenetic characterization of microbial community imbalances in human inflammatory bowel diseases. *Proc. Natl. Acad. Sci. U.S.A.* 104, 13780–13785. doi: 10.1073/pnas.0706625104

Furet, J.-P., Firmesse, O., Gourmelon, M., Bridonneau, C., Tap, J., Mondot, S., et al. (2009). Comparative assessment of human and farm animal faecal microbiota using real-time quantitative PCR. *FEMS Microbiol. Ecol.* 68, 351–362. doi: 10.1111/j.1574-6941.2009.00671.x

Furet, J. P., Kong, L. C., Tap, J., Poitou, C., Basdevant, A., Bouillot, J. L., et al. (2010). Differential adaptation of human gut microbiota to bariatric surgery-induced weight loss: links with metabolic and low-grade inflammation markers. *Diabetes* 59, 3049–3057. doi: 10.2337/db10-0253

Gopalakrishnan, V., Spencer, C. N., Nezi, L., Reuben, A., Andrews, M. C., Karpinets, T. V., et al. (2017). Gut microbiome modulates response to anti–PD-1 immunotherapy in melanoma patients. *Science* 359, 97–103. doi: 10.1126/science.aan4236

Gophna, U., Sommerfeld, K., Gophna, S., Doolittle, W. F., and Veldhuyzen van Zanten, S. J. (2006). Differences between tissue-associated intestinal microfloras of patients with Crohn's disease and ulcerative colitis. *J. Clin. Microbiol.* 44, 4136–4141. doi: 10.1128/JCM.01004-06

Graessler, J., Qin, Y., Zhong, H., Zhang, J., Licinio, J., Wong, M. L., et al. (2012). Metagenomic sequencing of the human gut microbiome before and after bariatric surgery in obese patients with type 2 diabetes: correlation with inflammatory and metabolic parameters. *Pharmacogenomics J.* 13, 514–522. doi: 10.1038/tpj.2012.43

Hansen, R., Russell, R. K., Reiff, C., Louis, P., McIntosh, F., Berry, S. H., et al. (2012). Microbiota of de-novo pediatric IBD: increased *Faecalibacterium prausnitzii* and reduced bacterial diversity in Crohn's but not in ulcerative colitis. *Am. J. Gastroenterol.* 107, 1913–1922. doi: 10.1038/ajg.2012.335

Jia, W., Whitehead, R. N., Griffiths, L., Dawson, C., Waring, R. H., Ramsden, D. B., et al. (2010). Is the abundance of *Faecalibacterium prausnitzii* relevant to Crohn's disease? *FEMS Microbiol. Lett.* 310, 138–144. doi: 10.1111/j.1574-6968.2010.02057.x

Joossens, M., Huys, G., Cnockaert, M., De Preter, V., Verbeke, K., Rutgeerts, P., et al. (2011). Dysbiosis of the faecal microbiota in patients with Crohn's disease and their unaffected relatives. *Gut* 60, 631–637. doi: 10.1136/gut.2010.223263

Kabeerdoss, J., Sankaran, V., Pugazhendhi, S., and Ramakrishna, B. S. (2013). *Clostridium leptum* group bacteria abundance and diversity in the fecal microbiota of patients with inflammatory bowel disease: a case-control study in India. *BMC Gastroenterol.* 13:20. doi: 10.1186/1471-230X-13-20

Kang, C.-S., Ban, M., Choi, E.-J., Moon, H.-G., Jeon, J.-S., Kim, D.-K., et al. (2013). Extracellular vesicles derived from gut microbiota, especially *Akkermansia muciniphila*, protect the progression of dextran sulfate sodium-induced colitis. *PLoS ONE* 8:e76520. doi: 10.1371/journal.pone.0076520

Lane, D. J. (1991). "16S/23S rRNA sequencing," in *Nucleic Acid Techniques in Bacterial Systematics*. eds E. Stackebrandt and M. Goodfellow (New York, NY: John Wiley and Sons), 115–175.

Lopez-Siles, M., Khan, T. M., Duncan, S. H., Harmsen, H. J., Garcia-Gil, L. J., and Flint, H. J. (2012). Cultured representatives of two major phylogroups of human colonic *Faecalibacterium prausnitzii* can utilize pectin, uronic acids, and host-derived substrates for growth. *Appl. Environ. Microbiol.* 78, 420–428. doi: 10.1128/AEM.06858-11

Lopez-Siles, M., Martinez-Medina, M., Abellà, C., Busquets, D., Sabat-Mir, M., Duncan, S. H., et al. (2015). Mucosa-associated *Faecalibacterium prausnitzii* phylotype richness is reduced in patients with inflammatory bowel disease. *Appl. Environ. Microbiol.* 81, 7582–7592. doi: 10.1128/AEM.02006-15

Lopez-Siles, M., Martinez-Medina, M., Busquets, D., Sabat-Mir, M., Duncan, S. H., Flint, H. J., et al. (2014). Mucosa-associated *Faecalibacterium prausnitzii* and *Escherichia coli* co-abundance can distinguish irritable bowel syndrome and inflammatory bowel disease phenotypes. *Int. J. Med. Microbiol.* 304, 464–475. doi: 10.1016/j.ijmm.2014.02.009

Lopez-Siles, M., Martinez-Medina, M., Surís-Valls, R., Aldeguer, X., Sabat-Mir, M., Duncan, S. H., et al. (2016). Changes in the abundance of *Faecalibacterium prausnitzii* phylogroups I and II in the intestinal mucosa of inflammatory bowel disease and patients with colorectal cancer. *Inflamm. Bowel Dis.* 22, 28–41. doi: 10.1097/MIB.0000000000000590

Lozupone, C., Faust, K., Raes, J., Faith, J. J., Frank, D. N., Zaneveld, J., et al. (2012). Identifying genomic and metabolic features that can underlie early successional and opportunistic lifestyles of human gut symbionts. *Genome Res.* 22, 1974–1984. doi: 10.1101/gr.138198.112

Lukovac, S., Belzer, C., Pellis, L., Keijser, B. J., de Vos, W. M., Montijn, R. C., et al. (2014). Differential modulation by *Akkermansia muciniphila* and *Faecalibacterium prausnitzii* of host peripheral lipid metabolism and histone acetylation in mouse gut organoids. *MBio* 5, e01438–e01414. doi: 10.1128/mBio.01438-14

Machiels, K., Joossens, M., Sabino, J., De Preter, V., Arijs, I., Eeckhaut, V., et al. (2013). A decrease of the butyrate-producing species *Roseburia hominis* and *Faecalibacterium prausnitzii* defines dysbiosis in patients with ulcerative colitis. *Gut* 63, 1275–1283. doi: 10.1136/gutjnl-2013-304833

Manichanh, C., Borruel, N., Casellas, F., and Guarner, F. (2012). The gut microbiota in IBD. *Nat. Rev. Gastroenterol. Hepatol.* 9, 599–608. doi: 10.1038/nrgastro.2012.152

Manichanh, C., Rigottier-Gois, L., Bonnaud, E., Gloux, K., Pelletier, E., Frangeul, L., et al. (2006). Reduced diversity of faecal microbiota in Crohn's disease revealed by a metagenomic approach. *Gut* 55, 205–211. doi: 10.1136/gut.2005.073817

Martín, R., Chain, F., Miquel, S., Lu, J., Gratadoux, J. J., Sokol, H., et al. (2014). The commensal bacterium *Faecalibacterium prausnitzii* is protective in DNBS-induced chronic moderate and severe colitis models. *Inflamm. Bowel Dis.* 20, 417–430. doi: 10.1097/01.MIB.0000440815.76627.64

Martín, R., Miquel, S., Benevides, L., Bridonneau, C., Robert, V., Hudault, S., et al. (2017). Functional characterization of novel *Faecalibacterium prausnitzii* strains isolated from healthy volunteers: a step forward in the use of *F. prausnitzii* as a Next-Generation Probiotic. *Front. Microbiol.* 8:1226. doi: 10.3389/fmicb.2017.01226

Martín, R., Miquel, S., Chain, F., Natividad, J. M., Jury, J., Lu, J., et al. (2015). *Faecalibacterium prausnitzii* prevents physiological damages in a chronic low-grade inflammation murine model. *BMC Microbiol.* 15:67. doi: 10.1186/s12866-015-0400-1

Martinez-Medina, M., Aldeguer, X., Gonzalez-Huix, F., Acero, D., and Garcia-Gil, L. J. (2006). Abnormal microbiota composition in the ileocolonic mucosa of Crohn's disease patients as revealed by polymerase chain reaction-denaturing gradient gel electrophoresis. *Inflamm. Bowel Dis.* 12, 1136–1145. doi: 10.1097/01.mib.0000235828.09305.0c

McLaughlin, S. D., Clark, S. K., Tekkis, P. P., Nicholls, R. J., and Ciclitira, P. J. (2010). The bacterial pathogenesis and treatment of pouchitis. *Therap. Adv. Gastroenterol.* 3, 335–348. doi: 10.1177/1756283X10370611

Mendoza Hernández, J. L., Lana Soto, R., and Díaz-Rubio, M. (2007). *Definiciones y Manifestaciones Clínicas Generales*. Madrid: Arán Ediciones S.L.

Miquel, S., Martín, R., Rossi, O., Bermúdez-Humarán, L., Chatel, J., Sokol, H., et al. (2013). *Faecalibacterium prausnitzii* and human intestinal health. *Curr. Opin. Microbiol.* 16, 255–261. doi: 10.1016/j.mib.2013.06.003

Mira-Pascual, L., Cabrera-Rubio, R., Ocon, S., Costales, P., Parra, A., Suarez, A., et al. (2015). Microbial mucosal colonic shifts associated with the development of colorectal cancer reveal the presence of different bacterial and archaeal biomarkers. *J. Gastroenterol.* 50, 167–179. doi: 10.1007/s00535-014-0963-x

Mondot, S., Kang, S., Furet, J. P., Aguirre de Carcer, D., McSweeney, C., Morrison, M., et al., (2011). Highlighting new phylogenetic specificities of Crohn's disease microbiota. *Inflamm. Bowel Dis.* 17, 185–192. doi: 10.1002/ibd.21436

Neef, A., and Sanz, Y. (2013). Future for probiotic science in functional food and dietary supplement development. *Curr. Opin. Clin. Nutr. Metab. Care* 16, 679–687. doi: 10.1097/MCO.0b013e328365c258

Nugent, S. G., Kumar, D., Rampton, D. S., and Evans, D. F. (2001). Intestinal luminal pH in inflammatory bowel disease: possible determinants and implications for therapy with aminosalicylates and other drugs. *Gut* 48, 571–577. doi: 10.1136/gut.48.4.571

Pineton de Chambrun, G., Peyrin-Biroulet, L., Lémann, M., and Colombel, J. F. (2010). Clinical implications of mucosal healing for the management of IBD. *Nat. Rev. Gastroenterol. Hepatol.* 7, 15–29. doi: 10.1038/nrgastro.2009.203

Png, C. W., Lindén, S. K., Gilshenan, K. S., Zoetendal, E. G., McSweeney, C. S., Sly, L. I., et al. (2010). Mucolytic bacteria with increased prevalence in IBD mucosa augment *in vitro* utilization of mucin by other bacteria. *Am. J. Gastroenterol.* 105, 2420–2428. doi: 10.1038/ajg.2010.281

Rajilić-Stojanović, M., Biagi, E., Heilig, H. G., Kajander, K., Kekkonen, R. A., Tims, S., et al. (2011). Global and deep molecular analysis of microbiota signatures

in fecal samples from patients with irritable bowel syndrome. *Gastroenterology* 141, 1792–1801. doi: 10.1053/j.gastro.2011.07.043

Rios-Covian, D., Gueimonde, M., Duncan, S. H., Flint, H. J., and de los Reyes-Gavilan, C. G. (2015). Enhanced butyrate formation by cross-feeding between *Faecalibacterium prausnitzii* and *Bifidobacterium adolescentis*. *FEMS Microbiol. Lett.* 362:fnv176. doi: 10.1093/femsle/fnv176

Rossi, O., Khan, M. T., Schwarzer, M., Hudcovic, T., Srutkova, D., Duncan, S. H., et al. (2015). *Faecalibacterium prausnitzii* strain HTF-F and its extracellular polymeric matrix attenuate clinical parameters in DSS-induced colitis. *PLoS ONE* 10:e0123013. doi: 10.1371/journal.pone.0123013

Routy, B., Le Chatelier, E., Derosa, L., Duong, C. P. M., Alou, M. T., Daillère, R., et al. (2017). Gut microbiome influences efficacy of PD-1-based immunotherapy against epithelial tumors. *Science* 359, 91–97. doi: 10.1126/science.aan3706

Sartor, R. B. (2006). Mechanisms of disease: pathogenesis of Crohn's disease and ulcerative colitis. *Nat. Clin. Pract. Gastroenterol. Hepatol.* 3, 390–407. doi: 10.1038/ncpgasthep0528

Sartor, R. B. (2008). Microbial influences in inflammatory bowel diseases. *Gastroenterology* 134, 577–594. doi: 10.1053/j.gastro.2007.11.059

Seksik, P., Sokol, H., Lepage, P., Vasquez, N., Manichanh, C., Mangin, I., et al. (2006). Review article: the role of bacteria in onset and perpetuation of inflammatory bowel disease. *Aliment. Pharmacol. Ther.* 24, 11–18. doi: 10.1111/j.1365-2036.2006.03053.x

Silverberg, M. S., Satsangi, J., Ahmad, T., Arnott, I. D., Bernstein, C. N., Brant, S. R., et al. (2005). Toward an integrated clinical, molecular and serological classification of inflammatory bowel disease: report of a working party of the 2005 Montreal World Congress of Gastroenterology. *Can. J. Gastroenterol.* 19, 5A–36A. doi: 10.1155/2005/269076

Sokol, H., Pigneur, B., Watterlot, L., Lakhdari, O., Bermúdez-Humarán, L. G., Gratadoux, J. J., et al. (2008). *Faecalibacterium prausnitzii* is an anti-inflammatory commensal bacterium identified by gut microbiota analysis of Crohn disease patients. *Proc. Natl. Acad. Sci. U.S.A.* 105, 16731–16736. doi: 10.1073/pnas.0804812105

Sokol, H., and Seksik, P. (2010). The intestinal microbiota in inflammatory bowel diseases: time to connect with the host. *Curr. Opin. Gastroenterol.* 26, 327–331. doi: 10.1097/MOG.0b013e328339536

Sokol, H., Seksik, P., Furet, J. P., Firmesse, O., Nion-Larmurier, I., Beaugerie, L., et al. (2009). Low counts of *Faecalibacterium prausnitzii* in colitis microbiota. *Inflamm. Bowel Dis.* 15, 1183–1189. doi: 10.1002/ibd.20903

Stoddard, S. F., Smith, B. J., Hein, R., Roller, B. R., and Schmidt, T. M. (2015). rrnDB: improved tools for interpreting rRNA gene abundance in bacteria and archaea and a new foundation for future development. *Nucleic Acids Res.* 43, D593–D598. doi: 10.1093/nar/gku1201

Swidsinski, A., Dörffel, Y., Loening-Baucke, V., Theissig, F., Rückert, J. C., Ismail, M., et al. (2011). Acute appendicitis is characterised by local invasion with *Fusobacterium nucleatum/necrophorum*. *Gut* 60, 34–40. doi: 10.1136/gut.2009.191320

Swidsinski, A., Loening-Baucke, V., Lochs, H., and Hale, L. P. (2005). Spatial organization of bacterial flora in normal and inflamed intestine: a fluorescence *in situ* hybridization study in mice. *World. J. Gastroenterol.* 11, 1131–1140. doi: 10.3748/wjg.v11.i8.1131

Swidsinski, A., Loening-Baucke, V., Vaneechoutte, M., and Doerffel, Y. (2008). Active Crohn's disease and ulcerative colitis can be specifically diagnosed and monitored based on the biostructure of the fecal flora. *Inflamm. Bowel Dis.* 14, 147–161. doi: 10.1002/ibd.20330

van Passel, M. W., Kant, R., Zoetendal, E. G., Plugge, C. M., Derrien, M., Malfatti, S. A., et al. (2011). The genome of *Akkermansia muciniphila*, a dedicated intestinal mucin degrader, and its use in exploring intestinal metagenomes. *PLoS ONE* 6:e16876. doi: 10.1371/journal.pone.0016876

Vermeiren, J., Van den Abbeele, P., Laukens, D., Vigsnaes, L. K., De Vos, M., Boon, N., et al. (2012). Decreased colonization of fecal *Clostridium coccoides/Eubacterium rectale* species from ulcerative colitis patients in an *in vitro* dynamic gut model with mucin environment. *FEMS Microbiol. Ecol.* 79, 685–696. doi: 10.1111/j.1574-6941.2011.01252.x

Weir, T. L., Manter, D. K., Sheflin, A. M., Barnett, B. A., Heuberger, A. L., and Ryan, E. P. (2013). Stool microbiome and metabolome differences between colorectal cancer patients and healthy adults. *PLoS ONE* 8:e70803. doi: 10.1371/journal.pone.0070803

Weisburg, W. G., Barns, S. M., Pelletier, D. A., and Lane, D. J. (1991). 16S ribosomal DNA amplification for phylogenetic study. *J. Bacteriol.* 173, 697–703.

Willing, B., Halfvarson, J., Dicksved, J., Rosenquist, M., Järnerot, G., Engstrand, L., et al. (2009). Twin studies reveal specific imbalances in the mucosa-associated microbiota of patients with ileal Crohn's disease. *Inflamm. Bowel Dis.* 15, 653–660. doi: 10.1002/ibd.20783

Wrzosek, L., Miquel, S., Noordine, M. L., Bouet, S., Joncquel Chevalier-Curt, M., Robert, V., et al. (2013). *Bacteroides thetaiotaomicron* and *Faecalibacterium prausnitzii* influence the production of mucus glycans and the development of goblet cells in the colonic epithelium of a gnotobiotic model rodent. *BMC Biol.* 11:61. doi: 10.1186/1741-7007-11-61

Conflict of Interest Statement: XA is a consultant for AbbVie, Janssen and Takeda, and has received honoraria for lectures, including services on speakers bureaus from AbbVie, MS-D, Janssen, Takeda, Shire, Zambon and Ferring. XA, LG-G, ML-S, and MM-M, have filed a European patent for a "Method for the detection, follow up and/or classification of intestinal diseases" (application number EP15382427).

The remaining authors declare that the research was conducted in the absence of any commercial or financial relationships that could be construed as a potential conflict of interest.

Copyright © 2018 Lopez-Siles, Enrich-Capó, Aldeguer, Sabat-Mir, Duncan, Garcia-Gil and Martinez-Medina. This is an open-access article distributed under the terms of the Creative Commons Attribution License (CC BY). The use, distribution or reproduction in other forums is permitted, provided the original author(s) and the copyright owner(s) are credited and that the original publication in this journal is cited, in accordance with accepted academic practice. No use, distribution or reproduction is permitted which does not comply with these terms.

frontiers in Cellular and Infection Microbiology

ORIGINAL RESEARCH
published: 12 July 2018
doi: 10.3389/fcimb.2018.00237

Akkermansia muciniphila as a Model Case for the Development of an Improved Quantitative RPA Microbiome Assay

Heather J. Goux[1], *Dimple Chavan*[1], *Mary Crum*[2], *Katerina Kourentzi*[2] and *Richard C. Willson*[1,2,3]*

[1] Department of Biology and Biochemistry, University of Houston, Houston, TX, United States, [2] Department of Chemical and Biomolecular Engineering, University of Houston, Houston, TX, United States, [3] Tecnológico de Monterrey-ITESM Campus Monterrey, Monterrey, Mexico

OPEN ACCESS

Edited by:
Pascale Alard,
University of Louisville, United States

Reviewed by:
Elisabeth Margaretha Bik,
uBiome, United States
James E. Graham,
University of Louisville, United States

***Correspondence:**
Richard C. Willson
willson@uh.edu

Specialty section:
This article was submitted to Microbiome in Health and Disease, a section of the journal Frontiers in Cellular and Infection Microbiology

Received: *11 December 2017*
Accepted: *20 June 2018*
Published: *12 July 2018*

Citation:
Goux HJ, Chavan D, Crum M, Kourentzi K and Willson RC (2018) Akkermansia muciniphila as a Model Case for the Development of an Improved Quantitative RPA Microbiome Assay. Front. Cell. Infect. Microbiol. 8:237. doi: 10.3389/fcimb.2018.00237

Changes in the population levels of specific bacterial species within the gut microbiome have been linked to a variety of illnesses. Most assays that determine the relative abundance of specific taxa are based on amplification and sequencing of stable phylogenetic gene regions. Such lab-based analysis requires pre-analytical sample preservation and storage that have been shown to introduce biases in the characterization of microbial profiles. Recombinase polymerase amplification (RPA) is an isothermal nucleic acid amplification method that employs commercially available, easy-to-use freeze-dried enzyme pellets that can be used to analyze specimens rapidly in the field or clinic, using a portable fluorometer. Immediate analysis of diverse bacterial communities can lead to a more accurate quantification of relative bacterial abundance. In this study, we discovered that universal bacterial 16S ribosomal DNA primers give false-positive signals in RPA analysis because manufacturing host *Escherichia coli* DNA is present in the RPA reagents. The manufacturer of RPA reagents advises against developing an RPA assay that detects the presence of *E. coli* due to the presence of contaminating *E. coli* DNA in the reaction buffer (www.twistdx.co.uk/). We, therefore, explored four strategies to deplete or fragment extraneous DNA in RPA reagents while preserving enzyme activity: metal-chelate affinity chromatography, sonication, DNA cleavage using methylation-dependent restriction endonucleases, and DNA depletion using anti-DNA antibodies. Removing DNA with anti-DNA antibodies enabled the development of a quantitative RPA microbiome assay capable of determining the relative abundance of the physiologically-important bacterium *Akkermansia muciniphila* in human feces.

Keywords: RPA, gut microbiome, *Akkermansia muciniphila*, bacterial quantification, point-of-need

INTRODUCTION

The human intestinal microbiome contains $\geq 10^{14}$ bacteria representing over 400 species (Ott et al., 2004). Recent publications have suggested that the composition of the gut microbiota is significantly associated with health and disease (Shreiner et al., 2015; Lloyd-Price et al., 2016; Lynch and Pedersen, 2016; Duvallet et al., 2017). Relatively small changes in bacterial levels from key taxonomic groups have been linked to a wide range of illnesses, including inflammatory bowel disease, Crohn's disease, colon cancer, and hyperglycemia (Watterlot et al., 2008; Kang et al., 2013; Scher et al., 2013; Scheperjans et al., 2015; Schneeberger et al., 2015; Dao et al., 2016; Rosa et al., 2017; Wong et al., 2017). The use of pro- or prebiotics or fecal microbiota transplantation have been shown to alter the microbial profile of the gut, in some cases improving health (Muegge, 2011; Petrof et al., 2013; Colman and Rubin, 2014; Cui et al., 2015; Plovier et al., 2016; Routy et al., 2018). Development of a method to monitor the abundance of beneficial microorganisms within the complex milieu of the gut microbiome is therefore of considerable interest.

A variety of techniques are available for analyzing microbiota composition, including small-subunit ribosomal RNA (16S rRNA) gene sequencing, whole-metagenome shotgun sequencing, quantitative polymerase chain reaction assays, and microbial culture (Morgan and Huttenhower, 2012). All prokaryotes harbor a 16S rRNA gene, which includes both conserved sequences and species-specific hypervariable regions. Well-developed databases (e.g., GreenGenes, Ribosomal Database Project, and Silva) are available to classify 16S rRNA sequence data at high taxonomic resolution for use in microbial population profiling. Sequencing short 16S rRNA gene segments often is more cost-effective than sequencing the entire metagenome and thus enables cohort studies large enough to identify statistically significant correlations with disease states (Morgan and Huttenhower, 2012; Hermann-Bank et al., 2013; Robinson et al., 2016). Although 16S rRNA sequencing is currently the favored tool for the detection of bacterial biomarkers, qPCR is faster, cheaper, and easier to interpret, making it the preferred method for biomarker validation (Watterlot et al., 2008; Kostic et al., 2012; Kang et al., 2013; Scher et al., 2013; Zhang et al., 2016). In addition, qPCR often enables more accurate quantification of specific species than 16S rRNA sequencing (Hermann-Bank et al., 2013). However, PCR and 16S detection methods can be subject to biases associated with pre-analytical sample preservation, storage, and DNA extraction (Robinson et al., 2016), leading to inaccuracies in fecal bacterial quantification. Reducing the amount of sample handling and eliminating sample storage can lead to a more accurate estimation of bacterial abundance within the gut.

Recombinase polymerase amplification (RPA) is an isothermal amplification nucleic acid detection method suitable for analysis of samples at the point of need (Euler et al., 2012a; Abd El Wahed et al., 2013, 2015; Rosser et al., 2015; Bonney et al., 2017; Kim and Lee, 2017). Rather than heat denaturation, RPA uses recombinases (*E. coli* RecA) to form a complex with signal stranded oligonucleotides (30–35 nt primers) and single strand binding proteins (SSBs) assist site-specific D-loop strand invasion (Piepenburg et al., 2006) of dsDNA. At a constant temperature of 37–42°C, *Sau* (*Staphylococcus aureus)* DNA polymerase performs primer-extension to generate a new strand of DNA. Much like PCR, the newly generated product goes on to become the template for future rounds of amplification. Incorporation of a cleavable self-quenched exo-probe or SYBR Green dye allows for real-time fluorescence monitoring of RPA assays, thus enabling quantitative analysis typically within 10–15 min (Crannell et al., 2014, 2015; Kim and Lee, 2016, 2017; Moore and Jaykus, 2017). As RPA utilizes freeze-dried, reaction-ready enzyme pellets (manufactured by TwistDx, Inc.) and a portable fluorometer, the technique can be readily adapted to field applications (Abd El Wahed et al., 2015). Immediate field-based analysis of diverse bacterial communities can lead to a more accurate quantification of relative bacterial abundance.

Although RPA can provide valuable data for quantifying bacterial taxa within the gut microbiome, transitioning from an exploratory 16S rRNA–based sequencing study to a PCR/RPA-based confirmatory study can be complicated by differences in the way taxonomic abundance is defined (Ott et al., 2004; Morgan and Huttenhower, 2012; Gloor et al., 2017). In real-time RPA, bacteria are quantified according to a standard curve with abundance defined in terms of gene copies per unit volume (Euler et al., 2012b; Crannell et al., 2014, 2015; Kim and Lee, 2017). By contrast, in 16S rRNA–based sequencing, bacterial abundance is estimated based on the fraction of total observed 16S rRNA sequences assignable to a particular taxonomic group (with the complication that the number of 16S rRNA genes per genome can vary; Robinson et al., 2016). Thus, correlations based on 16S rRNA–based sequencing are relative rather than absolute (Ott et al., 2004); as such, subsequent quantitative PCR/RPA data should ideally be reported in terms of relative abundance. One way this has been achieved in gut bacterial PCR studies is by calculating the ratio of group-specific to total 16S rRNA abundance (Hermann-Bank et al., 2013; Brukner et al., 2015; Zhang et al., 2016). This method can be easily adapted to RPA to quantify target organisms.

The importance of accurate quantification of specific organisms within the gut microbiome can be illustrated by the case of diabetes, which affected 9.4% of Americans (30.3 million individuals) in 2015 (Centers for Disease Control and Prevention, 2017). *Akkermansia muciniphila* is a gram-negative, anaerobic, mucin-degrading bacterium commonly found in high abundance in the human gut. Low abundance of *A. muciniphila* has been linked to hyperglycemia, glucose intolerance, obesity, and type 2 diabetes (Everard et al., 2011, 2013; Louis et al., 2016; Yassour et al., 2016). *A. muciniphila* is also a key producer of short-chain fatty acids in the gut, which have been shown to inhibit inflammation and aid in metabolic dysregulation (Dao et al., 2016). In several mouse studies, administering *A. muciniphila* to diabetic subjects improved their metabolic functions and aided in weight loss (Greer et al., 2016; Plovier et al., 2016; Hänninen et al., 2017). The medical community may soon need an inexpensive

screening tool for identifying individuals with lower fecal *A. muciniphila* abundance that could benefit from therapeutic intervention. We, therefore, chose *A. muciniphila* as a model organism in developing a quantitative RPA microbiome assay.

During assay development, we found that non-specific amplification occurred using 16S rRNA universal primer pairs in the absence of added DNA template, reducing the accuracy of total bacterial load quantification. Amplification of residual *Escherichia coli* production-host DNA contained in the recombinant RPA reagents was identified as the confounding factor and was confirmed by Sanger sequencing. Relative *A. muciniphila* abundance is calculated from the ratio of *A. muciniphila* to total 16S rRNA abundance. Therefore, an inability to quantify the total bacterial load precludes accurate estimation of the relative abundance of *A. muciniphila*. To resolve this issue, we explored four strategies to deplete or destroy extraneous *E. coli* DNA while preserving RPA reagent functionality: (1) metal-chelate affinity capture; (2) sonication; (3) methylation-dependent restriction endonuclease digestion; and (4) DNA capture/removal using anti-DNA antibodies. We show that removal of interfering DNA using anti-DNA antibodies was the most effective strategy. Using RPA reagents treated with anti-DNA antibodies, we then constructed a quantitative total bacterial standard curve and determined the relative abundance of *A. muciniphila* in a human fecal sample to demonstrate the application of the quantitative RPA microbiome assay.

MATERIALS AND METHODS

Design of Bacteria-Specific Primers

It is suggested that RPA primers be 30–35 nt long for optimal amplification of the template. Only 9% of previously published RPA primers are below 30 nt in length (Daher et al., 2016). RPA was attempted with widely-used 16S universal primers (primer set 2; **Table 1**) which resulted in a significant delay in amplification. We, therefore, undertook to design our own bacteria-specific primers 28–35 nt in length and with GC content of 30–70%. Highly-conserved regions within the 16S rRNA gene were chosen as the targets for bacteria-specific RPA primers. When designing a 16S gene specific universal primer, it is likely that large increases in primer length would lead to an increase in the number of mismatches. However, guidelines for RPA primer design are not as stringent as those for the design of PCR primers. Longer RPA primers tolerate some additional mismatches while still achieving adequate amplification (Daher et al., 2015). The National Center for Biotechnology Information BLAST tool was used to test each primer's potential match to all publicly-available bacteria genome sequences. A match was defined for this purpose as less than six total mismatches and less than four mismatches in the last six 3′ nucleotides of either the primer or the target sequence. Primer sequences complementary to human DNA were identified using BLAST and excluded in order to reduce the probability of amplifying human DNA. The free-energy calculation function of the OligoAnalyzer tool (http://www.idtdna.com/analyzer/Applications/OligoAnalyzer) was used to assess the potential formation of secondary structures (primer dimers and hairpins) and avoid inter- or intra-molecular interactions with a ΔG of < -6 kcal.mol^{-1}.

During *A. muciniphila* specific primer design, two different *A. muciniphila* 16S rRNA gene reference sequences (American Type Culture Collection [ATCC] strain BAA-835; accession number NR_074436.1 and accession number NR_042817.1) were downloaded from GenBank (http://www.ncbi.nlm.nih.gov/genbank) and aligned using SeaView (Gascuel et al., 2010) to identify species-specific conserved sequences within the 16S rRNA gene variable region. The newly-developed *A. muciniphila* specific primers (primer set 3, **Table 1**) were tested for species-specificity using an NCBI BLAST search tool to confirm zero mismatches to all 39 *A. muciniphila* genomes in the GenBank reference genome database. The NCBI BLAST tool was also used to test each primer's off-target specificity to all publicly-available bacteria genome sequences outside of *A. muciniphila*. The reverse primer was found to be 100% matched to two off-target organisms, *Haloferula rosa* and *Luteolibacter algae* (Verrucomicrobia phylum). *Luteolibacter algae* and *H. rosa* are two species commonly found in marine environments (Yoon et al., 2008; He et al., 2017) and are not known to inhabit the human gut in significant abundance. Using data from the U.S. NIH Human Microbiome Project and the search engine EZ Bio Cloud (https://www.ezbiocloud.net/resources/human_microbiome) we found no presence of *L. algae* and *H. rosa* in stool. The *Akkermansia* genus dominates the Verrucomicrobia population found in the human gut (Dubourg et al., 2013). When found in the gut, the abundance of these species is not enough to significantly affect the calculation of *A. muciniphila* abundance (0–5% of total reads; Zhang et al., 2015).

Genomic DNA Standards

E. coli strain 1532 (ATCC 35218) was streaked onto a 5% sheep's blood agar plate (Becton, Dickinson and Company; Franklin Lakes, NJ) and incubated for 12 h at 37°C. Genomic DNA (gDNA) was isolated from *E. coli* cultures using an UltraClean Microbial DNA Isolation kit (Mo Bio Laboratories; Carlsbad, CA). The absorbance of isolated *E. coli* and commercially obtained *A. muciniphila* gDNA (strain ATCC BAA-835) was measured at 230, 260, and 280 nm using a Nanodrop 1000 (NanoDrop Instruments, Wilmington, DE). The 260/280 and 260/230 absorbance ratios were $\geq$2.0, confirming gDNA purity. The gDNA concentration, expressed as genome copies per μL, was calculated using the absorbance at 260 nm, the extinction coefficient of double-stranded DNA (0.020 μg^{-1} mL cm^{-1}), the average molar weight of a DNA base pair (650 g mol^{-1}), the size of each reference strain's genome (*E. coli* ATCC 35218, 4.64 Mbp; *A. muciniphila* ATCC BAA-835, 2.66 Mbp), and Avogadro's number. gDNA aliquots (10 μL) were stored at −20°C and used as RPA standards. Ten-fold serial dilutions of both *E. coli* and *A. muciniphila* gDNA were made using nuclease-free deionized water. Finally, 2 or 5 μL of template (100–10^7 copies of *E. coli* or *A. muciniphila* gDNA) were added to quantitative RPA and PCR reactions.

TABLE 1 | General bacteria- and *Akkermansia muciniphila*–specific primer pairs.

Primer set	Specificity	Sequence (5′-3′)	Length (nt)	References
PRIMER SET 1				
Fwd	Bacteria	att gaa gag ttt gat cat ggc tca gat t	28	This work
Rvs		ccg tgt ctc agt tcc agt gtg gct ggt c	28	
PRIMER SET 2				
P338f	Bacteria	act cct acg gga ggc agc ag	20	Muyzer et al., 1993; Schneeberger et al., 2015
P518r		att acc gcg gct gct gg	17	
PRIMER SET 3				
Fwd	*A. muciniphila*	gcg tag gct gtt tcg taa gtc gtg tgt gaa ag	32	This work
Rvs		gag tgt tcc cga tat cta cgc att tca	30	
PRIMER SET 4				
Fwd	*A. muciniphila*	cag cac gtg aag gtg ggg	18	Collado et al., 2007; Schneeberger et al., 2015; Guo et al., 2016
Rvs		cct tgg ggt tgg ctt cag at	20	
PRIMER SET 5				
515f	Bacteria	gtg cca gcm gcc gcg gta a	18	Caporaso et al., 2011
806r		gga cta chv ggg twt cta at	20	

Quantitative Real-Time RPA

Real-time RPA reactions were performed using a TwistAmp Basic kit (TwistDx, Cambridge, UK, TABAS03KIT) with primers purchased from Integrated DNA Technologies (Coralville, IA). Master mix (45.5 μL) containing 420 nM primers (primer pair set 1 or 2, **Table 1**), SYBR green dye I (ThermoFisher Scientific, Product #S7567; 45,500-fold dilution of stock concentration), and TwistAmp rehydration buffer was prepared and distributed into TwistAmp Basic reaction tubes. Next, 2 or 5 μL of template (100–10^6 copies of *E. coli* or *A. muciniphila* gDNA standard) and 2.5 μL of 280 mM magnesium acetate (MgAc) were added to the reaction mix to initiate the amplification reaction. Tubes were then placed into an Agilent MxPro 3005 real-time PCR machine (Agilent Technologies, Santa Clara, CA). Fluorescence (excitation, 497 nm; detection, 520 nm) was measured every 15 s for 60 min at 37°C.

Strategies for Removing Extraneous DNA From RPA Reagents

Strategy 1: Removing DNA Using Metal-Chelate Affinity Capture

Chelating Sepharose fast-flow beads (25 μL; catalog no. 17057502, GE Healthcare; cross-linked 6% agarose functionalized with iminodiacetic acid groups) were charged according to the manufacturer's protocol with Ni^{2+} ions to enable interaction with aromatic DNA base nitrogen atoms (Murphy et al., 2003; Cano et al., 2005) and then resuspended in 70 μL of 60 mM Tris buffer (pH 7) containing 1 M NaCl. Four TwistDx TwistAmp RPA reaction pellets were rehydrated in 70 μL of TwistDx Rehydration Buffer. The bead and RPA reagent suspensions were combined and mixed on a rotator at end-over-end at 3 rpm for 2 h at 4°C. The mixture was then centrifuged at 5,500 *xg* for 2 min to remove the beads, and the supernatant was aliquoted into four PCR tubes (35 μL per tube). Master mix (47.5 μL) containing 505 μM primers and SYBR green dye (47,500-fold dilution of stock solution) was added to each tube along with 2 μL of *E. coli* gDNA standard (100 copies per μL). Next, 2.5 μL of 280 mM MgAc was added to the PCR tubes, which were then placed into an Agilent MxPro 3005 Real-Time PCR machine and amplified at 37°C.

Strategy 2: DNA Shearing by Sonication

Individual TwistAmp RPA Reaction pellets were reconstituted with 29.5 μL of TwistDx Rehydration Buffer, placed on ice, and sonicated at a amplitude of 40 for 10 cycles (3 s on, 7 s off) using an ultrasonic homogenizer (Model 150V/T, Biologics Inc.). Next, 29.5 μL of the sonicated suspension and 16 μL of master mix (containing 1.5 μM primer set 1 and 16,000-fold dilution of SYBR green dye) were pipetted into new PCR tubes. Template (2 μL; 100 *E. coli* gDNA copies per μL) and 2.5 μL of 280 mM MgAc were added to initiate RPA, and the tubes were placed into an Agilent MxPro 3005 real-time PCR machine for amplification.

Strategy 3: Methylation-Dependent Endonuclease Digestion

RPA pellets were suspended in 29.5 μL of Rehydration Buffer with 0–140 units of DpnI restriction endonuclease (New England Biolabs, product #R0176S) and incubated for 15 or 60 min at 37°C, with or without 14 mM MgAc, to cleave methylated *E. coli* gDNA at Gm_6ATC restriction sites. After digestion, tubes with treated pellet solution were mixed with 47.5 μL of master mix containing 505 μM primers and SYBR green dye (47,500-fold dilution of stock solution). Finally, 2 μL (100 copies) of *E. coli* gDNA standard and 2.5 μL of 280 mM MgAc were added to the tube caps and spun down in a microcentrifuge to simultaneously initiate the RPA reactions.

Strategy 4: DNA Depletion Using Anti-DNA Antibodies

Anti-dsDNA antibodies coupled to amine-modified magnetic particles were prepared as follows. Nine hundred microliters of 55.6 μg mL^{-1} anti-dsDNA antibody (#ab27156, Abcam) in 100 mM sodium acetate buffer (pH 5.4) was added to 45 μL of 0.1 M $NaIO_4$. After 30 min of incubation at room

temperature (RT), oxidized antibodies were concentrated using 100-kDa Amicon Ultra centrifugal filters (Millipore, Billerica, MA, USA) and diluted to 500 μL at 100 μg mL^{-1} in 200 mM sodium carbonate buffer (pH 9.6). Next, 3.1-μm Promag amine microspheres (200 μL; 1×10^8 particles; Bangs Laboratories Inc.) were washed and resuspended in 500 μL of 200 mM sodium carbonate buffer (pH 9.6) and then added to the oxidized antibodies. After incubation at RT for 2 h, 15 μL of 5 M $NaCNBH_3$, 1 M NaOH was added to the reaction and incubated for an additional 30 min at RT. Next, 75 μL of 1 M hydroxylamine was added, and the mixture was incubated for 30 min. The antibody-functionalized magnetic particles were washed 3 times and stored at 4°C in phosphate-buffered saline (PBS) (final concentration, 1×10^5 particles per μL).

To remove extraneous DNA, TwistAmp Basic kit freeze-dried pellets (TwistDx) were reconstituted in 29.5 μL of TwistDx Rehydration Buffer and transferred to a low-binding microcentrifuge tube containing 2×10^5 antibody-functionalized magnetic beads in 2 μL of buffer. The microcentrifuge tube was placed on a rotator and incubated for 30 min at 4°C, after which the beads were removed using a magnet, and the solution was transferred to new tubes in 29.5-μL aliquots. Master mix (47.5 μL) containing 505 μM primers and SYBR green dye (47,500-fold dilution of the stock solution) was added to each tube along with *E. coli* gDNA (100 genome copies per μL) in 2 μL. Finally, 2.5 μL of 280 mM MgAc was added to the tube caps and spun in a microcentrifuge to simultaneously initiate RPA.

qPCR Assays

Real-time PCR standard curves were prepared with 10-fold serial dilutions of gDNA standards (*E. coli* ATCC 35218 or *A. muciniphila* ATCC BAA-835) using previously-validated primer pairs (16S rRNA bacteria-specific primer set 2, or *A. muciniphila* specific primer set 4, **Table 1**). qPCR was performed in 20-μL reaction volumes containing 550 nM primers (1.1 μL of 10 μM), a 1× concentration of Brilliant III Ultra-Fast SYBR green qPCR master mix (10 μL of 2× commercial stock conc.; Agilent Technologies), and 2 or 5 μL of template. Amplification curves, baselines, and threshold cycles were calculated using Agilent MxPro 3005P software as described below.

Threshold Time and Cycle Parameters for RPA and qPCR Reactions

MxPro software (Agilent Technologies) was used to normalize baseline fluorescence and calculate RPA threshold times from raw fluorescence data. Using a linear least mean squares algorithm, the baseline function was calculated by fitting the raw fluorescence in the first 3 min of the reaction to a first-order function. Baseline-corrected fluorescence was obtained by subtracting the baseline from the raw fluorescence to plot an amplification curve. For each assay, threshold fluorescence was defined as the point at which the fluorescence exceeded the average baseline-corrected fluorescence by three standard deviations, located in the exponential region of the amplification curve. The threshold time or cycle was calculated as the time or cycle at which the reaction met the threshold fluorescence. For each assay, average threshold cycle ($n = 3$) was plotted against copies of gDNA per reaction on semi-logarithmic axes to generate a regression line.

Determining Total Bacterial and *A. muciniphila* Abundance

An anonymized human fecal sample from a deceased Caucasian female with a medical history of hypoglycemia and hypothyroidism was obtained from Analytical Biological Services Inc. Three micrograms of DNA (15 ng/μL) was isolated from 220 mg of the fecal sample using QIAamp DNA Stool mini kit (catalog no. 51504, Qiagen). Nucleic acid purity was confirmed by a 260 nm/280 nm absorbance ratio of 1.83 using Nanodrop™. Either 3 or 7.5 ng of isolated DNA (2- or 5-μL of a 10-fold dilution of the stock concentration) was run as the template in quantitative RPA and PCR assays. Average threshold time (RPA) or cycle (PCR) and relative standard curves were used to determine the number of *E. coli* or *A. muciniphila* gDNA copies per 15 ng of the isolated DNA. Finally, the relative *A. muciniphila* abundance was calculated as the ratio of *A. muciniphila* gDNA copies per μL to the number of bacterial gDNA copies per μL.

For both *A. muciniphila* (ATCC BAA-835) and *E. coli* (ATCC 35218) gDNA standards, the 16S rRNA gene sequences from the GenBank (accession nos. NR_074436.1 and EF436579, respectively) were aligned to the complete genome sequences of *A. muciniphila* (accession no. NC_010655.1) and *E. coli* (accession NZ_KK583188.1) using the NCBI BLAST. This resulted in three and seven matches (100% in identity and composition) for *A. muciniphila* and *E. coli*, respectively. Thus, to calculate the 16S rRNA gene copies for each standard, the genomic DNA copies were multiplied by the number of 16rRNA gene copies per genome (3 for *A. muciniphila* and 7 for *E. coli*).

Sequencing-Based Detection

The composition of the fecal microbiome was independently characterized using 16S rRNA sequencing. A QIAamp DNA Stool mini kit was used to isolate DNA from the fecal sample. SeqWright Genomic Services (Houston, TX) generated and validated a library of 300-bp amplicons (MiSeq Reagent kit v3, MS-102-3001) using the extracted DNA and a universal primer pair (primer set 5; **Table 1**) spanning the 16S rRNA V4 region (Caporaso et al., 2011). Sequencing was performed on an Illumina MiSeq instrument with 250-bp paired-end reads. Reads were then uploaded to the Sequencing Read Archive (BioProjectID: PRJNA472995) and Illumina Basespace Sequencing Hub for sequencing analysis. Kraken Metagenomics software was used to assign taxonomic labels to each read using a k-mer–based algorithm. The relative abundance of *A. muciniphila* was then calculated by comparing the number of reads classified as *A. muciniphila* to the total number of bacterial reads.

RESULTS

Identification of *Escherichia coli* DNA Contamination in RPA Reagents

With unmodified RPA reagents, amplification was observed with primer set 1 in reactions containing 100–1,000,000 copies of *E. coli* gDNA in 10.3 min essentially independent of

initial template concentration (standard deviation: 60 s, range: 10–11 min); no-template controls also showed amplification in 9.5 min ($n = 1$) (Figure S1). To confirm that the newly designed primer pair (primer set 1) was bacteria-specific, the amplification curves generated using primer set 1 were compared to amplification curves generated using the previously published and validated universal primer set 2 (**Table 1**, Figure S1). Amplification was observed with primer set 2 in reactions containing 100–1,000,000 copies of *E. coli* gDNA in 24.2 min (standard deviation: 150 s, range: 23.2–25.8 min), essentially independent of template concentration; the no-template control also showed amplification in 24.8 min ($n = 1$). A difference in primer length is the cause of the large jump in threshold time that is observed when no-template control reactions are tested with the two universal primer pairs. The manufacturer of the RPA reagent (TwistDx) recommends that RPA primers be 30–35 nt long. When RPA reactions are tested with PCR-size primers (15–22 nt in length), reactions will take longer to achieve threshold fluorescence than when reactions are tested with primers of the recommended length.

Amplicons generated from the no-template reaction with primer set 1 were purified using a QIAquick PCR Purification kit. To determine if primer dimers were contributing to unintended amplification, the purified RPA product was analyzed by gel electrophoresis to show the expected ∼330-bp single band. To determine the phylogenic origin of the amplicon, the product was Sanger sequenced (Genewiz, Houston, TX) and the sequencing traces analyzed with Sequence Scanner 2 (Applied Biosystems, Foster City, CA) to generate a consensus sequence. The consensus sequence was aligned against NCBI's 16S ribosomal RNA database using nBLAST to show the highest similarity (99–100% identity) when aligned with a portion of the 16S rRNA gene in *E. coli*. Information provided by the manufacturer indicated that essential enzymes in RPA reagents are produced in an *E. coli* expression host. We, therefore, hypothesized that DNA from the *E. coli* vector is present in the RPA reaction pellets and amplified when 16S rRNA universal primers are used.

Strategies for Removing Extraneous DNA From RPA Reagents

Removing DNA Using Metal-Chelate Affinity Capture

As the purines of single-stranded nucleic acids contain an imidazole ring similar to that of the histidines recognized in "His_6-tagging," they exhibit a strong affinity for chelated transition metal ions (Murphy et al., 2003; Cano et al., 2005). Thus, we hypothesized that Ni-IDA immobilized metal affinity chromatography (IMAC) agarose beads would be an effective means of selectively binding and removing extraneous DNA from RPA reagents.

RPA reaction pellets were first reconstituted in rehydration buffer and then incubated with Ni^{+2}-loaded IDA sepharose particles, as described in section Materials and Methods. The particles were removed by centrifugation, and the resulting supernatant was tested using primer set 1 in real-time RPA reactions spiked with 100 copies of *E. coli* gDNA (data not shown). Amplification curves generated using Ni-treated, and untreated reagents were indistinguishable, indicating that: (1) there was no significant decline in reaction efficiency after incubation with the IMAC resin; (2) RPA proteins exhibited low nonspecific (or His-tag) binding to Ni-IDA sepharose beads; and (3) little, if any, DNA was removed during the treatment of RPA pellets. Given our previous finding that Ni-IDA affinity is specific to single-stranded nucleic acids with exposed purine bases (Murphy et al., 2003; Cano et al., 2005), this result suggests that the majority of the residual DNA in the RPA reagents is double-stranded.

DNA Shearing by Sonication

Sonication is widely used in next-generation sequencing protocols to shear genomic DNA into fragments of as little as 150–200 bp. Gel electrophoresis analysis of the product generated from primer set 2, and no-template control reactions showed a single band, ∼300 bp in length. Thus, we hypothesized that sonicating the reaction pellet would render the contaminating DNA un-amplifiable in downstream RPA reactions. No-template reactions with sonicated reagents reached the threshold fluorescence, on average, 60 s earlier than reactions with untreated reagents (Figure S2). Thus, we concluded that: (1) RPA reagents are tolerant of the degree of sonication applied, and (2) sonicating RPA pellets was not sufficient to shear extraneous DNA to such a degree as to impair amplification.

This result is consistent with previous studies which showed increases in amplification efficiency when samples are sonicated before PCR (Golenberg et al., 1996; Veal et al., 2012). Fragmenting genomic DNA into ∼1 kb segments suggests facilitation of DNA dehybridization in GC-rich regions for quicker binding of polymerase at recognition sites and enhanced strand amplification.

Methylation-Dependent Endonuclease Digestion

DpnI is a methylation-dependent restriction endonuclease that cleaves DNA prepared from *E. coli* dam^+ strains but not PCR-amplified DNA (Glickman, 1980; Barnes et al., 2014). The DpnI cleavage site (5′-Gm_6ATC) was found to occur twice within the region of predicted amplification in the *E. coli* 16S rRNA gene (Figure S3). Thus, pre-treating RPA reagents with DpnI restriction enzymes should digest and render the extraneous DNA un-amplifiable.

Laborious removal of DpnI after incubation and prior to initiation of the RPA reaction likely would be unnecessary. As RPA reactions are isothermal, they commence immediately upon mixing of the reagents. This continuous amplification leads to prompt generation of synthetic products (Piepenburg et al., 2006). If sample (reaction template) and primers are simultaneously added to the DpnI-treated pellet, a portion of the sample DNA is likely to evade DpnI cleavage, allowing it to be amplified during the first round of RPA. The resulting unmethylated synthetic products are impervious to DpnI enzymatic cleavage and are available to act as a template in subsequent rounds of amplification.

No-template RPA reactions that contained pellets pre-treated for 15 min with 20 units of DpnI showed only a 90-s delay in threshold time when compared with reactions using untreated

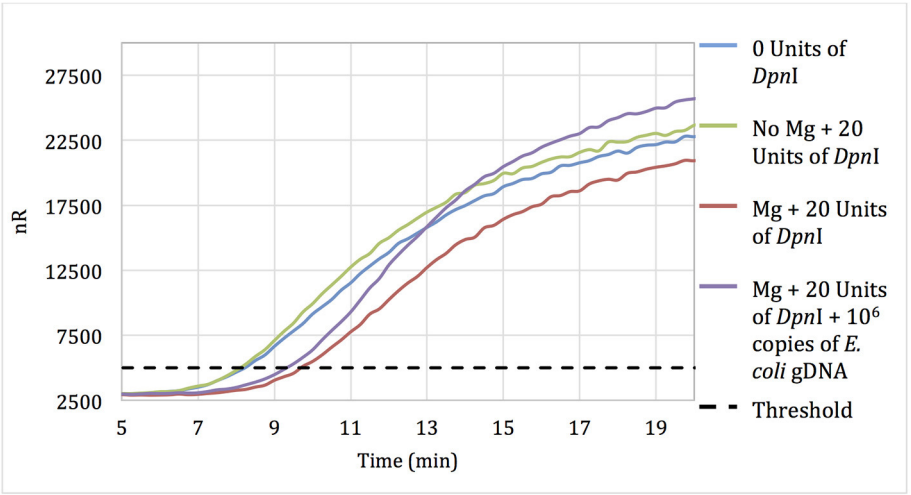

FIGURE 1 | Amplification curves of RPA reactions carried out using primer set 1 and untreated reagents (blue) or reagents pre-treated with 20 units of DpnI for 15 min (red). Reagents pre-treated with DpnI and spiked with 10^6 copies of *E. coli* gDNA (purple); reagents pre-treated with DpnI in the absence of MgAc (green).

pellets, suggesting that some but not all of the extraneous DNA was digested during DpnI treatment (**Figure 1**). Negative control reactions with pellets incubated with DpnI in the absence of magnesium (DpnI's co-factor) showed the same threshold time as reactions using untreated RPA reagent.

Increasing the DpnI digestion time from 15 to 60 min resulted in no increase in the threshold time difference between no-template reactions with treated and untreated RPA reagent. However, increasing the DpnI concentration 5- or 7-fold resulted in a 2.75 and 5.5-min increases in the threshold time, respectively (data not shown). Results indicate that treating RPA reagents with DpnI can digest and render a significant proportion of contaminating DNA un-amplifiable in subsequent applications.

DNA Depletion Using Anti-DNA Antibodies

Magnetic particles conjugated with anti-DNA antibodies with affinity for both dsDNA and ssDNA were used to treat RPA reagents, as described in section Materials and Methods. No-template RPA reactions that were pretreated with anti-dsDNA antibody magnetic particles showed a 3-min later threshold time than reactions involving untreated reagents (**Figure 2**). These data demonstrate that treating RPA reagents with anti-dsDNA antibody magnetic particles removes a significant proportion of extraneous DNA.

Reactions with treated reagents showed a 1.75-min earlier threshold time when spiked with 100 copies of *E. coli* gDNA compared with reactions with treated reagents in the absence of spiked *E. coli* gDNA (**Figure 2**). These data indicate that treatment with anti-dsDNA antibody magnetic particles does not significantly remove proteins necessary for RPA amplification.

Both DpnI treatment and anti-dsDNA antibody magnetic particles effectively removed extraneous DNA, with similar efficiencies, from RPA reagents. Treating RPA reagents with 100 units of DpnI showed a 2.75 min delay in threshold time when compared to reactions with untreated reagents. RPA reagents treated with anti-dsDNA antibody showed a comparable delay of 3 min in threshold time when compared to reactions with untreated reagents.

The cost of RPA reagents is ∼$5 per reaction; these reagents can be treated to remove extraneous DNA with 100 units of DpnI at a cost of $3.33, or using anti-DNA antibody and magnetic particles for $2.25 per reaction. Thus later work employed the slightly less-expensive anti-DNA magnetic particles.

Quantitative Bacterial Detection Using RPA

To determine the detection range of the assay based on DNA-depleted reagents, 10-fold serial dilutions of *E. coli* gDNA standards were spiked into RPA reactions containing RPA reagents pre-treated with anti-ds DNA antibody magnetic particles (**Figure 3A**). Two replicates for concentrations ranging from 10^6 to 10^3 *E. coli* gDNA copies per reaction and two no-template control reactions were performed. Threshold time versus log copy number of *E. coli* gDNA was fit to a semi-logarithmic regression line to generate a standard curve (**Figure 3B**).

To demonstrate that the total bacterial load in a clinically relevant sample can be quantified using RPA, DNA was isolated from a human fecal sample (Analytical Biological Services, Inc.) and amplified in RPA reactions. Based on the *E. coli* standard curve, the total bacterial load of the fecal sample was 1.01×10^7 bacterial gDNA copies per 15 ng of isolated gDNA.

The same fecal sample was also re-analyzed using real-time PCR. A total of 2 μL of each *E. coli* gDNA standard dilution was spiked into PCR reactions containing previously published pan bacteria–specific primers (**Table 1**, primer set 2; $n = 3$). Threshold cycle was plotted against log copies of *E. coli* gDNA per reaction to generate a standard curve (Figure S4), which was then used to calculate the total bacterial load of the fecal sample as 5.58×10^6 bacterial gDNA copies per 15 ng of isolated DNA. The total bacterial load of the stool sample quantified by qPCR differed

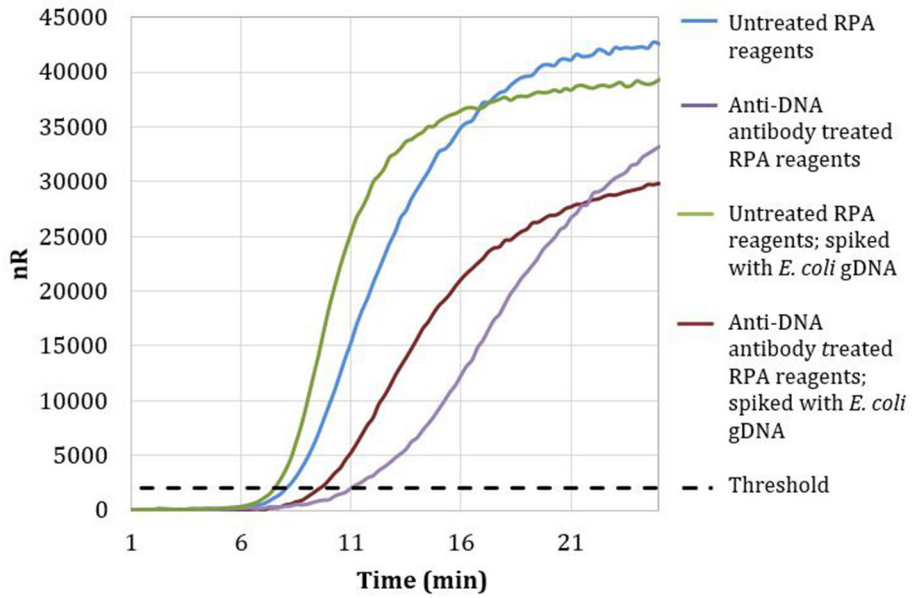

FIGURE 2 | Amplification curves of RPA reactions carried out with RPA primer set 1 and untreated (blue) or treated (purple) reagents. Untreated reactions spiked with 100 copies of *E. coli* gDNA (green) exhibited a threshold time of 7.25 min, whereas anti-DNA antibody treated reactions spiked with 100 copies of *E. coli* gDNA (maroon) exhibited a threshold time of 9.5 min.

by less than two-fold from the total bacterial load estimated by quantitative RPA (1.01×10^7 bacterial gDNA copies per 15 ng of isolated gDNA).

Development of the *A. muciniphila* Assay

Absolute *A. muciniphila* Abundance

Akkermansia muciniphila gDNA (0–1,000,000 copies; ATCC BAA-835) was amplified using real-time SYBR Green-RPA with *A. muciniphila*–specific primers designed in this work (**Table 1**, primer set 3). The amplification curves were used to determine threshold time values and generate a standard curve (log copy number gDNA vs. threshold cycle, **Figure 4**). Reactions run with no added template (NTC) exhibited an average threshold time of 10.8 ± 0.42 min ($n = 3$). Reactions spiked with 1,000 copies *E. coli* gDNA (ATCC 35218) exhibited an average threshold time insignificantly different from that of the NTC (10.6 min; $n = 3$).

Five microliters of a 10-fold dilution of gDNA isolated from the fecal sample (15 ng gDNA per μl) was run as a template in RPA reactions to yield an average threshold time of 6.05 ± 0.1 min ($n = 3$). The standard curve (**Figure 4**) was then used to quantify the absolute load of *A. muciniphila* as 2.99×10^5 gDNA copies per 15 ng of DNA isolated from the fecal sample.

The absolute *A. muciniphila* concentration in the fecal sample was separately determined by qPCR using primer set 4 (**Table 1**), which reportedly enables determination of the absolute abundance of *A. muciniphila* via qPCR (Collado et al., 2007; Schneeberger et al., 2015; Guo et al., 2016). The absolute *A. muciniphila* load of the fecal sample was estimated based on the qPCR semi-logarithmic regression line as 8.91×10^4 gDNA copies per reaction, or 1.78×10^5 gDNA copies per 15 ng of isolated gDNA (Figure S5), quite similar to the absolute *A. muciniphila* load of the fecal sample as determined using RPA (2.99×10^5 bacterial gDNA copies per 15 ng of isolated gDNA).

Relative *A. muciniphila* Abundance

Relative *A. muciniphila* abundance was calculated as the ratio of *A. muciniphila* 16S copies to total bacterial 16S copies using both qPCR (using primer sets 2 and 4) and RPA (using primer sets 1 and 3) to show a relative abundance of 1.36 and 1.29%, respectively. The relative *A. muciniphila* abundance of the fecal sample was determined using RPA from $3 \times 2.99 \times 10^5$ *A. muciniphila* 16S copies per 15 ng of gDNA divided by $7 \times 1.01 \times 10^7$ bacterial 16S copies per 15 ng of gDNA) and from PCR 5.34×10^5 *A. muciniphila* 16S copies/3.91×10^7 bacterial 16S copies) as $3 \times 1.78 \times 10^5$ *A. muciniphila* 16S copies per 15 ng of gDNA divided by $7 \times 5.58 \times 10^6$ bacterial 16S copies per 15 ng of gDNA.

In 16S rRNA gene sequencing, relative *A. muciniphila* abundance was defined as the ratio of *A. muciniphila* reads to the total number of bacterial reads. In 16S rRNA sequencing, the fecal sample produced 14,358,714 reads, of which 14,285,134 (99.5%) were taxonomically classified as bacteria. A total of 297,040 reads (2.07% of all reads) were classified as *A. muciniphila* ATCC BAA-835–specific, in good agreement with the RPA result.

When compared to sequencing, RPA gave a slightly lower relative *A. muciniphila* abundance in the fecal sample. This result could have been due to off-target amplification of the bacteria-specific primers. Note that the accuracy of the relative *A. muciniphila* abundance RPA assay, as with all nucleic acid-based assays, is highly dependent upon the quality of the primers.

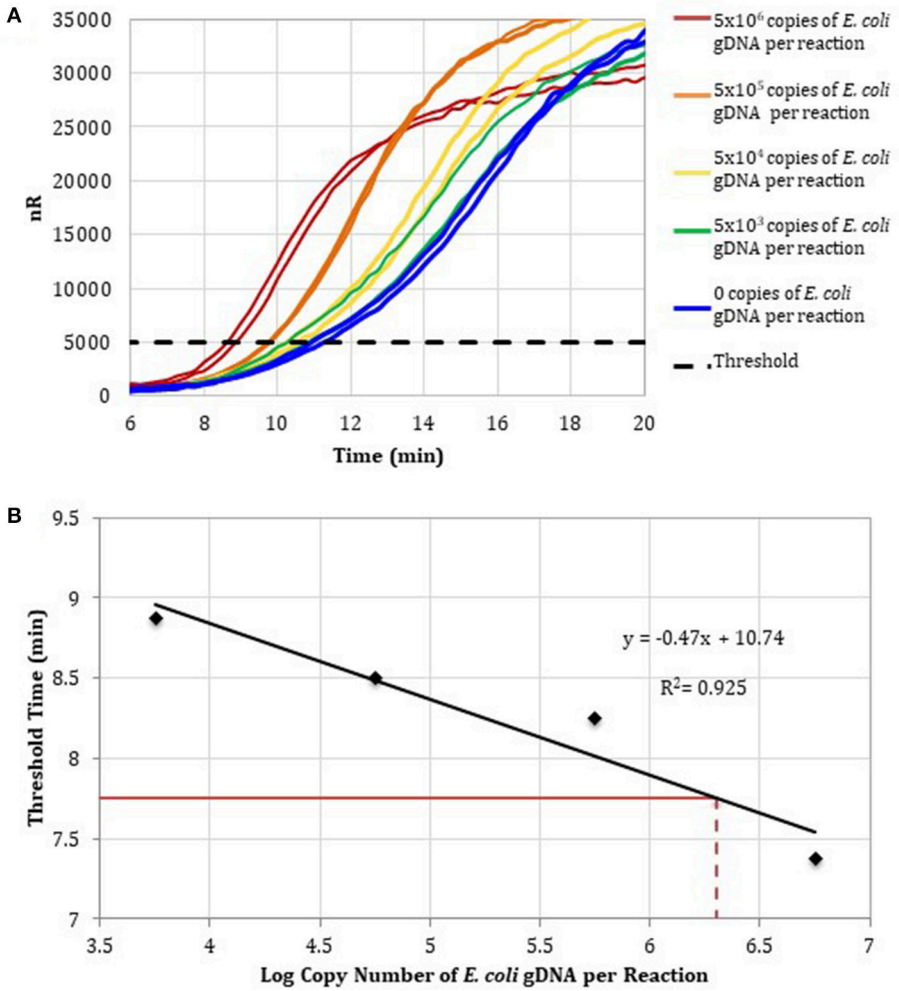

FIGURE 3 | (A) RPA amplification curves generated using the primer set 1, 0–10^6 copies of *E. coli* gDNA (2 μL per reaction; $n = 2$), and RPA reagents pre-treated with anti-dsDNA antibody-coupled magnetic particles. **(B)** RPA standard curve was generated using the average threshold times calculated from measurements in **(A)** ($n = 2$). The fecal DNA exhibited an average threshold time of 7. 75 min (solid red line) and an estimated load of 6.3-log copies of bacterial gDNA per reaction (dotted red line) or a total bacterial load of 1.01×10^7 bacterial gDNA copies per 15 ng of isolated gDNA.

RPA assay sensitivity could perhaps be improved by increasing the primer specificity.

DISCUSSION

Many microbial taxonomic groups have been identified as beneficial, detrimental, or simply indicative of a wide range of health conditions. As the number of organisms of interest expands, so does the need for inexpensive, accurate, and quantitative measurement of bacterial abundance within the gut. Unlike qPCR or 16S sequencing, RPA enables field-based testing. Recombinase polymerase amplification (RPA) is an isothermal nucleic acid amplification method that employs commercially available, easy-to-use freeze-dried, reaction-ready enzyme pellets that can be used to analyze specimens rapidly in the field, using a portable fluorometer. Analyzing complex microbial communities immediately after sampling can lead to a more accurate quantification of relative bacterial abundance. RPA is a method that is quickly growing in usage and range of applications (Piepenburg et al., 2008; Kim and Easley, 2011; Loo et al., 2013; Shin et al., 2013; Xu et al., 2014; Tortajada-Genaro et al., 2015; Daher et al., 2016; Yamanaka et al., 2017).

While many groups have developed RPA assays that demonstrate species-specific detection (Euler et al., 2012b; Ahmed et al., 2014; Krõlov et al., 2014; Clancy et al., 2015; Liljander et al., 2015; Cabada et al., 2017), there has been no development of an RPA assay that performs bacterial-specific detection. This gap is due to a high level of *E. coli* DNA in commercial RPA reagents. This paper is the first to offer a solution to this contamination. After successfully removing the contaminating DNA, we proceeded to demonstrate successful RPA quantification of bacteria in a stool sample.

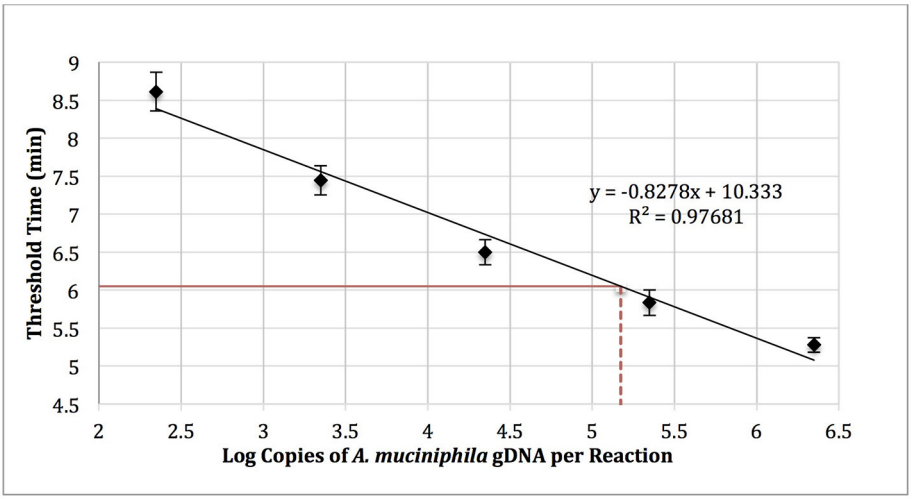

FIGURE 4 | RPA standard curve of *A. muciniphila* gDNA (0-1,000,000 copies; ATCC BAA-835) amplified using real-time SYBR green-RPA and primer set 1 ($n = 3$). The average threshold time of a 10-fold dilution of the fecal sample gDNA was 6.05 ± 0.1 min (solid red line, $n = 3$). The estimated load was 1.48×10^5 copies of *A. muciniphila* gDNA per reaction (dotted red line) or 2.99×10^5 copies of *A. muciniphila* gDNA per 15 ng of DNA isolated from the fecal sample.

In this proof-of-concept study we enabled the estimation of the relative abundance of *A. muciniphila* in human fecal DNA and demonstrated the promise of RPA as an inexpensive and accurate tool for measuring gut microbiome marker organisms. *A. muciniphila* appears to play a pivotal role in insulin resistance and inflammation. Furthermore, low abundance of *A. muciniphila* in the human gut is found to correlate with obesity. More recent studies indicate that *A. muciniphila* can influence the effectiveness of certain cancer immunotherapy drugs (Gopalakrishnan et al., 2018; Routy et al., 2018). Altering patients' gut microbiota to be rich in *A. muciniphila* may increase the fraction of individuals who respond to cancer immunotherapies. Given the short time *A. muciniphila* has been studied, the multitude of studies that support its role as a beneficial bacterium suggests its important role in human health. The medical community may soon need an inexpensive screening tool for identifying individuals with low fecal *A. muciniphila* abundance. To further assess the analytical accuracy and sensitivity of *Akkermansia muciniphila* detection with RPA more fecal samples should be tested.

AUTHOR CONTRIBUTIONS

HG helped conceive the project, designed and executed experiments, and wrote the manuscript. DC helped to design and perform experiments, and edited the manuscript. MC helped to interpret and conceive the project, and edited the manuscript. KK interpreted experiments, and helped to write and edit the manuscript. RW conceived the project, interpreted experiments, and helped to write and edit the manuscript.

ACKNOWLEDGMENTS

This work was supported by the FEMSA Foundation and the National Science Foundation, www.nsf.gov, (Grant Number 1759440).

SUPPLEMENTARY MATERIAL

The Supplementary Material for this article can be found online at: https://www.frontiersin.org/articles/10.3389/fcimb.2018.00237/full#supplementary-material

REFERENCES

Abd El Wahed, A., El-Deeb, A., El-Tholoth, M., Abd El Kader, H., Ahmed, A., Hassan, S., et al. (2013). A portable reverse transcription recombinase polymerase amplification assay for rapid detection of foot-and-mouth disease virus. *PLoS ONE* 8:e71642. doi: 10.1371/journal.pone.0071642

Abd El Wahed, A., Weidmann, M., and Hufert, F. T. (2015). Diagnostics-in-a-Suitcase: development of a portable and rapid assay for the detection of the emerging avian influenza A (H7N9) virus. *J. Clin. Virol.* 69, 16–21. doi: 10.1016/j.jcv.2015.05.004

Ahmed, A., van der Linden, H., and Hartskeerl, R. A. (2014). Development of a recombinase polymerase amplification assay for the detection of pathogenic Leptospira. *Int. J. Environ. Res. Public Health* 11, 4953–4964. doi: 10.3390/ijerph110504953

Barnes, H. E., Liu, G., Weston, C. Q., King, P., Pham, L. K., Waltz, S., et al. (2014). Selective microbial genomic DNA isolation using restriction endonucleases. *PLoS ONE* 9:e109061. doi: 10.1371/journal.pone.0109061

Bonney, L. C., Watson, R. J., Afrough, B., Mullojonova, M., Dzhuraeva, V., Tishkova, F., et al. (2017). A recombinase polymerase amplification assay for rapid detection of Crimean-Congo Haemorrhagic fever Virus infection. *PLoS Negl. Trop. Dis.* 11:e0006013. doi: 10.1371/journal.pntd.0006013

Brukner, I., Longtin, Y., Oughton, M., Forgetta, V., and Dascal, A. (2015). Assay for estimating total bacterial load: relative qPCR normalisation of bacterial

load with associated clinical implications. *Diagn. Microbiol. Infect. Dis.* 83, 1–6. doi: 10.1016/j.diagmicrobio.2015.04.005

Cabada, M. M., Malaga, J. L., Castellanos-Gonzalez, A., Bagwell, K. A., Naeger, P. A., Rogers, H. K., et al. (2017). Recombinase polymerase amplification compared to real-time polymerase chain reaction test for the detection of *Fasciola hepatica* in human stool. *Am. J. Trop. Med. Hyg.* 96, 341–346. doi: 10.4269/ajtmh.16-0601

Cano, T., Murphy, J. C., Fox, G. E., and Willson, R. C. (2005). Separation of genomic DNA from plasmid DNA by selective renaturation with immobilized metal affinity capture. *Biotechnol. Prog.* 21, 1472–1477. doi: 10.1021/bp050155g

Caporaso, J. G., Lauber, C. L., Walters, W. A., Berg-Lyons, D., Lozupone, C. A., Turnbaugh, P. J., et al. (2011). Global patterns of 16S rRNA diversity at a depth of millions of sequences per sample. *Proc. Natl. Acad. Sci. U.S.A.* 108(Suppl 1), 4516–4522. doi: 10.1073/pnas.1000080107

Centers for Disease Control and Prevention (2017). *National Diabetes Statistics Report, 2017*. Atlanta, GA: Centers for Disease Control and Prevention, US Dept of Health and Human Services. Available online at: https://www.cdc.gov/diabetes/data/statistics/statistics-report.html

Clancy, E., Higgins, O., Forrest, M. S., Boo, T. W., Cormican, M., Barry, T., et al. (2015). Development of a rapid recombinase polymerase amplification assay for the detection of Streptococcus pneumoniae in whole blood. *BMC Infect. Dis.* 15:481. doi: 10.1186/s12879-015-1212-5

Collado, M. C., Derrien, M., Isolauri, E., De Vos, W. M., and Salminen, S. (2007). Intestinal integrity and *Akkermansia muciniphila*, a mucin-degrading member of the intestinal microbiota present in infants, adults, and the elderly. *Appl. Environ. Microbiol.* 73, 7767–7770. doi: 10.1128/AEM.01477-07

Colman, R. J., and Rubin, D. T. (2014). Fecal microbiota transplantation as therapy for inflammatory bowel disease: a systematic review and meta-analysis. *J. Crohns. Colitis* 8, 1569–1581. doi: 10.1016/j.crohns.2014.08.006

Crannell, Z. A., Rohrman, B., and Richards-Kortum, R. (2014). Quantification of HIV-1 DNA using real-time recombinase polymerase amplification. *Anal. Chem.* 86, 5615–5619. doi: 10.1021/ac5011298

Crannell, Z. A., Rohrman, B., and Richards-Kortum, R. (2015). Development of a quantitative recombinase polymerase amplification assay with an internal positive control. *J. Vis. Exp.* doi: 10.3791/52620

Cui, B., Feng, Q., Wang, H., Wang, M., Peng, Z., Li, P., et al. (2015). Fecal microbiota transplantation through mid-gut for refractory Crohn's disease: safety, feasibility, and efficacy trial results. *J. Gastroenterol. Hepatol.* 30, 51–58. doi: 10.1111/jgh.12727

Daher, R. K., Stewart, G., Boissinot, M., and Bergeron, M. G. (2016). Recombinase polymerase amplification for diagnostic applications. *Clin. Chem.* 62, 947–958. doi: 10.1373/clinchem.2015.245829

Daher, R. K., Stewart, G., Boissinot, M., Boudreau, D. K., and Bergeron, M. G. (2015). Influence of sequence mismatches on the specificity of recombinase polymerase amplification technology. *Mol. Cell. Probes* 29, 116–121. doi: 10.1016/j.mcp.2014.11.005

Dao, M. C., Everard, A., Aron-Wisnewsky, J., Sokolovska, N., Prifti, E., Verger, E. O., et al. (2016). *Akkermansia muciniphila* and improved metabolic health during a dietary intervention in obesity: relationship with gut microbiome richness and ecology. *Gut* 65, 426–436. doi: 10.1136/gutjnl-2014-308778

Dubourg, G., Lagier, J. -C., Armougom, F., Robert, C., Audoly, G., Papazian, L., et al. (2013). High-level colonisation of the human gut by Verrucomicrobia following broad-spectrum antibiotic treatment. *Int. J. Antimicrob. Agents* 41, 149–155. doi: 10.1016/j.ijantimicag.2012.10.012

Duvallet, C., Gibbons, S. M., Gurry, T., Irizarry, R. A., and Alm, E. J. (2017). Meta-analysis of gut microbiome studies identifies disease-specific and shared responses. *Nat. Commun.* 8, 1784.

Euler, M., Wang, Y., Nentwich, O., Piepenburg, O., Hufert, F. T., and Weidmann, M. (2012a). Recombinase polymerase amplification assay for rapid detection of Rift Valley fever virus. *J. Clin. Virol.* 54, 308–312. doi: 10.1016/j.jcv.2012.05.006

Euler, M., Wang, Y., Otto, P., Tomaso, H., Escudero, R., Anda, P., et al. (2012b). Recombinase polymerase amplification assay for rapid detection of *Francisella tularensis*. *J. Clin. Microbiol.* 50, 2234–2238. doi: 10.1128/JCM.06504-11

Everard, A., Belzer, C., Geurts, L., Ouwerkerk, J. P., Druart, C., Bindels, L. B., et al. (2013). Cross-talk between *Akkermansia muciniphila* and intestinal epithelium controls diet-induced obesity. *Proc. Natl. Acad. Sci. U.S.A.* 110, 9066–9071. doi: 10.1073/pnas.1219451110

Everard, A., Lazarevic, V., Derrien, M., Girard, M., Muccioli, G. G., Muccioli, G. M., et al. (2011). Responses of gut microbiota and glucose and lipid metabolism to prebiotics in genetic obese and diet-induced leptin-resistant mice. *Diabetes* 60, 2775–2786. doi: 10.2337/db11-0227

Gascuel, O., Gouy, M., and Lyon, D. (2010). SeaView version 4: a multiplatform graphical user interface for sequence alignment and phylogenetic tree building. *Mol. Biol. Evol.* 27, 221–224. doi: 10.1093/molbev/msp259

Glickman, B. W. (1980). *Escherichia coli* mutator mutants deficient in methylation-instructed DNA mismatch correction. *Proc. Natl. Acad. Sci. U.S.A.* 77, 1063–1067. doi: 10.1073/pnas.77.2.1063

Gloor, G. B., Macklaim, J. M., Pawlowsky-Glahn, V., and Egozcue, J. J. (2017). Microbiome datasets are compositional: and this is not optional. *Front. Microbiol.* 8:2224. doi: 10.3389/fmicb.2017.02224

Golenberg, E. M., Bickel, A., and Weihs, P. (1996). Effect of highly fragmented DNA on PCR. *Nucleic Acids Res.* 24, 5026–5033. doi: 10.1093/nar/24.24.5026

Gopalakrishnan, V., Spencer, C. N., Nezi, L., Reuben, A., Andrews, M. C., Karpinets, T. V., et al. (2018). Gut microbiome modulates response to anti-PD-1 immunotherapy in melanoma patients. *Science* 359, 97–103. doi: 10.1126/science.aan4236

Greer, R. L., Dong, X., Moraes, A. C., Zielke, R. A., Fernandes, G. R., Peremyslova, E., et al. (2016). *Akkermansia muciniphila* mediates negative effects of IFNγ on glucose metabolism. *Nat. Commun.* 7:13329. doi: 10.1038/ncomms13329

Guo, X., Zhang, J., Wu, F., Zhang, M., Yi, M., and Peng, Y. (2016). Different subtype strains of *Akkermansia muciniphila* abundantly colonize in southern China. *J. Appl. Microbiol.* 120, 452–459. doi: 10.1111/jam.13022

Hänninen, A., Toivonen, R., Pöysti, S., Belzer, C., Plovier, H., Ouwerkerk, J. P., et al. (2017). *Akkermansia muciniphila* induces gut microbiota remodelling and controls islet autoimmunity in NOD mice. *Gut*. doi: 10.1136/gutjnl-2017-314508. [Epub ahead of print].

He, S., Stevens, S. L. R., Chan, L. -K., Bertilsson, S., Glavina Del Rio, T., Tringe, S. G., et al. (2017). Ecophysiology of freshwater verrucomicrobia inferred from metagenome-assembled genomes. *mSphere* 2:e00277-17. doi: 10.1128/mSphere.00277-17

Hermann-Bank, M., Skovgaard, K., Stockmarr, A., Larsen, N., and Mølbak, L. (2013). The Gut Microbiotassay: a high-throughput qPCR approach combinable with next generation sequencing to study gut microbial diversity. *BMC Genomics* 14:788. doi: 10.1186/1471-2164-14-788

Kang, D. -W., Park, J. G., Ilhan, Z. E., Wallstrom, G., Labaer, J., Adams, J. B., et al. (2013). Reduced incidence of Prevotella and other fermenters in intestinal microflora of autistic children. *PLoS ONE* 8:e68322. doi: 10.1371/journal.pone.0068322

Kim, J., and Easley, C. J. (2011). Isothermal DNA amplification in bioanalysis: strategies and applications. *Bioanalysis* 3, 227–239. doi: 10.4155/bio.10.172

Kim, J. Y., and Lee, J.-L. (2016). Rapid detection of salmonella enterica serovar enteritidis from eggs and chicken meat by real-time recombinase polymerase amplification in comparison with the two-step real-time PCR. *J. Food Saf.* 36, 402–411. doi: 10.1111/jfs.12261

Kim, J. Y., and Lee, J.-L. (2017). Development of a multiplex real-time recombinase polymerase amplification (RPA) assay for rapid quantitative detection of *Campylobacter coli* and jejuni from eggs and chicken products. *Food Control* 73, 1247–1255. doi: 10.1016/j.foodcont.2016.10.041

Kostic, A. D., Gevers, D., Pedamallu, C. S., Michaud, M., Duke, F., Earl, A. M., et al. (2012). Genomic analysis identifies association of Fusobacterium with colorectal carcinoma. *Genome Res.* 22, 292–298. doi: 10.1101/gr.126573.111

Krõlov, K., Frolova, J., Tudoran, O., Suhorutsenko, J., Lehto, T., Sibul, H., et al. (2014). Sensitive and rapid detection of *Chlamydia trachomatis* by recombinase polymerase amplification directly from urine samples. *J. Mol. Diagn.* 16, 127–135. doi: 10.1016/j.jmoldx.2013.08.003

Liljander, A., Yu, M., O'Brien, E., Heller, M., Nepper, J. F., Weibel, D. B., et al. (2015). Field-applicable recombinase polymerase amplification assay for rapid detection of *Mycoplasma capricolum* subsp. capripneumoniae. *J. Clin. Microbiol.* 53, 2810–2815. doi: 10.1128/JCM.00623-15

Lloyd-Price, J., Abu-Ali, G., and Huttenhower, C. (2016). The healthy human microbiome. *Genome Med.* 8, 51. doi: 10.1186/s13073-016-0307-y

Loo, J. F., Lau, P. M., Ho, H. P., and Kong, S. K. (2013). An aptamer-based bio-barcode assay with isothermal recombinase polymerase amplification for cytochrome-c detection and anti-cancer drug screening. *Talanta* 115, 159–165. doi: 10.1016/j.talanta.2013.04.051

Louis, S., Tappu, R. -M., Damms-Machado, A., Huson, D. H., and Bischoff, S. C. (2016). Characterization of the gut microbial community of obese patients following a weight-loss intervention using whole metagenome shotgun sequencing. *PLoS ONE* 11:e0149564. doi: 10.1371/journal.pone.0149564

Lynch, S. V., and Pedersen, O. (2016). The human intestinal microbiome in health and disease. *N. Engl. J. Med.* 375, 2369–2379. doi: 10.1056/NEJMra1600266

Moore, M. D., and Jaykus, L. -A. (2017). Development of a recombinase polymerase amplification assay for detection of epidemic human noroviruses. *Sci. Rep.* 7:40244. doi: 10.1038/srep40244

Morgan, X. C., and Huttenhower, C. (2012). Chapter 12: Human microbiome analysis. *PLoS Comput. Biol.* 8:e1002808. doi: 10.1371/journal.pcbi.1002808

Muegge, B. D. (2011). Diet drives convergence in gut microbiome functions across mammalian phylogeny and within humans. *Science* 332, 970–974. doi: 10.1126/science.1198719

Murphy, J. C., Jewell, D. L., White, K. I., Fox, G. E., and Willson, R. C. (2003). Nucleic acid separations utilizing immobilized metal affinity chromatography. *Biotechnol. Prog.* 19, 982–986. doi: 10.1021/bp025563o

Muyzer, G., Waal, E. C. D. E., and Uitierlinden, A. G. (1993). Profiling of complex microbial populations by denaturing gradient gel electrophoresis analysis of polymerase chain reaction-amplified genes coding for 16s rRNA. *Appl. Environ. Microbiol.* 59, 695–700.

Ott, S. J., Musfeldt, M., Ullmann, U., Hampe, J., and Schreiber, S. (2004). Quantification of intestinal bacterial populations by real-time PCR with a universal primer set and minor groove binder probes: a global approach to the enteric flora. 42, 2566–2572. doi: 10.1128/JCM.42.6.2566-2572.2004

Petrof, E. O., Gloor, G. B., Vanner, S. J., Weese, S. J., Carter, D., Daigneault, M. C., et al. (2013). Stool substitute transplant therapy for the eradication of Clostridium difficile infection: " RePOOPulating " the gut. *Microbiome* 1, 1–12. doi: 10.1186/2049-2618-1-3

Piepenburg, O., Williams, C. H., and Armes, N. A. (2008). *Methods for Multiplexing Recombinase Polymerase Amplification*. US Patent. Available online at: https://patentimages.storage.googleapis.com/16/58/ef/149158a9aa42f4/US7435561.pdf (Accessed May 14, 2018).

Piepenburg, O., Williams, C. H., Stemple, D. L., and Armes, N., A. (2006). DNA detection using recombination proteins. *PLoS Biol.* 4:e204. doi: 10.1371/journal.pbio.0040204

Plovier, H., Everard, A., Druart, C., Depommier, C., Van Hul, M., Geurts, L., et al. (2016). A purified membrane protein from *Akkermansia muciniphila* or the pasteurized bacterium improves metabolism in obese and diabetic mice. *Nat. Med.* 23, 107–113. doi: 10.1038/nm.4236

Robinson, C. K., Brotman, R. M., and Ravel, J. (2016). Intricacies of assessing the human microbiome in epidemiologic studies. *Ann. Epidemiol.* 26, 311–321. doi: 10.1016/j.annepidem.2016.04.005

Rosa, B. A., Hallsworth-pepin, K., Martin, J., Wollam, A., and Mitreva, M. (2017). Genome sequence of Christensenella minuta DSM 22607. *Genome Announc.* 5, 4–5. doi: 10.1128/genomeA.01451-16

Rosser, A., Rollinson, D., Forrest, M., and Webster, B. L. (2015). Isothermal Recombinase Polymerase amplification (RPA) of Schistosoma haematobium DNA and oligochromatographic lateral flow detection. *Parasit. Vectors* 8:446. doi: 10.1186/s13071-015-1055-3

Routy, B., Le Chatelier, E., Derosa, L., Duong, C. P. M., Alou, M. T., Daillère, R., et al. (2018). Gut microbiome influences efficacy of PD-1–based immunotherapy against epithelial tumors. *Science* 359, 91–97. doi: 10.1126/science.aan3706

Scheperjans, F., Aho, V., Pereira, P., B., Koskinen, K., and Paulin, L., Pekkonen, E., et al. (2015). Gut microbiota are related to Parkinson's disease and clinical phenotype. *Mov. Disord.* 30, 350–358. doi: 10.1002/mds.26069

Scher, J. U., Sczesnak, A., Longman, R. S., Segata, N., Ubeda, C., Bielski, C., et al. (2013). Expansion of intestinal *Prevotella copri* correlates with enhanced susceptibility to arthritis. *Elife* 2:e01202. doi: 10.7554/eLife.01202

Schneeberger, M., Everard, A., Gómez-Valadés, A. G., Matamoros, S., Ramírez, S., Delzenne, N. M., et al. (2015). *Akkermansia muciniphila* inversely correlates with the onset of inflammation, altered adipose tissue metabolism and metabolic disorders during obesity in mice. *Sci. Rep.* 5:16643. doi: 10.1038/srep16643

Shin, Y., Perera, A. P., Kim, K. W., and Park, M. K. (2013). Real-time, label-free isothermal solid-phase amplification/detection (ISAD) device for rapid detection of genetic alteration in cancers. *Lab Chip* 13, 2106–2114. doi: 10.1039/c3lc50129a

Shreiner, A. B., Kao, J. Y., and Young, V. B. (2015). The gut microbiome in health and in disease. *Curr. Opin. Gastroenterol.* 31, 69–75. doi: 10.1097/MOG.0000000000000139

Tortajada-Genaro, L. A., Santiago-Felipe, S., Amasia, M., Russom, A., and Maquieira, Á. (2015). Isothermal solid-phase recombinase polymerase amplification on microfluidic digital versatile discs (DVDs). *RSC Adv.* 5, 29987–29995. doi: 10.1039/C5RA02778K

Veal, C. D., Freeman, P. J., Jacobs, K., Lancaster, O., Jamain, S., Leboyer, M., et al. (2012). A mechanistic basis for amplification differences between samples and between genome regions. *BMC Genomics* 13:455. doi: 10.1186/1471-2164-13-455

Watterlot, L., Lakhdari, O., Bermu, L. G., Sokol, H., Bridonneau, C., Furet, J.-P., et al. (2008). *Faecalibacterium prausnitzii* is an anti-inflammatory commensal bacterium identified by gut microbiota analysis of Crohn disease patients. *Proc. Natl. Acad. Sci. U.S.A.* 105, 16731–16736. doi: 10.1073/pnas.0804812105

Wong, S. H., Kwong, T. N. Y., Chow, T. -C., Luk, A. K. C., Dai, R. Z. W., Nakatsu, G., et al. (2017). Quantitation of faecal Fusobacterium improves faecal immunochemical test in detecting advanced colorectal neoplasia. *Gut* 66, 1441–1448. doi: 10.1136/gutjnl-2016-312766

Xu, C., Li, L., Jin, W., and Wan, Y. (2014). Recombinase polymerase amplification (RPA) of CaMV-35S promoter and nos terminator for rapid detection of genetically modified crops. *Int. J. Mol. Sci.* 15, 18197–18205. doi: 10.3390/ijms151018197

Yamanaka, E. S., Tortajada-Genaro, L. A., and Maquieira, Á. (2017). Low-cost genotyping method based on allele-specific recombinase polymerase amplification and colorimetric microarray detection. *Microchim. Acta* 184, 1453–1462. doi: 10.1007/s00604-017-2144-0

Yassour, M., Lim, M. Y., Yun, H. S., Tickle, T. L., Sung, J., Song, Y. -M., et al. (2016). Sub-clinical detection of gut microbial biomarkers of obesity and type 2 diabetes. *Genome Med.* 8:17. doi: 10.1186/s13073-016-0271-6

Yoon, J., Matsuo, Y., Katsuta, A., Jang, J.-H., Matsuda, S., Adachi, K., et al. (2008). *Haloferula rosea* gen. nov., sp. nov., *Haloferula harenae* sp. nov., *Haloferula phyci* sp. nov., *Haloferula helveola* sp. nov. and *Haloferula sargassicola* sp. nov., five marine representatives of the family Verrucomicrobiaceae within the phylum "Verrucomicrobia." *Int. J. Syst. Evol. Microbiol.* 58, 2491–2500. doi: 10.1099/ijs.0.2008/000711-0

Zhang, A. N., Mao, Y., and Zhang, T. (2016). Development of quantitative real-time PCR assays for different clades of "Candidatus Accumulibacter." *Sci. Rep.* 6:23993. doi: 10.1038/srep23993

Zhang, H., Sparks, J. B., Karyala, S. V., Settlage, R., and Luo, X. M. (2015). Host adaptive immunity alters gut microbiota. *ISME J.* 9, 770–781. doi: 10.1038/ismej.2014.165

Conflict of Interest Statement: The authors declare that the research was conducted in the absence of any commercial or financial relationships that could be construed as a potential conflict of interest.

The reviewer JG and handling Editor declared their shared affiliation.

Copyright © 2018 Goux, Chavan, Crum, Kourentzi and Willson. This is an open-access article distributed under the terms of the Creative Commons Attribution License (CC BY). The use, distribution or reproduction in other forums is permitted, provided the original author(s) and the copyright owner(s) are credited and that the original publication in this journal is cited, in accordance with accepted academic practice. No use, distribution or reproduction is permitted which does not comply with these terms.

frontiers in Cellular and Infection Microbiology

ORIGINAL RESEARCH
published: 21 June 2018
doi: 10.3389/fcimb.2018.00190

Intestinal Inflammation in Chilean Infants Fed With Bovine Formula vs. Breast Milk and Its Association With Their Gut Microbiota

Juan C. Ossa, Dominique Yáñez, Romina Valenzuela, Pablo Gallardo, Yalda Lucero and Mauricio J. Farfán**

Departamento de Pediatría y Cirugía Infantil, Facultad de Medicina, Hospital Dr. Luis Calvo Mackenna, Universidad de Chile, Santiago, Chile

Introduction: Compared to bovine formula (BF), breast milk (BM) has unique properties. In the newborn intestine, there is a homeostatic balance between the counterparts of the immune system, which allows a physiological inflammation, modulated by the gut microbiota. Many studies have attempted to understand the effect of BF vs. BM, and the changes in the gut microbiota, but few also focus on intestinal inflammation.

Methods: We conducted a cohort study of newborn infants during their first 3 months. In stool samples taken at 1 and 3 months (timepoints T1 and T3), we quantified calprotectin, IL-8 and α1-antitrypsin by ELISA and we evaluated the expression of *IL8* and *IL1β* genes by RT-qPCR. To determine the microbiota composition, the 16S rRNA gene was amplified and sequenced using 454 pyrosequencing. Sequences were clustered into operational taxonomic units (OTUs).

Results: In total 15 BM and 10 BF infants were enrolled. In the BM group, we found calprotectin and α1-antitrypsin levels were significantly elevated at T3 compared to T1; no differences were found between T1 and T3 in the BF group. A comparison between the BM and BF groups showed that calprotectin levels at T1 were lower in the BM than the BF group; this difference was not observed at T3. For IL-8 levels, we found no differences between groups. A gene expression analysis of the *IL8* and *IL1β* genes showed that infants from the BF group at T1 have a significantly increased expression of these markers compared to the BM group. Gut microbiota analyses revealed that the phylum Bacteroidetes was higher in BM than BF, whereas Firmicutes were higher in BF. A redundancy analysis and ANOVA showed BM has a community structure statistically different to BF at T1 but not at T3. Compared to BF, BM at T1 showed a higher representation of *Enterococcus*, *Streptococcus*, *Enterobacter*, *Lactococcus,* and *Propionibacterium*.

Conclusions: We found a basal state of inflammation in the infants' intestine based on inflammation markers. One month after birth, infants receiving BF exhibited higher levels of inflammation compared to BM.

Keywords: intestinal inflammation, bovine formula, breast milk, gut microbiota, infant cohort

OPEN ACCESS

Edited by:
Pascale Alard,
University of Louisville, United States

Reviewed by:
Young Min Kwon,
University of Arkansas, United States
Erdong Cheng,
University of Pittsburgh Cancer Institute, United States

***Correspondence:**
Juan C. Ossa
jcossa@gmail.com
Mauricio J. Farfán
mfarfan@med.uchile.cl

Received: *12 December 2017*
Accepted: *17 May 2018*
Published: *21 June 2018*

Citation:
Ossa JC, Yáñez D, Valenzuela R, Gallardo P, Lucero Y and Farfán MJ (2018) Intestinal Inflammation in Chilean Infants Fed With Bovine Formula vs. Breast Milk and Its Association With Their Gut Microbiota. Front. Cell. Infect. Microbiol. 8:190. doi: 10.3389/fcimb.2018.00190

INTRODUCTION

Breast milk (BM) has been and will continue to be the ideal type of nutrition for every term or pre-term newborn. The WHO recommends exclusive breastfeeding for the first 6 months of life, with supplemental breastfeeding until 2 years old and beyond (Hoddinott et al., 2008). Compared to bovine formula milk (BF), BM contains nutrients, hormones, growth factors, immunoglobulins, cytokines and bacteria which confer protection against many diseases, such as necrotizing enterocolitis, respiratory and gastrointestinal infections, allergy, celiac disease, obesity, diabetes type I and II (Horta et al., 2007; Le Huërou-Luron et al., 2010). In the healthy newborn intestine, the counterparts of the immune system allow the mucosa to display a physiological inflammation, a result of the immune response to diet and bacteria in the intestinal lumen (Fiocchi, 1997). Gut microbiota starts to develop *in utero*, inherited from the mother, and is later influenced by the mode of delivery and the newborn feeding pattern (Bäckhed et al., 2012). Nowadays, gut microbiota plays a key role in maturation and maintenance of the immune system, food metabolism, intestinal epithelial cell homeostasis, protection against pathogens and neural development of the gut-brain axis (Hill and Artis, 2010; Lathrop et al., 2011). The shift in the composition of a healthy microbiota to an unhealthy one is called dysbiosis. Currently, many enteric and non-enteric diseases have been associated with dysbiosis of the gut microbiota (Arrieta et al., 2014).

Most studies have attempted to understand the effect of BF or BM on the gut microbiota composition showing that BF feeding is associated with microbiota with lower abundance of Bacteroides, and higher Clostridia compared to BM-fed infants. Regarding Bifidobacteria, there is a controversy as to whether they are lower in number and frequency in BF than BM. Also, BF-fed infants exhibit higher counts of Enterobacteriaceae than BM-fed infants (Guaraldi and Salvatori, 2012; Fan et al., 2014). Other studies have shown the effect of diet on the intestinal cell homeostasis in healthy neonates by either analyzing gene expression from exfoliated epithelial cells or protein levels in stools. Although several inflammatory markers as well as inflammatory gene expression have been evaluated in stool or serum in infant, few studies have addressed diet in the newborn looking at intestinal inflammation and its relation to changes in gut microbiota composition (Chapkin et al., 2010; Savino et al., 2010). Considering the above, using a non-invasive technique based on stool analysis, we conducted a 3-month cohort study of newborn infants who are either in the exclusive BM or BF to determine inflammatory markers in stool and gut microbiota composition.

METHODS

Study Design

We conducted a 3-month cohort study following 2 groups of newborn infants who are fed exclusively either with BM or BF. All infants were recruited from the maternity ward of Hospital Luis Tisné in Santiago, Chile. In order to associate the effect of diet with inflammation marker levels and the microbiota composition over the 3-month period, a collection of stool samples were taken at 1 (timepoint T1) and 3 (timepoint T3) months of life, within a range of ± 5 days. The timepoints were chosen due to the limited knowledge about the intestinal inflammation and its association with gut microbiota under 6 months.

Patients

Inclusion Criteria. We enrolled infants born at term (38–42 weeks of gestation), vaginally delivered, and described healthy at the time of discharge from the hospital. For enrollment, all the infants had to be receiving BM or BF exclusively. The BF group also included infants who were in BM and receiving formula supplements $\geq$20% of the volume ingested that day. *Exclusion Criteria*. We excluded from the study infants or mothers who during the study period received antibiotics, probiotics, steroidal or non-steroidal anti-inflammatory drugs 1 month prior to enrollment. Also, we excluded from the study mothers hospitalized other than for delivery, for surgical intervention, serious infection, or with any sign or symptom of infection or gastrointestinal disease (diarrhea, vomiting, fever).

Clinical Assessment

During recruitment, a complete clinical interview was done to take the history regarding pregnancy, delivery mode, birth weight, frequency and quantity of feeding, stool frequency, family composition, number of siblings, history of allergy, gastrointestinal and other systemic disorders in the family, family income and household environment (number of rooms, water supply and pets in the home).

Sample Collection

A stool sample was obtained from the infants during the endpoints described above. Samples were collected during a clinical visit to our center, the Hospital Luis Calvo Mackenna, Santiago, Chile. In case that the infant has no stool during the visit, a home kit for the parents was given to take the sample and store it in a sterile container to be transported to our center within the following 6 h. Stool samples were divided into at least 4 aliquots and stored at -80°C.

Ethics

This study was done in accordance with the recommendations of the Declaration of Helsinki. The study protocol was approved by the ethical committees of the Servicio de Salud Metropolitano Oriente and Hospital Luis Tisné. Written informed consent was obtained from all parents on behalf of their infants.

Inflammatory Protein Markers Determination

ELISA commercial kits for stool samples were used for the analysis of calprotectin (IDK® calprotectin ELISA, Immunodiagnostik, Germany) and α1-antitrypsin (IDK®

α1-antitrypsin ELISA, Immunodiagnostik, Germany). Samples were processed as directed by the manufacturer. For IL-8, we determined the concentration of these markers by ELISA as previously described (Harrington et al., 2005).

Gene Expression Assay

RNA was isolated from the stool sample using the Stool Total RNA Purification Kit (Norgen Biotek) according to the manufacturer's instructions. Then, cDNA was synthesized using the First Strand cDNA Synthesis Kit (ThermoFisher Scientific) and RT-qPCR was carried out with the TaqMan Gene Expression Assay (ThermoFisher Scientific) and specific TaqMan probes for *IL8*, *IL1β,* and *GADPH* genes as previously described (Bennett et al., 2009; Chapkin et al., 2010). The *GADPH* gene was used as a housekeeping gene to normalize the expression of *IL8* and *IL1β*. Changes in cycle threshold (ΔCT) values for each gene were obtained at T1 and T3. The mean of the ΔCT of the BM group was used as a reference for the fold expression changes in the BF group.

Pyrosequencing and Operational Taxonomic Unit (OTU) Assignment

Total DNA was extracted from stool samples using the QIAamp Fast DNA Stool Mini Kit (Qiagen) and stored at −20°C until PCR amplification. The 16S rRNA gene was amplified in a two-step process. First, the 16S rRNA gene was amplified using the primers GM3 and 1492R, and then a nested PCR was performed using the GM3-PS forward primer and a different 907-PS reverse primer for each sample in a 7-cycle reaction as described (Gallardo et al., 2017). Amplicons were purified and the concentration of the purified product was determined. Equimolar mixtures of the amplicons (10–12 samples each) were shipped to Macrogen Inc. (Seoul, Korea) for pyrosequencing. Pyrosequencing of each mix was done through 454 GS-FLX using a 1/8 plate. Sequence trimming and OTU assignment were performed by Macrogen using CD-HIT-DUP and QIIME (Caporaso et al., 2010) according to their standard protocol [cutoff of 97% of sequence identity at species level for OTU assignment and using the 11th version of RDP-16s rDNA database as reference (http://rdp.cme.msu.edu/index.jsp)]. The sequence data reported in this study have been deposited in the European Nucleotide Archive (ENA) database, under accession number PRJEB25846.

Statistics

Gene expression and protein results are expressed as means ± standard error of the mean (SEM). Comparison of results between multiple groups was performed using one-way analysis of variance (ANOVA) and the Tukey-Kramer multiple comparisons test for results between the different experimental groups. For the OTU comparison analysis we used a non-parametric bootstrapping method, the Mann-Whitney u test. Differences with a $P < 0.05$ were considered statistically significant. Analyses were performed using Prism6 (GraphPad, San Diego, California, USA). Redundancy analysis (RDA) of OTU composition was done using the "vegan" package of version 3.4.2 of the R software, as described by Gallardo et al. (2017). The abundance of each taxa was normalized by the total diversity per sample prior to any group comparison. For the taxonomic analysis, the abundance of each taxa was normalized by the total diversity per sample prior to any group comparison.

RESULTS

Patient Demographic

During the study, 25 patients were recruited, 15 in the BM and 10 in the BF group. There were no differences between gender or birth weight and lengths. The number of stools/day was lower in the BF group (2.5 vs. 4.4), but this difference was not statistically significant. All the patients had the same average number of relatives in the home. Regarding pets and allergies, all the families had pets and 50% of the patients in both groups had a history of first-grade atopy (atopic dermatitis or asthma or allergic rhinitis or food allergy). Finally, family income was similar in both groups. **Table 1** summarizes these findings.

BF-Fed Infants Showed Higher Intestinal Inflammation Than BM-Fed Infants

We quantified the levels of inflammatory markers calprotectin, IL-8 and α1-antitrypsin in stool samples by ELISA. In the BM group, we found calprotectin and α1-antitrypsin levels were significantly higher at T3 than at T1. No differences were found between T1 and T3 in the BF group (**Figures 1A,B**). A comparison of the BM and BF groups showed that calprotectin levels at T1 were lower in the BM group; this difference was not observed at T3 (**Figure 1A**). For IL-8 levels, we found no difference between groups (**Figure 1C**).

Gene expression analysis of *IL8* and *IL1β* genes showed that infants from the BF group have a significantly increased expression of these markers (2.3 ± 0.45 and 2.3 ± 0.4-folds, respectively) at T1 compared to the BM group. At T3, no difference was found in the expression of these genes (**Figure 2**).

BF-Fed Infants Harbor a Different Intestinal Microbiota Than BM-Fed Infants

The taxonomic analysis showed a total number of 140 OTUs, 28 exclusively present in the BM group and 23 in the BF group. Shared OTUs among groups was only 2 at T1, but at T3 the number of shared OTUs increased to 48. When comparing the

TABLE 1 | Patient demographics of BM and BF groups.

Patient characteristics	BM group ($n = 15$)	BF group ($n = 10$)	p-value
Sex (F/M)	7/8	6/4	ns
Birth weight avg. (gr)	3,457	3,400	ns
Birth length avg. (cm)	51	50.2	ns
Stools per day avg.	4.4	2.5	ns
Family members avg. (n)	5	5	ns
History 1st degree atopy	50%	50%	ns
Pets at home	60%	80%	ns

ns, not significant.

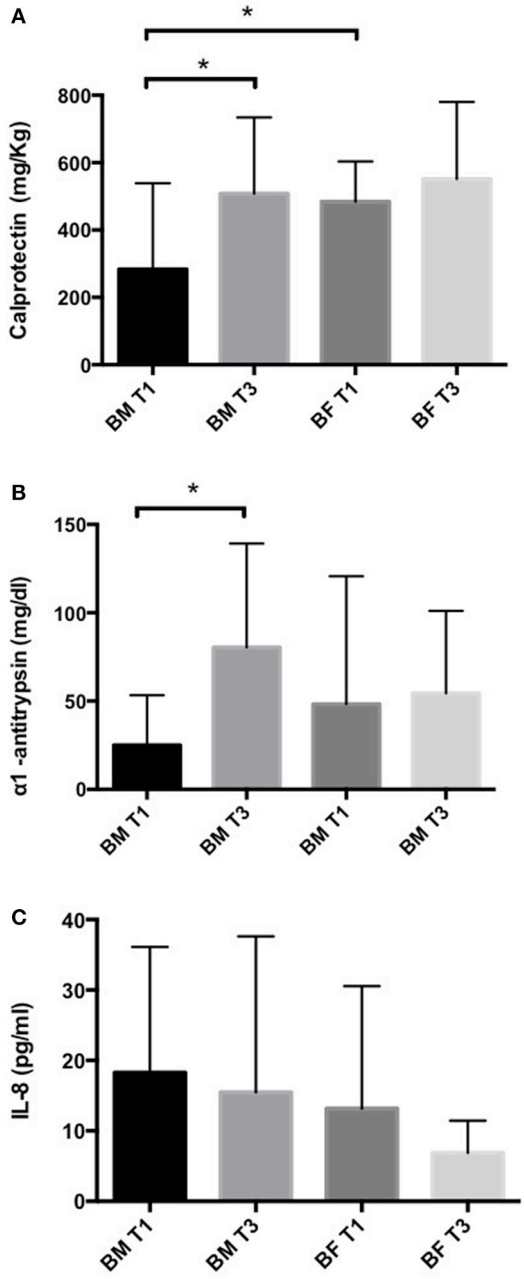

FIGURE 1 | Inflammatory markers in stool samples of infants fed with BM or BF. Concentration of calprotectin **(A)**, α1-antitrypsin **(B)** and IL-8 **(C)** in stool samples from BM and BF groups were determined by ELISA. *$p < 0.05$.

microbiota at T1, BM-fed newborns had 22 exclusive OTUs compared to 6 in the BF group (**Figure 3**). At phylum level, we found the BM group had a lower Firmicutes proportion (20 and 23%) than the BF group (38 and 42%) at T1 and T3. By contrast, a higher Bacteroides presence at T1 and T3 was found in the BF group (38 and 47%) than in the BM group (16 and 25%), respectively. The Firmicutes/Bacteroides ratio was lower in the BM group than the BF group at T1 (0.5 vs. 2.4) and at T3 (0.5 vs. 1.7). The proportions of Proteobacteria and Actinobacteria were similar among all groups. At genus level, the most abundant genera in all groups were *Escherichia/Shigella* and *Bacteroides*, followed by *Parabacteroides*, *Lechnospiracea,* and *Veillonela* (**Figure 4**).

A comparison of OTUs at genus level showed that the BF group had a higher representation of *Enterococcus* ($p = 0.001$), *Streptococcus* ($p = 0.001$), *Enterobacter* ($p = 0.01$), *Lactococcus* ($p = 0.03$) and *Propionibacterium* ($p = 0.04$) than the BM group at T1. At T3, the BM group had a higher representation of *Sutterella* ($p = 0.04$) and *Parabacteroides* ($p = 0.04$), whereas BF-fed infants had higher number of *Streptococus* ($p = 0.01$).

A RDA analysis of OTU composition showed a significant difference between BM and BF groups at T1 (**Figure 5A**), but not at T3 (**Figure 5B**).

DISCUSSION

Breastfeeding confers important benefits on the infant and protection from many diseases, most of them associated with changes in the intestinal tract environment. Few studies have endeavored to address the effect of diet and intestinal inflammation on the newborn. Here, we have shown in a cohort study that BF-fed infants have a higher intestinal inflammation defined by an increased concentration of calprotectin and α1-antitrypsin in stool samples taken 1 month after birth (T1) compared to an infant fed exclusively with BM. Even though these differences were not observed 2 months later (T3), our data support the role of BM in the low-grade inflammation compared to BF-fed infants 1 month after birth. Calprotectin and α1-antitrypsin are markers that specifically express protein loss and inflammation as seen in several gastrointestinal disorders, such as allergies and inflammatory bowel diseases (Poullis et al., 2002; Saarinen et al., 2002). Previous reports have compared the calprotectin levels in stools in healthy infants, BM vs., BF (median age 51 days old). Interestingly, the stool calprotectin level was higher in the BM group than in the BF group, suggesting a possible degree of local inflammation in the intestine in the BM infants (Savino et al., 2010). In another study, no differences were found in the stool calprotectin level between BM and BF newborns at 3 months old (Rosti et al., 2011). Similar to our findings but with a different approach, Kainonen et al., using a cohort of infants fed with BM and BF at high risk for the development of allergies, compared the levels of INF-γ, TNF-α, and IL-2 (proinflammatory), IL-5 and IL-4 (allergy) and IL-10 and TGF-β2 (anti-inflammatory). The BM group showed significantly lower proinflammatory markers in serum compared to the BF group, and the TGF-β2 levels in the BF group were significantly lower than in the BM group. These findings lasted up to 1 year, despite supplementation with solid food in both groups. Finally, they suggested BM had an immunomodulatory role "protecting" against inflammation (Kainonen et al., 2012). Possible mechanisms in breast milk dampening inflammation might involve its components, including immunoglobulins, cytokines such as IL-10, defensing, macrophage colony stimulating factors secreted

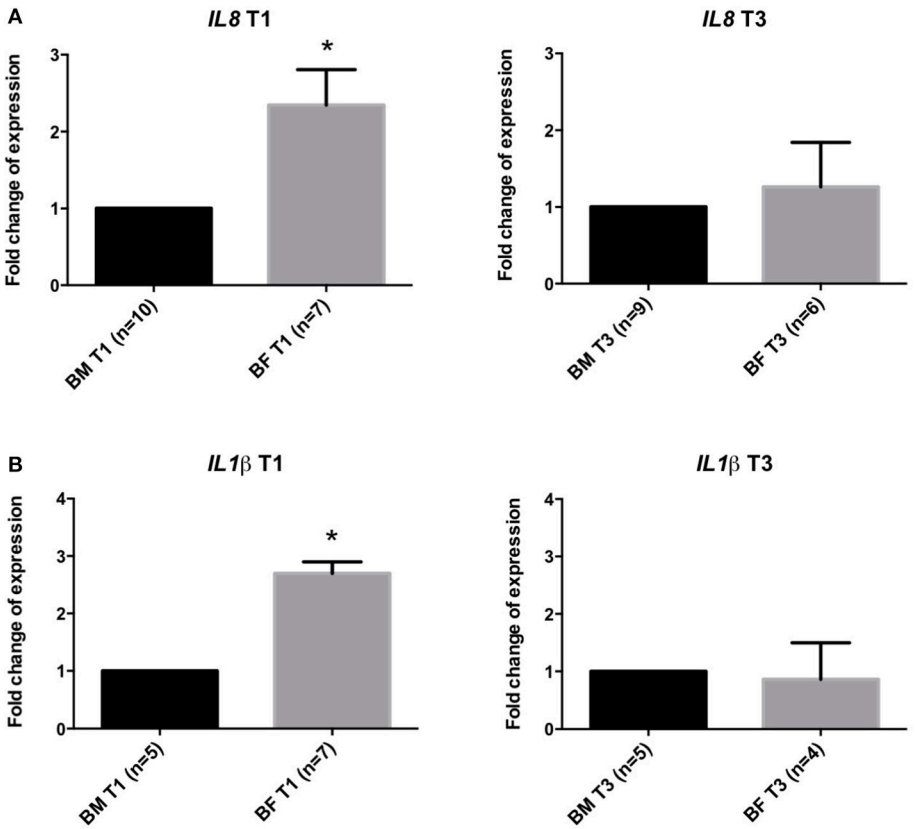

FIGURE 2 | Gene expression analysis in stool samples of infants fed with BM or BF. Gene expression at timepoints T1 and T3 of *IL8* **(A,B)** and *IL1β* genes in stool samples from BF group compared to BM group. Changes in cycle threshold (ΔCT) values for each gene, normalized to GAPDH gene, were obtained at T1 and T3. The mean of the ΔCT of BM group was used as a control for the ΔCT expression in the BF group compared to the BM group. $^{*}p < 0.05$.

by mammary epithelial cells and TGFβ produced by leukocytes present in the milk (Hennet and Borsig, 2016). In light of our results, the contribution of calprotectin and α1-antitrypsin in the gut homeostasis in infants merits further investigation.

We also quantified IL-8 in stools, but no significant differences were found between the groups. Although IL-8 is a pivotal molecule that orchestrates tissue inflammation, its role in intestinal inflammation in healthy children is not well characterized. In order to clarify the involvement of this cytokine, we decided to evaluate the expression of the *IL8* gene and another pro-inflammatory gene, *IL-1β*, in stool samples. We found a significantly increased expression of both genes in the BF group compared to the BM group at T1 but not at T3, suggesting that both genes might have a role in BM in ameliorating inflammation in the first month.

Microbiota has emerged as an important environmental factor in the inflammation of several gut diseases in children (Lu and Ni, 2015). In healthy infants, microbiota might play an important role in gut homeostasis. Our data suggest that the gut microbiota of the BM group clearly differs from the BF infants at T1 (**Figure 5**). BF harbors more Firmicutes and fewer Bacteroidetes, exhibiting a higher Firmicutes/Bacteroidetes (F/B) ratio than the BM group at T1 and T3, which is in line with previous data in healthy newborns (Mariat et al., 2009). A similar increase in Firmicutes has been seen in babies initially born by cesarean section (Hill et al., 2017). Interestingly, obesity is associated with an abundance of Firmicutes and a depletion of Bacteroidetes, where the interrelation of short-chain fatty acids fermented by bacteria plus the lipopolysaccharide from gram negative bacteria will induce inflammation and obesity (Chakraborti, 2015; Koliada et al., 2017). At genus level, we found that the BF group had a significantly higher amount of *Enterococcus*, *Enterobacter* and also *Streptococcus* than the BM group at T1, and all of these had been shown to be responsible for sepsis in early neonates as well in animal models receiving BF (Nakayama et al., 2003; Simonsen et al., 2014). These observations might be associated with a difference in calprotectin levels found in the BM group at this timepoint. Interestingly, in the BM group the calprotectin and α1-antitrypsin levels were higher at T3 than at T1, and these genera were found to be more abundant at T3 than at T1, suggesting that species belonging to these genera might be linked to gut inflammation. Our data support the idea that diet induces microbial changes that can induce inflammation and that BM reduces the inflammation burden, modulating the microbiota and thus maintaining intestinal homeostasis.

Our study has limitations. The number of patients included in the study was small, a situation that might be explained by the number of mothers who currently breastfeed their child exclusively in the first months of life. In the gut microbiota analysis, we could not identify any Bifidobacterium known to be present in newborn samples, despite other studies having found differences in their abundance between BF and BM (Penders et al., 2006; Hascoët et al., 2011). These results may possibly be attributed to the sequencing platform used (454 pyrosequencing). New sequencing platforms will make it possible to overcome this issue in future projects. Another limitation was the number of cytokines and genes evaluated. Although calprotectin, IL-8 and α1-antitrypsin are key markers of intestinal inflammation, there are several markers that could be explored. The development of new multiplex analyte platforms validated for stool samples will provide a broader picture of the molecules involved in intestinal homeostasis in infants.

In conclusion, using non-invasive methods in stools we found a basal state of inflammation baseline in the infant's intestine based on inflammation markers. At 1 month after birth, infants receiving BF exhibited higher levels of inflammation than BM in terms of changes in the microbiota composition. These results

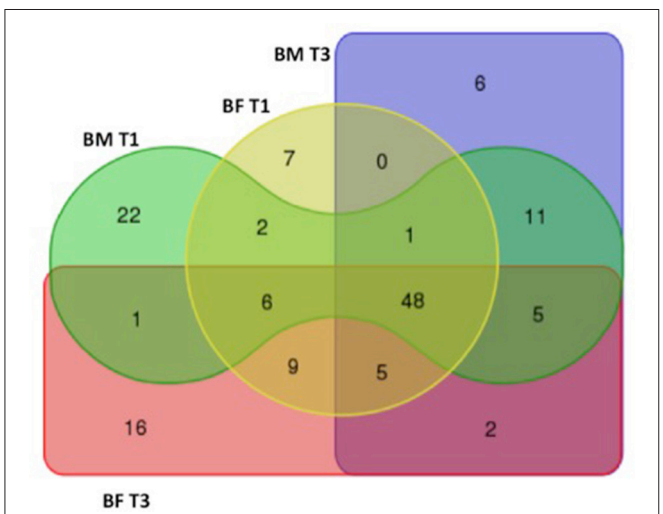

FIGURE 3 | Distribution of the OTUs among groups. Venn diagram showing the distribution of the 140 OTUs found at BM T1 (green), BM T3 (purple), BF T1 (yellow), and BF T3 (red) timepoints.

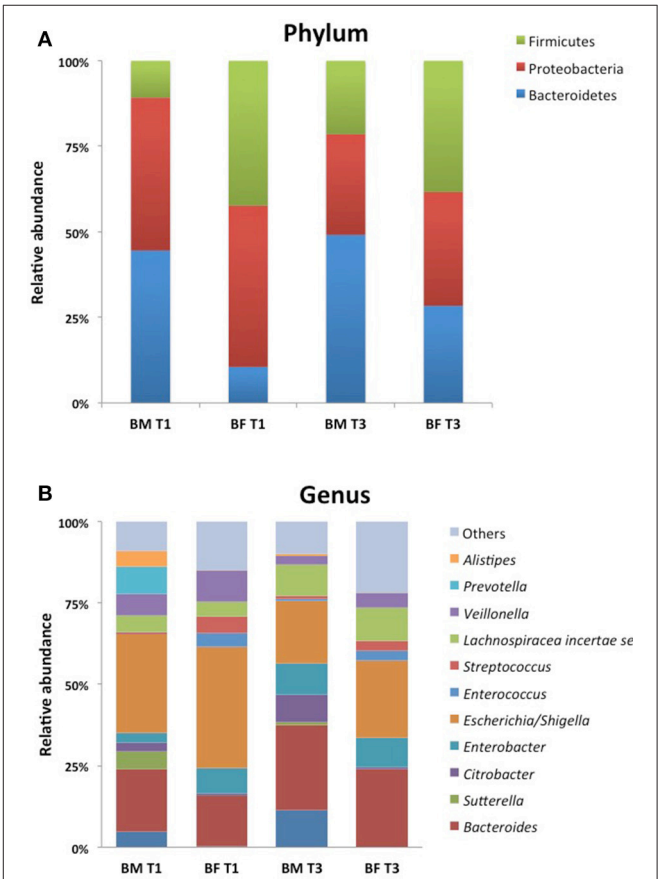

FIGURE 4 | Community profile at different taxonomic levels. Relative abundance of taxa at Phylum **(A)** and Genus **(B)** level of the 10 most abundant taxa. Each color represents a different taxonomic unit. Less representative taxa were grouped as "other".

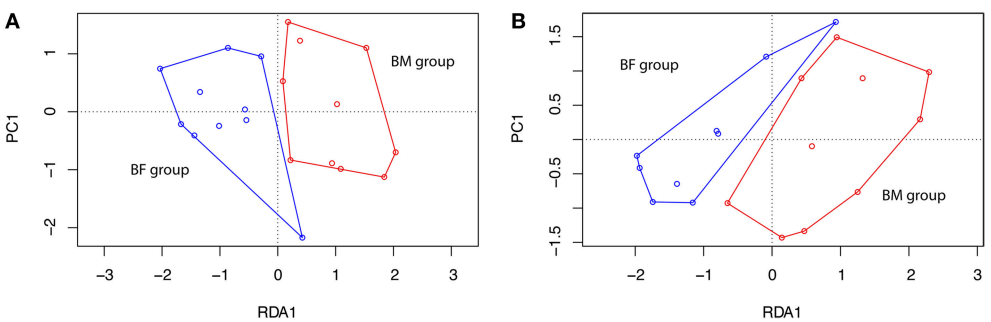

FIGURE 5 | Redundancy analysis at timepoints T1 and T3. A redundancy analysis (RDA) was conducted using sample classification as the explanatory matrix and relative OTU diversity as the response matrix at **(A)** T1, 1 month and **(B)** T3, 3 months. Data was normalized with a double square root transformation. Sample grouping and axis significance were analyzed by ANOVA (RDA T1 $p = 0.003$, RDA T3 $p = 0.238$).

might signify that BM has a protective role in ameliorating inflammation, modulating the intestinal microbiota during the first months of life.

AUTHOR CONTRIBUTIONS

JO participated in the study design, data acquisition, data interpretation, manuscript writing and final approval of the manuscript. DY participated in the sample collection and analysis. RV participated in the cohort enrollment and sample collection. PG participated in the microbiota data analysis and manuscript writing. YL participated in the study design and data interpretation. MF participated in the study design, data acquisition, data interpretation, manuscript writing and final approval of the manuscript.

ACKNOWLEDGMENTS

This work was supported by FONDECYT grants 11130374 to JO and 1160426 to MF.

REFERENCES

Arrieta, M. C., Stiemsma, L. T., Amenyogbe, N., Brown, E. M., and Finlay, B. (2014). The intestinal microbiome in early life: health and disease. *Front. Immunol.* 5:427. doi: 10.3389/fimmu.2014.00427

Bäckhed, F., Fraser, C. M., Ringel, Y., Sanders, M. E., Sartor, R. B., Sherman, P. M. et al. (2012). Defining a healthy human gut microbiome: current concepts, future directions, and clinical applications. *Cell Host Microbe* 12, 611–622. doi: 10.1016/j.chom.2012.10.012

Bennett, W. E. Jr, González-Rivera, R., Shaikh, N., Magrini, V., Boykin, M., Warner, B. B., et al., (2009). A Method for isolating and analyzing human mRNA from newborn stool. *J. Immunol. Methods* 349, 56–60. doi: 10.1016/j.jim.2009.07.013

Caporaso, J. G., Kuczynski, J., Stombaugh, J., Bittinger, K., Bushman, F. D., Costello, E. K., et al. (2010). QIIME allows analysis of high-throughput community sequencing data. *Nat. Methods* 7, 335–336. doi: 10.1038/nmeth.f.303

Chakraborti, C. K. (2015). New-found link between microbiota and obesity. *World J. Gastrointest. Pathophysiol.* 6, 110–119. doi: 10.4291/wjgp.v6.i4.110

Chapkin, R. S., Zhao, C., Ivanov, I., Davidson, L. A., Goldsby, J. S., Lupton, J. R., et al. (2010). Noninvasive stool-based detection of infant gastrointestinal development using gene expression profiles from exfoliated epithelial cells. *Am. J. Physiol. Gastrointest. Liver Physiol.* 298, G582–G589. doi: 10.1152/ajpgi.00004.2010

Fan, W., Huo, G., Li, X., Yang, L., and Duan, C. (2014). Impact of diet in shaping gut microbiota revealed by a comparative study in infants during the six months of life." *J. Microbiol. Biotechnol.* 24, 133–143. doi: 10.4014/jmb.1309.09029

Fiocchi, C. (1997). Intestinal inflammation: a complex interplay of immune and nonimmune cell interactions. *Am. J. Physiol.* 273(4 Pt 1), G769–G775. doi: 10.1152/ajpgi.1997.273.4.G769

Gallardo, P., Izquierdo, M., Vidal, R. M., Chamorro-Veloso, N., Rosselló-Móra, R., O'Ryan, M., et al. (2017). Distinctive gut microbiota is associated with diarrheagenic escherichia coli infections in chilean children. *Front. Cell. Infect. Microbiol.* 7:424. doi: 10.3389/fcimb.2017.00424

Guaraldi, F., and Salvatori, G. (2012). Effect of breast and formula feeding on gut microbiota shaping in newborns. *Front. Cell. Infect. Microbiol.* 2:94. doi: 10.3389/fcimb.2012.00094

Harrington, S. M., Strauman, M. C., Abe, C. M., and Nataro, J. P., (2005). Aggregative adherence fimbriae contribute to the inflammatory response of epithelial cells infected with enteroaggregative *Escherichia coli*. *Cell Microbiol.* 7, 1565–1578. doi: 10.1111/j.1462-5822.2005.00588.x

Hascoët, J. M., Hubert, C., Rochat, F., Legagneur, H., Gaga, S., Emady-Azar, S., et al. G. (2011). Effect of formula composition on the development of infant gut microbiota. *J. Pediatr. Gastroenterol. Nutr.* 52, 756–762. doi: 10.1097/MPG.0b013e3182105850

Hennet, T., and Borsig, L. (2016). Breastfed at Tiffany's. *Trends Biochem. Sci.* 41, 508–518. doi: 10.1016/j.tibs.2016.02.008

Hill, C. J., Lynch, D. B., Murphy, K., Ulaszewska, M., Jeffery, I. B., O'Shea, C. A., et al. (2017). Evolution of gut microbiota composition from birth to 24 weeks in the INFANTMET Cohort. *Microbiome* 5:4. doi: 10.1186/s40168-016-0213-y

Hill, D. A., and Artis, D. (2010). Intestinal bacteria and the regulation of immune cell homeostasis. *Annu. Rev. Immunol.* 28, 623–667. doi: 10.1146/annurev-immunol-030409-101330

Hoddinott, P., Tappin, D., and Wright, C. (2008). Breast feeding. *BMJ* 336, 881–887. doi: 10.1136/bmj.39521.566296.BE

Horta, B. L., Bahl, R., Martinés, J. C., Victora, C. G., and World Health Organization (2007). *Evidence on the Long-Term Effects of Breast-Feeding: Systematic Reviews and Meta-Analyses.* Geneva: WHO Library Cataloguing-in-Publication Data.

Kainonen, E., Rautava, S., and Isolauri, E. (2012). Immunological programming by breast milk creates an anti-inflammatory cytokine milieu in breast-fed infants compared to formula-fed infants. *Br. J. Nutr.* 109, 1962–1970. doi: 10.1017/S0007114512004229

Koliada, A., Syzenko, G., Moseiko, V., Budovska, L., Puchkov, K., Perederiy, V., et al. (2017). Association between body mass index and Firmicutes/Bacteroidetes ratio in an adult Ukrainian population. *BMC Microbiol.* 17:120. doi: 10.1186/s12866-017-1027-1

Lathrop, S. K., Bloom, S. M., Rao, S. M., Nutsch, K., Lio, C. W., Santacruz, N. et al. (2011). Peripheral education of the immune system by colonic commensal microbiota. *Nature* 478, 250–254. doi: 10.1038/nature10434

Le Huërou-Luron, I., Blat, S., and Boudry, G. (2010). Breast- v. formula-feeding: impacts on the digestive tract and immediate and long-term health effects. *Nutr. Res. Rev.* 23, 23–36. doi: 10.1017/S0954422410000065

Lu, C. Y., and Ni, Y. H. (2015). Gut microbiota and the development of pediatric diseases. *J. Gastroenterol.* 50, 720–726. doi: 10.1007/s00535-015-1082-z

Mariat, D., Firmesse, O., Levenez, F., Guimaraes, V., Sokol, H., Dore, J., et al. P. (2009). The Firmicutes/Bacteroidetes ratio of the human microbiota changes with age. *BMC Microbiol.* 9:123. doi: 10.1186/1471-2180-9-123

Nakayama, M., Yajima, M., Hatano, S., Yajima, T., and Kuwata, T. (2003). Intestinal adherent bacteria and bacterial translocation in breast-fed and formula-fed rats in relation to susceptibility to infection. *Pediatr. Res.* 54, 364–371. doi: 10.1203/01.PDR.0000077482.28990.2D

Penders, J., Thijs, C., Vink, C., Stelma, F. F., Snijders, B., Kummeling, I., et al. (2006). Factors influencing the composition of the intestinal microbiota in early infancy. *Pediatrics* 118, 511–521. doi: 10.1542/peds.2005-2824

Poullis, A., Foster, R., Northfield, T. C., and Mendall, M. A. (2002). Review article: faecal markers in the assessment of activity in inflammatory bowel disease. *Aliment Pharmacol. Ther.* 16, 675–681. doi: 10.1046/j.1365-2036.2002.01196

Rosti, L., Braga, M., Fulcieri, C., Sammarco, G., Manenti, B., and Costa, E. (2011). Formula milk feeding does not increase the release of the inflammatory marker calprotectin, compared to human milk. *Pediatr. Med. Chir.* 33, 178–181.

Saarinen, K. M., Sarnesto, A., and Savilahti, E. (2002). Markers of inflammation in the feces of infants with cow's milk allergy. *Pediatr. Allergy Immunol.* 13, 188–194. doi: 10.1034/j.1399-3038.2002.01027

Savino, F., Castagno, E., Calabrese, R., Viola, S., Oggero, R., and Miniero, R. (2010). High faecal calprotectin levels in healthy, exclusively breast-fed infants. *Neonatology* 97, 299–304. doi: 10.1159/000255161

Simonsen, K. A., Anderson-Berry, A. L., Delair, S. F., and Davies, H. D. (2014). Early-onset neonatal sepsis. *Clin. Microbiol. Rev.* 27, 21–47. doi: 10.1128/CMR.00031-13

Conflict of Interest Statement: The authors declare that the research was conducted in the absence of any commercial or financial relationships that could be construed as a potential conflict of interest.

Copyright © 2018 Ossa, Yáñez, Valenzuela, Gallardo, Lucero and Farfán. This is an open-access article distributed under the terms of the Creative Commons Attribution License (CC BY). The use, distribution or reproduction in other forums is permitted, provided the original author(s) and the copyright owner are credited and that the original publication in this journal is cited, in accordance with accepted academic practice. No use, distribution or reproduction is permitted which does not comply with these terms.

frontiers in Cellular and Infection Microbiology

GENERAL COMMENTARY
published: 20 June 2018
doi: 10.3389/fcimb.2018.00212

Commentary: Reducing Viability Bias in Analysis of Gut Microbiota in Preterm Infants at Risk of NEC and Sepsis

Gemma Agustí[1] *and Francesc Codony*[2]*

[1] Departament d'Òptica i Optometria, Universitat Politècnica de Catalunya-Barcelona Tech, Terrassa, Spain, [2] Laboratori Municipal - Aigües de Mataró, Mataró, Spain

Keywords: viability PCR, live-dead distinction, analysis bias, microbiome, PMA

A commentary on

Reducing Viability Bias in Analysis of Gut Microbiota in Preterm Infants at Risk of NEC and Sepsis

by Young, G. R., Smith, D. L., Embleton, N. D., Berrington, J. E., Schwalbe, E. C., Cummings, S. P., et al. (2017). Front. Cell. Infect. Microbiol. 7:237. doi: 10.3389/fcimb.2017.00237

The recent work by Young et al. (2017) demonstrates the importance of obtaining accurate data when analyzing the microbial community in real-life complex samples. These authors showed that an analysis of gut microbiota samples from preterm infants who at risk of necrotizing enterocolitis (NEC) and sepsis could be biased if the analysis includes DNA from dead cells. The study used a viability PCR (vPCR) approach to overcome this obstacle. Notably, vPCR uses specific photoreactive dye that cannot cross intact cell membranes. When a sample is incubated with this dye and exposed to light, the dye irreversibly binds to DNA in dead cells that have damaged cell membranes. This step effectively neutralizes the DNA and prevents it from being detected by PCR.

Regarding the importance of removing DNA from dead cells during microbial analysis, similar conclusions have been drawn by studies of, for example, environmental samples (Carini et al., 2016) and clinical specimens (Rogers et al., 2013). We agree with this premise and encourage others to use vPCR in microbial analysis, but caution that proper sample preparation is required for this technique.

vPCR methodology is theoretically simple to use since it requires only a reagent and a light source; however, as with many techniques, a lack of practical experience with the technique led the authors to overlook some important considerations. vPCR is still relatively new, with the first paper by Nogva et al. (2003). The scientific community has developed strategies and general rules for optimizing the vPCR workflow; some of these strategies were reviewed by Fittipaldi et al. (2012). More recent work has demonstrated that during sample manipulation, plastic can contribute to false positive results. Indeed, the walls of microtubes can retain free DNA, thereby preventing the nucleic acid from interacting with the reagent. Accordingly, the DNA fraction on the walls of the microtubes is not neutralized, and when it is detected, it is incorrectly assigned to the live DNA fraction (Agustí et al., 2017). This is only one example of how technical issues during early sample treatment steps can affect the conclusions of the analysis. For this reason, it is our opinion that despite the valuable conclusions, some microbiome analyses based on vPCR have hidden weaknesses.

In the paper by Young et al. (2017), the authors analyzed stool samples that were suspended in PBS, but the pH and the oxygen levels of standard PBS solutions were not optimal for

OPEN ACCESS

Edited by:
Pascale Alard,
University of Louisville, United States

Reviewed by:
Morgan Langille,
Dalhousie University, Canada

***Correspondence:**
Francesc Codony
francesc.codony@aiguesmataro.cat

Received: *22 June 2017*
Accepted: *05 June 2018*
Published: *20 June 2018*

Citation:
Agustí G and Codony F (2018) Commentary: Reducing Viability Bias in Analysis of Gut Microbiota in Preterm Infants at Risk of NEC and Sepsis. Front. Cell. Infect. Microbiol. 8:212. doi: 10.3389/fcimb.2018.00212

ensuring the viability of the cells in the stool samples. Therefore, the sample handling steps themselves could have affected the viability of some cells in the specimen. For example, only half of the anaerobic microorganisms from the mammalian large bowel survive exposure to O_2 for 5 min, and this percentage decreases to 3–5% after 20 min of exposure (Brusa et al., 1989). This effect is quite predictable and easy to understand; however, other important aspects, such as centrifugation (Peterson et al., 2012), the time between sample collection and storage (Cuthbertson et al., 2014), and freeze/thawing (Cuthbertson, 2015) can also lead to bias in culture-independent analysis.

The authors evaluated the effect of freezing the samples and concluded that freeze/thawing did not change the results for the stool samples. However, factors other than storage were not considered, so it remains unclear whether their conclusions were influenced by additional biases.

The work of Young et al. is valuable, and the conclusions very clearly show the importance of overcoming bias due to DNA from dead cells in a microbial diversity analysis. We suggest that an additional warning about the importance of appropriate sample handling would be helpful to readers who may wish to conduct similar analyses.

AUTHOR CONTRIBUTIONS

Both authors reviewed the original work and wrote this commentary.

REFERENCES

Agustí, G., Fittipaldi, M., and Codony, F. (2017). False-positive viability PCR results: an association with microtubes. *Curr. Microbiol.* 74, 377–380. doi: 10.1007/s00284-016-1189-3

Brusa, T., Canzi, E., Pacini, N., Zanchi, R., and Ferrari, A. (1989). Oxygen tolerance of anaerobic bacteria isolated from human feces. *Curr. Microbiol.* 19, 39. doi: 10.1007/BF01568901

Carini, P., Marsden, P. J., Leff, J. W., Morgan, E. E., Strickland, M. S., and Fierer, N. (2016). Relic DNA is abundant in soil and obscures estimates of soil microbial diversity. *Nat. Microbiol.* 19:16242. doi: 10.1038/nmicrobiol.2016.242

Cuthbertson, L., Rogers, G. B., Walker, A. W., Oliver, A., Hafiz, T., Hoffman, L. R., et al. (2014). Time between collection and storage significantly influences bacterial sequence composition in sputum samples from cystic fibrosis respiratory infections. *J. Clin. Microbiol.* 52, 3011–3016. doi: 10.1128/JCM.00764-14

Cuthbertson, L., Rogers, G. B., Walker, A. W., Oliver, A., Hoffman, L. R., Carroll, M. P., et al., (2015). Implications of multiple freeze-thawing on respiratory samples for culture-independent analyses. *J. Cyst. Fibros.* 14, 464–467. doi: 10.1016/j.jcf.2014.10.004

Fittipaldi, M., Nocker, A., and Codony, F. (2012). Progress in understanding preferential detection of live cells using viability dyes in combination with DNA amplification. *J. Microbiol. Methods.* 91, 276–289. doi: 10.1016/j.mimet.2012.08.007

Nogva, H. K., Drømtorp, S. M., Nissen, H., and Rudi, K. (2003). Ethidium monoazide for DNA based differentiation of viable and dead bacteria by 5'-nuclease PCR. *Biotechniques* 34, 812–813.

Peterson, B. W., Sharma, P. K., van der Mei, H. C., and Busscher, H. J. (2012). Bacterial cell surface damage due to centrifugal compaction. *Appl. Environ. Microbiol.* 78, 120–125. doi: 10.1128/AEM.06780-11

Rogers, G. B., Cuthbertson, L., Hoffman, L. R., Wing, P. A., Pope, C., Hooftman, D. A., et al. (2013). Reducing bias in bacterial community analysis of lower respiratory infections. *ISME J.* 7, 697–706. doi: 10.1038/ismej.2012.145

Young, G. R., Smith, D. L., Embleton, N. D., Berrington, J. E, Schwalbe, E. C, Cummings, S. P. et al. (2017). Reducing Viability Bias in Analysis of Gut Microbiota in Preterm Infants at Risk of NEC and Sepsis. *Front. Cell. Infect. Microbiol.* 7:237. doi: 10.3389/fcimb.2017.00237

Conflict of Interest Statement: The authors declare that the research was conducted in the absence of any commercial or financial relationships that could be construed as a potential conflict of interest.

Copyright © 2018 Agustí and Codony. This is an open-access article distributed under the terms of the Creative Commons Attribution License (CC BY). The use, distribution or reproduction in other forums is permitted, provided the original author(s) and the copyright owner are credited and that the original publication in this journal is cited, in accordance with accepted academic practice. No use, distribution or reproduction is permitted which does not comply with these terms.

frontiers in Cellular and Infection Microbiology

GENERAL COMMENTARY
published: 04 April 2018
doi: 10.3389/fcimb.2018.00104

Commentary: Bacteriophage transfer during faecal microbiota transplantation in *Clostridium difficile* infection is associated with treatment outcome

Blessing O. Anonye[1,2]*

[1] Microbiology and Infection Unit, Division of Biomedical Sciences, Warwick Medical School, Coventry, United Kingdom,
[2] Warwick Integrative Synthetic Biology Centre, School of Life Sciences, University of Warwick, Coventry, United Kingdom

Keywords: bacteriophages, gut microbiota, fecal microbiota transplantation, *C. difficile* infection, *Caudovirales*

A commentary on

Bacteriophage transfer during faecal microbiota transplantation in *Clostridium difficile* infection is associated with treatment outcome
by Zuo T., Wong S. H., Lam K., Lui R., Cheung K., Tang W., et al. (2017). Gut 67, 634–643. doi: 10.1136/gutjnl-2017-313952

OPEN ACCESS

Edited by:
Till Strowig,
Helmholtz-Zentrum für Infektionsforschung, Germany

Reviewed by:
Joseph Sorg,
Texas A&M University, United States
Xingmin Sun,
University of South Florida, United States
V. K. Viswanathan,
University of Arizona, United States

***Correspondence:**
Blessing O. Anonye
b.anonye@warwick.ac.uk

Received: *25 October 2017*
Accepted: *19 March 2018*
Published: *04 April 2018*

Citation:
Anonye BO (2018) Commentary: Bacteriophage transfer during faecal microbiota transplantation in Clostridium difficile infection is associated with treatment outcome. Front. Cell. Infect. Microbiol. 8:104. doi: 10.3389/fcimb.2018.00104

Fecal microbiota transplantation (FMT) has been used as a treatmentof last resort for recurrent *C. difficile* infections (CDI) with a cure rate of 85–90% after the first FMT (van Nood et al., 2013; Jiang et al., 2017). Several studies have examined the changes that occur in the bacterial community that leads to reestablishment of the intestinal microbiota (Fuentes et al., 2014; Seekatz et al., 2014; Staley et al., 2016). However, studies that have investigated the role of viruses in FMT are limited (Broecker et al., 2016a,b, 2017; Ott et al., 2017).

Recently, Zuo and colleagues performed metagenomics sequencing of virus like particles on fecal samples from patients with CDI and healthy controls to determine if bacteriophages were associated with restoration of the intestinal microbiota after FMT (Zuo et al., 2017). Prior to FMT, the patients had increased abundance of *Caudovirales* with decreased diversity, richness and evenness when compared to healthy controls. Longitudinal studies of patients who received FMT ($n = 9$) and standard therapy, vancomycin ($n = 5$) demonstrated that FMT led to the transfer of viruses from the donor to the recipients (Zuo et al., 2017).

The patients that were administered FMT were divided into two groups of "responders" and "non-responders" based on whether they were cured of CDI or recurred after FMT. In particular, after FMT, they noticed a significant decrease in the abundance of *Caudovirales* and increase in richness of donor-derived *Caudovirales* in the enteric virome of the patients (Zuo et al., 2017). There was a correlation between donor viral richness and the patients responding to FMT. Of the two-thirds that were cured after FMT, four of the donors had higher *Caudovirales* richness when compared to the non-responders group where the donor *Caudovirales* richness was lower (Zuo et al., 2017). When compared to the non-responders, the remaining two donors had a similar ($n = 1$ for non-responder donor) or slightly higher *Caudovirale* richness.

Furthermore, lower abundance of the family, *Microviridae* was observed in the patients before FMT when compared to the controls but this increased after FMT. Fifteen viral species were found to be enriched between FMT responders and non-responders. Viral species belonging to the *Microviridae* family such as *Eel River Basin pequenovirus* was the most abundant in the responders (Zuo et al., 2017).

Moreover, Zuo et al. performed 16S rRNA gene sequencing to determine changes in the bacterial community and noted increase in *Lachnospiraceae* and *Ruminococcaceae* families (Zuo et al., 2017). However, there was no significant difference between donor transferred bacteria between FMT responders and non-responders. Interestingly, vancomycin treatment had no significant effect on the viral community (*Caudovirales*) of those who responded to the antibiotic therapy. However, the bacterial community was significantly affected (Zuo et al., 2017).

Broecker et al. investigated the long term bacterial and virome changes in a patient after FMT for recurrent CDI, and found the virome at several months post-FMT related to the donor virome (Broecker et al., 2016a,b). Similarly, Ott and colleagues recently demonstrated that sterile fecal filtrates from donor feces was effective in treating recurrent CDI in five patients (Ott et al., 2017). They showed that the "phagebiota" of a recipient at 6 weeks post-FMT was similar to the fecal filtrate from the donor (Ott et al., 2017). These findings indicate that apart from live bacteria, other components of the microbiota such as bacteriophages, antimicrobial compounds or metabolites contribute to reestablishment of the intestinal microbiota in FMT.

There is no doubt that bacteriophages play a role in the intestinal microbiota with a potential to alter the composition and function of the host microbiota. The question is what constitutes a healthy gut phageome and how do they influence the human gut microbiota? Most of the phages in healthy human gut microbiota belong to the *Caudovirales* order and from the family *Microviridae* which have double and single stranded DNA respectively (Kim et al., 2011; Manrique et al., 2016). As seen above in recurrent CDI, increased diversity, richness and evenness of the *Caudovirales* was implicated in the efficacy of FMT. However, in other intestinal diseases, it is not clear cut as to the role of *Caudovirales* likely due to other risk factors involved (Norman et al., 2015). For example, *Caudovirales* richness was observed in patients with inflammatory bowel disease (Norman et al., 2015).

The next question one may be tempted to ask is, how stable is the "phagebiota" in individuals and what are the effects of antibiotic perturbations on the phageome? Research by Ly et al. showed that transmission of viruses was common between members of the same household over a 6-month period (Ly et al., 2016). Treatment of healthy individuals living in a particular household with the antibiotics, amoxicillin or azithromycin for 7 days did not affect the composition of viruses in the intestinal microbiota (Ly et al., 2016).

These studies have highlighted the underappreciated role viruses play in addition to bacterial colonization in the intestinal microbiota. However, as individual phages are specific in action toward their bacterial host, it would be advantageous to isolate phages that target pathogenic bacteria such as *C. difficile,* though this is not trivial. Indeed, previous work revealed that using a single phage, ΦCD27 (Meader et al., 2010, 2013) or a combination of phages led to the inhibition of *C. difficile* growth *in vitro* and *in vivo* (Nale et al., 2016a,b). Recently, a combination of four phages was found to totally inhibit *C. difficile* growth in a batch fermentation model spiked with feces from four healthy volunteers (Nale et al., 2018).

Much work remains to be done on phage therapy for *C. difficile* infection. The ability to develop a synthetic mixture of phages as treatment for infectious diseases, will go a long way in this era of antibiotic resistance. Not only will this be beneficial in severe CDI, but could also be useful as a therapy for other diseases related to the intestinal microbiota.

AUTHOR CONTRIBUTIONS

The author confirms being the sole contributor of this work and approved it for publication.

FUNDING

BA received a small Warwick Integrative Synthetic Biology (WISB) grant. WISB is a BBSRC/EPSRC Synthetic Biology Research Centre (grant ref: BB/M017982/1) funded under the UK Research Councils' Synthetic Biology for Growth programme.

REFERENCES

Broecker, F., Klumpp, J., and Moelling, K. (2016a). Long-term microbiota and virome in a Zürich patient after fecal transplantation against *Clostridium difficile* infection. *Ann. N. Y. Acad. Sci.* 1372, 29–41. doi: 10.1111/nyas.13100

Broecker, F., Klumpp, J., Schuppler, M., Russo, G., Biedermann, L., Hombach, M., et al. (2016b). Long-term changes of bacterial and viral compositions in the intestine of a recovered *Clostridium difficile* patient after fecal microbiota transplantation. *Cold Spring Harb. Mol. Case Stud.* 2:a000448. doi: 10.1101/mcs.a000448

Broecker, F., Russo, G., Klumpp, J., and Moelling, K. (2017). Stable core virome despite variable microbiome after fecal transfer. *Gut Microbes* 8, 214–220. doi: 10.1080/19490976.2016.1265196

Fuentes, S., van Nood, E., Tims, S., Heikamp-de Jong, I., ter Braak, C. J., Keller, J. J., et al. (2014). Reset of a critically disturbed microbial ecosystem: faecal transplant in recurrent *Clostridium difficile* infection. *ISME J.* 8, 1621–1633. doi: 10.1038/ismej.2014.13

Jiang, Z. D., Ajami, N. J., Petrosino, J. F., Jun, G., Hanis, C. L., Shah, M., et al. (2017). Randomised clinical trial: faecal microbiota transplantation for recurrent *Clostridium difficile* infection – fresh, or frozen, or lyophilised microbiota from a small pool of healthy donors delivered by colonoscopy. *Aliment. Pharmacol. Ther.* 45, 899–908. doi: 10.1111/apt.13969

Kim, M. S., Park, E. J., Roh, S. W., and Bae, J. W. (2011). Diversity and abundance of single-stranded DNA viruses in human feces. *Appl. Environ. Microbiol.* 77, 8062–8070. doi: 10.1128/aem.06331-11

Ly, M., Jones, M. B., Abeles, S. R., Santiago-Rodriguez, T. M., Gao, J., Chan, I. C., et al. (2016). Transmission of viruses via our microbiomes. *Microbiome* 4, 64. doi: 10.1186/s40168-016-0212-z

Manrique, P., Bolduc, B., Walk, S. T., van der Oost, J., de Vos, W. M., and Young, M. J. (2016). Healthy human gut phageome. *Proc. Natl. Acad. Sci. U.S.A.* 113, 10400–10405. doi: 10.1073/pnas.1601060113

Meader, E., Mayer, M. J., Gasson, M. J., Steverding, D., Carding, S. R., and Narbad, A. (2010). Bacteriophage treatment significantly reduces viable Clostridium difficile and prevents toxin production in an *in vitro* model system. *Anaerobe* 16, 549–554. doi: 10.1016/j.anaerobe.2010.08.006

Meader, E., Mayer, M. J., Steverding, D., Carding, S. R., and Narbad, A. (2013). Evaluation of bacteriophage therapy to control *Clostridium difficile* and toxin production in an *in vitro* human colon model system. *Anaerobe* 22, 25–30. doi: 10.1016/j.anaerobe.2013.05.001

Nale, J. Y., Chutia, M., Carr, P., Hickenbotham, P. T., and Clokie, M. R. (2016a). 'Get in early'; biofilm and Wax Moth (*Galleria mellonella*) models reveal new insights into the therapeutic potential of *Clostridium difficile* bacteriophages. *Front. Microbiol.* 7:1383. doi: 10.3389/fmicb.2016.01383

Nale, J. Y., Redgwell, T. A., Millard, A., and Clokie, M. R. J. (2018). Efficacy of an optimised bacteriophage cocktail to clear *Clostridium difficile* in a batch fermentation model. *Antibiotics* 7:13. doi: 10.3390/antibiotics7010013

Nale, J. Y., Spencer, J., Hargreaves, K. R., Buckley, A. M., Trzepinski, P., Douce, G. R., et al. (2016b). Bacteriophage combinations significantly reduce clostridium difficile growth *in vitro* and proliferation *in vivo*. *Antimicrob. Agents Chemother.* 60, 968–981. doi: 10.1128/aac.01774-15

Norman, J. M., Handley, S. A., Baldridge, M. T., Droit, L., Liu, C. Y., Keller, B. C., et al. (2015). Disease-specific Alterations in the enteric virome in inflammatory bowel disease. *Cell* 160, 447–460. doi: 10.1016/j.cell.2015.01.002

Ott, S. J., Waetzig, G. H., Rehman, A., Moltzau-Anderson, J., Bharti, R., Grasis, J. A., et al. (2017). Efficacy of sterile fecal filtrate transfer for treating patients with *Clostridium difficile* Infection. *Gastroenterology* 152, 799.e797–811.e797. doi: 10.1053/j.gastro.2016.11.010

Seekatz, A. M., Aas, J., Gessert, C. E., Rubin, T. A., Saman, D. M., Bakken, J. S., et al. (2014). Recovery of the gut microbiome following fecal microbiota transplantation. *MBio* 5:e00893-14. doi: 10.1128/mBio.00893-14

Staley, C., Kelly, C. R., Brandt, L. J., Khoruts, A., and Sadowsky, M. J. (2016). Complete microbiota engraftment is not essential for recovery from recurrent *Clostridium difficile* infection following fecal microbiota transplantation. *MBio* 7:e01965-16. doi: 10.1128/mBio.01965-16

van Nood, E., Vrieze, A., Nieuwdorp, M., Fuentes, S., Zoetendal, E. G., de Vos, W. M.,et al. (2013). Duodenal infusion of donor feces for recurrent *Clostridium difficile*. *N. Engl. J. Med.* 368, 407–415. doi: 10.1056/NEJMoa1205037

Zuo, T., Wong, S. H., Lam, K., Lui, R., Cheung, K., Tang, W., et al. (2017). Bacteriophage transfer during faecal microbiota transplantation in *Clostridium difficile* infection is associated with treatment outcome. *Gut* 67, 634–643. doi: 10.1136/gutjnl-2017-313952

Conflict of Interest Statement: The author declares that the research was conducted in the absence of any commercial or financial relationships that could be construed as a potential conflict of interest.

Copyright © 2018 Anonye. This is an open-access article distributed under the terms of the Creative Commons Attribution License (CC BY). The use, distribution or reproduction in other forums is permitted, provided the original author(s) and the copyright owner are credited and that the original publication in this journal is cited, in accordance with accepted academic practice. No use, distribution or reproduction is permitted which does not comply with these terms.

frontiers in Cellular and Infection Microbiology

REVIEW
published: 26 February 2018
doi: 10.3389/fcimb.2018.00060

Mycotoxin: Its Impact on Gut Health and Microbiota

*Winnie-Pui-Pui Liew and Sabran Mohd-Redzwan**

Department of Nutrition and Dietetics, Faculty of Medicine and Health Sciences, Universiti Putra Malaysia, Serdang, Malaysia

The secondary metabolites produced by fungi known as mycotoxins, are capable of causing mycotoxicosis (diseases and death) in human and animals. Contamination of feedstuffs as well as food commodities by fungi occurs frequently in a natural manner and is accompanied by the presence of mycotoxins. The occurrence of mycotoxins' contamination is further stimulated by the on-going global warming as reflected in some findings. This review comprehensively discussed the role of mycotoxins (trichothecenes, zearalenone, fumonisins, ochratoxins, and aflatoxins) toward gut health and gut microbiota. Certainly, mycotoxins cause perturbation in the gut, particularly in the intestinal epithelial. Recent insights have generated an entirely new perspective where there is a bi-directional relationship exists between mycotoxins and gut microbiota, thus suggesting that our gut microbiota might be involved in the development of mycotoxicosis. The bacteria–xenobiotic interplay for the host is highlighted in this review article. It is now well established that a healthy gut microbiota is largely responsible for the overall health of the host. Findings revealed that the gut microbiota is capable of eliminating mycotoxin from the host naturally, provided that the host is healthy with a balance gut microbiota. Moreover, mycotoxins have been demonstrated for modulation of gut microbiota composition, and such alteration in gut microbiota can be observed up to species level in some of the studies. Most, if not all, of the reported effects of mycotoxins, are negative in terms of intestinal health, where beneficial bacteria are eliminated accompanied by an increase of the gut pathogen. The interactions between gut microbiota and mycotoxins have a significant role in the development of mycotoxicosis, particularly hepatocellular carcinoma. Such knowledge potentially drives the development of novel and innovative strategies for the prevention and therapy of mycotoxin contamination and mycotoxicosis.

Keywords: mycotoxicosis, intestine, hepatocellular carcinoma, trichothecene, zearalenone, fumonisin, ochratoxin, aflatoxin

OPEN ACCESS

Edited by:
Venkatakrishna Rao Jala, University of Louisville, United States

Reviewed by:
Gabriela Del Valle Perdigon, Consejo Nacional de Ciencia y Tecnología - CONICET, Argentina
Alinne Castro, Universidade Católica Dom Bosco, Brazil

****Correspondence:***
Sabran Mohd-Redzwan
mohdredzwan@upm.edu.my;
mohd.redzwan.sabran@gmail.com

Received: *10 October 2017*
Accepted: *12 February 2018*
Published: *26 February 2018*

Citation:
Liew W-P-P and Mohd-Redzwan S (2018) Mycotoxin: Its Impact on Gut Health and Microbiota. Front. Cell. Infect. Microbiol. 8:60. doi: 10.3389/fcimb.2018.00060

BACKGROUND

The momentum of scientific paper publication toward mycotoxin is an increasing trend where 16,821 papers were recorded in Scopus since the first mycotoxin, aflatoxin (AF) was identified in the year 1965. Data clearly showed the significance of mycotoxin research which will be further discussed later in this review paper. Nevertheless, the global health issue arose from mycotoxin is still frequently ignored in many low-income countries, where mycotoxins affect staple foods (Wild and Gong, 2010). The exposure is long-term and often at high

doses, regretfully these particular regions are the least regulated in terms of agricultural practices and human exposure. The attention only has been paid in the richer nations of the world, to meet stringent import regulations on mycotoxin contamination (Battilani et al., 2016). To date, the world still desires for a more accurate evidence-based on mycotoxins and human health, as well as a better biomarker of exposure and data from studies of disease distribution. Current data are valid to justify and respond to reduce exposure in vulnerable populations (Freire and da Rocha, 2017). The implementation of more practical and affordable mycotoxin removal techniques at the household level to effectively reduce exposure are becoming increasingly important. When mycotoxins are introduced into the organism from food, they first come to interact with the gastrointestinal (GI) tract (Assunção et al., 2016). The GI tract is where the gut microbiota resides: it is known for its role in modulating the immune system and digestive processes. Gut microbiota work in concert with the GI tract protects the host from the toxicity of mycotoxins. Accordingly, integration of microbial-based approaches through maintaining a healthy gut microbiota is highly demanded.

MYCOTOXINS

Mycotoxins, the low molecular mass (MW ∼700 Da) secondary metabolites mainly produced by *Aspergillus*, *Penicillium*, and *Fusarium* are highly noxious substances on animals and humans. However, not all mycotoxin are classified as such, for example, Penicillin, is widely used an antibiotic (Speight, 2012). The structural form of mycotoxins varies from simple four C compounds, e.g., moniliformin, to complex substances such as the phomopsins (Zain, 2011). Fungal proliferation and production of mycotoxins rise naturally due to environmental factors, especially during tropical conditions (Mohd-Redzwan et al., 2013). Besides, the downstream processing such as poor harvesting practices, improper storage and less than optimal conditions during transportation, processing, and marketing can also contribute to the growth of fungi and increase the risk of the major food spoilage agent caused by mycotoxin production (Khazaeli et al., 2014). Due to their ubiquitous nature of fungi, mycotoxins have been increasingly attracting the concern of health organizations where their occurrence in foods cannot be ignored and already poses risk to consumers (Jahanian, 2016).

IMPORTANCE OF RESEARCH ON MYCOTOXIN

Occurrence of Mycotoxicosis

Notably, it has been estimated that 25% of the world's crops such as nuts, cereals, and rice are contaminated by mold and fungal growth, as reviewed by the United Nations Food and Agriculture Organization and the World Health Organization (Pandya and Arade, 2016). The toxic effect of mycotoxins on animal and human health is referred to as mycotoxicosis. Exposure to mycotoxins is mostly by ingestion but also occurs by the dermal and inhalation routes. The extent of adverse effects of mycotoxins on human or animals health mainly depends on the extent of exposure (dosage and period), type of mycotoxins, physiological and nutritional status as well as possible synergistic effects of other chemicals to which the animals or humans are exposed (Gajecka et al., 2013). In 1960, interest on mycotoxins was initiated by the occurrence of Turkey X disease caused by AF, which killed more than 100,000 turkeys. Subsequently, it was found that AFs are carcinogenic and cause hepatocellular carcinoma (HCC) in animals and humans, and this has stimulated research on mycotoxins (Peraica et al., 1999). Since then, around 400 mycotoxins are known, but AFs, ochratoxins, zearalenone (ZEA), fumonisins (FBs) and trichothecenes are mostly focused on public health issues (Ates et al., 2013). Mycotoxin exposure is not only limited to pure mycotoxins but also masked mycotoxin which formed when plants protect themselves by conjugating mycotoxins to biopolymers. In addition, some people are more susceptible to getting mycotoxicosis than others, and this is due to the pharmacogenetic variability where specific gene mutations such as cytochrome p450 (CYP 450) genes could either increase or decrease the metabolic activity (cytotoxicity) of the challenging mycotoxins (Sun et al., 2016). For instance, in both *in vivo* (Muhammad et al., 2017) and *in vitro* (Lewis et al., 2000) studies, CYPs' 1A2 and 3A4 appear as the most important enzymes that increased metabolism of AFB1 to its active form, AFB1-8,9-epoxide and subsequently to AFB1-DNA adduct formation, in which the biomarker has been linked to the development of liver cancer (Ceccaroli et al., 2015).

Chronic mycotoxicosis causes a greater impact on human health. Mycotoxin can induce diverse and powerful toxic effects in test systems: some are carcinogenic, mutagenic, teratogenic, estrogenic, hemorrhagic, immunotoxic, nephrotoxic, hepatotoxic, dermatoxic and neurotoxic (Milićević et al., 2010). Frequently, mycotoxicosis remains unrecognized by medical professionals. Mycotoxicosis can be weighed when a disease appears in several persons, with no obvious connection to a known etiological agent, such as microorganisms (Viegas et al., 2015).

Future Prospect: Impact of Growing Population and Ongoing Climate Change on Mycotoxin

By the year 2030, the world's population is estimated to reach 8.2 billion people, and with 842 million people estimated as having been undernourished in the period of the year 2011–2013, food supply will definitely present a growing challenge in the next decades (FAO, 2014). This scenario will, in turn, have a tremendous negative impact on food supply (FAO, 2014). It is worth to note that the presence of hazardous substances (e.g., mycotoxins) also limits or reduces the marketability of food products in international markets (Anater et al., 2016).

There is now widespread consensus that the earth is warming at an unprecedented rate (Medina et al., 2015). The geographic distribution and production of the crop, as well as the phyllosphere microflora of crops, are expected to be strongly affected by climate change. For instance, mycotoxigenic

Aspergillus flavus are able to grow under high temperatures and drought conditions. The resilient growth of *A. flavus* under extreme heat and dry condition is an expected and emerging dilemma mainly in the Mediterranean and other temperate regions (Logrieco et al., 2003). For example, the impacts of climate change have been observed in Serbia, where no contamination occurred previously, but prolonged hot and dry weather in the year 2012 resulted in 69% of maizes contaminated with AFs (Medina et al., 2015). A similar case also found in Hungary, where the increase in AFs contamination may be due to climate change conditions (Dobolyi et al., 2013).

The world's largest agri-food exporters include countries such as Brazil and Argentina and parts of Asia including China and India are identified as hot spots for impacts of climate change (Ray et al., 2012). Thus, from a food security perspective, a more accurate prediction of impacts of climate change on mycotoxins need to be addressed to prevent compromised food sustainability which possibly resulting in negative social consequences.

GASTROINTESTINAL TRACT

The GI tract is an organ within humans and other animals which responsible for food ingestion, digestion, energy and nutrients absorption, immune response, as well as elimination of waste products (feces) (Celi et al., 2017). The architecture of the GI tract is intended to facilitate these functions. The basic feature of GI tract is a muscular tube lined by a mucous membrane and comprised four layers forming a continuous passage. All segments of the GI tract are divided into four layers: mucosa, submucosa, muscularis propria, and serosa (Jaladanki and Wang, 2016). The mucosa is made up of three layers (epithelium, lamina propria, and muscular mucosae). The entire mucosa rests on the submucosa, beneath which is the muscularis propria. The outermost layer is named as the serosa. The complex infolding at mucosa layer forms an immense surface area for the most efficient nutrient absorption. The submucosa contains arteries, veins, inflammatory cells, lymphatics, and autonomic nerves. The muscularis mucosa is a thin layer of smooth muscle that forms the basis of peristalsis. While, the serosa is made of connective tissue that contains blood vessels, nerves, and fat (Jaladanki and Wang, 2016).

The epithelium layer at the innermost of mucosa is of vital importance for intestinal barrier function. The intestinal epithelium is one layer of thin cells lining the gut lumen. The epithelial contains enterocytes, enteroendocrine, and goblet cells at villi, whereas the Paneth cells, located under the crypts (Fink and Koo, 2016). It acts as a barrier to block the entry of harmful agents such as pathogens, toxins, and foreign antigens. Besides, it is also an important site for nutrient absorption including electrolytes, dietary nutrients, and water via its selective permeable membrane (Constantinescu and Chou, 2016). Each intestinal epithelial cell is connected by desmosomes, tight junctions (TJs), and adherens junctions (AJs). The AJs and desmosomes are responsible for the mechanical linkage of adjacent cells. Whereas, the TJs control the intercellular space and regulate selective paracellular ionic solute transport (Capaldo et al., 2014). Above the epithelium lies a complex microflora which is recognized as gut microbiota and the role of gut microbiota will be discussed later in this review article. The selective permeable barrier of mucosal epithelium establishes the interplay between the intestinal immune system and the luminal contents.

Mycotoxins and Gut Health

Upon ingestion of contaminated food or feed, the GI tract is particularly affected by mycotoxin. Generally, intestinal barrier in the GI tract functions as a filter against harmful mycotoxins. However, some mycotoxins have been found to exert their detrimental effects in the GI tract. For example, mycotoxins can alter the normal intestinal functions such as barrier function and nutrient absorption. Some mycotoxins also affect the histomorphology of intestine. The impacts of mycotoxins include trichothecenes, zearalenone, fumonisins, ochratoxins, and AFs on general and gut health will be comprehensively reviewed.

Trichothecenes

Fusarium graminearum is the main fungi species that produces tricothecenes. All tricothecenes contain an epoxide at the C12, C13 positions, which is responsible for their toxicological activity (Nathanail et al., 2015). T-2 toxin (Type A) and DON (Type B) are the major mycotoxins that cause toxicity to humans and animals via oral ingestion (Nathanail et al., 2015).

During World War II, a biological weapon caused an acute syndrome consists of cough, sore throat, dyspnea, bloody nasal discharge, and fever was reported by Soviet scientists (Pitt and Miller, 2016). Twenty years later, T-2 mycotoxin was discovered when civilians consumed wheat that was unintentionally contaminated with Fusarium fungi (Pitt and Miller, 2016). A human toxicosis due to ingestion of moldy rice contaminated with T-2 toxin has been reported in China. According to Wang Z. et al. (1993), 65% of patients developed food poisoning symptoms such as chills, nausea, abdominal distension, dizziness, vomiting, thoracic stuffiness, abdominal pain, and diarrhea. Similar to T-2 toxicity, victims of DON outbreak suffered from vomiting syndromes (Etzel, 2014). Several outbreaks of acute DON toxicity in human have been reported in India, China, and the USA (Etzel, 2014).

Trichothecenes toxic effects in animals (dairy cattle, swines, broilers, and rats) include decreased plasma glucose, reduced blood cell and leukocyte count, weight loss, alimentary toxic aleukia, as well as pathological changes in the liver and stomach (Adhikari et al., 2017). The mechanism involved in T-2 and DON toxicity is generally via oxidative stress-mediated deoxyribonucleic acid (DNA) damage and apoptosis (Wu et al., 2014). Furthermore, T-2 and DON are well-known inhibitors of protein synthesis resulting from the binding of peptidyl-transferase, which is located in the 60s ribosomal subunit (Yang et al., 2017).

In the GI tract, a decreased absorption of glucose was observed following T-2 and DON intoxication resulted from suppressed SGLT1 (glucose transporter) mRNA expression. Apart from the glucose absorption, SGLT1 also responsible for water reabsorption, thus reduction of SGLT1 transporter induces diarrhea as well (Grenier and Applegate, 2013).

The weight loss effect of trichothecenes involved neuroendocrine factors and cytokines. DON and T-2 elevated concentrations of the indoleamines, serotonin and 5-hydroxy-3-indoleacetic acid (HIAA) in all brain regions (Wang J. et al., 1993). These neuroendocrine factors can affect the secretion of both anorexigenic and/or orexigenic hormones (Maresca, 2013). Through increasing gene expression of anorexia-inducing proinflammatory cytokines such as interleukin-1β (IL-1β), interleukin-6 (IL-6) and tumor necrosis factor-α (TNF-α), trichothecenes exacerbate the condition of anorexia (Wu et al., 2015). In addition, DON and T-2 also induced the release of the satiety hormones, peptide YY (PYY) and cholecystokinin (CCK), which are critical mediators of anorexia (Wu et al., 2015).

Using animal models, trichothecenes was found to induce necrotic lesions in the GI tract (Kolf-Clauw et al., 2013). A shortening of villi height was also observed in trichothecenes-treated animals (swine, poultry, and rat model). The changes on villi were due to activation of the apoptotic pathway by trichothecenes, which in turn leads to nutrition malabsorption (Alizadeh et al., 2015). Furthermore, results obtained from *in vivo* and *in vitro* studies showed that trichothecenes increased intestinal permeability. Using porcine epithelial cell, trichothecenes increased the intestinal permeability by lowering tight junction proteins expression (Osselaere et al., 2013). In addition, previous studies revealed a significant ($P < 0.05$) decreased in the number of goblet cells that secrete mucin in trichothecenes-treated animals. Mucin is primarily involved in the gut barrier function (Pinton and Oswald, 2014). The disruption in the integrity of intestinal epithelium allows the entry of the pathogen into the gut lumen (Lessard et al., 2015). Besides, trichothecenes have been linked with a decreased level of IL-8 in the intestine, which is responsible for pathogen removal (Kadota et al., 2013). Overall, trichothecenes exert negative impacts on GI tracts specifically on the gut absorption, integrity, and immunity.

Zearalenone

Zearalenone (ZEA) is a mycotoxin that primarily produced by *Fusarium graminearum* and *Fusarium culmorum* in foods and feeds. The high rate of co-occurrence of ZEA with FBs and DON indicates that these mycotoxins might be involved in a wide range of synergistic and additive interactions. ZEA has been linked to scabby grain toxicosis occurred in Japan, China, Australia, and the USA, with symptoms including nausea, vomiting, and diarrhea (Liao et al., 2009).

It is well recognized that ZEA is a non-steroidal estrogenic mycotoxin that is implicated in the reproductive disorders of farm animals (swines, cattle, and sheep) and hyperoestrogenic syndromes in humans (Kotowicz et al., 2014). Toxicological studies of ZEA revealed its effects on the reproductive system, including enlarged uterus, altered reproductive tract, decreased fertility, as well as abnormal level of progesterone and estradiol. Besides, the ingestion of ZEA during pregnancy reduced fetal weight and survival rate of embryo (Zhang et al., 2014). This phenomenon can be explained through the structure of ZEA. ZEA has a structure which allows it to bind to the mammalian estrogen receptor, although with lower affinity compared to the natural-occurring estrogens (Hueza et al., 2014). Besides, ZEA has also been shown to be hepatotoxic, haematotoxic, immunotoxic and genotoxic (Zhou et al., 2017).

Although the reproductive organ is the main target for ZEA to induce toxicity, the adverse effects of ZEA on GI tracts have been reported. The effects of ZEA ingestion on the GI tract are not as detrimental compared to the other mycotoxins. Studies using intestinal epithelial cells showed that ZEA induced cell death without altering the cell integrity as indicated by transepithelial electrical resistance (Marin et al., 2015). In contrast, it was discovered that the metabolites of ZEA (α- and β-zearalenol) significantly ($P < 0.05$) decreased the cell integrity. The study showed that ZEA and its metabolites acted differently in the gut (Marin et al., 2015). Abassi et al. (2016) demonstrated that ZEA enhanced cell proliferation, increased colony formation and fastened cell migration of colon carcinoma cell line HCT116. Another study also showed that ZEA down-regulated the expression of tumor-suppressor genes (PCDH11X, DKK1, and TC5313860) in intestinal cells (Taranu et al., 2015). In fact, the modulation of gene expression was responsible for the carcinogenic effects of ZEA. Nevertheless, swines ingested ZEA did not showed changes in the height of villi, the thickness of the mucosa, and number of goblet cells (Gajecka et al., 2016a,b; Lewczuk et al., 2016). In brief, ZEA plays a negative role in gut health although no apparent histological changes have been observed.

Fumonisins

Fusarium verticillioides is the major producer of fumonisins, where fumonisin B1 (FB1) is the most abundant in nature (Lerda, 2017). In contrast to most mycotoxins, which are hydrophobic in nature, fumonisins are hydrophilic compounds, which hinders its discovery until 1988 (Gelderblom et al., 1988). Human epidemiological studies in South Africa, Italy, and China revealed that the esophageal cancer is related to the intake of corn grains containing fumonisins (Chilaka et al., 2017). Another epidemic of neural tube defects (birth defects of the brain, spine, or spinal cord) occurred along the Texas-Mexico border, China and South Africa were also found to be associated with fumonisins-contaminated corn consumption (Ortiz et al., 2015). In animals, fumonisins have been found to cause pulmonary edema and hydrothorax in swines; leukoencephalomalacia in equine; and HCC in rats (da Rocha et al., 2014).

FB1 shares the same structure as cellular sphingolipids (Masching et al., 2016). Sphingolipids are responsible for neurological and immunological diseases, as well as cancer. Normal degradation of sphingolipids to ceramide requires sphingomyelinase and ceramidase (Boini et al., 2017). However, FB1 disturbs sphingolipids metabolism via ceramide synthase inhibition which leads to sphingosine accumulation in cells (Masching et al., 2016). FB1 elevates sphingosine levels in urine, serum, kidney, liver, and small intestine. The abnormal turnover of sphingosine induced cytotoxicity, oxidative stress, apoptosis in cells (Hahn et al., 2015).

Using intestinal cell lines (IPEC-1, Caco-2, and HT29), Minervini et al. (2014) found FB1 decreased the cell viability and proliferation in a concentration-dependent manner. A possible

mechanism has been suggested through the accumulation of sphinganine by FB1. In the intestinal epithelial cells, sphinganine accumulation blocked G0/G1 phase in cell and resulted in growth inhibition and apoptosis (Angius et al., 2015). The accumulation of sphinganine also altered glycoprotein distribution in the jejunum and caused an increase in transepithelial passage of FB1 (Yamazoe et al., 2017). In addition, FB1 altered the integrity of intestinal barrier by suppressing tight junction (TJ) protein expression level (Romero et al., 2016). The increase in intestinal permeability, in turn, promotes translocation of bacteria (Kelly et al., 2015).

Besides, high levels of FB1 also induced an overgrowth in intestinal goblet cell of broiler and swine (Alassane-Kpembi and Oswald, 2015). Goblet-cell hyperplasia is associated with increased mucin secretion. However, continuous hypersecretion of mucins might deplete the number of goblet cells, resulting in devastation of mucus barrier (Johansson and Hansson, 2016). Previous studies conducted using intestinal cell lines (IPEC-1, Caco-2, and HT29) showed that FB1 was able to regulate immune responses. Upon LPS exposure to the FB1-treated cell line, a reduction in IL-8 synthesis was detected (Minervini et al., 2014). Such reduction could be responsible for a low number of polymorphonuclear leukocytes (PMNs) recruited to infection sites, thus leading to the ineffective elimination of pathogen from the gut (Brazil et al., 2013). Generally, in the gut, FB1 increased intestinal cell apoptosis, reduced intestinal barrier and caused immune dysfunction.

Ochratoxin

Ochratoxin is mainly produced by *Aspergillus species* and *Penicillium species*. Ochratoxin A (OTA) is the most prevalent and relevant fungal toxin of this group (Liuzzi et al., 2017). The main target site of OTA is kidney. Previous findings from animals showed OTA is a potent renal carcinogen (Russo et al., 2016). The International Agency for Research on Cancer (IARC) categorized OTA as possibly carcinogenic to humans under Group 2B carcinogen. Apart from that, OTA is an immunosuppressive, teratogenic, and nephrotoxic compound (Ladeira et al., 2017).

In human studies, OTA is associated with kidney diseases, such as Balkan endemic nephropathy (BEN). BEN is a chronic tubulointerstitial disease which slowly progressed into terminal renal failure. Indeed, a 15 years study confirmed that BEN is correlated with upper urothelial tract cancer (Rouprêt et al., 2015). Furthermore, OTA has been associated with the occurrence of upper urothelial tract cancer (Fahmy et al., 2014). However, a systemic review by Bui-Klimke and Wu (2015) revealed that there is no significant evidence for human health risks associated with OTA exposure based on the epidemiological data. The modes of toxic action of OTA are identified through the blockage of protein synthesis and energy production, the formation of DNA adduct formation, apoptosis, as well as the induction of oxidative stress (Kőszegi and Poór, 2016). Moreover, recent studies showed OTA triggered autism via epigenetic mechanism (Mezzelani et al., 2016).

Other than its adverse effects on the kidney, previous studies also revealed the gut changes induced by OTA. OTA altered nutrition absorption in the intestine. *In vitro* studies demonstrated that OTA decreased glucose absorption via SGLT1 transporter (Peraica et al., 2011). In addition, OTA-treated animals experienced faster and more harmful parasite infections (provoked by *Eimeria acervulina* and *E. adenoeides*) in chicks and turkey compared to control. The results showed that animals fed with OTA had higher lesion and oocyst indexes in the intestine and more damage at mucosa (Manafi et al., 2011). This can be explained by the increased intestinal permeability in the presence of OTA. In addition, results from immunoblotting and immunofluorescence showed that the expression of TJ proteins responsible for intestinal integrity was significantly ($P < 0.05$) suppressed by OTA (McLaughlin et al., 2004). Besides, OTA-induced oxidative stress also can alter intestinal permeability (Anderson et al., 2016). The oxidative stress induced by OTA has been found to be associated with the apoptosis in the intestinal IPEC-J2 cells (Wang et al., 2017). A study by Solcan et al. (2015) on OTA-fed broilers revealed there is a decrease in villi height and increase in apoptosis of intestinal epithelial cells. Similar results were obtained from another study using broiler model (Qu et al., 2017). Inflammation pathway in the intestine was also affected by OTA. The expression of inflammation-related cytokines (IL-8, IL-6, IL-17A, IL-12, and IL-18) was significantly ($P < 0.05$) decreased in the intestine of the piglets exposed to the toxin (Marin et al., 2017). The alteration of immune system renders the gut vulnerability to infection. OTA exerted its effect on gut via the reduction of nutrient absorption, disruption of intestinal permeability, cell apoptosis, and modulation of immune system.

Aflatoxin

AF is a mycotoxin produced by *Aspergillus flavus* and *Aspergillus parasiticus*. The most common mycotoxin found in human food and animal feed is AFB1. In fact, AFB1 is the most potent hepatocarcinogen recognized in mammals and listed as Group I carcinogen by IARC (Muhammad et al., 2017). Liver is the main target site of AFB1. Cumulative evidences from human and animals revealed a strong linkage occurs between AFB1 and HCC. While, acute aflatoxicosis induced abdominal pain, vomiting, edema, and death (Mohd-Redzwan et al., 2013).

Aflatoxicosis outbreak has been recorded four times in Kenya from 2004 to 2014, with near to 600 individuals were affected and 211 deaths were reported from the tragic outbreak (Awuor et al., 2017). As discussed earlier, p450 enzymes in the liver metabolize AFB1 into AFB1-8,9-exo-epoxide. The highly reactive exo-epoxides form derivatives with DNA, RNA and proteins which subsequently react with the p53 tumor suppressor gene. The reaction generates AFB1-N7-Gua which is then converted to its stabilized form, AFB1-formamidopyrimidine (AFB1-FABY) adduct. AFB1-FABY causes transversion of guanine (G) to thymine (T), which leads to mutation and malignant transformation (Kew, 2013). In addition to the hepatotoxicity of AFB1 mentioned above, other adverse effects include growth retardation, immunosuppression, and genotoxicity have been reported (Kumar et al., 2017).

Like most of the mycotoxins, AFB1 compromised the health of GI tracts. Colon cell line (Caco-2) was used in *in vitro* experiment to determine the AFB1 toxicity in the intestine. AFB1 significantly ($P < 0.05$) inhibited cell growth, increased lactate

dehydrogenase activity and caused genetic damage. It is found that the mechanism of AFB1 cytotoxicity are associated with reactive oxygen species (ROS) generation, which leads to the damage of cell membrane and DNA (Zhang et al., 2015). Besides, transepithelial electrical resistance assay showed a reduction in intestinal Caco-2 cells' integrity after AFB1 treatment (Romero et al., 2016).

Similar result has been observed in *in vivo* study where AFB1 affects intestinal barrier function in broiler model as indicated by an increased ratio of lactulose to rhamnose ratio in the plasma (Chen et al., 2016). Several studies on broiler exposed to AFB1 showed that the density (weight/length) of intestine was reduced (Hossein and Gurbuz, 2015). An increase of apoptotic events was found in the jejunum, accompanied with elevated apoptotic markers (Bax and caspase-3) mRNA expression level. Moreover, the increased apoptosis was corresponded to a lower jejunal villi height as found in the other studies (Peng et al., 2014; Zheng et al., 2017). Another study by Akinrinmade et al. (2016) demonstrated intestinal injuries induced by AFB1 in rats. In the AFB1-fed rat, leucocyte and lymphocyte infiltration were observed at lamina propria of the intestinal mucosa. In the duodenum and ileum, AFB1 exposure caused intestinal lesions such as the development of sub-epithelial space and villi degeneration. The adverse effects on the gut from AFB1 exposure include the disruption of intestinal barrier, cell proliferation, cell apoptosis, and immune system. Although AFB1 is the most life-threatening mycotoxin, yet its toxicity on the gut is comparable to the other mycotoxins.

GUT MICROBIOTA

The gut microbiota represents an ensemble of microorganisms including bacteria, viruses, and fungi that harbor within the GI tracts of living organisms. In the past, gut microbiota studies have been focused on the association of single pathogenic organisms with human health. Non-pathogenic microbes were previously thought to be benign as compared to the pathogens (Holmes et al., 2011). Nevertheless, the gut microbiota has recently become a blooming research area (Hoffmann et al., 2013).

The rapid rise of remarkable and cost-effective next-generation DNA sequencing methods provide an effective approach to study the composition of the host microbiota. Metagenomic sequencing and amplicon sequencing using specific genes markers are established to replace culture-independent methods for host microbiota analysis (Kuczynski et al., 2012). The amplified sequences resulting read abundance, which reflects the microbial diversity. The advances in molecular biology have provided innovative ways to entangle the complex microbial communities. Using the methods, it has been revealed that majority of microorganisms resides in the gut cannot be cultured outside the host. In the human, for instance, approximately 80% of the total bacterial species in the gut failed to be cultured under laboratory conditions (Guarner and Malagelada, 2003). Besides, these methods also revealed differences in gut bacterial community between anatomical sites, between individuals, and between healthy and diseased states. The findings have completely transformed the view of mammals biology (Weinstock, 2012). As such, growing interest has led to an increasing research into the communities of non-pathogenic microbes that inhabit the human body, and the need to describe the genomes of these organisms to understand the human microbiota has been recognized.

The composition of the gut microbiota varies significantly at the relative ratios of dominant phyla, genera, and species. In particular, stable and healthy gut microbiota is generally indicated by the rich diversity of gut bacteria (Mosca et al., 2016). The rapid development of gut microbiota study has revealed its significant role in maintaining human health. The involvement of gut microbiota in nutrition, metabolism, and immune function has been well established. The gut microbiota allows the host to metabolize a vast range of dietary substrates. For example, the metabolism of carbohydrate is a major catalytic function of the microbiota. The gut microbiota (specifically *Bacteroides, Bifidobacterium, Enterobacterium, Fecalibacterium,* and *Roseburia*) assist in the fermentation of complex polysaccharides that escaped proximal digestion (Jandhyala et al., 2015). The fermentation process produces monosaccharides and short chain fatty acids (SCFAs) which include acetate, butyrate, and propionate that are rich energy sources for the host (Jandhyala et al., 2015). Similarly, metabolism pathways of proteins, bile, and phytochemicals, as well as vitamins synthesis by the microbiota, has been also elucidated (Rowland et al., 2017).

Apart from that, the gut microbiota protects the host against infections via several mechanisms. The microbes reside in the gut modulate the population of pathogenic microorganisms via competitive exclusion for attachment sites and nutrient (Donaldson et al., 2016). The significance of gut microbiota in the development of immunity can be readily appreciated from the study of germ-free (GF) mice. By comparison to normal mice, GF mice which have a lack of microbiota have been shown to exhibit irregularities in cytokines profile, contain poorly formed local and systemic lymphoid structures as well as the abnormal level of immune cells (Sekirov et al., 2010). Furthermore, accumulating recent data demonstrated that the functions of gut microbiota further extend beyond the gut. Mechanisms studies suggesting that microbial metabolites have taken the role by sending signals to peripheral organs, including the liver, adipose tissue, pancreas, cardiovascular system, lung, and even to the brain (Lv et al., 2017).

It is widely recognized that the composition of gut microbiota in newborns is obtained from mothers during delivery (Dominguez-Bello et al., 2010). While the alteration in the composition of the gut microbiota is mediated by numerous factors including dietary changes (Cani and Everard, 2016), development of disorders and diseases (Hand et al., 2016), genetics as well as stressful experiences (Karl et al., 2017). Sufficient evidence has revealed the inter-relationship between dietary habit and the intestinal microbiota composition (Cani and Everard, 2016). For example, high fat diet renders the host to harbor a gut microbiota enriched in the phylum *Firmicutes* and depleted in *Bacteriodetes*. Besides, high fat diet has been also identified to promote proliferation of specific bacterial strains such as Enterobacteriaceae, which may increase

intestinal lipopolysaccharide and subsequently increase gut permeability as well as triggering inflammation (Bibbò et al., 2016). On the other hand, a diet rich in fiber has been observed to modulate gut microbiota by altering fermentative metabolites and intestinal pH. Fermentation of fiber by the colonic microbiota produces SCFAs, wherein the metabolites play a significant role in regulating pH in the intestine. It has been demonstrated that a decrease in pH is able to significantly ($P < 0.05$) decrease the population of Bacteriodetes spp. and members of Enterobacteriaceae while promoting the growth of beneficial butyrate-producing microorganisms (Duncan et al., 2009).

On the other hand, studies revealed that the host genotype contributes remarkably to the resemblances in the gut microbial taxa. The genes linked with microbial taxa are particularly responsible for diet sensing, immunity, and metabolism (Goodrich et al., 2016b). Moreover, data showed a family belongs to the Firmicutes and Christensenellaceae has the highest heritability. The presence of Christensenellaceae in the gut is frequently associated with low serum triglyceride levels observed in lean and healthy human phenotype (van Opstal and Bordenstein, 2015). In genotype factor studies, monozygotic twins which developed from one zygote are often used as the subjects. As compared to dizygotic twins, it has been shown that there is a higher carriage of *Methanobrevibacter smithii* in monozygotic twins. *M. smithii* has also found to be related with leanness (Goodrich et al., 2016a). Besides, numerous studies have linked genetic loci with population of gut bacteria in mice and humans. For instance, *LCT* gene which encodes for lactase-phlorizin hydrolase. Single nucleotide polymorphisms (SNPs) in *LCT* are directly correlated with lactose intolerance and the abundance of lactose-metabolizing bacteria, specifically *Bifidobacterium* (Lerner et al., 2017).

Recently, the occurrence of diseases has often been linked consequentially to dysbiosis of gut microbiota. A wide range of gut microbiota-related diseases have been revealed include autism, asthma, colon cancer, Crohn's Disease, irritable bowel syndrome (IBS), food allergies, cardiovascular disease, obesity, diabetes, eczema and hepatic encephalopathy, mental disorders (Kamada et al., 2013; Sommer and Bäckhed, 2013; Korem et al., 2015). For instance, bacterial overgrowth in the small intestine is commonly observed in patients with IBS. An investigation using 16S rRNA-based microbiota profiling approaches on IBS subjects revealed quantitative and qualitative changes in both mucosal and fecal gut microbiota (Simrén et al., 2012; Collins, 2014). The findings suggested that the gut microbiota balance was compromised in the events of gut inflammation. The dysbiosis of gut microbiota initiates mucosal innate immune responses and increases intestinal permeability. Subsequently, translocation of pathogens occurs, and harmful metabolites can enter the intestinal epithelium. Such events in the gut further exacerbate the severity of diseases (Collins, 2014). Apart from that, evidence showed that the gut microbiota-derived products (SCFA, neurotransmitters, enzymes, and toxins) can be absorbed from the gut, and subsequently affect the metabolic phenotype of the host (Lee and Hase, 2014). In addition, metabolites from the host are transported into the gut via the enterohepatic circulation and serve as substrates for the microbiota. These processes give rise to an interspecies cross-talk between the host genome and the gut microbiota (Lee and Hase, 2014).

Regrettably, fewer studies have discussed on the importance of the minorities such as virus, commensal fungi, archaea, and protozoa. The gut virome comprised plant-derived viruses, giant viruses, and abundant (90%) bacteriophages. Pathogenicity of gut viruses includes gastroenteritis, pneumonitis, and diarrhea (Scarpellini et al., 2015). Whereas, fungal communities in the gut mainly consist of the Ascomycota, Basidiomycota, and Zygomycota. *Candida* species have been primarily associated in inflammatory bowel diseases (IBD), Crohn's disease (CD), ulcerative colitis (UC), obesity and gut inflammation (Sam et al., 2017). Undeniably, the gut microbiota influences almost all system resides in our body, which is of vital importance for survival, therefore, maintaining a balanced microbiota is essentially important.

The Bi-directional Interaction between Mycotoxin and the Gut Microbiota

Gut microbiota represents an important bridge between environmental substances and host metabolism. Findings found that gut microbiota, particularly in animals have profound interactions with ingested mycotoxins. Microbes reside in the gut aid host in the mycotoxin removal process through metabolizing or binding to the mycotoxins. Although some microbes possess the mycotoxin removal ability, it is noteworthy to mention that bacteria from the same genus, however, are unable to remove mycotoxin. Interestingly, few studies also demonstrated that mycotoxins can alter the gut microbiota. Such findings suggested that there is a bi-directional interaction occurs between mycotoxin and the gut microbiota. Evidence of disturbance on gut microbiota modulation induced by mycotoxin only had been studied on animal and the results have been summarized (**Table 1**). The changes in gut microbiota can be observed up to species level in some of the studies using advance molecular approaches. However, the compositions of gut microbiota are greatly influenced by various factors during the experiment. Confounding factors affecting microbial composition and function may include diet (Cani and Everard, 2016), the exposure of environmental chemical and antibiotics (Claus et al., 2017), genetic background (Goodrich et al., 2016b), as well as the mental health condition (stress) of the host (Karl et al., 2017). These factors can explain that the microbiota in same species may not be able to reduce the level of mycotoxins. Besides, the changes in gut microbiota due to the presence of mycotoxin may contribute by some uncontrolled variables. Contrasting data obtained from different studies in this review further highlight the significance of confounding factors toward the outcome of studies. Nonetheless, a well-controlled study designs is essential to ensure repeatable studies with consistent results.

Deoxynivalenol

A study has demonstrated the ability of gut microbiota to remove deoxynivalenol (DON) using an *in vitro* study (He et al., 1992). It was reported that the microorganisms in large intestines

TABLE 1 | *In vivo* experiments: Gut microbiota alteration by mycotoxins.

No	Subjects	Age	Comparison	No. of subjects	Treatment period	Methods	Taxonomic findings	Functional findings	References
1	Male Swedish Landrace x Yorkshire pigs; SPF	Not specified, 20 kg	Post-valve T-caecum cannulas pig treated with 0.05 mg DON/kg BW /day: Before and after exposure to feces from pigs with DON de-epoxidation ability	5	Daily for 10 weeks	Terminal restriction fragment length polymorphism (T-RFLP)	No difference could be detected in the T-RFLP profiles in the intestinal microflora between samples from pigs before and after acquiring the ability to de-epoxidate trichothecenes.	The deoxynivalenol de-epoxidation ability was found in fecal and ileal, 1 week after the pigs were exposed to feces from pigs known to have the de-epoxidation ability.	Eriksen et al., 2002
2	Large White pigs; SPF	9-week-old	Healthy and DON (2.8 mg/kg) treated rat	24	Daily for 4 weeks	Capillary Electrophoresis Single-Stranded Conformation Polymorphism (CE-SSCP)	The species richness index was significantly increased by DON exposure.	A significant reduction of daily weight gain was observed in piglets exposed to the contaminated diet when compared to control.	Waché et al., 2008
3	Male Sprague-Dawley rats; GF	8 weeks old, 120–150 g	Germ-free rats inoculated with human fecal: Untreated and treated with DON (100mg/kg BW)	20	Daily for 4 weeks	Real-time PCR	DON significantly increased Bacteroides/Prevotella group and decreased concentration levels for *Escherichia coli.*	-	Saint-Cyr et al., 2013
4	Female Wistar rats; Pregnant	Not specified	Healthy pregnant rat fed with normal diet and DON-contaminated diet (10 mg/kg)	24	Daily for 4 weeks	16S sequencing	No difference could be detected in the intestinal microflora between control group and DO-treated group.	DON exacerbates the DNA damage induced by *E. coli* producing colibactin	Payros et al., 2017
5	Large-White piglets; SPF	4 weeks old, 41.6 kg	Healthy piglets fed with normal diet and diet containing 12 mg/kg of fumonisins (Mixture of FB1 and FB2)	48	Daily for 63 days	Capillary Electropho-resis Single-Stranded Conformation Polymorphism (CE-SSCP)	Fumonisins decreased the fecal microbiota SSCP-profiles similarity between the fumonisins treated and the untreated control group.	Fumonisins affected sphingolipid [sphinganine (Sa) and sphingosine (So)] metabolism.	Burel et al., 2013
6	Male Fischer 344 rats	6–7 weeks old	Healthy and OTA (70 and 210 μg/kg BW) treated rat	18	5 days/ week for 4 weeks	16S rRNA and shotgun sequencing	OTA increased Lactobacillaceae and decreased Bacteroidaceae in relative abundance. In genus level, Bacteroides, Dorea, Escherichia, Oribacterium, Ruminococcus, and Syntrophococcus were decreased and Lactobacillus increased. Facultative anaerobes were increased whereas anaerobes were reduced.	Changes in functional genes of gut microbiota including signal transduction, carbohydrate transport, transposase, amino acid transport system, and mismatch repair were observed.	Guo et al., 2014
7	Male Fischer 344 rats	5-weeks old, 120–130 g	Healthy and AFB1 treated rat; control, low (5 mg AFB1/kg BW), medium (25 mg/kg BW), high (75 mg/kg BW)	20	5 days/ week for 4 weeks	16S sequencing	Fecal: Clostridiales and Bacteroidales were increased in a dose-dependent manner of AFB1. In contrast, Lactobacillales from Firmicutes, Streptococcus sp. and Lactococcus sp. were decreased in a dose-dependent manner of AFB1 exposure.	-	Wang et al., 2015

(Continued)

TABLE 1 | Continued

No	Subjects	Age	Comparison	No. of subjects	Treatment period	Methods	Taxonomic findings	Functional findings	References
8	Male Broiler chicks	1 day old	Healthy and AFB1 treated rat; control, 2 ppm, 1.5 ppm, 1 ppm daily	240	Daily for 21 days	Differential Agar (deMan Rogosa Sharpe for LAB; MacConkey for Gram-negative bacteria	AFB1 significantly reduced total LAB in chickens that received 1 ppm AFB1. In chickens fed with 2 and 1.5 ppm AFB1, the total number of Gram-negative bacteria and LAB were significantly increased.	AFB1 increased the heterophils-to-lymphocyte ratio. The villus length in both duodenum and ileum increased significantly by AFB1 as well as a reduction in duodenum crypt.	Schmeits et al., 2014
9	Female BALB/c mice	Not specified	Germfree and conventional microflora mice treated with AFB1 (10 mg/kg P.O) or dimethylsulfoxide (control)	12	1 h	CFU counts	Liver: Greater numbers of bacterial mutants were recovered from the conventional flora mice than from the germfree mice after AFB1 treatment.	Potentiated toxic effects.	Rowland, 1988
10	Gilts	25 ± 2 kg	Healthy and mycotoxin mixture treated gilts; control, 40 μg ZEA/kg BW + 12 μg DON/kg BW	75	Daily for 6 weeks	Differential Agar	ZEA and DON mixture significantly reduced amounts of *Clostridium perfringens*, *Escherichia coli*, and Enterobacteriaceae but increased the biodiversity.	Mixture of ZEA and DON increased amino acid metabolism in microbiota.	Piotrowska et al., 2014
11	Dairy calves	Less than 1 month and mature calf	Mycotoxin [aflatoxin (1–3 ppb) and fumonisin (50–350 ppb)] induced HE calf: Untreated and treated with Celmanax®/Dairyman's Choice™	From 3 production sites (Not specified)	Daily for 14 days	CFU counts	Fecal: Aflatoxin and fumonisin increased Shiga Toxin-producing *Escherichia coli* (STEC).	Aflatoxin exposure affects the STEC-secreted cytotoxin composition indicated by increasing intracellular Ca^{2+} concentrations corresponding to increased cytotoxicity.	Baines et al., 2013

of broilers were able to transform DON into de-epoxy-DON. The gut microbes of broiler were further shown to transform DON to the less toxic metabolite, de-epoxy-DON via epoxide reductase. Similar findings have been observed in other studies using microbial content from the broiler intestine (Lun et al., 1988; Young et al., 2007). Some other studies have also shown that intestinal microorganisms of other animal species including rat (Worrell et al., 1989) and swine (Kollarczik et al., 1994) possess the same ability. However, no alteration was found when swines' intestines content was used in the study conducted by He et al. (1992).

Apart from these, mycotoxin degrading bacteria had been isolated from intestinal content for extensive studies. Microbiological selection strategies guided by PCR DGGE (denaturing gradient gel electrophoresis) had been employed to isolate DON-transforming bacteria and the isolates obtained belong to four different bacterial groups; Anaerofilum, Bacillus Clostridiales, and Collinsella (Yu H. et al., 2010). In addition, a microbial community, namely microbial culture C133 from catfish digesta was screened, and capable to completely transformed DON to de-epoxy-DON after 96 h incubation (Guan et al., 2009). Several intestinal bacterial strains have been identified as biological trichothecene detoxification agent via *in vitro* screening and microbial analyses in other recent reviews (Hathout and Aly, 2014). Interestingly, a study showed the ability to metabolize DON can be obtained via gut microbiota transfer in swine. However, the transfer of gut microbiota revealed no changes in the DNA-profiles of the gut bacterial composition (Eriksen et al., 2002).

Several studies have been done on the interaction of DON toward the gut microbiota. Consumption of feed contaminated with DON for a time duration of 4 weeks has been shown to exert minor effect on the total number of fecal aerobic mesophilic bacteria and anaerobic sulfite-reducing bacteria in swine. Although there was no effect of DON on microbial diversity, the richness index was significantly ($P < 0.05$) increased by DON exposure (Waché et al., 2008). In another study by Saint-Cyr et al. (2013), GF male rats were inoculated with fecal flora from healthy human, in order to investigate the human gut microbial changes induced by DON. By using real-time PCR quantification, a significant increase of Bacteroides/Prevotella group and decreased concentration levels of *Escherichia coli* were observed after feeding the rats with DON for 4 weeks ($P < 0.05$). In human, the shift in the proportion of Bacteroides is highly associated with diseases as individuals with Crohn's disease or celiac diseases often exhibit a higher abundance of Bacteroides than healthy individuals (Kamada, 2016). A recent study, however, revealed that DON has no significant changes in the diversity and relative abundance of gut microbiota based on 16S rRNA microbiota analysis (Payros et al., 2017).

T-2 Toxin

Gratz et al. (2017) demonstrated that masked T-2 toxin was released as a parent mycotoxin by human gut microbiota, and thereby contribute to mycotoxin exposure. Trichothecene mycotoxins are generally known as ribotoxic stress inducer which effectively blocks eukaryotic 28S rRNA. Thus, in theoretical aspect, the T-2 toxin would not interfere with bacterial protein translation and growth as suggested by Schmeits et al. (2014). Nevertheless, this is in contrast to the observation seen in a study conducted by Tenk et al. (1982). It was shown that the administration of T-2 toxin for 1 week was sufficient to induce a substantial increase in the aerobic bacteria count in the intestine of swines and rats (Tenk et al., 1982). While the bacterial populations have been shown to be greatly affected by trichothecene, the mechanism which causes the perturbation of bacterial population remains to be elucidated.

Zearalenone

An *in vitro* experiment demonstrated that zearalenone compounds were converted into unknown metabolites by human gut microbiota (Gratz et al., 2017). The first study on the effect of ZEA on gut microbiota has been carried out by Piotrowska et al. (2014). The changes in gut microbiota were evaluated using Biolog EcoPlate method which only allows the quantification of culturable bacteria. After 6 weeks of ZEA ingestion, the data showed the concentration of *Clostridium perfringens, Enterobacteriaceae*, and *E. coli* was significantly reduced ($P < 0.05$).

Fumonisins

Using capillary electrophoresis single-stranded conformation polymorphism (CE-SSCP), it is shown that fumonisins decreased the fecal microbiota SSCP-profiles similarity of the fumonisins-treated swines, compared to the untreated control group. The results indicated that there is an increase in the diversity of microbiota. The balance of the digestive microbiota was transiently but markedly affected after 63 days of chronic exposure to fumonisin, which consists of a mixture of FB1 and FB2 (Burel et al., 2013).

Ochratoxin A

A study investigating the effect of OTA on gut microbiota using bioreactors has been carried out by Ouethrani et al. (2013), in which each bioreactor represents different parts of the adult human gut (Ouethrani et al., 2013). Based on the study, the gut microbiota degradation of OTA and microbiota diversity alteration were observed only at the descending colon after 1-week exposure to OTA. PCR-TTGE targeting *Lactobacilli* populations showed that *Lactobacillus reuteri* present during the start-up period, was permanently disappeared at the end of the OTA treatment period accompanied by some minor changes in the bifidobacteria population. The alteration was explained by a significant reduction in acetic, butyric and total SCFA concentration ($P < 0.05$). The reduction of beneficial microbes, lactobacillus and bifidobacteria indicated that the OTA shifted the microbiota balance and possibly led to impaired immunity.

In vivo study in rat demonstrated that OTA treatment decreased the diversity of the gut microbiota (Guo et al., 2014). The authors also reported that the relative abundance of Lactobacillaceae was increased whereas the Bacteroidaceae was decreased. Moreover, at the genus level, the OTA decreased the population of Bacteroides, Dorea, Escherichia, Oribacterium, Ruminococcus, and Syntrophococcus, while increased the

number of Lactobacillus. The results showed Lactobacillus was more resistant to OTA and Lactobacillus may play a role in OTA detoxification process. Apart from that, it was also reported that the total facultative anaerobes were increased by the OTA treatment. In fact, the increase in facultative anaerobes was often observed in individuals with health complication (Shimizu et al., 2011) as well as in the elderly (Rudi and Avershina, 2015). This may further suggest that the OTA may cause negative effects on the host health via gut microbiota modulation.

Aflatoxin

In contrast to the intense research on AFB1 untoward effects, little information is available in regard to the outcomes of AFB1 on the gut microbiota. The findings from Wang et al. (2015) suggested that AFB1 could alter the gut microbiota in a dose-dependent manner. AFB1 decreased phylogenetical diversity but increased evenness of community composition. Although there was no changes at the phylum level, some lactic acid bacteria were significantly ($P < 0.05$) reduced in the presence of AFB1 (Wang et al., 2015). The reduction of LAB in animals treated with a lower dosage of AFB1 explains the severe immune malfunction induced by lower dosage of AFB1 (Qian et al., 2014).

A recent study showed that AFB1 at a dosage level of 1 ppm significantly ($P < 0.05$) reduced total LAB in the broiler. In contrast, the total number of Gram-negative bacteria and LAB were significantly ($P < 0.05$) increased in the group of broiler fed with 1.5 and 2 ppm of AFB1 (Galarza-Seeber et al., 2016). Besides, it has also been reported that 2.5 ppm of AFB1 increased the production of total volatile fatty acids in broilers, which suggested the association of higher dosage of AFB1 with a higher prevalence of LAB in the intestine (Kubena et al., 2001). Interestingly, a separate study showed greater numbers of bacterial mutants were recovered from mice exposed to AFB1 (Rowland, 1988). The data implies that the genotoxic effects of AFB1 not only affecting the host, but the gut microbiota as well.

Combination of Mycotoxins

On the other hand, the effect of a combination of mycotoxins on the modulation of gut microbiota has also been investigated. The exposure of gilts to ZEA and DON was found to pose an adverse impact on mesophilic aerobic bacteria. In particular, the amounts of *C. perfringens*, *E. coli*, and other bacteria in the family *Enterobacteriaceae* were reduced significantly after the 6th week of the experiment ($P < 0.05$). Nevertheless, the biodiversity of microorganisms in the gut was increased. Apart from that, an increase in the metabolism of amino acid by the gut microbiota was also observed. It was suggested that the increased metabolism of amino acid may be detrimental due to the formation of biogenic amines and procarcinogenic compounds (Piotrowska et al., 2014). Besides, a study confirmed AF and fumonisin mixture increased Shiga Toxin-producing *E. coli* (STEC) level in fecal (Baines et al., 2013). The composition of STEC-secreted cytotoxin was affected as reflected in the elevated concentration of intracellular Ca^{2+} with a corresponding increase in cytotoxicity. Mycotoxins are capable of altering the microbial balance of the intestine. Furthermore, the possible pathway proposed is via oxidative stress induced by mycotoxins (Vinderola and Ritieni, 2014). Nonetheless, the mechanisms by which mycotoxins affect the gut bacterial composition however remain unclear.

THE ROLE OF GUT MICROBIOTA IN THE DEVELOPMENT OF MYCOTOXICOSIS: HCC

Chronic mycotoxicosis, such as HCC results from a high dosage of mycotoxins' contamination. Such pathogenesis generally involves the formation of DNA adducts, regulation of DNA methylation, and alteration of gene expression (Dai et al., 2017; Zhu et al., 2017). Interestingly, gut microbiota perturbation is found to be one of the factors influencing mycotoxin-induced HCC and its association is described in **Figure 1**. The development of HCC in mice induced by a combination of diethylnitrosamine (DEN) and hepatotoxin carbon tetrachloride (CCl4), a model that features several characteristics of chronically injured livers in which human HCC mostly arises, is prevented via gut sterilization. The same study also showed that mice that were grown in specific GF conditions demonstrated fewer and smaller tumors as compared with those grown under specific pathogen free (SPF) conditions (Dapito et al., 2012). In a toxic model of hepatocarcinogenesis, Yu L. X. et al. (2010) found that the depletion of host microflora suppresses tumor formation. Treatment of rats with antibiotic targeting gram-negative organisms (polymyxin B and neomycin) markedly reduced the size and number of HCC nodules after injection of DEN, which induces HCC.

Some specific bacterial species are also found to be correlated with HCC development. Studies showed that the intestinal colonization by *Helicobacter hepaticus* induced HCC, and the DNA of *Helicobacter* ssp. is only present in liver biopsies from HCC patients, not in control samples (Gargano and Hughes, 2014). Findings from both animal and human studies demonstrated that liver cirrhosis and HCC stimulate an intestinal dysbiosis as well as a significant increase population of the *E. coli* and *Atopobium* cluster, coupled with a significant ($P < 0.05$) reduction in the percentages of beneficial microbes such as Lactobacillus group, Bifidobacterium group, and Enterococcus group (Zhang et al., 2012). Besides, hepatocarcinogenesis is found to be related to the increased lipopolysaccharides (LPS) levels which are commonly produced by pathogens in several studies (Zhang et al., 2012).

Probiotics are known for their roles in gut health and microbiota restoration. In addition, many strains of probiotics possess the ability to reduce the level of mycotoxins, particularly via binding. Treatment with probiotics mixture, Prohep [*Lactobacillus rhamnosus* GG, heat-inactivated VSL#3, and viable *E. coli* Nissle 1917 (1:1:1)] successfully relieved the microbial imbalance and hepatic inflammation, which further decreased liver tumor growth (Li et al., 2016). A human study by El-Nezami et al. (2006) demonstrated a statistically significant decrease (up to 55% at 5th week; $P < 0.05$) of urinary AFB-N7-guanine level in the probiotic (*L. rhamnosus* LC705 and *Propionibacterium freudenreichii* subsp. *shermanii*)

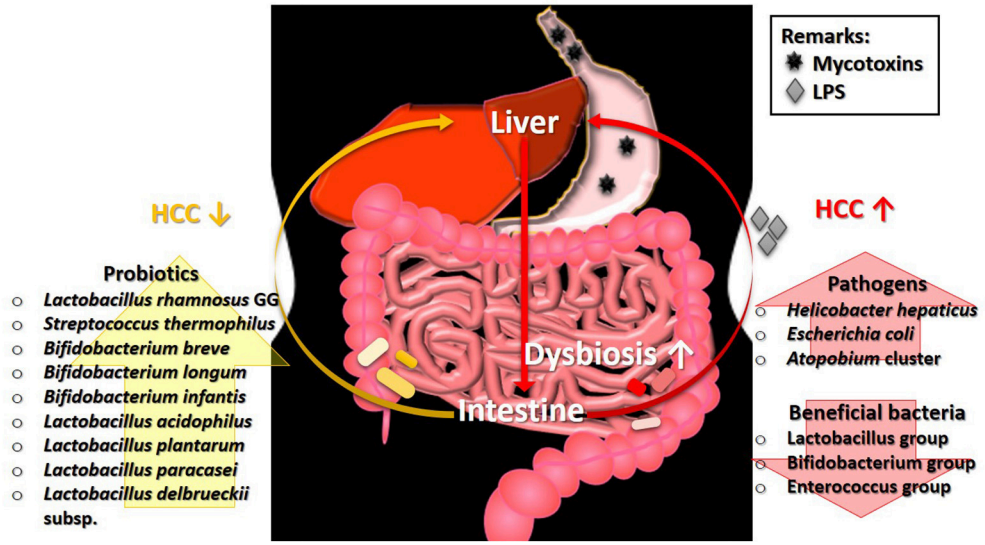

FIGURE 1 | The involvement of gut microbiota in the pathogenesis of HCC. Ingestion of mycotoxin-contaminated foods induces HCC, which eventually leads to the intestinal dysbiosis. The perturbation of microbial balance in the intestine causes a decrease of beneficial gut bacteria. Without the protection from beneficial bacteria, the growth of pathogens will expand rapidly and produce high level of LPS. The presence of LPS exacerbates the condition of HCC. Restoration of gut microbiota balance via intake of probiotics can alleviate the tumorigenic effects in HCC. HCC, hepatocellular carcinoma; LPS, lipopolysaccharide.

mixture group compared to the placebo group. Similar finding was found by Mohd Redzwan et al. (2016) where serum AFB1-lys level were significantly lower ($P < 0{\cdot}05$) in the *Lactobacillus casei* Shirota supplemented individuals. Besides, hepatic transcriptome in AFB1-induced HCC was positively altered by probiotics (Monson et al., 2015). Probiotic supplement reduces the biologically available effective toxic dose of mycotoxin coupled with its gut microbiota normalization ability, offer an effective dietary approach to decrease the risk of liver cancer. As shown in these studies, the restoration of gut microbiota equilibrium offers protection and treatment effects in HCC whereas the occurrence of HCC is linked to the higher abundance of pathogens as illustrated in **Figure 1**. The linkage of microbiota and HCC is undeniably important to understand the mechanism involved in the pathogenesis of HCC.

CONCLUSIONS

This concise review has attempted to draw together the keyworks to highlight the crucial interaction between mycotoxins, the gut, and the gut microbiota in human and animal health. The mycotoxins and gut microbiota studies have revealed meaningful interactions. The uptake of mycotoxin and subsequent tissue distribution are governed by GI tract absorption, and the presence of microbiota at the GI tract can affect the intestinal barrier causing different (maximal or limited) bioavailability of these fungal compounds. The gut microbiota can vary within the same species, thus different reactions toward mycotoxin can be observed as discussed in this review article. In addition, mycotoxins disrupt the gut microbiota balance, and thereby dysregulate intestinal functions and impair local immune response, which may eventually result in systemic toxicity that leads to chronic mycotoxicosis, HCC. The severity of HCC condition can be positively governed by restoration of gut microbiota balance and gut health via probiotics administration. Probiotic which generally helps restore the natural harmony of gut microbiota coupled with its mycotoxins reducing ability could increase its health-promoting value. Regardless, more studies are needed to elucidate the interaction between the gut microbiota and mycotoxin and the implication of such interaction for mycotoxicosis prevention/treatment.

AUTHOR CONTRIBUTIONS

SM-R and W-P-PL provided the conception and the structure of the article. W-P-PL wrote the draft. SM-R and W-P-PL revised the article and approved the final version to be published.

FUNDING

Research grant GP-IPM/2016/9480100 from Universiti Putra Malaysia.

ACKNOWLEDGMENTS

The authors would like to acknowledge financial support through research grant GP-IPM/2016/9480100 from Universiti Putra Malaysia (UPM). W-P-PL would like to thank UPM [Graduate Research Fellowship, GRF] and Ministry of Higher Education Malaysia (MoHE) [MyBrain15 Program] for the scholarships.

REFERENCES

Abassi, H., Ayed-Boussema, I., Shirley, S., Abid, S., Bacha, H., and Micheau, O. (2016). The mycotoxin zearalenone enhances cell proliferation, colony formation and promotes cell migration in the human colon carcinoma cell line HCT116. *Toxicol. Lett.* 254, 1–7. doi: 10.1016/j.toxlet.2016.04.012

Adhikari, M., Negi, B., Kaushik, N., Adhikari, A., Al-Khedhairy, A. A., Kaushik, N. K., et al. (2017). T-2 mycotoxin: toxicological effects and decontamination strategies. *Oncotarget* 8, 33933–33952. doi: 10.18632/oncotarget.15422

Akinrinmade, F. J., Akinrinde, A. S., and Amid, A. (2016). Changes in serum cytokine levels, hepatic and intestinal morphology in aflatoxin B1-induced injury: modulatory roles of melatonin and flavonoid-rich fractions from *Chromolena odorata*. *Mycotoxin Res.* 32, 53–60. doi: 10.1007/s12550-016-0239-9

Alassane-Kpembi, I., and Oswald, I. P. (2015). "Effect of feed contaminants on intestinal health of monogastric farm animals," in *Intestinal Health: Key to Maximise Growth Performance in Livestock*, ed T. Niewold (Wageningen: Academic Publishers), 89–95. doi: 10.3920/978-90-8686-792-9_7

Alizadeh, A., Braber, S., Akbari, P., Garssen, J., and Fink-Gremmels, J. (2015). Deoxynivalenol impairs weight gain and affects markers of gut health after low-dose, short-term exposure of growing pigs. *Toxins* 7, 2071–2095. doi: 10.3390/toxins7062071

Anater, A., Manyes, L., Meca, G., Ferrer, E., Luciano, F. B., Pimpão, C. T., et al. (2016). Mycotoxins and their consequences in aquaculture: a review. *Aquaculture* 451, 1–10. doi: 10.1016/j.aquaculture.2015.08.022

Anderson, G., Seo, M., Berk, M., Carvalho, A. F., and Maes, M. (2016). Gut permeability and microbiota in Parkinson's disease: role of depression, tryptophan catabolites, oxidative and nitrosative stress and melatonergic pathways. *Curr. Pharm. Des.* 22, 6142–6151. doi: 10.2174/1381612822666160906161513

Angius, F., Spolitu, S., Uda, S., Deligia, S., Frau, A., Banni, S., et al. (2015). High-density lipoprotein contribute to G0-G1/S transition in Swiss NIH/3T3 fibroblasts. *Sci. Rep.* 5:17812. doi: 10.1038/srep17812

Assunção, R., Martins, C., Dupont, D., and Alvito, P. (2016). Patulin and ochratoxin a co-occurrence and their bioaccessibility in processed cereal-based foods: a contribution for Portuguese children risk assessment. *Food Chem. Toxicol.* 96, 205–214. doi: 10.1016/j.fct.2016.08.004

Ates, E., Mittendorf, K., Stroka, J., and Senyuva, H. (2013). Determination of *Fusarium mycotoxins* in wheat, maize and animal feed using on-line clean-up with high resolution mass spectrometry. *Food Addit. Contamin.* 30, 156–165. doi: 10.1080/19440049.2012.729162

Awuor, A. O., Yard, E., Daniel, J. H., Martin, C., Bii, C., Romoser, A., et al. (2017). Evaluation of the efficacy, acceptability and palatability of calcium montmorillonite clay used to reduce aflatoxin B1 dietary exposure in a crossover study in Kenya. *Food Addit. Contamin.* 34, 93–102. doi: 10.1080/19440049.2016.1224933

Baines, D., Sumarah, M., Kuldau, G., Juba, J., Mazza, A., and Masson, L. (2013). Aflatoxin, fumonisin and shiga toxin-producing *Escherichia coli* infections in calves and the effectiveness of Celmanax®/Dairyman's choice™ applications to eliminate morbidity and mortality losses. *Toxins* 5, 1872–1895. doi: 10.3390/toxins5101872

Battilani, P., Stroka, J., and Magan, N. (2016). Foreword: mycotoxins in a changing world. *World Mycot. J.* 9, 647–651. doi: 10.3920/WMJ2016.x004

Bibbò, S., Ianiro, G., Giorgio, V., Scaldaferri, F., Masucci, L., Gasbarrini, A., et al. (2016). The role of diet on gut microbiota composition. *Eur. Rev. Med. Pharmacol. Sci.* 20, 4742–4749.

Boini, K. M., Xia, M., Koka, S., Gehr, T., and Li, P. -L. (2017). Sphingolipids in obesity and related complications. *Front. Biosci.* 22, 96–116. doi: 10.2741/4474

Brazil, J. C., Louis, N. A., and Parkos, C. A. (2013). The role of polymorphonuclear leukocyte trafficking in the perpetuation of inflammation during inflammatory bowel disease. *Inflamm. Bowel Dis.* 19, 1556–1565. doi: 10.1097/MIB.0b013e318281f54e

Bui-Klimke, T. R., and Wu, F. (2015). Ochratoxin A and human health risk: a review of the evidence. *Crit. Rev. Food Sci. Nutr.* 55, 1860–1869. doi: 10.1080/10408398.2012.724480

Burel, C., Tanguy, M., Guerre, P., Boilletot, E., Cariolet, R., Queguiner, M., et al. (2013). Effect of low dose of fumonisins on pig health: immune status, intestinal microbiota and sensitivity to Salmonella. *Toxins* 5, 841–864. doi: 10.3390/toxins5040841

Cani, P. D., and Everard, A. (2016). Talking microbes: when gut bacteria interact with diet and host organs. *Mol. Nutr. Food Res.* 60, 58–66. doi: 10.1002/mnfr.201500406

Capaldo, C. T., Farkas, A. E., and Nusrat, A. (2014). Epithelial adhesive junctions. *F1000Prime Rep.* 6:13. doi: 10.12703/P6-1

Ceccaroli, C., Pulliero, A., Geretto, M., and Izzotti, A. (2015). Molecular fingerprints of environmental carcinogens in human cancer. *J. Environ. Sci. Health* 33, 188–228. doi: 10.1080/10590501.2015.1030491

Celi, P., Cowieson, A., Fru-Nji, F., Steinert, R., Kluenter, A. -M., and Verlhac, V. (2017). Gastrointestinal functionality in animal nutrition and health: new opportunities for sustainable animal production. *Anim. Feed Sci. Technol.* 234, 88–100. doi: 10.1016/j.anifeedsci.2017.09.012

Chen, X., Naehrer, K., and Applegate, T. (2016). Interactive effects of dietary protein concentration and aflatoxin B1 on performance, nutrient digestibility, and gut health in broiler chicks. *Poult. Sci.* 95, 1312–1325. doi: 10.3382/ps/pew022

Chilaka, C. A., De Boevre, M., Atanda, O. O., and De Saeger, S. (2017). The status of *Fusarium* mycotoxins in Sub-Saharan Africa: a review of emerging trends and post-harvest mitigation strategies towards food control. *Toxins* 9:19. doi: 10.3390/toxins9010019

Claus, S. P., Guillou, H., and Ellero-Simatos, S. (2017). The gut microbiota: a major player in the toxicity of environmental pollutants? *Npj Biofilms Microbiomes* 3**:**17001. doi: 10.1038/npjbiofilms.2017.1

Collins, S. M. (2014). A role for the gut microbiota in IBS. *Nat. Rev. Gastroenterol. Hepatol.* 11, 497–505. doi: 10.1038/nrgastro.2014.40

Constantinescu, C. S., and Chou, I. J. (2016) "Intestinal bacterial antigens, toxin-induced pathogenesis and immune cross-reactivity in neuromyelitis optica and multiple sclerosis," in *Neuro-Immuno-Gastroenterology*, eds C. S. Constantinescu, R. Arsenescu, and V. Arsenescu (Cham: Springer), 227–236. doi: 10.1007/978-3-319-28609-9_13

Dai, Y., Huang, K., Zhang, B., Zhu, L., and Xu, W. (2017). Aflatoxin B1-induced epigenetic alterations: an overview. *Food Chem. Toxicol.* 109(Pt 1), 683–689. doi: 10.1016/j.fct.2017.06.034

Dapito, D. H., Mencin, A., Gwak, G. -Y., Pradere, J. -P., Jang, M. -K., Mederacke, I., et al. (2012). Promotion of hepatocellular carcinoma by the intestinal microbiota and TLR4. *Cancer Cell* 21, 504–516. doi: 10.1016/j.ccr.2012.02.007

da Rocha, M. E. B., Freire, F. D. C. O., Maia, F. E. F., Guedes, M. I. F., and Rondina, D. (2014). Mycotoxins and their effects on human and animal health. *Food Control* 36, 159–165. doi: 10.1016/j.foodcont.2013.08.021

Dobolyi, C., Sebok, F., Varga, J., Kocsubé, S., Szigeti, G., Baranyi, N., et al. (2013). Occurrence of aflatoxin producing *Aspergillus flavus* isolates in maize kernel in Hungary. *Acta Alimentaria* 42, 451–459. doi: 10.1556/AAlim.42.2013.3.18

Dominguez-Bello, M. G., Costello, E. K., Contreras, M., Magris, M., Hidalgo, G., Fierer, N., et al. (2010). Delivery mode shapes the acquisition and structure of the initial microbiota across multiple body habitats in newborns. *Proc. Natl. Acad. Sci. U.S.A.* 107, 11971–11975. doi: 10.1073/pnas.1002601107

Donaldson, G. P., Lee, S. M., and Mazmanian, S. K. (2016). Gut biogeography of the bacterial microbiota. *Nat. Rev. Microbiol.* 14, 20–32. doi: 10.1038/nrmicro3552

Duncan, S. H., Louis, P., Thomson, J. M., and Flint, H. J. (2009). The role of pH in determining the species composition of the human colonic microbiota. *Environ. Microbiol.* 11, 2112–2122. doi: 10.1111/j.1462-2920.2009.01931.x

El-Nezami, H. S., Polychronaki, N. N., Ma, J., Zhu, H., Ling, W., Salminen, E. K., et al. (2006). Probiotic supplementation reduces a biomarker for increased risk of liver cancer in young men from Southern China. *Am. J. Clin. Nutr.* 83, 1199–1203. doi: 10.1093/ajcn/83.5.1199

Eriksen, G. S., Pettersson, H., Johnsen, K., and Lindberg, J. (2002). Transformation of trichothecenes in ileal digesta and faeces from pigs. *Arch. Anim. Nutr.* 56, 263–274. doi: 10.1080/00039420214343

Etzel, R. A. (2014). Reducing malnutrition: time to consider potential links between stunting and mycotoxin exposure? *Pediatrics* 134, 4–6. doi: 10.1542/peds.2014-0827

Fahmy, N., Woo, M., Alameldin, M., MacDonald, K., Goneau, L. W., Cadieux, P., et al. (2014). Ochratoxin A is not detectable in renal and testicular tumours. *Can. Urol. Assoc. J.* 8, 40–46. doi: 10.5489/cuaj.1240

FAO (2014). *Economic Analysis of Supply and Demand for Food up to 2030*. Special Focus on Fish and Fishery Products, Rome.

Fink, J., and Koo, B.-K. (2016). "Clonal evolution of stem cells in the gastrointestinal tract," in *Advances in Experimental Medicine and Biology: Stem Cells, Pre-neoplasia, and Early Cancer of the Upper Gastrointestinal Tract*, eds M. Jansen and N. Wright (Cham: Springer), 11–25. doi: 10.1007/978-3-319-41388-4_2

Freire, F. D. C. O., and da Rocha, M. E. B. (2017). "Impact of mycotoxins on human health," in *Fungal Metabolites*, eds J. M. Mérillon and K. Ramawat (Cham: Springer), 239–261. doi: 10.1007/978-3-319-25001-4_21

Gajecka, M., Stopa, E., Tarasiuk, M., Zielonka, Ł., and Gajecki, M. (2013). The expression of type-1 and type-2 nitric oxide synthase in selected tissues of the gastrointestinal tract during mixed mycotoxicosis. *Toxins* 5, 2281–2292. doi: 10.3390/toxins5112281

Gajecka, M., Tarasiuk, M., Zielonka, Ł., Dabrowski, M., and Gajecki, M. (2016a). Risk assessment for changes in the metabolic profile and body weights of pre-pubertal gilts during long-term monotonic exposure to low doses of zearalenone (ZEN). *Res. Vet. Sci.* 109, 169–180. doi: 10.1016/j.rvsc.2016.07.013

Gajecka, M., Zielonka, Ł., and Gajecki, M. (2016b). Activity of Zearalenone in the Porcine Intestinal Tract. *Molecules* 22:18. doi: 10.3390/molecules22010018

Galarza-Seeber, R., Latorre, J. D., Bielke, L. R., Kuttappan, V. A., Wolfenden, A. D., Hernandez-Velasco, X., et al. (2016). Leaky gut and mycotoxins: Aflatoxin B1 does not increase gut permeability in broiler chickens. *Front. Veter. Sci.* 3:10. doi: 10.3389/fvets.2016.00010

Gargano, L. M., and Hughes, J. M. (2014). Microbial origins of chronic diseases. *Annu. Rev. Public Health* 35, 65–82. doi: 10.1146/annurev-publhealth-032013-182426

Gelderblom, W., Jaskiewicz, K., Marasas, W., Thiel, P., Horak, R., Vleggaar, R., et al. (1988). Fumonisins–novel mycotoxins with cancer-promoting activity produced by *Fusarium moniliforme*. *Appl. Environ. Microbiol.* 54, 1806–1811.

Goodrich, J. K., Davenport, E. R., Beaumont, M., Jackson, M. A., Knight, R., Ober, C., et al. (2016a). Genetic determinants of the gut microbiome in UK twins. *Cell Host Microbe* 19, 731–743. doi: 10.1016/j.chom.2016.04.017

Goodrich, J. K., Davenport, E. R., Waters, J. L., Clark, A. G., and Ley, R. E. (2016b). Cross-species comparisons of host genetic associations with the microbiome. *Science* 352, 532–535. doi: 10.1126/science.aad9379

Gratz, S. W., Dinesh, R., Yoshinari, T., Holtrop, G., Richardson, A. J., Duncan, G., et al. (2017). Masked trichothecene and zearalenone mycotoxins withstand digestion and absorption in the upper GI tract but are efficiently hydrolyzed by human gut microbiota *in vitro*. *Mol. Nutr. Food Res.* 61:1600680. doi: 10.1002/mnfr.201600680

Grenier, B., and Applegate, T. J. (2013). Modulation of intestinal functions following mycotoxin ingestion: meta-analysis of published experiments in animals. *Toxins* 5, 396–430. doi: 10.3390/toxins5020396

Guan, S., He, J., Young, J. C., Zhu, H., Li, X. -Z., Ji, C., et al. (2009). Transformation of trichothecene mycotoxins by microorganisms from fish digesta. *Aquaculture* 290, 290–295. doi: 10.1016/j.aquaculture.2009.02.037

Guarner, F., and Malagelada, J. -R. (2003). Gut flora in health and disease. *Lancet* 361, 512–519. doi: 10.1016/S0140-6736(03)12489-0

Guo, M., Huang, K., Chen, S., Qi, X., He, X., Cheng, W. -H., et al. (2014). Combination of metagenomics and culture-based methods to study the interaction between ochratoxin a and gut microbiota. *Toxicol. Sci.* 141, 314–323. doi: 10.1093/toxsci/kfu128

Hahn, I., Nagl, V., Schwartz-Zimmermann, H. E., Varga, E., Schwarz, C., Slavik, V., et al. (2015). Effects of orally administered fumonisin B 1 (FB 1), partially hydrolysed FB 1, hydrolysed FB 1 and N-(1-deoxy-d-fructos-1-yl) FB 1 on the sphingolipid metabolism in rats. *Food Chem. Toxicol.* 76, 11–18. doi: 10.1016/j.fct.2014.11.020

Hand, T. W., Vujkovic-Cvijin, I., Ridaura, V. K., and Belkaid, Y. (2016). Linking the microbiota, chronic disease, and the immune system. *Trends Endocrinol. Metabol.* 27, 831–843. doi: 10.1016/j.tem.2016.08.003

Hathout, A. S., and Aly, S. E. (2014). Biological detoxification of mycotoxins: a review. *Ann. Microbiol.* 64, 905–919. doi: 10.1007/s13213-014-0899-7

He, P., Young, L., and Forsberg, C. (1992). Microbial transformation of deoxynivalenol (vomitoxin). *Appl. Environ. Microbiol.* 58, 3857–3863.

Hoffmann, C., Dollive, S., Grunberg, S., Chen, J., Li, H., Wu, G. D., et al. (2013). Archaea and fungi of the human gut microbiome: correlations with diet and bacterial residents. *PLoS ONE* 8:e66019. doi: 10.1371/journal.pone.0066019

Holmes, E., Li, J. V., Athanasiou, T., Ashrafian, H., and Nicholson, J. K. (2011). Understanding the role of gut microbiome–host metabolic signal disruption in health and disease. *Trends Microbiol.* 19, 349–359. doi: 10.1016/j.tim.2011.05.006

Hossein, A., and Gurbuz, Y. (2015). Aflatoxins in poultry nutrition. *Kahramanmaraş Sütçü Imam Üniversitesi Doga Bilimleri Dergisi* 18, 1–5. doi: 10.18016/ksujns.98227

Hueza, I. M., Raspantini, P. C. F., Raspantini, L. E. R., Latorre, A. O., and Górniak, S. L. (2014). Zearalenone, an estrogenic mycotoxin, is an immunotoxic compound. *Toxins* 6, 1080–1095. doi: 10.3390/toxins6031080

Jahanian, E. (2016). Mycotoxin-induced toxicity; an updated mini-review on the current concepts. *Immunopathol. Persa* 2:e11.

Jaladanki, R. N., and Wang, J. Y. (2016). "Regulation of gastrointestinal mucosal growth," in *Colloquium Series on Integrated Systems Physiology: From Molecule to Function to Disease*, eds N. D. Granger and J. Granger (Princeton, NJ: Morgan and Claypool), i–132. doi: 10.4199/C00028ED1V01Y201103ISP015

Jandhyala, S. M., Talukdar, R., Subramanyam, C., Vuyyuru, H., Sasikala, M., and Reddy, D. N. (2015). Role of the normal gut microbiota. *World J. Gastroenterol.* 21, 8787–8803. doi: 10.3748/wjg.v21.i29.8787

Johansson, M. E., and Hansson, G. C. (2016). Immunological aspects of intestinal mucus and mucins. *Nat. Rev. Immunol.* 16, 639–649. doi: 10.1038/nri.2016.88

Kadota, T., Furusawa, H., Hirano, S., Tajima, O., Kamata, Y., and Sugita-Konishi, Y. (2013). Comparative study of deoxynivalenol, 3-acetyldeoxynivalenol, and 15-acetyldeoxynivalenol on intestinal transport and IL-8 secretion in the human cell line Caco-2. *Toxicol. in Vitro* 27, 1888–1895. doi: 10.1016/j.tiv.2013.06.003

Kamada, N. (2016). P-192 unraveling the functional role of dysbiosis in Crohn's disease. *Inflamm. Bowel Dis.* 22:S67. doi: 10.1097/01.MIB.0000480309.65025.5a

Kamada, N., Seo, S. -U., Chen, G. Y., and Núñez, G. (2013). Role of the gut microbiota in immunity and inflammatory disease. *Nat. Rev. Immunol.* 13, 321–335. doi: 10.1038/nri3430

Karl, J. P., Margolis, L. M., Madslien, E. H., Murphy, N. E., Castellani, J. W., Gundersen, Y., et al. (2017). Changes in intestinal microbiota composition and metabolism coincide with increased intestinal permeability in young adults under prolonged physiologic stress. *Am. J. Physiol. Gastroint. Liver Physiol.* 312, G559–G571. doi: 10.1152/ajpgi.00066.2017

Kelly, J. R., Kennedy, P. J., Cryan, J. F., Dinan, T. G., Clarke, G., and Hyland, N. P. (2015). Breaking down the barriers: the gut microbiome, intestinal permeability and stress-related psychiatric disorders. *Front. Cell. Neurosci.* 9:392. doi: 10.3389/fncel.2015.00392

Kew, M. C. (2013). Aflatoxins as a cause of hepatocellular carcinoma. *J. Gastroint. Liver Dis.* 22, 305–310.

Khazaeli, P., Najafi, M. L., Bahaabadi, G. A., Shakeri, F., and Naghibzadeh tahami, A. (2014). Evaluation of aflatoxin contamination in raw and roasted nuts in consumed Kerman and effect of roasting, packaging and storage conditions. *Life Sci. J.* 10, 578–583.

Kolf-Clauw, M., Sassahara, M., Lucioli, J., Rubira-Gerez, J., Alassane-Kpembi, I., Lyazhri, F., et al. (2013). The emerging mycotoxin, enniatin B1, down-modulates the gastrointestinal toxicity of T-2 toxin *in vitro* on intestinal epithelial cells and *ex vivo* on intestinal explants. *Arch. Toxicol.* 87, 2233–2241. doi: 10.1007/s00204-013-1067-8

Kollarczik, B., Gareis, M., and Hanelt, M. (1994). *In vitro* transformation of the Fusarium mycotoxins deoxynivalenol and zearalenone by the normal gut microflora of pigs. *Nat. Toxins* 2, 105–110. doi: 10.1002/nt.2620020303

Korem, T., Zeevi, D., Suez, J., Weinberger, A., Avnit-Sagi, T., Pompan-Lotan, M., et al. (2015). Growth dynamics of gut microbiota in health and disease inferred from single metagenomic samples. *Science* 349, 1101–1106. doi: 10.1126/science.aac4812

Kőszegi, T., and Poór, M. (2016). Ochratoxin A: molecular interactions, mechanisms of toxicity and prevention at the molecular level. *Toxins* 8:111. doi: 10.3390/toxins8040111

Kotowicz, N. K., Frac, M., and Lipiec, J. (2014). The importance of Fusarium fungi in wheat cultivation–pathogenicity and mycotoxins production: a review. *J. Anim. Plant Sci.* 21, 3326–3243.

Kubena, L., Bailey, R., Byrd, J., Young, C., Corrier, D., Stanker, L., et al. (2001). Cecal volatile fatty acids and broiler chick susceptibility to *Salmonella*

typhimurium colonization as affected by aflatoxins and T-2 toxin. *Poult. Sci.* 80, 411–417. doi: 10.1093/ps/80.4.411

Kuczynski, J., Lauber, C. L., Walters, W. A., Parfrey, L. W., Clemente, J. C., Gevers, D., et al. (2012). Experimental and analytical tools for studying the human microbiome. *Nat. Rev. Genetics* 13, 47–58. doi: 10.1038/nrg3129

Kumar, P., Mahato, D. K., Kamle, M., Mohanta, T. K., and Kang, S. G. (2017). Aflatoxins: a global concern for food safety, human health and their management. *Front. Microbiol.* 7:2170. doi: 10.3389/fmicb.2016.02170

Ladeira, C., Frazzoli, C., and Orisakwe, O. E. (2017). Engaging one health for non-communicable diseases in Africa: perspective for mycotoxins. *Front. Public Health* 5:266. doi: 10.3389/fpubh.2017.00266

Lee, W. -J., and Hase, K. (2014). Gut microbiota-generated metabolites in animal health and disease. *Nat. Chem. Biol.* 10, 416–424. doi: 10.1038/nchembio.1535

Lerda, D. (2017). Fumonisins in foods from Cordoba (Argentina), presence: mini review. *Toxicol. Open Access* 3:125. doi: 10.4172/2476-2067.1000125

Lerner, A., Arleevskaya, M., Schmiedl, A., and Matthias, T. (2017). Microbes and viruses are bugging the gut in celiac disease. are they friends or foes? *Front. Microbiol.* 8:1392. doi: 10.3389/fmicb.2017.01392

Lessard, M., Savard, C., Deschene, K., Lauzon, K., Pinilla, V. A., Gagnon, C. A., et al. (2015). Impact of deoxynivalenol (DON) contaminated feed on intestinal integrity and immune response in swine. *Food Chem. Toxicol.* 80, 7–16. doi: 10.1016/j.fct.2015.02.013

Lewczuk, B., Przybylska-Gornowicz, B., Gajecka, M., Targonska, K., Ziółkowska, N., Prusik, M., et al. (2016). Histological structure of duodenum in gilts receiving low doses of zearalenone and deoxynivalenol in feed. *Exp. Toxicol. Pathol.* 68, 157–166. doi: 10.1016/j.etp.2015.11.008

Lewis, C., Smith, J., Anderson, J., and Freshney, R. (2000). Increased cytotoxicity of food-borne mycotoxins toward human cell lines *in vitro* via enhanced cytochrome p450 expression using the MTT bioassay. *Mycopathologia* 148, 97–102. doi: 10.1023/A:1007130923558

Li, J., Sung, C. Y. J., Lee, N., Ni, Y., Pihlajamäki, J., Panagiotou, G., et al. (2016). Probiotics modulated gut microbiota suppresses hepatocellular carcinoma growth in mice. *Proc. Natl. Acad. Sci. U.S.A.* 113, E1306–E1315. doi: 10.1073/pnas.1518189113

Liao, C. -D., Chiueh, L. -C., and Shih, D. Y. -C. (2009). Determination of zearalenone in cereals by high-performance liquid chromatography and liquid chromatography-electrospray tandem mass spectrometry. *J. Food Drug Anal.* 17, 52–58.

Liuzzi, V. C., Fanelli, F., Tristezza, M., Haidukowski, M., Picardi, E., Manzari, C., et al. (2017). Transcriptional analysis of Acinetobacter sp. neg1 capable of degrading ochratoxin A. *Front. Microbiol.* 7:2162. doi: 10.3389/fmicb.2016.02162

Logrieco, A., Bottalico, A., Mulé, G., Moretti, A., and Perrone, G. (2003). Epidemiology of toxigenic fungi and their associated mycotoxins for some Mediterranean crops. *Eur. J. Plant Pathol.* 109, 645–667. doi: 10.1023/A:1026033021542

Lun, A., Moran, E., Young, L., and McMillan, E. (1988). Disappearance of deoxynivalenol from digesta progressing along the chicken's gastrointestinal tract after intubation with feed containing contaminated corn. *Bull. Environ. Contam. Toxicol.* 40, 317–324. doi: 10.1007/BF01689086

Lv, G., Cheng, N., and Wang, H. (2017). The gut microbiota, tumorigenesis, and liver diseases. *Engineering* 3, 110–114. doi: 10.1016/J.ENG.2017.01.017

Manafi, M., Mohan, K., and Ali, M. N. (2011). Effect of ochratoxin A on coccidiosis-challenged broiler chicks. *World Mycotoxin J.* 4, 177–181. doi: 10.3920/WMJ2010.1234

Maresca, M. (2013). From the gut to the brain: journey and pathophysiological effects of the food-associated trichothecene mycotoxin deoxynivalenol. *Toxins* 5, 784–820. doi: 10.3390/toxins5040784

Marin, D. E., Motiu, M., and Taranu, I. (2015). Food contaminant zearalenone and its metabolites affect cytokine synthesis and intestinal epithelial integrity of porcine cells. *Toxins* 7, 1979–1988. doi: 10.3390/toxins7061979

Marin, D. E., Pistol, G. C., Gras, M. A., Palade, M. L., and Taranu, I. (2017). Comparative effect of ochratoxin A on inflammation and oxidative stress parameters in gut and kidney of piglets. *Regul. Toxicol. Pharmacol.* 89, 224–231. doi: 10.1016/j.yrtph.2017.07.031

Masching, S., Naehrer, K., Schwartz-Zimmermann, H.-E., Sărăndan, M., Schaumberger, S., Dohnal, I., et al. (2016). Gastrointestinal degradation of fumonisin B1 by carboxylesterase fumD prevents fumonisin induced alteration of sphingolipid metabolism in turkey and swine. *Toxins* 8:84. doi: 10.3390/toxins8030084

McLaughlin, J., Padfield, P. J., Burt, J. P., and O'Neill, C. A. (2004). Ochratoxin A increases permeability through tight junctions by removal of specific claudin isoforms. *Am. J. Physiol. Cell Physiol.* 287, C1412–C1417. doi: 10.1152/ajpcell.00007.2004

Medina, Á., Rodríguez, A., and Magan, N. (2015). Climate change and mycotoxigenic fungi: impacts on mycotoxin production. *Curr. Opin. Food Sci.* 5, 99–104. doi: 10.1016/j.cofs.2015.11.002

Mezzelani, A., Raggi, M., Marabotti, A., and Milanesi, L. (2016). Ochratoxin A as possible factor trigging autism and its male prevalence via epigenetic mechanism. *Nutr. Neurosci.* 19, 43–46. doi: 10.1179/1476830515Z.000000000186

Milićević, D. R., Škrinjar, M., and Baltić, T. (2010). Real and perceived risks for mycotoxin contamination in foods and feeds: challenges for food safety control. *Toxins* 2, 572–592. doi: 10.3390/toxins2040572

Minervini, F., Garbetta, A., D'Antuono, I., Cardinali, A., Martino, N. A., Debellis, L., et al. (2014). Toxic mechanisms induced by fumonisin B1 mycotoxin on human intestinal cell line. *Arch. Environ. Contam. Toxicol.* 67, 115–123. doi: 10.1007/s00244-014-0004-z

Mohd-Redzwan, S., Jamaluddin, R., Mutalib, A., Sokhini, M., and Ahmad, Z. (2013). A mini review on aflatoxin exposure in Malaysia: past, present and future. *Front. Microbiol.* 4:334. doi: 10.3389/fmicb.2013.00334

Mohd Redzwan, S., Mutalib, M. S. A., Wang, J. -S., Ahmad, Z., Kang, M. -S., Nasrabadi, E. N., et al. (2016). Effect of supplementation of fermented milk drink containing probiotic *Lactobacillus casei* Shirota on the concentrations of aflatoxin biomarkers among employees of Universiti Putra Malaysia: a randomised, double-blind, cross-over, placebo-controlled study. *Br. J. Nutr.* 115, 39–54. doi: 10.1017/S0007114515004109

Monson, M. S., Settlage, R. E., Mendoza, K. M., Rawal, S., El-Nezami, H. S., Coulombe, R. A., et al. (2015). Modulation of the spleen transcriptome in domestic turkey (*Meleagris gallopavo*) in response to aflatoxin B1 and probiotics. *Immunogenetics* 67, 163–178. doi: 10.1007/s00251-014-0825-y

Mosca, A., Leclerc, M., and Hugot, J. P. (2016). Gut microbiota diversity and human diseases: should we reintroduce key predators in our ecosystem? *Front. Microbiol.* 7:455. doi: 10.3389/fmicb.2016.00455

Muhammad, I., Sun, X., Wang, H., Li, W., Wang, X., Cheng, P., et al. (2017). Curcumin successfully inhibited the computationally identified CYP2A6 enzyme-mediated bioactivation of aflatoxin B1 in arbor acres broiler. *Front. Pharmacol.* 8:143. doi: 10.3389/fphar.2017.00143

Nathanail, A. V., Varga, E., Meng-Reiterer, J., Bueschl, C., Michlmayr, H., Malachova, A., et al. (2015). Metabolism of the Fusarium mycotoxins T-2 toxin and HT-2 toxin in wheat. *J. Agric. Food Chem.* 63, 7862–7872. doi: 10.1021/acs.jafc.5b02697

Ortiz, C. S., Richards, C., Terry, A., Parra, J., and Shim, W. -B. (2015). Genetic variability and geographical distribution of mycotoxigenic *Fusarium verticillioides* strains isolated from maize fields in Texas. *Plant Pathol. J.* 31, 203–211. doi: 10.5423/PPJ.OA.02.2015.0020

Osselaere, A., Santos, R., Hautekiet, V., De Backer, P., Chiers, K., Ducatelle, R., et al. (2013). Deoxynivalenol impairs hepatic and intestinal gene expression of selected oxidative stress, tight junction and inflammation proteins in broiler chickens, but addition of an adsorbing agent shifts the effects to the distal parts of the small intestine. *PLoS ONE* 8:e69014. doi: 10.1371/journal.pone.0069014

Ouethrani, M., Van de Wiele, T., Verbeke, E., Bruneau, A., Carvalho, M., Rabot, S., et al. (2013). Metabolic fate of ochratoxin A as a coffee contaminant in a dynamic simulator of the human colon. *Food Chem.* 141, 3291–3300. doi: 10.1016/j.foodchem.2013.05.157

Pandya, J. P., and Arade, P. C. (2016). Mycotoxin: a devil of human, animal and crop health. *Adv. Life Sci.* 5, 3937–3941.

Payros, D., Dobrindt, U., Martin, P., Secher, T., Bracarense, A. P. F., Boury, M., et al. (2017). The food contaminant deoxynivalenol exacerbates the genotoxicity of gut microbiota. *MBio* 8:e00007-17. doi: 10.1128/mBio.00007-17

Peng, X., Zhang, S., Fang, J., Cui, H., Zuo, Z., and Deng, J. (2014). Protective roles of sodium selenite against aflatoxin B1-induced apoptosis of jejunum in broilers. *Int. J. Environ. Res. Public Health* 11, 13130–13143. doi: 10.3390/ijerph111213130

Peraica, M., Flajs, D., Mladinic, M., Zeljezic, D., Eror, D. B., Koepsell, H., et al. (2011). Oxidative stress and Na^+-glucose cotransporters Sglt1 and

Sglt2 in kidneys of ochratoxin A-treated rats. *Toxicol. Lett.* 205:S275. doi: 10.1016/j.toxlet.2011.05.933

Peraica, M., Radic, B., Lucic, A., and Pavlovic, M. (1999). Toxic effects of mycotoxins in humans. *Bull. World Health Organ.* 77, 754–766.

Pinton, P., and Oswald, I. P. (2014). Effect of deoxynivalenol and other Type B trichothecenes on the intestine: a review. *Toxins* 6, 1615–1643. doi: 10.3390/toxins6051615

Piotrowska, M., Slizewska, K., Nowak, A., Zielonka, Ł., Zakowska, Z., Gajecka, M., et al. (2014). The effect of experimental fusarium mycotoxicosis on microbiota diversity in porcine ascending colon contents. *Toxins* 6, 2064–2081. doi: 10.3390/toxins6072064

Pitt, J. I., and Miller, J. D. (2016). A concise history of mycotoxin research. *J. Agric. Food Chem.* 65, 7021–7033. doi: 10.1021/acs.jafc.6b04494

Qian, G., Tang, L., Guo, X., Wang, F., Massey, M. E., Su, J., et al. (2014). Aflatoxin B1 modulates the expression of phenotypic markers and cytokines by splenic lymphocytes of male F344 rats. *J. Appl. Toxicol.* 34, 241–249. doi: 10.1002/jat.2866

Qu, D., Huang, X., Han, J., and Man, N. (2017). Efficacy of mixed adsorbent in ameliorating ochratoxicosis in broilers fed ochratoxin a contaminated diets. *Ital. J. Anim. Sci.* 16, 573–579. doi: 10.1080/1828051X.2017.1302822

Ray, D. K., Ramankutty, N., Mueller, N. D., West, P. C., and Foley, J. A. (2012). Recent patterns of crop yield growth and stagnation. *Nat. Commun.* 3:1293. doi: 10.1038/ncomms2296

Romero, A., Ares, I., Ramos, E., Castellano, V., Martínez, M., Martínez-Larrañaga, M. -R., et al. (2016). Mycotoxins modify the barrier function of Caco-2 cells through differential gene expression of specific claudin isoforms: protective effect of illite mineral clay. *Toxicology* 353, 21–33. doi: 10.1016/j.tox.2016.05.003

Rouprêt, M., Babjuk, M., Compérat, E., Zigeuner, R., Sylvester, R. J., Burger, M., et al. (2015). European association of urology guidelines on upper urinary tract urothelial cell carcinoma: 2015 update. *Eur. Urol.* 68, 868–879. doi: 10.1016/j.eururo.2015.06.044

Rowland, I., Gibson, G., Heinken, A., Scott, K., Swann, J., Thiele, I., et al. (2017). Gut microbiota functions: metabolism of nutrients and other food components. *Eur. J. Nutr.* doi: 10.1007/s00394-017-1445-8. [Epub ahead of print].

Rowland, I. R. (1988). Interactions of the gut microflora and the host in toxicology. *Toxicol. Pathol.* 16, 147–153. doi: 10.1177/019262338801600207

Rudi, K., and Avershina, E. (2015). The composition of the gut microbiota throughout life, with an emphasis on early life. *Microb. Ecol. Health Dis.* 26:26050. doi: 10.3402/mehd.v26.26050

Russo, P., Capozzi, V., Spano, G., Corbo, M. R., Sinigaglia, M., and Bevilacqua, A. (2016). Metabolites of microbial origin with an impact on health: ochratoxin A and biogenic amines. *Front. Microbiol.* 7:482. doi: 10.3389/fmicb.2016.00482

Saint-Cyr, M. J., Perrin-Guyomard, A., Houée, P., Rolland, J. -G., and Laurentie, M. (2013). Evaluation of an oral subchronic exposure of deoxynivalenol on the composition of human gut microbiota in a model of human microbiota-associated rats. *PLoS ONE* 8:e80578. doi: 10.1371/journal.pone.0080578

Sam, Q. H., Chang, M. W., and Chai, L. Y. A. (2017). The fungal mycobiome and its interaction with gut bacteria in the host. *Int. J. Mol. Sci.* 18:330. doi: 10.3390/ijms18020330

Scarpellini, E., Ianiro, G., Attili, F., Bassanelli, C., De Santis, A., and Gasbarrini, A. (2015). The human gut microbiota and virome: potential therapeutic implications. *Digest. Liver Dis.* 47, 1007–1012. doi: 10.1016/j.dld.2015.07.008

Schmeits, P. C., Katika, M. R., Peijnenburg, A. A., van Loveren, H., and Hendriksen, P. J. (2014). DON shares a similar mode of action as the ribotoxic stress inducer anisomycin while TBTO shares ER stress patterns with the ER stress inducer thapsigargin based on comparative gene expression profiling in Jurkat T cells. *Toxicol. Lett.* 224, 395–406. doi: 10.1016/j.toxlet.2013.11.005

Sekirov, I., Russell, S. L., Antunes, L. C. M., and Finlay, B. B. (2010). Gut microbiota in health and disease. *Physiol. Rev.* 90, 859–904. doi: 10.1152/physrev.00045.2009

Shimizu, K., Ogura, H., Hamasaki, T., Goto, M., Tasaki, O., Asahara, T., et al. (2011). Altered gut flora are associated with septic complications and death in critically ill patients with systemic inflammatory response syndrome. *Dig. Dis. Sci.* 56, 1171–1177. doi: 10.1007/s10620-010-1418-8

Simrén, M., Barbara, G., Flint, H. J., Spiegel, B. M., Spiller, R. C., Vanner, S., et al. (2012). Intestinal microbiota in functional bowel disorders: a Rome foundation report. *Gut* 62, 159–176. doi: 10.1136/gutjnl-2012-302167

Solcan, C., Pavel, G., Floristean, V., Chiriac, I., Slencu, B., and Solcan, G. (2015). Effect of ochratoxin A on the intestinal mucosa and mucosa-associated lymphoid tissues in broiler chickens. *Acta Vet. Hung.* 63, 30–48. doi: 10.1556/AVet.2015.004

Sommer, F., and Bäckhed, F. (2013). The gut microbiota—masters of host development and physiology. *Nat. Rev. Microbiol.* 11, 227–238. doi: 10.1038/nrmicro2974

Speight, N. (2012). "Mycotoxin-related illness," in *Advancing Medicine with Food and Nutrients, 2nd Edn.*, ed I. Kohlstadt (Boca Raton, FL: CRC Press; Taylor & Francis Group), 821–850.

Sun, L. -H., Zhang, N. -Y., Zhu, M. -K., Zhao, L., Zhou, J. -C., and Qi, D.-S. (2016). Prevention of aflatoxin B1 hepatoxicity by dietary selenium is associated with inhibition of cytochrome P450 isozymes and up-regulation of 6 selenoprotein genes in chick liver. *J. Nutr.* 146, 655–661. doi: 10.3945/jn.115.224626

Taranu, I., Braicu, C., Marin, D. E., Pistol, G. C., Motiu, M., Balacescu, L., et al. (2015). Exposure to zearalenone mycotoxin alters *in vitro* porcine intestinal epithelial cells by differential gene expression. *Toxicol. Lett.* 232, 310–325. doi: 10.1016/j.toxlet.2014.10.022

Tenk, I., Fodor, E., and Szathmáry, C. (1982). The effect of pure Fusarium toxins (T-2, F-2, DAS) on the microflora of the gut and on plasma glucocorticoid levels in rat and swine. *Zentralblatt für Bakteriologie, Mikrobiologie und Hygiene. 1. Abt. Originale. A, Medizinische Mikrobiologie, Infektionskrankheiten und Parasitologie* 252, 384–393.

van Opstal, E. J., and Bordenstein, S. R. (2015). Rethinking heritability of the microbiome. *Science* 349, 1172–1173. doi: 10.1126/science.aab3958

Viegas, C., Pinheiro, A. C., Sabino, R., Viegas, S., Brandão, J., and Veríssimo, C. (2015). *Environmental Mycology in Public Health: Fungi and Mycotoxins Risk Assessment and Management*. Cambridge, UK: Academic Press; Elsevier.

Vinderola, G., and Ritieni, A. (2014). Role of probiotics against mycotoxins and their deleterious effects. *J. Food Res.* 4:10. doi: 10.5539/jfr.v4n1p10

Waché, Y. J., Valat, C., Postollec, G., Bougeard, S., Burel, C., Oswald, I. P., et al. (2008). Impact of deoxynivalenol on the intestinal microflora of pigs. *Int. J. Mol. Sci.* 10, 1–17. doi: 10.3390/ijms10010001

Wang, H., Chen, Y., Zhai, N., Chen, X., Gan, F., Li, H., et al. (2017). Ochratoxin A induced apoptosis of IPEC-J2 cells through ROS-mediated mitochondrial permeability transition pore opening pathway. *J. Agric. Food Chem.* 65, 10630–10637. doi: 10.1021/acs.jafc.7b04434

Wang, J., Fitzpatrick, D., and Wilson, J. (1993). Effect of dietary T-2 toxin on biogenic monoamines in discrete areas of the rat brain. *Food Chem. Toxicol.* 31, 191–197. doi: 10.1016/0278-6915(93)90093-E

Wang, J., Tang, L., Glenn, T. C., and Wang, J. -S. (2015). Aflatoxin B1 induced compositional changes in gut microbial communities of male F344 rats. *Toxicol. Sci.* 150, 54–63. doi: 10.1093/toxsci/kfv259

Wang, Z., Feng, J., and Tong, Z. (1993). Human toxicosis caused by moldy rice contaminated with fusarium and T-2 toxin. *Biomed. Environ. Sci.* 6, 65–70.

Weinstock, G. M. (2012). Genomic approaches to studying the human microbiota. *Nature* 489, 250–256. doi: 10.1038/nature11553

Wild, C. P., and Gong, Y. Y. (2010). Mycotoxins and human disease: a largely ignored global health issue. *Carcinogenesis* 31, 71–82. doi: 10.1093/carcin/bgp264

Worrell, N., Mallett, A., Cook, W., Baldwin, N., and Shepherd, M. (1989). The role of gut micro-organisms in the metabolism of deoxynivalenol administered to rats. *Xenobiotica* 19, 25–32. doi: 10.3109/00498258909034673

Wu, Q. -H., Wang, X., Yang, W., Nüssler, A. K., Xiong, L. -Y., Kuča, K., et al. (2014). Oxidative stress-mediated cytotoxicity and metabolism of T-2 toxin and deoxynivalenol in animals and humans: an update. *Arch. Toxicol.* 88, 1309–1326. doi: 10.1007/s00204-014-1280-0

Wu, W., Zhou, H. -R., Pan, X., and Pestka, J. J. (2015). Comparison of anorectic potencies of the trichothecenes T-2 toxin, HT-2 toxin and satratoxin G to the Ipecac alkaloid emetine. *Toxicol. Rep.* 2, 238–251. doi: 10.1016/j.toxrep.2014.12.010

Yamazoe, Y., Koyama, N., and Kumagai, S. (2017). Possible role of phosphatidylcholine and sphingomyelin on fumonisin B1-mediated toxicity. *Food Safety* 5, 75–97. doi: 10.14252/foodsafetyfscj.2017004

Yang, L., Tu, D., Zhao, Z., and Cui, J. (2017). Cytotoxicity and apoptosis induced by mixed mycotoxins (T-2 and HT-2 toxin) on primary hepatocytes of broilers *in vitro*. *Toxicon* 129, 1–10. doi: 10.1016/j.toxicon.2017.01.001

Young, J. C., Zhou, T., Yu, H., Zhu, H., and Gong, J. (2007). Degradation of trichothecene mycotoxins by chicken intestinal microbes. *Food Chem. Toxicol.* 45, 136–143. doi: 10.1016/j.fct.2006.07.028

Yu, H., Zhou, T., Gong, J., Young, C., Su, X., Li, X. -Z., et al. (2010). Isolation of deoxynivalenol-transforming bacteria from the chicken intestines using the approach of PCR-DGGE guided microbial selection. *BMC Microbiol.* 10:182. doi: 10.1186/1471-2180-10-182

Yu, L. X., Yan, H. X., Liu, Q., Yang, W., Wu, H. P., Dong, W., et al. (2010). Endotoxin accumulation prevents carcinogen-induced apoptosis and promotes liver tumorigenesis in rodents. *Hepatology* 52, 1322–1333. doi: 10.1002/hep.23845

Zain, M. E. (2011). Impact of mycotoxins on humans and animals. *J. Saudi Chem. Soc.* 15, 129–144. doi: 10.1016/j.jscs.2010.06.006

Zhang, H. -L., Yu, L. -X., Yang, W., Tang, L., Lin, Y., Wu, H., et al. (2012). Profound impact of gut homeostasis on chemically-induced pro-tumorigenic inflammation and hepatocarcinogenesis in rats. *J. Hepatol.* 57, 803–812. doi: 10.1016/j.jhep.2012.06.011

Zhang, J., Zheng, N., Liu, J., Li, F., Li, S., and Wang, J. (2015). Aflatoxin B1 and aflatoxin M1 induced cytotoxicity and DNA damage in differentiated and undifferentiated Caco-2 cells. *Food Chem. Toxicol.* 83, 54–60. doi: 10.1016/j.fct.2015.05.020

Zhang, Y., Jia, Z., Yin, S., Shan, A., Gao, R., Qu, Z., et al. (2014). Toxic effects of maternal zearalenone exposure on uterine capacity and fetal development in gestation rats. *Reprod. Sci.* 21, 743–753. doi: 10.1177/1933719113512533

Zheng, Z., Zuo, Z., Zhu, P., Wang, F., Yin, H., Peng, X., et al. (2017). A study on the expression of apoptotic molecules related to death receptor and endoplasmic reticulum pathways in the jejunum of AFB1-intoxicated chickens. *Oncotarget* 8:89655. doi: 10.18632/oncotarget.20333

Zhou, H., George, S., Hay, C., Lee, J., Qian, H., and Sun, X. (2017). Individual and combined effects of aflatoxin B 1, deoxynivalenol and zearalenone on HepG2 and RAW 264.7 cell lines. *Food Chem. Toxicol.* 103, 18–27. doi: 10.1016/j.fct.2017.02.017

Zhu, L., Zhang, B., Dai, Y., Li, H., and Xu, W. (2017). A review: epigenetic mechanism in ochratoxin a toxicity studies. *Toxins* 9:113. doi: 10.3390/toxins9040113

Conflict of Interest Statement: The authors declare that the research was conducted in the absence of any commercial or financial relationships that could be construed as a potential conflict of interest.

Copyright © 2018 Liew and Mohd-Redzwan. This is an open-access article distributed under the terms of the Creative Commons Attribution License (CC BY). The use, distribution or reproduction in other forums is permitted, provided the original author(s) and the copyright owner are credited and that the original publication in this journal is cited, in accordance with accepted academic practice. No use, distribution or reproduction is permitted which does not comply with these terms.

frontiers in Cellular and Infection Microbiology

REVIEW
published: 08 February 2018
doi: 10.3389/fcimb.2018.00029

Clostridioides difficile Biology: Sporulation, Germination, and Corresponding Therapies for *C. difficile* Infection

Duolong Zhu[1], *Joseph A. Sorg*[2] *and Xingmin Sun*[1]*

[1] Department of Molecular Medicine, Morsani College of Medicine, University of South Florida, Tampa, FL, United States,
[2] Department of Biology, Texas A&M University, College Station, TX, United States

Clostridioides difficile is a Gram-positive, spore-forming, toxin-producing anaerobe, and an important nosocomial pathogen. Due to the strictly anaerobic nature of the vegetative form, spores are the main morphotype of infection and transmission of the disease. Spore formation and their subsequent germination play critical roles in *C. difficile* infection (CDI) progress. Under suitable conditions, *C. difficile* spores will germinate and outgrow to produce the pathogenic vegetative form. During CDI, *C. difficile* produces toxins (TcdA and TcdB) that are required to initiate the disease. Meanwhile, it also produces spores that are responsible for the persistence and recurrence of *C. difficile* in patients. Recent studies have shed light on the regulatory mechanisms of *C. difficile* sporulation and germination. This review is to summarize recent advances on the regulation of sporulation/germination in *C. difficile* and the corresponding therapeutic strategies that are aimed at these important processes.

Keywords: *C. difficile*, spores, germination, CDI, sporulation

OPEN ACCESS

Edited by:
Nathan W. Schmidt,
University of Louisville, United States

Reviewed by:
Paul Edward Carlson,
Food and Drug Administration, United States
Peter Mullany,
University College London, United Kingdom

***Correspondence:**
Xingmin Sun
sun5@health.usf.edu

Received: *30 October 2017*
Accepted: *23 January 2018*
Published: *08 February 2018*

Citation:
Zhu D, Sorg JA and Sun X (2018) Clostridioides difficile Biology: Sporulation, Germination, and Corresponding Therapies for C. difficile Infection. Front. Cell. Infect. Microbiol. 8:29. doi: 10.3389/fcimb.2018.00029

INTRODUCTION

Clostridioides difficile (formerly *Clostridium difficile*; Lawson et al., 2016; Oren and Garrity, 2016) is a Gram-positive, spore-forming, toxin-producing, anaerobic bacterium which has established itself as a leading cause of nosocomial antibiotic-associated diarrhea in the developed countries (Sebaihia et al., 2006). It is found widely in the mammalian gastrointestinal (GI) tract and can cause toxin-mediated *C. difficile* infections (CDI) that range from mild diarrhea to pseudomembranous colitis and potential death (Lessa et al., 2012). *C. difficile* causes over 500,000 infections per year in the United States alone, resulting in an estimated 29,000 deaths and an estimated cost of $1–3 billion (Dubberke and Olsen, 2012; Lessa et al., 2015). Currently, antibiotics are the standard treatments for CDI (i.e., vancomycin, metronidazole, or fidaxomicin; Evans and Safdar, 2015). Though effective, CDI recurrence after the initial treatment can still reach up to 15–35% in treated patients (Leffler and Lamont, 2015). Though recurrence is not fully understood, one of the reasons for high recurrence rate is that *C. difficile* spores may still be present within the patients gut and germinate to the vegetative form after completion or discontinuation of antibiotic treatment (Cornely et al., 2012). Meanwhile, poor host immune response to *C. difficile* and frequent disruption of the normal gut flora may also contribute to the high recurrence rate (Johnson, 2009). Due to the inherent antibiotic resistance of *C. difficile* cells and high prevalence of CDI in some hospitals, the Centers for Disease Control and Prevention (CDC) has listed *C. difficile* as "an urgent threat"

regarding the antibiotic associated threats to the United States (Centres for Disease Control and Prevention (US), 2013).

Because *C. difficile* is an obligate anaerobic pathogen, the vegetative cells are unable to survive outside of a host in the aerobic environment. When *C. difficile* cells meet certain environmental stimuli (e.g., nutrient deprivation, quorum sensing, and other unidentified stress factors), they will initiate a sporulation pathway to produce sufficient dormant spores to survive in extreme situations (Setlow, 2006; Rodriguez-Palacios and LeJeune, 2011; Deakin et al., 2012; Higgins and Dworkin, 2012). *C. difficile* pathogenesis relies on the formation of aerotolerant dormant spores which allows *C. difficile* to persist within the host and to disseminate through patient-to-patient contact/environmental contamination (Britton and Young, 2012). In the host GI tract, the dormant spores must germinate from dormancy to form the actively growing vegetative cells which produce the toxins that cause the primary symptoms of the disease. Under suitable conditions, when germinant receptors sense the presence of small molecules (germinants), spore germination will be induced (Sorg and Sonenshein, 2008).

Recent studies have focused on the regulatory mechanisms of *C. difficile* sporulation/germination to gain insight into these important processes. However, when compared to other well-studied organisms such as *Bacillus subtilis* and *Clostridium perfringens*, our knowledge of *C. difficile* spore biology still lags far behind. In this review, we will discuss recent progresses in the field of *C. difficile* spore biology, specifically on the sporulation and germination processes and their implications for CDI treatment.

C. DIFFICILE SPORULATION

Sporulation Program

Though the signals/molecules that trigger *C. difficile* sporulation have not been identified, based on studies in other organisms, it is likely that environmental stimuli such as nutrient limitation, quorum sensing, and other unidentified stress factors are involved (Higgins and Dworkin, 2012). In fact, though the mechanism is not well-defined, a recent report has suggested that quorum sensing is important for *C. difficile* spore formation (Darkoh et al., 2016). As described in other spore-forming bacteria (e.g., *B. subtilis*), the main process of *C. difficile* sporulation contains four morphogenetic stages (**Figure 1**; Edwards and McBride, 2014; Gil et al., 2017): (I) an asymmetric septation generates a smaller compartment (SC) and a larger mother cell (MC); (II) the MC engulfs the SC (now the forespore) in a phagocytic-like event resulting in a forespore being wholly contained within the MC's cytoplasm; (III) the spore cortex and coat layers are assembled; (IV) the MC lyses and releases the mature spore into the surrounding environment. Though the mechanisms that initiate spore formation may differ between organisms, the overall spore architecture is conserved among endospore-forming bacteria. Located in the center of the mature spore is the core. The spore core contains the genomic DNA, mRNA, ribosomes, protein, and is very rich in pyridine-2,6-dicarboxylic acid (DPA), commonly as a calcium salt (CaDPA). The spore core is surrounded by an inner membrane, a peptidoglycan-containing germ cell wall, a specialized peptidoglycan-containing cortex, an outer membrane and layers of coat protein (**Figure 1**; Edwards and McBride, 2014; Gil et al., 2017). In some *C. difficile* strains, an exosporium layer surrounds the coat, but not all spore-forming bacteria and not all *C. difficile* strains have this layer (thus this layer is not shown in **Figure 1**).

Regulator CodY and CcpA

Environmental stimuli (e.g., nutrient deprivation or quorum sensing) could trigger *C. difficile* sporulation. Previous studies in *Bacillus* and *Clostridioides* species have revealed that the CodY and CcpA nutritional sensor proteins work as negative regulators of sporulation (**Figure 2**; Duncan et al., 1995; Hofmeister et al., 1995; Karow et al., 1995; Londoño-Vallejo and Stragier, 1995; Antunes et al., 2012; Nawrocki et al., 2016; Serrano et al., 2016). Among the genes CodY regulates are genes involved in spore formation including *spo0A*, *rapA*, *rapC*, *rapE*, *sinI/R*, *sigH*, and *kinB*. Recently, Edwards et al. demonstrated that the oligopeptide permease genes *app* and *opp*, and the putative sporulation regulator genes *sinI* and *sinR*, were regulated by CodY to suppress the initiation of *C. difficile* sporulation (Edwards et al., 2014). Previous studies indicated that the variability of CodY-dependent regulation is an important contributor to virulence and sporulation in current epidemic isolates (Bennett et al., 2007; Majerczyk et al., 2008; van Schaik et al., 2009). But, to date, the regulatory mechanisms by which CodY affects sporulation are not fully understood because the factors that initiate sporulation in *C. difficile* are still being identified.

CcpA, a LacI family DNA-binding transcriptional regulator, works as a global transcriptional regulator that responds to the availability of carbohydrates (Deutscher et al., 2006). The CcpA sequence and structure are conserved in *C. difficile*, and has high homology to other pathogens (identity $\geq$62% analyzed with NCBI website), such as *Staphylococcus aureus*, *Clostridium perfringens,* and *Clostridium perfringens*. CcpA represses the use of alternative carbon sources and positively regulates sugar uptake, fermentation, and amino acid metabolism (Fujita, 2009). In the past few years, CcpA has been shown to regulate several virulence-associated genes. For example, it regulates the expression of the *S. aureus* α-hemolysin (*hla*), enterotoxins A, B, and C (*sea*, *seb*, and *sec*) genes, the *C. perfringens* enterotoxin (*cpe*) gene, and the *Bacillus anthracis atxA* and protective antigen (*pagA*) genes (Varga et al., 2004; Seidl et al., 2006; Chiang et al., 2011). Moreover, CcpA also plays critical role in the control of colonization, antibiotic resistance, and biofilm formation (Seidl et al., 2006; Varga et al., 2008). In *C. difficile,* CcpA directly regulates the PaLoc genes (*tcdR*, *tcdB*, *tcdA,* and *tcdC*) to mediate glucose-dependent repression of toxin production and indirectly regulates *C. difficile* sporulation (Antunes et al., 2011).

Sporulation Progress

Studies have revealed the master transcriptional regulator Spo0A plays the critical role during *C. difficile* sporulation (Deakin et al., 2012). In all studied endospore-forming bacteria, Spo0A must be phosphorylated (Spo0A-P) by a histidine kinase to become

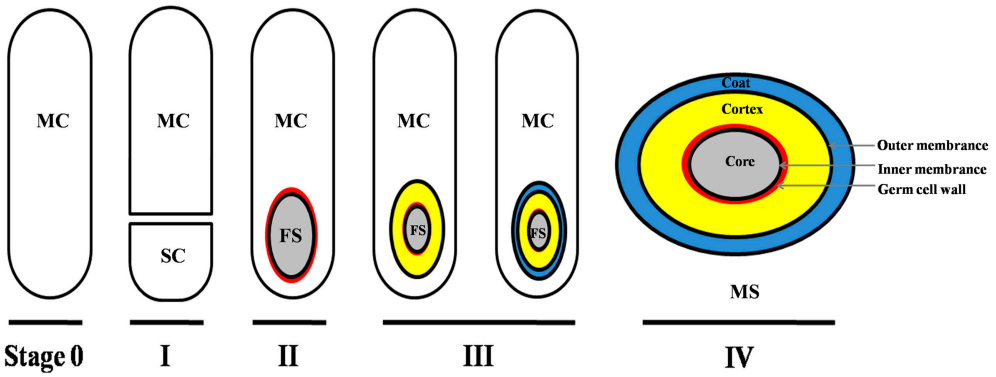

FIGURE 1 | Main morphogenetic stages of the sporulation process and structure of *C. difficile* spore. This figure was drawn based on the references (Edwards and McBride, 2014; Gil et al., 2017). The main layers of spore structure are shown in this figure (IV). Some *C. difficile* strains have exosporium, while some have not. The exosporium structure was not shown in this figure. MC, mother cell compartment; SC, smaller compartment; FS, forespore compartment; MS, mature spore.

activated. In *Bacilli*, these histidine kinases (Kin) are found on the plasma membrane and lead to the phosphorylation of Spo0A through Spo0F/Spo0B phosphotransfer system. *C. difficile* does not encode orthologs of these kinases or the phosphotransfer system. However, previous studies have demonstrated five putative orphan histidine kinases {CD1352 [CD630_13520; *cprK* (McBride and Sonenshein, 2011)], CD1492 (CD630_14920), CD1579 (CD630_15790), CD1949 (CD630_19490), and CD2492 (CD630_24920)} in *C. difficile* strain 630 genome that could potentially phosphorylate Spo0A (**Figure 2**; Underwood et al., 2009). A ClosTron mutation in CD2492 (CD630_24920) resulted in a decreased capacity of the resulting strain to generate spores compared to the WT parent. However, this mutant still generated spores (∼4%) suggesting that other histidine kinases can phosphorylate Spo0A or lead to Spo0A phosphorylation (Underwood et al., 2009). In support of this hypothesis, CD1579 (CD630_15790) was shown to autophosphorylate and transfer a phosphate directly to Spo0A (Underwood et al., 2009). Importantly though, the authors did not complement their CD2492 ClosTron mutation, which could have polar effects on downstream genes. In contrast, Childress et al. found that a markerless deletion of CD1492 (CD630_14920) was an inhibitor of sporulation and suppresses spore formation (Childress et al., 2016). This phenotype could be complemented by expression of the wild type allele. Currently, the function of the other putative orphan histidine kinases and their ability to phosphorylate Spo0A are unclear.

Recently, RstA was found to be a novel, positive regulator of sporulation initiation in *C. difficile* (**Figure 2**; Edwards et al., 2016). RstA positively affects the initiation of *C. difficile* sporulation through its peptide-interacting domain (TPR), and negatively regulates toxin production and mobility by affecting the flagellar-specific sigma factor (SigD) expression. But a detailed pathway on the regulation of sporulation initiation by RstA is not fully appreciated. The authors hypothesized that RstA may be a *C. difficile* global transcriptional regulator, similar to the broad physiological roles that the RNPP (Rap/NprR/PlcR/PrgX) proteins play in other bacteria (Edwards et al., 2016).

Spo0A functions as a critical regulator for sporulation by regulating sporulation-specific RNA polymerase sigma factors, especially for σ^E, σ^F, σ^G, and σ^K (Fimlaid and Shen, 2015). These σ factors activate compartment-specific transcriptional regulation during *B. subtilis* sporulation and are also conserved in *Clostridium* species. σ^E and σ^K are MC-specific, and σ^F and σ^G are specific to the developing forespore. The sporulation regulatory pathway of sigma factors in *C. difficile* is illustrated in **Figure 2**: (1) σ^F is activated in the forespore soon after polar septation, and it controls early stages of development in this compartment. σ^F becomes active when the anti-sigma factor SpoIIAB (ADP form) binds to the anti-anti-sigma factor SpoIIAA in its unphosphorylated form, while SpoIIE catalyzes dephosphorylation; (2) σ^F activity leads to expression of SpoIIR, which interacts with the membrane-bound protease SpoIIGA (SpoIIGA is responsible for the cleavage of pro-σ^E through trans-septum signaling, yielding active σ^E); (3) after σ^F and σ^E become specifically active in the forespore and MC, respectively, the MC engulfs the forespore; (4) σ^E activity leads to expression of SpoIIIA-H, which works with σ^F-controlled SpoIIQ to form a channel in the inner and outer forespore membranes. SpoIIIAH and SpoIIQ localize to the asymmetric septum and the engulfing membranes and interact in the intermembrane space via their extracytoplasmic domains; (5) σ^E-controlled SpoIIID activates σ^K in the MC (Haraldsen and Sonenshein, 2003; Fimlaid et al., 2013; Pereira et al., 2013; Paredes-Sabja et al., 2014; Saujet et al., 2014). Though many of the factors that control spore formation are conserved in *C. difficile*, there are some differences in the sporulation program between *C. difficile* and *B. subtilis*. For instance (**Figure 2**), pro-σ^k is not encoded by *C. difficile*, but the mature σ^k is produced directly in *C. difficile*, σ^E activation is dispensable for σ^G activation, σ^G activation is dispensable for σ^K activation, and σ^K is responsible for transcribing the germinant receptors while σ^G is responsible in *B. subtilis* (Fimlaid et al., 2013; Pereira et al., 2013). Importantly, the FS line of gene expression occurs largely independently of the MC line of gene expression. Moreover, σ^G can be activated before σ^E and σ^K, indicating that the order/sequence of sigma factor

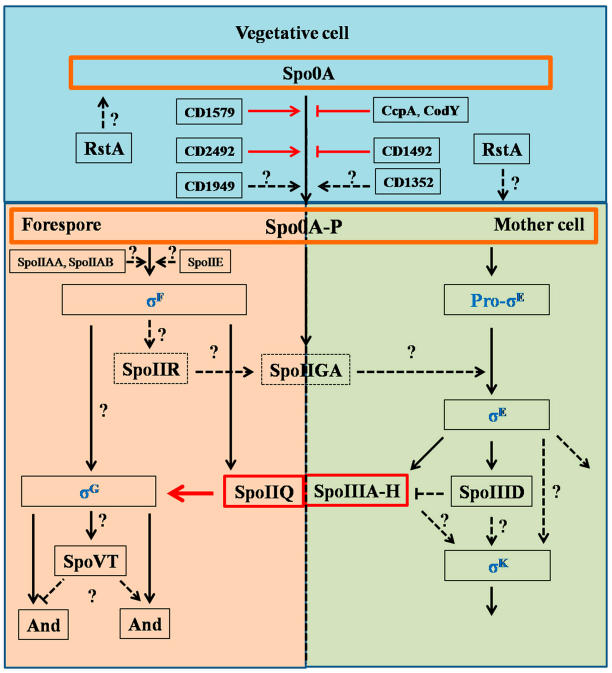

FIGURE 2 | Regulation pathways of *C. difficile* sporulation. This figure was drawn based on the references (Fimlaid et al., 2013; Fimlaid and Shen, 2015). Regulation of box SpoIIQ, SpoIIA-H, CD1579 (CD630_15790), CD1492 (CD630_14920), CD2492 (CD630_24920), CcpA, CodY, and RstA were added in this figure based on the recent advances in *C. difficile* sporulation. CD1492 (CD630_14920), CcpA, and CodY were the negative regulators in sporulation pathways. Function of SpoIIQ-SpoIIAH complex was characterized by Pinho group, recently (Serrano et al., 2016). Spo0A and Spo0A-P were scheduled in orange boxes, four sigma factors were colored in blue. Dashed boxes indicate that the function of the proteins in regulation pathways has not been identified. Black arrows indicate the regulatory relationship between the factors has been confirmed, dashed arrows indicate the regulatory relationship between the factors has not been tested, red arrows, stops and boxes indicate the function of proteins and the correlation of factors has been confirmed recently. Question marks indicate that there is suggestive, but no conclusive experimental evidence.

activation is not as tightly controlled in *C. difficile* as it is in *B. subtilis*.

Finally, and in another departure from the model of spore formation in *B. subtilis*, a recent article by Ribis and colleagues used a TargeTron-based gene disruption demonstrated that the SpoVM protein is not required for spore formation/maturation (Ribis et al., 2017). SpoVM is a small protein that is expressed in the MC that recognizes the positive curvature of outer membrane of the developing forespore and embeds itself there. In *B. subtilis*, SpoVM recruits the SpoIVA scaffolding protein which polymerizes and surrounds the forespore. Subsequently, the coat is deposited onto the polymerized SpoIVA protein. In *C. difficile*, a *spoVM* mutation resulted in a modest defect in spore production (<5-fold), but their resistance properties are not different from a wildtype spore. This phenotype could be complemented through chromosomal complementation of the wild type allele. However, and importantly, the mutation in *spoVM* lead to a mislocalization of the coat proteins to one pole of the developing forespore and the coat extended into the MC cytoplasm; SpoIVA still polymerized on the surface of the forespore.

C. DIFFICILE SPORE GERMINATION

Germination Program

In most organisms, spore germination is induced when specific germinant receptors sense the presence of small molecules (germinants; Setlow, 2003). To date, germination has been most-studied in *Bacillus* spp. and it contains three main steps (Paredes-Sabja et al., 2011, 2014): (I) germinant (e.g., nucleosides, sugars, amino acids, and/or ions) binding with their cognate Ger-type receptors (GerAA-AB-AC) at the inner spore membrane to trigger the release of monovalent cations (H^+, Na^+, and K^+) and the large amount of CaDPA stored within the core, in exchange for water; (II) CaDPA release and core rehydration leads to the activation of spore cortex lytic enzymes (SCLEs) SleB and CwlJ; (III) activated SleB and CwlJ degrade the peptidoglycan cortex layer, which allows for full core rehydration and resumption of metabolism in the spore core.

Germinant Recognition/Signaling

Germination of *C. difficile* spores is the first step for initiating CDI. *C. difficile* spore germination is activated in response to certain host-derived bile salt germinants [e.g., taurocholic acid (TCA)/cholic acid derivatives] and amino acids (e.g., glycine or alanine; Sorg and Sonenshein, 2008). Chenodeoxycholic acid-derivatives (a compound structurally similar to cholic acid but lacking the 12α-hydroxyl group) are competitive inhibitors of cholic acid-mediated germination (Francis et al., 2013b). Though the Ger-type germinant receptors have been widely studied in many organisms, including *C. perfringens* and *Clostridium botulinum/sporogenes*, *C. difficile* does not encode orthologs of the *gerA* germinant. Instead, *C. difficile* spores use the subtilisin-like, CspC pseudoprotease as the bile acid germinant receptor (**Figure 3**; Paredes-Sabja et al., 2008; Francis et al., 2013a, 2015; Wang S. W. et al., 2015; Bhattacharjee et al., 2016; Francis and Sorg, 2016). *C. difficile* packages three subtilisin-like serine proteases proteins, CspA, CspB, and CspC, into the spore. In *C. difficile*, CspB, and CspA are encoded as a *cspBA* gene fusion, where the CspA portion of CspBA lacks an intact catalytic triad (Adams et al., 2013; Kevorkian et al., 2016). The CspBA fusion protein undergoes interdomain cleavage during spore formation, leading to the separation of CspB and CspA, which are transported into the spore by unknown mechanisms. *cspC* is encoded downstream of *cspBA* and, similar to *cspA*, encodes an incomplete catalytic triad. Despite the loss of apparent catalytic activity, *cspC* (and *cspA*) important for *C. difficile* spore germination. Interruption of the *cspC* coding region through ethyl methanesulfonate (EMS)-generated SNPs and TargeTron methods abrogates spore germination, and certain SNPs in the *cspC* sequence also affect germinant specificity (Francis et al., 2013a). Similarly, though *cspA* lacks an intact catalytic triad, *cspA* is essential for spore germination by controlling the levels of CspC into the developing spore (Francis et al., 2013a; Kevorkian et al., 2016). Only CspB contains an intact catalytic triad and,

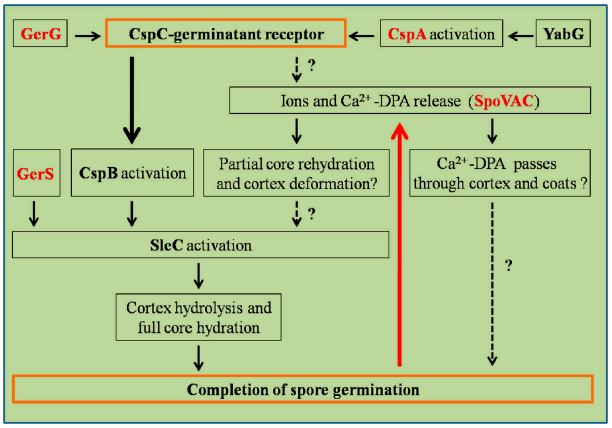

FIGURE 3 | Regulation pathways of *C. difficile* spore germination. This figure was drawn based on the references (Paredes-Sabja et al., 2011; Fimlaid et al., 2013). Regulation of box GerG, GerS, CspA, and SpoVAC texted in red were drawn in this figure based on the recent advances in *C. difficile* spore germination. GerS, GerG, and SpoVAC proteins were characterized by Shen group, recently (Fimlaid et al., 2015; Donnelly et al., 2016, 2017). CspC-germinant receptor and completion of germination were scheduled in the orange boxes. Black arrows indicate the regulatory relationship between the factors has been confirmed, dashed arrows indicate the regulatory relationship between the factors has not been tested. Thick black/red arrow indicates central signal pathway in germination progress. Question marks indicate that there is suggestive, but no conclusive experimental evidence.

thus, is hypothesized to be important for activating the SCLE, pro-SleC, to its active, cortex-degrading form (Kevorkian et al., 2016).

Activation of the cortex hydrolase SleC depends on the CspB protease, which cleaves the N-terminal pro sequence from the protein. Activated SleC degrades the cortex leading to CaDPA release from the spore core in response to osmotic swelling sensed at the inner spore membrane as a result of cortex degradation (Francis and Sorg, 2016). The osmotic pressure at the inner spore membrane is regulated by SpoVAC (a mechanosensing protein), which allows CaDPA release from the core (Velásquez et al., 2014; Donnelly et al., 2016; Francis and Sorg, 2016). Strikingly, inactivation of either the CspC or SleC inhibited cortex degradation and CaDPA release. These results suggest that the CspC is required for CaDPA release and that cortex degradation precedes CaDPA release, opposite to what occurs in *B. subtilis* (Francis and Sorg, 2016). These studies suggest that the process of *C. difficile* spore germination appears to occur in an outside-in manner, while in *B. subtilis*, the signal appears to travel from the inside-out (Francis and Sorg, 2016).

GerG and GerS Regulators of Spore Germination

Recently, GerG and GerS were identified as important players in *C. difficile* spore germination (**Figure 3**; Fimlaid et al., 2015; Donnelly et al., 2017). Donnelly et al. identified the *C. difficile*-specific protein GerG as an important player in the *C. difficile* germination process (Donnelly et al., 2017). A deletion of *C. difficile gerG* resulted in spores with germination defects and reduced responsiveness to bile salt germinants. This phenotype was likely due to the decrease in the incorporation of the CspC, CspB, and CspA germination proteins into spores; this phenotype could be complemented *in trans*. Similarly, Fimlaid et al. identified another regulator of *C. difficile* spore germination using TargeTron-based gene disruption (Fimlaid et al., 2015). The GerS lipoprotein functions as a critical regulator in *C. difficile* spore germination (Fimlaid et al., 2015). In this study, the *gerS* mutant has a severe germination defect and fails to degrade cortex; this phenotype could be complemented *in trans*. Interestingly, *C. difficile gerS* mutant spores still cleave pro-SleC to its active form, suggesting that either cortex is not appropriately modified for SleC-recognition or that SleC is bound to other proteins that GerS regulates (Fimlaid et al., 2015). Importantly, loss of GerS attenuated the *C. difficile* virulence in the hamster infection model (Fimlaid et al., 2015). Because GerG and GerS are found exclusively in *C. difficile*, GerG and GerS proteins could be the potential targets to develop *C. difficile*-specific anti-infective therapies.

Activators and Inhibitors of *C. difficile* Spore Germination

Bile-acid mediated germination is essential for *C. difficile* spore germination and CDI in mammalian GI tract. Bile acids are the end products of cholesterol metabolism in liver and are essential for lipoprotein, glucose, drug, and energy metabolism (Chiang, 2009; Howerton et al., 2011). In humans, cholic acid (CA) and chenodeoxycholic acid (CDCA) are two main primary bile acids (PBAs) that are conjugated with either taurine or glycine. Though most of the bile acids secreted into the gut are reabsorbed and recycled back to the liver to be used in other rounds of digestion, some escape hepatic recirculation and enter the large intestine where they become acted upon by the colonic microbiome. Here, the conjugated bile acids become deconjugated due to the action of bile salt hydrolases that are expressed on the cell surfaces of many different bacteria. Subsequently, a small subset of the colonic microbiome will take up and 7α-dehydroxylate the PBAs to form secondary bile acids (SBAs; Ridlon et al., 2006). About 50 different chemically distinct SBAs [e.g., deoxycholate (DCA), lithocholate (LCA), ursodeoxycholate (UDCA), isodeoxycholate (iDCA), and isolithocholate (iLCA)] can be found in human large intestine (Setchell et al., 1983). Recently, Thanissery et al. have analyzed the impact of gut microbial derived SBAs on *C. difficile* life cycle, specifically, the differences in inhibition efficiency of spore germination, growth, and toxin activity among of DCA, iDCA, LCA, iLCA, UDCA, ωMCA, and HDCA in clinically relevant *C. difficile* strains R20291 and CD196 (ribotype 027), M68 and CF5 (017), 630 (012), BI9 (001), and M120 (078) (Thanissery et al., 2017). Not surprisingly, the authors found these cholic acid- and chenodeoxycholic acid-derivatives all impacted the *C. difficile* life cycle; the sensitivity varied by strain and SBA.

Although bile acids are essential to activate *C. difficile* spore germination, they are not sufficient to activate germination on

their own. Amino acid co-germinants are also required for spore germination (Sorg and Sonenshein, 2008; Howerton et al., 2011; Shrestha and Sorg, 2017; Shrestha et al., 2017). However, different amino acids function as co-germinants with different spore germination efficiencies. Glycine is the most effective co-germinant in *C. difficile*, while alanine is most-often used as co-germinant in *B. subtilis* and other organisms. In *B. subtilis*, L-alanine interacts with the GerAA-AB-AC germinant receptor to trigger CaDPA release from the spore core and subsequent cortex hydrolysis. However, D-alanine competitively-inhibits L-alanine-mediated spore germination in *B. subtilis* (Yasuda and Tochikubo, 1984). In *C. difficile*, L-alanine can also function as a co-germinant with TCA to stimulate spore germination (Shrestha et al., 2017). Though D-alanine is unable to inhibit L-alanine-mediated *C. difficile* spore germination, unlike what is observed in *B. subtilis*, D-alanine can work as a co-germinant to trigger *C. difficile* spore germination in defined medium (Shrestha and Sorg, 2017; Shrestha et al., 2017). In order for D-alanine to function as a good co-germinant, an alanine racemase (Alr2) should be present in the *C. difficile* spore. Alr2 interconverts L-alanine and D-alanine (Shrestha et al., 2017). Interestingly, *C. difficile* Alr2 can also interconvert L- and D-serine, and both of these amino acids can act as co-germinants for *C. difficile* spore germination (Shrestha et al., 2017). Building on this work, Shrestha et al. found that many different amino acids are co-germinants when tested at 37°C (Shrestha and Sorg, 2017). In this work, two different *C. difficile* strains responded to a hierarchy of amino acid co-germinants. For UK1 and M68 strains, glycine was the most effective co-germinant (EC_{50} = ∼200 μM) and L-alanine, taurine, and L-glutamine were also good co-germinants (Shrestha and Sorg, 2017). Interestingly, amino acids that regulate important physiological processes were not co-germinants (L-isoleucine, L-leucine and L-valine).

Recently, Kochan et al. identified a critical role for Ca^{2+} during *C. difficile* spore germination (Kochan et al., 2017). In their study, they found that *C. difficile* spores cannot germinate in rich medium supplemented with TCA but without Ca^{2+}, indicating that Ca^{2+} is indispensable for spore germination. The authors suggested that it works together with glycine to stimulate germination; however, Ca^{2+} may play a role in the activity of the CspB serine protease, the CspC germinant receptor, the CspA pseudoprotease, or in the activity of the cortex hydrolase. Other subtilisin-like proteases require Ca^{2+} for activity (Siezen and Leunissen, 1997) and some cortex-degrading enzymes also require Ca^{2+}. Though no Ca^{2+} was found in the CspB crystal structure, the structures of CspC and CspA have yet to be determined. Thus, Ca^{2+} may not function as a co-germinant with glycine, but, rather, as an essential cofactor for *C. difficile* spore germination. However, and importantly, the role of Ca^{2+} during *C. difficile* spore germination was also verified in the murine model. *Ex vivo* assays with mouse ileal contents that were depleted with chelex resin (to remove Ca^{2+}) did not support germination of *C. difficile* spores (Kochan et al., 2017). This work provided a novel potential strategy for CDI control by modulating intestinal Ca^{2+} concentration.

In summary, although several main components of spore sporulation/germination machinery of *C. difficile* have been identified and characterized, several questions remain regarding how *C. difficile* decides when to enter the sporulation pathway. Moreover, though the Csp pseudoproteases are important for germination, how they interact with and transmit the bile acid signal are still unknown. Further detailed work is necessary to characterize these important aspects of *C. difficile* physiology.

TREATMENTS OF CDI BASED ON SPORULATION/GERMINATION

Currently, the standard treatment of CDI is the use of vancomycin, metronidazole, or fidaxomicin, each of which has some level of recurring disease due to the continued insult to the colonic microbiome and the presence of spores within the colon/environment (Allen et al., 2013). To meet this challenge, non-antibiotic and immune-based therapies against CDI have been developed, such as anti-toxins, vaccines, fecal microbiota transplant (FMT), and anti-germination-based compounds (Gerding et al., 2008; Howerton et al., 2013; Kociolek and Gerding, 2016). Many anti-toxins and vaccines for CDI have been developed in the past two decades (Cox et al., 2013; Monteiro et al., 2013; Mathur et al., 2014; Zhao et al., 2014; Wang Y. K. et al., 2015; Yang et al., 2015; Qiu et al., 2016). Though these treatments can effectively decrease the morbidity and mortality of CDI, most of the anti-toxins and vaccines cannot suppress *C. difficile* colonization and kill *C. difficile* spores. Therefore, with these treatments, there are still risks of potential CDI relapse in the host.

Instead of merely neutralizing *C. difficile* toxins in host, strategies which can directly decrease *C. difficile* colonization, kill the vegetative cells, and suppress sporulation/germination are desirable treatments for CDI. FMT is an effective strategy to reconstruct the gut microbiota to suppress *C. difficile* colonization, especially for patients who have multiple bouts of recurring disease and who have failed conventional treatment methods (Borody and Khoruts, 2012; Weingarden et al., 2014; Khoruts and Sadowsky, 2016; Kim et al., 2016). Although FMT is deemed relatively safe and low-cost, the unappealing aesthetics of the procedure is often a concern of patients (Sampath et al., 2013; Varier et al., 2015). Because the *C. difficile* spore form is necessary for dissemination and persistence, sporulation/germination are critical steps for CDI. Thus, it is worth developing therapeutic strategies for disrupting *C. difficile* disease transmission and spread according to *C. difficile* spore biology. Basing on the progress of *C. difficile* spore germination, the PBA CDCA and secondary bile acids LCA, UDCA, and iLCA are potent inhibitors of *C. difficile* spore germination (Sorg and Sonenshein, 2010; Zhang and Klaassen, 2010; Heeg et al., 2012). Moreover, several mouse-derived bile acids, such as α-muricholic acid, β-muricholic acid, and ω-muricholic acid inhibit *C. difficile* spore germination and growth (Francis et al., 2013b). Excitingly, synthesized bile acid analogs, such as CAmSA, methylchenodeoxycholic acid diacetate, and compound

21b (derived from UDCA) have been identified to inhibit *C. difficile* spore germination (Sorg and Sonenshein, 2009; Howerton et al., 2013; Stoltz et al., 2017). Of these compounds, CAmSA showed promise in inhibiting/delaying *C. difficile* disease in a mouse model of CDI. These anti-germination-based strategies could work in a couple of different ways. (i) High risk patients who are to be treated with antibiotics could also take an anti-germinant to prevent the germination of spores within the host's gut. This patient continues to take the anti-germinant during and post-antibiotic treatment so that the normal, colonic, microbiome has a chance to repopulate and provide natural protection against CDI. (ii) Patients with CDI could take the recommended course of antibiotics plus the anti-germinants. This strategy would prevent recurring disease by allowing the microbiome to re-establish colonization resistance post-antibiotic treatment. Because both strategies block germination, and thus downstream events (vegetative growth, toxin production, and spore formation), anti-germination therapy would limit the presence of spores within the surrounding environment because *C. difficile* would not have a chance to expand in population and produce spores. In contrast germination-inducing strategies are a viable option for environmental cleanup; inducing *in vivo* germination has the potential for toxin-production and, thus, exacerbation of symptoms. Due to the inherent nature of the dormant spore, harsh chemicals (e.g., bleach) are required to clean environmental surfaces. But by germinating the spores in the environment, the germinated spores become susceptible to a wider range of sanitizing agents (Nerandzic and Donskey, 2010, 2013, 2017; Nerandzic et al., 2016). More studies should be investigated for further application of germination inhibitors.

CONCLUDING AND REMARKS

Although much has been learned about the sporulation/germination processes of *C. difficile* and the different therapeutic strategies for CDI, many key questions related to regulation pathways of sporulation/germination processes remain unanswered. Thus, much work remains to be done to further understand *C. difficile* spore biology and develop new efficient approaches for CDI treatment: (1) It is expected that further work will allow us to fully understand the mechanisms of the initiation of sporulation by identifying the proteins that are involved in Spo0A phosphorylation; (2) Due to the relevance of spore germination with CDI progression, it is worth defining how the bile acid germinant receptor, CspC, and the unidentified glycine germinant receptor regulate CaDPA release and cortex degradation; (3) More alternative therapeutic strategies for CDI disease need to be developed based on the knowledge of *C. difficile* sporulation/germination.

AUTHOR CONTRIBUTIONS

All authors listed, have made a substantial, direct, and intellectual contribution to the work; DZ wrote and revised this manuscript; JS and XS revised this manuscript.

ACKNOWLEDGMENTS

This work was supported in part by National Institutes of Health grants (K01-DK092352, R21-AI113470, R03-DK112004, R01-AI132711) to XS, and was also supported by awards 5R01AI116895 and 1U01AI124290 to JS from the National Institute of Allergy and Infectious Diseases.

REFERENCES

Adams, C. M., Eckenroth, B. E., Putnam, E. E., Doublie, S., and Shen, A. (2013). Structural and functional analysis of the CspB protease required for Clostridium spore germination. *PLoS Pathog.* 9:e1003165. doi: 10.1371/journal.ppat.1003165

Allen, C. A., Babakhani, F., Sears, P., Nguyen, L., and Sorg, J. A. (2013). Both fidaxomicin and vancomycin inhibit outgrowth of *Clostridium difficile* spores. *Antimicrob. Agents Ch*. 57, 664–667. doi: 10.1128/AAC.01611-12

Antunes, A., Martin-Verstraete, I., and Dupuy, B. (2011). CcpA-mediated repression of *Clostridium difficile* toxin gene expression. *Mol. Microbiol.* 79, 882–899. doi: 10.1111/j.1365-2958.2010.07495.x

Antunes, A., Camiade, E., Monot, M., Courtois, E., Barbut, F., Sernova, N. V., et al. (2012). Global transcriptional control by glucose and carbon regulator CcpA in *Clostridium difficile*. *Nucleic Acids Res.* 40, 10701–10718. doi: 10.1093/nar/gks864

Bennett, H. J., Pearce, D. M., Glenn, S., Taylor, C. M., Kuhn, M., Sonenshein, A. L., et al. (2007). Characterization of relA and codY mutants of *Listeria monocytogenes*: identification of the CodY regulon and its role in virulence. *Mol. Microbiol.* 63, 1453–1467. doi: 10.1111/j.1365-2958.2007.05597.x

Bhattacharjee, D., McAllister, K. N., and Sorg, J. A. (2016). Germinants and their receptors in Clostridia. *J. Bacteriol.* 198, 2767–2775. doi: 10.1128/JB.00405-16

Borody, T. J., and Khoruts, A. (2012). Fecal microbiota transplantation and emerging applications. *Nat. Rev. Gastroenterol. Hepatol.* 9, 88–96. doi: 10.1038/nrgastro.2011.244

Britton, R. A., and Young, V. B. (2012). Interaction between the intestinal microbiota and host in *Clostridium difficile* colonization resistance. *Trends Microbiol.* 20, 313–319. doi: 10.1016/j.tim.2012.04.001

Centres for Disease Control and Prevention (US) (2013). *Antibiotic Resistance Threats in the United States, 2013*. Atlanta, GA: Centres for Disease Control and Prevention, US Department of Health and Human Services.

Chiang, C., Bongiorni, C., and Perego, M. (2011). Glucose-dependent Aactivation of *Bacillus anthracis* toxin gene expression and virulence requires the carbon catabolite protein CcpA. *J. Bacteriol.* 193, 52–62. doi: 10.1128/JB.01656-09

Chiang, J. Y. (2009). Bile acids: regulation of synthesis. *J. Lipid Res.* 50, 1955–1966. doi: 10.1194/jlr.R900010-JLR200

Childress, K. O., Edwards, A. N., Nawrocki, K. L., Anderson, S. E., Woods, E. C., and McBride, S. M. (2016). The phosphotransfer protein CD1492 represses sporulation initiation in *Clostridium difficile*. *Infect. Immun.* 84, 3434–3444. doi: 10.1128/IAI.00735-16

Cornely, O. A., Miller, M. A., Louie, T. J., Crook, D. W., and Gorbach, S. L. (2012). Treatment of first recurrence of *Clostridium difficile* infection: fidaxomicin versus vancomycin. *Clin. Infect. Dis.* 55, S154–S161. doi: 10.1093/cid/cis462

Cox, A. D., St Michael, F., Aubry, A., Cairns, C. M., Strong, P. C., Hayes, A. C., et al. (2013). Investigating the candidacy of a lipoteichoic acid-based glycoconjugate as a vaccine to combat *Clostridium difficile* infection. *Glycoconjugate J.* 30, 843–855. doi: 10.1007/s10719-013-9489-3

Darkoh, C., Odo, C., and DuPont, H. L. (2016). Accessory gene regulator-1 locus is essential for virulence and pathogenesis of *Clostridium difficile*. *Mbio* 7:e01237. doi: 10.1128/mBio.01237-16

Deakin, L. J., Clare, S., Fagan, R. P., Dawson, L. F., Pickard, D. J., West, M. R., et al. (2012). The *Clostridium difficile* spo0A gene is a persistence and transmission factor. *Infect. Immun.* 80, 2704–2711. doi: 10.1128/IAI.00147-12

Deutscher, J., Francke, C., and Postma, P. W. (2006). How phosphotransferase system-related protein phosphorylation regulates carbohydrate metabolism in bacteria. *Microbiol. Mol. Biol. R.* 70, 939–1031. doi: 10.1128/MMBR.00024-06

Donnelly, M. L., Fimlaid, K. A., and Shen, A. (2016). Characterization of *Clostridium difficile* spores lacking either SpoVAC or dipicolinic acid synthetase. *J. Bacteriol.* 198, 1694–1707. doi: 10.1128/JB.00986-15

Donnelly, M. L., Li, W., Li, Y. Q., Hinkel, L., Setlow, P., and Shen, A. (2017). A *Clostridium difficile*-specific, gel-forming protein required for optimal spore germination. *Mbio* 8:e02085-16. doi: 10.1128/mBio.02085-16

Dubberke, E. R., and Olsen, M. A. (2012). Burden of *Clostridium difficile* on the healthcare system. *Clin. Infect. Dis.* 55, S88–SS92. doi: 10.1093/cid/cis335

Duncan, L., Alper, S., Arigoni, F., Losick, R., and Stragier, P. (1995). Activation of cell-specific transcription by a serine phosphatase at the site of asymmetric division. *Science* 270, 641–644. doi: 10.1126/science.270.5236.641

Edwards, A. N., and McBride, S. M. (2014). Initiation of sporulation in *Clostridium difficile*: a twist on the classic model. *FEMS Microbiol. Lett.* 358, 110–118. doi: 10.1111/1574-6968.12499

Edwards, A. N., Nawrocki, K. L., and McBride, S. M. (2014). Conserved oligopeptide permeases modulate sporulation initiation in *Clostridium difficile*. *Infect. Immun.* 82, 4276–4291. doi: 10.1128/IAI.02323-14

Edwards, A. N., Tamayo, R., and McBride, S. M. (2016). A novel regulator controls *Clostridium difficile* sporulation, motility and toxin production. *Mol. Microbiol.* 100, 954–971. doi: 10.1111/mmi.13361

Evans, C. T., and Safdar, N. (2015). Current trends in the epidemiology and outcomes of *Clostridium difficile* infection. *Clin. Infect. Dis.* 60, S66–S71. doi: 10.1093/cid/civ140

Fimlaid, K. A., and Shen, A. (2015). Diverse mechanisms regulate sporulation sigma factor activity in the Firmicutes. *Curr. Opin. Microbiol.* 24, 88–95. doi: 10.1016/j.mib.2015.01.006

Fimlaid, K. A., Bond, J. P., Schutz, K. C., Putnam, E. E., Leung, J. M., Lawley, T. D., et al. (2013). Global analysis of the sporulation pathway of *Clostridium difficile*. *PLoS Genet.* 9:e1003660. doi: 10.1371/journal.pgen.1003660

Fimlaid, K. A., Jensen, O., Donnelly, M. L., Francis, M. B., Sorg, J. A., and Shen, A. (2015). Identification of a novel lipoprotein regulator of *Clostridium difficile* spore germination. *PLoS Pathog.* 11:e1005239. doi: 10.1371/journal.ppat.1005239

Francis, M. B., and Sorg, J. A. (2016). Dipicolinic acid release by germinating *Clostridium difficile* spores occurs through a mechanosensing mechanism. *Msphere* 1:e00306-16. doi: 10.1128/mSphere.00306-16

Francis, M. B., Allen, C. A., Shrestha, R., and Sorg, J. A. (2013a). Bile acid recognition by the *Clostridium difficile* germinant receptor, CspC, is important for establishing infection. *PLoS Pathog.* 9:e1003356. doi: 10.1371/journal.ppat.1003356

Francis, M. B., Allen, C. A., and Sorg, J. A. (2013b). Muricholic acids inhibit *Clostridium difficile* spore germination and growth. *PLoS ONE* 8:e7365310. doi: 10.1371/journal.pone.0073653

Francis, M. B., Allen, C. A., and Sorg, J. A. (2015). Spore cortex hydrolysis precedes dipicolinic acid release during *Clostridium difficile* spore germination. *J. Bacteriol.* 197, 2276–2283. doi: 10.1128/JB.02575-14

Fujita, Y. (2009). Carbon catabolite control of the metabolic network in *Bacillus subtilis*. *Biosci. Biotechnol. Biochem.* 73, 245–259. doi: 10.1271/bbb.80479

Gerding, D. N., Muto, C. A., and Owens, R. C. (2008). Treatment of *Clostridium difficile* infection. *Clin. Infect. Dis.* 46, S32–S42. doi: 10.1086/521860

Gil, F., Lagos-Moraga, S., Calderon-Romero, P., Pizarro-Guajardo, M., and Paredes-Sabja, D. (2017). Updates on *Clostridium difficile* spore biology. *Anaerobe* 45, 3–9. doi: 10.1016/j.anaerobe.2017.02.018

Haraldsen, J. D., and Sonenshein, A. L. (2003). Efficient sporulation in *Clostridium difficile* requires disruption of the σK gene. *Mol. Microbiol.* 48, 811–821. doi: 10.1046/j.1365-2958.2003.03471.x

Heeg, D., Burns, D. A., Cartman, S. T., and Minton, N. P. (2012). Spores of *Clostridium difficile* clinical isolates display a diverse germination response to bile salts. *PLoS ONE* 7:e32381. doi: 10.1371/journal.pone.0032381

Higgins, D., and Dworkin, J. (2012). Recent progress in *Bacillus subtilis* sporulation. *FEMS Microbiol. Rev.* 36, 131–148. doi: 10.1111/j.1574-6976.2011.00310.x

Hofmeister, A. E., Londonovallejo, A., Harry, E., Stragier, P., and Losick, R. (1995). Extracellular signal protein triggering the proteolytic activation of a developmental transcription factor in *Bacillus subtilis*. *Cell* 83, 219–226. doi: 10.1016/0092-8674(95)90163-9

Howerton, A., Ramirez, N., and Abel-Santos, E. (2011). Mapping interactions between germinants and *Clostridium difficile* spores. *J. Bacteriol.* 193, 274–282. doi: 10.1128/JB.00980-10

Howerton, A., Patra, M., and Abel-Santos, E. (2013). A new strategy for the prevention of *Clostridium difficile* infection. *J. Infect. Dis.* 207, 1498–1504. doi: 10.1093/infdis/jit068

Johnson, S. (2009). Recurrent *Clostridium difficile* infection: a review of risk factors, treatments, and outcomes. *J. Infect.* 58, 403–410. doi: 10.1016/j.jinf.2009.03.010

Karow, M. L., Glaser, P., and Piggot, P. J. (1995). Identification of a gene, spoIIR that links the activation of σE to the transcriptional activity of σF during sporulation in *Bacillus subtilis*. *Proc. Natl. Acad. Sci. U.S.A.* 92, 2012–2016. doi: 10.1073/pnas.92.6.2012

Kevorkian, Y., Shirley, D. J., and Shen, A. (2016). Regulation of *Clostridium difficile* spore germination by the CspA pseudoprotease domain. *Biochimie* 122, 243–254. doi: 10.1016/j.biochi.2015.07.023

Khoruts, A., and Sadowsky, M. J. (2016). Understanding the mechanisms of faecal microbiota transplantation. *Nat. Rev. Gastroenterol. Hepatol.* 13, 508–516. doi: 10.1038/nrgastro.2016.98

Kim, H. B., Wang, Y., and Sun, X. (2016). A detrimental role of immunosuppressive drug, dexamethasone, during *Clostridium difficile* infection in association with a gastrointestinal microbial shift. *J. Microbiol. Biotechnol.* 26, 567–571. doi: 10.4014/jmb.1512.12017

Kochan, T. J., Somers, M. J., Kaiser, A. M., Shoshiev, M. S., Hagan, A. K., Hastie, J. L., et al. (2017). Intestinal calcium and bile salts facilitate germination of *Clostridium difficile* spores. *PLoS Pathog.* 13:e1006443. doi: 10.1371/journal.ppat.1006443

Kociolek, L. K., and Gerding, D. N. (2016). Breakthroughs in the treatment and prevention of *Clostridium difficile* infection. *Nat. Rev. Gastroenterol. Hepatol.* 13, 150–160. doi: 10.1038/nrgastro.2015.220

Lawson, P. A., Citron, D. M., Tyrrell, K. L., and Finegold, S. M. (2016). Reclassification of *Clostridium difficile* as *Clostridioides difficile* (Hall and O'Toole 1935) Prevot 1938. *Anaerobe* 40, 95–99. doi: 10.1016/j.anaerobe.2016.06.008

Leffler, D. A., and Lamont, J. T. (2015). *Clostridium difficile* infection. *New Engl. J. Med.* 373, 287–288. doi: 10.1056/NEJMra1403772

Lessa, F. C., Gould, C. V., and McDonald, L. C. (2012). Current status of *Clostridium difficile* infection epidemiology. *Clin. Infect. Dis.* 55, S65–S70. doi: 10.1093/cid/cis319

Lessa, F. C., Winston, L. G., McDonald, L. C., and Difficil, E. I. P. C. (2015). Burden of *Clostridium difficile* infection in the United States. *N. Engl. J. Med.* 372, 2369–2370. doi: 10.1056/NEJMoa1408913

Londoño-Vallejo, J. A., and Stragier, P. (1995). Cell-cell signaling pathway activating a developmental transcription factor in *Bacillus subtilis*. *Gene Dev.* 9, 503–508. doi: 10.1101/gad.9.4.503

Majerczyk, C. D., Sadykov, M. R., Luong, T. T., Lee, C., Somerville, G. A., and Sonenshein, A. L. (2008). *Staphylococcus aureus* CodY negatively regulates virulence gene expression. *J. Bacteriol.* 190, 2257–2265. doi: 10.1128/JB.01545-07

Mathur, H., Rea, M. C., Cotter, P. D., Ross, R. P., and Hill, C. (2014). The potential for emerging therapeutic options for *Clostridium difficile* infection. *Gut Microbes* 5, 696–710. doi: 10.4161/19490976.2014.983768

McBride, S. M., and Sonenshein, A. L. (2011). Identification of a genetic locus responsible for antimicrobial peptide resistance in *Clostridium difficile*. *Infect. Immun.* 79, 167–176. doi: 10.1128/IAI.00731-10

Monteiro, M. A., Ma, Z. C., Bertolo, L., Jiao, Y., Arroyo, L., Hodgins, D., et al. (2013). Carbohydrate-based *Clostridium difficile* vaccines. *Expert Rev. Vaccines* 12, 421–431. doi: 10.1586/erv.13.9

Nawrocki, K. L., Edwards, A. N., Daou, N., Bouillaut, L., and McBride, S. M. (2016). CodY-dependent regulation of sporulation in *Clostridium difficile*. *J. Bacteriol.* 198, 2113–2130. doi: 10.1128/JB.00220-16

Nerandzic, M. M., and Donskey, C. J. (2010). Triggering germination represents a novel strategy to enhance killing of *Clostridium difficile* spores. *PLoS ONE* 5:e12285. doi: 10.1371/journal.pone.0012285

Nerandzic, M. M., and Donskey, C. J. (2013). Activate to eradicate: inhibition of *Clostridium difficile* spore outgrowth by the synergistic effects of osmotic activation and nisin. *PLoS ONE* 8:e54740. doi: 10.1371/journal.pone.0054740

Nerandzic, M. M., and Donskey, C. J. (2017). Sensitizing *Clostridium difficile* spores with germinants on skin and environmental surfaces represents a new strategy for reducing spores via ambient mechanisms. *Pathog. Immun*. 2, 404–421 doi: 10.20411/pai.v2i3.221

Nerandzic, M. M., Sankar, C. T., Setlow, P., and Donskey, C. J. (2016). A cumulative spore killing approach: synergistic sporicidal activity of dilute peracetic acid and ethanol at low pH against *Clostridium difficile* and *Bacillus subtilis* spores. *Open Forum. Infect. Dis.* 3:ofv206. doi: 10.1093/ofid/ofv206

Oren, A., and Garrity, G. M. (2016). Notification of changes in taxonomic opinion previously published outside the IJSEM. *Int. J. Syst. Evol. Microbiol.* 66, 2469–2470. doi: 10.1099/ijsem.0.001150

Paredes-Sabja, D., Torres, J. A., Setlow, P., and Sarker, M. R. (2008). *Clostridium perfringens* spore germination: characterization of germinants and their receptors. *J. Bacteriol.* 190, 1190–1201. doi: 10.1128/JB.01748-07

Paredes-Sabja, D., Setlow, P., and Sarker, M. R. (2011). Germination of spores of Bacillales and Clostridiales species: mechanisms and proteins involved. *Trends Microbiol.* 19, 85–94. doi: 10.1016/j.tim.2010.10.004

Paredes-Sabja, D., Shen, A., and Sorg, J. A. (2014). *Clostridium difficile* spore biology: sporulation, germination, and spore structural proteins. *Trends Microbiol.* 22, 406–416. doi: 10.1016/j.tim.2014.04.003

Pereira, F. C., Saujet, L., Tome, A. R., Serrano, M., Monot, M., Couture-Tosi, E., et al. (2013). The spore differentiation pathway in the enteric pathogen *Clostridium difficile*. *PLoS Genet.* 9:e1003782. doi: 10.1371/journal.pgen.1003782

Qiu, H. Y., Cassan, R., Johnstone, D., Han, X. B., Joyee, A. G., McQuoid, M., et al. (2016). Novel *Clostridium difficile* anti-toxin (TcdA and TcdB) humanized monoclonal antibodies demonstrate *in vitro* neutralization across a broad spectrum of clinical strains and *in vivo* potency in a hamster spore challenge model. *PLoS ONE* 11:e0157970. doi: 10.1371/journal.pone.0157970

Ribis, J. W., Ravichandran, P., Putnam, E. E., Pishdadian, K., and Shen, A. (2017). The conserved spore coat protein SpoVM is largely dispensable in *Clostridium difficile* spore formation. *Msphere* 2:e00315-17. doi: 10.1128/mSphere.00315-17

Ridlon, J. M., Kang, D. J., and Hylemon, P. B. (2006). Bile salt biotransformations by human intestinal bacteria. *J. Lipid Res.* 47, 241–259. doi: 10.1194/jlr.R500013-JLR200

Rodriguez-Palacios, A., and LeJeune, J. T. (2011). Moist-heat resistance, spore aging, and superdormancy in *Clostridium difficile*. *Appl. Environ. Microbiol.* 77, 3085–3091. doi: 10.1128/AEM.01589-10

Sampath, K., Levy, L. C., and Gardner, T. B. (2013). Fecal transplantation: beyond the aesthetic. *Gastroenterology* 145, 1151–1153. doi: 10.1053/j.gastro.2013.09.015

Saujet, L., Pereira, F. C., Henriques, A. O., and Martin-Verstraete, I. (2014). The regulatory network controlling spore formation in *Clostridium difficile*. *FEMS Microbiol. Lett.* 358, 1–10. doi: 10.1111/1574-6968.12540

Sebaihia, M., Wren, B. W., Mullany, P., Fairweather, N. F., Minton, N., Stabler, R., et al. (2006). The multidrug-resistant human pathogen *Clostridium difficile* has a highly mobile, mosaic genome. *Nat. Genet.* 38, 779–786. doi: 10.1038/ng1830

Seidl, K., Stucki, M., Ruegg, M., Goerke, C., Wolz, C., Harris, L., et al. (2006). *Staphylococcus aureus* CcpA affects virulence determinant production and antibiotic resistance. *Antimicrob. Agents. Chemother.* 50, 1183–1194. doi: 10.1128/AAC.50.4.1183-1194.2006

Serrano, M., Crawshaw, A. D., Dembek, M., Monteiro, J. M., Pereira, F. C., Pinho, M. G., et al. (2016). The SpoIIQ-SpoIIIAH complex of *Clostridium difficile* controls forespore engulfment and late stages of gene expression and spore morphogenesis. *Mol. Microbiol.* 100, 204–228. doi: 10.1111/mmi.13311

Setchell, K. D., Lawson, A. M., Tanida, N., and Sjovall, J. (1983). General-methods for the analysis of metabolic profiles of bile-acids and related-compounds in feces. *J. Lipid Res.* 24, 1085–1100.

Setlow, P. (2003). Spore germination. *Curr. Opin. Microbiol.* 6, 550–556. doi: 10.1016/j.mib.2003.10.001

Setlow, P. (2006). Spores of *Bacillus subtilis*: their resistance to and killing by radiation, heat and chemicals. *J. Appl. Microbiol.* 101, 514–525. doi: 10.1111/j.1365-2672.2005.02736.x

Shrestha, R., and Sorg, J.A. (2017). Hierarchical recognition of amino acid co-germinants during *Clostridioides difficile* spore germination. *Anaerobe* 49, 41–47. doi: 10.1016/j.anaerobe.2017.12.001

Shrestha, R., Lockless, S. W., and Sorg, J. A. (2017). A *Clostridium difficile* alanine racemase affects spore germination and accommodates serine as a substrate. *J. Biol. Chem.* 292, 10735–10742. doi: 10.1074/jbc.M117.791749

Siezen, R. J., and Leunissen, J. A. (1997). Subtilases: the superfamily of subtilisin-like serine proteases. *Protein Sci.* 6, 501–523. doi: 10.1002/pro.5560060301

Sorg, J. A., and Sonenshein, A. L. (2008). Bile salts and glycine as cogerminants for *Clostridium difficile* spores. *J. Bacteriol.* 190, 2505–2512. doi: 10.1128/JB.01765-07

Sorg, J. A., and Sonenshein, A. L. (2009). Chenodeoxycholate is an inhibitor of *Clostridium difficile* spore germination. *J. Bacteriol.* 191, 1115–1117. doi: 10.1128/JB.01260-08

Sorg, J. A., and Sonenshein, A. L. (2010). Inhibiting the initiation of *Clostridium difficile* spore germination using analogs of chenodeoxycholic acid, a bile acid. *J. Bacteriol.* 192, 4983–4990. doi: 10.1128/JB.00610-10

Stoltz, K. L., Erickson, R., Staley, C., Weingarden, A. R., Romens, E., Steer, C. J., et al. (2017). Synthesis and biological evaluation of bile acid analogues inhibitory to *Clostridium difficile* spore germination. *J. Med. Chem.* 60, 3451–3471. doi: 10.1021/acs.jmedchem.7b00295

Thanissery, R., Winston, J. A., and Theriot, C. M. (2017). Inhibition of spore germination, growth, and toxin activity of clinically relevant C. difficile strains by gut microbiota derived secondary bile acids. *Anaerobe* 45, 86-100. doi: 10.1016/j.anaerobe.2017.03.004

Underwood, S., Guan, S., Vijayasubhash, V., Baines, S. D., Graham, L., Lewis, R. J., et al. (2009). Characterization of the sporulation initiation pathway of *Clostridium difficile* and its role in toxin production. *J. Bacteriol.* 191, 7296–7305. doi: 10.1128/JB.00882-09

van Schaik, W., Chateau, A., Dillies, M. A., Coppee, J. Y., Sonenshein, A. L., and Fouet, A. (2009). The global regulator CodY regulates toxin gene expression in *Bacillus anthracis* and is required for full virulence. *Infect. Immun.* 77, 4437–4445. doi: 10.1128/IAI.00716-09.

Varga, J., Stirewalt, V. L., and Melville, S. B. (2004). The CcpA protein is necessary for efficient sporulation and enterotoxin gene (cpe) regulation in *Clostridium perfringens*. *J. Bacteriol.* 186, 5221–5229. doi: 10.1128/JB.186.16.5221-5229.2004

Varga, J. J., Therit, B., and Melville, S. B. (2008). Type IV Pili and the CcpA protein are needed for maximal biofilm formation by the gram-positive anaerobic pathogen *Clostridium perfringens*. *Infect. Immun.* 76, 4944–4951. doi: 10.1128/IAI.00692-08

Varier, R. U., Biltaji, E., Smith, K. J., Roberts, M. S., Kyle Jensen, M., LaFleur, J., et al. (2015). Cost-effectiveness analysis of fecal microbiota transplantation for recurrent *Clostridium difficile* infection. *Infect. Control Hosp. Epidemiol.* 36, 438–444. doi: 10.1017/ice.2014.80

Velásquez, J., Schuurman-Wolters, G., Birkner, J. P., Abee, T., and Poolman, B. (2014). *Bacillus subtilis* spore protein SpoVAC functions as a mechanosensitive channel. *Mol. Microbiol.* 92, 813–823. doi: 10.1111/mmi.12591

Wang, S., Shen, A., Setlow, P., and Li, Y. Q. (2015). Characterization of the dynamic germination of individual *Clostridium difficile* spores using raman spectroscopy and differential interference contrast microscopy. *J. Bacteriol.* 197, 2361–2373. doi: 10.1128/JB.00200-15

Wang, Y. K., Yan, Y. X., Kim, H. B., Ju, X. H., Zhao, S., Zhang, K., et al. (2015). A chimeric protein comprising the glucosyltransferase and cysteine proteinase domains of toxin B and the receptor binding domain of toxin A induces protective immunity against *Clostridium difficile* infection in mice and hamsters. *Hum. Vacc. Immunother.* 11, 2215–2222. doi: 10.1080/21645515.2015.1052352

Weingarden, A. R., Chen, C., Bobr, A., Yao, D., Lu, Y. W., Nelson, V. M., et al. (2014). Microbiota transplantation restores normal fecal bile acid composition in recurrent *Clostridium difficile* infection. *Am. J. Physiol. Gastrointest Liver Physiol.* 306, G310–G319. doi: 10.1152/ajpgi.00282.2013

Yang, Z. Y., Ramsey, J., Hamza, T., Zhang, Y. R., Li, S., Yfantis, H. G., et al. (2015). Mechanisms of protection against *Clostridium difficile* infection by the

monoclonal antitoxin antibodies actoxumab and bezlotoxumab. *Infect. Immun.* 83, 822–831. doi: 10.1128/IAI.02897-14

Yasuda, Y., and Tochikubo, K. (1984). Relation between D-glucose and L-alanine and D-alanine in the initiation of germination of *Bacillus subtilis* spore. *Microbiol. Immunol.* 28, 197–207. doi: 10.1111/j.1348-0421.1984.tb00671.x

Zhang, Y., and Klaassen, C. D. (2010). Effects of feeding bile acids and a bile acid sequestrant on hepatic bile acid composition in mice. *J. Lipid Res.* 51, 3230–3242. doi: 10.1194/jlr.M007641

Zhao, S., Ghose-Paul, C., Zhang, K., Tzipori, S., and Sun, X. (2014). Immune-based treatment and prevention of *Clostridium difficile* infection. *Hum. Vacc. Immunother.* 10, 3522–3530. doi: 10.4161/21645515.2014.980193

Conflict of Interest Statement: The authors declare that the research was conducted in the absence of any commercial or financial relationships that could be construed as a potential conflict of interest.

Copyright © 2018 Zhu, Sorg and Sun. This is an open-access article distributed under the terms of the Creative Commons Attribution License (CC BY). The use, distribution or reproduction in other forums is permitted, provided the original author(s) and the copyright owner are credited and that the original publication in this journal is cited, in accordance with accepted academic practice. No use, distribution or reproduction is permitted which does not comply with these terms.

frontiers in Cellular and Infection Microbiology

ORIGINAL RESEARCH
published: 23 January 2018
doi: 10.3389/fcimb.2018.00005

Identification and Characterization of Blood and Neutrophil-Associated Microbiomes in Patients with Severe Acute Pancreatitis Using Next-Generation Sequencing

Qiurong Li†, Chenyang Wang†, Chun Tang†, Xiaofan Zhao, Qin He and Jieshou Li*

Research Institute of General Surgery, Jinling Hospital, Medical School, Nanjing University, Nanjing, China

Infectious complications are a leading cause of death for patients with severe acute pancreatitis (SAP). Yet, our knowledge about details of the blood microbial landscape in SAP patients remains limited. Recently, some studies have reported that the peripheral circulation harbors a diverse bacterial community in healthy and septic subjects. The objective of this study was to examine the presence of the blood bacterial microbiome in SAP patients and its potential role in the development of infectious complications. Here we conducted a prospective observational study on a cohort of 50 SAP patients and 12 healthy subjects to profile the bacterial composition in the blood. The patients were subgrouped into uninfected ($n = 17$), infected ($n = 16$), and septic ($n = 17$) cases. Applying 16S rDNA-based next-generation sequencing technique, we investigated blood and neutrophil-associated microbiomes in SAP patients, and assessed their connections with immunological alterations. Based on the sequencing data, a diverse bacterial microbiota was found in peripheral blood and neutrophils from the healthy and SAP subjects. As compared to healthy controls, the blood and neutrophil-associated microbiomes in the patients were significantly altered, with an expansion in Bacteroidetes and Firmicutes as well as a decrease in Actinobacteria. Variations in the microbiome composition in patients were associated with immunological disorders, including altered lymphocyte subgroups, elevated levels of serum cytokines and altered proteomic profiles of neutrophils. However, no significant compositional difference was observed between the patient subgroups, implying that the microbiota alterations might not be linked to presence/absence of infectious complications in SAP. Together, we present an initial description of the blood and neutrophil-associated bacterial profiles in SAP patients, offering novel evidence for the existence of the blood microbiome. Identification of the blood microbiome provides novel insights into characteristics and diagnostics of bacteremia in the patients. Further study is required to assess the possible implications of the blood microbiome in health and diseases.

Keywords: blood microbiome, neutrophil-associated microbiome, severe acute pancreatitis, sepsis, next-generation sequencing, proteomics

OPEN ACCESS

Edited by:
Michele Marie Kosiewicz, University of Louisville, United States

Reviewed by:
Renate Lux, UCLA School of Dentistry, United States
Michael F. Minnick, University of Montana, United States

***Correspondence:**
Qiurong Li
liqiurongjue@126.com

†*These authors have contributed equally to this work.*

Received: *05 May 2017*
Accepted: *09 January 2018*
Published: *23 January 2018*

Citation:
Li Q, Wang C, Tang C, Zhao X, He Q and Li J (2018) Identification and Characterization of Blood and Neutrophil-Associated Microbiomes in Patients with Severe Acute Pancreatitis Using Next-Generation Sequencing. Front. Cell. Infect. Microbiol. 8:5. doi: 10.3389/fcimb.2018.00005

INTRODUCTION

Severe acute pancreatitis (SAP) is a terrible disease, associated with a mortality rate in the range of 20–50% (Nathens et al., 2004; Garg et al., 2005; Noor et al., 2011). Among the cases with SAP, up to 80% of deaths are attributed to infectious complications and multiple organ dysfunction syndromes (MODS) (Garg et al., 2005). Despite antibiotic prophylaxis in the management of SAP, the incidence of systemic infections is still surprisingly high (Villatoro et al., 2010). Infectious complications have become a major concern in SAP, especially cases of pancreatic necrosis (Medich et al., 1993). Accumulating evidence has suggested that systemic infections in SAP patients are mainly derived from invasion by gut organisms (Schmid et al., 1999; Noor et al., 2011). Yet, the molecular mechanisms behind the development of systemic infections in SAP are not fully known.

During the last two decades, bacterial translocation has been thought to be a major source causing systemic infection and MODS in SAP patients (MacFie et al., 1999; Cicalese et al., 2001). Enteric bacteria could cross the impaired intestinal barrier to reach peripheral circulation, leading to infected pancreatic necrosis and sepsis (Ammori et al., 1999). Just like in patients who underwent sepsis following severe trauma, burn, major operative intervention and other causes, cultures of blood specimens in SAP patients complicated by sepsis are often negative, even in the presence of infected pancreatic necrosis (Sainio et al., 1995; Ammori et al., 2003). As a result, specific interventions against infections are probably delayed in some cases, causing lethal complications. It is quite possible that enteric bacteria may translocate into systemic circulation, but escape from detection by standard culture methods. Utilization of new techniques, such as polymerase chain reaction or matrix-assisted laser desorption ionization–time of flight, to some extent, has improved the ability to detect bloodstream pathogens (Ecker et al., 2010; Buehler et al., 2016), however, our knowledge on the blood-microbial landscape in septic patients is still limited. Appling a culture-independent method, we observed that bloodstream invasion by multiple gut organisms (commonly 5–8 bacterial species) contributed to the development of bacteremia in SAP patients (Li et al., 2013a). Owing to insensitivity of this approach to low-abundance microbial sequences (Muyzer et al., 1993), the bacterial taxonomic richness in the blood of the patients was most likely underestimated. As a result, a deeper exploration of the blood bacterial composition and diversity with emerging molecular techniques might be needed. Recent studies with 16S rDNA-based high-throughput sequencing showed that a diverse microbiota is present in the blood of septic patients (Grumaz et al., 2016; Gosiewski et al., 2017) and healthy individuals (Païssé et al., 2016). Although its biological and clinical significance remains to be further explored, discovery of a blood microbiome might represent an important step toward a better understanding of the microbial world of the human body and its relationships with health and diseases. Therefore, it is urgently needed to ascertain whether a rich microbiota is harbored in blood of SAP patients using culture-independent next-generation sequencing techniques to better understand the development of bacteremia and infectious complications.

The complex network of immune cells and specialized molecules has evolved to defend against pathogens. Various types of immune cells, including neutrophils, monocytes, and lymphocytes, could integrate microbial signals to govern the inflammatory response, together maintaining the homeostasis of systemic circulation (Akira et al., 2006). Recent studies have revealed that sepsis is probably the sequelae of a cascade of events starting with a local inflammatory response against organisms derived from the gut (Bosmann and Ward, 2013). When pathogens invade, the innate immune system recognizes microbial molecules and kicks off an inflammatory response (Akira et al., 2006). Activation of neutrophils could induce excessive production of pro-inflammatory cytokines and disrupt the balance of the pro- and anti-inflammatory response, leading to an overwhelming imbalance (Delano et al., 2011; Bosmann and Ward, 2013). As the first-line responder against pathogens, the neutrophils play a central role for elimination of bacterial infection. Some pathogens can be engulfed and gain entry to the cells (Appelberg, 2007), shaping the neutrophil-associated microbiomes (NAMs). The functional impairment of neutrophils could disrupt the dynamic balance between internalization and clearance of pathogens (Amulic et al., 2012; Hotchkiss et al., 2013; Matthew et al., 2016), likely altering the membership of the neutrophil-associated microbiome and causing infection. However, the composition of the community in neutrophils and its role in sepsis remains uncharacterized. Elucidation of changes of the NAMs and the potential connection with host immunological disorders would be helpful for better understanding the mechanism of sepsis pathogenesis in SAP patients.

Here we performed 16S rDNA-based sequencing on the blood and neutrophils of SAP patients to profile the microbial landscape in peripheral circulation and estimated its potential connection with the development of bacteremia and infectious complications. In addition, we dissected the immune cell repertoires in blood and the proteomic profiles of neutrophils through a fluorescence activated cell sorting (FACS) approach and quantitative proteomics analysis, and examined the relationships of blood microbiota alterations with immunological disorders in SAP patients.

MATERIALS AND METHODS

Ethics Statement

All participants provided written informed consent upon enrollment. Studies were approved by the Human Subjects Institutional Committee of Jinling Hospital and were conducted in accordance with all relevant guidelines and regulations.

Study Populations and Experimental Design

Fifty patients who underwent SAP and admitted to the Department of General Surgery, Jinling Hospital, between March 2014 and March 2016, were enrolled in this study. Acute pancreatitis was diagnosed in accordance with clinical symptoms and at least 3 times the upper limit of normal value in serum amylase or evidence on computed tomographic scan of

the abdomen (Bradley, 1993). SAP is defined as the presence or absence of organ failure and/or local complications, such as pancreatic necrosis, abscess or pseudocyst (Bradley, 1993). Based on the presence or absence of infectious symptoms, the patients were distributed into three subgroups: uninfected ($n = 17$), infected ($n = 16$) and septic ($n = 17$) (**Table 1**). Septic patients were identified according to the presence of suspected or documented infections and an acute increase in the Sequential (Sepsis-related) Organ Failure Assessment (SOFA) score of 2 points or more (Singer et al., 2016). The infected patients were defined as having suspected or documented infections but an absence of emerging organ dysfunction, and uninfected cases showing no infectious signs. The patients' clinical characteristics, such as demographic data, clinical diagnoses, comorbidities, vital signs, hematologic and chemical data, blood gas analyses, blood cultures, Acute Physiology and Chronic Health Examination-II (APACHE-II) score and SOFA scores, were recorded (Supplementary Table 1). Twelve healthy volunteers who had no infectious signs and no elevated level of serum CRP served as control subjects. Subjects <18 or more than 70 years old were excluded in this study. Blood samples from enrolled patients and healthy subjects were collected for high-throughput sequencing, quantitative proteomics analysis of peripheral neutrophils, and measurement of blood immune cell subpopulations.

Sampling and Neutrophil Isolation

Peripheral blood was sterilely collected at the days in which sepsis was definitely diagnosed and immediately delivered to our laboratory. The sample was then divided into 3 aliquots of 200 μL in the biosafety cabinet and stored at −80°C. Another portion (2 mL) of each sample was immediately used for isolation of neutrophils with commercially Ficoll-dextran reagents. Neutrophil-rich pellets were subjected to hypotonic lysis of the remaining erythrocytes with E-lysis. Cell pellets were resuspended in DMEM supplemented with 10% FCS (heat inactivated). Cells were incubated in polypropylene tubes (Falcon/Becton Dickinson, Cambridge, UK) to prevent adherence. The purity of neutrophils was >95%, as assessed by $CD16^+$ cell by flow cytometry. Isolated neutrophils were stored at −80°C until DNA extraction and proteomics analysis.

DNA Extraction and Polymerase Chain Reaction (PCR)

DNA from whole blood and isolated neutrophils was extracted with the QIAamp DNA Mini Kit (Qiagen, Valencia, CA) following the manufacturer's instructions. For extraction of neutrophil DNA, a bead-beating step (FastPrep machine for 45 s at setting 5.5, Bio 101) after the addition of the RLT buffer was done to enhance cell lysis. The hypervariable V3 region of the 16S rRNA gene was amplified using universal primer set 357f (5′-TACGGGAGGCAGCAG-3′) and 518r (5′-ATTACCGCGGCTGCTGG-3′) (Li et al., 2013b). An aliquot of DNA (100 ng) recovered from the blood and neutrophils was added into a reaction mixture, and PCR reactions were carried out with a touchdown thermocycling program. The cycling was as follows: initial denaturation at 94°C for 5 min, 30 s at 94°C (denaturation), 30 s at 65°C (annealing), and 30 s at 68°C (elongation) with a 0.5°C touchdown every second cycle during annealing for 20 cycles, followed by 15 cycles with an annealing temperature of 56°C and a final cycle consisting of 5 min at 68°C. The purity and correct size of the resulting PCR amplicons (approximately 190 bp) were assessed on 1% agarose gels, stained with ethidium bromide (5 μg/mL) and visualized under UV light. To ascertain the specificity of the primers (no eukaryotic, mitochondrial, or Archea DNA targeted), we sequenced the PCR products (∼10 ng each sample) by Sanger technologies. The sequencing results showed that only 16S rDNA bacterial fragments were yielded from the amplification, confirming the specificity of the primers.

To ensure absence of false positive amplifications, we conducted real-time quantitative PCR with the primer set (357f/518r) to test for possible bacterial contaminants from the reagents (PCR mixtures, solutions for DNA extraction and sterile water) and consumables. The standard curve for the quantification was performed by generating a series of 10-fold dilutions from 5×10^3 to 5×10^8 of 16S rRNA gene copies per reaction using plasmid DNA containing the complete 16S rRNA gene sequence of an *E. coli* DH5α strain. Amplifications of samples and standard dilutions were performed in duplicates on the AB7500 real time PCR system (Life Technologies, CA). The quality of the amplifications was assessed by melting curves. The data showed that the background signal, represented by negative controls (NC), was far lower than those of blood samples (Supplementary Figure 1), indicating the absence of bacterial DNA contaminants from reagents and consumables.

DNA Library Construction and 16S rRNA Gene Sequencing

PCR products were purified with Agencourt AMPure beads (BeckmanCoulter). An aliquot (50 ng) of purified DNA was used for construction of barcoded libraries using the Ion Plus Fragment Library Kit (Life Technologies). In this step, a sample-specific "DNA molecular tag (barcode)," a 14-base semirandom sequence, was intended to uniquely identify original template molecules. DNA concentrations of the libraries were estimated with a Qubit dsDNA HS kit. Libraries for each run were diluted to 26 pM for template preparation. Emulsion PCR was carried out using the Ion OneTouchTM 200 Template Kit v2 (Life Technologies). Sequencing of amplicon libraries was conducted on 316 v2 chips using the Ion Torrent PGM system with the Ion Sequencing 200 kit (Life Technologies). After sequencing, the individual sequence reads were filtered by the PGM software to remove low quality and polyclonal sequences. All PGM quality-approved, trimmed and filtered data were exported as FASTQ files.

The sequence data were deposited in the NCBI Bioproject and the Sequence Read Archive with accession codes PRJNA428535 and SRP128069, respectively.

Sequence Processing and Quality Control

Sequenced files were online converted to FASTA format and were filtered to remove low-quality sequences with the Galaxy

TABLE 1 | Demographics of study population.

		Uninfected (*N* = 17)	Infected (*N* = 16)	Septic (*N* = 17)	Healthy (*N* = 12)
Age		43.1 ± 11.5	40.4 ± 12.1	47.3 ± 10.7	29.2 ± 3.8
Male (%)		9 (53)	10 (63)	11 (65)	10 (83)
Female (%)		8 (47)	6 (37)	6 (35)	2 (17)
APACHE II scores		4 ± 2	9 ± 1	15 ± 3	0
SOFA scores		0.06 ± 0.24	0.44 ± 0.11	6.47 ± 3.45	0
Lac (mmol/L)		1.3 ± 0.5	1.2 ± 0.5	2.4 ± 2.7	N/A
C-reactive protein (mg/L)		59.5 ± 37.1	133.4 ± 77.3	196.1 ± 71.2	N/A
Hematologic analysis	White blood cell count ($\times 10^9$/L)	8.7 ± 2.5	12.8 ± 7.5	16.9 ± 14.6	6.7 ± 1.1
	Neutrophil percentage (%)	76.3 ± 7.3	83.3 ± 6.3	86.4 ± 8.2	62.4 ± 10.1
	Lymphocyte percentage (%)	14.0 ± 5.5	9.8 ± 5.1	7.8 ± 5.0	27.8 ± 9.4
	Hematocrit	0.30 ± 0.039	0.27 ± 0.045	0.28 ± 0.059	0.43 ± 0.030
	Platelet ($\times 10^9$/L)	276 ± 86	207 ± 92	186 ± 139	257 ± 70.9
Liver function	Total protein (g/L)	55.7 ± 6.6	54.1 ± 6.9	51.6 ± 6.2	74.1 ± 4.9
	Albumin (g/L)	32.8 ± 3.4	30.9 ± 3.3	29.6 ± 2.8	47.1 ± 2.2
	Total bilirubin (μmol/L)	9.8 ± 5.1	16.4 ± 17.2	40.5 ± 8.7	11.9 ± 2.8
	Direct bilirubin (μmol/L)	5.0 ± 2.6	9.5 ± 14.0	29.9 ± 9.0	4.1 ± 1.2
	Indirect bilirubin (μmol/L)	4.8 ± 2.8	6.9 ± 4.3	10.6 ± 6.8	7.8 ± 1.9
Renal function	Creatinine (μmol/L)	58 ± 50	103 ± 133	136 ± 120	72 ± 21
	Urea N (mmol/L)	7.4 ± 12.1	6.1 ± 5.0	8.9 ± 7.0	5.8 ± 1.4
	Uric acid (μmol/L)	203 ± 105	166 ± 95	219 ± 134	299 ± 110
Blood coagulation	Prothrombin time (s)	13.0 ± 0.9	15.6 ± 6.1	16.4 ± 4.6	12.4 ± 1.0
	Partial thromboplastin time (s)	37.3 ± 7.2	53.9 ± 31.3	59.6 ± 28.9	28.8 ± 2.3
	International normalized ratio	1.14 ± 0.080	1.36 ± 0.54	1.43 ± 0.41	1.08 ± 0.089
	Fibrinogen (mg/dL)	4.44 ± 0.81	4.21 ± 1.18	4.10 ± 1.09	2.63 ± 0.64
Infection	Microbiologically confirmed (%)	0	25.0	35.3	0
	Clinically proven or suspected (%)	0	100.0	100.0	0
Type of organisms	Gram-positive (%)	0	6.3	5.9	0
	Gram-negative (%)	0	18.7	23.5	0
	Fungus (%)	0	0	5.9	0

N/A, no available.

projects (https://usegalaxy.org/). A mean quality score of ≥20 and a minimum length of 150 bp for the coupled V3 region were required. The resulting sequences were then aligned online to operational taxonomic units (OTUs) (97% identity) with the CD-HIT (http://weizhong-lab.ucsd.edu/cdhit_454/cgi-bin/index.cgi) (Li and Godzik, 2006). Sequences that did not match the defined core region of the seed alignment were manually removed. OTUs were classified taxonomically to bacterial genera using the Ribosomal Database Project (RDP) classifier with a 50% bootstrap threshold (http://rdp.cme.msu.edu/classifier/classifier.jsp) (Wang et al., 2007).

Protein Extraction, Digestion, and iTRAQ Labeling

Isolated neutrophils were thawed and resuspended in lysis buffer of cold acetone containing 10% trichloroacetic acid (TCA) and 10 mM dithiothreitol (DTT) and sonicated for 3 times on ice to enhance cell lysis. The protein pellets were then collected by centrifuging and resuspended in a buffer (7 M urea, 2 M thiourea, 4% CHAPS, 30 mM, Tris–HCl pH 8.0), containing 1 mM phenylmethylsulfonyl fluoride (PMSF), 2 mM ethylenediaminetetraacetic acid (EDTA) and 10 mM DTT. Samples were again sonicated and centrifuged and subsequently, the supernatant was reduced and alkylated by 10 mM DTT and 55 mM iodoacetamide (IAA). The treated proteins were precipitated with chilled acetone (1:4) at −20°C overnight. The precipitants were resuspended in 500 mM triethylammonium bicarbonate (TEAB), then sonicated and centrifuged as above. The protein content of the supernatant was determined using the Bradford method. The resulting proteins (∼100 μg) of each sample were digested by and then labeled with 6-plex iTRAQ reagents containing 6 different stable-isotope (126–131) covalent mass tags (Applied Biosystems) according to the manufacturer's protocol.

Peptide Fractionation and Mass Spectrometry (MS) Analysis

The labeled peptides were pooled, eluted and resolved into 10 fractions using an Ultremex SCX column containing 5-μm particles (Phenomenex, USA). The eluted fractions were desalted using a Strata X C18 column (Phenomenex, USA) and dried under vacuum. Each fraction was resuspended in a certain volume of buffer A (2% acetonitrile, 0.1% formic acid, pH3.0) and centrifuged at 20,000 × g for 10 min. The final concentration of peptide was about 0.5 μg/μl on average in each fraction. Supernatant was loaded on a Nano ACQUITY UPLC system using the autosampler. The peptides were subjected to nanoelectrospray ionization followed by tandem mass spectrometry (MS/MS) in a LTQ-Orbitrap (Thermo Fisher Science, USA) coupled online to the HPLC. Intact peptides were detected in the Orbitrap at a resolution of 60,000. Peptides were selected for MS/MS using high energy collision dissociation (HCD) operating mode with a normalized collision energy setting of 45%. LC-MS/MS was operated in positive ion mode as described. The analytical condition was set at a linear gradient from 0 to 60% of buffer B (CH_3CN) in 150 min, and a flow rate of 200 nL/min. Ion fragments were detected on the LTQ. A data-dependent procedure that alternated between one MS scan followed by eight MS/MS scans was applied for the eight most abundant precursor ions above a threshold ion count of 5,000 in the MS survey scan. The electrospray voltage applied was 1,500 V. Automatic gain control (AGC) was used to prevent overfilling of the ion trap; 1×10^4 ions were accumulated in the ion trap for generation of HCD spectra. For MS scans, the m/z scan range was 350 to 2,000 Da.

MS Data Processing, Protein Quantization, and Functional Annotation

The MS/MS spectra acquired from precursor ions were submitted to Maxquant (version 1.2.2.5) using the following search parameters: the database for the search was Uniprot proteome (version 20140418); the enzyme was trypsin (full cleavage); dimethylation labeling for quantification; the dynamic modifications were set for oxidized Met (+16); carbamidomethylation of cysteine was set as static modification; MS/MS tolerance was set at 10 ppm; the minimum peptide length was 6; the false detection rates for both peptides and proteins were all set below 0.01. All identified peptides had an ion score above the identity threshold, and a protein was considered identified if at least one such unique peptide match was apparent for the protein. Individual quantitative samples were normalized within each acquisition run according to the algorithm described in i-Tracker (Shadforth et al., 2005). The logic algorithm for set operations was applied to further screen for differentially expressed proteins identified in the present study. Gene Ontology (GO) functional annotation was carried out using Blast2GO software (Conesa et al., 2005).

Flow Cytometry

Blood specimens were freshly collected for assessment of lymphocyte subsets, cell apoptosis, and HLA-DR expression on monocytes. For measurement of cell apoptosis, mononuclear cells were prepared by density gradient centrifugation with Ficoll-Paque (Stem cell Technologies), and were then stained by Annexin V-PE, 7-ADD-PerCP, and fluorescein-labeled mAbs against CD4, or CD8, respectively. Assessment of T lymphocyte subsets, HLA-DR and T-helper (Th) cells was performed using commercial kits (BD Biosciences). After activation with phorbol myristate acetate and ionomycin, immunostaining was performed using fluorescein-labeled mAbs against CD4, interferon-gama (INF-γ), interleukin (IL)-4 and IL-17 (BD Pharmingen). A logical gate combining $CD4^+$ cells and their scatter properties was used for the phenotypes of Th1, Th2, and Th17 cells. The proportions of the peripheral naïve CD4 T cells ($CD3^+CD4^+CCR7^+CD45RA^{high}CD28^+$), naïve CD8 T cells ($CD3^+CD8^+CCR7^+CD45RA^{high}CD28^+$), memory CD4 T cells ($CD3^+CD4^+CD45RA^-$), memory CD8 T cells ($CD3^+CD8^+CD45RA^-$), effector memory ($CD3^+CD8^+CCR7^-CD45RA^-$), and terminal effector memory ($CD3^+CD8^+CCR7^-CD45RA^{high}CD28^-$) were also measured, respectively (Qi et al., 2014). All data were acquired on a Becton Dickinson FACSCanto II and analyzed with CellQuest software (BD Biosciences).

Assay of Serum Cytokines

Measurement of serum TNF-α, IL-1β, IL-6, IL-10, IL-18, and IFN-γ levels was performed in duplicate with enzyme-linked immunosorbent assay (ELISA) kits (R&D Systems, Abingdon, UK).

Statistical Analysis

Quantitative data are represented as means ± standard deviation (SD). Statistical analysis was performed by one-way analysis of variance (ANOVA) followed by the Holm-Sidak test using SPSS software (version 12.0). A $P < 0.05$ was considered significant. The species richness in the bacterial microbiota was estimated by the OTU numbers at the same sequencing depth, which was compared to reflect the difference of the microbiota diversity between groups. Correlation between two variances was estimated using linear regression analysis with a Pearson's test in R software (http://www.r-project.org/). Heatmaps were generated for non-scaled, non-normalized titer data using a Euclidean distance function with complete linkage clustering or non-clustering in R using the package pheatmap (version 3.1.1). Principal component analysis was conducted with Canoco software for Windows 4.5 (Microcomputer Power, Ithaca, NY). The output matrix containing the relative abundance of OTUs per sample was processed with the linear discriminant analysis effect size (LEfSe) algorithm (Segata et al., 2011) using an alpha cutoff of 0.05 and an effect size cutoff of 2.0.

RESULTS

Characterization of Bacterial Microbiomes in Peripheral Blood of SAP Patients

To characterize the bacterial communities possibly present in systemic circulation, we sequenced 16S rRNA gene amplicons of blood samples from 50 patients with SAP and 12 healthy subjects.

The patients were classified into three groups: uninfected (n = 17), infected (n = 16), and septic (n = 17) (**Table 1** and Supplementary Table 1). Prior to sequencing, we conducted a quantitative polymerase chain reaction (qPCR) assay to determine the concentration of 16S rRNA gene copies in the whole blood of each subject (Supplementary Figure 1). The numbers of 16S rDNA copies in blood were significantly higher in the infected and septic patients than in healthy controls (on average 1.38×10^8 copies per milliliter) ($P < 0.01$) (Supplementary Figure 1D). After sequencing the 16S rDNA amplicons, we generated over 80,000 sequences for each sample, and unique sequences were clustered into 14,526 OTUs (97% ID). Taxonomic classification showed that these OTUs were assigned into 335 bacterial genera, mainly affiliated with the four major phyla: Proteobacteria, Bacteroidetes, Firmicutes and Actinobacteria (Supplementary Figure 2A). An average of 204 OTUs (range: 50–694) were obtained from the patients' samples (Supplementary Figure 2B), indicating that a diverse bacterial microbiome, rather than one or several bacterial species as thought previously, was present in peripheral circulation of the patients. Surprisingly, we also observed a highly diverse microbiota in the blood of healthy subjects (on average 360 OTUs, range: 265–520) (Supplementary Figure 2B). As compared to healthy controls, the species richness of the blood microbiota, estimated by the number of OTUs (at the same sequencing depth), was significantly reduced in SAP patients ($P < 0.05$) (Supplementary Figure 2B). Additionally, the composition of the microbiota was profoundly distinct between the patients and healthy controls, characterized by severe depletion of Actinobacteria ($P < 0.0001$) and an overgrowth of Bacteroidetes in the former ($P < 0.05$) (Supplementary Figure 2C). At the class level, we saw a marked increase in Bacteroidia and Clostridia, and a striking reduction in Actinobacteriae, Flavobacteriia and Bacilli in the patients vs. healthy controls ($P < 0.05$) (Supplementary Figure 2C). Principal component analysis (PCA) of the weighted UniFrac distances, based on the data of genus-level relative abundance, showed a clear separation of the patients' samples from healthy controls along PC1 and PC2, indicating the differences of the microbiota profiles between them (Supplementary Figure 2D). However, no significant difference was found in the microbiota structures across the patient groups, as scattered distribution of their sample dots in the PCA plot.

Potential Source of the Blood Microbiota in SAP Patients

To track the possible source of blood microbiomes, we compared our sequences to the 16S rRNA gene dataset from the National Center for Biotechnology Information (NCBI) (The Human Microbiome Project Consortium, 2012). Consequently, an average of 87.0% (range: 73.5–98.3%) of the blood microbiome memberships across individuals were taxonomically classified as known commensal or pathogenic bacteria colonizing the human gut, far higher than those from other sites (Supplementary Figure 3A). Given the dominance of the putative gut-derived organisms within the niches, we estimated their contribution to the microbiome-wide alterations in SAP patients (**Figure 1A**). The counts of the OTUs likely affiliated with the gut organisms was markedly declined in patients relative to the healthy controls ($P < 0.05$) (Supplementary Figure 3B). Comparison of phylum-level proportions indicated pronounced variations of the putative gut-derived organisms in patients, displaying similar patterns vs. the microbiome-wide changes (**Figure 1B** and Supplementary Figure 2C). The Bacteroidetes was overrepresented while Actinobacteria was markedly decreased in all patient groups ($P < 0.05$) (**Figure 1B**), followed by a striking increase in the ratios of the relative abundance between both phyla compared to those of healthy subjects (Supplementary Figure 4A). The ratios between Firmicutes and Actinobacteria rose (Supplementary Figure 4B), which was mainly due to significant decline in Actinobacteria in the blood of the patients. Such changes in the predominant phyla provided compelling evidence indicating that the putative gut-derived bacterial composition was significantly altered in patients (Supplementary Figure 3C). Class-level analyses showed highly consistent changes with those of the aggregate microbiota (**Figure 1B** and Supplementary Figure 2C), suggesting that shifts of the putative gut-derived organisms contributed predominantly to the blood microbiome-wide alterations in patients. At the genus level, 20 of the putative gut-derived bacterial genera, including *Bacteroides* (10.5 ± 9.2%), *Escherichia/Shigella* (9.0 ± 4.6%), *Acinetobacter* (8.9 ± 4.9%), *Stenotrophomonas* (also likely derived from soils) (8.5 ± 4.8%), *Serratia* (4.9 ± 2.8%), *Pseudomonas* (also likely as soil-derived) (4.5 ± 2.8%), *Rhizobium* (also likely as soil-derived) (3.0 ± 2.4%), *Prevotella* (1.9 ± 2.1%), *Corynebacterium* (also likely derived from skin or soils) (1.5 ± 1.7%) and so on, dominated the blood microbiota in patients (average relative abundance >1%) (**Figure 1C**). These bacterial genera were also abundant in healthy controls; however, their proportions were significantly distinct from those of patients (**Figure 1C**). The genera *Bacteroides*, *Stenotrophomonas*, *Serratia*, *Rhizobium*, *Prevotella*, *Staphylococcus,* and *Paracoccus* were markedly expanded in the blood of the patients, regardless of the illness severities ($P < 0.05$, vs. healthy controls) (**Figure 1C**). Interestingly, some bacterial genera, such as *Rhizobium*, *Phascolarctobacterium*, *Alistipes*, *Parabacteroides*, *Faecalibacterium*, *Paraprevotella,* and *Clostridium XlVa*, were present in the patients, but not detected in healthy subjects. In contrast, the genera *Acinetobacter*, *Lactococcus*, *Dietzia*, *Flavobacterium*, *Pseudomonas*, *Corynebacterium, Sphingobium,* and *Brevundimonas,* were consistently decreased in the patients ($P < 0.05$, vs. healthy controls). Of them, some bacterial genera were commonly considered to be potentially pathogenic or probiotic, and were probably of special importance for the blood microbiome alterations in patients (Supplementary Figure 5). Like the blood microbiota-wide analysis, the sample dots, representing the putative gut-derived bacterial communities, displayed highly similar distributions in the PCA plots (**Figure 1D** and Supplementary Figure 2D), indicating that altered abundance of putative gut-originated organisms was predominantly responsible for the microbiome-wide alteration in patients. To further identify taxonomic differences in the microbiomes between the patients and healthy subjects, we conducted a linear discriminant analysis (LDA) effect size

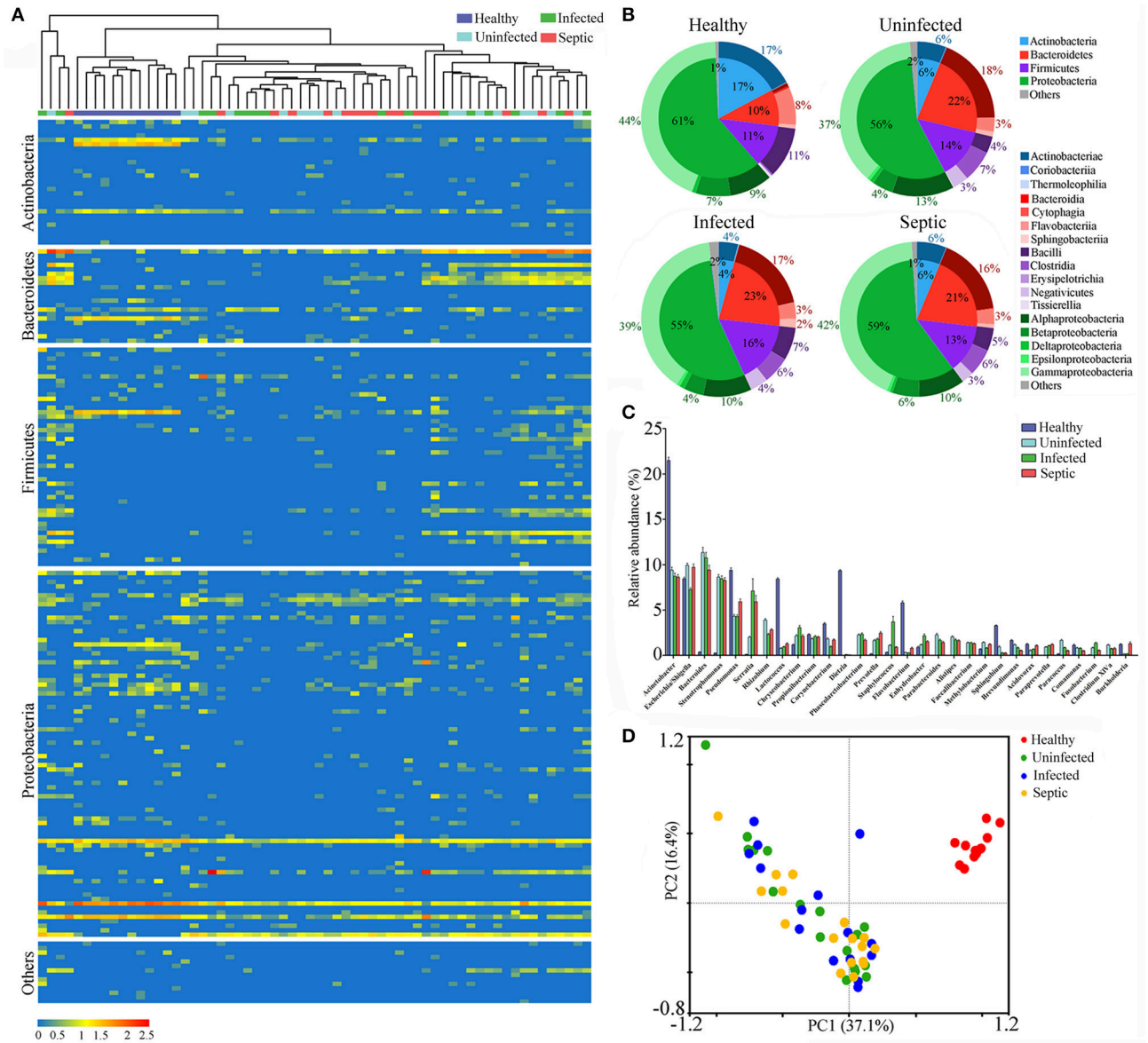

FIGURE 1 | Characterization of the blood bacterial microbiomes potentially derived from the gut. **(A)** Heatmap showing the abundance of the putative gut-derived bacterial genera identified by taxonomic classification. The data represent the Log10 values of the operational taxonomic unit (OTU) counts each genus. The clustering relationships across the blood samples are shown in the upper panel. **(B)** The pie charts indicating the composition of the putative gut-derived organisms in the blood microbiota at the phylum and class levels. **(C)** Comparisons in the relative proportions of the top 30 bacterial genera among groups. **(D)** The plot of principal component analysis (PCA) showing the difference of the microbial community structures.

(LEfSe) algorithm. Consistent with the findings mentioned above (**Figure 1B**), the changes of the blood microbiome in patients were primarily sourced from the classes Bacteroidia, Clostridia, Actinobacteriae, Flavobacteriia and Bacilli (Supplementary Figure 6).

Identification of Diverse Bacterial Microbiome within Neutrophils

To define the configurations of neutrophil-associated microbiomes, also termed as NAMs, we isolated peripheral neutrophils from the patients and healthy subjects, and sequenced the 16S rDNA amplicons obtained from the cells. We observed that a surprisingly diverse microbiome was present within the neutrophils both in patients and in healthy subjects, as indicated by several hundreds to thousands of unique OTUs. Similar to the blood microbiomes, the OTUs obtained from the neutrophil specimens were mainly classified into the four phyla: Proteobacteria, Bacteroidetes, Firmicutes and Actinobacteria (Supplementary Figure 7A). A notable expansion of OTUs numbers was seen in the infected or septic patients ($P < 0.01$)

(Supplementary Figure 7B), implying that the neutrophils in these cases might capture more diverse bacteria than in healthy controls. Viewing the microbiota profile, we found that the increase of species richness in infected or septic patients was mainly due to over-presence of certain bacteria belonging to the phyla Bacteroidetes and Firmicutes ($P < 0.05$, vs. healthy controls) (Supplementary Figure 7C). The proportions of the classes Bacteroidia, Clostridia, and Negativicutes were significantly expanded in the patients, whilst Actinobacteriae, Flavobacteriia, Gammaproteobacteria and Betaproteobacteria were markedly declined ($P < 0.05$, vs. healthy controls) (Supplementary Figure 7C). The PCA plots showed that the majority of the patients' sample dots, were distant from those of the healthy controls, suggesting that the NAM shifted toward aberrant configuration in patients (Supplementary Figure 7D).

Next we determined the potential origin of the neutrophil-associated microbiome, obtaining similar results with that of the blood microbiota. The organisms that presumably derived from the gut constituted the major component of the neutrophil-associated microbiome, with high abundance proportions (on average 83.1% of the aggregate, range: 63.7 to 94.8%) across all samples (Supplementary Figure 8A). The putative gut-derived organisms in neutrophils were profoundly diverse (**Figures 2A,B**), and especially in infected and septic patients, the counts of the OTUs and bacterial genera were far more than in healthy controls ($P < 0.01$) (**Figure 2C**). As compared to healthy controls, the most significant shifts of the bacterial communities in neutrophils of patients were the increases in the Bacteroidetes and Firmicutes, together with a profound reduction in Actinobacteria and Proteobacteria ($P < 0.01$) (**Figure 2D**). The ratios between Bacteroidetes or Firmicutes and Actinobacteria were significantly higher in the patients than those of healthy microbiotas ($P < 0.01$) (Supplementary Figure 8B). At the class level, the bacterial microbiomes in neutrophils differed markedly between the patients and healthy individuals, mainly characterized by an expansion in Bacteroidia, Clostridia and Negativicutes, as well as a reduction in Actinobacteriae, Flavobacteriia, Gammaproteobacteria, and Betaproteobacteria ($P < 0.01$) (**Figure 2D**). The proper proportions of such bacterial taxons appeared to be disrupted, indicating significant alterations in the neutrophil-associated microbiomes of the patients. The PCA plot, based on the relative abundance of the putative gut- derived bacterial genera, indicated that the microbiome memberships were distinguished between healthy controls and patients (**Figure 2E**). To explore the bacterial phylotypes associated with the shifts of the neutrophil-associated microbiomes in the patients, we compared the relative abundance of some specific bacterial genera that were often included in the potentially pathogenic and probiotic organisms (Supplementary Figure 9A). Of them, the potentially pathogenic organisms, including *Bacteroides*, *Stenotrophomonas*, *Clostridium* XIVa, *Fusobacterium*, *Eubacterium,* and *Serratia* were more enriched in the patients than healthy individuals ($P < 0.05$) (Supplementary Figure 9B). However, the genera *Acinetobacter*, *Lactococcus*, *Corynebacterium*, *Flavobacterium*, *Pseudomonas*, *Bifidobacterium*, *Legionella,* and *Anaerococcus* were significantly less abundant in the patients ($P < 0.05$, vs. Healthy controls) (Supplementary Figure 9B). Further, we conducted the linear discriminant analysis (LDA) effect size (LEfSe), indicating the variations of the neutrophil-associated microbiomes in patients (Supplementary Figure 10). In total, the neutrophil-associated microbiome in the patients was distinct from that of healthy subjects, which probably had important implications in the development of bacteremia and systemic infection.

Associations between Immune Traits and Blood Microbiome in SAP Patients

Next we characterized a wide range of circulating immune cell subtypes in the peripheral blood samples from the patients and healthy controls. As shown in the **Figure 3A**, the percentages of $CD4^+$ and $CD8^+$ T lymphocyte subsets were both reduced in the septic patients ($P < 0.01$, vs. healthy controls). The proportions of naïve T cells ($CD4^+$, $CD8^+$) were also decreased strikingly in the infected and septic cases, whilst the memory T cells were increased compared to those of healthy subjects ($P < 0.01$). In addition, the counts of the total lymphocytes, $CD4^+$ and $CD8^+$ T lymphocytes were significantly decreased in the patients ($P < 0.01$, vs. healthy controls), reaching the minimum values in septic cases (**Figure 3C**). By contrast, a significant increase in $CD8^+$ T cell apoptosis was observed in the infected and septic patients ($P < 0.001$) (**Figure 3B**). The apoptosis of $CD4^+$ T cells was also increased in uninfected, infected and septic cases, while a significantly statistical difference was only found between septic patients and healthy controls ($P < 0.05$). Of special note, the septic patients displayed a strong proinflammatory cytokine profile, characterized by increased release of IL-1β, IL-2, IL-6, TNF-α, and IFN-γ in the serum ($P < 0.001$) (**Figure 3B**).

The blood and neutrophil-associated microbiomes of the patients were distinctfrom those of healthy subjects, raising a question of whether shifts of the microbiomes were related to the immunological disorders in patients. To address it, we examined relationships between specific clades of the microbiomes and the immunological parameters in patients (**Figure 4**). We observed that some bacterial genera associated with the neutrophils, such as *Acinetobacter*, *Bacteriodes*, *Stenotrophomonas*, *Serratia*, *Pseudomonas*, *Chryseobacterium*, *Methylobacterium*, *Clostridium*, *Enterococcus*, *Lactococcus*, and *Oscillibacter*, etc., were correlated either positively or negatively with T lymphocyte subsets, especially naïve and memory T cells, in the septic patients (**Figure 4**). Similarly, some of the bacterial phylotypes showed strong correlation with the immunological traits in the uninfected and infected patients. The majority of these bacteria in the neutrophil-associated microbiomes were closely associated with the changes of serum cytokine levels in patients (Supplementary Figure 11). However, the bacterial genera that closely correlated to the lymphocyte subsets and serum cytokine concentrations were relatively fewer in healthy controls. In addition, some bacterial taxa in the peripheral blood were significantly correlative with the immunological parameters both in patients and in healthy subjects (Supplementary Figures 12, 13). Clearly, the changes of the blood and neutrophil-associated microbiomes were strongly linked to immunological disorders of patients.

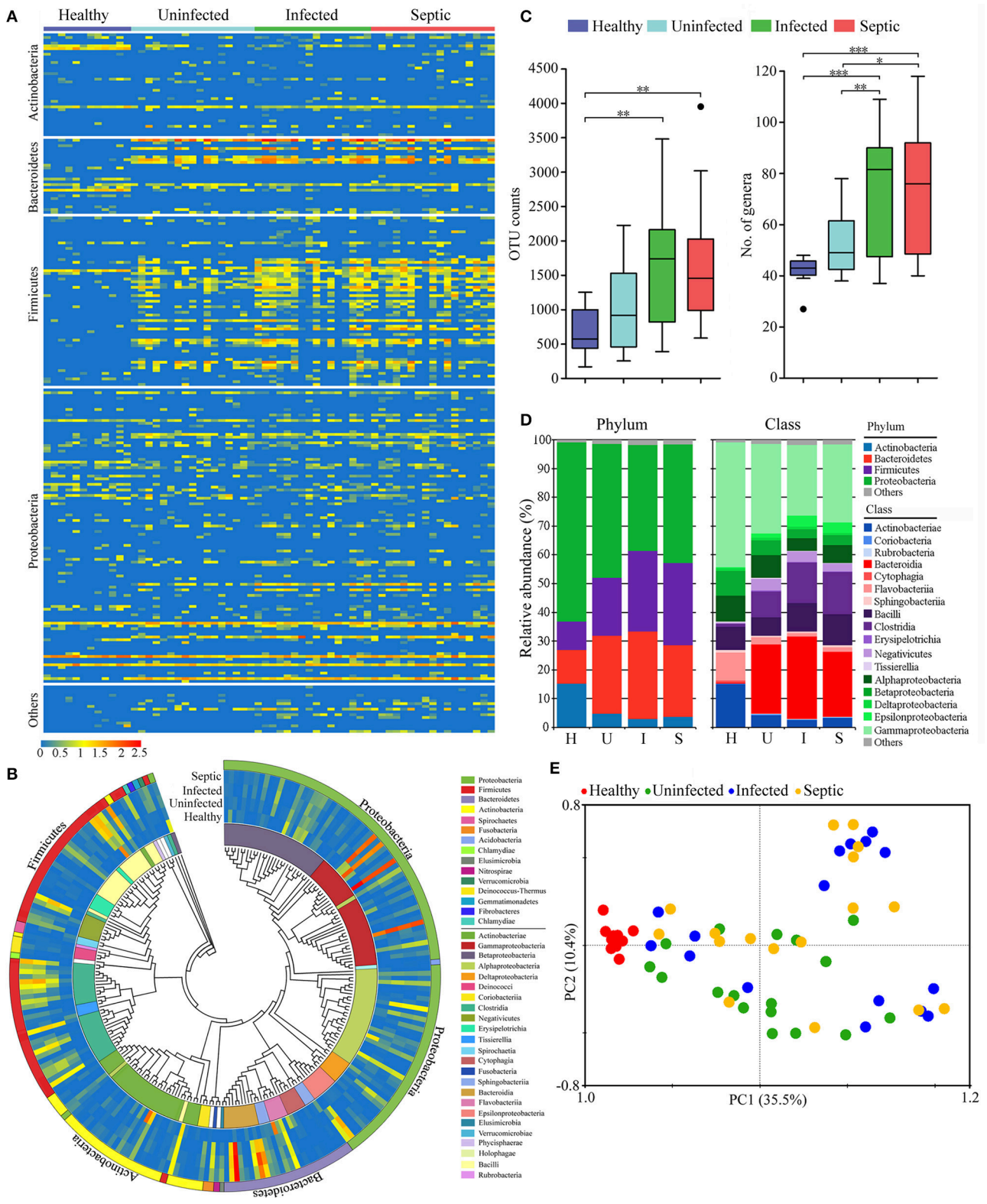

FIGURE 2 | Phylogenetic compositions of putative gut-derived organisms in the neutrophil-associated microbiomes (NAMs). **(A)** Heatmap exhibiting the composition of the bacterial genera likely originated from the gut in peripheral neutrophils. **(B)** The phylogenetic analysis of the putative gut-derived bacterial composition of the NAMs. The data presented in the heatmap represent the means of the Log10 values of the operational taxonomic unit (OTU) counts from each group. **(C)** Differences

(Continued)

FIGURE 2 | of the counts the OTUs and genera affiliated with the putative gut-derived organisms in the NAMs. *$P < 0.05$; **$P < 0.01$; ***$P < 0.001$. **(D)** Changes of the predominant bacterial composition in the NAMs at the phylum and class levels. The letters "H," "U," "I," and "S" represent the healthy, uninfected, infected and septic groups, respectively. **(E)** Principal component analysis (PCA) of weighted UniFrac distances, based on the relative abundance of each genus, displaying the compositional differences of the NAMs.

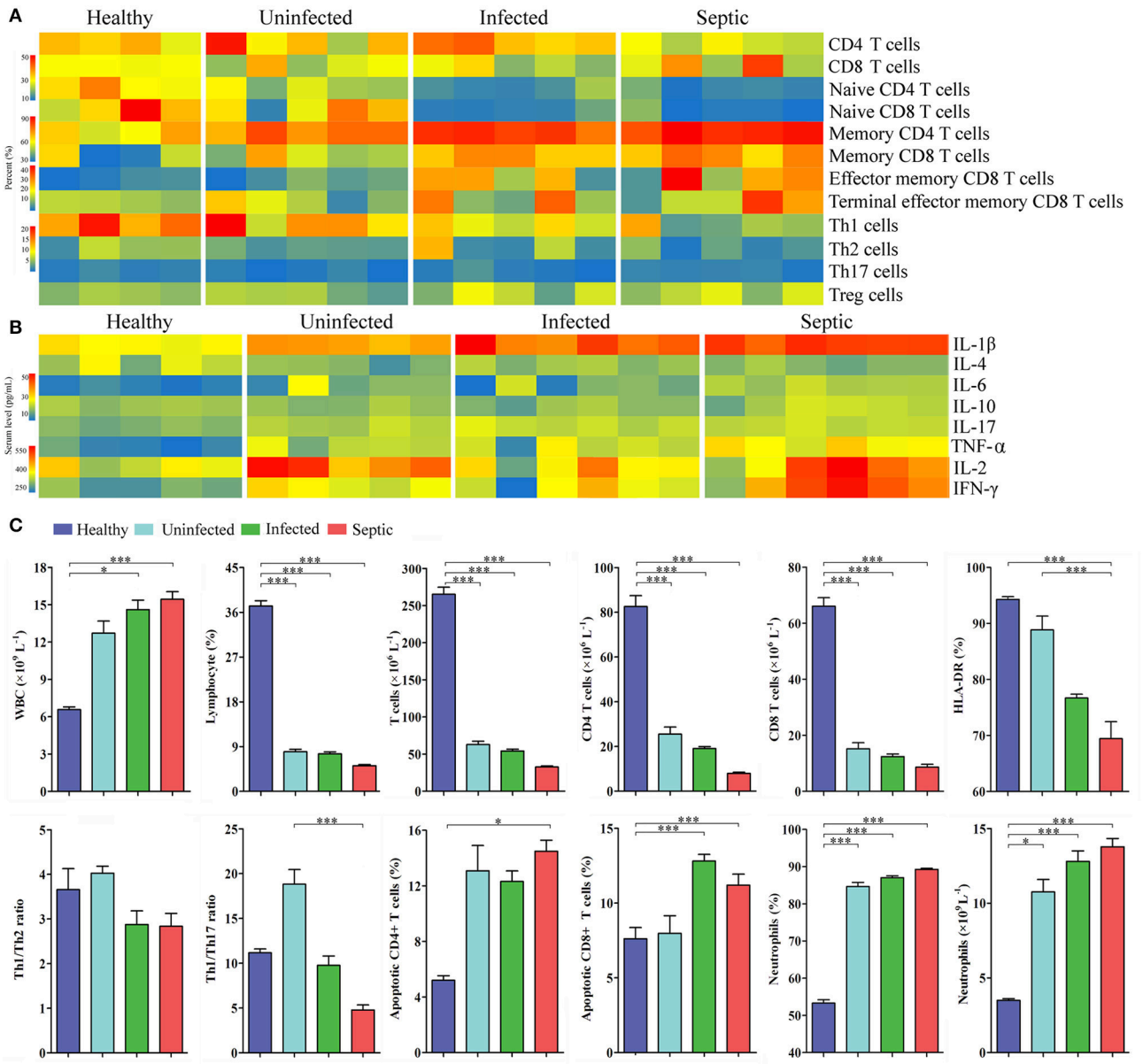

FIGURE 3 | Changes in the peripheral immune cell subpopulations and serum cytokines. **(A)** Heatmap displaying the variations of the lymphocyte subsets in SAP patients compared to healthy controls. **(B)** Profiles of the serum cytokines in patients and healthy controls. **(C)** The graphs indicate the changes of T-helper cell subsets, apoptotic lymphocytes and neutrophils, together with the counts of peripheral immune cells in patients. *$P < 0.05$; ***$P < 0.001$.

Changes of Neutrophil Proteomic Profiles and Its Connection with Alterations of Blood Microbiome

We further performed comparative proteomic analysis on peripheral neutrophils derived from healthy and SAP subjects in an attempt to link cell functional changes to the microbiome alterations. A total of 296 proteins were characterized as differentially expressed, were then annotated and clustered into six categories involved in biological functions of neutrophils, including innate immune defense, immune response, cytokine

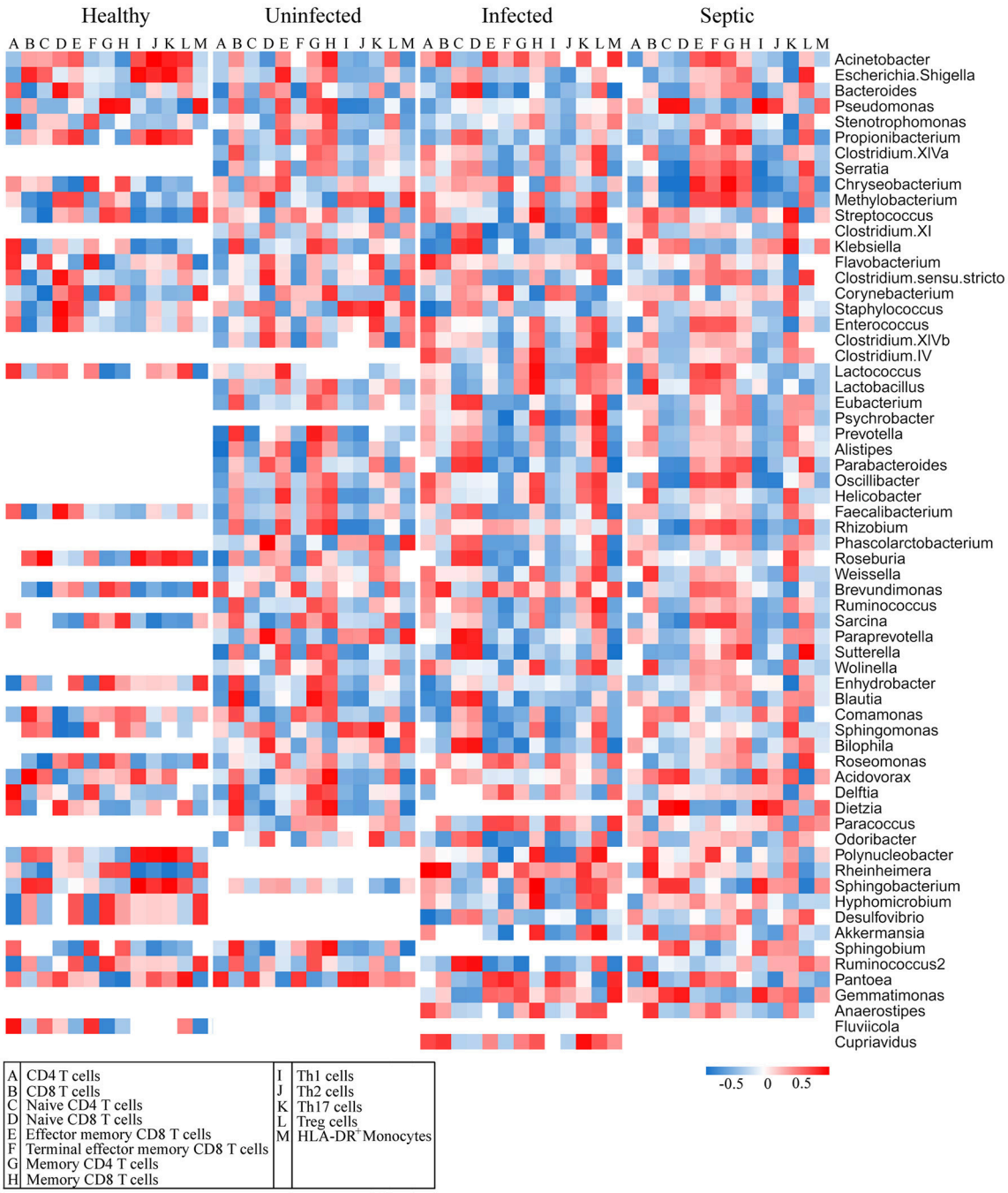

FIGURE 4 | Correlations of the predominant bacterial genera in the neutrophils with the subpopulations of peripheral lymphocytes. The data presented in the heatmap indicate the correlation coefficient between variances.

release, cell apoptosis, cell structure, and metabolic activity (Supplementary Table 2). As shown in the **Figure 5A**, the expression profiles of these proteins were dramatically varied in SAP patients with sepsis and healthy controls. Of these, the proteins closely involved in bactericidal activities of neutrophil, such as lysozyme C (LYZ), eosinophil cationic protein (RNASE3), myeloperoxidase (MPO), neutrophil defensin 3 (DEFA4), properdin (CFP) and bactericidal permeability-increasing protein (BPI), were significantly down-regulated in septic patients, indicating that the dysfunction of innate immunity might be present in septic cases. We also compared the expression profiles of some known immune response-associated proteins, as characterized by significant down-regulations for a vast majority of these proteins in SAP patients (**Figure 5A**).

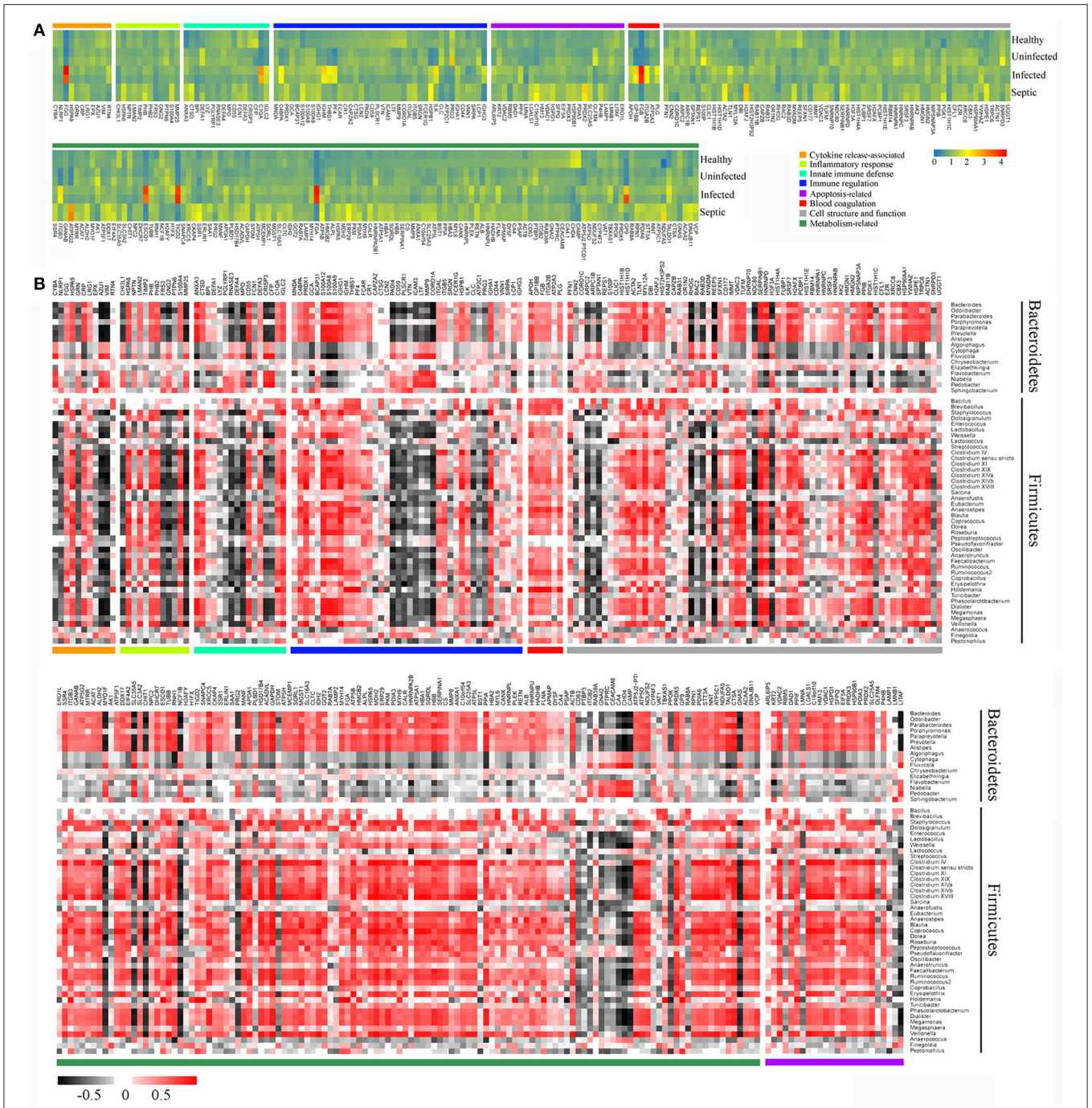

FIGURE 5 | Association between alterations of neutrophil proteomics profiling and dysbiotic microbiota**. (A)** Heatmap showing the changes of the relative abundance of expressed-differentially proteins in neutrophils. **(B)** Correlations between the expressed-differentially proteins of neutrophils and the predominant bacterial genera from the neutrophil-associated microbiomes. The data indicate the correlation coefficient between variances.

The changes in the protein expressions were likely, at least in part, involved in the immunosuppression in SAP patients with sepsis. Of special note, matrix metallopeptidase 9 (MMP9), a protein prompting leukocyte transendothelial migration, was significantly declined in septic patients, suggesting the presence of neutrophil dysfunction. The expression of the proteins involved in modulation of proinflammatory cytokines was strikingly up-regulated in septic patients, probably having implication for establishment of the uncontrollable inflammatory response. Similarly, the expression of some proteins associated

with cell apoptosis was increased in septic patients, which may help to explain delayed neutrophil apoptosis in sepsis. In addition, an over-representation in metabolism-related proteins was observed in the septic patients, when compared against the data set from healthy persons. Basing on the observations, we provide indirect evidence indicating that the function of neutrophils might be impaired in SAP patients with sepsis.

Next we conducted a Pearson's correlation analysis to associate the differentially expressed proteins of neutrophils with microbiome memberships (**Figure 5B**). Our data showed that changes of the protein expression in neutrophils were closely associated with specific bacterial taxons of the microbiome. As shown in **Figure 5B,** most of the proteins in the functional clusters of innate immune defense, immune response and cytokine production correlated negatively with compositional changes of the neutrophil-associated microbiome, especially the memberships of the phyla Bacteroidetes and Firmicutes. On the contrary, a majority of the proteins involved in the apoptosis and metabolic activities of neutrophils correlated positively with the members of the microbiomes.

DISCUSSION

To our knowledge, this is the first prospective observational case series exploring the microbial landscape in peripheral blood and neutrophils in SAP patients, as well as their potential links with the immunological disorders of the patients. Through this study, we identified diverse bacterial microbiomes within peripheral blood and neutrophils, and discovered that the microbiome is altered in SAP patients. More importantly, the abundance changes in certain members of the microbiomes are closely linked to the immunological disorders of the patients. Our findings provide emerging evidence supporting the presence of the blood microbiome and give us novel insights into induction of bacteremia in SAP patients.

Recent studies have begun to document that human blood contains an authentic microbiome, which could contribute significantly to the development of sepsis (Grumaz et al., 2016; Gosiewski et al., 2017) and several chronic diseases (Amar et al., 2013; Rajendhran et al., 2013; Dinakaran et al., 2014). Yet, whether a diverse bacterial community is present in blood of SAP patients remains an unanswered question. Through the fingerprinting approach of 16S rRNA amplicons, we have recently demonstrated that multiple bacterial species are commonly seen in blood of patients with SAP (Li et al., 2013a), but without deep sequencing data it was not possible to define the microbial landscape in blood and its potential role in pathogenesis of sepsis. Herein we conduct 16S rRNA gene sequencing to characterize the bacterial profile present in blood of SAP patients. We show that the peripheral blood in SAP patients has a diverse bacterial microbiota, dominated by the phyla Proteobacteria, Actinobacteria, Bacteroidetes, and Firmicutes, which is consistent with previous reports (Amar et al., 2013; Rajendhran et al., 2013; Dinakaran et al., 2014). Furthermore, the blood microbiome in SAP patients appears dysbiotic, as revealed by loss of species richness and changes of predominant bacterial taxa relative to healthy controls. Together with the findings, we suggest that the perturbation of blood microbiota, which likely represents a disease-provoking state, might be involved in the progression of sepsis. Prior studies have reported that dysbiosis of the blood microbiome is an independent risk factor of cardiovascular disease, indicating its potentially pathological role (Amar et al., 2013; Rajendhran et al., 2013; Dinakaran et al., 2014). In total, our investigations based on culture-independent techniques have shown a previously unappreciated complexity of the blood bacterial microbiome in SAP patients, also forcing reconsideration of the mechanisms of sepsis pathogenesis and exacerbations.

Intestinal dysbiosis and bacterial translocation are common in critically ill patients, and there is strong evidence that the translocation of bacteria and their products across the intestinal barrier drives the progression of sepsis (Dickson, 2016; Alverdy and Krezalek, 2017). Our understanding of the concept of translocation of one or several organisms from the gut is founded on culture-based studies (MacFie et al., 1999; MacFie, 2004). Recently, Dickson and colleagues have demonstrated that the lung microbiome is enriched with gut-associated bacteria in sepsis and acute respiratory distress syndrome, providing strong evidence for gut–lung translocation of bacterial microbiota (Dickson et al., 2016). The observations prompted us to re-consider the current opinion of bacterial translocation from the gut to systemic circulation. Our data presented here reveal that the blood microbiome is mainly composed of gut-associated organisms in SAP patients, which is similar to the results in the lung microbiome (Dickson et al., 2016). It is therefore speculated that a bacterial consortium from the gut, rather than single or several organisms, might migrate into systemic circulation during sepsis. A longitudinal study of paired stool and blood specimens will be required to determine the true prevalence for gut-blood translocation of bacterial microbiota in sepsis. Nonetheless, the significant correlation between circulating bacteria and clinical manifestations offers evidence that the blood microbiome may play an important role in sepsis, even in the absence of gut–blood translocation.

Innate immune cells and microorganisms in blood are highly interactive, maintaining a delicate balance between defending against infection and eliciting an excessive inflammatory response (Nathan, 2006). Given the critical role of neutrophils in eradication of pathogens, we sought to characterize the composition of neutrophil-associated microbiomes and explore potential roles in the alteration of blood microbiome in SAP. We show that the neutrophils contain a diverse microbiome, and the microbiota composition is significantly altered in SAP patients, consistent with the findings from the blood microbiome. Proteomic analysis of the neutrophils shows that the function of neutrophils is likely disturbed, especially in septic patients, as revealed by reframing of the protein profiles. The bactericidal effector function of neutrophils, represented by decreased antibacterial peptide production (Flannagan et al., 2009), is probably restricted in SAP patients with sepsis. Another prominent feature of neutrophils is decreased expression of MMP9, possibly contributing to impairment of cell migration during systemic infections (Kolaczkowska et al.,

2009). The observations indicate that the neutrophil function is probably collapsed, leading to impaired intracellular bacterial clearance and compositional shifts of NAMs in sepsis. Further investigations with neutrophil killing/phagocytosis assays will be needed to provide direct evidence linking the blood microbiome alterations seen in SAP patients with neutrophil dysfunction.

Unlike other organs, the blood was originally presumed to be sterile, and microbes were thought to be present in circulation only in sepsis cases. But, in recent years, the presence of bacterial 16S rRNA genes has been reported in the circulation of healthy individuals (Potgieter et al., 2015; Païssé et al., 2016). In this study, we have added evidence suggesting that the peripheral blood harbors a diverse bacterial microbiota in healthy individuals, consistent with the previous reports (Païssé et al., 2016). Interestingly, the blood microbiota is enriched with the putative gut-derived bacteria, implying that translocation of intestinal bacteria may play a critical role in shaping the unique microbiota. Previous studies have demonstrated that intestinal bacterial translocation could be a normal physiological event, and under healthy conditions the enteric organisms can move across the "intact" intestinal epithelium into normally sterile tissues including blood, contributing to development of systemic and/or organ immune system (Brenchley and Douek, 2012; Wiest et al., 2014). Quite contrary to the traditional concept that circulating blood is sterile in health, the blood may harbor a commensal microbiome, which is likely to be altered during disease.

In spite of compelling evidence indicating the existence of blood microbiome in SAP patients, our study has several limitations. The primary limitation is that the results are based on sequencing of 16S rRNA genes, which is not sufficient to determine if a live microbiota is present in the circulation. It is required for metatranscriptomic studies to validate the presence/absence of a live bacterial microbiome in the blood. Another limitation is that 16S rDNA-based community profiling only provides information on the microbiota composition. Future studies will be needed to move from taxonomic description to detailed, metagenomics-based functional characterizations of the microbiota. Additionally, the number of individuals sampled in our study is relatively small, and thus it will be important to validate these observations with increasingly larger and more sophisticated human cohort studies.

In summary, we have presented compelling evidence that the blood contains a diverse bacterial microbiome in SAP patients. We also have identified the unique compositional signature of the blood and neutrophil-associated microbiomes that could distinguish SAP patients from healthy controls. More importantly, our data reveal potential links between the alterations in the blood and neutrophil-associated microbiomes and the immunological disorders in SAP patients. Yet, the possible involvement of blood microbiome variations in the development of systemic infection remains uncertain in SAP patients. Here we have only just begun to delineate the outline of the blood microbiome, and further investigations would likely provide novel insights into its roles in health and diseases.

AUTHOR CONTRIBUTIONS

QL, CW, and JL conceived of the work. QL and CW designed experiments and analyzed data. CW, CT, XZ, and QH enrolled the patients, collected samples, performed the experiments, and prepared the figures and tables. CW wrote the article and revised it critically for important intellectual content. QL reviewed and revised the manuscript. All authors read and approved the final version of the manuscript for submission.

FUNDING

This work was supported by the grants from the National Basic Research Program (973 Program) in China (2013CB531403) and National High-tech R&D Program (863 Program) of China (2012AA021007).

SUPPLEMENTARY MATERIAL

The Supplementary Material for this article can be found online at: https://www.frontiersin.org/articles/10.3389/fcimb.2018.00005/full#supplementary-material

REFERENCES

Akira, S., Uematsu, S., and Takeuchi, O. (2006). Pathogen recognition and innate immunity. *Cell* 124, 783–801. doi: 10.1016/j.cell.2006.02.015

Alverdy, J. C., and Krezalek, M. A. (2017). Collapse of the microbiome, emergence of the pathobiome, and the immunopathology of sepsis. *Crit. Care Med.* 45, 337–347 doi: 10.1097/CCM.0000000000002172

Amar, J., Lange, C., Payros, G., Garret, C., Chabo, C., Lantieri, O., et al. (2013). Blood microbiota dysbiosis is associated with the onset of cardiovascular events in a large general population: the D.E.S.I.R. study. *PLoS ONE* 8:e54461. doi: 10.1371/journal.pone.0054461

Ammori, B. J., Fitzgerald, P., Hawkey, P., and McMahon, M. J. (2003). The early increase in intestinal permeability and systemic endotoxin exposure in patients with severe acute pancreatitis is not associated with systemic bacterial translocation: molecular investigation of microbial DNA in the blood. *Pancreas* 26, 18–22. doi: 10.1097/00006676-200301000-00004

Ammori, B. J., Leeder, P. C., King, R. F., Barclay, G. R., Martin, I. G., Larvin, M., et al. (1999). Early increase in intestinal permeability in patients with severe acute pancreatitis: correlation with endotoxemia, organ failure, and mortality. *J. Gastrointest. Surg.* 3, 252–262. doi: 10.1016/S1091-255X(99)80067-5

Amulic, B., Cazalet, C., Hayes, G. L., Metzler, K. D., and Zychlinsky, A. (2012). Neutrophil function: from mechanisms to disease. *Annu. Rev. Immunol.* 30, 459–489. doi: 10.1146/annurev-immunol-020711-074942

Appelberg, R. (2007). Neutrophils and intracellular pathogens: beyond phagocytosis and killing. *Trends Microbiol.* 15, 87–92. doi: 10.1016/j.tim.2006.11.009

Bosmann, M., and Ward, P. A. (2013). The inflammatory response in sepsis. *Trends Immunol.* 34, 129–136. doi: 10.1016/j.it.2012.09.004

Bradley, E. L. III. (1993). A clinically based classification system for acute pancreatitis. Summary of the International Symposium on Acute Pancreatitis,

Atlanta, GA, September 11 through 13, 1992. *Arch. Surg.* 128, 586–590. doi: 10.1001/archsurg.1993.01420170122019

Brenchley, J. M., and Douek, D. C. (2012). Microbial translocation across the GI tract. *Annu. Rev. Immunol.* 30, 149–173. doi: 10.1146/annurev-immunol-020711-075001

Buehler, S. S., Madison, B., Snyder, S. R., Derzon, J. H., Cornish, N. E., Saubolle, M. A., et al. (2016). Effectiveness of practices to increase timeliness of providing targeted therapy for inpatients with bloodstream infections: a laboratory medicine best practices systematic review and meta-analysis. *Clin. Microbiol. Rev.* 29, 59–103. doi: 10.1128/CMR.00053-14

Cicalese, L., Sahai, A., Sileri, P., Rastellini, C., Subbotin, V., Ford, H., et al. (2001). Acute pancreatitis and bacterial translocation. *Dig. Dis. Sci.* 46, 1127–1132. doi: 10.1023/A:1010786701289

Conesa, A., Götz, S., García-Gómez, J. M., Terol, J., Talón, M., and Robles, M. (2005). Blast2GO: a universal tool for annotation, visualization and analysis in functional genomics research. *Bioinformatics* 21, 3674–3676. doi: 10.1093/bioinformatics/bti610

Delano, M. J., Thayer, T., Gabrilovich, S., Kelly-Scumpia, K. M., Winfield, R. D., Scumpia, P. O., et al. (2011). Sepsis induces early alterations in innate immunity that impact mortality to secondary infection. *J. Immunol.* 186, 195–202. doi: 10.4049/jimmunol.1002104

Dickson, R. P. (2016). The microbiome and critical illness. *Lancet Respir. Med.* 4, 59–72. doi: 10.1016/S2213-2600(15)00427-0

Dickson, R. P., Singer, B. H., Newstead, M. W., Falkowski, N. R., Erb-Downward, J. R., Standiford, T. J., et al. (2016). Enrichment of the lung microbiome with gut bacteria in sepsis and the acute respiratory distress syndrome. *Nat. Microbiol.* 1:161113. doi: 10.1038/nmicrobiol.2016.113

Dinakaran, V., Rathinavel, A., Pushpanathan, M., Sivakumar, R., Gunasekaran, P., and Rajendhran, J. (2014). Elevated levels of circulating DNA in cardiovascular disease patients: metagenomic profiling of microbiome in the circulation. *PLoS ONE* 9:e105221. doi: 10.1371/journal.pone.0105221

Ecker, D. J., Sampath, R., Li, H., Massire, C., Matthews, H. E., Toleno, D., et al. (2010). New technology for rapid molecular diagnosis of bloodstream infections. *Expert Rev. Mol. Diagn.* 10, 399–415. doi: 10.1586/erm.10.24

Flannagan, R. S., Cosio, G., and Grinstein, S. (2009). Antimicrobial mechanisms of phagocytes and bacterial evasion strategies. *Nat. Rev. Microbiol.* 7, 355–366. doi: 10.1038/nrmicro2128

Garg, P. K., Madan, K., Pande, G. K., Khanna, S., Sathyanarayan, G., Bohidar, N. P., et al. (2005). Association of extent and infection of pancreatic necrosis with organ failure and death in acute necrotizing pancreatitis. *Clin. Gastroenterol. Hepatol.* 3, 159–166. doi: 10.1016/S1542-3565(04)00665-2

Gosiewski, T., Ludwig-Galezowska, A. H., Huminska, K., Sroka-Oleksiak, A., Radkowski, P., Salamon,. D., et al. (2017). Comprehensive detection and identification of bacterial DNA in the blood of patients with sepsis and healthy volunteers using next-generation sequencing method -the observation of DNAemia. *Eur. J. Clin. Microbiol. Infect. Dis.* 36, 329–336. doi: 10.1007/s10096-016-2805-7

Grumaz, S., Stevens, P., Grumaz, C., Decker, S. O., Weigand, M. A., Hofer, S., et al. (2016). Next-generation sequencing diagnostics of bacteremia in septic patients. *Genome Med.* 8:73. doi: 10.1186/s13073-016-0326-8

Hotchkiss, R. S., Monneret, G., and Payen, D. (2013). Sepsis-induced immunosuppression: from cellular dysfunctions to immunotherapy. *Nat. Rev. Immunol.* 13, 862–874. doi: 10.1038/nri3552

Kolaczkowska, E., Grzybek, W.-R. N., Piccard, H., Plytycz, B., Arnold, B., and Opdenakker, G. (2009). Neutrophil elastase activity compensates for a genetic lack of matrix metalloproteinase 9 (MMP 9) in leukocyte infiltration in a model of experimental peritonitis. *J. Leukoc. Biol.* 85, 374–381. doi: 10.1189/jlb.0808460

Li, Q., Wang, C., Tang, C., He, Q., Li, N., and Li, J. (2013a). Bacteremia in the patients with acute pancreatitis as revealed by 16S rRNA gene-based techniques. *Crit. Care Med.* 41, 1938–1950. doi: 10.1097/CCM.0b013e31828a3dba

Li, Q., Wang, C. Y., Tang, C., He, Q., Li, N., and Li, J. S. (2013b). Reciprocal interaction between intestinal microbiota and mucosal lymphocyte in cynomolgus monkeys after alemtuzumab treatment. *Am. J. Transplant.* 13, 899–910. doi: 10.1111/ajt.12148

Li, W., and Godzik, A. (2006). Cd-hit: A fast program for clustering and comparing large sets of protein or nucleotide sequences. *Bioinformatics* 22, 1658–1659. doi: 10.1093/bioinformatics/btl158

MacFie, J. (2004). Current status of bacterial translocation as a cause of surgical sepsis. *Br. Med. Bull.* 71, 1–11. doi: 10.1093/bmb/ldh029

MacFie, J., O'Boyle, C., Mitchel, C. J., Buckley, P. M., Johnstone, D., and Sudworth, P. (1999). Gut origin of sepsis: a prospective study investigating associations between bacterial translocation, gastric microflora, and septic morbidity. *Gut* 45, 223–228. doi: 10.1136/gut.45.2.223

Matthew, J., Delano, A., and Ward, P. (2016). Sepsis-induced immune dysfunction: can immune therapies reduce mortality? *J. Clin. Invest.* 126, 23–31. doi: 10.1172/JCI82224

Medich, D. S., Lee, T. K., Melhem, M. F., Rowe, M. I., Schraut, W. H., and Lee, K. K. (1993). Pathogenesis of pancreatic sepsis. *Am. J. Surg.* 165, 46–50. doi: 10.1016/S0002-9610(05)80403-9

Muyzer, G., de Waal, E. C., and Uitterlinden, A. G. (1993). Profiling of complex microbial populations by denaturing gradient gel electrophoresis analysis of polymerase chain reaction amplified genes coding for 16S rRNA. *Appl. Environ. Microbiol.* 59, 695–700.

Nathan, C. (2006). Neutrophils and immunity: Challenges and opportunities. *Nat. Rev. Immunol.* 6, 173–182. doi: 10.1038/nri1785

Nathens, A. B., Curtis, J. R., Beale, R. J., Cook, D. J., Moreno, R. P., Romand, J. A., et al. (2004). Management of the critically ill patient with severe acute pancreatitis. *Crit. Care Med.* 32, 2524–2536. doi: 10.1097/01.CCM.0000148222.09869.92

Noor, M. T., Radhakrishna, Y., Kochhar, R., Ray, P., Wig, J. D., Sinha, S. K., et al. (2011). Bacteriology of infection in severe acute pancreatitis. *JOP* 12, 19–25. Available online at: http://www.joplink.net/prev/201101/12.html

Païssé, S., Valle, C., Servant, F., Courtney, M., Burcelin, R., Amar, J., et al. (2016). Comprehensive description of blood microbiome from healthy donors assessed by 16S targeted metagenomic sequencing. *Transfusion* 56, 1138–1147. doi: 10.1111/trf.13477

Potgieter, M., Bester, J., Kell, D. B., and Pretorius, E. (2015). The dormant blood microbiome in chronic, inflammatory diseases. *FEMS Microbiol. Rev.* 39, 567–591. doi: 10.1093/femsre/fuv013

Qi, Q., Liu, Y., Cheng, Y., Glanville, J., Zhang, D., Lee, J. Y., et al. (2014). Diversity and clonal selection in the human T-cell repertoire. *Proc. Natl Acad. Sci. U.S.A.* 111, 13139–13144. doi: 10.1073/pnas.1409155111

Rajendhran, J., Shankar, M., Dinakaran, V., Rathinavel, A., and Gunasekaran, P. (2013). Contrasting circulating microbiome in cardiovascular disease patients and healthy individuals. *Int. J. Cardiol.* 68, 5118–5120. doi: 10.1016/j.ijcard.2013.07.232

Sainio, V., Kemppaainen, E., Puolakkainen, P., Taavitsainen, M., Kivisaari, L., Valtonen, V., et al. (1995). Early antibiotic treatment in acute necrotising pancreatitis. *Lancet* 346, 663–667. doi: 10.1016/S0140-6736(95)92280-6

Schmid, S. W., Uh, W., Friess, H., Malfertheiner, P., and Büchler, M. W. (1999). The role of infection in acute pancreatitis. *Gut* 45, 311–316. doi: 10.1136/gut.45.2.311

Segata, N., Izard, J., Waldron, L., Gevers, D., Miropolsky, L., Garrett, W. S., et al. (2011). Metagenomic biomarker discovery and explanation. *Genome Biol.* 12:R60. doi: 10.1186/gb-2011-12-6-r60

Shadforth, I. P., Dunkley, T. P., Lilley, K. S., and Bessant, C. (2005). i-Tracker: for quantitative proteomics using iTRAQ. *BMC Genomics* 6:145. doi: 10.1186/1471-2164-6-145

Singer, M., Deutschman, C. S., Seymour, C. W., Shankar-Hari, M., Annane, D., Bauer, M., et al. (2016). The third international consensus definitions for sepsis and septic shock (Sepsis-3). *JAMA* 315, 801–810. doi: 10.1001/jama.2016.0287

The Human Microbiome Project Consortium (2012). Structure, function and diversity of the healthy human microbiome. *Nature* 486, 207–214. doi: 10.1038/nature11234

Villatoro, E., Mulla, M., and Larvin, M. (2010). Antibiotic therapy for prophylaxis against infection of pancreatic necrosis in acute pancreatitis (Review). *Cochrane Database Syst. Rev.* 12:CD002941. doi: 10.1002/14651858.CD002941.pub3

Wang, Q., Garrity, G. M., Tiedje, J. M., and Cole, J. R. (2007). Naive Bayesian classifier for rapid assignment of rRNA sequences into the new bacterial taxonomy. *Appl. Environ. Microbiol.* 73, 5261–5267. doi: 10.1128/AEM.00062-07

Wiest, R., Lawson, M., and Geuking, M. (2014). Pathological bacterial translocation in liver cirrhosis. *J. Hepatol.* 60, 197–209. doi: 10.1016/j.jhep.2013.07.044

Conflict of Interest Statement: The authors declare that the research was conducted in the absence of any commercial or financial relationships that could be construed as a potential conflict of interest.

Copyright © 2018 Li, Wang, Tang, Zhao, He and Li. This is an open-access article distributed under the terms of the Creative Commons Attribution License (CC BY). The use, distribution or reproduction in other forums is permitted, provided the original author(s) or licensor are credited and that the original publication in this journal is cited, in accordance with accepted academic practice. No use, distribution or reproduction is permitted which does not comply with these terms.

frontiers in Cellular and Infection Microbiology

ORIGINAL RESEARCH
published: 30 November 2017
doi: 10.3389/fcimb.2017.00489

Microbiota Modulate Anxiety-Like Behavior and Endocrine Abnormalities in Hypothalamic-Pituitary-Adrenal Axis

Ran Huo[1, 2, 3†], Benhua Zeng[4†], Li Zeng[2, 5†], Ke Cheng[1, 2†], Bo Li[1, 2, 3], Yuanyuan Luo[1, 2], Haiyang Wang[2], Chanjuan Zhou[1], Liang Fang[1], Wenxia Li[4], Rong Niu[4], Hong Wei[4] and Peng Xie[1, 2, 3, 5*]*

[1] Department of Neurology, Yongchuan Hospital, Chongqing Medical University, Chongqing, China, [2] Institute of Neuroscience and the Collaborative Innovation Center for Brain Science, Chongqing Medical University, Chongqing, China, [3] Key Laboratory of Clinical Laboratory Diagnostics (Ministry of Education), Department of Laboratory Medicine, Chongqing Medical University, Chongqing, China, [4] Department of Laboratory Animal Science, College of Basic Medical Sciences, Third Military Medical University, Chongqing, China, [5] Department of Neurology, First Affiliated Hospital of Chongqing Medical University, Chongqing Medical University, Chongqing, China

OPEN ACCESS

Edited by:
Michele Marie Kosiewicz, University of Louisville, United States

Reviewed by:
Valerio Iebba, Sapienza Università di Roma, Italy
Guoqiang Zhu, Yangzhou University, China

***Correspondence:**
Hong Wei
weihong63528@163.com
Peng Xie
xiepeng@cqmu.edu.cn

[†] *These authors have contributed equally to this work.*

Received: *23 July 2017*
Accepted: *13 November 2017*
Published: *30 November 2017*

Citation:
Huo R, Zeng B, Zeng L, Cheng K, Li B, Luo Y, Wang H, Zhou C, Fang L, Li W, Niu R, Wei H and Xie P (2017) Microbiota Modulate Anxiety-Like Behavior and Endocrine Abnormalities in Hypothalamic-Pituitary-Adrenal Axis. Front. Cell. Infect. Microbiol. 7:489. doi: 10.3389/fcimb.2017.00489

Intestinal microbes are an important system in the human body, with significant effects on behavior. An increasing body of research indicates that intestinal microbes affect brain function and neurogenesis, including sensitivity to stress. To investigate the effects of microbial colonization on behavior, we examined behavioral changes associated with hormones and hormone receptors in the hypothalamic-pituitary-adrenal (HPA) axis under stress. We tested germ-free (GF) mice and specific pathogen-free (SPF) mice, divided into four groups. A chronic restraint stress (CRS) protocol was utilized to induce external pressure in two stress groups by restraining mice in a conical centrifuge tube for 4 h per day for 21 days. After CRS, Initially, GF restraint-stressed mice explored more time than SPF restraint-stressed mice in the center and total distance of the OFT. Moreover, the CRH, ACTH, CORT, and ALD levels in HPA axis of GF restraint-stressed mice exhibited a significantly greater increase than those of SPF restraint-stressed mice. Finally, the Crhr1 mRNA levels of GF CRS mice were increased compared with SPF CRS mice. However, the Nr3c2 mRNA levels of GF CRS mice were decreased compared with SPF CRS mice. All results revealed that SPF mice exhibited more anxiety-like behavior than GF mice under the same external stress. Moreover, we also found that GF mice exhibited significant differences in, hormones, and hormone receptors compared with SPF mice. In conclusion, Imbalances of the HPA axis caused by intestinal microbes could affect the neuroendocrine system in the brain, resulting in an anxiety-like behavioral phenotype. This study suggested that intervention into intestinal microflora may provide a new approach for treating stress-related diseases.

Keywords: intestinal microbes, HPA axis, CRS model, microbiota-gut-brain axis, stress-related diseases

INTRODUCTION

The intestine is the largest system in the mammalian body, containing 100 trillion organisms. Intestinal microbial flora are established in early life in mammals, and affect the host's physiological function (Grenham et al., 2011; Lozupone et al., 2012; Heitlinger et al., 2017). Recent studies also have reported that intestinal microbial steady-state imbalances can cause a range of metabolic diseases (Wen et al., 2008; Henaomejia et al., 2012; Koren et al., 2012). A number of studies have explored the mechanisms of intestinal microorganisms, and a range of microbe-related diseases have been discovered and explored in neuropsychiatric subjects. However, the precise mechanisms of action of intestinal microbial flora remain unclear. Among the known pathogenetic mechanisms, several mental illnesses have been linked to the hypothalamic-pituitary-adrenal (HPA) axis (Schatzberg et al., 2014; Fries et al., 2015).

According to the long-standing HPA axis imbalance theory, hormone imbalance is closely associated with psychiatric diseases. A range of factors, including exercise, anxiolytic drugs, and sexual experience, can interfere with the secretion of stress hormones related to the HPA axis (Romero, 2004). Meanwhile, stress-related psychiatric disorders are closely related to imbalances in the HPA axis (Jacobson, 2014; van Bodegom et al., 2017), including anxiety disorders, social anxiety disorder, and post-traumatic stress disorder (Wirtz et al., 2007). Several studies have reported that changes in HPA axis hormones vary between stimulus type and rat variety, and can be used as an index of the intensity of a stressor (Girotti et al., 2006). In addition, one study found that plasma hormone levels (adrenocorticotropic hormone, ACTH; cortisol, CORT) were increased in the HPA axis after exposure to various stressors for 30 min (Hueston et al., 2011) and decreased to baseline levels within a certain time after the termination of acute stress (Dhabhar et al., 1997). The glucocorticoid receptor (GR) and the mineralocorticoid receptor (MR) mediate regulation of CORT gene expression (Arriza et al., 1987), which illustrates that hormonal changes in the HPA axis may are associated with changes in receptor levels. Interestingly, previous studies have found microbes are closely connection between HPA axis and behavior (Moya-Pérez et al., 2017).

In recent studies, GF mice are widely used as a tool for assessing the role of intestinal microbes, which have been found to affect mouse brain function and behavior (Luczynski et al., 2016). In addition, an increasing body of research has examined the effects of intestinal microbes in the HPA axis and microbiota-gut-brain axis using GF animals and antibiotic intervention (Foster, 2015; Zeng et al., 2016). Studies in which stool is transplanted from patients into the intestine of germ-free (GF) mice have revealed that gut microbiota can affect animals' behavior through the microbiota-gut-brain axis (Bercik et al., 2011; Cryan and Dinan, 2012; Zheng et al., 2016b). In the HPA axis, the hypothalamus is considered the starting point of the HPA axis, and previous studies have shown that levels of hormone concentration and hormone receptors in this brain region are altered under acute pressure (Crumeyrolle-Arias et al., 2014; Zhu et al., 2014). To create artificial chronic stress, the chronic restraint stress (CRS) model is classical and widely used to induce external pressure to detect the relationship between chronic pressure and diseases (Andrus et al., 2012). On the basis of this previous research, we hypothesized that intestinal microbial stabilization disorders would affect behavioral changes through the HPA axis using the CRS model in mice.

In the current study, to assess the effects of intestinal microbes on the HPA axis, we first examined behavior, hormone levels and receptor expression in the HPA axis using the CRS model in both GF and SPF mice. Then behavior was analyzed to assess whether differences in intestinal microbes play an important role in behavioral changes in mice.

MATERIALS AND METHODS

Animals

GF Kunming (KM) and SPF KM mice (male; 6 weeks old) were provided by the Experimental Animal Center of the Third Military Medical University (Chongqing, China) and bred at the Experimental Animal Center of the Third Military Medical University (GB 14922.2-2011). GF mice were kept and subjected to the CRS protocol in sterile isolators until the beginning of the behavioral tests. Weekly fecal samples were collected from GF mice and monitored using cultures of aerobic and anaerobic microbes to ensure the reliability of sterile feeding conditions. SPF mice were kept and subjected to the CRS protocol in barrier system with 10,000 cleanliness level and noise $\leq$60 dB. All animals were group-housed in Macrolon cages (37 cm long, 26 cm wide, 17 cm high) and fed with autoclaved chow and water. Animal room conditions were maintained with a constant temperature of 22 $\pm$ 2°C, relative humidity 55 $\pm$ 5% under a 12 h light-12 h dark cycles (lights on at 8:00 a.m.). The experimental protocols were in accord with the National Institutes of Health Guide for the Care and Use of Laboratory Animals (NIH Publication No. 80-23), revised in 1996. Moreover, the Ethics Committee of Chongqing Medical University approved all the experiments.

Chronic Restraint Stress (CRS) Procedure

All mice were acclimatized to the standard experimental environment for 7 days before the test session (Liu et al., 2016). GF and SPF mice were subjected to an established chronic physical restraint protocol. They were placed in the 50 ml multiple breathable hollows (0.5 mm diameter, 12 holes) conical centrifuge tubes (Wong et al., 2016). This restraint vessel was adapted to the animal's body size, and no pain was involved. Mice were restrained in the pipe for 4 h (from 13:00 to 17:00), with 20 h of rest time each day for 21 days. Mice were deprived of food and water during restraint then given food and water after each restraint experiment (Zafir and Banu, 2007). Mice were released into the cage to receive water and food immediately after the experiment. This restraint procedure was approved by the Ethics Committee of Chongqing Medical University. The details of the experimental procedure are shown in **Figure 1**.

Behavioral Procedures

In each experiment, GF and SPF mice (n = 28–32 in each group) were removed from the bacteria isolator, and

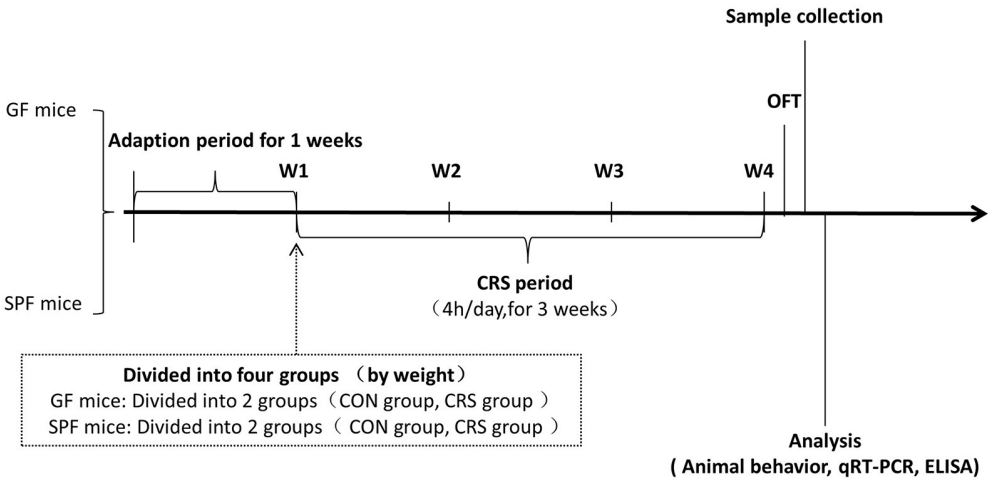

FIGURE 1 | Animal treatment and experimental procedure. W1, animal adaptation time; Animals were grouped on the last day of the first week; W1–W4, CRS period. GF mice, germ-free mice; SPF mice, specific pathogen-free mice; CRS, chronic restraint stress; OFT, open field test; qRT-PCR, quantitative real-time PCR; ELISA, enzyme-linked immunosorbent assay.

placed in the experimental environment for at least 1 h. The whole experimental environment was insulated to maintain a temperature of 22 ± 2°C, and humidity of 55 ± 5%. The trajectory of each mouse was recorded with a video tracking system linked to a computer. Trajectories were analyzed and quantified using the SMART2.5 software package (Panlab, Barcelona, Spain).

Open Field Test (OFT)

Mice were gently placed in the center of the apparatus and allowed to move freely. The device was constructed from opaque black paper (45 × 45 × 45 cm), and had no distinctive odor. The position placing each mouse was the fixed edge of the device. After each test, 70% ethanol was utilized to clean feces and remove odor. The test time was 6 min: 1 min to adapt, and 5 min for testing. The whole experimental process was recorded with a video tracking system. Correlative indices were measured in the last 5 min (Kim et al., 2012; Zhang et al., 2016; Zhou et al., 2016).

Sample Collection and Preparation

After the experimental period, mice were euthanized with 10% chloral hydrate (400 mg/kg; Chen et al., 2015). Mice were perfused with ice physiological saline (0.9% NaCl, Nongfu Spring Company Limited, Hangzhou, China). The whole brain was dissected and immediately placed in liquid nitrogen. All tissue samples were stored in a refrigerator at −80°C (Wang et al., 2016).

Hormonal Measurement

To quantify changes in HPA axis hormones in the hypothalamus tissue, the concentrations of ACTH, corticotropin-releasing hormone (CRH), CORT, and aldosterone (ALD) were analyzed using an enzyme-linked immunosorbent (ELISA) kit (ACTH, least detectable dose, 0.22 pg/ml, percent coefficient of variation, 5.38%, MD Bioproducts, USA; CRH, least detectable dose, 0.19 ng/ml, percent coefficient of variation, 6.54%; CORT, least detectable dose, 0.19 ng/ml, percent coefficient of variation, 6.66%; ALD, least detectable dose, 18.75 pg/ml, percent coefficient of variation, 4.73%; Elabscience Biotechnology Co., Ltd. China). Hypothalamus tissue was weighed, then minced into small pieces, which were homogenized in 1 g: 9 ml phosphate-buffered saline (PBS; Hyclone Co., USA) with protease inhibitor (Roche, Germany). We allowed samples and reagents to equilibrate to room temperature (22–25°C) before performing the assay. Each procedure was carried out according to the kit instructions, on ice.

Hormonal concentrations from each sample were calculated from the standard curve using CurveExpert 1.30 software (Daniel G. Hyams Co., USA) in accordance with the manufacturer's recommendations and normalized for hypothalamus tissue homogenate protein measured with the BCA method using enhanced BCA protein assay kit (Beyotime Co., China). The ELISA reaction was recorded at the corresponding wavelength using a microplate reader (Bio-Rad Co., USA).

Hormone-Related Receptor Measurement

Total RNA was extracted from frozen hypothalamus tissue using an RNA mini kit (Ambion, USA) on ice. All experimental procedures were in accord with the kit instructions, followed by reverse-transcribed into DNA using a PrimeScript RT Reagent Kit (Takara, Toyoto, Japan). The cycling conditions were: three cycles of reverse transcription reaction at 37°C for 15 min and reverse transcriptase inactivation reaction at 85°C for 5 s. The mRNA values in the hypothalamus were quantified using qRT-PCR (Roche, Germany). The cycling conditions were: 10 min preincubation at 95°C and 40 cycles of DNA amplification at 95°C for 10 s, 60°C for 30 s, and 72°C for 35 s. Primer

sequences were acquired using Primerbank (Harvard, USA), and synthesized by a biotechnology company (Sangon Biotech, Shanghai, China). The primer sequences for Crhr1fwd were as follows: 5′-gggcagcccgtgtgaattatt-3′, rev: 5′-atgacggcaatgtggtagtgc-3′; for Crhr2fwd:5′-catccaccacgtccgagac-3′, rev:5′-ctcgccaggattgacaaagaa-3′; for Mc2rfwd:5′-acaccgcaagaaataactccg-3′, rev:5′-aggaggacaatcaagttctcca-3′; for Nr3c1fwd:5′-agctccccctggtagagac-3′, rev:5′-ggtgaagacgcagaaaccttg-3′; for Nr3c2fwd:5′-gaagagccccctctgtttgcag-3′, rev:5′-tccttgagtgatgggactgtg-3′; for Gapdhfwd:5′-AGGTCGGTGTGAACGGATTTG-3′, rev:5′-TGTAGACCATGTAGTTGAGGTCA-3′. The corresponding mRNA content was standardized with Gapdh mRNA, and data expression was normalized with respect to the corresponding control group. All data were quantified with LightCycler 96 SW 1.1 analysis software (Roche, Germany). Hormonal receptor levels (Crhr1, Crhr2, Mc2r, Nr3c1, Nr3c2) were analyzed using quantitative real-time polymerase chain reaction (qRT-PCR; Roche, Germany) assay.

Statistical Analysis

All data were calculated as single data points superimposed to boxplots. The ELISA data, PCR data, and behavioral data were analyzed using two-way analysis of variance (ANOVA) assay with SPSS 20.0 (IBM North America, New York, NY, USA). In all cases, $p < 0.05$ were considered statistically significant.

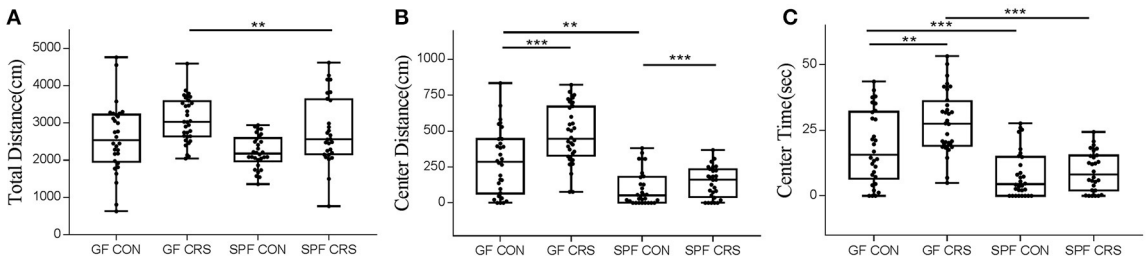

FIGURE 2 | Differences in open field test performance between groups. In the open field test (OFT): total distance (locomotor activity) traveled [**A**, $F_{(3, 116)} = 4.961$], distance in central activity [**B**, $F_{(3, 116)} = 7.949$] and time spent in the center [**C**, $F_{(3, 116)} = 5.658$] for GF CRS mice and SPF CRS mice were compared with the naive group. All values were presented as single data points superimposed to boxplots ($n = 28$–32 in each group). $^{**}p < 0.01$, $^{***}p < 0.001$.

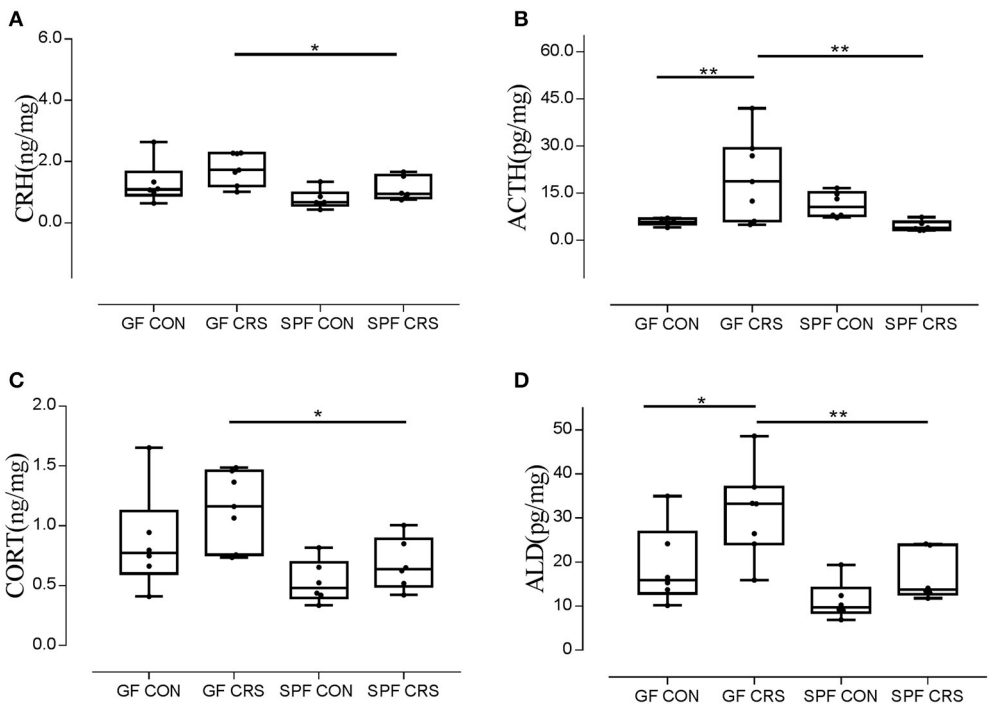

FIGURE 3 | Ratios of CRH, ACTH, CORT, and ALD levels relative to protein in hypothalamus tissue homogenates in control group and CRS group. ($n = 6$–7 in each group). The concentrations of CRH, ACTH, CORT, and ALD in tissue homogenates were measured with an ELISA kit. The concentrations of CRH, ACTH, CORT, and ALD were calculated as ng or pg/mg, hypothalamus protein homogenates. The values were presented as single data points superimposed to boxplots. [**A**, $F_{(3, 21)} = 0.794$; **B**, $F_{(3, 21)} = 6.197$; **C**, $F_{(3, 21)} = 0.990$; **D**, $F_{(3, 21)} = 1.450$]. $^{*}p < 0.05$, $^{**}p < 0.01$.

RESULTS

Changes in Behaviors between GF and SPF Mice

In order to determine whether the microbial colonization can alter behavior in mice, the OFT was used to assess behavior. Two-way ANOVA revealed that the SPF stressed control group moved a shorter total distance in the OFT compared with the GF stressed group ($p < 0.01$). Other groups did not show significant differences (**Figure 2A**). GF non-stressed control animals moved a significantly greater distance than SPF non-stressed mice in the center of the OFT ($p < 0.01$), and GF stressed animals moved a greater distance than GF non-stressed mice ($p < 0.001$). Mice in the SPF CRS group moved a greater distance in the center than those in the SPF non-CRS group ($p < 0.001$; **Figure 2B**). GF control mice spent less time exploring than GF stressed animals ($p < 0.01$)in the center of the OFT. In addition, the results revealed that GF control mice spent more time exploring than SPF control animals ($p < 0.001$), and GF restraint-stressed mice explored more time than SPF restraint-stressed mice ($p < 0.001$) in the center of the OFT (**Figure 2C**).

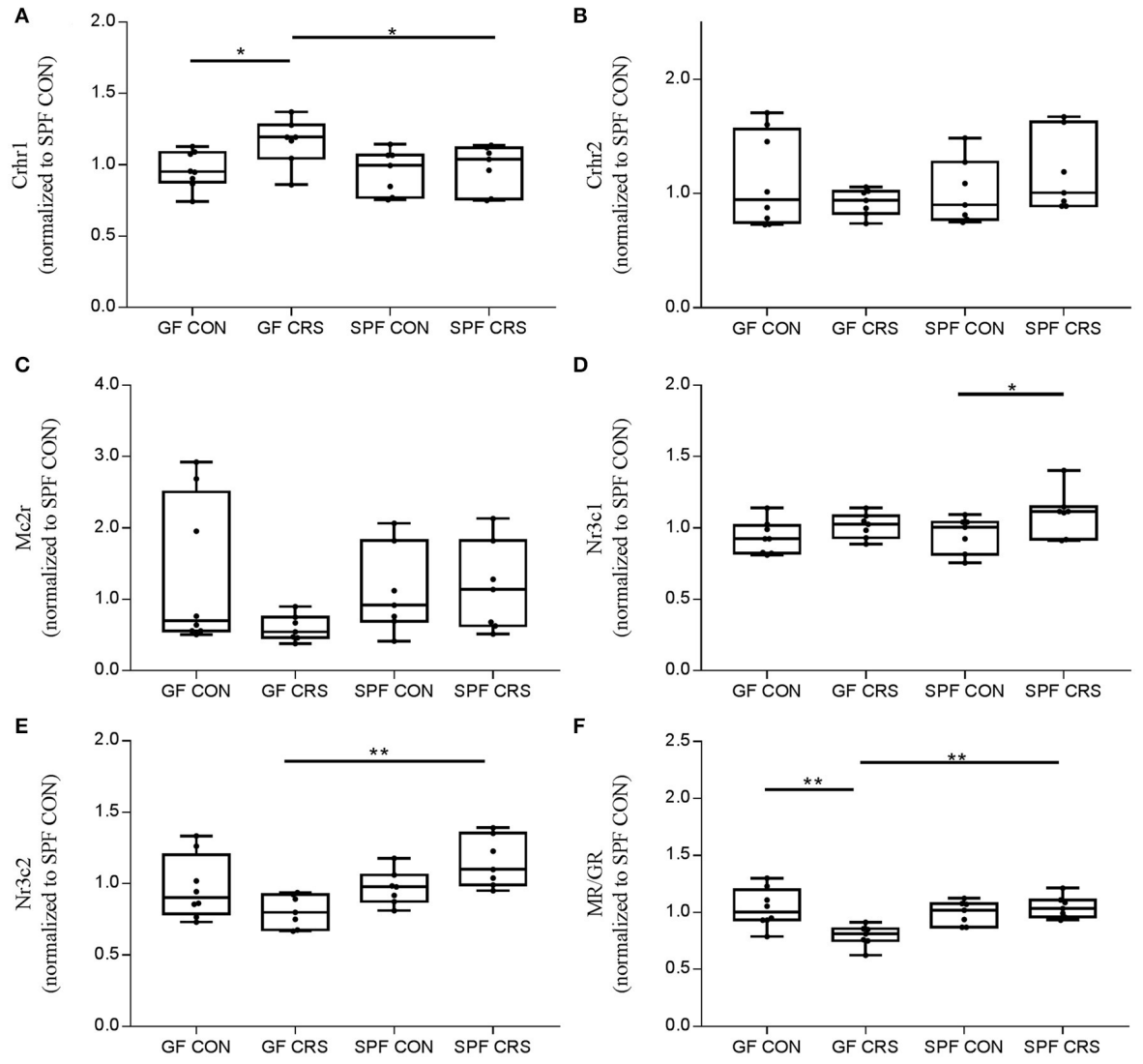

FIGURE 4 | Validation of hormone receptors and mineralocorticoid receptor (MR) / glucocorticoid receptor (GR) expression changes in the hypothalamus. Expression of hormone receptors and MR/GR was assessed in GF mice, GF CRS mice, SPF mice, and SPF CRS mice ($n = 7$–8 in each group). The data were analyzed using two-way ANOVA. Crhr1, corticotropin releasing hormone receptor 1, CRFR1; Crhr2, corticotropin releasing hormone receptor 2, CRFR2; Mc2r, melanocortin 2 receptor, ACTHR; Nr3c1, nuclear receptor subfamily 3, group C, member 1, glucocorticoid receptor, GR; Nr3c2, nuclear receptor subfamily 3, group C, member 2, mineralocorticoid receptor, MR. **(A)** shows the hormone receptor change in HPA axis. [**A**, $F_{(3, 25)} = 0.315$; **B**, $F_{(3, 25)} = 5.012$;**C**, $F_{(3, 25)} = 5.005$; **D**, $F_{(3, 25)} = 0.373$; **E**, $F_{(3, 25)} = 1.813$]. The MR/GR expression ratio was calculated to assess receptor disorder [$F_{(3, 25)} = 1.711$, **F**]. The values were presented as single data points superimposed to boxplots $^*p < 0.05$, $^{**}p < 0.01$. All data were normalized to SPF control mice.

Hormonal Dysfunction of the HPA Axis

We examined hormone and receptor levels in hypothalamic tissue. To assess changes in HPA axis-related hormones, hormonal levels were measured using ELISA in hypothalamus homogenates. As shown in **Figure 3A**, the CRH levels of GF restraint-stressed mice exhibited a significantly greater increase than those of SPF restraint-stressed mice ($p < 0.05$). The concentrations of ACTH in GF restraint-stressed mice homogenates were higher than in the GF control group ($p < 0.01$) and SPF restraint-stressed mice ($p < 0.01$; **Figure 3B**). The results revealed a trend toward increased CORT concentration in the GF restraint-stressed group compared with the SPF restraint-stressed group ($p < 0.05$; **Figure 3C**). ALD levels in GF restraint-stressed mice were also increased in hypothalamus homogenates compared with GF control group ($p < 0.05$) and SPF restraint-stressed mice ($p < 0.01$; **Figure 3D**).

Changes in Hormone Receptor mRNA

To investigate the link between hormone levels and hormone receptor mRNA, receptor mRNA in the mouse hypothalamus was quantified using qRT-PCR. **Figure 4** shows the changes in receptor levels among the groups. As expected, the Crhr1 mRNA levels of GF CRS mice were increased compared with GF control ($p < 0.05$) and SPF CRS mice ($p < 0.05$; **Figure 4A**). However, Nr3c1 mRNA expression in SPF control mice was decreased compared with SPF CRS mice ($p < 0.05$; **Figure 4D**), and Nr3c2 mRNA expression was decreased in GF CRS mice compared with SPF CRS mice ($p < 0.01$; **Figure 4E**). de Kloet (2014) demonstrated that the MR/GR balance plays an important role in mediating the function of CORT in the brain, and that dysfunction of MR/GR expression can occur in specific pathological, emotional, and cognitive conditions (Brinks et al., 2007). To detect whether MR/GR expression had changed, we calculated the ratio of MR to GR and found that MR/GR decreased in GF CRS mice compared with GF control mice ($p < 0.01$). A decrease was also found in SPF CRS mice ($p < 0.01$; **Figure 4F**).

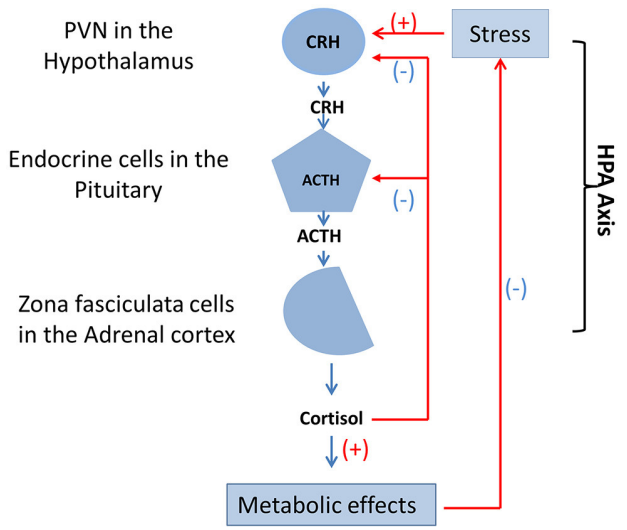

FIGURE 5 | Function and mutual adjustment of HPA axis. The HPA axis contains three cell types that secrete three different hormones: neurons of the PVN in the hypothalamus secrete CRH, endocrine cells in the pituitary secrete ACTH, and zona fasciculata cells in the adrenal cortex secrete cortisol. Stress, drugs, and diseases produce positive feedback regulation of neurons in the of the medial parvocellular portion of the PVN. In addition, cortisol that could result in metabolic effects produces direct negative feedback suppression of endocrine cells in the pituitary and CRH neurons of the PVN in the hypothalamus, respectively. HPA axis, hypothalamic-pituitary-adrenal axis; PVN, hypothalamic paraventricular nucleus; CRH, corticotropin-releasing hormone; ACTH, adrenocorticotropic hormone.

DISCUSSION

In our study, behavioral tests showed that GF control mice exhibited an increase in the distance traveled and time spent in the center of the OFT compared with SPF control mice, consistent with previous reports (Zeng et al., 2016; Zheng et al., 2016b). The GF mice without non-intestinal microbial colonization moved a greater total distance in the OFT and spent more time in the center, compared with SPF mice with intestinal microbes after CRS. This finding indicates that SPF mice with intestinal microbes exhibited increased anxiety-like behavior under the same pressure. Previous studies demonstrated that GF F344 rats were more likely to exhibit anxiety-like behavior than SPF rats (Crumeyrolle-Arias et al., 2014; Desbonnet et al., 2014; Wong et al., 2016; Zheng et al., 2016a,b). However, some studies found no relationship between intestinal microbes and animal behavior. The effects of intestinal microbes and physiological state on psychopathology are still debated. We then found that behavioral changes were largely consistent with changes in hormones, both in the presence of intestinal microbes and non-intestinal microbes. In addition, the results showed that hormones in GF CRS mice were significantly upregulated compared with SPF CRS mice in the HPA axis, in accord with previous reports (Sudo et al., 2004). This mechanism may be related to changes in CRH-signaling, glucocorticoids, or GR, which mediate behavior in the central nervous system (Owens and Nemeroff, 1991).

Although, some previous studies reported that anxiety- and trauma-related disorders were not consistent with simultaneous changes in the HPA axis, it is well established that these disorders are associated with an imbalance in the HPA axis (Smith et al., 1989; Baker et al., 1999; Jacobson, 2014). The current results revealed that GF CRS mice exhibited anti-anxiety behavior accompanied by HPA axis over-activity compared with SPF CRS mice. This novel finding may be related to our use of hypothalamus tissue, whereas many previous studies used plasma. The HPA axis has a complex feedback mechanism, and intestinal microbes may regulate behavior through the endocrine system, which may subsequently induce overactivity in the HPA axis.

Our examination of hormone receptors also indicated hormone dysfunction in the hypothalamus. Previous studies reported that hormone receptor gene knockout mice and mice given hormone receptor antagonists exhibited modulation of stress-coping behaviors (Boyle et al., 2005). GR is widely

expressed in most cell types throughout the body (De Kloet et al., 2000). GR and MR act as ligand-activated transcription factors and affect gene transcription, playing an important role in glucocorticoid function (Reul and Kloet, 1985). In addition, researchers have reported that changes of GR or MR levels in the hippocampus are associated with HPA axis dysfunction in mood-related illness, although findings have been inconsistent, with some studies finding that GR mRNA is decreased in depression, and other studies reporting that GR mRNA in the hippocampus was unchanged (Webster et al., 2002). At the same time, down-regulated MR and GR expression, and changes in MR/GR ratio have been reported in stress-induced rats (Medina et al., 2013). In the current study, we also used the MR/GR expression ratio to assess receptor diversification in the hypothalamus after behavioral changes. The results revealed changes in MR/GR expression and the action of intestinal microbes.

Intestinal microbes constitute a large and complex ecosystem in the intestinal wall of animals, affecting physiological and neuronal function, as well as animal behavior, via the microbiota-gut-brain axis and metabolites. Taken together with the behavioral and hormonal variations described above, the current results indicate that intestinal microbes play a critical role in influencing behavior and HPA-axis regulatory imbalance under external stress. Recent research suggests that intestinal microbes affect the host's physiology, metabolism and immunology, as well as nervous system development and brain function, through the microbiota-brain-gut axis (Collins and Bercik, 2009; Fu et al., 2015; Yano et al., 2015). Interestingly, Bercik et al. (2011) reported that adult mice given microbial agents via oral absorption showed changes in exploratory behavior and brain-derived neurotrophic factor (BDNF) expression in the hippocampus, while no change was observed with intraperitoneal injection of the same agent.

Studies have also reported that high intestinal permeability, bacterial translocation, and inflammatory factors are an important factor in mental disorders. Intestinal microflora mediate a series of neurotrophic factors, BDNF, and proteins (Ait-Belgnaoui et al., 2005). Intestinal microbial immune disorders are associated with aberrant neurodevelopment, and inappropriate use of antibiotics inhibits short-chain-fatty-acids (SCFAs) and the interaction between toll-like receptors and Treg cells. Moreover, the HPA axis (**Figure 5**) is affected by the peripheral nervous system (PNS), infection, and stress. The proportion of carbohydrates in food and dietary structure can also affect HPA axis activity (Keating et al., 2004; Glover et al., 2010; Ronald et al., 2010; Smith et al., 2013).

In addition, we speculated that intestinal microbes might cause intestinal metabolic changes through the intestinal microbial-gut-brain axis pathway. Metabolites may then pass through the intestinal wall, into blood circulation and through the blood-brain-barrier (BBB). The central nervous system (CNS) may then be affected by products of bacterial metabolism, causing hormone and receptor dysfunction, as well as behavioral changes.

First, intestinal microbes through enterochromaffin (EC) cells control the synthesis of 5-HT, which could be involved in brain function (Yano et al., 2015). Second, microbes may have an important relationship with the CNS through the inflammatory pathway, possibly activating local or systemic immune responses through the vagus nerve to influence the activity of the brain-gut axis (Borovikova et al., 2000; Wang et al., 2003). Third, SCFAs produced by intestinal bacterial fermentation have an immunomodulatory function, stimulating the link between the sympathetic nerve and nerve cells through G-protein-coupled receptor 41 (GPR41) and 43 (GPR43; Kimura et al., 2011). This might regulate the balance of microgliacytes, and mediate the release of intestinal peptide from endocrine cells to affect brain-gut axis activity (Wren and Bloom, 2007). In addition, this may mediate 5-HT synthesis in EC cells, which provides the CNS termination signal (Yano et al., 2015). Finally, intestinal microbes regulate tryptophan metabolism, which affects brain function and plays an important role in serotonin synthesis in the CNS (Ben-Ari, 2013). Moreover, intestinal microbes may also produce dopamine, γ-aminobutyric acid, histamine and acetylcholine, regulating the function of CNS and the stability of the HPA axis (Thomas et al., 2012; Barrett et al., 2014). In accord with this notion, the microbiota-gut-brain axis is considered to function as a bidirectional regulation mechanism of animal behavior (Wong et al., 2016).

The current study involved several limitations that should be considered. First, we did not use multiple behavioral paradigms to examine behavior more comprehensively. Moreover, this experiment did not clarify which intestinal microbial flora induced behavioral and endocrine changes in mice. Thus, more in-depth examination of the possible mechanisms involved should be conducted in follow-up research. In addition, in future studies we plan to re-colonize known microorganisms or probiotics into the intestine to regulate the connection between the intestine and the brain in mice, then utilize the corresponding intestinal microbe antibiotics, hormone or receptor antagonists to interfere with the connection, to further reveal the functional mechanisms of microorganisms in the HPA axis.

CONCLUSIONS

Based on previous research, in the current study we predicted that intestinal microbes would be an important factor in balancing the HPA axis. Imbalances of the HPA axis caused by intestinal microbes can affect the neuroendocrine system in the brain, resulting in an anxiety-like behavioral phenotype. The current findings suggest the possibility that novel treatments could be developed for stress-related diseases, including anxiety disorders, by direct or indirect intervention in intestinal microbial flora with currently available drug treatments.

AUTHOR CONTRIBUTIONS

RH, BZ, BL, YL, HyW, CZ, LF, WL, and RN: Performed experiments; LZ, RH, PX, and HW: Designed the study; RH and KC: Wrote the manuscript; All authors reviewed and approved the manuscript prior to its submission.

FUNDING

This work was supported by The National Key Research and Development Program of China (2017YFA0505700),

the National Natural Science Foundation of China (grant no. 81401140 and grant no. 81601207), and China Postdoctoral Science Foundation funded project (2017M612923).

ACKNOWLEDGMENTS

We thank the Third Military Medical University (Chongqing, China) for providing animals and experimental conditions.

REFERENCES

Ait-Belgnaoui, A., Bradesi, S., Fioramonti, J., Theodorou, V., and Bueno, L. (2005). Acute stress-induced hypersensitivity to colonic distension depends upon increase in paracellular permeability: role of myosin light chain kinase. *Pain* 113, 141–147. doi: 10.1016/j.pain.2004.10.002

Andrus, B. M., Blizinsky, K., Vedell, P. T., Dennis, K., Shukla, P. K., Schaffer, D. J., et al. (2012). Gene expression patterns in the hippocampus and amygdala of endogenous depression and chronic stress models. *Mol. Psychiatry* 17, 49–61. doi: 10.1038/mp.2010.119

Arriza, J. L., Weinberger, C., Cerelli, G., Glaser, T. M., Handelin, B. L., Housman, D. E., et al. (1987). Cloning of human mineralocorticoid receptor complementary DNA: structural and functional kinship with the glucocorticoid receptor. *Science* 237, 268–275. doi: 10.1126/science.3037703

Baker, D. G., West, S. A., Nicholson, W. E., Ekhator, N. N., Kasckow, J. W., Hill, K. K., et al. (1999). Serial CSF corticotropin-releasing hormone levels and adrenocortical activity in combat veterans with posttraumatic stress disorder. *Am. J. Psychiatry* 156, 585–588.

Barrett, E., Ross, R. P., O'Toole, P. W., Fitzgerald, G. F., and Stanton, C. (2014). γ-Aminobutyric acid production by culturable bacteria from the human intestine. *J. Appl. Microbiol.* 116, 1384–1386. doi: 10.1111/j.1365-2672.2012.05344.x

Ben-Ari, Y. (2013). Neuropaediatric and neuroarchaeology: understanding development to correct brain disorders. *Acta Paediatr.* 102, 331–334. doi: 10.1111/apa.12161

Bercik, P., Denou, E., Collins, J., Jackson, W., Lu, J., Jury, J., et al. (2011). The intestinal microbiota affect central levels of brain-derived neurotropic factor and behavior in mice. *Gastroenterology* 141, 599–609. doi: 10.1053/j.gastro.2011.04.052

Borovikova, L. V., Ivanova, S., Zhang, M., Yang, H., Botchkina, G. I., Watkins, L. R., et al. (2000). Vagus nerve stimulation attenuates the systemic inflammatory response to endotoxin. *Nature* 405, 458–462. doi: 10.1038/35013070

Boyle, M. P., Brewer, J. A., Funatsu, M., Wozniak, D. F., Tsien, J. Z., Izumi, Y., et al. (2005). Acquired deficit of forebrain glucocorticoid receptor produces depression-like changes in adrenal axis regulation and behavior. *Proc. Natl. Acad. Sci. U.S.A.* 102, 473–478. doi: 10.1073/pnas.0406458102

Brinks, V., van der Mark, M. H., de Kloet, E. R., and Oitzl, M. S. (2007). Differential MR/GR activation in mice results in emotional states beneficial or impairing for cognition. *Neural Plast.* 2007:90163. doi: 10.1155/2007/90163

Chen, G., Yang, D., Yang, Y., Li, J., Cheng, K., Tang, G., et al. (2015). Amino acid metabolic dysfunction revealed in the prefrontal cortex of a rat model of depression. *Behav. Brain Res.* 278, 286–292. doi: 10.1016/j.bbr.2014.05.027

Collins, S. M., and Bercik, P. (2009). The relationship between intestinal microbiota and the central nervous system in normal gastrointestinal function and disease. *Gastroenterology* 136, 2003–2014. doi: 10.1053/j.gastro.2009.01.075

Crumeyrolle-Arias, M., Jaglin, M., Bruneau, A., Vancassel, S., Cardona, A., Daugé, V., et al. (2014). Absence of the gut microbiota enhances anxiety-like behavior and neuroendocrine response to acute stress in rats. *Psychoneuroendocrinology* 42, 207–217. doi: 10.1016/j.psyneuen.2014.01.014

Cryan, J. F., and Dinan, T. G. (2012). Mind-altering microorganisms: the impact of the gut microbiota on brain and behaviour. *Nat. Rev. Neurosci.* 13, 701–712. doi: 10.1038/nrn3346

de Kloet, E. R. (2014). From receptor balance to rational glucocorticoid therapy. *Endocrinology* 155, 2754–2769. doi: 10.1210/en.2014-1048

De Kloet, E. R., Van Acker, S. A., Sibug, R. M., Oitzl, M. S., Meijer, O. C., Rahmouni, K., et al. (2000). Brain mineralocorticoid receptors and centrally regulated functions. *Kidney Int.* 57, 1329–1336. doi: 10.1046/j.1523-1755.2000.00971.x

Desbonnet, L., Clarke, G., Shanahan, F., Dinan, T., and Cryan, J. (2014). Microbiota is essential for social development in the mouse. *Mol. Psychiatry* 19, 146–148. doi: 10.1038/mp.2013.65

Dhabhar, F. S., Mcewen, B. S., and Spencer, R. L. (1997). Adaptation to prolonged or repeated stress – comparison between rat strains showing intrinsic differences in reactivity to acute stress. *Neuroendocrinology* 65, 360–368. doi: 10.1159/000127196

Foster, J. (2015). S.20.04 Gut-brain communication: how the microbiome influences anxiety and depression. *Eur. Neuropsychopharmacol.* 25, S141. doi: 10.1016/S0924-977X(15)30098-5

Fries, G. R., Vasconcelosmoreno, M. P., Gubert, C., Sartori, J., Eisele, B., Ferrari, P., et al. (2015). Hypothalamic-pituitary-adrenal axis dysfunction and illness progression in bipolar disorder. *Int. J. Neuropsychopharmacol.* 18, 1630–1635. doi: 10.1093/ijnp/pyu043

Fu, J., Bonder, M. J., Cenit, M. C., Tigchelaar, E., Maatman, A., Dekens, J. A., et al. (2015). The gut microbiome contributes to a substantial proportion of the variation in blood lipids. *Circ. Res.* 117, 817–824. doi: 10.1161/CIRCRESAHA.115.306807

Girotti, M., Pace, T. W., Gaylord, R. I., Rubin, B. A., Herman, J. P., and Spencer, R. L. (2006). Habituation to repeated restraint stress is associated with lack of stress-induced c-fos expression in primary sensory processing areas of the rat brain. *Neuroscience* 138, 1067–1081. doi: 10.1016/j.neuroscience.2005.12.002

Glover, V., O'connor, T., and O'Donnell, K. (2010). Prenatal stress and the programming of the HPA axis. *Neurosci. Biobehav. Rev.* 35, 17–22. doi: 10.1016/j.neubiorev.2009.11.008

Grenham, S., Clarke, G., Cryan, J. F., and Dinan, T. G. (2011). Brain–gut–microbe communication in health and disease. *Front. Physiol.* 2:94. doi: 10.3389/fphys.2011.00094

Heitlinger, E., Ferreira, S. C. M., Thierer, D., Hofer, H., and East, M. L. (2017). The intestinal eukaryotic and bacterial biome of spotted hyenas: the impact of social status and age on diversity and composition. *Front. Cell. Infect. Microbiol.* 7:262. doi: 10.3389/fcimb.2017.00262

Henaomejia, J., Elinav, E., Jin, C., Hao, L., Mehal, W. Z., Strowig, T., et al. (2012). Inflammasome-mediated dysbiosis regulates progression of NAFLD and obesity. *Nature* 482, 179–185. doi: 10.1038/nature10809

Hueston, C. M., Barnum, C. J., Eberle, J. A., Ferraioli, F. J., Buck, H. M., and Deak, T. (2011). Stress-dependent changes in neuroinflammatory markers observed after common laboratory stressors are not seen following acute social defeat of the Sprague Dawley rat. *Physiol. Behav.* 104, 187–198. doi: 10.1016/j.physbeh.2011.03.013

Jacobson, L. (2014). Hypothalamic-pituitary-adrenocortical axis: neuropsychiatric aspects. *Compr. Physiol.* 4, 715–738. doi: 10.1002/cphy.c130036

Keating, D. J., Rychkov, G. Y., Adams, M. B., Holgert, H., McMillen, I. C., and Roberts, M. L. (2004). Opioid receptor stimulation suppresses the adrenal medulla hypoxic response in sheep by actions on Ca^{2+} and K^{+} channels. *J. Physiol.* 555, 489–502. doi: 10.1113/jphysiol.2003.056176

Kim, C. S., Chang, P. Y., and Johnston, D. (2012). Enhancement of dorsal hippocampal activity by knockdown of HCN1 channels leads to anxiolytic- and antidepressant-like behaviors. *Neuron* 75, 503–516. doi: 10.1016/j.neuron.2012.05.027

Kimura, I., Inoue, D., Maeda, T., Hara, T., Ichimura, A., Miyauchi, S., et al. (2011). Short-chain fatty acids and ketones directly regulate sympathetic nervous system via G protein-coupled receptor 41 (GPR41). *Proc. Natl. Acad. Sci. U.S.A.* 108, 8030–8035. doi: 10.1073/pnas.1016088108

Koren, O., Goodrich, J. K., Cullender, T. C., Spor, A., Laitinen, K., Bäckhed, H. K., et al. (2012). Host remodeling of the gut microbiome and metabolic changes during pregnancy. *Cell* 150, 470–480. doi: 10.1016/j.cell.2012.07.008

Liu, L., Zhou, X., Zhang, Y., Liu, Y., Yang, L., Pu, J., et al. (2016). The identification of metabolic disturbances in the prefrontal cortex of the chronic restraint stress rat model of depression. *Behav. Brain Res.* 305, 148. doi: 10.1016/j.bbr.2016.03.005

Lozupone, C. A., Stombaugh, J. I., Gordon, J. I., Jansson, J. K., and Knight, R. (2012). Diversity, stability and resilience of the human gut microbiota. *Nature* 489, 220–230. doi: 10.1038/nature11550

Luczynski, P., Neufeld, M. V., Oriach, C. S., Clarke, G., Dinan, T. G., and Cryan, J. F. (2016). Growing up in a bubble: using germ-free animals to assess the influence of the gut microbiota on brain and

behavior. *Int. J. Neuropsychopharmacol.* 19:pyw020. doi: 10.1093/ijnp/pyw020

Medina, A., Seasholtz, A. F., Sharma, V., Burke, S., Bunney, W., Myers, R. M., et al. (2013). Glucocorticoid and mineralocorticoid receptor expression in the human hippocampus in major depressive disorder. *J. Psychiatr. Res.* 47, 307–314. doi: 10.1016/j.jpsychires.2012.11.002

Moya-Pérez, A., Perez-Villalba, A., Benítez-Páez, A., Campillo, I., and Sanz, Y. (2017). Bifidobacterium CECT 7765 modulates early stress-induced immune, neuroendocrine and behavioral alterations in mice. *Brain Behav. Immun.* 65, 43–56. doi: 10.1016/j.bbi.2017.05.011

Owens, M. J., and Nemeroff, C. B. (1991). Physiology and pharmacology of corticotropin-releasing factor. *Pharmacol. Rev.* 43, 425.

Reul, J. M., and de Kloet, E. R. (1985). Two receptor systems for corticosterone in rat brain: microdistribution and differential occupation. *Endocrinology* 117, 2505–2511. doi: 10.1210/endo-117-6-2505

Romero, L. M. (2004). Physiological stress in ecology: lessons from biomedical research. *Trends Ecol. Evol.* 19, 249–255. doi: 10.1016/j.tree.2004.03.008

Ronald, A., Pennell, C. E., and Whitehouse, A. J. (2010). Prenatal maternal stress associated with ADHD and autistic traits in early childhood. *Front. Psychol.* 1:223. doi: 10.3389/fpsyg.2010.00223

Schatzberg, A. F., Keller, J., Tennakoon, L., Lembke, A., Williams, G., Kraemer, F. B., et al. (2014). HPA axis genetic variation, cortisol and psychosis in major depression. *Mol. Psychiatry* 19, 220–227. doi: 10.1038/mp.2013.129

Smith, M. A., Davidson, J., Ritchie, J. C., Kudler, H., Lipper, S., Chappell, P., et al. (1989). The corticotropin-releasing hormone test in patients with posttraumatic stress disorder. *Biol. Psychiatry* 26, 349–355. doi: 10.1016/0006-3223(89)90050-4

Smith, P. M., Howitt, M. R., Panikov, N., Michaud, M., Gallini, C. A., Bohlooly-y, M., et al. (2013). The microbial metabolites, short-chain fatty acids, regulate colonic Treg cell homeostasis. *Science* 341, 569–573. doi: 10.1126/science.1241165

Sudo, N., Chida, Y., Aiba, Y., Sonoda, J., Oyama, N., Yu, X. N., et al. (2004). Postnatal microbial colonization programs the hypothalamic-pituitary-adrenal system for stress response in mice. *J. Physiol.* 558, 263–275. doi: 10.1113/jphysiol.2004.063388

Thomas, C. M., Hong, T., van Pijkeren, J. P., Hemarajata, P., Trinh, D. V., Hu, W. et al. (2012). Histamine derived from probiotic *Lactobacillus reuteri* suppresses TNF via modulation of PKA and ERK Signaling. *PLoS ONE* 7:e31951. doi: 10.1371/journal.pone.0031951

van Bodegom, M. V., Homberg, J. R., and Henckens, M. J. A. G. (2017). Modulation of the hypothalamic-pituitary-adrenal axis by early life stress exposure. *Front. Cell. Neurosci.* 11:87. doi: 10.3389/fncel.2017.00087

Wang, H., Yu, M., Ochani, M., Amella, C. A., Tanovic, M., Susarla, S., et al. (2003). Nicotinic acetylcholine receptor α7 subunit is an essential regulator of inflammation. *Nature* 421, 384–388. doi: 10.1038/nature01339

Wang, W., Guo, H., Zhang, S. X., Li, J., Cheng, K., Bai, S. J., et al. (2016). Targeted metabolomic pathway analysis and validation revealed glutamatergic disorder in the prefrontal cortex among chronic social defeat stress mice model of depression. *J. Proteome Res.* 15, 3784–3792. doi: 10.1021/acs.jproteome.6b00577

Webster, M. J., Knable, M. B., O'grady, J., Orthmann, J., and Weickert, C. S. (2002). Regional specificity of brain glucocorticoid receptor mRNA alterations in subjects with schizophrenia and mood disorders. *Mol. Psychiatry* 7, 985–994. doi: 10.1038/sj.mp.4001139

Wen, L., Ley, R. E., Volchkov, P. Y., Stranges, P. B., Avanesyan, L., Stonebraker, A. C., et al. (2008). Innate immunity and intestinal microbiota in the development of Type 1 diabetes. *Nature* 455, 1109–1113. doi: 10.1038/nature07336

Wirtz, P. H., von Känel, R., Emini, L., Ruedisueli, K., Groessbauer, S., Maercker, A., et al. (2007). Evidence for altered hypothalamus-pituitary-adrenal axis functioning in systemic hypertension: blunted cortisol response to awakening and lower negative feedback sensitivity. *Psychoneuroendocrinology* 32, 430–436. doi: 10.1016/j.psyneuen.2007.02.006

Wong, M., Inserra, A., Lewis, M., Mastronardi, C., Leong, L., Choo, J., et al. (2016). Inflammasome signaling affects anxiety-and depressive-like behavior and gut microbiome composition. *Mol. Psychiatry* 21,797–805. doi: 10.1038/mp.2016.46

Wren, A. M., Bloom, S. R. (2007). Gut hormones and appetite control. *Gastroenterology* 132, 2116–2130. doi: 10.1053/j.gastro.2007.03.048

Yano, J. M., Yu, K., Donaldson, G. P., Shastri, G. G., Ann, P., Ma, L., et al. (2015). Indigenous bacteria from the gut microbiota regulate host serotonin biosynthesis. *Cell* 161, 264–276. doi: 10.1016/j.cell.2015.02.047

Zafir, A., and Banu, N. (2007). Antioxidant potential of fluoxetine in comparison to *Curcuma longa* in restraint-stressed rats. *Eur. J. Pharmacol.* 572, 23–31. doi: 10.1016/j.ejphar.2007.05.062

Zeng, L., Zeng, B., Wang, H., Li, B., Huo, R., Zheng, P., et al. (2016). Microbiota modulates behavior and protein kinase C mediated cAMP response element-binding protein signaling. *Sci. Rep.* 6:29998. doi: 10.1038/srep29998

Zhang, S., Wang, W., Li, J., Cheng, K., Zhou, J., Zhu, D., et al. (2016). Behavioral characterization of CD36 knockout mice with SHIRPA primary screen. *Behav. Brain Res.* 299, 90–96. doi: 10.1016/j.bbr.2015.11.027

Zheng, P., Cheng, K., Zeng, L., Zhou, C. J., and Xie, P. (2016a). A new pathway for the gut microbiota to modulate the brain: activation of pattern-recognition receptors by microbial products. *Mol. Psychiatry* 22, 162–163. doi: 10.1038/mp.2016.210

Zheng, P., Zeng, B., Zhou, C., Liu, M., Fang, Z., Xu, X., et al. (2016b). Gut microbiome remodeling induces depressive-like behaviors through a pathway mediated by the host's metabolism. *Mol. Psychiatry* 21, 786–796. doi: 10.1038/mp.2016.44

Zhou, J., Liu, Z., Yu, J., Han, X., Fan, S., Shao, W. et al. (2016). Quantitative proteomic analysis reveals molecular adaptations in the hippocampal synaptic active zone of chronic mild stress-unsusceptible rats. *Int. J. Neuropsychopharmacol.* 19:pyv100. doi: 10.1093/ijnp/pyv100

Zhu, L.-J., Liu, M.-Y., Li, H., Liu, X., Chen, C., Han, Z., et al. (2014). The different roles of glucocorticoids in the hippocampus and hypothalamus in chronic stress-induced HPA axis hyperactivity. *PLoS ONE* 9:e97689. doi: 10.1371/journal.pone.0097689

Conflict of Interest Statement: The authors declare that the research was conducted in the absence of any commercial or financial relationships that could be construed as a potential conflict of interest.

Copyright © 2017 Huo, Zeng, Zeng, Cheng, Li, Luo, Wang, Zhou, Fang, Li, Niu, Wei and Xie. This is an open-access article distributed under the terms of the Creative Commons Attribution License (CC BY). The use, distribution or reproduction in other forums is permitted, provided the original author(s) or licensor are credited and that the original publication in this journal is cited, in accordance with accepted academic practice. No use, distribution or reproduction is permitted which does not comply with these terms.

frontiers in Cellular and Infection Microbiology

ORIGINAL RESEARCH
published: 26 October 2017
doi: 10.3389/fcimb.2017.00455

Alteration of Gut Microbiota and Inflammatory Cytokine/Chemokine Profiles in 5-Fluorouracil Induced Intestinal Mucositis

Hong-Li Li†, Lan Lu†, Xiao-Shuang Wang, Li-Yue Qin, Ping Wang, Shui-Ping Qiu, Hui Wu, Fei Huang, Bei-Bei Zhang, Hai-Lian Shi and Xiao-Jun Wu**

Shanghai Key Laboratory of Compound Chinese Medicines, The Ministry of Education (MOE) Key Laboratory for Standardization of Chinese Medicines, Institute of Chinese Materia Medica, Shanghai University of Traditional Chinese Medicine, Shanghai, China

Disturbed homeostasis of gut microbiota has been suggested to be closely associated with 5-fluorouracil (5-Fu) induced mucositis. However, current knowledge of the overall profiles of 5-Fu-disturbed gut microbiota is limited, and so far there is no direct convincing evidence proving the causality between 5-Fu-disturbed microbiota and colonic mucositis. In mice, in agreement with previous reports, 5-Fu resulted in severe colonic mucositis indicated by weight loss, diarrhea, bloody stool, shortened colon, and infiltration of inflammatory cells. It significantly changed the profiles of inflammatory cytokines/chemokines in serum and colon. Adhesion molecules such as vascular cell adhesion molecule-1 (VCAM-1), intercellular adhesion molecule-1 (ICAM-1), and VE-Cadherin were increased. While tight junction protein occludin was reduced, however, zonula occludens-1 (ZO-1) and junctional adhesion molecule-A (JAM-A) were increased in colonic tissues of 5-Fu treated mice. Meanwhile, inflammation related signaling pathways including NF-κB and mitogen activated protein kinase (MAPKs) in the colon were activated. Further study disclosed that 5-Fu diminished bacterial community richness and diversity, leading to the relative lower abundance of Firmicutes and decreased Firmicutes/Bacteroidetes (F/B) ratio in feces and cecum contents. 5-Fu also reduced the proportion of Proteobacteria, Tenericutes, Cyanobacteria, and Candidate division TM7, but increased that of Verrucomicrobia and Actinobacteria in feces and/or cecum contents. The fecal transplant from healthy mice prevented body weight loss and colon shortening of 5-Fu treated mice. In addition, the fecal transplant from 5-Fu treated mice reduced body weight and colon length of vancomycin-pretreated mice. Taken together, our study demonstrated that gut microbiota was actively involved in the pathological process of 5-Fu induced intestinal mucositis, suggesting potential attenuation of 5-Fu induced intestinal mucositis by manipulating gut microbiota homeostasis.

Keywords: gut microbiota, 5-fluorouracil, intestinal mucositis, inflammatory chemokines/cytokines, fecal transplantation

OPEN ACCESS

Edited by:
Michele Marie Kosiewicz, University of Louisville, United States

Reviewed by:
Valerio Iebba, Sapienza Università di Roma, Italy
Nour Eissa, University of Manitoba, Canada

***Correspondence:**
Hai-Lian Shi
shihailian2003@163.com
Xiao-Jun Wu
xiaojunwu320@126.com

† These authors have contributed equally to this work.

Received: *20 January 2017*
Accepted: *09 October 2017*
Published: *26 October 2017*

Citation:
Li H-L, Lu L, Wang X-S, Qin L-Y, Wang P, Qiu S-P, Wu H, Huang F, Zhang B-B, Shi H-L and Wu X-J (2017) Alteration of Gut Microbiota and Inflammatory Cytokine/Chemokine Profiles in 5-Fluorouracil Induced Intestinal Mucositis. Front. Cell. Infect. Microbiol. 7:455. doi: 10.3389/fcimb.2017.00455

INTRODUCTION

Gastrointestinal microbiota plays an important role in the maintenance of human health (Figlewicz, 2008; Zhao, 2013; Patel et al., 2016). Healthy gastrointestinal microbiota characterized by high rich and diverse bacteria (Vandeputte et al., 2016) interacts with mucosal epithelium and is responsible for normal substance metabolism, immune response and intestinal angiogenesis (Stringer et al., 2009a,b; Candela et al., 2014). Disturbed gut microbiota has been revealed to induce many disorders, such as metabolic diseases (obesity and diabetes) (Philippot et al., 2013), inflammatory bowel diseases (Tung et al., 2011), multiple sclerosis, and even psychiactric diseases such as depression (Wang and Kasper, 2014). More and more evidences suggest that sustained homeostasis of gut microbiota seems to benefit the recovery of many diseases.

Cancer chemotherapeutic agents have been found to interfere with the homeostasis of gut microbiota. For instance, irinotecan, a cytotoxic chemotherapy agent for colon cancer, can induce the alteration of β-glucuronidase producing bacteria of intestinal microflora (Stringer et al., 2007). Ipilimumab, a CTLA-4 blocker, even has to exert its anticancer effect through the interaction between *Bacteroides fragilis* (*B. fragilis*) and *B.fragilis*-specific T cells (Vétizou et al., 2015). 5-fluorouracil (5-Fu), the first-line chemotherapeutic agent for the therapy of metastatic colorectal cancer, induces gastrointestinal adverse events such as diarrhea, hemorrhage and intestinal mucositis in clinic, which not only diminish its therapeutic efficacy but also increase patient's suffering (Sonis et al., 2004; Stringer et al., 2009b). Administration of probiotics ameliorates 5-Fu induced intestinal mucositis in mice (Justino et al., 2014; Yeung et al., 2015), suggesting possible causality between the gastrointestinal microbiota and the disease. In rats, 5-Fu treatment changes the relative abundance of microbiota from several genera in gastrointestine, including *Clostridium*, *Lactobacillus, Enterococcus, Bacteroides, Straphylococcus, Streptococcus,* and *Escherichia* (Stringer et al., 2007). However, due to the limited techniques at that time, the profiling of the gastrointestinal microbiota was incomplete. In addition, the detailed function of gut microbiota in 5-Fu-induced gastrointestinal mucositis has not been well clarified yet.

In 5-Fu-induced mucositis rodents, chemokines/cytokines such as chemokine-1, 2, 9 (CXCL1, CXCL2, CXCL9), and interleukine-4 (IL-4) are elevated, which is accompanied with intestinal epithelium damage. Further study disclosed that CXCL9 is closely related to the intestinal damage, while IL-4 as a pro-inflammatory cytokine can increase intestinal epithelium permeability (Prisciandaro et al., 2012; Soares et al., 2013; Wang and Kasper, 2014; Lu et al., 2015; Sakai et al., 2016). NF-κB and mitogen activated protein kinase (MAPK) pathways can be activated in the small intestine of 5-Fu induced mucositis (Liu et al., 2013). However, the reciprocal association among the overall profiles of 5-Fu-induced inflammatory cytokines/chemokines, alteration of tight junction and adhesion proteins and cellular signaling pathways has not been elucidated, especially in colon tissue.

Although disturbed homeostasis of gut microbiota has been suggested to be closely associated with the adverse effect of 5-Fu, current knowledge of the overall profiles of 5-Fu-disturbed gut microbiota is limited, and so far there is no direct convincing evidence that can prove the causality between 5-Fu-disturbed microbiota and colonic mucositis. The present study was aimed to provide the overall profile of 5-Fu-disturbed gut microbiota by direct sequencing of 16S rRNA gene in cecum contents and feces of colonic mucositis mice using high throughput Miseq sequencing technologies. Meanwhile, the influence of 5-Fu on the inflammatory cytokines/chemokines, adhesion molecules, tight junction molecules as well as MAPK and NF-κB pathways in colonic tissues of mice was investigated. And the fecal transplantation experiments were conducted to elucidate the causality between gut microbiota and colonic mucositis. Our findings confirmed the important role of gut microbiota in 5-Fu induced intestinal mucositis and may provide novel therapy regimen for patients suffered from 5-Fu induced intestinal mucositis.

Abbreviations: 5-Fu, 5-fluorouracil; MPO, myeloperoxidase; IFN-γ, interferon-γ; IL-1/6, interleukin-1/6; TNF-α, tumor necrosis factor-α; CXCL1/5/9/13, chemokine (C-X-C motif) ligand 1/5/9/13; IL-22 R1, interleukin-22 receptor 1; IL-12 R2, interleukin-12 receptor 2; VCAM-1, vascular cell adhesion molecule-1; ICAM-1, intercellular adhesion molecule-1; G-CSF, granulocyte colony stimulating factor; GM-CSF, granulocyte-macrophage colony stimulating factor; BSA, bovine serum albumin; MAPK, mitogen activated protein kinase; ERK, extracellular signal-regulated kinase; SAPK/JNK, stress activated protein kinase/jun N-terminal kinase; p-ERK, phosphorylated extracellular signal-regulated kinase; p-JNK, phosphorylated jun N-terminal kinase; iNOS, inducible NO synthase; ZO-1, zonula occludens-1; JAM-A, junctional adhesion molecule-A.

MATERIALS AND METHODS

Animals and Mucositis Induction

Male BALB/c mice, 4-week old, obtained from Shanghai SLAC Laboratory Animal Co. Ltd. (SYXK2014-008, Shanghai, China) were housed under a 12 h light/dark cycle at room temperature ($23 \pm 2^{\circ}C$) with access to food and water *ad libitum*. Two weeks later, the mice were randomly divided into two groups, namely control group and 5-Fu group ($n = 10$/group). According to Huang et al's method (Huang et al., 2009), to induce mucositis, the 5-Fu group mice were intraperitoneally administered with 5-Fu (50 mg/kg) once daily for 3 days. Meanwhile, the control group mice were intraperitoneally administered with 0.9% saline. All animal experiments were conducted complying with the Institutional Animal Care guidelines approved by the Experimental Animal Ethical Committee of Shanghai University of Traditional Chinese Medicine.

Mucositis Assessment and Samples Collection

Body weight, diarrhea and bloody stool of mice were recorded daily for the assessment of mucositis. Diarrhea grade was evaluated based on the consistency of stool, using the modified parameters as described previously (Leocádio et al., 2015): 0, normal; 1, slightly wet; 2, moderate wet; 3, loose; 4, watery stool. At the last day (day 7), the grade of blood stool was assessed by a commercial testing paper (BASO diagnostics Inc. China) with the following scores: 0, normal; 1, slight bleeding; 2, moderate

bleeding; 3, severe bleeding; 4, visible bleeding. Meanwhile, the feces were collected and stored at −80°C. Then the mice were sacrificed under anesthesia, and the entire small intestine and colon were excised after removal of fat tissue and their length were measured. The colon tissues near the cecum were either fixed in 10% formalin (w/v) or snap frozen in liquid nitrogen for further analysis.

Protein Chip analysis

Colon tissues were homogenized with cell lysis buffer containing protease inhibitor cocktail on ice and centrifuged at 12,000 rpm for 15 min at 4°C. The supernatant was collected and subjected to concentration measurement using BCA method. Afterwards, all protein samples were diluted to the same concentration. Inflammatory/anti-inflammatory cytokines in the samples were measured by RayBio® Mouse Cytokine Antibody Arrays according to the manufacturer's protocol.

Histopathological Assessment

Fixed colon tissue samples were embedded in paraffin, sectioned in 4 μm-thick slices, and stained with hematoxylin-eosin. The morphological alteration and inflammatory cell infiltration were observed under microscope (Olympus BX61VS).

Immunohistochemistry

The endogenous peroxidases in 4 μm-thick slices were deactivated by incubation with 3% H_2O_2 for 10 min. For antigen retrieval, the sections were soaked in 10 mM citrate buffer solution (pH 6.0) and heated twice in a microwave oven. After washed thoroughly with PBS (pH7.4), the sections were blocked with 3% BSA in tris buffered saline (TBS) for 20 min, then incubated with anti-myeloperoxidase antibody (anti-MPO) (1:200, #SH0022, Skyhobio) and anti-p65 (1:400, #SH0023, Skyhobio) antibodies overnight at 4°C followed by incubation with HRP-conjugated secondary antibody (#K5007, Dako) for 50 min. The sections were further incubated with DAB-H_2O_2 solution (#K5007, Dako), counterstained with hematoxylin, dehydrated with ethanol and sealed in resinene for microscopic observation.

Quantitative Polymerase Chain Reaction (qPCR)

Total RNA was extracted from colon tissues using TRIzol reagent (Life Technologies). cDNA was generated from total RNA with the RevertAid First Strand cDNA Synthesis Kit (Thermo). The primers (GeneRay) used in PCR amplification were listed in **Table 1**. Quantitative PCR was performed with SYBR Premix EX Taq under the following conditions: 95°C, 30 s; then followed by 40 cycles (95°C, 5 s; 60°C, 34 s); finally 95°C, 15 s; 60°C, 1 min; 95°C, 15 s. Quantity of target genes calculated by the comparative C_t method was normalized to that of β-actin (internal reference) in the same sample (Araújo et al., 2015).

Multiplex Immunoassays

Serum was collected by centrifugation at 4,000 rpm for 10 min at 4°C. Colon segments were homogenized in cell lysis buffer, then the supernatants were collected through centrifugation at 12,000 rpm for 15 min. Concentrations of 13 cytokines in the supernatants and serum were measured by ProcartaPlex® Mix&Match Mouse 13-plex [including interleukin-6 (IL-6), tumor necrosis factor-α (TNF-α), interleukin-10 (IL-10), interleukin-12p-70 (IL-12p70), interleukin-21 (IL-21), interleukin-22 (IL-22), interleukin-31 (IL-31), granulocyte colony stimulating factor (G-CSF), granulocyte-macrophage colony stimulating factor (GM-CSF), Leptin, RANTES, chemokine-5 (CXCL5), and chemokine-1 (CXCL1)] according to the manufacturer's recommendation.

TABLE 1 | The primers used in qPCR analysis.

Genes	Forward primer	Reverse primer
IFN-γ	ATTGCGGGGTTGTATCTGGG	GGGTCACTGCAGCTCTGAAT
IL-1β	TTTGAAGTTGACGGACCCC	TGTGCTGCTGCGAGATTTG
IL-6	ACCACGGCCTTCCCTACTTC	CATTTCCACGATTTCCCAGA
TNF-α	GGAACACGTCGTGGGATAATG	GGCAGACTTTGGATGCTTGTT
CXCL5	GTTCATCTCGCCATTCATGC	GCGGCTATGACTGAGGAAGG
CXCL9	GGAGTTCGAGGAACCCTAGTG	GGGATTTGTAGTGGATCGTGC
CXCL13	GGCCACGGTATTCTGGAAGC	GGGCGTAACTTGAATCCGA TCTA
CXCL1	GGCTTCCTTATGTTCAAAC AGGG	GCCGTTACTCGGGTAAATTACA
CD11b	GGTCGGCAAGCAACTGATTT	CAACTTGCATTATGGCATCCA
IL-22 R1	GACTCCATTTGCGTCATCGC	CCTGTCACCGTGTGTCATCA
IL-10 R2	TGGAGCCGTGGACAACTTAC	ATGGCCACAATCCAGGAAGG
VCAM-1	GAACCCAAACAGAGGCAGAG	GGTATCCCATCACTTGAGCAG
ICAM-1	CGCTGTGCTTTGAGAACTGT	AGGTCCTTGCCTACTTGCTG
VE-Cadherin	CGCCAACATCACGGTCAA	ACGGTTAGCGTGCTGGTTC
Occludin	ATGGCAAGCGATCATACCC	TTCCTGCTTTCCCCTTCG
β-actin	CGGTTCCGATGCCCTGAGG CTCTT	CGTCACACTTCATGATGGAA TTGA

ELISA Assay

Concentration of CXCL9 in serum and supernatants of colonic tissues was quantified by CXCL9 ELISA assay kit (Abcam, UK) according to manufacturer's instruction.

Western Blot Analysis

Colon tissues were homogenized and lysed in RIPA buffer supplemented with protease inhibitor cocktail on ice. After centrifugation at 12,000 rpm for 15 min at 4°C, the supernatant was collected and its protein concentration was determined by BCA method. Total protein (60 μg) from each sample was separated by SDS-PAGE and transferred onto PVDF membrane by wet transfer approach. Then PVDF membranes were blocked with 5% (w/v) bovine serum albumin (BSA) solution and incubated with different primary antibodies against p-p65 (1:1000, #3033L, Cell Signal Technology), p-IκBα (1:500, #2859S, CST), p-p38 MAPK (1:1000, #4511, CST), phosphorylated extracellular signal-regulated kinase (p-ERK1/2, 1:1000, #9154, CST), phosphorylated jun N-terminal kinase (p-JNK, 1:1000, #4668, CST), p38 MAPK (1:1000, #9212, CST), extracellular signal-regulated kinase (ERK1/2, 1:1000, #4695, CST), stress activated protein kinase/jun N-terminal kinase (SAPK/JNK, 1:1000, #9252S, CST), inducible

NO synthase (iNOS, 1:1000, #ab204017, Abcam), VCAM-1(1:2000, #3540-1, Epitomics), ICAM-1 (1:1000, #3482-1, Epitomics), Occludin (1:2000, #GTX85016, GeneTex), ZO-1 (1:500, #ab59720, Abcam), JAM-A (1:500, # sc-37049, Santa cruz) and β-actin (1:2000, #12413, CST) overnight at 4°C. After washed with 1 × PBS containing 0.1% (v/v) Tween-20, the membranes were incubated with respective secondary antibodies. The protein bands were visualized with ECL-prime kit. Quantification of target protein was performed by measuring integral optic density of respective target proteins with Tanon Gis software.

16S rRNA Miseq Sequencing and Bioinformatic Analysis

Microbial genomic DNA was extracted from cecum contents and feces using a QIAamp DNA Stool Mini Kit according to the manufacturer's instructions. The resultant DNA extracts were used for the PCR amplification. Quantification of the PCR products was performed on FTC-3000TM real-time PCR instrument. The V3-V4 region of 16S rRNA gene of gut microbiota was sequenced using Illumina MiSeq 2 × 300 bp high throughput platform. The bioinformatic analysis was conducted as described previously (MacIntyre et al., 2015). The generated 16S rRNA gene sequences were analyzed using the bioinformatic software package Mothur with MiSeq SOP Pipeline. The paired reads were assembled using make.contigs. Screen.seqs command was used to remove low quality reads using the following filtering parameters, maxambig = 0, minlength = 200 and maxlength = 580, maxhomop = 8. The remained sequences were simplified using the unique.seqs command to generate a unique set of sequences, then aligned with the SILVA databases (version 119). The screen.seqs command was implemented again to keep within our defined criteria using the following parameters: start = 12,878, end = 28,464. The filter.seqs was used to remove empty columns from our alignment. Further de-noise sequences were pre-clustered using the pre.cluster command (http://www.mothur.org/wiki/Pre.cluster) allowing for up to 4 differences between sequences. Then reads were checked for chimeras using UCHIME algorithm and the chimeric sequences were removed by the chimera.uchime command with default parameters. To classify (classify.seqs) the sequences, the SILVA 119 database was used with a confidence threshold of 80%. The non-bacterial sequences were deleted. The distance matrix between the aligned sequences was generated by the dist.seqs command. Finally, these sequences were clustered to OTUs (operational taxonomic units) at 97% sequence identity (furthest neighbor method). A majority of consensus taxonomy for each OTU was obtained by the classify.otu command with default parameters.

Fecal Transplantation

For healthy fecal transplantation experiment, 24 mice were randomly divided into three groups: Control, 5-Fu and 5-Fu+feces ($n = 8$/group). Both 5-Fu group and 5-Fu+feces group mice were injected intraperitoneally with 5-Fu (50 mg/kg/day) for 3 days. For 5-Fu+feces group mice, they were additionally administered with the fecal suspension from normal mice via oral gavage from day 1 to day 7 once a day. For 5-Fu-treated fecal transplantation experiment, 40 mice were randomly divided into four groups, namely Control, 5-Fu, Con-feces and 5-Fu-feces ($n = 10$/group). The mice in Control and 5-Fu groups were treated as aforementioned. Fecal pellets from Control group and 5-Fu group mice were collected and suspended in sterile PBS. For Con-feces group and 5-Fu-feces group mice, they were pretreated with vancomycin (100 mg/kg) for 3 days (Ubeda et al., 2013; Warn et al., 2016), then were administered with respective fecal suspension from Control group or 5-Fu group mice by oral gavage for 11 days. Body weight, diarrhea, and bloody stool of mice were recorded daily. At last, the mice were sacrificed under anesthesia and the length of entire colon after removal of fat tissue was measured.

Statistical Analysis

Each value was presented as mean ± S.E.M. Differences between two groups were analyzed by un-paired Student's *t*-test using PrismDemo 5. In all cases, the value of $P < 0.05$ was considered statistically significant.

RESULTS

5-Fu Induced Colonic Mucositis

Consistent with previous studies (Pereira et al., 2016), body weight of 5-Fu-treated mice was dramatically decreased from day 2 to day 7 after 5-Fu treatment (**Figure 1A**, $P < 0.05$ or $P < 0.001$), compared with the control mice. Meanwhile, severe diarrhea was found in 5-Fu group mice from day 5 to day 7 (**Figure 1B**, $P < 0.001$). At day 7, severe bloody stool was found in 5-Fu treated mice (**Figure 1C**). Shortened intestine indicates the increased contraction ability (Dou et al., 2013), while the shortened colon is closely associated with severe diarrhea. In our experiments, the small intestine length of 5-Fu treated mice was not changed compared to that of the control (**Figure 1D**). By contrast, the colon length of 5-Fu treated mice was significantly shortened (**Figures 1E,F**, $P < 0.001$) and the cecum of 5-Fu treated mice seemed to be smaller (**Figure 1E**). Moreover, 5-Fu treatment injured mucosal epithelium and disrupted crypt-villus structures, which was accompanied with enhance cellular infiltration (HE staining) and neutrophil (MPO staining) infiltration (**Figures 1G,H**).

5-Fu Altered Inflammatory Cytokine and Chemokine Profiles

Although previous studies exposed the alteration of several inflammatory factors in 5-Fu induced intestinal mucositis (Justino et al., 2014; Lu et al., 2015), the changed profile of the other inflammatory factors involved in the process has not been explored. In present study, a mouse inflammation antibody array (40 inflammatory factors) was employed to preliminarily examine the alteration of inflammatory factor profile. As shown in **Figure 2A**, compared to the control, 5-Fu seemed to elevate the protein levels of KC (CXCL1), LIX (CXCL5), MIG (CXCL9), B-lymphocyte chemoattractant (BLC), IL-6 and sTNFR I (>1.5-fold) but decrease that of G-CSF, IL-12p40/p70, RANETS, CD30L, Fractalkine, IL-10, IL12p70, Leptin, and TIMP-2 (>1.3-fold) in colonic tissues. In terms of mRNA expression of the cytokines/chemokines, 5-Fu treatment induced the mRNA

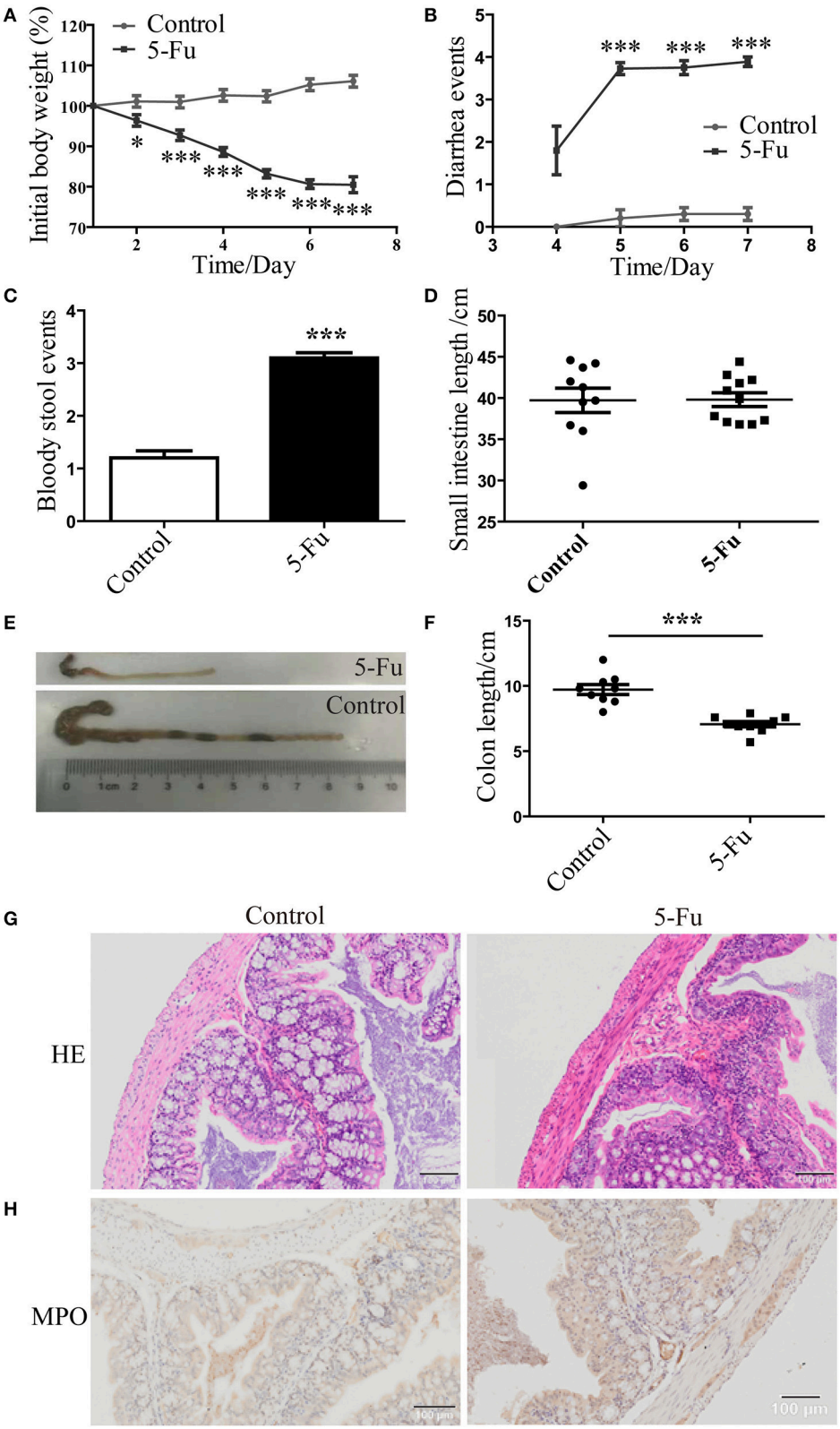

FIGURE 1 | 5-Fu induced mucositis and colon shortening in mice. **(A)** 5-Fu induced body weight changes. Data were plotted as percentage of initial body weight. **(B)** The occurrence of diarrhea. Data represented the evaluation scores of diarrhea. **(C)** The bloody stool events measured by BASO testing paper. **(D)** The small intestine length. **(E,F)** The colon length. **(G)** HE staining of colonic sections. **(H)** MPO staining of colonic sections. Values were expressed as mean ± S.E.M ($n = 10$/group). Data were analyzed by *t*-test. $^{*}P < 0.05$, $^{***}P < 0.001$ vs. control group.

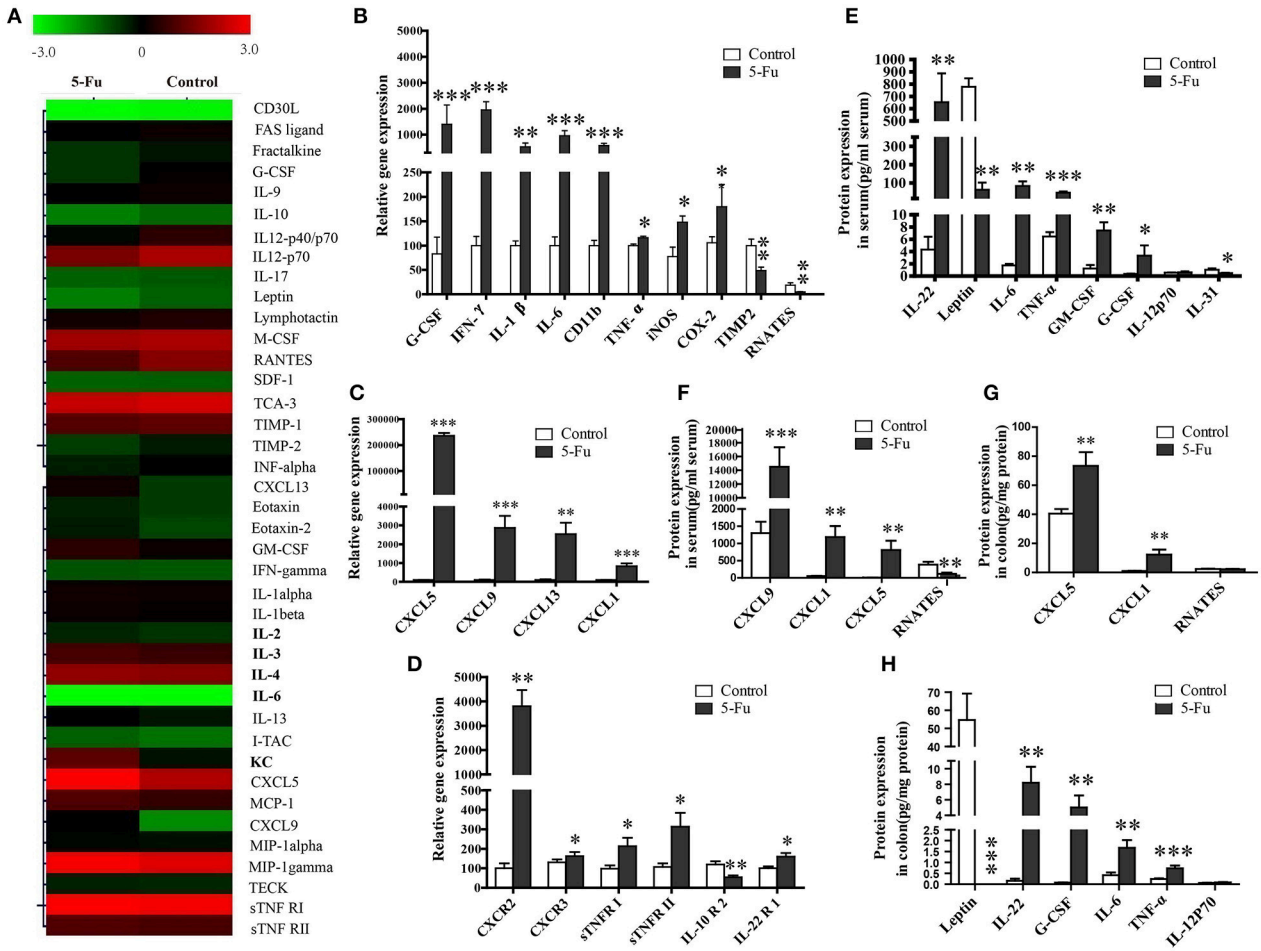

FIGURE 2 | 5-Fu induced the alteration of inflammatory chemokines/cytokines in colonic tissues or serum at protein and gene expression levels. **(A)** The alteration of inflammatory chemokines/cytokines in colonic tissue measured by protein chip analysis. **(B–D)** The inflammatory chemokines/cytokines gene expression measured by qPCR assay. **(E,F)** 5-Fu induced the alteration of inflammatory chemokines/cytokines in serum. **(G,H)** 5-Fu induced the alteration of inflammatory chemokines/cytokines in colonic tissues. Values were expressed as mean ± S.E.M ($n = 10$/group). Data were analyzed by *t*-test. $^{*}P < 0.05$, $^{**}P < 0.01$, $^{***}P < 0.001$ vs. control group.

expression of G-CSF, CD11b, iNOS, COX-2, interferon-γ (IFN-γ), IL-1β, IL-6, TNF-α, CXCL5, CXCL9, CXCL13, and CXCL1 (**Figures 2B,C**, $P < 0.05$, $P < 0.01$ or $P < 0.001$), but decreased that of TIMP2 and RNATES in colonic tissues. Moreover, as shown in **Figure 2D**, 5-Fu treatment modulated the mRNA expression of cytokine/chemokine receptors, as it up-regulated the mRNA expression of chemokine (C-X-C motif) receptor 2, 3 (CXCR2, CXCR3), sTNFR I, sTNFR II and interleukin-22 receptor 1 (IL-22R1), however, down-regulated that of interleukin-10 receptor 2 (IL-10R2). In order to further confirm the changes of inflammatory factors, the multiplex immunoassays and ELISA assay were performed, respectively. As illustrated in **Figures 2E,F**, in serum of 5-Fu-induced mice, the protein levels of CXCL9, CXCL1 (KC), CXCL5, IL-22, IL-6, TNF-α, GM-CSF, and G-CSF were significantly increased ($P < 0.05$, $P < 0.01$, or $P < 0.001$), but that of RNATES, Leptin, and IL-31 were significantly decreased ($P < 0.05$, $P < 0.01$, or $P < 0.001$). Similarly, in colonic tissues of 5-Fu-induced mice, the protein levels of IL-22, G-CSF, IL-6, TNF-α, CXCL1 (KC), and CXCL5 were significantly elevated (**Figures 2G,H**, $P < 0.01$ or $P < 0.001$), while that of Leptin was significantly reduced ($p < 0.001$). By contrast, protein level of IL-12p70 did not change in both serum and colonic tissues.

5-Fu Modulated the Expression of Tight Junctions (TJ) and Adhesion Proteins

Tight junction supports the integral intestinal epithelial barrier structure and barrier function, which is disrupted under inflammation (Capaldo et al., 2017; Chang et al., 2017). Adhesion molecules mediate the attachment of lymphocytes, neutrophils and inflammatory cells to the endothelial cells under inflammatory condition (Erbeldinger et al., 2017; Kim et al., 2017). As shown in **Figure 3**, 5-Fu treatment induced significant mRNA expression of adhesion molecules, VCAM-1, ICAM-1,

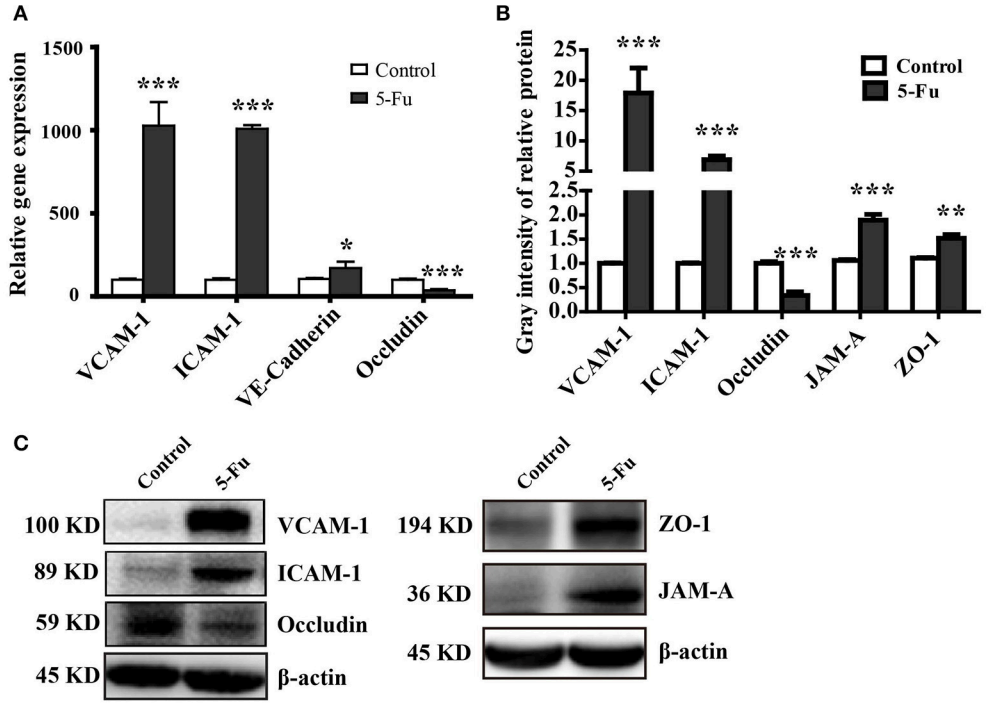

FIGURE 3 | 5-Fu regulated the expression of tight junction and adhesion molecules in colonic tissues. **(A)** 5-Fu regulated gene expression of tight junction and adhesion molecule measured by qPCR analysis ($n = 6$/group). **(B,C)** 5-Fu regulated protein expression of occludin, VCAM-1, ICAM-1, JAM-A, and ZO-1($n =$ 3-4/group). β-actin was used as the endogenous reference. Values were expressed as mean ± S.E.M. Data were analyzed by *t*-test. $^{*}P < 0.05$, $^{**}P < 0.01$, $^{***}P < 0.001$ vs. control group.

and VE-Cadherin ($P < 0.001$, $P < 0.001$, and $P < 0.05$) as well as the protein expression of VCAM-1 and ICAM-1 ($P < 0.001$) in colon. However, in terms of tight junction proteins, 5-Fu decreased mRNA and protein expression of occludin ($P < 0.001$, $P < 0.001$). But 5-Fu increased the protein level of JAM-A and ZO-1 ($P < 0.001$ and $P < 0.01$).

5-Fu Activated MAPK and NF-κB Pathway Signaling

MAPK and NF-κB pathways are closely associated with inflammation (Park et al., 2013). To determine whether MAPK and NF-κB pathways were involved in 5-Fu-induced colonic mucositis, we further assessed the effect of 5-Fu treatment on the activation of signaling molecules, including ERK1/2, JNK, p38 MAPK, IκB and NF-κB. As shown in **Figure 4**, 5-Fu enhanced the phosphorylation of ERK1/2, JNK, p38 MAPK, IκB and NF-κB as well as the protein expression of iNOS in the colon ($P < 0.001$, or $P < 0.01$). Moreover, 5-Fu treatment increased the expression of activated NF-κB in the intestinal epithelial cells (**Figure 4E**). All of these results indicated that 5-Fu treatment resulted in the activation of MAPK and NF-κB signaling pathways.

5-Fu Altered Bacterial Diversity and Community Composition

Gut microbiota has been indicated in inflammatory bowel disease (Terán-Ventura et al., 2014; Patel et al., 2016). Alteration of gut microbiota composition may affect the function of mucosal immune system, resulting in the intestinal inflammation (Autenrieth and Baumgart, 2017; Etienne-Mesmin et al., 2017; Holleran et al., 2017). Therefore, to clarify the change of gut microbiota of 5-Fu treated mice, the diversity and composition of gut microbiota in cecum contents and feces were analyzed by Miseq sequencing. The Chao community richness and Shannon diversity were used to estimate within-community diversity (α-diversity). Sequencing of 16S rRNA gene V3-V4 region of gut microbiota showed that 5-Fu greatly decreased the community richness of microbiota in both feces and cecum contents, compared with the controls (**Figure 5A**, $P < 0.001$). It significantly decreased the Shannon diversity in cecum contents but not that in feces of mice (**Figures 5B,C**, $P < 0.01$). Unweighted UniFrac PCoA analysis demonstrated that there was a significant difference between control and 5-Fu treated mice regarding beta-diversity at OTUs level (**Figures 5D,E**). These results indicated that 5-Fu treatment led to the richness and diversity loss in the bacterial community, especially in cecum contents.

The four major phyla in the feces and cecum contents were Bacteroidetes, Verrucomicrobia, Firmicutes, and Proteobacteria (**Figures 6A,B**, Table S1), among which Bacteroidetes and Verrucomicrobia were the relatively abundant ones. 5-Fu treatment remarkably decreased the relative abundance of Firmicutes, Proteobacteria, and Cyanobacteria at phyla level in feces ($P < 0.05$ or $P < 0.01$). However, 5-Fu increased the

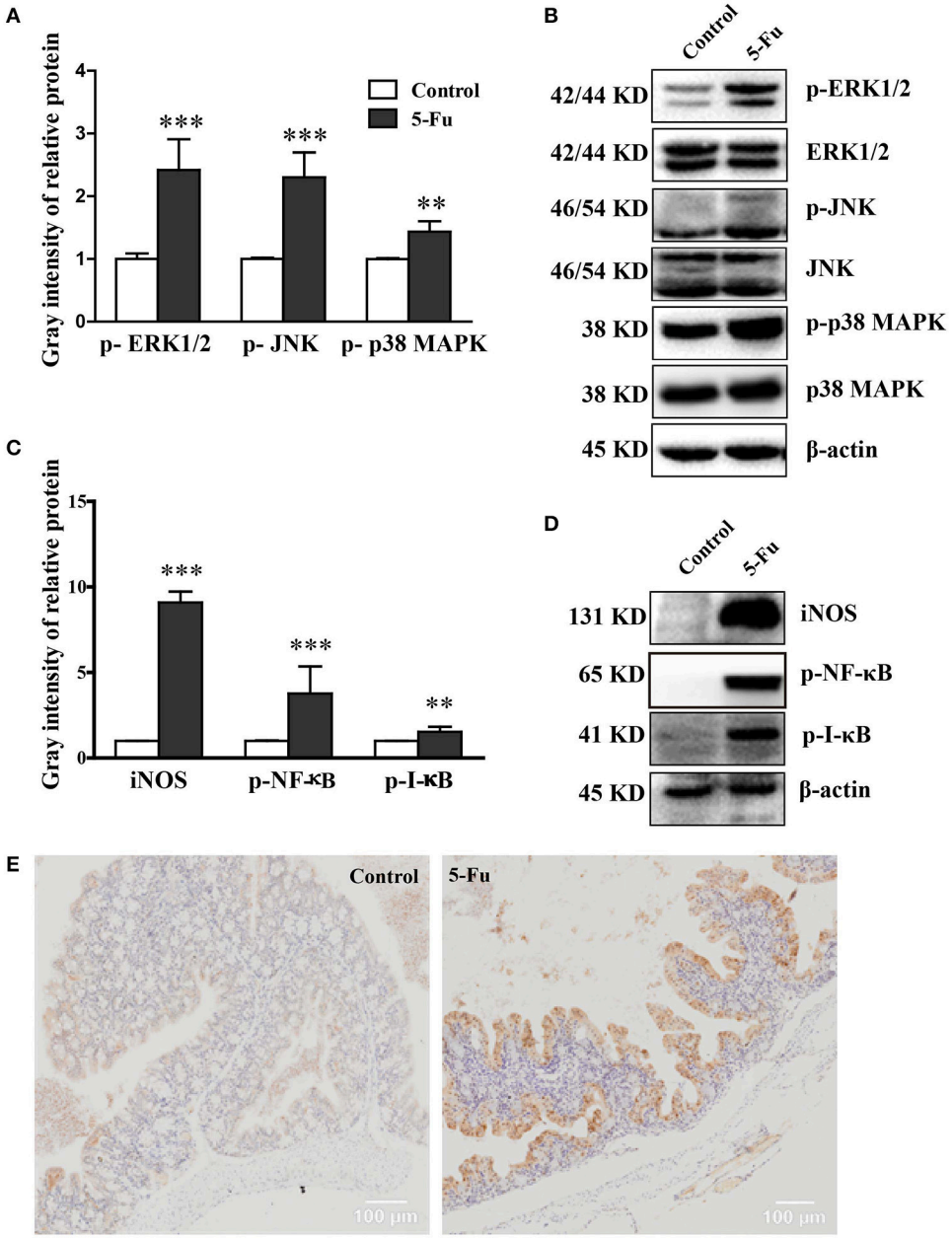

FIGURE 4 | 5-Fu activated NF-κB and MAPK signaling pathways in colonic tissues. **(A,B)** 5-Fu treatment enhanced the protein expression of p-ERK1/2, p-JNK, and p-p38 MAPK. **(C,D)** 5-Fu treatment elevated the protein expression of iNOS, p-NF-κB, and p-I-κB. **(E)** 5-Fu treatment increased the expression of activated NF-κB in the colonic epithelial cells. Values were expressed as mean ± S.E.M (n = 3/group). Data were analyzed by t-test. $^{**}P < 0.01$, $^{***}P < 0.001$ vs. control group.

abundance of Verrucomicrobia ($P < 0.05$), although it also reduced that of Firmicutes and Cyanobacteria ($P < 0.01$) in cecum contents. In addition, 5-Fu significantly decreased the ratio of Firmicutes/Bacteroidetes (F/B) in cecum contents and feces (**Figure 6C**, $p < 0.001$, $p < 0.05$). Further correlation analysis (**Figures 6D,E**) showed that F/B ratio positively correlated with body weight change (Spearman's $R = 0.7761$, $P < 0.001$ in cecum; Spearman's $R = 0.6525$, $P < 0.05$ in feces). More information about gut microbiota in cecum contents and feces could be found in Supplementary Data (Tables S1–12).

Disturbed Gut Microbiota was Involved in Body Weight Loss and Colon Shortening in 5-Fu Induced Colonic Mucositis

As shown in **Figure 7A**, from day 4, fecal transplantation significantly rescued the body weight loss of mice induced by 5-Fu treatment ($P < 0.05$). Furthermore, at day 7, fecal microbiota

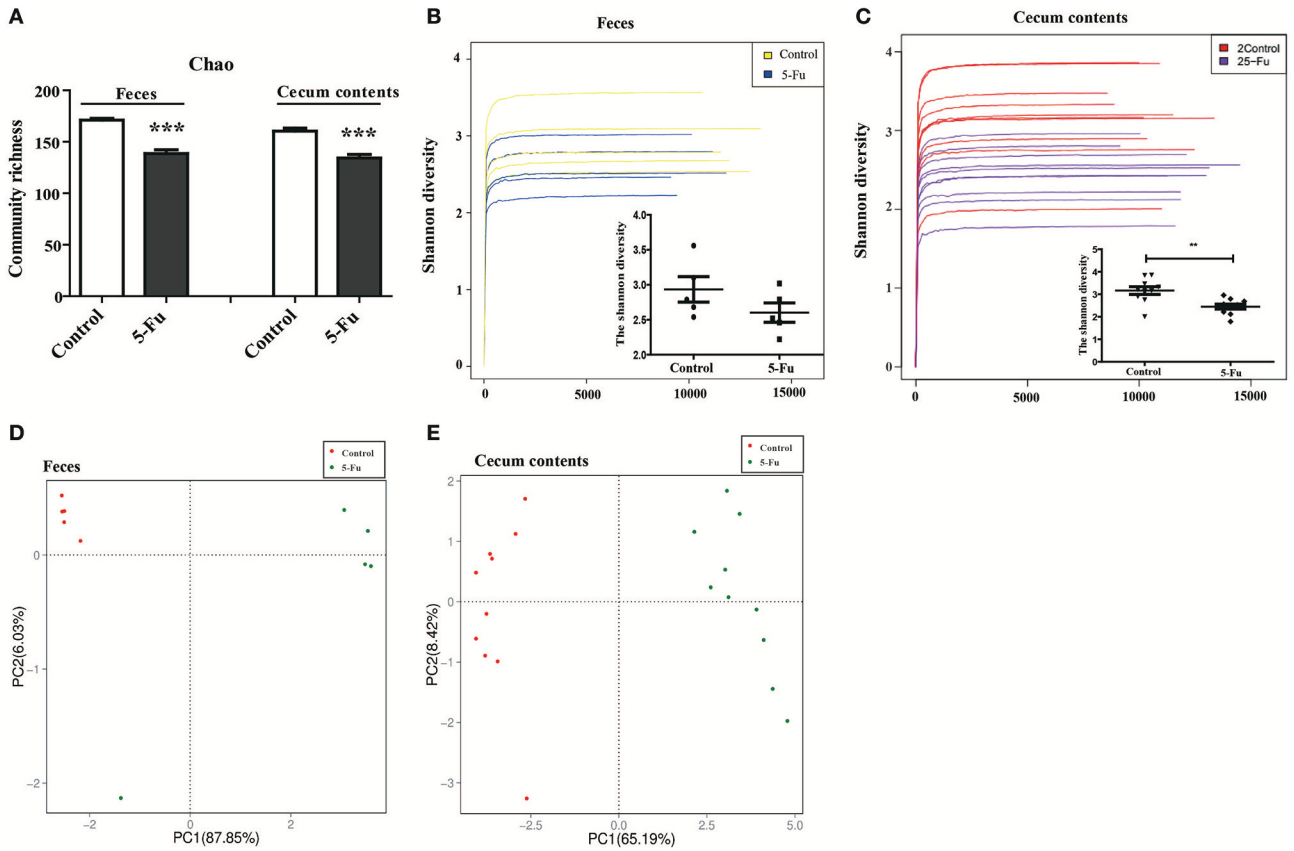

FIGURE 5 | 5-Fu decreased the richness and diversity of gut microbiota in feces and cecum contents of mice. **(A)** 5-Fu decreased the richness of gut microbiota in feces and cecum contents. Chao is an estimator of the community richness. **(B,C)** 5-Fu decreased the diversity of gut microbiota in feces (**B**, Shannon index curves and Shannon diversity histogram) and cecum contents (**C**, Shannon index curves and Shannon diversity histogram). **(D,E)** The unweighted UniFrac PCoA results of feces **(D)** and cecum contents **(E)** for beta-diversity at OTUs level. Values were expressed as mean ± S.E.M (n = 5/group, feces; n = 10/group, cecum contents). Data were analyzed by t-test. $^{**}P < 0.01$, $^{***}P < 0.001$ vs. control group.

transplantation prevented the shortening of colon induced by 5-Fu treatment (**Figures 7B,C**) ($P < 0.01$). In another experiment, to assess the effect of fecal microbiota on 5-Fu induced colonic mucositis, the vancomycin-pretreated mice were transplanted with feces from Control and 5-Fu group mice, respectively. As shown in **Figures 7D–F**, compared to mice transplanted with normal feces, mice transplanted with feces from 5-Fu treated mice showed significant body weight loss and shortened colon. These results implicated that disturbed gut microbiota contributed to the induction of intestinal mucositis in 5-Fu treated mice.

DISCUSSION

Although previous studies have indicated that gut microbiota plays an important role in 5-Fu induced gastrointestinal mucositis (Stringer et al., 2009b; Chang et al., 2012; Gao et al., 2014), however, none of them described the causal relationship in a systemic way. In present study, we analyzed the alteration of gut microbiota and inflammatory cytokine/chemokine profiles with relatively systemic methods. Our findings showed that, besides small intestine mucositis, 5-Fu also induced colonic mucositis. Both gut microbiota and inflammatory cytokine/chemokine profiles were altered significantly, which was accompanied with mucosal barrier disruption and inflammatory signaling pathway activation. Further studies revealed that fecal transplant from healthy mice alleviated the severity of colonic mucositis, while that from 5-Fu treated mice seemed to induce significant symptoms of colonic mucositis. Our results indicated that the recovery of homeostasis of gut microbiota by fecal transplantation might facilitate the relief of gastrointestinal mucositis induced by 5-Fu.

Pro-inflammatory cytokines and anti-inflammatory factors play a critical role in inflammatory bowel diseases (Stringer et al., 2009b). The expression levels of IL-6, TNF-α, IL-1β, IFN-γ, CXCL1 were shown to increase in small intestine of 5-Fu-induced intestinal mucositis mice (Soares et al., 2011, 2013; Chang et al., 2012; Yasuda et al., 2013; Yeung et al., 2015). In present study, IL-6, TNF-α, IL-1β were remarkably increased in serum and/or colon tissue at both mRNA and protein levels in 5-Fu induced colonic mucositis mice. Meanwhile, 5-Fu elevated the levels of IFN-γ, G-CSF, GM-CSF, and CD11b,

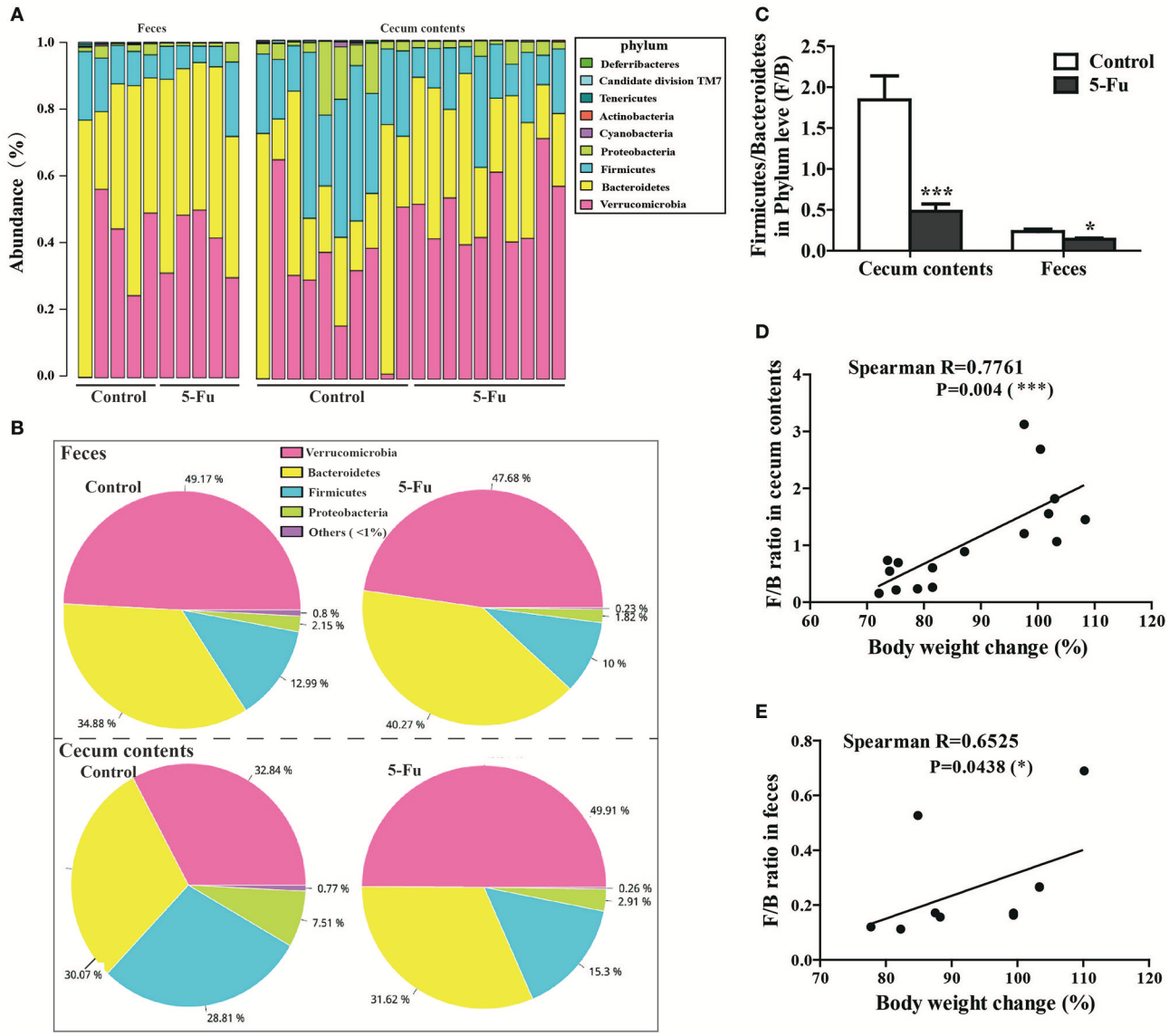

FIGURE 6 | 5-Fu treatment changed the gut microflora community composition at phylum level in feces and cecum contents of mice. **(A)** The bar diagram of bacterial community distribution in cecum contents (n = 10/group) and feces (n = 5/group) at phylum level, respectively. **(B)** The pie charts depicting the mean relative abundance for feces and cecum contents at phylum level, respectively. **(C)** 5-Fu treatment down-regulated the ratio of F/B in cecum contents and feces. **(D)** The correlation between body weight changes and F/B ratio in cecum contents. **(E)** The correlation between body weight changes and F/B ratio in feces. Values were expressed as mean ± S.E.M (n = 5/group, feces; n = 10/group, cecum contents). Data were analyzed by t-test. $^{*}P < 0.05$, $^{***}P < 0.001$ vs. control group.

while decreased that of RNATES and IL-31. Interestingly, leptin, a hormone produced and secreted by adipose tissue, muscle and stomach, was also detected in colonic tissue. And, 5-Fu could significantly decrease leptin both in serum and colonic tissues. Leptin treatment has been shown to promote intestinal recovery and enhance enterocyte turnover in a rat model of methotrexate-induced mucositis (Sukhotnik et al., 2009). The decreased leptin in serum and colon might partly reflect the excerbation of colonic mucositis induced by 5-Fu. CXCL9 treatment has been disclosed to attenuate 5-Fu induced mucositis (Han et al., 2011), however, it exacerbates 5-Fu induced acute intestinal damage (Lu et al., 2015). Therefore, further investigation is needed to clarify the effect of CXCL9 on 5-Fu induced mucositis. So far the role of CXCL5 in 5-Fu induced mucositis has not been elucidated yet. CXCL13 mediates T cell recruitment and participates in the regulation of inflammatory response (Hui et al., 2015). IL-22 produced by T cells and NK cells participates in tumorigenesis and tumor progression, and mediates chemoresistance (Wu et al., 2014), which is enhanced in colon of 5-Fu induced mice (Sakai et al., 2013). In present study, 5-Fu treatment significantly modulated the levels of CXCL5, CXCL9, CXCL13, and IL-22 in serum and/or colonic tissues. Moreover, 5-Fu increased gene

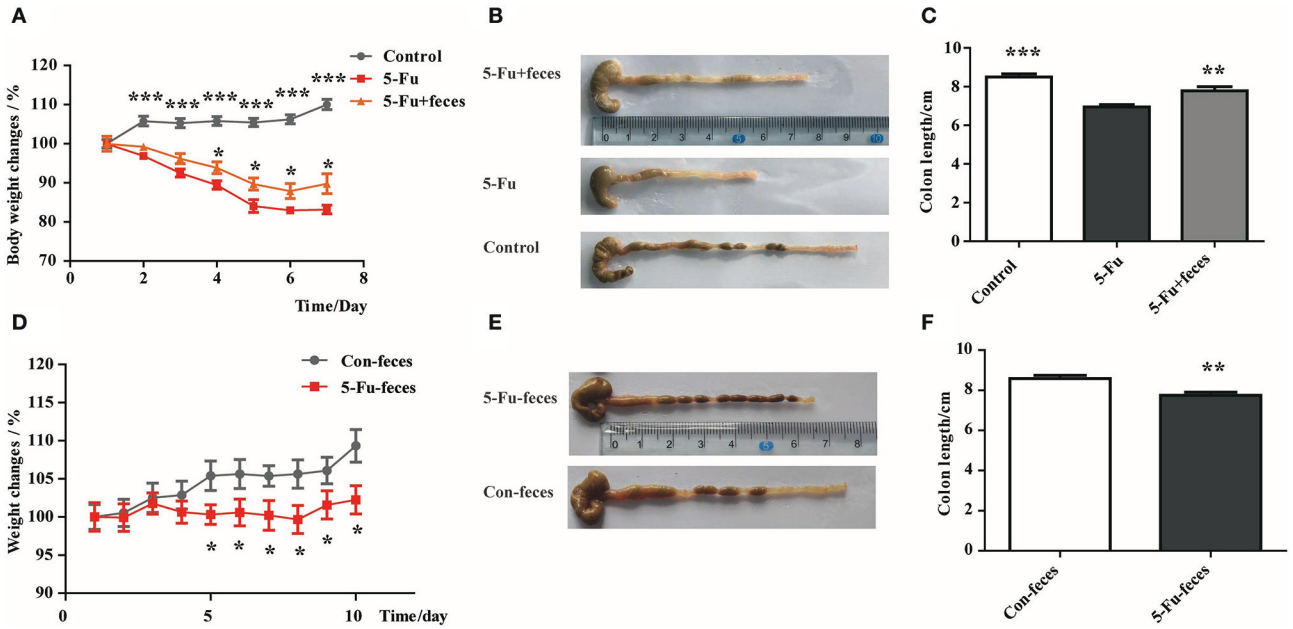

FIGURE 7 | Disturbed gut microbiota resulted in body weight loss and colon shortening in 5-Fu treated mice. **(A)** Normal fecal microbiota transplantation inhibited 5-Fu induced body weight loss. Data plotted as percentage of initial body weight. **(B,C)** The effect of normal fecal microbiota transplantation on colon length. Values were expressed as mean ± S.E.M ($n = 7$/group). Data were analyzed by *t*-test. $^{*}P < 0.05$, $^{**}P < 0.01$, $^{***}P < 0.001$ vs. 5-Fu group. **(D)** Fecal microbiota transplantation from 5-Fu treated mice induced body weight loss in mice pretreated with vancomycin. Data were plotted as percentage of initial body weight. **(E,F)** The effect of fecal microbiota transplantation from 5-Fu treated mice on colon length in vancomycin pretreated mice. Values were expressed as mean ± S.E.M ($n =$ 10/group). Data were analyzed by *t*-test. $^{*}P < 0.05$, $^{**}P < 0.01$ vs. control group.

expression of CXCR2 (receptor of CXCL1, CXCL5), CXCR3 (receptor of CXCL9), sTNFRI and sTNFRII (receptors of TNF-α), and IL-22R1 (receptor of IL-22), while reduced that of IL-10R2 (receptor of IL-10) in colonic tissue. All of these results implicated that 5-Fu induced colonic mucositis along with significant inflammatory responses.

TJs maintain the intestinal mucosal barrier (Yang et al., 2015). Reduction of TJs expression always indicates the increased intestinal epithelial permeability (Park et al., 2015; Yang et al., 2015). Chemotherapeutic drug could increase intestinal epithelial barrier permeability via reducing protein expression of TJs (Beutheu Youmba et al., 2012). Inflammatory infiltration is a characteristic of mucositis, which is triggered by the increased adhesion molecules in intestinal endothelia that attract the circulating inflammatory cells including neutrophils, T lymphocyte cells, B lymphocyte cells to gather in the inflammatory sites (Erbeldinger et al., 2017; Kim et al., 2017). The inflammatory cells further accelerate the modification of tight junction, thereby increase intestinal permeability leading to the disruption of mucosal barrier (Leocádio et al., 2015). The elevated pro-inflammatory cytokines induced by 5-Fu have been shown to account for the loss of tight junction proteins of small intestine, such as occludin and claudin-1, and result in diarrhea (Patel et al., 2016). In colonic tissues, our results demonstrated that 5-Fu treatment disrupted tight junction as the expression of occludin was down-regulated at both mRNA and protein levels. Surprisingly, ZO-1 protein was upregulated by 5-Fu in our study. It is well-known that ZO-1 is a cytoplasmic scaffolding protein, which is breakdown or redistributed under TNF-α-induced inflammatory condition (Chen et al., 2017; Watari et al., 2017). However it did not show significant change in mucosa of 5-Fu-induced small intestine (Song et al., 2013) or irinotecan-induced gut toxicity (Wardill et al., 2014), suggesting that its specific role on mucosal barrier under these inflammatory conditions. We don't know whether there is a compensatory mechanism in ZO-1, because of the decreased expression of occludin in 5-Fu induced colonic mucositis. Meanwhile, adhesion proteins such as ICAM-1, VCAM-1, JAM-A, and VE-Cadherin were increased by 5-Fu. These results indicated that 5-Fu treatment might increase the colonic epithelial barrier permeability through decreasing TJ proteins and up-regulating adhesion proteins to recruit inflammatory cells to colonic epithelium, and then enhance the translocation of gut microbiota in the mucosa to promote the inflammation.

NF-κB and MAPK pathways can be activated by many inflammatory chemokines/cytokines, which may result in a pro-inflammatory chemokines/cytokines positive feedback (Zimmerman et al., 2008; Tung et al., 2011; Chang et al., 2012; Jiang et al., 2012; Song et al., 2013; Candela et al., 2014; Dou et al., 2014; Yeung et al., 2015). And their activation in the small intestine has been shown to be involved in 5-Fu induced mucositis (Liu et al., 2013). Also, methotrexate (MTX) treatment increased intestinal permeability partially related to the decreased TJs protein expression through MAPK and NF-κB

pathways (Beutheu Youmba et al., 2012). In agreement with the report, in our study, enhanced phosphorylation of NF-κB and MAPK pathway molecules were also found in colonic tissue of 5-Fu treated mice, indicating their active participation in regulating expression of tight junction proteins and colonic proinflammatory cytokines/chemokines in the pathogenesis of 5-Fu induced colonic mucositis.

Disturbed gut microbiota, in either diversity or abundance, has been found to play an important role in the pathological development of inflammatory bowel diseases (Juste et al., 2014; Rangel et al., 2016). At genus level, 5-Fu treatment has been shown to decrease *Clostridium*, *Lactobacillus, Streptococcus* and *Enterococcus* and increase *Escherichia* in rat jejunum or colon (Stringer et al., 2007, 2009b). Different from the findings in rat, in present study, 5-Fu significantly decreased *Odoribacter*, *Candidatus Saccharimonas* and *Marvinbryantia*, and increased *Helicobacter* and *Thalassospira* in mouse feces. Moreover, 5-Fu significantly changed the abundance of *Blautia*, *Alistipes*, *Coprococcus, Roseburia*, *Akkermansia*, *Bilophila, Candidatus Saccharimonas,* and *Mucispirillum* in mouse cecum contents. The difference between our findings and previous reports might reflect the variable microbiota profiles affected by multiple factors such as environment, diet, gender, age, and species. At phylum level, microbiota low in Firmicutes has been disclosed to enhance the intestinal sensitivity to inflammation (Natividad et al., 2015). Decreased abundance of Ruminococcaceae and Lachnospiraceae families belong to Firmicutes phylum is found to be associated with inflammatory states (Knip and Siljander, 2016). On the contrary, cocktail of Ruminococcaceae and Lachnospiraceae families can efficiently reverse experimental colitis induced by dextran sodium sulfate (DSS) (Natividad et al., 2015). The ratio of Firmicutes/Bacteroidetes seems to be important for the maintenance of physiological state as the relative abundance of Firmicutes/Bacteroidetes influences body weight of animals, especially in metabolic diseases (Turnbaugh et al., 2006; Kassinen et al., 2007; Remely et al., 2014). Proteobacteria has been shown to play a crucial and active role in overall gut metabolism and host response despite their low abundance (Pérez-Cobas et al., 2013). Cyanobacteria inhibits inflammation by production of anti-inflammatory pitinoic acids B and C (Montaser et al., 2013). On the contrary, Verrucomicrobia appears to contribute to inflammation as their abundance bloomed in mice treated with DSS (Nagalingam et al., 2011). In present study, 5-Fu reduced the richness and diversity of gut microbiota, the relative abundance of Lachnospiraceae and Ruminococcaceae families (Tables S4, S10) accompanied with a lower ratio of Firmicutes/Bacteroidetes. Moreover, 5-Fu lessened the relative abundance of Proteobacteria, Candidate division TM7 and Cyanobacteria while increased that of Verrucomicrobia and Actinobacteria. These results implicated the active involvement of the microbiota in 5-Fu induced colonic mucositis. We also found that there was significant positive correlation between body weight changes and F/B ratio in feces and cecum contents. Our further results showed that fecal transplantation from normal mice could partly reverse the body weight loss and colon length decrease of 5-Fu treated mice. Moreover, feces from 5-Fu treated mice could also result in body weight loss and colon length decrease in normal mice pretreated with vancomycin. These results demonstrated that gut microbiota dysfunction at least partly accounted for the mucositis induced by 5-Fu. And the increased colonic epithelial barrier permeability induced by 5-Fu, would promote the translocation of gut bacteria in the intestinal mucosa, then to increase the inflammatory response (Escobedo et al., 2014; Mayer et al., 2015; Severance et al., 2016; Leung and Yimlamai, 2017).

In summary, our results indicated that 5-Fu induced mucositis might be partly mediated by the disturbance of gut microbiota. Since modulation gut microbiota by administration of probiotics or certain gut microbiota metabolite seemed to benefit 5-Fu-induced mucositis (Justino et al., 2014; González-Sarrías et al., 2015; An and Ha, 2016; Flórez et al., 2016), our findings provided potential novel therapeutic strategy for patients suffered from 5-Fu induced intestinal mucositis by manipulation of specific gut microbiota.

AUTHOR CONTRIBUTIONS

HS and XWu designed all the experiments, analyzed data and wrote the paper, and the performances of HS and XWu were equal in this study. HL and LL carried out the main experiments, and the performances of HL and LL were equal in this study; XWang, LQ, PW, SQ, and HWu performed parts of experiments. FH, and BZ provided valuable suggestions for this study and helped to draft the manuscript. All authors read and approved the final manuscript.

ACKNOWLEDGMENTS

This work was supported by the National Natural Science Foundation of China (81603354, 81673626), Shanghai Eastern Scholar Program (2013-59), and Shanghai E-research Institute of Bioactive Constituent in TCM plan.

SUPPLEMENTARY MATERIAL

The Supplementary Material for this article can be found online at: https://www.frontiersin.org/articles/10.3389/fcimb.2017.00455/full#supplementary-material

REFERENCES

An, J., and Ha, E. M. (2016). Combination therapy of *Lactobacillus plantarum* Supernatant and 5-Fluouracil increases chemosensitivity in colorectal cancer cells. *J. Microbiol. Biotechnol.* 26, 1490–1503. doi: 10.4014/jmb.1605.05024

Araújo, C. V., Lazzarotto, C. R., Aquino, C. C., Figueiredo, I. L., Costa, T. B., Alves, L. A., et al. (2015). Alanyl-glutamine attenuates 5-fluorouracil-induced intestinal mucositis in apolipoprotein E-deficient mice. *Braz J. Med. Biol. Res*, 48, 493–501. doi: 10.1590/1414-431X20144360

Autenrieth, D. M., and Baumgart, D. C. (2017). [Microbiome and Gut Inflammation]. *Dtsch. Med. Wochenschr.* 142, 261–266. doi: 10.1055/s-0042-111608

Beutheu Youmba, S., Belmonte, L., Galas, L., Boukhettala, N., Bôle-Feysot, C., Déchelotte, P., et al. (2012). Methotrexate modulates tight junctions through NF-κB, MEK, and JNK pathways. *J. Pediatr. Gastroenterol. Nutr.* 54, 463–470. doi: 10.1097/MPG.0b013e318247240d

Candela, M., Turroni, S., Biagi, E., Carbonero, F., Rampelli, S., Fiorentini, C., et al. (2014). Inflammation and colorectal cancer, when microbiota-host mutualism breaks. *World J. Gastroenterol.* 20, 908–922. doi: 10.3748/wjg.v20.i4.908

Capaldo, C. T., Powell, D. N., and Kalman, D. (2017). Layered defense: how mucus and tight junctions seal the intestinal barrier. *J. Mol. Med. (Berl.)* 95, 927–934. doi: 10.1007/s00109-017-1557-x

Chang, C. T., Ho, T. Y., Lin, H., Liang, J. A., Huang, H. C., Li, C. C., et al. (2012). 5-Fluorouracil induced intestinal mucositis via nuclear factor-kappaB activation by transcriptomic analysis and *in vivo* bioluminescence imaging. *PLoS ONE* 7:e31808. doi: 10.1371/journal.pone.0031808

Chang, X., Zhao, L., Wang, J., Lu, X., and Zhang, S. (2017). Sini-san improves duodenal tight junction integrity in a rat model of functional dyspepsia. *BMC Complement Altern. Med.* 17:432. doi: 10.1186/s12906-017-1938-2

Chen, Q., Chen, O., Martins, I. M., Hou, H., Zhao, X., Blumberg, J. B., et al. (2017). Collagen peptides ameliorate intestinal epithelial barrier dysfunction in immunostimulatory Caco-2 cell monolayers via enhancing tight junctions. *Food Funct.* 8, 1144–1151. doi: 10.1039/c6fo01347c

Dou, W., Zhang, J., Ren, G., Ding, L., Sun, A., Deng, C., et al. (2014). Mangiferin attenuates the symptoms of dextran sulfate sodium-induced colitis in mice via NF-κB and MAPK signaling inactivation. *Int. Immunopharmacol.* 23, 170–178. doi: 10.1016/j.intimp.2014.08.025

Dou, W., Zhang, J., Sun, A., Zhang, E., Ding, L., Mukherjee, S., et al. (2013). Protective effect of naringenin against experimental colitis via suppression of Toll-like receptor 4/NF-kappaB signalling. *Br. J. Nutr.* 110, 599–608. doi: 10.1017/S0007114512005594

Erbeldinger, N., Rapp, F., Ktitareva, S., Wendel, P., Bothe, A. S., Dettmering, T., et al. (2017). Measuring leukocyte adhesion to (primary) endothelial cells after photon and charged particle exposure with a dedicated laminar flow chamber. *Front. Immunol.* 8:627. doi: 10.3389/fimmu.2017.00627

Escobedo, G., López-Ortiz, E., and Torres-Castro, I. (2014). Gut microbiota as a key player in triggering obesity, systemic inflammation and insulin resistance. *Rev. Invest. Clin.* 66, 450–459.

Etienne-Mesmin, L., Chassaing, B., and Gewirtz, A. T. (2017). Tryptophan: a gut microbiota-derived metabolites regulating inflammation. *World J. Gastrointest. Pharmacol. Ther.* 8, 7–9. doi: 10.4292/wjgpt.v8.i1.7

Figlewicz, D. A. (2008). Comments on Fornai et al. (PNAS/ Feb 2008). *Amyotroph Lateral Scler.* 9, 125–126. doi: 10.1080/17482960802066643

Flórez, A. B., Sierra, M., Ruas-Madiedo, P., and Mayo, B. (2016). Susceptibility of lactic acid bacteria, bifidobacteria and other bacteria of intestinal origin to chemotherapeutic agents. *Int. J. Antimicrob. Agents* 48, 547–550. doi: 10.1016/j.ijantimicag.2016.07.011

Gao, J., Gao, J., Qian, L., Wang, X., Wu, M., Zhang, Y., et al. (2014). Activation of p38-MAPK by CXCL4/CXCR3 axis contributes to p53-dependent intestinal apoptosis initiated by 5-fluorouracil. *Cancer Biol Ther.* 15, 982–991. doi: 10.4161/cbt.29114

González-Sarrías, A., Tomé-Carneiro, J., Bellesia, A., Tomás-Barberán, F. A., and Espín, J. C. (2015). The ellagic acid-derived gut microbiota metabolite, urolithin A, potentiates the anticancer effects of 5-fluorouracil chemotherapy on human colon cancer cells. *Food Funct.* 6, 1460–1469. doi: 10.1039/c5fo00120j

Han, X., Wu, Z., Di, J., Pan, Y., Zhang, H., Du, Y., et al. (2011). CXCL9 attenuated chemotherapy-induced intestinal mucositis by inhibiting proliferation and reducing apoptosis. *Biomed. Pharmacother.* 65, 547–554. doi: 10.1016/j.biopha.2011.03.008

Holleran, G., Lopetuso, L. R., Ianiro, G., Pecere, S., Pizzoferrato, M., Petito, V., et al. (2017). Gut microbiota and inflammatory bowel disease: so far so gut. *Minerva Gastroenterol Dietol.* 63, 373–384. doi: 10.23736/S1121-421X.17.02386-8

Huang, T. Y., Chu, H. C., Lin, Y. L., Ho, W. H., Hou, H. S., Chao, Y. C., et al. (2009). Minocycline attenuates 5-fluorouracil-induced small intestinal mucositis in mouse model. *Biochem. Biophys. Res. Commun.* 384, 634–639. doi: 10.1016/j.bbrc.2009.09.041

Hui, W., Zhao, C., and Bourgoin, S. G. (2015). LPA Promotes T Cell Recruitment through Synthesis of CXCL13. *Mediators Inflamm.* 2015:248492. doi: 10.1155/2015/248492

Jiang, Y., Lü, X., Man, C., Han, L., Shan, Y., Qu, X., et al. (2012). Lactobacillus acidophilus induces cytokine and chemokine production via NF-kappaB and p38 mitogen-activated protein kinase signaling pathways in intestinal epithelial cells. *Clin. Vaccine Immunol.* 19, 603–608. doi: 10.1128/CVI.05617-11

Juste, C., Kreil, D. P., Beauvallet, C., Guillot, A., Vaca, S., Carapito, C., et al. (2014). Bacterial protein signals are associated with Crohn's disease. *Gut* 63, 1566–1577. doi: 10.1136/gutjnl-2012-303786

Justino, P. F., Melo, L. F., Nogueira, A. F., Costa, J. V., Silva, L. M., Santos, C. M., et al. (2014). Treatment with *Saccharomyces boulardii* reduces the inflammation and dysfunction of the gastrointestinal tract in 5-fluorouracil-induced intestinal mucositis in mice. *Br. J. Nutr.* 111, 1611–1621. doi: 10.1017/S0007114513004248

Kassinen, A., Krogius-Kurikka, L., Mäkivuokko, H., Rinttil,ä, T., Paulin, L., Corander, J., et al. (2007). The fecal microbiota of irritable bowel syndrome patients differs significantly from that of healthy subjects. *Gastroenterology* 133, 24–33. doi: 10.1053/j.gastro.2007.04.005

Kim, M. K., Park, H. J., Kim, Y., Kim, H. J., Bae, S. K., Bae, M. K., et al. (2017). Gastrin-releasing peptide induces monocyte adhesion to vascular endothelium by upregulatingendothelial adhesion molecules. *Biochem. Biophys. Res. Commun.* 485, 542–549. doi: 10.1016/j.bbrc.2017.01.058

Knip, M., and Siljander, H. (2016). The role of the intestinal microbiota in type 1 diabetes mellitus. *Nat. Rev. Endocrinol.* 12, 154–167. doi: 10.1038/nrendo.2015.218

Leocádio, P. C., Antunes, M. M., Teixeira, L. G., Leonel, A. J., Alvarez-Leite, J. I., Machado, D. C., et al. (2015). L-arginine pretreatment reduces intestinal mucositis as induced by 5-FU in mice. *Nutr. Cancer* 67, 486–493. doi: 10.1080/01635581.2015.1004730

Leung, D. H., and Yimlamai, D. (2017). The intestinal microbiome and paediatric liver disease. *Lancet Gastroenterol. Hepatol.* 2, 446–455. doi: 10.1016/S2468-1253(16)30241-2

Liu, Z., Xi, J., Schröder, S., Wang, W., Xie, T., Wang, Z., et al. (2013). Chimonanthus nitens var. salicifolius Aqueous Extract Protects against 5-Fluorouracil Induced Gastrointestinal Mucositis in a Mouse Model. *Evid. Based Compl. Alternat. Med.* 2013:789263. doi: 10.1155/2013/789263

Lu, H., Liu, H., Wang, J., Shen, J., Weng, S., Han, L., et al. (2015). The chemokine CXCL9 exacerbates chemotherapy-induced acute intestinal damage through inhibition of mucosal restitution. *J. Cancer Res. Clin. Oncol.* 141, 983–992. doi: 10.1007/s00432-014-1869-y

MacIntyre, D. A., Chandiramani, M., Lee, Y. S., Kindinger, L., Smith, A., Angelopoulos, N., et al. (2015). The vaginal microbiome during pregnancy and the postpartum period in a European population. *Sci. Rep.* 5: 8988. doi: 10.1038/srep08988

Mayer, E. A., Tillisch, K., and Gupta, A. (2015). Gut/brain axis and the microbiota. *J. Clin. Invest.* 125, 926–938. doi: 10.1172/JCI76304

Montaser, R., Paul, V. J., and Luesch, H. (2013). Modular strategies for structure and function employed by marine cyanobacteria: characterization and synthesis of pitinoic acids. *Org. Lett.* 15, 4050–4053. doi: 10.1021/ol401396u

Nagalingam, N. A., Kao, J. Y., and Young, V. B. (2011). Microbial ecology of the murine gut associated with the development of dextran sodium sulfate-induced colitis. *Inflamm. Bowel Dis.* 17, 917–926. doi: 10.1002/ibd.21462

Natividad, J. M., Pinto-Sanchez, M. I., Galipeau, H. J., Jury, J., Jordana, M., Reinisch, W., et al. (2015). Ecobiotherapy rich in firmicutes decreases susceptibility to colitis in a humanized gnotobiotic mouse model. *Inflamm. Bowel. Dis.* 21, 1883–1893. doi: 10.1097/MIB.0000000000000422

Park, H. Y., Kim, T. H., Kim, C. G., Kim, G. Y., Kim, C. M., Kim, N. D., et al. (2013). Purpurogallin exerts anti-inflammatory effects in lipopolysaccharide-stimulated BV microglial cells through the inactivation of the NF-κB and MAPK signaling pathways. *Int. J. Mol. Med.* 32, 1171–1178. doi: 10.3892/ijmm.2013

Park, H. Y., Kunitake, Y., Hirasaki, N., Tanaka, M., and Matsui,T. (2015). Theaflavins enhance intestinal barrier of Caco-2 Cell monolayers through the expression of AMP-activated protein kinase-mediated Occludin, Claudin-1, and ZO-1. *Biosci. Biotechnol. Biochem.* 79, 130–137. doi: 10.1080/09168451.2014.951027

Patel, T., Bhattacharya, P., and Das, S. (2016). Gut microbiota: an indicator to gastrointestinal tract diseases. *J. Gastrointest. Cancer* 47, 232–238. doi: 10.1007/s12029-016-9820-x

Pereira, V. B., Melo, A. T., Assis-Júnior, E. M., Wong, D. V., Brito, G. A., Almeida, P. R., et al. (2016). A new animal model of intestinal mucositis induced by the combination of irinotecan and 5-fluorouracil in mice. *Cancer Chemother Pharmacol.* 77, 323–332. doi: 10.1007/s00280-015-2938-x

Pérez-Cobas, A. E., Gosalbes, M. J., Friedrichs, A., Knecht, H., Artacho, A., Eismann, K., et al. (2013). Gut microbiota disturbance during antibiotic therapy: a multi-omic approach. *Gut* 62, 1591–1601. doi: 10.1136/gutjnl-2012-303184

Philippot, L., Raaijmakers, J. M., Lemanceau, P., and van der Putten, W. H. (2013). Going back to the roots: the microbial ecology of the rhizosphere. *Nat. Rev. Microbiol.* 11, 789–799. doi: 10.1038/nrmicro3109

Prisciandaro, L. D., Geier, M. S., Chua, A. E., Butler, R. N., Cummins, A. G., Sander, G. R., et al. (2012). Probiotic factors partically prevent changes to caspase 3 and 7 activation and transepithelial electrical resistance in a model of 5-fluorouracil-induced epithelial cell damage. *Support Care Cancer* 20, 3205–3210. doi: 10.1007/s00520-012-1446-3

Rangel, I., Ganda Mall, J. P., Willén, R., Sjöberg, F., and Hultgren-Hörnquist, E. (2016). Degree of colitis correlates with microbial composition and cytokine responses in colon and caecum of Galphai2-deficient mice. *FEMS Microbiol. Ecol.* 92:fiw098. doi: 10.1093/femsec/fiw098

Remely, M., Aumueller, E., Merold, C., Dworzak, S., Hippe, B., Zanner, J., et al. (2014). Effects of short chain fatty acid producing bacteria on epigenetic regulation of FFAR3 in type 2 diabetes and obesity. *Gene* 537, 85–92. doi: 10.1016/j.gene.2013.11.081

Sakai, H., Kai, Y., Oguchi, A., Kimura, M., Tabata, S., Yaegashi, M., et al. (2016). Curcumin inhibits 5-Fluorouracil-induced Up-regulation of CXCL1 and CXCL2 of the colon associated with attenuation of diarrhoea development. *Basic Clin. Pharmacol. Toxicol.* 119, 540–547. doi: 10.1111/bcpt.12619

Sakai, H., Sagara, A., Matsumoto, K., Hasegawa, S., Sato, K., Nishizaki, M., et al. (2013). 5-Fluorouracil induces diarrhea with changes in the expression of inflammatory cytokines and aquaporins in mouse intestines. *PLoS ONE* 8:e54788. doi: 10.1371/journal.pone.0054788

Severance, E. G., Yolken, R. H., and Eaton, W. W. (2016). Autoimmune diseases, gastrointestinal disorders and the microbiome in schizophrenia: more than a gut feeling. *Schizophr. Res.* 176, 23–25. doi: 10.1016/j.schres.2014.06.027

Soares, P. M., Lima-Junior, R. C., Mota, J. M., Justino, P. F., Brito, G. A., Ribeiro, R. A., et al. (2011). Role of platelet-activating factor in the pathogenesis of 5-fluorouracil-induced intestinal mucositis in mice. *Cancer Chemother. Pharmacol.* 68, 713–720. doi: 10.1007/s00280-010-1540-5

Soares, P. M., Mota, J. M., Souza, E. P., Justino, P. F., Franco, A. X., Cunha, F. Q., et al. (2013). Inflammatory intestinal damage induced by 5-fluorouracil requires IL-4. *Cytokine* 61, 46–49. doi: 10.1016/j.cyto.2012.10.003

Song, M. K., Park, M. Y., and Sung, M. K. (2013). 5-Fluorouracil-induced changes of intestinal integrity biomarkers in BALB/c mice. *J. Cancer Prev.* 18, 322–329. doi: 10.15430/JCP.2013.18.4.322

Sonis, S. T., Elting, L. S., Keefe, D., Peterson, D. E., Schubert, M., Hauer-Jensen, M., et al. (2004). Perspectives on cancer therapy-induced mucosal injury: pathogenesis, measurement, epidemiology, and consequences for patients. *Cancer* 100, 1995–2025. doi: 10.1002/cncr.20162

Stringer, A. M., Gibson, R. J., Bowen, J. M., and Keefe, D. M. (2009a). Chemotherapy-induced modifications to gastrointestinal microflora: evidence and implications of change. *Curr. Drug Metab.* 10, 79–83. doi: 10.2174/138920009787048419

Stringer, A. M., Gibson, R. J., Bowen, J. M., Logan, R. M., Yeoh, A. S., and Keefe, D. M. (2007). Chemotherapy-induced mucositis: the role of gastrointestinal microflora and mucins in the luminal environment. *J. Support Oncol.* 5, 259–267.

Stringer, A. M., Gibson, R. J., Logan, R. M., Bowen, J. M., Yeoh, A. S., Hamilton, J., et al. (2009b). Gastrointestinal microflora and mucins may play a critical role in the development of 5-Fluorouracil-induced gastrointestinal mucositis. *Exp. Biol. Med. (Maywood)* 234, 430–441. doi: 10.3181/0810-RM-301

Sukhotnik, I., Mogilner, J. G., Shteinberg, D., Karry, R., Lurie, M., Ure, B. M., et al. (2009). Leptin accelerates enterocyte turnover during methotrexate-induced intestinal mucositis in a rat. *Cancer Biol. Ther.* 8, 899–906. doi: 10.4161/cbt.8.10.8128

Terán-Ventura, E., Aguilera, M., Vergara, P., and Martínez, V. (2014). Specific changes of gut commensal microbiota and TLRs during indomethacin-induced acute intestinal inflammation in rats. *J. Crohns Colitis.* 8, 1043–1054. doi: 10.1016/j.crohns.2014.02.001

Tung, D., Cheung, P. H., Tudor, G., Booth, C., and Saha, S. (2011). *In vivo* effects of immunomodulators in a murine model of Fluorouracil-induced mucositis. *Curr. Ther. Res. Clin. Exp.* 72, 262–272. doi: 10.1016/j.curtheres.2011.11.003

Turnbaugh, P. J., Ley, R. E., Mahowald, M. A., Magrini, V., Mardis, E. R., and Gordon, J. I. (2006). An obesity-associated gut microbiome with increased capacity for energy harvest. *Nature* 444, 1027–1031. doi: 10.1038/nature05414

Ubeda, C., Bucci, V., Caballero, S., Djukovic, A., Toussaint, N. C., Equinda, M., et al. (2013). Intestinal microbiota containing *Barnesiella* species cures vancomycin-resistant Enterococcusfaecium colonization. *Infect. Immun.* 81. 965–973. doi: 10.1128/IAI.01197-12

Vandeputte, D., Falony, G., Vieira-Silva, S., Tito, R. Y., Joossens, M., and Raes, J. (2016). Stool consistency is strongly associated with gut microbiota richness and composition, enterotypes and bacterial growth rates. *Gut* 65, 57–62. doi: 10.1136/gutjnl-2015-309618

Vétizou, M., Pitt, J. M., Daillère, R., Lepage, P., Waldschmitt, N., Flament, C., et al. (2015). Anticancer immunotherapy by CTLA-4 blockade relies on the gut microbiota. *Science* 350, 1079–1084. doi: 10.1126/science.aad1329

Wang, Y., and Kasper, L. H. (2014). The role of microbiome in central nervous system disorders. *Brain Behav. Immun.* 38, 1–12. doi: 10.1016/j.bbi.2013.12.015

Wardill, H. R., Bowen, J. M., Al-Dasooqi, N., Sultani, M., Bateman, E., Stansborough, R., et al. (2014). Irinotecan disrupts tight junction proteins within the gut: implications for chemotherapy-induced gut toxicity. *Cancer Biol. Ther.* 15, 236–244. doi: 10.4161/cbt.27222

Warn, P., Thommes, P., Sattar, A., Corbett, D., Flattery, A., Zhang, Z., et al. (2016). Disease Progression and Resolution in Rodent Models of Clostridium difficile Infection and Impact of Antitoxin Antibodies and Vancomycin. *Antimicrob Agents Chemother* 60, 6471–6482. doi: 10.1128/AAC.00974-16

Watari, A., Sakamoto, Y., Hisaie, K., Iwamoto, K., Fueta, M., Yagi, K., et al. (2017). Rebeccamycin Attenuates TNF-alpha-Induced Intestinal Epithelial Barrier Dysfunction by Inhibiting Myosin Light Chain Kinase Production. *Cell Physiol. Biochem.* 41, 1924–1934. doi: 10.1159/000472367

Wu, T., Wang, Z., Liu, Y., Mei, Z., Wang, G., Liang, Z., et al. (2014). Interleukin 22 protects colorectal cancer cells from chemotherapy by activating the STAT3 pathway and inducing autocrine expression of interleukin 8. *Clin. Immunol.* 154, 116–126. doi: 10.1016/j.clim.2014.07.005

Yang, F., Wang, A., Zeng, X., Hou, C., Liu,H., and Qiao, S. (2015). Lactobacillus reuteri I5007 modulates tight junction protein expression in IPEC-J2 cells with LPSstimulation and in newborn piglets under normal conditions. *BMC Microbiol.* 15:32. doi: 10.1186/s12866-015-0372-1

Yasuda, M., Kato, S., Yamanaka, N., Iimori, M., Matsumoto, K., Utsumi, D., et al. (2013). 5-HT(3) receptor antagonists ameliorate 5-fluorouracil-induced intestinal mucositis by suppression of apoptosis in murine intestinal crypt cells. *Br. J. Pharmacol.* 168, 1388–1400. doi: 10.1111/bph.12019

Yeung, C. Y., Chan, W. T., Jiang, C. B., Cheng, M. L., Liu, C. Y., Chang, S. W., et al. (2015). Amelioration of Chemotherapy-Induced Intestinal Mucositis by Orally Administered Probiotics in a Mouse Model. *PLoS ONE* 10:e0138746. doi: 10.1371/journal.pone.0138746

Zhao, L. (2013). The gut microbiota and obesity: from correlation to causality. *Nat. Rev. Microbiol.* 11, 639–647. doi: 10.1038/nrmicro3089

Zimmerman, N. P., Vongsa, R. A., Wendt, M. K., and Dwinell, M. B. (2008). Chemokines and chemokine receptors in mucosal homeostasis at the intestinal epithelial barrier in inflammatory bowel disease. *Inflamm. Bowel Dis.* 14, 1000–1011. doi: 10.1002/ibd.20480

Conflict of Interest Statement: The authors declare that the research was conducted in the absence of any commercial or financial relationships that could be construed as a potential conflict of interest.

Copyright © 2017 Li, Lu, Wang, Qin, Wang, Qiu, Wu, Huang, Zhang, Shi and Wu. This is an open-access article distributed under the terms of the Creative Commons Attribution License (CC BY). The use, distribution or reproduction in other forums is permitted, provided the original author(s) or licensor are credited and that the original publication in this journal is cited, in accordance with accepted academic practice. No use, distribution or reproduction is permitted which does not comply with these terms.

frontiers in Cellular and Infection Microbiology

ORIGINAL RESEARCH
published: 11 October 2017
doi: 10.3389/fcimb.2017.00444

The Influence of Proton Pump Inhibitors on the Fecal Microbiome of Infants with Gastroesophageal Reflux—A Prospective Longitudinal Interventional Study

Christoph Castellani[1], Georg Singer[1], Karl Kashofer[2], Andrea Huber-Zeyringer[1], Christina Flucher[1], Margarita Kaiser[1] and Holger Till[1]*

[1] Department of Paediatric and Adolescent Surgery, Medical University of Graz, Graz, Austria, [2] Institute of Pathology, Medical University of Graz, Graz, Austria

Proton pump inhibitors (PPIs) are the standard therapy for gastroesophageal reflux disease. In adults, PPI treatment is associated with *Clostridium difficile* infections (CDI). In contrast to adults the microbiome of infants develops from sterility at birth toward an adult-like profile in the first years of life. The effect of PPIs on this developing microbiome has never been studied. The aim of the present study was to determine the effect of oral PPIs on the fecal microbiome in infants with gastroesophageal reflux disease (GERD). In this prospective longitudinal study 12 infants with proven GERD received oral PPIs for a mean period of 18 weeks (range 8–44). Stool samples were collected before ("before PPI") and 4 weeks after initiation of PPI therapy ("on PPI"). A third sample was obtained 4 weeks after PPI discontinuation ("after PPI"). The fecal microbiome was determined by NGS based 16S rDNA sequencing. This trial was registered with clinicaltrials.gov (NCT02359604). In a comparison of "before PPI" and "on PPI" neither α- nor β-diversity changed significantly. On the genus level, however, the relative abundances showed a decrease of *Lactobacillus* and *Stenotrophomonas* and an increase of *Haemophilus*. After PPI therapy there was a significant increase of α- and β-diversity. Additionally, the relative abundances of the phyla Firmicutes, Bacteroidetes, and Proteobacteria were significantly changed and correlated to patients' age and the introduction of solid foods. PPI treatment has only minor effects on the fecal microbiome. After discontinuation of PPI treatment the fecal microbiome correlated to patients' age and nutrition.

Keywords: proton pump inhibitors, microbiome, infants, GERD, *Clostridium difficile*

OPEN ACCESS

Edited by:
Nathan W. Schmidt,
University of Louisville, United States

Reviewed by:
Gena D. Tribble,
University of Texas Health Science Center at Houston, United States
Xingmin Sun,
University of South Florida, United States

***Correspondence:**
Georg Singer
georg.singer@medunigraz.at

Received: *12 July 2017*
Accepted: *29 September 2017*
Published: *11 October 2017*

Citation:
Castellani C, Singer G, Kashofer K, Huber-Zeyringer A, Flucher C, Kaiser M and Till H (2017) The Influence of Proton Pump Inhibitors on the Fecal Microbiome of Infants with Gastroesophageal Reflux—A Prospective Longitudinal Interventional Study. Front. Cell. Infect. Microbiol. 7:444. doi: 10.3389/fcimb.2017.00444

INTRODUCTION

Gastroesophageal reflux (GER) is a common finding in infants caused by temporary relaxations of the immature lower esophageal sphincter (LES) (Vandenplas et al., 2007). With maturation of the LES in the first year of life GER events often decrease. Some infants, however, may develop gastroesophageal reflux disease (GERD) associated with vomiting, feeding problems, pain, esophagitis, failure to thrive and/or recurrent respiratory infections (Rudolph et al., 2001; Colletti and Di Lorenzo, 2003).

In these infants conservative therapy includes upright positioning, increased feeding frequencies with lower amounts and food thickeners (Hollwarth, 2012). Nevertheless, some children may require acid suppression therapy with proton pump inhibitors (PPI). In adults, possible side effects of prolonged PPI therapy include an increased risk of community acquired enteritis and *Clostridium difficile* infections (CDI) (Janarthanan et al., 2012; Bouwknegt et al., 2014; McDonald et al., 2015).

The influence of PPI therapy on the intestinal microbiome has only been studied in adults under PPI therapy demonstrating dramatic changes of both the gastric and esophageal microbial communities (Amir et al., 2014). Furthermore, examinations of fecal samples have shown an increased abundance of *Enterococcae* and *Streptococcae* as well as decreased *Clostridiales*, associated with an increased risk of CDI (Freedberg et al., 2015b). Recent reports also describe an increased risk of CDI infections in infants under acid suppression treatment (Brown et al., 2015; Freedberg et al., 2015a). The exact pathophysiological mechanism of this association, however, is poorly understood. The two most common theories are (1) PPI directly affect the microbial environment by increasing the gastric pH and/or (2) PPI directly target bacterial proton pumps containing P-type ATPase enzymes (Vesper et al., 2009).

The gut microbiome in infancy develops from sterility at birth to an adult-like profile [dominated by the phyla Firmicutes (50–70% total bacterial numbers), Bacteroidetes (10–30%), Proteobacteria (up to 10%) and Actinobacteria (up to 10%), (Eckburg et al., 2005)] within the first years of life (Palmer et al., 2007; Yatsunenko et al., 2012). In this period a longitudinal investigation of fecal samples has revealed an increase of the total number of colonizing bacteria as well as unstable and heterogenic relative abundances of the different phyla (Palmer et al., 2007). Thus, data derived from the "stable" microbiome in adults are not representative for infants (Palmer et al., 2007; Yatsunenko et al., 2012).

PPI-associated changes of the microbiome have not been studied in infancy yet. Therefore, the aim of this prospective longitudinal interventional investigation was to assess the influence of oral PPI therapy on the fecal microbiome of infants with proven GERD.

MATERIALS AND METHODS

According to our institutional protocol all patients with suspected GERD undergo 24 h-pH-impedance monitoring (24 h-pH-MII). After ethical approval (Ethical Committee of the Medical University of Graz, 26-429 ex 13/14) and informed consent of parents or legal guardians patients younger than 1 year with proven GERD were enrolled in this study between November 2014 and August 2016. Patients with relevant additional diagnoses were excluded. This trial was registered with clinicaltrials.gov (NCT02359604).

A first stool sample was taken before initiation of PPI therapy, stored in a PSP® Spin Stool DNA Kit (Stratec molecular GmbH, Berlin, Germany) and frozen at −21°C until further processing ("*before PPI*" sample). According to our protocol all patients received 1 mg/kg body weight oral esomeprazole daily. After 4 weeks of PPI treatment a second stool sample was collected and stored as described ("*on PPI*" sample). The duration of PPI therapy depended on the patients' clinical symptoms. A third sample was collected 4 weeks after discontinuation of PPI therapy ("*after PPI*" sample). None of the patients received antibiotics or other acid suppressants during the course of the study. Dietary habits were recorded.

DNA Isolation, 16s Library Preparation and Sequencing

Frozen stool samples were thawed and a peanut sized stool sample was thoroughly mixed in 500 µl PBS. 250 µl of the suspension were mixed with 250 µl bacterial lysis buffer from the MagnaPure LC DNA Isolation Kit III (Bacteria, Fungi) (Roche, Mannheim, Germany) and transferred to MagnaLyser green bead tubes (Roche, Mannheim, Germany) for mechanical lysis performed two times at 6,500 rpm for 30 s in a MagnaLyser instrument (Roche, Mannheim, Germany). After bead beating 25 µl lysozyme (100 mg/ml) were added to the samples for enzymatic lysis and incubated at 37°C for 30 min followed by incubation with 43 µl Proteinase K (20 mg/ml) at 65°C for 1 h. Heat inactivation of enzymes was performed at 95°C for 10 min. Samples were centrifuged at 13,000 rpm for 5 min and 100 µl of the lysed samples were transferred to the Magna Pure instrument and DNA was purified according to manufacturer's instructions. PCR and library preparation with hypervariable regions V1-2 were performed as described before (Klymiuk et al., 2016) with 2 µl of total DNA per 25 µl PCR reaction in triplicates using primers 27f (AGAGTTTGATCCTGGCTCAG) and 357r (CTGCTGCCTYCCGTA) yielding a 330 bp long insert. Triplicates were pooled, amplification was verified by checking on a 1% agarose gel and sequencing library was normalized, indexed, and quantified according to Klymiuk et al. (2016). The pooled sample library was sequenced on a MiSeqII desktop sequencer (Illumina, Eindhoven, Netherlands) with v3 600 cycles chemistry (Illumina, Eindhoven, Netherlands) according to the manufacturer's instructions at 6 pM with 20% PhiX (Illumina, Eindhoven, Netherlands) in one run.

Sequence reads were submitted to the NCBI Sequence Read Archive (https://www.ncbi.nlm.nih.gov/sra/?term=SRP119055).

Microbiome Analysis

Sequencing reads were processed with scripts of the QIIME platform. Briefly, reads were clustered to Operational Taxonomic Units (OTU) using the pick_open_reference_otus.py script and uclust algorithm based on the greengenes database (gg_otus-13_8-release) and a 97% identity threshold. OTUs were visualized as OTU tables, bar charts and PCOA plots. Alpha diversity measurements (observed species and chao1) and beta-diversity measurements (unweighted unifrac) were derived using the respective QIIME tools. Group significance for all categories was determined with the Adonis test, while individual species difference was quantified by Kruskall-Wallis tests and pairwise comparisons by Mann-Whitney-U-test. The Adonis test computes R2 (effect size) and pseudo-P values of categories by first identifying the relevant centroids of the data and then calculating the squared deviations from these points. After

that, significance tests are performed using *F*-tests based on sequential sums of squares from permutations of the raw data. Adonis tests were performed in R (2.15.1) using the vegan package. Significance of differences in alpha diversity was calculated by non-parametric two-sample *t*-test using Monte Carlo permutations to calculate the *p*-value. Lefse analysis was performed for all categories as described previously (Segata et al., 2011).

RESULTS

36 stool samples ($n = 12$ "before PPI", $n = 12$ "on PPI," $n = 12$ "after PPI") of 12 patients (8 male, 4 female) were included. The mean gestational age was 38 weeks (STD 2.0; range 35–41 weeks). Patients had a mean birth weight of 2,794 g (STD 468; range 2,100–3,688 g) and a mean birth length of 48.8 cm (STD 2.6; range 44–53 cm).

Patients were included at a mean age of 5.2 months (STD 3.2; range 0.5–10.2 months). All patients suffered from GERD. The data of their 24 h-pH-MII is shown in **Table 1**. The patients' nutrition at the time of stool sampling is displayed in **Table 2**. The mean duration of PPI treatment was 18 weeks (STD 11; range 8–44).

PPI Therapy Had No Influence on α- and β-Diversity

In the within-individual comparison ("before PPI" vs. "on PPI"), oral PPI treatment did not influence α-diversity (Chao1 index; $p = 0.729$, **Figure 1**). Additionally, β-diversity did not change when comparing "*before PPI*" and "*on PPI*" (unweighted UniFrac; $p = 0.913$).

PPI Treatment Caused Only Minimal Changes in the Fecal Microbiome

Taxa summary plots at the phylum and class level at the different time points tested are depicted in **Figure 2**. On the genus level, PPI therapy caused a significant decrease of *Lactobacillus* and of *Stenotrophomonas*. Additionally, there was a significant increase of *Haemophilus* (**Table 3**). Although Streptococcus increased under PPI therapy none of the bacteria associated with an elevated risk of CDI in adults (*Streptococcus, Enterococcus*, *Clostridiaceae*) were significantly altered (**Figure 3**). There was no significant correlation between the results of impedance testing and the corresponding microbiome ("*before PPI*") ($p > 0.10$).

The Third Sample ("after PPI") Showed Increasing α- und β-Diversities and Altered Relative Abundances in Correlation with Patients' Age and Dietary Habits

The α-diversity significantly increased over the time of the experiment ($p = 0.003$ for the comparison "*before PPI*" to "*after*

TABLE 1 | Results of the 24 h-pH-MII before initiation of oral PPI therapy ($n = 12$).

	AET	ABET	WABET	NABET	TBET	NRA	NRWA	NRNA	NRT
	%	%	%	%	%	*n*	*n*	*n*	*n*
Mean	7.3	1.0	0.8	0	1.8	34.3	25.4	0.4	60.0
STD	4.9	0.8	0.6	0	0.9	21.4	19.9	1.2	21.1
MIN	0.6	0.2	0.1	0	0.4	9.0	8.0	0.0	30.0
MAX	16.3	2.9	2.0	0.1	3.5	73.0	75.0	4.0	96.0

AET, acid exposure time (pH < 4); ABET, acidic bolus exposure time (pH < 4); WABET, weakly acidic bolus exposure time (4 ≤ pH < 7); NABET, non-acidic bolus exposure time (pH ≥ 7); TBET, total bolus exposure time; NRA, number of acidic refluxes; NRWA, number of weakly acidic refluxes; NRNA, number of non-acidic refluxes; NRT, total number of refluxes.

TABLE 2 | Nutrition of the infants at the three different time points of stool sampling ($n = 12$).

ID	1st sample	2nd sample	3rd sample
	Before PPI	On PPI	After PPI
1	MM	MM	MM
2	FM	FM	FM/SF
3	MM/FM	FM	FM/SF
4	MM/FM	FM	FM/SF
5	FM	FM	FM/SF
6	FM	FM	FM/SF
7	FM	FM/SF	FM/SF
8	MM/SF	FM/SF	FM/SF
9	MM/FM	FM/SF	FM/SF
10	FM	FM/SF	FM/SF
11	MM/SF	FM/SF	FM/SF
12	MM/SF	MM/SF	FM/SF

MM, mother's milk; FM, formula; SF, solid food.

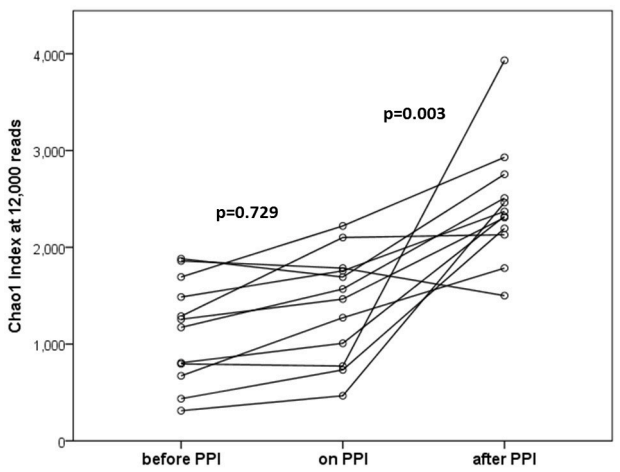

FIGURE 1 | α-diversities (Chao1 index at 12,000 reads) at the three time points tested ($n = 12$ per time point). In the within-individual comparison there was no statistically significant difference after 4 weeks of PPI treatment ($p = 0.729$). Four weeks after discontinuation of PPI therapy α-diversities were significantly increased ($p = 0.003$ for "after PPI" vs. "before PPI" and "on PPI." Lines connect individuals.

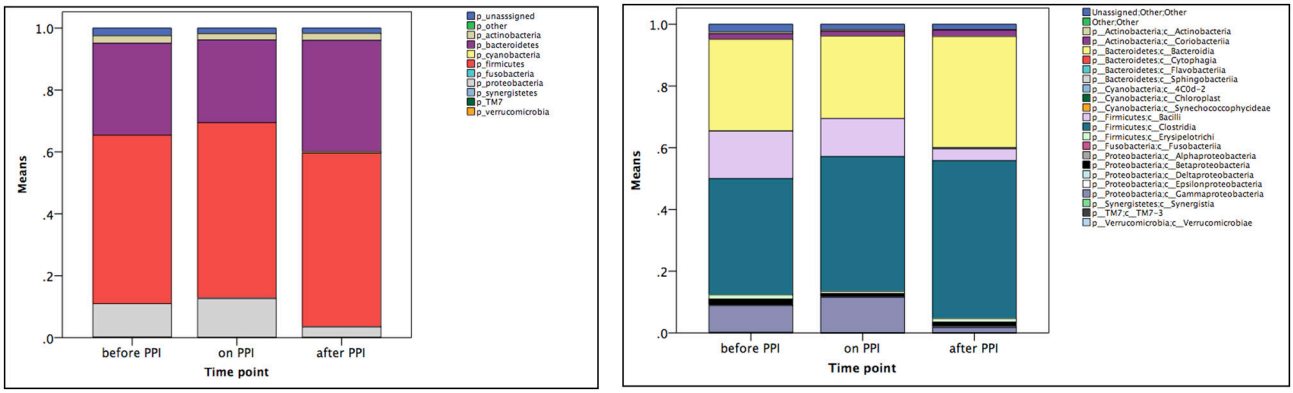

FIGURE 2 | Mean taxa summary plots at the phylum (left panel) and class (right panel) level at the three different time points measured ($n = 12$ per time point).

PPI" and $p = 0.003$ for the comparison "*on PPI*" and "*after PPI*"). Furthermore, the β-diversity significantly changed throughout the experiment ($p = 0.003$ comparing "*before PPI*" and "*after PPI*" and $p = 0.001$ comparing "*on PPI*" and "*after PPI*"). For the relative abundances the majority of changes was also seen in comparison to the third sample and occurred in the Firmicutes phylum (**Table 3**). A correlation was found between these microbial changes and the patients' age ($p = 0.062$) and nutrition ($p = 0.001$).

DISCUSSION

This study is the first to address fecal microbial changes under PPI treatment in infants. In contrast to most studies reported in adults GERD was not only suspected in our patients, but proven by impedance monitoring prior to enrollment and PPI therapy. Notably, we were able to find a completely different response to PPIs in infants than previously described in adults.

Up to now the majority of studies investigating the effect of PPI on gut microbiota have compared adult PPI users to non-users. Two large series have reported significant decreases of the overall fecal microbial diversity under PPI treatment (Imhann et al., 2016; Jackson et al., 2016). However, to assess the exact effect of PPIs on individuals a longitudinal investigation of the same patients on and off PPI is required. Presently there is only one study in 12 adults which has addressed this issue reporting no significant changes of the fecal microbial diversity (Freedberg et al., 2015b). Similarly, our investigation with the same sample size in infants showed no significant changes of α- and β-diversity under PPI treatment.

Regarding relative bacterial abundances under PPI several reports with varying findings in adult patients have been published. Overall, *Streptococcus*, *Enterococcus,* and *Clostridiales* were most commonly affected in this population. Imhan et al., for instance, have described significant increases of *Enterococcus*, *Streptococcus,* and *E. coli* under PPI therapy (Imhann et al., 2016). Another group has found increased abundances of *Streptococcaceae*, *Lactobacillaceae*, *Pasteurellaceae*, *Corynebacteriaceae,* and *Micrococcaceae* (amongst others) and decreases of *Lachnospiraceae*, *Ruminococcaceae,* and *Erysipelotrichaceae (Jackson et al., 2016)*. Furthermore, an observation of fecal samples of long-term PPI users has revealed an increase of *Lachnospiraceae*, *Erysipelotrichaceae,* and *Streptococcaceae (Clooney et al., 2016)*. In contrast to adults our investigation in infants revealed only minor changes of the relative microbial abundances under PPI therapy.

In adults, an increased risk of *Clostridium difficile* infections (CDI) under PPI therapy has been postulated. In detail, increases of *Enterococcae* and *Streptococcae* combined with decreases of *Clostridiales* were reported in association with an increased risk of CDI (Freedberg et al., 2015b). Similarly, recent pediatric studies have reported an increased risk of CDI under acid suppression therapy (Brown et al., 2015). First reports about associations between PPI and CDI infections in infants (Freedberg et al., 2015a) rely on culture-based retrospective investigations only. In our series we have found a non-significant increase of *Streptococcus* and *Clostridiaceae* under PPI treatment (compare **Figure 3**). These results further fuel recent controversial discussions regarding the association between CDI and PPI (Leffler and Lamont, 2015; Faleck et al., 2016).

The majority of changes in our series were seen when comparing the microbiome between "*before PPI*" and "*on PPI*" to "*after PPI.*" While we cannot rule out the possibility that the removal of PPI treatment may cause a temporary flux in diversity, other studies showing an increasing diversity with increasing infants' age (Hill et al., 2017) support the physiological development of the intestinal microbiome as the underlying reason for this finding. Additionally, the correlation between the relative abundances and patients' age/nutrition also suggests the developing microbiome of infants as the most likely cause for these alterations.

One possible limitation of the present study includes the lack of a control group without PPI treatment. However, recent investigations of the developing microbiome have shown a marked variability and heterogeneity of the fecal microbiome within the first years of life (Palmer et al., 2007; Yatsunenko et al., 2012). This makes the selection of infants for a representative

TABLE 3 | Mean relative abundances (RA) at the different levels.

Phylum	Class	Order	Family	Genus	Before PPI	On PPI	After PPI
Firmicutes					0.544	0.565	0.551
	Clostridia	*Clostridiales*	*Ruminococcaceae*		0.040	0.044	$0.095^{*\#}$
				Oscillospira	3.1×10^{-3}	1.7×10^{-3}	$6.4 \times 10^{-3*\#}$
				Faecalibacterium	3.3×10^{-3}	3.7×10^{-3}	9.2×10^{-3}
				Ruminococcus	2.9×10^{-3}	2.1×10^{-3}	$5.1 \times 10^{-3*\#}$
			Veillonellaceae		0.128	0.107	$0.056^{*\#}$
				Veilonella	0.119	0.096	$0.026^{*\#}$
				Phascolarctobacterium	0	3.7×10^{-7}	$9.3 \times 10^{-3*}$
			Lachnospiraceae		0.115	0.158	0.249^{*}
				Lachnospira	4.3×10^{-3}	0.016	$0.018^{*\#}$
				Blautia	0.015	0.017	$0.036^{*\#}$
				Coprococcus	6.8×10^{-3}	7.5×10^{-3}	$0.022^{*\#}$
				Dorea	4.8×10^{-4}	1.3×10^{-4}	$1.3 \times 10^{-3*\#}$
				Anaerostiges	7.2×10^{-5}	0	0
	Bacilli	*Lactobacillales*	*Lactobacillaceae*	*Lactobacillus*	2.6×10^{-4}	$2.9 \times 10^{-5*}$	$3.4 \times 10^{-5*}$
	Erysipelotrichi	*Erysipelotrichales*	*Erysipelotrichaceae*	*Eubacterium*	2.6×10^{-3}	5.5×10^{-4}	$3.7 \times 10^{-3*\#}$
				Coprobacillus	3.2×10^{-5}	1.2×10^{-4}	$1.8 \times 10^{-3*\#}$
Bacteroidetes					0.302	0.272	0.376
	Bacteroidea	*Bacteroidales*	*Rikenellaceae*	*Bacteroides*	6.3×10^{-5}	4.8×10^{-5}	$0.010^{\#}$
Proteobacteria					0.11	0.13	0.03^{*}
	Gammaproteobacteria				0.087	0.117	$0.017^{*\#}$
		Enterobacteriales	*Enterobacteriaceae*	*Escherichia*	0.086	0.110	$0.017^{*\#}$
		Xanthomonadales	*Xanthomonadaceae*	*Stenotrophomonas*	5.1×10^{-5}	$1.6 \times 10^{-6*}$	$1.6 \times 10^{-6*\#}$
		Pasteurellales	*Pasteurellaceae*	*Haemophilus*	0	$2.3 \times 10^{-5*}$	1.8×10^{-6}
Acinetobacteria					0.024	0.020	0.023
	Coriobacteria	*Coriobacteriales*	*Coriobacteriaceae*	*Adlercreutzia*	0	0	3.7×10^{-5}
Cyanobacteria					2.2×10^{-5}	3.1×10^{-6}	3.8×10^{-3}
Verrucomicrobia					1.7×10^{-3}	0	4.9×10^{-4}
Fusobacteria					5.4×10^{-4}	1.5×10^{-3}	4.1×10^{-4}
TM7					2.3×10^{-5}	4.5×10^{-5}	7.0×10^{-5}

*$p < 0.05$ vs. "before PPI"; $^{\#}p < 0.05$ vs. "on PPI." Significant increases under PPI therapy are colored in blue, significant decreases in red.

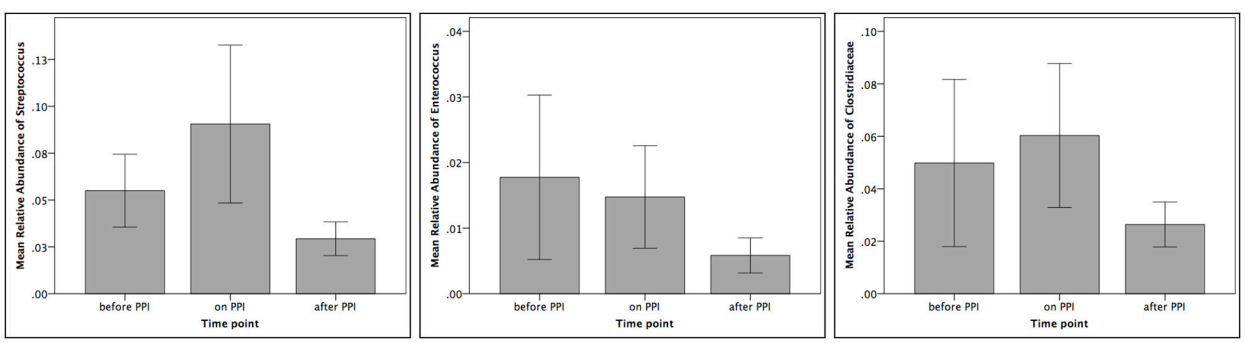

FIGURE 3 | Relative abundances of *Streptococcus*, *Enterococcus* and *Clostridiaceae* at the three different time points tested ($n = 12$ per time point).

and comparable control group difficult. In accordance to the literature we have found a constant increase of α-diversity in our samples (Palmer et al., 2007). This further substantiates the developing microbiome as a reason for the changes encountered in the third sample of this series. In our longitudinal intra-individual comparison, the same patient is investigated on and off PPI and thus serves as his/her own control. Another limitation is the relatively small number of included infants. However, the sample size resembles that of the only longitudinal study in adult patients (Freedberg et al., 2015b). Our setting also takes care of the heterogeneity of the microbiome in infants and the different age of our patients upon inclusion because the patients are compared by dependent tests within themselves (intra-individual).

Finally, we have only measured the fecal microbiome and could not include samples from other parts of the gastrointestinal (GI) tract. The fecal microbiome is easily accessible and the obtained results can be compared to adult studies (Freedberg et al., 2015b; Clooney et al., 2016; Imhann et al., 2016; Jackson et al., 2016). However, the fecal microbiome does not necessarily represent the whole GI-tract (Haange et al., 2012) and possible alterations of the microbial diversity of the upper GI-tract under PPI treatment are subject for further investigations.

Since we were not able to demonstrate any relevant changes under PPI therapy one might question whether a PPI dosage of 1 mg/kg/day esomeprazole was sufficient. Theoretically, our findings could be caused by inadequate acid suppression. Although we did not repeat impedance monitoring "*on PPI*" we could demonstrate that our institutional protocol and PPI dosage was effective in a previous examination (Castellani et al., 2014). Additionally, the symptoms caused by the GERD resolved in all our patients under PPI therapy suggesting adequate acid suppression.

In conclusion, oral PPI therapy did not have relevant impact on the development of the infant fecal microbiome at a sensitive time of life in our series. Microbial changes associated with an increased risk of CDI infection described in adults did not reach statistical significance in this study. The majority of alterations occurred through the course of time and is correlated to patients' age and nutrition representing the normal development of the microbiome. Future studies are required to investigate possible microbial changes of the upper GI-tract under PPI treatment.

AUTHOR CONTRIBUTIONS

CC and GS performed the statistics and wrote the manuscript; KK performed the microbiome analysis and performed the biostatistics; AH recruited the patients and collected the samples; CF and MK analyzed the data and assisted to draft the manuscript; HT coordinated the project and critically reviewed the manuscript.

REFERENCES

Amir, I., Konikoff, F. M., Oppenheim, M., Gophna, U., and Half, E. E. (2014). Gastric microbiota is altered in oesophagitis and Barrett's oesophagus and further modified by proton pump inhibitors. *Environ. Microbiol.* 16, 2905–2914. doi: 10.1111/1462-2920.12285

Bouwknegt, M., Van Pelt, W., Kubbinga, M. E., Weda, M., and Havelaar, A. H. (2014). Potential association between the recent increase in campylobacteriosis incidence in the Netherlands and proton-pump inhibitor use - an ecological study. *Euro Surveill.* 19:20873. doi: 10.2807/1560-7917.ES2014.19.32.20873

Brown, K. E., Knoderer, C. A., Nichols, K. R., and Crumby, A. S. (2015). Acid-suppressing agents and risk for *Clostridium difficile* infection in pediatric patients. *Clin. Pediatr. (Phila).* 54, 1102–1106. doi: 10.1177/0009922815569201

Castellani, C., Huber-Zeyringer, A., Bachmaier, G., Saxena, A. K., and Hollwarth, M. E. (2014). Proton pump inhibitors for reflux therapy in infants: effectiveness determined by impedance pH monitoring. *Pediatr. Surg. Int.* 30, 381–385. doi: 10.1007/s00383-013-3458-6

Clooney, A. G., Bernstein, C. N., Leslie, W. D., Vagianos, K., Sargent, M., Laserna-Mendieta, E. J., et al. (2016). A comparison of the gut microbiome between long-term users and non-users of proton pump inhibitors. *Aliment. Pharmacol. Ther.* 43, 974–984. doi: 10.1111/apt.13568

Colletti, R. B., and Di Lorenzo, C. (2003). Overview of pediatric gastroesophageal reflux disease and proton pump inhibitor therapy. *J. Pediatr. Gastroenterol. Nutr.* 37(Suppl. 1), S7–S11. doi: 10.1097/00005176-200311001-00003

Eckburg, P. B., Bik, E. M., Bernstein, C. N., Purdom, E., Dethlefsen, L., Sargent, M., et al. (2005). Diversity of the human intestinal microbial flora. *Science* 308, 1635–1638. doi: 10.1126/science.1110591

Faleck, D. M., Salmasian, H., Furuya, E. Y., Larson, E. L., Abrams, J. A., and Freedberg, D. E. (2016). Proton pump inhibitors do not increase risk for *Clostridium difficile* infection in the intensive care unit. *Am. J. Gastroenterol.* 111, 1641–1648. doi: 10.1038/ajg.2016.343

Freedberg, D. E., Lamouse-Smith, E. S., Lightdale, J. R., Jin, Z., Yang, Y. X., and Abrams, J. A. (2015a). Use of acid suppression medication is associated with risk for c. difficile infection in infants and children: a population-based study. *Clin. Infect. Dis.* 61, 912–917. doi: 10.1093/cid/civ432

Freedberg, D. E., Toussaint, N. C., Chen, S. P., Ratner, A. J., Whittier, S., Wang, T. C., et al. (2015b). Proton pump inhibitors alter specific taxa in the human gastrointestinal microbiome: a crossover trial. *Gastroenterology* 149, 883–885.e9. doi: 10.1053/j.gastro.2015.06.043

Haange, S. B., Oberbach, A., Schlichting, N., Hugenholtz, F., Smidt, H., Von Bergen, M., et al. (2012). Metaproteome analysis and molecular genetics of rat intestinal microbiota reveals section and localization resolved species distribution and enzymatic functionalities. *J. Proteome Res.* 11, 5406–5417. doi: 10.1021/pr3006364

Hill, C. J., Lynch, D. B., Murphy, K., Ulaszewska, M., Jeffery, I. B., O'shea, C. A., et al. (2017). Evolution of gut microbiota composition from birth to 24 weeks in the INFANTMET Cohort. *Microbiome* 5:4. doi: 10.1186/s40168-016-0213-y

Hollwarth, M. (2012). "Gastroesophageal Reflux Disease," in *Pediatric Surgery*, eds A. G. Coran, N. S. Adzick, T. M. Krummel, J. M. Laberge, R. Shamberger and A. Caldamone (Philadelphia, PA: Saunders), 947–958.

Imhann, F., Bonder, M. J., Vich Vila, A., Fu, J., Mujagic, Z., Vork, L., et al. (2016). Proton pump inhibitors affect the gut microbiome. *Gut* 65, 740–748. doi: 10.1136/gutjnl-2015-310376

Jackson, M. A., Goodrich, J. K., Maxan, M. E., Freedberg, D. E., Abrams, J. A., Poole, A. C., et al. (2016). Proton pump inhibitors alter the composition of the gut microbiota. *Gut* 65, 749–756. doi: 10.1136/gutjnl-2015-310861

Janarthanan, S., Ditah, I., Adler, D. G., and Ehrinpreis, M. N. (2012). *Clostridium difficile*-associated diarrhea and proton pump inhibitor therapy: a meta-analysis. *Am. J. Gastroenterol.* 107, 1001–1010. doi: 10.1038/ajg.2012.179

Klymiuk, I., Bambach, I., Patra, V., Trajanoski, S., and Wolf, P. (2016). 16S based microbiome analysis from healthy subjects' skin swabs stored for different storage periods reveal phylum to genus level changes. *Front. Microbiol.* 7:2012. doi: 10.3389/fmicb.2016.02012

Leffler, D. A., and Lamont, J. T. (2015). *Clostridium difficile* Infection. *N. Engl. J. Med.* 373, 287–288. doi: 10.1056/NEJMra1403772

McDonald, E. G., Milligan, J., Frenette, C., and Lee, T. C. (2015). Continuous proton pump inhibitor therapy and the associated risk of recurrent *Clostridium difficile* infection. *JAMA Intern. Med.* 175, 784–791. doi: 10.1001/jamainternmed.2015.42

Palmer, C., Bik, E. M., Digiulio, D. B., Relman, D. A., and Brown, P. O. (2007). Development of the human infant intestinal microbiota. *PLoS Biol.* 5:e177. doi: 10.1371/journal.pbio.0050177

Rudolph, C. D., Mazur, L. J., Liptak, G. S., Baker, R. D., Boyle, J. T., Colletti, R. B., et al. (2001). Guidelines for evaluation and treatment of gastroesophageal reflux in infants and children: recommendations of the North American Society for Pediatric Gastroenterology and Nutrition. *J. Pediatr. Gastroenterol. Nutr.* 32(Suppl. 2), S1–31. doi: 10.1097/00005176-200100002-00001

Segata, N., Izard, J., Waldron, L., Gevers, D., Miropolsky, L., Garrett, W. S., et al. (2011). Metagenomic biomarker discovery and explanation. *Genome Biol.* 12:R60. doi: 10.1186/gb-2011-12-6-r60

Vandenplas, Y., Salvatore, S., Devreker, T., and Hauser, B. (2007). Gastro-oesophageal reflux disease: oesophageal impedance versus pH monitoring. *Acta Paediatr.* 96, 956–962. doi: 10.1111/j.1651-2227.2007.00306.x

Vesper, B. J., Jawdi, A., Altman, K. W., Haines, G. K. III., Tao, L., and Radosevich, J. A. (2009). The effect of proton pump inhibitors on the human microbiota. *Curr. Drug Metab.* 10, 84–89. doi: 10.2174/138920009787048392

Yatsunenko, T., Rey, F. E., Manary, M. J., Trehan, I., Dominguez-Bello, M. G., Contreras, M., et al. (2012). Human gut microbiome viewed across age and geography. *Nature* 486, 222–227. doi: 10.1038/nature 11053

Conflict of Interest Statement: The authors declare that the research was conducted in the absence of any commercial or financial relationships that could be construed as a potential conflict of interest.

Copyright © 2017 Castellani, Singer, Kashofer, Huber-Zeyringer, Flucher, Kaiser and Till. This is an open-access article distributed under the terms of the Creative Commons Attribution License (CC BY). The use, distribution or reproduction in other forums is permitted, provided the original author(s) or licensor are credited and that the original publication in this journal is cited, in accordance with accepted academic practice. No use, distribution or reproduction is permitted which does not comply with these terms.

frontiers in Cellular and Infection Microbiology

ORIGINAL RESEARCH
published: 21 September 2017
doi: 10.3389/fcimb.2017.00417

Helicobacter pylori CagA Protein Negatively Regulates Autophagy and Promotes Inflammatory Response via c-Met-PI3K/Akt-mTOR Signaling Pathway

Na Li[1,2,3†], Bin Tang[1,2,4†], Yin-ping Jia[1], Pan Zhu[1], Yuan Zhuang[2], Yao Fang[1,2], Qian Li[1], Kun Wang[1,2], Wei-jun Zhang[2], Gang Guo[2], Tong-jian Wang[3], You-jun Feng[5], Bin Qiao[3], Xu-hu Mao[1]* and Quan-ming Zou[2]**

[1] Department of Clinical Microbiology and Immunology, Southwest Hospital & College of Medical Laboratory Science, Third Military Medical University, Chongqing, China, [2] Department of Microbiology and Biochemical Pharmacy, National Engineering Research Center for Immunobiological Products, College of Pharmacy, Third Military Medical University, Chongqing, China, [3] Institute of Cardiovascular Disease, General Hospital of Jinan Military Region, Jinan, China, [4] Emei Sanatorium of PLA Rocket Force, Emeishan, China, [5] Department of Medical Microbiology and Parasitology, Zhejiang University School of Medicine, Hangzhou, China

OPEN ACCESS

Edited by:
Pascale Alard,
University of Louisville, United States

Reviewed by:
Mario M. D'Elios,
University of Florence, Italy
Nagendran Tharmalingam,
Brown University, United States

***Correspondence:**
Bin Qiao
cijnmd@126.com
Xu-hu Mao
mxh95xy@tom.com
Quan-ming Zou
qmzou2007@163.com

† These authors have contributed equally to this work.

Received: *23 July 2017*
Accepted: *08 September 2017*
Published: *21 September 2017*

Citation:
Li N, Tang B, Jia Y, Zhu P, Zhuang Y, Fang Y, Li Q, Wang K, Zhang W, Guo G, Wang T, Feng Y, Qiao B, Mao X and Zou Q (2017) Helicobacter pylori CagA Protein Negatively Regulates Autophagy and Promotes Inflammatory Response via c-Met-PI3K/Akt-mTOR Signaling Pathway. Front. Cell. Infect. Microbiol. 7:417. doi: 10.3389/fcimb.2017.00417

Cytotoxin-associated-gene A (CagA) of *Helicobacter pylori* (*H. pylori*) is a virulence factor that plays critical roles in *H. pylori*-induced gastric inflammation. In the present study, gastric biopsies were used for genotyping *cagA* and *vacA* genes, determining the autophagic activity, and the severity of gastric inflammation response. It was revealed that autophagy in gastric mucosal tissues infected with *cagA*$^+$ *H. pylori* strains was lower than the levels produced by *cagA*$^-$ *H. pylori* strains, accompanied with accumulation of SQSTM1 and decreased LAMP1 expression. *In vitro,* deletion mutant of *cagA* gene resulted in increased autophagic activity, and decreased expression of SQSTM1 and cytokines, whereas over-expression of CagA down-regulated the starvation-induced autophagy, and induced more production of the cytokines. Moreover, the production of the cytokines was increased by inhibition of autophagy, but decreased by enhancement of autophagy. Deletion of CagA decreased the ability to activate Akt kinase at Ser-473 site and increased autophagy. c-Met siRNA significantly affected CagA-mediated autophagy, and decreased the level of p-Akt, p-mTOR, and p-S6. Both c-Met siRNA and MK-2206 could reverse inflammatory response. *H. pylori* CagA protein negatively regulates autophagy and promotes the inflammation in *H. pylori* infection, which is regulated by c-Met-PI3K/Akt-mTOR signaling pathway activation.

Keywords: ***Helicobacter pylori*, autophagy, CagA, c-Met, SQSTM1**

INTRODUCTION

Helicobacter pylori (H. pylori) is a Gram-negative bacterium causing gastritis, peptic ulcer disease and gastric adenocarcinoma (Suerbaum and Michetti, 2002). Although *H. pylori* could induce strong inflammation, it is not able to clear the bacterium, resulting in persistent infection. Cytotoxin-associated gene A (CagA), one of *H. pylori* virulence factors, is an effector secreted by the type IV secretion system into gastric epithelial cells, and undergoes tyrosine phosphorylation,

and activates a series of intracellular signal transduction reactions, resulting in severe tissue inflammation and damage (Gunn et al., 1998). Generally, *H. pylori* strains expressing CagA protein is more virulent, and leading to severe gastritis (Fischer et al., 2001). CagA is able to activate the transcription factor, NF-κB, and translocate it into the nucleus, where it up-regulates transcription of interlukin-8 (IL-8), a chemotactic and inflammatory cytokine (Brandt et al., 2005). However, the specific mechanism that CagA-positive strains induce inflammation remains unclear.

Macroautophagy (hereafter autophagy) has an important role in controlling intracellular environment. The damaged cell organelles, proteins, or invading microorganisms are sequestered into autophagosomes, and finally delivered into autolysosomes for degradation (Shintani and Klionsky, 2004). In the case of infection of pathogenic microorganism, the final consequence of the infection was decided by the evolving struggle between the host cells and invading microbes, and autophagy plays a critical role in the struggle. A number of important pathogens could be degraded by autolysosomes, such as, *Listeria monocytogenes* (Py et al., 2007), group A Streptococcus (Nakagawa et al., 2004), and *Francisella tularensis* (Cremer et al., 2009). However, some pathogenic bacteria also develop some mechanisms to subvert autophagy to survive in cells, eventually leading to the occurrence of various diseases, such as, Shigella (Kayath et al., 2010) and *Mycobacterium tuberculosis* (Shin et al., 2010).

It has been demonstrated that the induction of autophagosome formation or autophagy depends on the vacuolating cytotoxin (VacA), which is another virulent factor of *H. pylori* (Terebiznik et al., 2009). In turn, autophagy can eliminate intracellular *H. pylori* and may decrease the stability of intracellular VacA and ameliorate toxin-mediated cellular vacuolation (Terebiznik et al., 2009), despite the fact that autophagy is not sufficient to block vacuole biogenesis and pathogenesis (Zavros and Rogler, 2012). Recently, Tsugawa et al. showed that intracellular CagA is degraded by autophagy and short lived in AGS cells (Tsugawa et al., 2012), but whether or not autophagy regulated by CagA in *H. pylori*-induced gastric inflammation have never been explored.

Therefore, the purpose of this article was to determine the effect of CagA on autophagy of gastric epithelial cells and the production of autophagy-regulated proinflammatory cytokines in *H. pylori* infection.

MATERIALS AND METHODS

Patients and Specimens

Consecutive patients who underwent upper endoscopy due to dyspeptic symptoms at Southwest Hospital, Chongqing, China during January 2013 and December 2014, were recruited. One hundred and six (49 women and 57 men with age of 43 ± 20 years) patients were eligible for enrollment into the *H. pylori* positive group if they had a positive [^{13}C] urea breath test, a positive rapid urease test, and *H. pylori* culture. Eleven (six women and five men with age of 35 ± 20 years) with normal gastric mucosa were eligible for enrollment into the *H. pylori* negative group, and the clinical characteristics are shown in Supplementary Table 2. The study was approved by the Institutional Review Board at Third Military Medical University, and all patients signed informed consent before participation. All experiments were performed in accordance with relevant guidelines and regulations.

H. pylori was successfully isolated from 106 patients, and genotyping for *cagA* and *vacA* was performed for 106 isolates. All *H. pylori* strains carry the *vacA* gene. To exclude the effect of VacA, the toxigenic vacA genotype ($vacA^{s1m1}$, 42 cases), expressing a functional VacA toxic, were excluded from the study. The rest of the cases include: normal control (11 cases), $cagA^{-}/vacA^{s1m2}$ (7 cases), $cagA^{+}/vacA^{s1m2}$ (57 cases). To ensure that approximately equal numbers of each group, 23 selective patients were chosen randomly for analyzing autophagy and inflammation, dividing into normal control (8 cases), $cagA^{-}/vacA^{s1m2}$ (7 cases), $cagA^{+}/vacA^{s1m2}$ (8 cases).

Evaluation of Inflammation Score for Gastric Biopsy Samples

The selected gastric biopsy samples among the genotype subgroups were obtained to perform H&E staining. The intensity of inflammation was evaluated independently by two pathologists according to previously established criteria. The degree of neutrophil infiltration, mononuclear cell infiltration, atrophy, and metaplasia was assessed according to the updated Sydney classification as follows: 0, absent; 1, minimal; 2, mild; 3, moderate; 4, marked. So the biopsies were from different stages of gastritis (Dixon et al., 1996).

Genotyping for cagA and vacA Genes

H. pylori infection status was detected by rapid urease test, bacterial culture, ^{13}C-urea breath test, and histological examination (Vaira et al., 1999). In patients with positive culture, *H. pylori* isolates were subcultured for a maximum of five passages, and genomic DNA was extracted to genotype for the *cagA* and *vacA* genes, as previously described (Argent et al., 2008). The primers used for PCR amplification and nucleotide sequencing are listed in Supplementary Table 1.

Cell Line and *H. pylori* Strains

AGS (a human gastric cancer cell line) purchased from the cell bank of Chinese Academy of Sciences, were cultured in F12 cell culture medium (Gibco, Grand Island, NY, USA, #11765-054) supplemented with 10% FBS (Gibco, #10099-141) in a humidified incubator (5% CO_2) at 37°C. The starvation condition was established by culturing the cells with serum-free medium for 4 h.

The wide-type $cagA^{+}/vacA^{+}$ *H. pylori* strain, NCTC11637 (*Hp*-WT, obtained from ATCC), *cagA*-knockout *H. pylori* with NCTC11637 background (*Hp*-Δ*cagA*, kindly provided by Dr. Sasakawa (Asahi et al., 2000; Suzuki et al., 2009) and *H. pylori cagA*-knockout complementation mutant (*Hp-c-cagA,* constructed by our group), were cultured on brain-heart infusion medium (10% rabbit blood) under microaerophilic conditions (5% O_2, 10% CO_2, and 85% N_2) at 37°C. *Hp-c-cagA* mutant was obtained by amplifying the cDNA fragments of *cagA* gene from the gene of NCTC11637 by polymerase chain reaction

(PCR), and the primers of PCR is following: forward: 5′-GCGCTCGAGATGACTAACGAACC-3′; reverse: 5′-GCGCTGCAGTTAAGATTTTTGG-3′. The product of PCR was digested with *Xho*I and *Pst*I, and then ligating the cDNA fragments of *cagA* gene between *cagA*-upstream and -downstream sequences cloned on the pHel3 shuttle vector. The pHel3 shuttle vector with *cagA* gene was electroporated into *Hp*-Δ*cagA* cells carrying the kanamycin resistance. *Hp-c-cagA* clones were cultured in brain-heart infusion medium as previous described.

AGS cells transfected with plasmids and/or siRNAs were infected with *Hp*-WT, *Hp*-Δ*cagA,* or *Hp-c-cagA,* respectively, with different multiplicity of infection (MOI = 10, 50, 100, 200), for 6 h. Cells without infection served as controls.

Reagents and Antibodies

Rapamycin (Rapa, R8781), 3-methyladenine (3-MA, M9281), bafilomycin A1 (Baf-A1, B1793), antibodies against ATG12 (WH0009140M1), MAP1LC3B (L7543), and ATG5 (WH0009474M1) were purchased from Sigma-Aldrich (Shanghai, CHINA), and MK-2206 2HCL (S1078) purchased from Selleckchem (Houston, TX, USA). Antibodies against Akt (9272), mTOR (2972), AMPK (2532), phospho-Akt (Ser473) (4060), LAMP1 (9091), phospho-mTOR (Ser2448) (5536), phospho-S6 ribosomal protein (Ser235/236) (2211), ribosomal protein (2217), phospho-c-Met (Y1234/Y1235) (4033), and c-Met (4560) were obtained from Cell Signaling Technology (Beverly, MA, USA), whereas antibodies against β-actin (sc-10731), VacA (sc-25790), CagA (sc-17450), phospho-tyrosine (PY99) (sc-7020) and SQSTM1 (sc-28359), and siRNAs specific for SQSTM1 (human, sc-29679), ATG12 (human, sc-72578), c-Met (human, sc-29397), and ATG5 (human, sc-41445), along with a control siRNA (sc-44230) were obtained from Santa Cruz Biotechnology (CA, USA).

Immunohistochemistry for SQSTM1

Gastric biopsy sections from patients infected with different genotypes of *H. pylori* were stained using SQSTM1 antibody (Enzo Life Sciences, BML-PW9860-0025) by the DAB reagent technique. SQSTM1 staining was assessed by three pathologists with no prior knowledge of the different groups, and scored as 0 (no staining), 1 (<10% of SQSTM1 staining), 2 (10–50% of SQSTM1 staining), or 3 (>50% of SQSTM1 staining).

Western Blotting, Quantitative RT-PCR, NF-κB Activity, and ELISA

The protein level of SQSTM1, LAMP1, phospho-mTOR (Ser2448), MAP1LC3B, ATG12, ATG5, AMPK, phospho-Akt (Ser473), Akt, mTOR, ribosomal protein, phospho-c-Met (Y1234/Y1235), c-Met, phospho-S6 ribosomal protein (Ser235/236), VacA, CagA, and phospho-tyrosine (PY99) were performed to determine by Western blotting in gastric tissues or AGS cells as described previously (Tang et al., 2015).

Trizol reagent (Invitrogen, 15596-026) was used to extract total RNA from gastric biopsy sections. qRT-PCR analysis of gastric biopsy sections from patients for the mRNA of *SQSTM1*, *BECN1*, *IL-8*, *TNF-α, β-actin,* and *IL-1β* were performed by using PrimeScript RT-PCR kits (Takara, Tokyo, Japan, DRR037), and run on a Bio-Rad IQ5 thermocycler (Bio-Rad Laboratories, Inc., Hercules, USA), *β-actin* as an internal control. The conditions for PCR were as follows: 1 cycle of 95°C for 30 s, 40 cycles of 95°C for 6 s, 60°C for 6 s, and 72°C for 31 s, and the primer sequences used are shown in Supplementary Table 1.

AGS cells were cotransfected with Renilla control vector (*pRL-TK*, Promega, #2241) and luciferase reporter vector *pNF-κB-TA-Luc* (Clontech, #631904) with lipofectamine 2000 (the ratio of 20:1) for 1 day, followed with *H. pylori* infection. The Dual-Luciferase Reporter Assay System (Promega, E1910) detected firefly luciferase activity and Renilla luciferase activity according to the manufacture's protocol.

The supernatant of AGS cells with different treatment were detected by DuoSet ELISA Development System (IL-8, IL-1β, and TNF-α; R&D, Minneapolis, USA) as our previous study (Tang et al., 2016).

Transfection of AGS With Plasmids and/or siRNAs

The *GFP-MAP1LC3B* plasmid and *RFP-MAP1LC3B* expression plasmid were kindly provided by Dr. Tamotsu Yoshimori (Department of Cell Biology, National Institute for Basic Biology, Presto, Japan) and Dr. Maria Colombo (Universidad Nacional de Cuyo, Mendoza, Argentina), respectively. The CagA expression plasmid, *pEGFP-C1-CagA* (*GFP-CagA*) (Asahi et al., 2000; Suzuki et al., 2009), was kindly provided by Dr. Chihiro Sasakawa. The *cagA* mutant plasmid, *pEGFP-C1-CagA-Mut* (*GFP-CagA-Mut*) was constructed by Life Technologies, Shanghai, China, and a series of CagA mutants with the Tyr residues of 899, 918, and 972 being substituted by Ala were generated from a plasmid-encoding fragment of *cagA* gene of *H. pylori* ATCC 26695 on pBluescript (Promega, Madison, USA) using a Gene Editor *in vitro* Site-Directed Mutagenesis System (Promega). These mutants were at the sites 2,695–2,697, 2,752–2,754, and 2,914–2,915 bp, respectively, started from the sequence ATG. Lipofectamine 2000 (Invitrogen, #11668019) was used to transfect plasmids and/or siRNAs into AGS cells. 3×10^6 AGS cells were seeded into a 100-mm dish and incubated with transfection complexes containing 100 nM siRNA for 24 h.

Immunoprecipitation Assays

AGS cells were harvested in RIPA buffer on crushed ice, and centrifuged at 6,000 rpm for 5 min, and commercial Lowry Assay (Bio-Rad DC) detected the concentration of protein. Five milligrams per milliliter of protein and 1 μg/μL anti-CagA (sc-17450, Santa Cruz Biotechnology) was incubated overnight at 4°C, then added 50 μL 50% protein A/G-sepharose bead suspension for 2 h, and washed three times with pre-cold RIPA buffer, and added 50 μL protein sample buffer to collect in each tube, and proteins detected by western blotting analysis.

Puncta Formation Assays

AGS cells were transfected with *GFP-MAP1LC3B* or *RFP-MAP1LC3B* plasmid for 24 h, following *H. pylori* infection for another 24 h. Radiance 2000 laser scanning confocal microscope detected the images of the cells, and image analysis with

LaserSharp 2000 software (Bio-Rad, San Francisco, CA) as our previous study (Tang et al., 2016). According to methods for monitoring GFP-LC3 and mRFP-GFP-LC3 puncta formation assays (Klionsky et al., 2007; Mizushima et al., 2010), the average number of MAP1LC3B puncta per cell in *GFP-MAP1LC3B* or *RFP-MAP1LC3B*-positive cells (200 cells per sample) was determined (Pattingre et al., 2005).

Cell Viability

AGS cell viability was assessed using an MTT assay (Sigma) according to the manufacturer's instructions. Five milligrams per liter of MTT was added to each wells of AGS cells for 1–2 h, and dissolved in MTT solubilization solution. The absorbance at 590 nm (A590) was determined for each well using a microplate reader (Bio-Rad). After subtracting the background absorbance, the A590 value of the treated cells was divided by that of the untreated cells to determine the percentage of viable cells.

MDC and AO Staining Assays

Monodansylcadaverine (MDC) and acridine orange (AO) staining was used to quantify the number of autolysosomes in AGS cells. Following treatment with *H. pylori* or transfection with plasmids/siRNAs, cells were stained with 10 mM MDC (sigma, 30432) and 1 mg/mL AO solution (sigma, A8097) at 37°C for 10 min, and fixed in 3% paraformaldehyde in PBS for 30 min. Photographs were obtained with a Radiance 2000 laser scanning confocal microscope (MDC, excitation wave length about 380 nm and emission filter 525 nm; AO, emission peak at 650 nm). The cells were then trypsinised and quantified by flow cytometry using a FACScan cytometer and CellQuest software (BD, New Jersey, USA). The percentage of cells with characteristic MDC or AO staining over the total cells was assessed.

Transmission Electron Microscopy

AGS cells or gastric biopsy sections were collected and fixed in 2% paraformaldehyde, 0.1% glutaraldehyde and 0.1 M sodium cacodylate buffer (pH 7.4) for 2 h, then post-fixed in 1% OsO4, 0.5% potassium ferricyanide in cacodylate buffer for 1.5 h, then dehydrated with graded alcohol, and embedded in straight resin. Ultrathin sections were counterstained with 0.3% lead citrate and detected by Philips EM420 electron microscope. The method of counting autophagosomes' numbers was followed as described previously by Yla-Anttila et al. (2009). Data obtained by scoring for the presence of autophagic vacuoles (autophagosomes, autolysosomes) profiles per cell profile on the sections, and a total of 35 cells were recorded for triplicate samples per condition per experiment.

Statistical Analyses

The Student *t*-test was used to analyze between two groups, and one-way analysis of variance (ANOVA) was used to analyze among multiple group data, and expressed as mean ± standard error (SEM). GraphPad Prism software (GraphPad, San Diego, CA) was used for all statistical analyses. For all inferential statistics a $P < 0.05$ was considered significant.

RESULTS

Autophagy Is Down-Regulated in Human Gastric Mucosa With CagA Positive *H. pylori*

The clinical characteristics of 117 patients with (106) and those without (11) *H. pylori* infection are shown in Supplementary Table 2. *H. pylori* was successfully isolated from 106 patients, and genotyping for *cagA* and *vacA*. All *H. pylori* strains carry the *vacA* gene. To exclude the effect of VacA, the toxigenic *vacA* genotype ($vacA^{s1m1}$), expressing a functional VacA toxic, were excluded from the study. In order to ensure that approximately equal numbers of each group, three equal groups were created for analyzing via random sampling methods, including normal control (8 cases), $cagA^{-}/vacA^{s1m2}$ (7 cases), $cagA^{+}/vacA^{s1m2}$ (8 cases).

To verify the effect of CagA in severe tissue inflammation, we evaluated the level of inflammation in gastric mucosa. Firstly, the degree of gastric inflammation was higher in patients infected with $cagA^{+}/vacA^{s1m2}$ strains than in those infected with $cagA^{-}/vacA^{s1m2}$ strains (**Figure 1A**). Notably, the mRNA levels of IL-8, TNF-α, and IL-1β in the gastric epithelial cells were significantly higher in patients infected with $cagA^{+}/vacA^{s1m2}$ strains than in patients without *H. pylori* infection or those infected with $cag^{-}/vacA^{s1m2}$ strains (**Figure 1B**).

Furthermore, we evaluate the autophagic activity in gastric mucosal tissues from patients infected with different genotypes *H. pylori*. The SQSTM1/p62 (sequestosome1) protein serves as a link between LC3 and ubiquitinated substrates (Wang et al., 2010). Dysfunctional autophagy could result in an accumulation of SQSTM1, which has been involved in promoting inflammation (Raju et al., 2012). Therefore, we detected the levels of SQSTM1 in human gastric biopsies. As shown in **Figure 2A**, accumulation of SQSTM1 in the gastric biospy with *H. pylori* infection was significantly higher than those uninfected normal control, and the accumulation of SQSTM1 was significantly higher in the gastric epithelium cells in patients infected with $cagA^{+}/vacA^{s1m2}$ strains than in those infected with $cagA^{-}/vacA^{s1m2}$ strains ($P < 0.001$) as determined by immunohistochemistry. Moreover, in patients infected with $cagA^{-}/vacA^{s1m2}$ strains, the ratio of microtubule-associated protein 1 light chain 3 beta-II (MAP1LC3B-II) to β-actin and the lysosomal-associated membrane protein 1 (LAMP1, the late endosomal lysosomal marker) protein levels was higher than that in patients infected with $cagA^{+}/vacA^{s1m2}$ strains, and the SQSTM1 protein levels increased in patients infected with CagA-positive *H. pylori* (**Figure 2B**). In addition, infection of $cagA^{+}/vacA^{s1m2}$ strains was significantly associated with increased levels of mRNA expression of SQSTM1 (Supplementary Figure 1A), but not of BECN1 (Supplementary Figure 1B). Furthermore, it was also revealed an increase in the number of autophagosomes in patients infected with $cagA^{-}/vacA^{s1m2}$ strains compared with that in $cagA^{+}/vacA^{s1m2}$ group in TEM analysis (**Figure 2C**). Both $cagA^{+}/vacA^{s1m2}$ and $cagA^{-}/vacA^{s1m2}$ groups displayed high autophagy activity than the normal control group. These findings indicate that *H. pylori* infection could induce inflammation response and autophagy activity in the gastric epithelium cells in

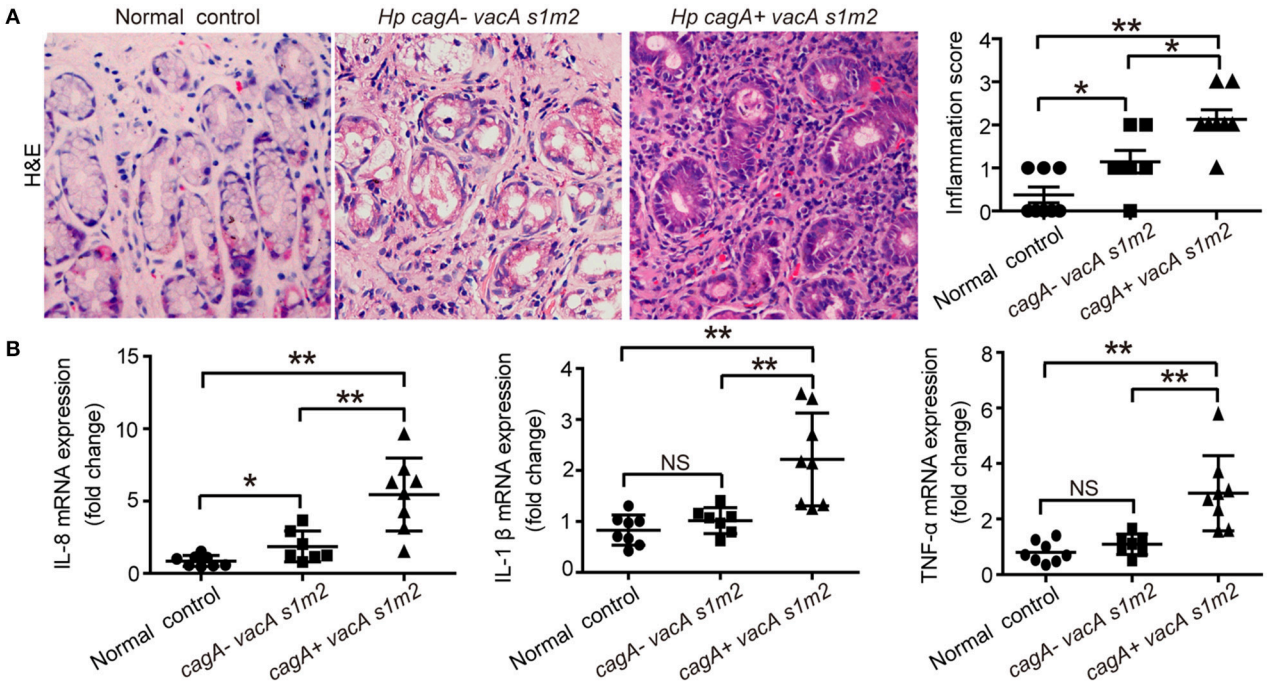

FIGURE 1 | The inflammatory response on gastric biopsies from patients infected with *cagA*$^{-}$/*vacA*^{s1m2} or *cagA*$^{+}$/*vacA*^{s1m2} strains of *H. pylori*. **(A)** Histological scores of inflammation (H&E staining) in the gastric mucosa of patients without *H. pylori* infection and those infected with *cagA*$^{-}$/*vacA*^{s1m2} or *cagA*$^{+}$/*vacA*^{s1m2} strains of *H. pylori*. The intensity of staining is shown in the right graph and the data are expressed as mean±SEM. **(B)** mRNA expression of proinflammatory cytokines in gastric mucosa of patients without *H. pylori* ($n = 8$), patients infected with *cagA*$^{-}$/*vacA*^{s1m2} ($n = 7$), and those infected with *cagA*$^{+}$/*vacA*^{s1m2} ($n = 8$). All real-time PCR data are normalized to β-actin and expressed as fold change. Experiments performed in triplicate showed consistent results. *$P < 0.05$, or **$P < 0.01$.

vivo, but CagA-positive *H. pylori* are associated with more severe inflammation, and down-regulates autophagic response *in vivo*.

CagA Could Inhibit the Generation of Autophagosomes in AGS Cells

To further validate the role of CagA in autophagy regulation, we next infected AGS cells with the *H. pylori* wide-type (*Hp*-WT), *H. pylori cagA*-knockout mutant (*Hp*-Δ*cagA*) or *H. pylori cagA*-knockout complementation (*Hp-c-cagA*) (MOI = 100:1), which strains the expression of VacA is similar during infection (Supplementary Figure 2A), and evaluated the kinetics of autophagosome formation by a *GFP-MAP1LC3B* puncta formation assay. Formation of MAP1LC3B puncta, peaked at 12 h and decreased at 24 h (**Figure 3A** and Supplementary Figure 2B). And compared with cells infected with *Hp*-WT or *Hp-c-cagA*, there was a significantly increased percentage of cells with formation of MAP1LC3B puncta for cells infected with *Hp*-Δ*cagA* (**Figure 3A**). TEM revealed an increase in the number of autophagic vacuoles (autophagosomes and autolysosomes) in AGS cells infected with *Hp*-Δ*cagA*-infected cells, compared with cells infected with *Hp*-WT or *Hp-c-cagA* (**Figure 3B**). Similar results were obtained in MDC (**Figure 3C** and Supplementary Figure 2D) and AO (**Figure 3D** and Supplementary Figure 2D) staining. Additionally, *Hp*-Δ*cagA* induced MAP1LC3B-II formation, and decreased SQSTM1 protein expression at a higher level, compared with *Hp*-WT or *Hp-c-cagA*, at 6, 12, and 24 h (**Figure 3E** and Supplementary Figure 2C). Furthermore, inhibition of autophagy by Baf-A1 challenge resulted in further accumulation of both MAP1LC3B-II and SQSTM1 in AGS cells after 6 h of *Hp*-WT or *Hp*-Δ*cagA* infection (**Figure 3F**), suggesting that *H. pylori* CagA did not inhibit the fusion of autophagosomes with lysosomes. Furthermore, under *Hp*-WT or *Hp*-Δ*cagA* infection, the levels of MAP1LC3B-II in AGS cells transfected with the CagA expression plasmid (*GFP-CagA)* were decreased in comparison to that in transfected-control cells (**Figure 3G**), suggesting that over-expression of CagA lead to further reduction of autophagic flux. Collectively, these data suggest that *H. pylori* CagA may inhibit the generation of autophagosomes in AGS cells.

CagA Down-Regulates Starvation-Induced Autophagy in AGS Cells

In order to eliminate the influence of *H. pylori* itself on autophagy, starvation-triggered autophagy was performed in AGS cells after transfecting the CagA expression plasmid (*GFP-CagA)* or tyrosine phosphorylation point mutant of CagA plasmid (*GFP-CagA-Mut*). At least 50% transfection efficiency was achieved for transfection of *GFP-CagA* and *GFP-CagA-Mut* in AGS (Supplementary Figure 3A). Although cell viability was influenced by starvation to a certain extent during the first 4 h, it appears not to be significantly influenced afterwards (Supplementary Figure 3B). During nutrient starvation, in the

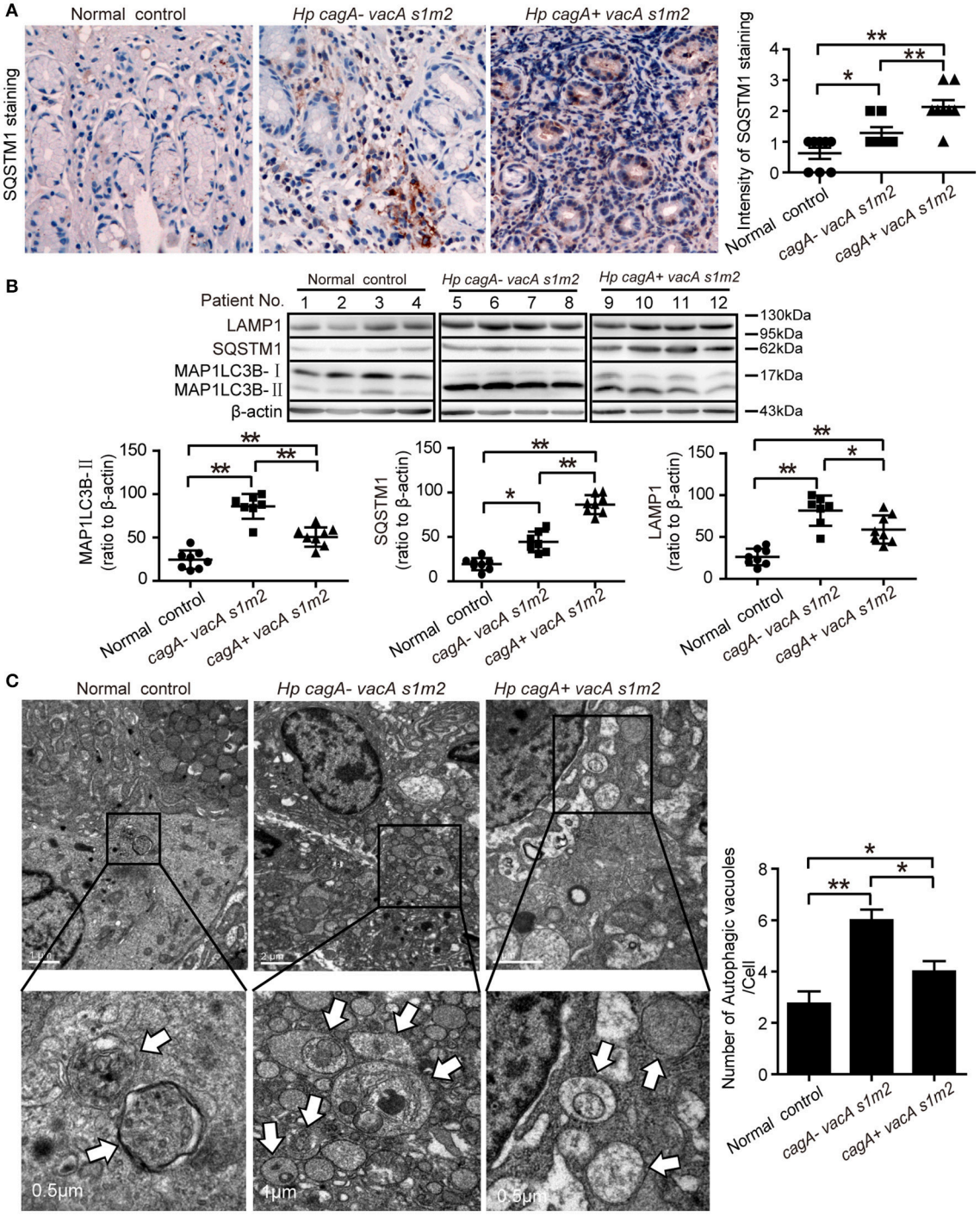

FIGURE 2 | Autophagy is down-regulated in human gastric mucosa of patients infected with CagA positive *H. pylori* strains. **(A)** Immunohistochemistry showing SQSTM1 expression in the gastric mucosa of patients without *H. pylori* infection and those infected with $cagA^{-}/vacA^{s1m2}$ or $cagA^{+}/vacA^{s1m2}$ strains of *H. pylori*. The intensity of staining is shown in the right graph and the data are expressed as mean ± SEM. **(B)** Western blot assay showing the protein levels of MAP1LC3B-II, SQSTM1 and LAMP1 in the gastric mucosa of patients of normal control (patients 1–4), $cagA^{-}/vacA^{s1m2}$(patients 5–8), and $cagA^{+}/vacA^{s1m2}$ (patients 9–12) with the rates to β-actin being illustrated in the graphs in which the data are expressed as mean ± SEM. **(C)** Transmission electron microscopy showing autophagosomes in gastric biopsy sections of patients without *H. pylori* infection and those infected with $cagA^{-}/vacA^{s1m2}$ or $cagA^{+}/vacA^{s1m2}$ strains of *H. pylori*. Normal controls are patients without *H. pylori* infection. The white arrows indicate the autophagosomes. The numbers of autophagic vacuoles per cell in each TEM section ($n = 35$ cells) are shown in the right graph and the data are expressed as mean ± SEM. Experiments performed in triplicate showed consistent results. $^{*}P < 0.05$, or $^{**}P < 0.01$.

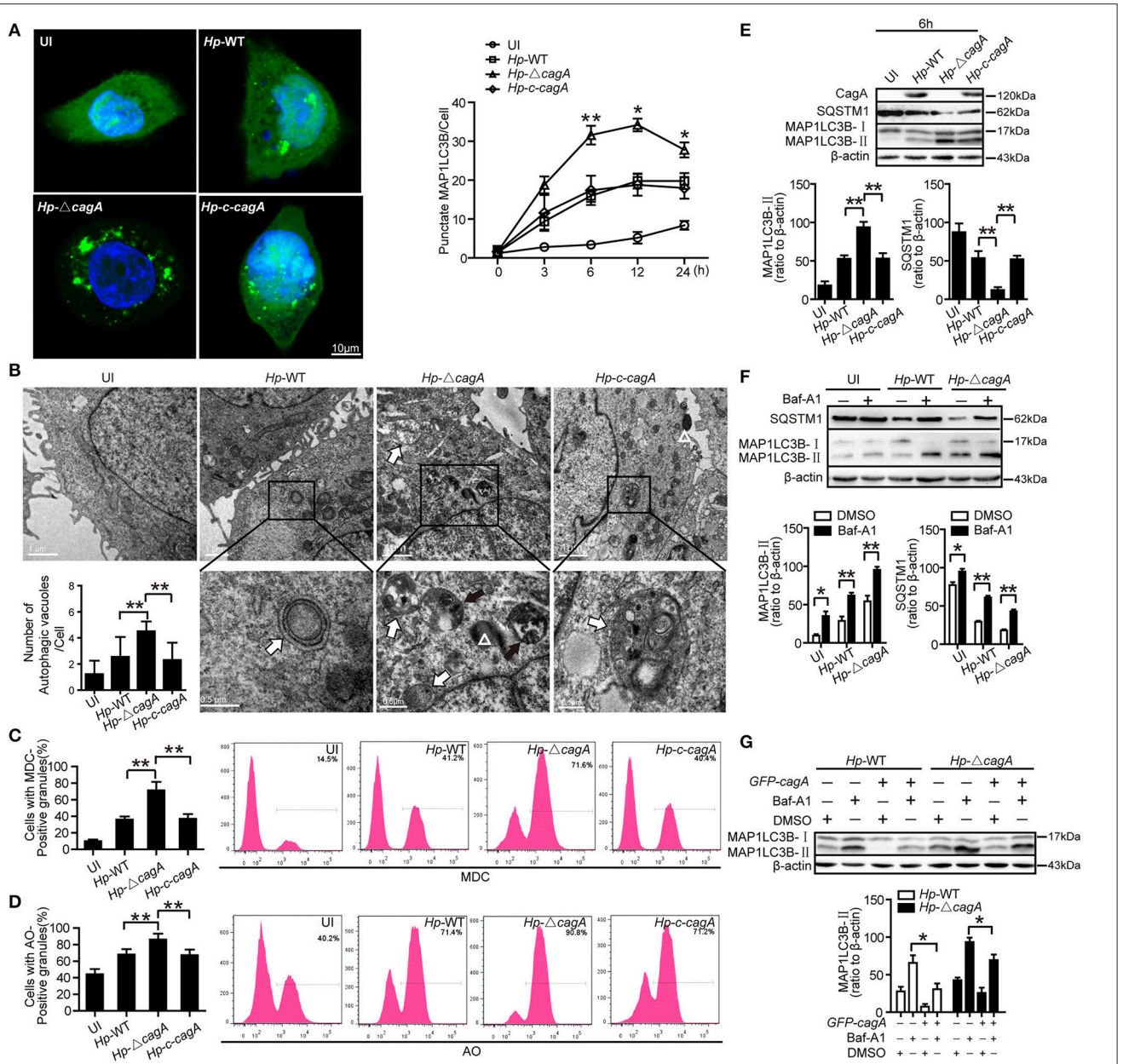

FIGURE 3 | CagA could inhibit the generation of autophagosomes in AGS cells. **(A)** Confocal microscopy showing AGS cells transfected with *GFP-MAP1LC3B* without *H. pylori* infection (UI), and transfected AGS cells with the wild type *H. pylori* (*Hp*-WT), the *cagA*-knockout *H. pylori* (*Hp*-Δ*cagA*) or the *cagA*-knockout complementation mutant *H. pylori* (*Hp-c-cagA*) (MOI = 100:1) infection for 6 h (left) and the indicated periods of time (right). Scale bars: 10 μm. The number of *GFP-MAP1LC3B* puncta in each cell ($n \geq 200$ cells) was counted. **(B)** Representative transmission electron microscopy showing AGS cells without *H. pylori* infection and those infected with *Hp*-WT, *Hp*-Δ*cagA,* or *Hp-c-cagA* (MOI = 100:1) for 6 h. The white arrows indicate autophagosomes, and the black arrows indicate autolysosomes, and the white triangle indicate *H. pylori*. The numbers of autophagic vacuoles per cell in each TEM section ($n = 35$ cells) are shown in the lower left graph and the data are expressed as mean ± SEM. **(C,D)** Flow cytometry showing MDC and AO staining of AGS cells 6 h after infection with *Hp*-WT, *Hp*-Δ*cagA,* or *Hp-c-cagA* (MOI = 100:1). **(E)** Western blotting showing the protein levels of CagA, SQSTM1, and MAP1LC3B-II with the rates of SQSTM1 and MAP1LC3B-II to β-actin in AGS cells infected with *Hp*-WT, *Hp*-Δ*cagA,* or *Hp-c-cagA* (MOI = 100:1) for 6 h. **(F)** Measurement of MAP1LC3B-II conversion and SQSTM1 in AGS cells infected with *Hp*-WT or *Hp*-Δ*cagA* (MOI = 100:1) for 6 h in the presence of Baf-A1 (10 nM). **(G)** AGS cells were transfected with *GFP-CagA,* and then infected with *Hp*-WT or *Hp*-Δ*cagA* (MOI = 100:1) for 6 h in the presence of Baf-A1 (10 nM). Results shown are representative of three independent experiments. $^{*}P < 0.05$, $^{**}P < 0.01$.

AGS cells transfected with *GFP-CagA* or *GFP-CagA-Mut*, there was a significant decrease in the number of autophagosomes as determined by TEM, compared with cells transfected with control plasmid ($P < 0.05$, **Figure 4A**). The ratio of MAP1LC3B-II to β-actin was also significantly decreased in cells transfected with *GFP-CagA* or *GFP-CagA-Mut* following

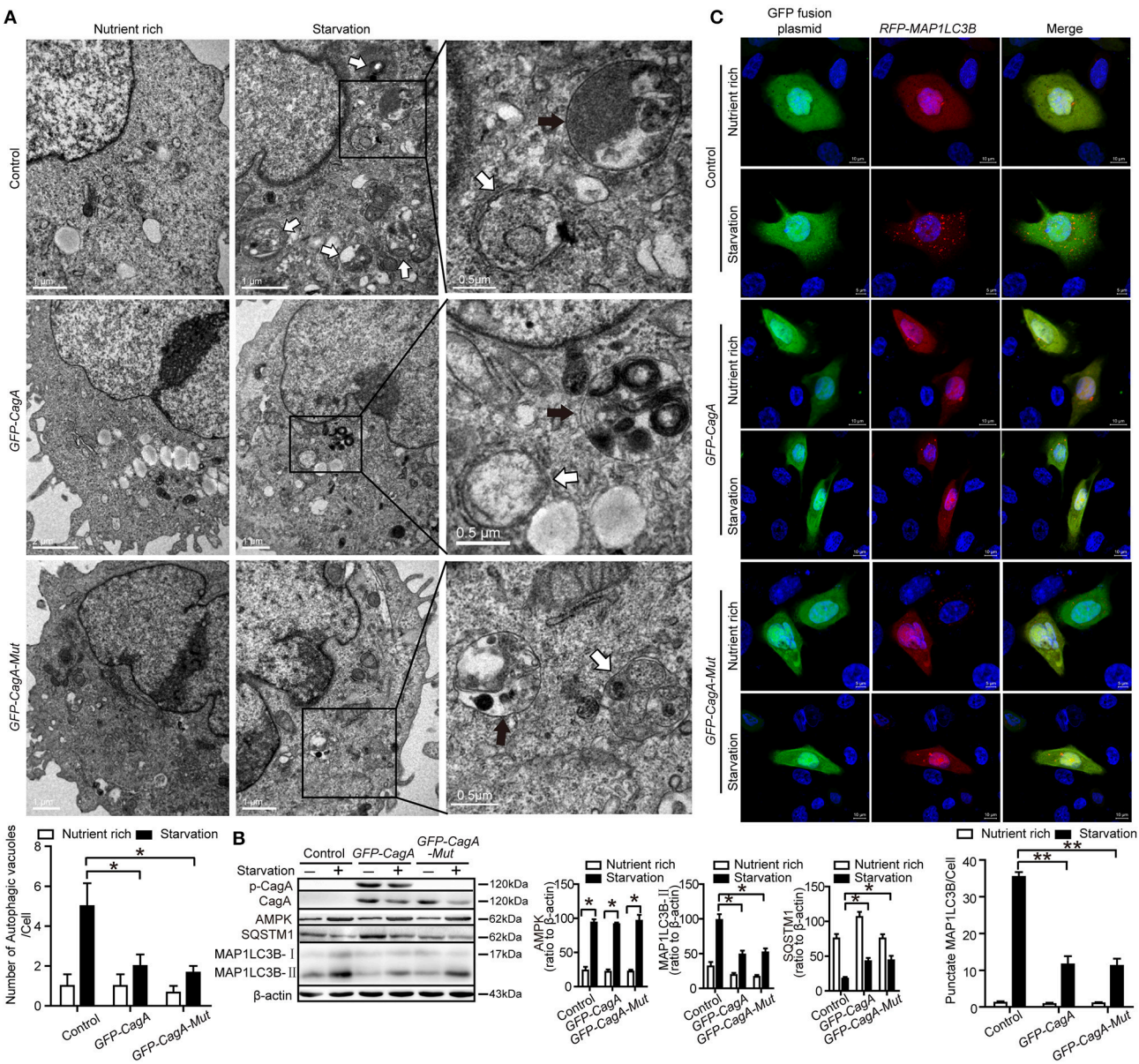

FIGURE 4 | CagA down-regulates starvation-induced autophagy in AGS cells. **(A)** Transmission electron microscopy showing autophagic vacuoles in AGS cells transfected with *GFP-CagA*, *GFP-CagA-Mut*, or a control (*pEGFP-C1*) plasmid before pretreatment of normal media or subjected to 4 h starvation. The white arrows indicate autophagosomes, and the black arrows indicate autolysosomes. The numbers of autophagic vacuoles per cell in each TEM section ($n = 35$ cells) are shown in the lower graph and the data are expressed as mean ± SEM. **(B)** Western blot assay showing MAP1LC3B-II conversion and expression of p-CagA, CagA, AMPK, and SQSTM1 in AGS cells transfected with *GFP-CagA*, *GFP-CagA-Mut*, or a control (*pEGFP-C1*) plasmid in the nutrient rich medium or 4 h starvation. **(C)** Confocal microscopy showing AGS cells co-transfected with *RFP-MAP1LC3B* and *GFP-CagA*, *GFP-CagA-Mut*, or a control (*pEGFP-C1*) plasmid in the nutrient rich medium or 4 h starvation. Scale bars: 5 or 10 μm. The number of *RFP-MAP1LC3B* puncta in each cell ($n \geq 200$ cells) was counted. Experiments were performed in triplicate, and all replicates showed similar results. $^{*}P < 0.05$, $^{**}P < 0.01$.

starvation treatment ($P < 0.05$, **Figure 4B**). Similarly, SQSTM1 expression was increased in cells transfected with *GFP-CagA* or *GFP-CagA-Mut* following starvation treatment ($P < 0.05$, **Figure 4B**). Interestingly, we observed that transfection with *GFP-CagA* or *GFP-CagA-Mut* had no effect on the expression of the AMP activated protein kinase (AMPK, an energy sensor; **Figure 4B**), indicating that CagA suppressed starvation-induced autophagy may not via the AMPK signal pathway. Furthermore, as shown in **Figure 4C**, the number of *RFP-MAP1LC3B* puncta in AGS cells co-transfected with *RFP-MAP1LC3B* and *GFP-CagA* was decreased after starvation treatment ($P < 0.05$). Taken together, these results suggest that CagA suppressed starvation-induced autophagy, which may not be dependent on tyrosine phosphorylation of CagA.

Autophagy Inhibition Increases Cytokines Production

To clarify the role of CagA in the inflammation, the expression of proinflammatory cytokines (IL-8, TNF-α, and IL-1β), which are involved in gastritis during *H. pylori* infection (Nakachi et al., 2000), was examined by ELISA assay. These cytokines were significantly higher in AGS cells infected with *Hp*-WT or *Hp-c-cagA* than in those infected with *Hp*-Δ*cagA* at different time points (**Figure 5A**). Moreover, These cytokines in AGS cells infected with *Hp*-WT and *Hp*-Δ*cagA* was increased following the increase of the bacterial load. AGS cells infected with *Hp*-WT produced greater amounts of the cytokines than cells infected with *Hp*-Δ*cagA* (**Figure 5B**).

We also examined the production of the cytokines with the autophagy enhancer (Rapa, Rapamycin) or inhibitors (3-MA or Baf-A1) treatment during *Hp*-WT and *Hp*-Δ*cagA* infection. The effects of two autophagy inhibitors, and one enhancer, are shown in Supplementary Figures 4A–C. Autophagy inhibitors significantly increased the cytokines and activated NF-κB, and enhancer Rapa decreased the ones in AGS cells infected *Hp*-Δ*cagA* infection (**Figure 5C** and Supplementary Figure 4E). After 24 h infection, the three proinflammatory cytokines were increased with the inhibitors in cells infected with *Hp*-WT and *Hp*-Δ*cagA* (Supplementary Figure 4F). Moreover, the production of proinflammatory cytokines and activity of NF-κB were significantly increased in AGS cells transfected with siRNAs for ATG5 or ATG12 upon *H. pylori* infection (**Figure 5D** and Supplementary Figure 4G). These data suggested that autophagy plays a critical role in the inflammation induced by *H. pylori*.

c-Met Is an Important Adaptor in CagA-mediated Autophagy Pathway

The previous study reported that CagA has been known to activate c-Met and the PI3K/AKT pathway (Churin et al., 2003). However, it is not clear whether c-Met could regulate autophagy. The wild type *H. pylori* infection activated c-Met in AGS cells (**Figure 6A**). CagA was coimmunoprecipitated with c-Met in AGS cells infection with *Hp*-WT (**Figure 6B**). This result was consistent with previous study (Oliveira et al., 2009). The effects of c-Met depletion through siRNA interference are shown in Supplementary Figure 4D. The number of *GFP-MAP1LC3B* puncta in c-Met siRNA group was higher than that of control group upon infection with the *Hp*-WT ($P < 0.05$, **Figure 6C**). It was a significant increase in the ratio of MAP1LC3B-II to β-actin in c-Met siRNA group than in the control siRNA upon infection with the *Hp*-WT ($P < 0.05$, **Figure 6D**). Furthermore, MDC and AO staining showed that c-Met siRNA group induced the formation of autophagolysosomes in AGS cells at a significantly higher level, compared with control siRNA group in AGS cells infected with *Hp*-WT ($P = 0.008$ and 0.018, respectively, **Figures 6E,F** and Supplementary Figure 5A). Moreover, in CagA-expressing AGS cells, the ratio of MAP1LC3B-II to β-actin significantly increased by c-Met siRNA regardless of infection status (**Figure 6G**). These results demonstrate that c-Met may be an important adaptor in CagA-mediated autophagy pathway.

CagA Regulates Autophagy through c-Met/Akt Signaling Pathway

Given that c-Met could activate PI3K/AKT/mTOR pathway (Lim and Walikonis, 2008; Tang et al., 2015), we hypothesized that PI3K/AKT/mTOR pathway might play an important role in the process of CagA-mediated autophagy. We analyzed the activation status of the key members of autophagy-related PI3K/Akt/mTOR pathways. As shown in **Figure 7A**, *Hp*-WT activated Akt kinase at Ser-473 site at a significantly higher level than did *Hp*-Δ*cagA* ($P = 0.018$), which was consistent with a previous report (Tabassam et al., 2009). Both *Hp*-WT and *Hp*-Δ*cagA* increased MAP1LC3B-II expression, but *Hp*-Δ*cagA* did at a significantly higher level than did *Hp*-WT (**Figure 7A**). There was a significant increase in the levels of phosphorylated mTOR (p-mTOR) and phosphorylated S6 ribosomal protein (p-S6) upon *Hp*-WT vs. *Hp*-Δ*cagA* (**Figure 7A**). Tyrosine phosphorylation of CagA did not affect the expression levels of proteins related to PI3K/Akt/mTOR pathway and autophagy in AGS cells (**Figure 7B**), whereas c-Met siRNA significantly decreased the level of p-Akt, p-mTOR, and p-S6, and increased MAP1LC3B-II levels (**Figure 7C**). Moreover, treatment of MK-2206, a specific inhibitor of Akt, abrogated Akt activation, and reversed the ratio of MAP1LC3B-II/β-action, and decreased the level of p-Akt, p-mTOR, and p-S6 (**Figure 7D**). Then, to investigate whether c-Met siRNA or MK-2206 reverse inflammatory response during *H. pylori* infection, we detected the expression of inflammatory cytokines. As shown in **Figure 7E**, there was a significant decrease in the production of proinflammatory cytokines in cells transfected with siRNA specific for c-Met upon infection. Similarly, the expression of inflammatory cytokines significantly decreased in AGS cells treated with MK2206 during infection (**Figure 7F**). Together, we concluded that the CagA-mediated autophagy pathway may be dependent on the c-Met/Akt signaling pathway, which could regulate the expression of inflammatory cytokines.

DISCUSSION

In the present study, we observed that (i) autophagy was down-regulated in gastric mucosal tissues infected with *cagA*+ positive *H. pylori* strains, with increased gastric inflammation; (ii) CagA inhibited autophagy and induced production of proinflammatory cytokines in AGS cells; (iii) CagA downregulated starvation-induced autophagy; (iv) Inhibition of autophagy enhanced *H. pylori*-induced cytokine production; (v) c-Met siRNA significantly affected CagA-mediated autophagy; and (vi) CagA regulates autophagy through c-Met/Akt signaling pathway. These findings indicate that CagA may act as a negative regulator of autophagy in *H. pylori*-induced inflammatory response. Specifically, given that inflammation and autophagy are major determinants of gastric malignancy (Mohri et al., 2012), it also opens a new avenue of research on gastric malignancies, especially prophylaxis and treatment.

Autophagy, as the quality control of the cellular environment, plays an important role in the protective response during infection (Deretic, 2010). However, a number of pathogens

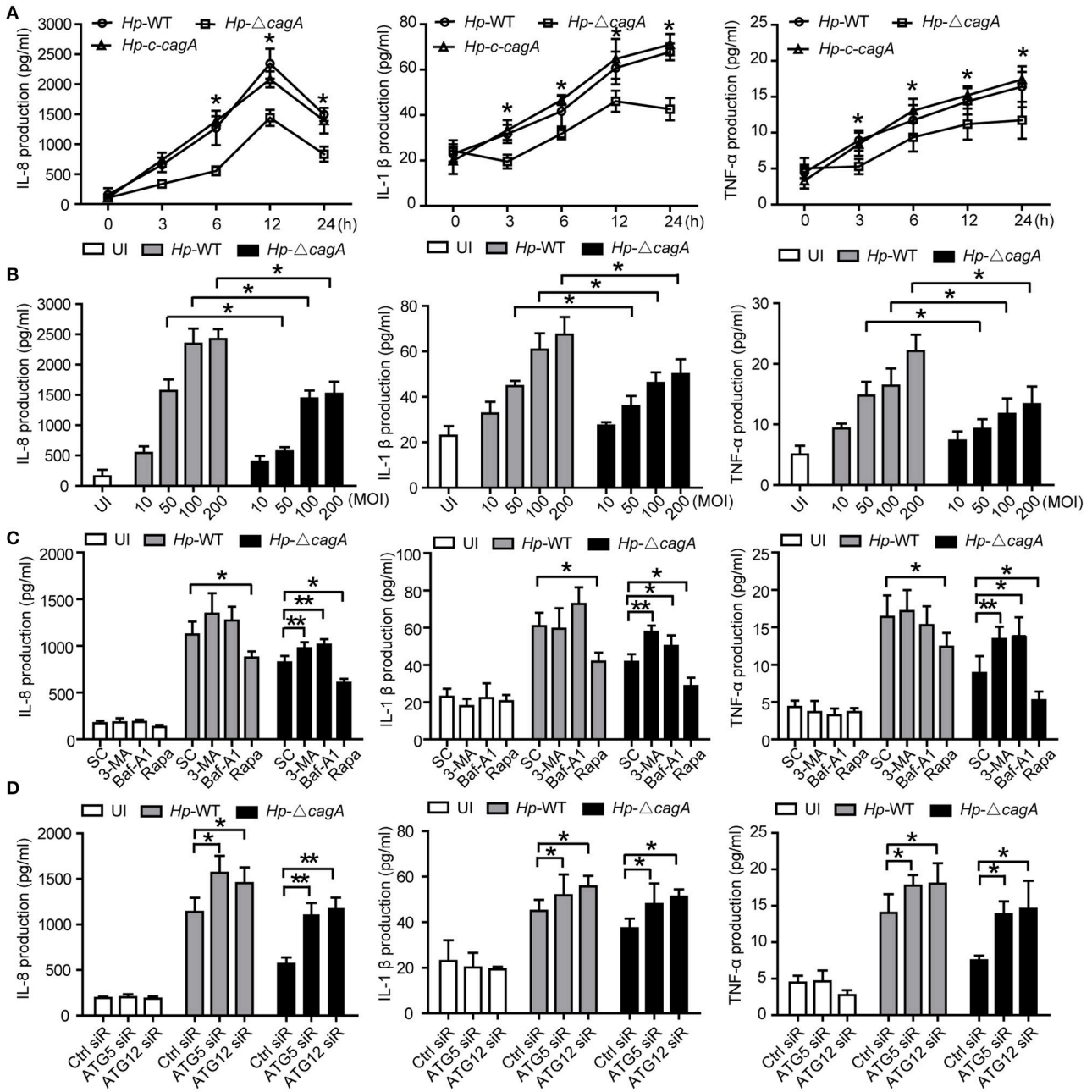

FIGURE 5 | Inhibition of autophagy enhances cytokines production induced by the cagA-knockout *H. pylori*. **(A,B)** Production of IL-8, IL-1β and TNF-α in AGS cells infected *Hp*-WT, *Hp*-Δ*cagA* or *Hp*-*c*-*cagA* at MOI of 100 for the indicated periods of time **(A)** or at different MOIs (10, 50, 100, and 200) for 12 h **(B)**, as assessed by enzyme-linked immunosorbent assay (ELISA). **(C)** After pretreatment of SC (solvent control, 0.1% DMSO), 3-MA (2 mM), Baf-A1 (10 nM) or Rapa (100 nM), AGS cells were infected with *Hp*-WT or *Hp*-Δ*cagA* (MOI = 100:1) for 6 h. Supernatants were assessed by ELISA for levels of IL-8, IL-1β, and TNF-α. **(D)** Production of IL-8, IL-1β, and TNF-α in AGS cells transfected with siRNA specific for ATG5 or ATG12 (50 nM) for 24 h and infected with *Hp*-WT or *Hp*-Δ*cagA* (MOI = 100) for 6 h, as assessed by ELISA. Data are presented as the mean ± SEM of three experiments. $^{*}P < 0.05$, $^{**}P < 0.01$.

could subvert autophagy to promote inflammation generation, the occurrence and promotion of tumor, and genetic instability (Deretic and Levine, 2009). Previous studies have reported that autophagosome formation was induced by VacA of *H. pylori in vitro* (Terebiznik et al., 2009), but VacA could also disrupt autophagic flux to promote the infection (Raju et al., 2012). In the present study, we demonstrated that CagA could inhibit autophagy, increased the production of proinflammatory cytokines and facilitated gastric inflammation. In gastric mucosal tissues, autophagy was downregulated in patients infected with CagA positive *H. pylori* strains, which was accompanied with an increased production of cytokines. To rule out the effect of

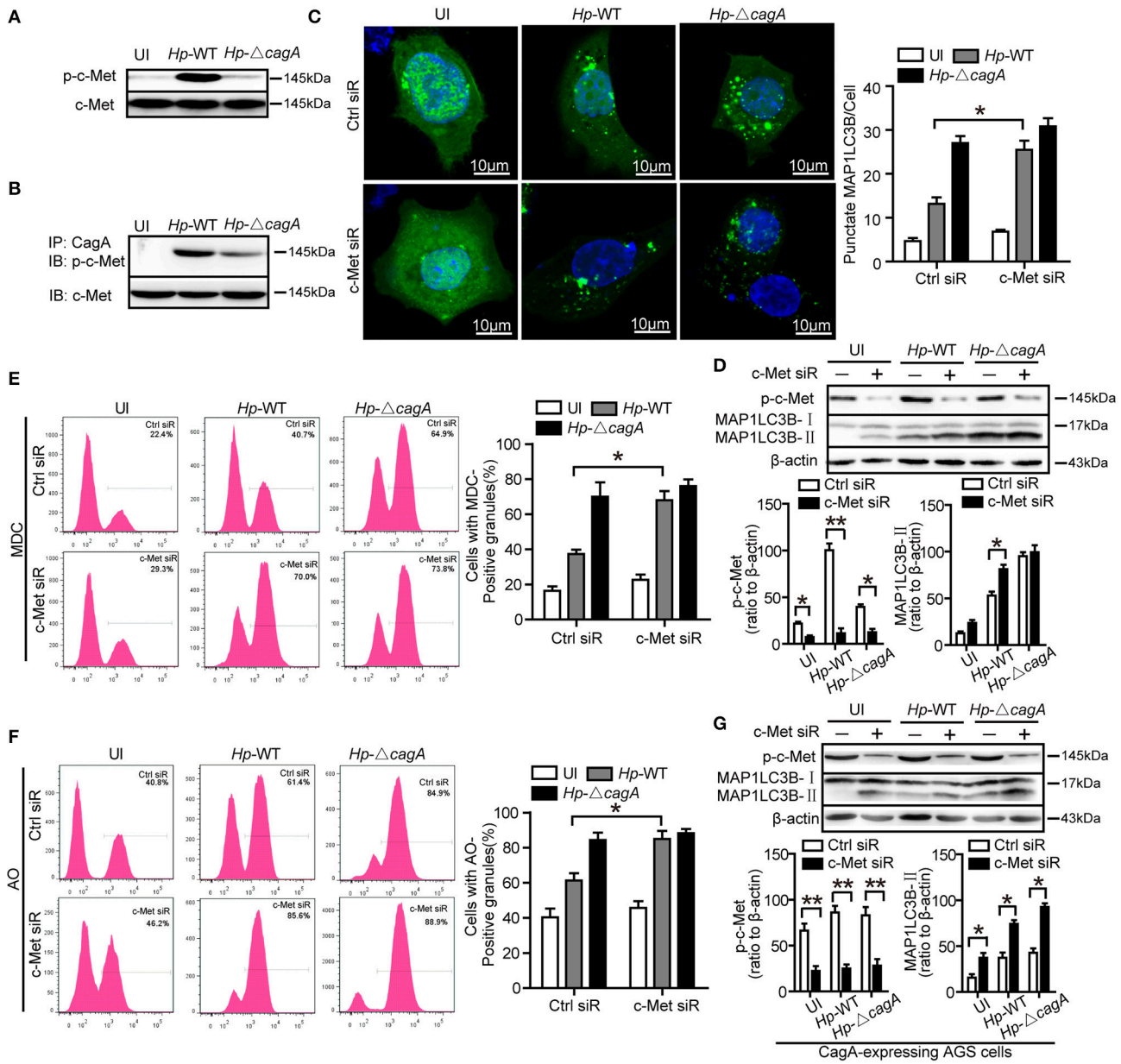

FIGURE 6 | c-Met is an important adaptor in CagA-mediated autophagy pathway. **(A,B)** AGS cells were infected with *Hp*-WT or *Hp*-Δ*cagA*, and p-c-Met and c-Met were detected by western blot. CagA was immunoprecipitated from lysates. Immunoprecipitates (IP) were subjected to SDS-PAGE and immunoblot (IB) analysis with anti-p-c-Met (top) or anti–c-Met (bottom) antibodies. **(C)** Confocal microscopy showing AGS cells co-transfected with *GFP-MAP1LC3B* plasmid and c-Met siRNAs or control siRNA for 24 h, and then infected with *Hp*-WT or *Hp*-Δ*cagA* for 6 h. The percentages of cells with MAP1LC3B punctas are shown in the right graph with data being expressed as means ± SEM of three experiments ($n \geq 200$ cells). **(D)** Western blot analysis of p-c-Met, MAP1LC3B-II conversion and β-actin in AGS cells transfected with c-Met siRNA or control siRNA and infected with *Hp*-WT or *Hp*-Δ*cagA* for 6 h. p-c-Met and MAP1LC3B-II band intensity was normalized to β-actin. **(E,F)** Flow cytometry showing MDC (upper panel) and AO (lower panel) staining of AGS cells transfected with c-Met siRNA or control siRNA and then infected with *Hp*-WT or *Hp*-Δ*cagA* for 6 h. **(G)** Western blot analysis of p-c-Met, MAP1LC3B-II conversion and β-actin in CagA-expressing AGS cells (AGS cells after transfecting the CagA expression plasmid, *GFP-CagA*) after transfected with c-Met siRNA or control siRNA and infected with *H. pylori* as described above. Experiments performed in triplicate showed consistent results. *$P < 0.05$, **$P < 0.01$.

VacA on autophagy, the toxigenic vacA genotype ($vacA^{s1m1}$), expressing a functional VacA toxic, were excluded from the study. We selectively recruited patients with *H. pylori* negative infection, ones infected with *H. pylori* $cagA^{-}/vacA^{s1m2}$ strains and ones infected with $cagA^{+}/vacA^{s1m2}$ strains in the present study. As shown in **Figures 2A–C**, the signaling molecules such as, lower MAP1LC3B-II conversion, SQSTM1 accumulation and decreased LAMP1 expression (late endosomal/lysosomal marker;

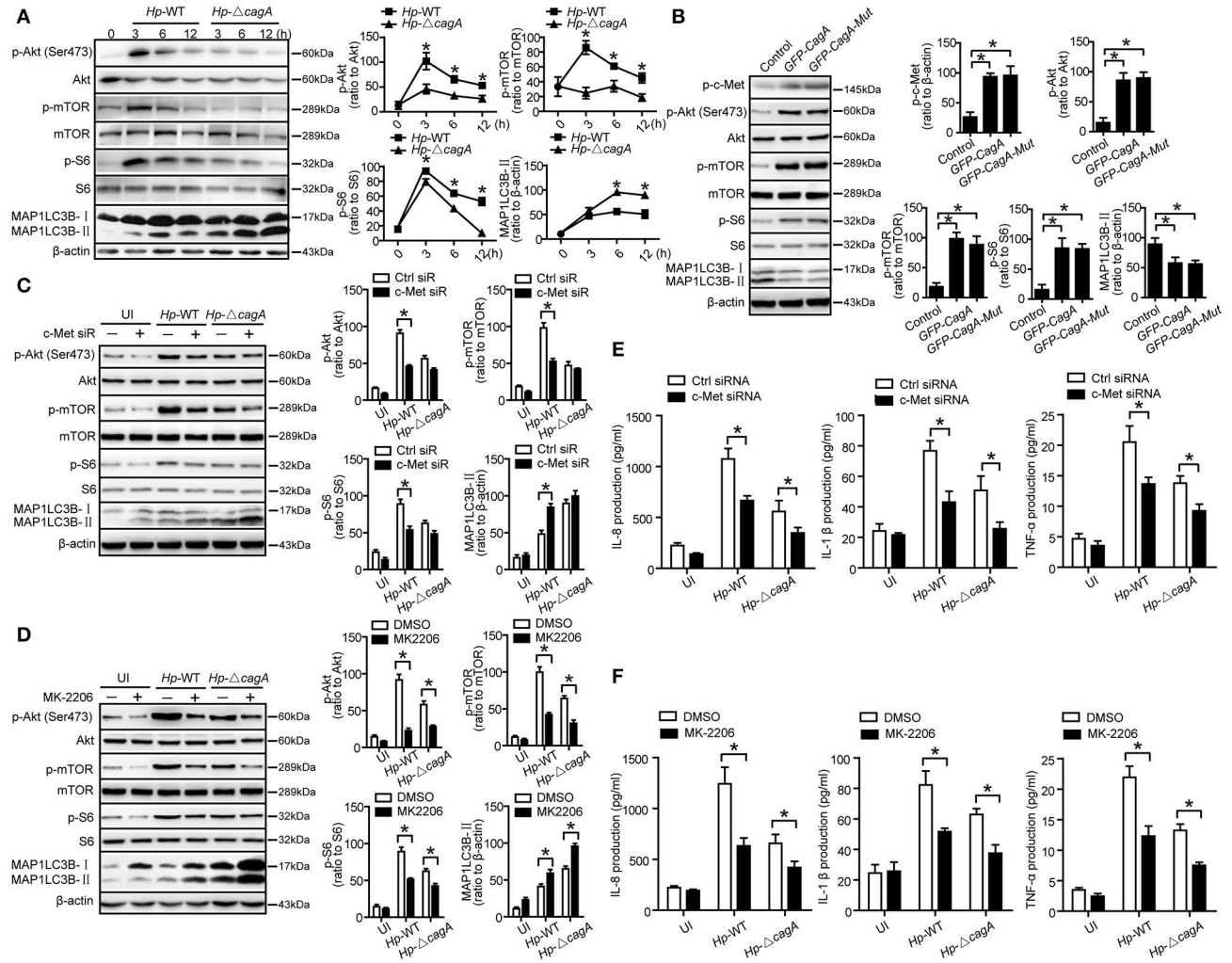

FIGURE 7 | CagA regulates autophagy through PI3K/AKT/mTOR pathway. **(A)** Expression of p-Akt(Ser473), Akt, p-mTOR, mTOR, p-S6, S6, MAP1LC3B-I, and MAP1LC3B-II in AGS cells infected with *Hp*-WT or *Hp*-Δ*cagA*(MOI = 100) at different time points. **(B)** Expression of p-Akt(Ser473), Akt, p-mTOR, mTOR, p-S6, S6, MAP1LC3B-I, and MAP1LC3B-II in AGS cells transfected with *GFP-CagA*, *GFP-CagA-Mut* or control plasmid. **(C)** Expression of p-Akt(Ser473), Akt, p-mTOR, mTOR, p-S6, S6, MAP1LC3B-I, and MAP1LC3B-II in AGS cells transfected c-Met siRNA or control siRNA (50 nM) for 24 h and then infected with *Hp*-WT or *Hp*-Δ*cagA* (MOI = 100) for 6 h. **(D)** Expression of p-Akt(Ser473), Akt, p-mTOR, mTOR, p-S6, S6, MAP1LC3B-I, and MAP1LC3B-II in AGS cells infected with *Hp*-WT or *Hp*-Δ*cagA* (MOI = 100) for 6 h with or without pre-treatment of MK-2206 (8 μM). **(E)** Production of IL-8, IL-1β and TNF-α in AGS cells transfected c-Met siRNA or control siRNA (50 nM) for 24 h and then infected with *Hp*-WT or *Hp*-Δ*cagA* (MOI = 100) for 6 h, as assessed by ELISA. **(F)** After pretreatment of DMSO or MK-2206 (8 μM), AGS cells were infected with *Hp*-WT or *Hp*-Δ*cagA* (MOI = 100:1) for 6 h. Supernatants were assessed by ELISA for levels of IL-8, IL-1β, and TNF-α. Experiments performed in triplicate showed consistent results. *$P < 0.05$.

Yu et al., 2010) in gastric mucosal tissues infected with $cagA^+$ *H. pylori* strains compared with $cagA^-$ *H. pylori* strains, which indicated that autophagic activity was decreased with increased gastric inflammation in patients infected with $cagA^+/vacA^{s1m2}$ strains. These results suggest that *H. pylori* CagA might induce inflammation by inhibiting autophagy. The intracellular CagA could be degraded by autophagy and short lived in AGS cells (Tsugawa et al., 2012). These finding suggest that induction of autophagy by *H. pylori* infection can degrade CagA by host cell defenses. Our observations indicate that persistent infection of bacterial exerts CagA to inhibit autophagy and induce inflammation.

Our observation that CagA is a negative regulatory factor for autophagy induced by *H. pylori* infection is consistent with findings of Deen's study (Deen et al., 2015), which showed that cagPAI of *H. pylori* has an inhibitory role in autophagy in macrophages. In addition, our results are also consistent with another study in which gastric biopsies from patients infected with $cagA^+/vacA^{s1m1}$ strains showed a significantly higher accumulation of SQSTM1 in the gastric epithelium compared with patients infected with a nonfunctional $cagA^-/vacA^{s2m2}$ strains (Raju et al., 2012). Given that tyrosine phosphorylation of CagA plays critical roles in the activation of many pathways (Moss et al., 2001; Boonyanugomol et al., 2011; Wandler and

Guillemin, 2012), we constructed the corresponding tyrosine phosphorylation mutants of the parent CagA (*GFP-CagA-Mut*). Our results demonstrated that tyrosine phosphorylation of CagA did not affect the PI3K/Akt/mTOR pathway, autophagy, and inflammation, suggesting that inhibition of autophagy is not dependent on tyrosine phosphorylation of CagA. Thus, the more specific mechanism of autophagy inhibited by CagA needs to be further investigated in the future.

It is well-established that autophagy plays critical roles in innate and adaptive immunity (Deretic et al., 2013), and disrupted autophagy is involved in secreting the proinflammatory cytokines, such as: IL-1α, IL-8, and IL-18 (Martins et al., 2015). Several studies have reported that autophagy may be an important mechanism for controlling inflammation in patients with Crohn's disease (Hampe et al., 2007; Rioux et al., 2007). Here, we demonstrated that autophagy inhibition enhanced the production of proinflammatory cytokines in *H. pylori* infection. SQSTM1, which is a major cargo ubiquitin-binding receptor in cells, is degraded by autolysosomes, and deficiencies of autophagy leads to accumulation of SQSTM1 (Wang et al., 2006). Moreover, SQSTM1 has further beneficial effects in NF-κB dependent cytokine production (Dupont et al., 2009). In the present study, there was a significant accumulation of SQSTM1 in the gastric mucosa of patients infected with CagA-positive *H. pylori* strains. When autophagy was inhibited, the activity of NF-κB was enhanced in AGS cells infected with mutant *H. pylori* strains (i.e., *Hp*-Δ*cagA*). These results suggested that autophagy inhibited by CagA leads to accumulation of SQSTM1, resulting in NF-κB dependent cytokine production.

CagA activates c-Met through its CRPIA (i.e., conserved repeat responsible for phosphorylation-independent activity) motif, which is critical for activation of PI3K/Akt signaling pathway and the pleiotropic transcriptional responses in *H. pylori* infection, including activation of NF-κB and β-catenin (Suzuki et al., 2009). Our data showed that, CagA was coimmunoprecipitated with c-Met in AGS cells during *H. pylori* infection, and siRNA silencing mediated c-Met knockdown in AGS enhanced the autophagy significantly in cells infected with wide-type *cagA*$^+$ *H. pylori* strain (i.e., *Hp*-WT). The PI3K/Akt signaling pathway participates in autophagy via mTOR, an autophagic regulators, resulting in autophagy suppression (Harashima et al., 2012). In the present study, we showed that CagA-positive *H. pylori* significantly increased the level of phosphorylated Akt at Ser473 and the levels of p-mTOR and p-S6 in AGS cells. The Akt inhibitor reversed the ratio of MAP1LC3B-II/β-actin in CagA-positive *H. pylori* infection, and blocked the level of phosphorylated Akt at Ser473. These findings clearly indicate that CagA inhibits autophagy via the c-Met-PI3K/Akt-mTOR signaling pathway.

Although CagA has already been reported to be a virulent factor in the inflammation induced by *H. pylori* infection, this is a new study demonstrating that CagA negatively regulates autophagy through c-Met-PI3K/Akt-mTOR signaling pathway, which is associated with increased expression of proinflammatory cytokines. Therefore, we postulate that inhibition of autophagy by CagA promotes gastric inflammation, which, in turn, initiates the multistep of gastric carcinogenesis (Correa, 1992). Moreover, given the pleiotropic actions of CagA, the interplay between CagA and autophagy regulation mechanism, which needs to be further investigated. A better understanding of the molecular mechanisms by which *H. pylori* infection modulates and interplays with autophagy will shed new insight into the development of more effective therapeutic strategies for *H. pylori* infection.

AUTHOR CONTRIBUTIONS

Conceived and designed the experiments: NL and BT. Performed the experiments: YJ, PZ, YZ, and YF. Analyzed the data: QL, KW, WZ, GG, and TW. Wrote the paper: YjF, BQ, XM, and QZ.

ACKNOWLEDGMENTS

Thanks Dr. Ji-qin Lian and Dr. Shi-ming Yang (Third Military Medical University, Chongqing, China) for editing of the manuscript, and Medjaden Bioscience Limited for assisting in the preparation of this manuscript. This work was supported by grants from National Natural Science Foundation of China (NSFC, 81301482 and 81501721).

SUPPLEMENTARY MATERIAL

The Supplementary Material for this article can be found online at: http://journal.frontiersin.org/article/10.3389/fcimb.2017.00417/full#supplementary-material

REFERENCES

Argent, R. H., Thomas, R. J., Aviles-Jimenez, F., Letley, D. P., Limb, M. C., El-Omar, E. M., et al. (2008). Toxigenic *Helicobacter pylori* infection precedes gastric hypochlorhydria in cancer relatives, and H. *pylori* virulence evolves in these families. *Clin. Cancer Res.* 14, 2227–2235. doi: 10.1158/1078-0432.CCR-07-2022

Asahi, M., Azuma, T., Ito, S., Ito, Y., Suto, H., Nagai, Y., et al. (2000). *Helicobacter pylori* CagA protein can be tyrosine phosphorylated in gastric epithelial cells. *J. Exp. Med.* 191, 593–602. doi: 10.1084/jem.191.4.593

Boonyanugomol, W., Chomvarin, C., Baik, S. C., Song, J. Y., Hahnvajanawong, C., Kim, K. M., et al. (2011). Role of cagA-positive *Helicobacter pylori* on cell proliferation, apoptosis, and inflammation in biliary cells. *Dig. Dis. Sci.* 56, 1682–1692. doi: 10.1007/s10620-010-1512-y

Brandt, S., Kwok, T., Hartig, R., Konig, W., and Backert, S. (2005). NF-kappaB activation and potentiation of proinflammatory responses by the *Helicobacter pylori* CagA protein. *Proc. Natl. Acad. Sci. U.S.A.* 102, 9300–9305. doi: 10.1073/pnas.0409873102

Churin, Y., Al-Ghoul, L., Kepp, O., Meyer, T. F., Birchmeier, W., and Naumann, M. (2003). *Helicobacter pylori* CagA protein targets the c-Met receptor and enhances the motogenic response. *J. Cell Biol.* 161, 249–255. doi: 10.1083/jcb.200208039

Correa, P. (1992). Human gastric carcinogenesis: a multistep and multifactorial process–first american cancer society award lecture on cancer epidemiology and prevention. *Cancer Res.* 52, 6735–6740.

Cremer, T. J., Amer, A., Tridandapani, S., and Butchar, J. P. (2009). *Francisella tularensis* regulates autophagy-related host cell signaling pathways. *Autophagy* 5, 125–128. doi: 10.4161/auto.5.1.7305

Deen, N. S., Gong, L., Naderer, T., Devenish, R. J., and Kwok, T. (2015). Analysis of the relative contribution of phagocytosis, lc3-associated phagocytosis, and canonical autophagy during *Helicobacter pylori* infection of macrophages. *Helicobacter* 20, 449–459. doi: 10.1111/hel.12223

Deretic, V. (2010). Autophagy in infection. *Curr. Opin. Cell Biol.* 22, 252–262. doi: 10.1016/j.ceb.2009.12.009

Deretic, V., and Levine, B. (2009). Autophagy, immunity, and microbial adaptations. *Cell Host Microbe* 5, 527–549. doi: 10.1016/j.chom.2009.05.016

Deretic, V., Saitoh, T., and Akira, S. (2013). Autophagy in infection, inflammation and immunity. *Nat. Rev. Immunol.* 13, 722–737. doi: 10.1038/nri3532

Dixon, M. F., Genta, R. M., Yardley, J. H., and Correa, P. (1996). Classification and grading of gastritis. The updated Sydney System. International Workshop on the Histopathology of Gastritis, Houston 1994. *Am. J. Surg. Pathol.* 20, 1161–1181. doi: 10.1097/00000478-199610000-00001

Dupont, N., Lacas-Gervais, S., Bertout, J., Paz, I., Freche, B., Van Nhieu, G. T., et al. (2009). Shigella phagocytic vacuolar membrane remnants participate in the cellular response to pathogen invasion and are regulated by autophagy. *Cell Host Microbe* 6, 137–149. doi: 10.1016/j.chom.2009.07.005

Fischer, W., Puls, J., Buhrdorf, R., Gebert, B., Odenbreit, S., and Haas, R. (2001). Systematic mutagenesis of the *Helicobacter pylori* cag pathogenicity island: essential genes for CagA translocation in host cells and induction of interleukin-8. *Mol. Microbiol.* 42, 1337–1348. doi: 10.1046/j.1365-2958.2001.02714.x

Gunn, M. C., Stephens, J. C., Stewart, J. A., Rathbone, B. J., and West, K. P. (1998). The significance of cagA and vacA subtypes of *Helicobacter pylori* in the pathogenesis of inflammation and peptic ulceration. *J. Clin. Pathol.* 51, 761–764. doi: 10.1136/jcp.51.10.761

Hampe, J., Franke, A., Rosenstiel, P., Till, A., Teuber, M., Huse, K., et al. (2007). A genome-wide association scan of nonsynonymous SNPs identifies a susceptibility variant for Crohn disease in ATG16L1. *Nat. Genet.* 39, 207–211. doi: 10.1038/ng1954

Harashima, N., Inao, T., Imamura, R., Okano, S., Suda, T., and Harada, M. (2012). Roles of the PI3K/Akt pathway and autophagy in TLR3 signaling-induced apoptosis and growth arrest of human prostate cancer cells. *Cancer Immunol. Immunother.* 61, 667–676. doi: 10.1007/s00262-011-1132-1

Kayath, C. A., Hussey, S., El Hajjami, N., Nagra, K., Philpott, D., and Allaoui, A. (2010). Escape of intracellular Shigella from autophagy requires binding to cholesterol through the type III effector, IcsB. *Microbes Infect.* 12, 956–966. doi: 10.1016/j.micinf.2010.06.006

Klionsky, D. J., Cuervo, A. M., and Seglen, P. O. (2007). Methods for monitoring autophagy from yeast to human. *Autophagy* 3, 181–206. doi: 10.4161/auto.3678

Lim, C. S., and Walikonis, R. S. (2008). Hepatocyte growth factor and c-Met promote dendritic maturation during hippocampal neuron differentiation via the Akt pathway. *Cell. Signal.* 20, 825–835. doi: 10.1016/j.cellsig.2007.12.013

Martins, J. D., Liberal, J., Silva, A., Ferreira, I., Neves, B. M., and Cruz, M. T. (2015). Autophagy and inflammasome interplay. *DNA Cell Biol.* 34, 274–281. doi: 10.1089/dna.2014.2752

Mizushima, N., Yoshimori, T., and Levine, B. (2010). Methods in mammalian autophagy research. *Cell* 140, 313–326. doi: 10.1016/j.cell.2010.01.028

Mohri, Y., Tanaka, K., Ohi, M., Toiyama, Y., Yasuda, H., Inoue, Y., et al. (2012). Inflammation-based prognostic score as a predictor of postoperative gastric cancer recurrence. *Anticancer Res.* 32, 4581–4584.

Moss, S. F., Sordillo, E. M., Abdalla, A. M., Makarov, V., Hanzely, Z., Perez-Perez, G. I., et al. (2001). Increased gastric epithelial cell apoptosis associated with colonization with cagA + *Helicobacter pylori* strains. *Cancer Res.* 61, 1406–1411.

Nakachi, N., Klein, T. W., Friedman, H., and Yamamoto, Y. (2000). *Helicobacter pylori* infection of human gastric epithelial cells induces IL-8 and TNFalpha, but not TGFbeta1 mRNA. *FEMS Immunol. Med. Microbiol.* 29, 23–26.

Nakagawa, I., Amano, A., Mizushima, N., Yamamoto, A., Yamaguchi, H., Kamimoto, T., et al. (2004). Autophagy defends cells against invading group A Streptococcus. *Science* 306, 1037–1040. doi: 10.1126/science.1103966

Oliveira, M. J., Costa, A. M., Costa, A. C., Ferreira, R. M., Sampaio, P., Machado, J. C., et al. (2009). CagA associates with c-Met, E-cadherin, and p120-catenin in a multiproteic complex that suppresses *Helicobacter pylori*-induced cell-invasive phenotype. *J. Infect. Dis.* 200, 745–755. doi: 10.1086/604727

Pattingre, S., Tassa, A., Qu, X., Garuti, R., Liang, X. H., Mizushima, N., et al. (2005). Bcl-2 antiapoptotic proteins inhibit Beclin 1-dependent autophagy. *Cell* 122, 927–939. doi: 10.1016/j.cell.2005.07.002

Py, B. F., Lipinski, M. M., and Yuan, J. (2007). Autophagy limits *Listeria monocytogenes* intracellular growth in the early phase of primary infection. *Autophagy* 3, 117–125. doi: 10.4161/auto.3618

Raju, D., Hussey, S., Ang, M., Terebiznik, M. R., Sibony, M., Galindo-Mata, E., et al. (2012). Vacuolating cytotoxin and variants in Atg16L1 that disrupt autophagy promote *Helicobacter pylori* infection in humans. *Gastroenterology* 142, 1160–1171. doi: 10.1053/j.gastro.2012.01.043

Rioux, J. D., Xavier, R. J., Taylor, K. D., Silverberg, M. S., Goyette, P., Huett, A., et al. (2007). Genome-wide association study identifies new susceptibility loci for Crohn disease and implicates autophagy in disease pathogenesis. *Nat. Genet.* 39, 596–604. doi: 10.1038/ng2032

Shin, D. M., Jeon, B. Y., Lee, H. M., Jin, H. S., Yuk, J. M., Song, C. H., et al. (2010). *Mycobacterium tuberculosis* eis regulates autophagy, inflammation, and cell death through redox-dependent signaling. *PLoS Pathog.* 6:e1001230. doi: 10.1371/journal.ppat.1001230

Shintani, T., and Klionsky, D. J. (2004). Autophagy in health and disease: a double-edged sword. *Science* 306, 990–995. doi: 10.1126/science.1099993

Suerbaum, S., and Michetti, P. (2002). *Helicobacter pylori* infection. *N. Engl. J. Med.* 347, 1175–1186. doi: 10.1056/NEJMra020542

Suzuki, M., Mimuro, H., Kiga, K., Fukumatsu, M., Ishijima, N., Morikawa, H., et al. (2009). *Helicobacter pylori* CagA phosphorylation-independent function in epithelial proliferation and inflammation. *Cell Host Microbe* 5, 23–34. doi: 10.1016/j.chom.2008.11.010

Tabassam, F. H., Graham, D. Y., and Yamaoka, Y. (2009). *Helicobacter pylori* activate epidermal growth factor receptor- and phosphatidylinositol 3-OH kinase-dependent Akt and glycogen synthase kinase 3beta phosphorylation. *Cell. Microbiol.* 11, 70–82. doi: 10.1111/j.1462-5822.2008.01237.x

Tang, B., Li, Q., Zhao, X. H., Wang, H. G., Li, N., Fang, Y., et al. (2015). Shiga toxins induce autophagic cell death in intestinal epithelial cells via the endoplasmic reticulum stress pathway. *Autophagy* 11, 344–354. doi: 10.1080/15548627.2015.1023682

Tang, B., Wang, K., Jia, Y. P., Zhu, P., Fang, Y., Zhang, Z. J., et al. (2016). *Fusobacterium nucleatum*-induced impairment of autophagic flux enhances the expression of proinflammatory cytokines via ROS in Caco-2 Cells. *PLoS ONE* 11:e0165701. doi: 10.1371/journal.pone.0165701

Terebiznik, M. R., Raju, D., Vazquez, C. L., Torbricki, K., Kulkarni, R., Blanke, S. R., et al. (2009). Effect of *Helicobacter pylori*'s vacuolating cytotoxin on the autophagy pathway in gastric epithelial cells. *Autophagy* 5, 370–379. doi: 10.4161/auto.5.3.7663

Tsugawa, H., Suzuki, H., Saya, H., Hatakeyama, M., Hirayama, T., Hirata, K., et al. (2012). Reactive oxygen species-induced autophagic degradation of *Helicobacter pylori* CagA is specifically suppressed in cancer stem-like cells. *Cell Host Microbe* 12, 764–777. doi: 10.1016/j.chom.2012.10.014

Vaira, D., Malfertheiner, P., Megraud, F., Axon, A. T., Deltenre, M., Hirschl, A. M., et al. (1999). Diagnosis of *Helicobacter pylori* infection with a new non-invasive antigen-based assay. HpSA European study group. *Lancet* 354, 30–33. doi: 10.1016/S0140-6736(98)08103-3

Wandler, A. M., and Guillemin, K. (2012). Transgenic expression of the *Helicobacter pylori* virulence factor CagA promotes apoptosis or tumorigenesis through JNK activation in Drosophila. *PLoS Pathog.* 8:e1002939. doi: 10.1371/journal.ppat.1002939

Wang, L., Dong, Z., Huang, B., Zhao, B., Wang, H., Zhao, J., et al. (2010). Distinct patterns of autophagy evoked by two benzoxazine derivatives in vascular endothelial cells. *Autophagy* 6, 1115–1124. doi: 10.4161/auto.6.8.13508

Wang, Q. J., Ding, Y., Kohtz, D. S., Mizushima, N., Cristea, I. M., Rout, M. P., et al. (2006). Induction of autophagy in axonal dystrophy and degeneration. *J. Neurosci.* 26, 8057–8068. doi: 10.1523/JNEUROSCI.2261-06.2006

Yla-Anttila, P., Vihinen, H., Jokitalo, E., and Eskelinen, E. L. (2009). Monitoring autophagy by electron microscopy in Mammalian cells. *Methods Enzymol.* 452, 143–164. doi: 10.1016/S0076-6879(08)03610-0

Yu, L., McPhee, C. K., Zheng, L., Mardones, G. A., Rong, Y., Peng, J., et al. (2010). Termination of autophagy and reformation of lysosomes regulated by mTOR. *Nature* 465, 942–946. doi: 10.1038/nature09076

Zavros, Y., and Rogler, G. (2012). Variants in autophagy genes affect susceptibility to both Crohn's disease and *Helicobacter pylori* infection. *Gastroenterology* 142, 1060–1063. doi: 10.1053/j.gastro.2012.03.012

Conflict of Interest Statement: The authors declare that the research was conducted in the absence of any commercial or financial relationships that could be construed as a potential conflict of interest.

Copyright © 2017 Li, Tang, Jia, Zhu, Zhuang, Fang, Li, Wang, Zhang, Guo, Wang, Feng, Qiao, Mao and Zou. This is an open-access article distributed under the terms of the Creative Commons Attribution License (CC BY). The use, distribution or reproduction in other forums is permitted, provided the original author(s) or licensor are credited and that the original publication in this journal is cited, in accordance with accepted academic practice. No use, distribution or reproduction is permitted which does not comply with these terms.

frontiers in Cellular and Infection Microbiology

ORIGINAL RESEARCH
published: 06 September 2017
doi: 10.3389/fcimb.2017.00392

Probiotics for the Treatment of Atopic Dermatitis in Children: A Systematic Review and Meta-Analysis of Randomized Controlled Trials

*Ruixue Huang[1], Huacheng Ning[1], Minxue Shen[2,3], Jie Li[2,3], Jianglin Zhang[2,3] and Xiang Chen[2,3]**

[1] Department of Occupational and Environmental Health, Xiangya School of Public Health, Central South University, Changsha, China, [2] Department of Dermatology, Xiangya Hospital, Central South University, Changsha, China, [3] Hunan Key Laboratory of Skin Cancer and Psoriasis, Xiangya Hospital, Central South University, Changsha, China

Objective: Atopic dermatitis (AD) is a prevalent, burdensome, and psychologically important pediatric concern. Probiotics have been suggested as a treatment for AD. Some reports have explored this topic; however, the utility of probiotics for AD remains to be firmly established.

Methods: To assess the effects of probiotics on AD in children, the PubMed/Medline, Cochrane Library Scopus, and OVID databases were searched for reports published in the English language.

Results: Thirteen studies were identified. Significantly higher SCORAD values favoring probiotics over controls were observed (mean difference [MD], −3.07; 95% confidence interval [CI], −6.12 to −0.03; $P < 0.001$). The reported efficacy of probiotics in children < 1 year old was −1.03 (95%CI, −7.05 to 4.99) and that in children 1–18 years old was −4.50 (95%CI, −7.45 to −1.54; $P < 0.001$). Subgroup analyses showed that in Europe, SCORAD revealed no effect of probiotics, whereas significantly lower SCORAD values were reported in Asia (MD, −5.39; 95%CI, −8.91 to −1.87). *Lactobacillus rhamnosus* GG (MD, 3.29; 95%CI, −0.30 to 6.88; $P = 0.07$) and *Lactobacillus plantarum* (MD, −0.70; 95%CI, −2.30 to 0.90; $P = 0.39$) showed no significant effect on SCORAD values in children with AD. However, *Lactobacillus fermentum* (MD, −11.42; 95%CI, −13.81 to −9.04), *Lactobacillus salivarius* (MD, −7.21; 95%CI, −9.63 to −4.78), and a mixture of different strains (MD, −3.52; 95%CI, −5.61 to −1.44) showed significant effects on SCORAD values in children with AD.

Conclusions: Our meta-analysis indicated that the research to date has not robustly shown that probiotics are beneficial for children with AD. However, caution is needed when generalizing our results, as the populations evaluated were heterogeneous. Randomized controlled trials with larger samples and greater power are necessary to identify the species, dose, and treatment duration of probiotics that are most efficacious for treating AD in children.

Keywords: probiotics, constipation, children, meta-analysis, randomized controlled trial

OPEN ACCESS

Edited by:
Pascale Alard,
University of Louisville, United States

Reviewed by:
Valerio Iebba,
Sapienza Università di Roma, Italy
Arianna Aceti,
Università di Bologna, Italy

****Correspondence:***
Xiang Chen
chenxiang_xy@126.com

Received: *19 May 2017*
Accepted: *22 August 2017*
Published: *06 September 2017*

Citation:
Huang R, Ning H, Shen M, Li J, Zhang J and Chen X (2017) Probiotics for the Treatment of Atopic Dermatitis in Children: A Systematic Review and Meta-Analysis of Randomized Controlled Trials. Front. Cell. Infect. Microbiol. 7:392. doi: 10.3389/fcimb.2017.00392

INTRODUCTION

Atopic dermatitis (AD), is one of the most common chronic inflammatory skin disorders among infants and children. AD is characterized by itching and recurrent eczematous lesions, and its incidence has increased worldwide over the past several decades. The current prevalence rate is 10–20% in infants and children (Weidinger and Novak, 2016). As the leading non-fatal medical skin disorder, AD imposes severe psychosocial burdens on pediatric patients and their families (Chamlin and Chren, 2010; Silverberg, 2016; Sidbury and Khorsand, 2017). AD is associated with high risks of allergy, asthma, and mental health issues (Sung et al., 2017). Infants and children with AD are typically treated with topical corticosteroids (TCS), antihistamines, and even antibiotics (Totri et al., 2017). However, these medications exert several adverse side effects, and AD symptoms may recur rapidly after treatment is stopped. Furthermore, long-term TCS use may trigger new-onset AD.

Probiotics is becoming increasingly attractive as a treatment option for some illnesses in children (Fuchs-Tarlovsky et al., 2016). Probiotics (live bacteria or yeasts) are not necessarily harmless, but they help to protect hosts from harmful bacteria (Mizock, 2015). When administered in adequate amounts, probiotics may play beneficial roles not only in the gastrointestinal tract but also in the gut–brain–skin axis (Ogden and Bielory, 2005; Dehingia et al., 2015; Huang et al., 2016; Huang and Hu, 2017). Several studies on the benefits of probiotics for pediatric AD patients have appeared over the past decades. In 2000, Pessi et al. reported that oral probiotics alleviated the clinical symptoms of gastrointestinal inflammation and AD (Pessi et al., 2000). Kirjavainen et al. (2003) reported lower *Bacteroides* counts in the fecal microflora of children with atopic eczema than in healthy infants and suggested that probiotics can be used to treat AD in children (Kirjavainen et al., 2003); however, some reports yielded contrasting results (Licari et al., 2015). For instance, Gruber et al. found that *Lactobacillus rhamnosus strain GG (LGG)* exerted no therapeutic effects in infants with mild-to-moderate AD (Gruber et al., 2007). Therefore, we systematically evaluated the effects of probiotics used to treat AD in children.

METHODS

Inclusion Criteria

The inclusion criteria for the meta-analysis were (1) RCTs of children aged ≤18 years in whom AD severity was graded by experienced dermatologists using the Severity scoring of atopic dermatitis: the SCORAD index (1993); Yoon et al. (2015) (2) that evaluated the use of any probiotic culture/strain/dose/therapy regimen (including studies on fermented yogurt; all dosage forms including tablets, powders, oil suspensions, and capsules were included). All results are presented as means ± standard deviation. However, if multiple reports evaluated the same group of patients, we selected only the most recent complete report. SCORAD, developed by the European Task Force on AD in 1993 (1993), assesses the AD area, clinical features, visual analog scale data, and clinical symptoms, and it is widely used to evaluate AD severity in children (Machura et al., 2008).

Exclusion Criteria

Studies that did not meet the inclusion criteria or that were published in languages other than English were excluded.

Search Process

Two individuals of our team searched the following databases from the times of the earliest records in 2000 to April 12, 2017: PubMed (https://www.ncbi.nlm.nih.gov/pubmed), Embase (https://www.embase.com/login), Cochrane Library (http://www.cochranelibrary.com/) and Scopus (https://www.elsevier.com/solutions/scopus) (available on the internet); and Ovid, Orbis, and the Web of Science (available at our university library with free downloads). The following search string was used in searching: [(infant OR infants) OR (neonate OR neonates) OR (newborn OR newborns) OR (toddler OR toddlers)] AND (probiotic OR probiotics OR pro-biotics OR probio*) AND (atopic dermatitis OR atopic eczema) OR (SCORAD) OR (atopic OR atopy) NOT (animals) NOT (adult). The references listed in each report were examined to allow us to retrieve additional information. We only reviewed works in the English language, thus not those in (for example) Korean or Chinese. Furthermore, conference abstracts were excluded, because they lacked detailed data.

Data Collection

The two individuals collected all data independently. The eligibility of studies was confirmed by both reviewers. A tabulation of study author(s), publication date, recruited numbers, probiotic strain(s), dosage, treatment duration, and treatment results was prepared (**Table 1**). If the study data were unclear, we attempted to contact the corresponding author via email to obtain further information.

Statistical Analysis

RevMan 5.3 software (Cochrane Collaboration, Nordic Cochrane Center, Copenhagen, Denmark; http://community.cochrane.org/tools/review-production-tools/revman-5/) was accessed to conduct the meta-analysis. SCORAD was commonly used to measure the efficacy of probiotics in children with AD. As the results were continuous data, the mean difference (MD) and 95%CI were calculated for statistical analyses, and either a randomized-effects model or fixed-effects model was used depending on whether heterogeneity was apparent. Subgroup assessment was performed with regard to different geographical status, infants aged <1 year, children aged between 1 and 18 years, different strains, and *LGG*. The c^2 test was used to identify statistical heterogeneity (Margolis and Mitra, 2017). The I^2 statistic was calculated to identify and quantify inconsistency. When I^2 was ≥ 50%, indicating significant heterogeneity, we used a random-effects model for meta-analysis. When I^2 was < 50% indicating no heterogeneity, we employed a fixed-effects model. Publication bias was assessed by constructing funnel plots. A two-tailed $P < 0.05$ was used to reflect statistical significance. Sensitivity analyses, also termed uncertainty analyses, were used to explore the extent to which our results and conclusions were altered by changes in the data or analysis approach (Alexander et al., 2016). If the conclusions did not change upon application of the sensitivity analysis, those conclusions were considered robust.

TABLE 1 | Characteristics of included RCTs for meta-analysis.

Study, year (country)	n	Age	Genus, species, and strain, duration	Dose	Outcome summary
Viljanen et al., 2005; Finland	220	1.4–11.9 months	*Lactobacillus rhamnosus strain GG (LGG)*; 4 weeks	5×10^9 cfu or mixture twice daily capsules	Positive effect of probiotics was seen only in IgE-sensitized infants
Weston et al., 2005; Austria	56	6–18 months	*LF; 8-week*	2×10^{10} CFU/g /d	Positive effect of probiotics was seen only in food-sensitized children
Folster-Holst et al., 2006; Germany	54	1–55 months	*Lactobacillus rhamnosus strain GG(LGG); 8-week*	10×10^9CFU	No significant difference between synbiotics and placebo
Gruber et al., 2007; Germany	102	3–12 months	*Lactobacillus rhamnosus strain GG(LGG); 8-week*	$>5 \times 10^9$CFU, twice daily orally	No significant difference between synbiotics and placebo
Niers et al., 2009; Netherland	98	1–24 months	*B. bifidobacterium infantis, LC. lactis W58; 24-week*	3×10^9CFU, once daily	No difference was observed among two groups
Wu et al., 2012; Taiwan	60	2–14 years	*Lactobacillus (LS), 8-week*	5×10^{10} CFU, twice daily	SCORAD decrease significantly in probiotic group compared to placebo group
Gerasimov et al., 2010; Ukraine	90	1–3 years	*Mixture (LA t BL)/synbiotics; 8-week*	5×10^{10} CFU, twice daily	SCORAD decrease significantly in probiotic group compared to placebo group
Woo et al., 2010; Korea	75	2–10 years	*Lactobacillus (LS2)/synbiotics; 12-week*	2×10^{10} CFU, twice daily	SCORAD decrease significantly in probiotic group compared to placebo group
Shafiei et al., 2011; Iran	41	1–36 months	*Seven strain probiotics plus prebiotic mixture; 2 months*	1×10^9CFU, once daily	No significant difference between probiotics and placebo
Gore et al., 2012; UK	133	3–6 months	*Lactobacillus (LP) or Bifidobacterium (BL); 12-week*	1×10^{10} CFU	No significant difference between probiotics and placebo
Han et al., 2012; Korea	83	1–13 years	*Lactobacillus (LP2); 12-week*	5×10^{10} CFU, twice daily	SCORAD decrease significantly in probiotic group compared to placebo
Yesilova et al., 2012; Turkey	39	1–12 years	*Mixture (BB2, LA, LC, LS2); 8-week*	4×10^{10} CFU, daily	SCORAD decrease significantly in probiotic group compared to placebo
Wang and Wang, 2015; Taiwan	220	1–28 years	*Lactobacillus paracasei(LP), Lactobacillus fermentum(LF), Mixture; 3 months*	LP,LF(2×10^{10} CFU,qd); Mixture(4×10^{10} CFU,qd)	SCORAD decrease significantly in probiotic group compared to placebo

In meta-analyses, sensitivity analyses are conducted by excluding studies one-by-one to identify those studies that materially affect the results (Copas and Shi, 2000). The risk of bias in each RCT was explored using the "risk of risk" tool in Revman software. The PRISMA statement published in 2009 aimed to improve the reporting of systematic reviews and meta-analyses. PRISMA defines an evidence-based minimum set of items to employ, and we followed this guideline (http://www.prisma-statement.org/). PRISMA features both a checklist and a flow diagram. We used the checklist to ensure that our study structure was appropriate and the flow diagram to map the numbers of records identified, included, and excluded, as well as the reasons for exclusion (Zhang et al., 2017). Publication bias was checked by drawing funnel plots, which are commonly used in systematic reviews and meta-analyses. Publication bias is considered absent if the study results are distributed in close proximity to the averages.

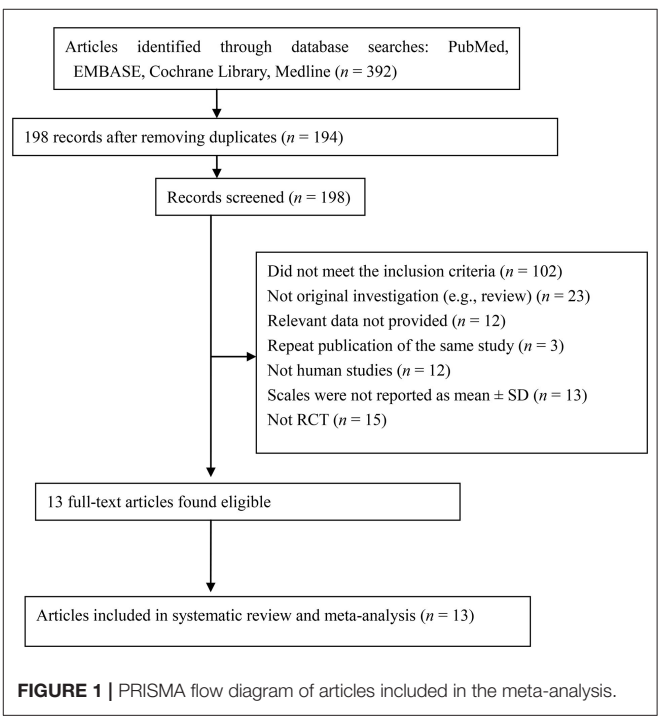

FIGURE 1 | PRISMA flow diagram of articles included in the meta-analysis.

RESULTS

Included Studies

The PRISMA flow diagram (**Figure 1**) shows how we selected the relevant reports. We initially screened 392 articles, excluded those that did not meet our inclusion criteria, and finally retained 26 articles. As some reports did not report data as means ± SD,

we contacted the corresponding authors by email. Unfortunately, we sent 13 emails and didn't receive any data suitable for inclusion in the meta-analysis. Ultimately, 13 studies involving 1,070 children fulfilled our selection criteria (**Table 1**).

Quality Assessment

Figure 2A shows the risk of bias within all enrolled RCTs, as adjudged by the two reviewers. **Figure 2B** presents the individual risks of bias, again as perceived by the reviewers. Both figures show that the risks of bias were rather low, because all were RCTs that adhered to high standards. Four studies divided children into probiotic intervention and control groups; two studies created three groups (probiotics, a placebo, and another intervention). Twelve studies were of double-blind design. All 13 studies reported baseline data including socioeconomic status and mean age; these did not differ significantly among the groups.

Probiotics and Children with AD

Data from 1,070 children (intervention group, 553; control group, 517) were assessed. The outcome of a random-effects

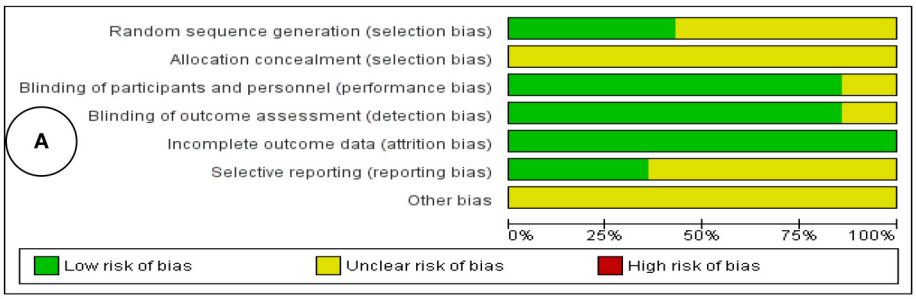

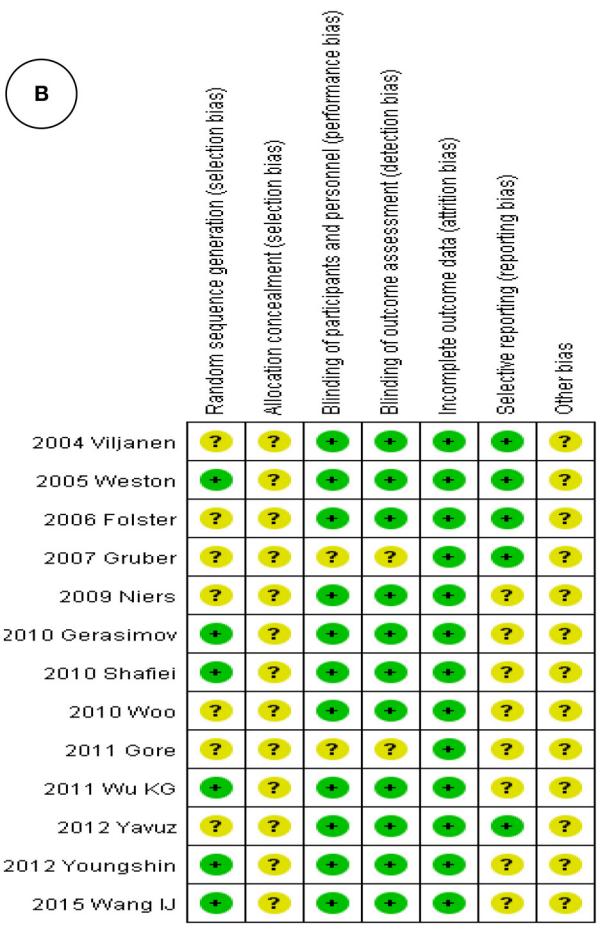

FIGURE 2 | (A) Risk of bias graph, with each risk of bias item presented as a percentage across all included studies. **(B)** Risk of bias summary, with each risk of bias item for each included study.

meta-analysis model involving all 13 trials is shown in **Figure 3**. Significant differences in SCORAD values favoring probiotics over the control were observed overall (MD, −3.07; 95%CI, −6.12 to −0.03; $P < 0.00001$). However, a high degree of heterogeneity was observed across these 14 trials ($I^2 = 87\%$).

Subgroup Analysis of Probiotics Efficacy by Age

All 13 trials involved children aged 0–18 years. We categorized the children into two groups: infants <1 year old and children 1–18 years old. Accordingly, five trials were included in the <1 year subgroup, and nine trials were included in the 1–18 years subgroup (**Figure 4**). The efficacy of probiotics in the former subgroup was −1.03 (95%CI, −7.05 to 4.99) and that in the latter subgroup was −4.50 (95%CI, −7.45 to −1.54; $P < 0.001$). However, a high degree of heterogeneity was observed among the <1 year subgroup ($I^2 = 94\%$).

Subgroup Assessment by Continent

Subgroup assessment by continent showed different effects. In Europe, probiotics showed no effect on SCORAD, whereas significantly lower SCORAD values were reported in Asia (MD, −5.39; 95%CI, −8.91 to −1.87). In Australia, the MD was −11.20 (95%CI, −13.76 to −8.64). However, there was heterogeneity among these trials (**Figure 5**).

Subgroup Assessment of Different Cultured Organisms

MD scoring compared to control and placebo interventions was performed by cultured organism group. *LGG* (MD, 3.29; 95%CI, −0.30 to 6.88; $P = 0.07$) and *LP* (MD, −0.70; 95%CI, −2.30 to 0.90; $P = 0.39$) showed no significant effects on SCORAD values in children. However, *LF* (MD, −11.42; 95%CI, −13.81 to −9.04), *LS* (MD, −7.21; 95%CI, −9.63 to −4.78), and a mixture of different strains (MD, −3.52; 95%CI, −5.61 to −1.44) showed significant effects on SCORAD values in children (**Figure 6**).

Publication Bias

We used RevMan software to draw funnel plots (**Figure 7**), wherein each dot represents data from a single RCT. A random-effects model was used to this end. The funnel plots were somewhat asymmetrical, thus indicating potential publication bias, perhaps attributable in part to the fact that we included only English-language publications and excluded conference abstracts. However, studies with positive outcomes are more

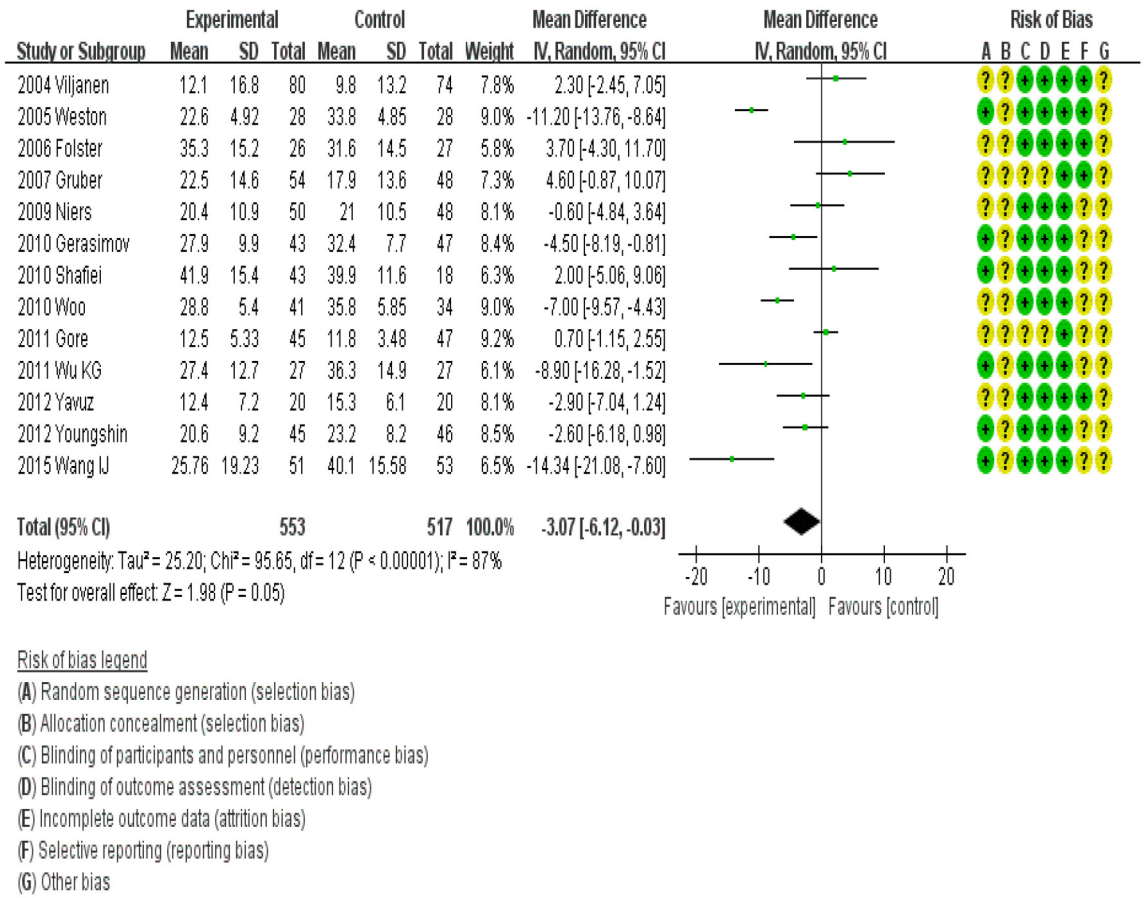

FIGURE 3 | MD scoring with probiotics treatment compared to control and placebo interventions. 95%CI, 95% confidence interval.

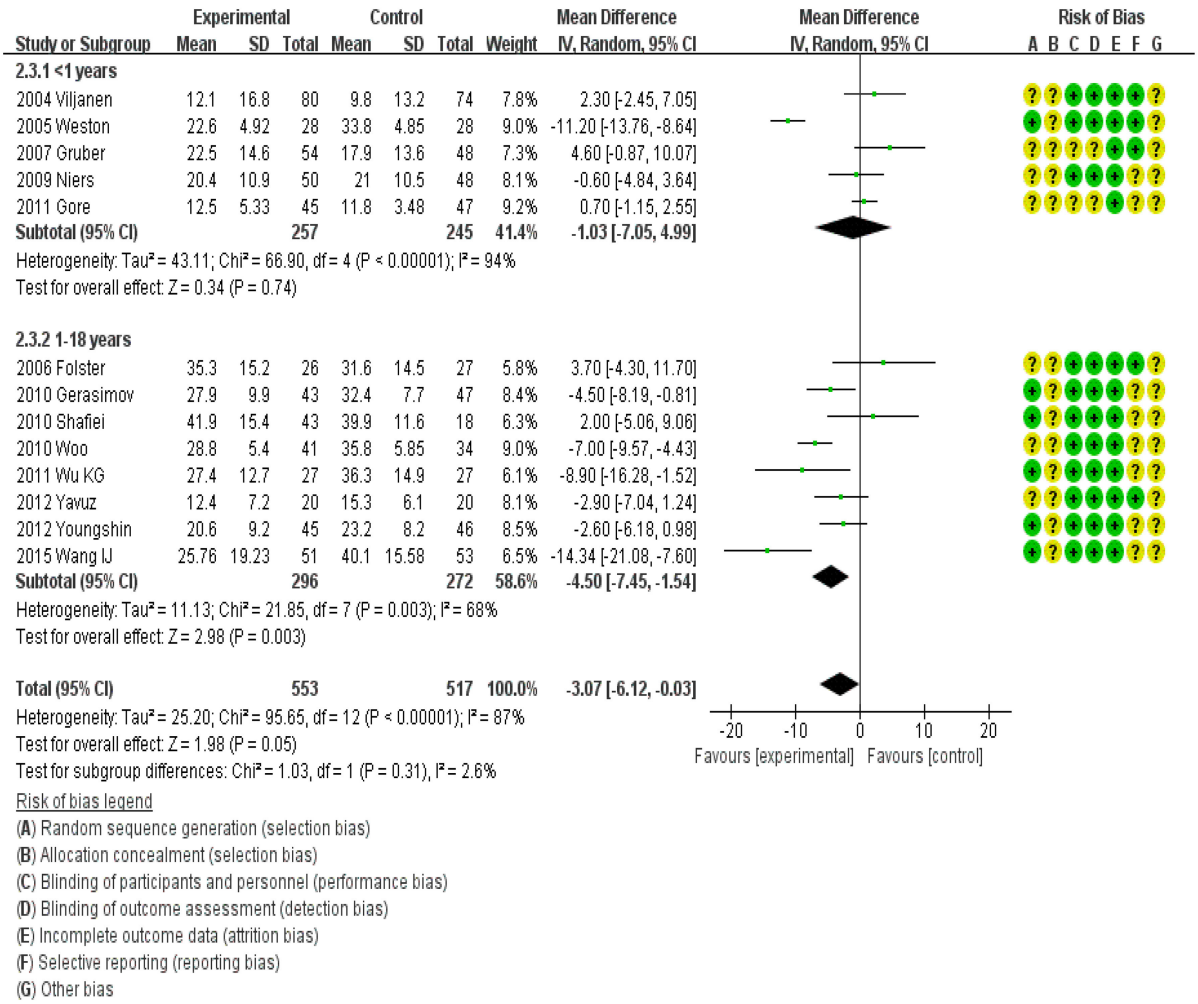

FIGURE 4 | MD scoring with probiotics treatment compared to control and placebo interventions by age group.

likely to be published than are those with negative outcomes, thus creating bias.

Sensitivity Testing

We performed sensitivity analyses to assess the relative influence of each study by excluding the studies one by one, and the results suggested no significant changes in effects with regard to subgroups.

DISCUSSION

Overall, the data suggested an overall benefit of probiotics supplementation in children with AD, and age-specific sub-analyses showed that probiotics effectively reduce SCORAD values in children aged 1–18 years. Geography-specific sub-analyses showed that probiotics effectively reduced SCORAD values in Asia, while no effect was observed for Europe. Strain-specific sub-analyses indicated that *Lactobacillus (LS), Lactobacillus fermentum (LF)*, and a probiotic mixture reduced SCORAD values in children with AD, while LGG and Lactobacillus plantarum (LP)showed no effect in children with AD.

Hippocrates (460–370) stated that "All diseases begin in the gut", which is the earliest suggestion that bacteria affect health (Hippocrates, 2002). Metchnikoff, known as the father of probiotics (Gordon, 2016), proposed that colonic bacteria afforded health benefits in aging adults. In recent decades, probiotics that aid in the resolution of pediatric atopic eczema have been investigated. Viljanen et al. explored probiotic effects on pediatric atopic eczema/dermatitis syndrome but found no significant difference between the treatment and control groups (Viljanen et al., 2005). Passeron et al. compared probiotics and prebiotics and found that both significantly improved AD manifestations in children (Passeron et al., 2006). Brouwer et al. evaluated the clinical and immunological effects of *Lactobacillus rhamnosus* (*LR*) supplementation in a hydrolyzed formula given to children with AD but found no significant effect (Brouwer et al., 2006). The cited authors suggested that the discrepancies between their results and those of other trials were likely attributable to differences in treatment timing and the strains

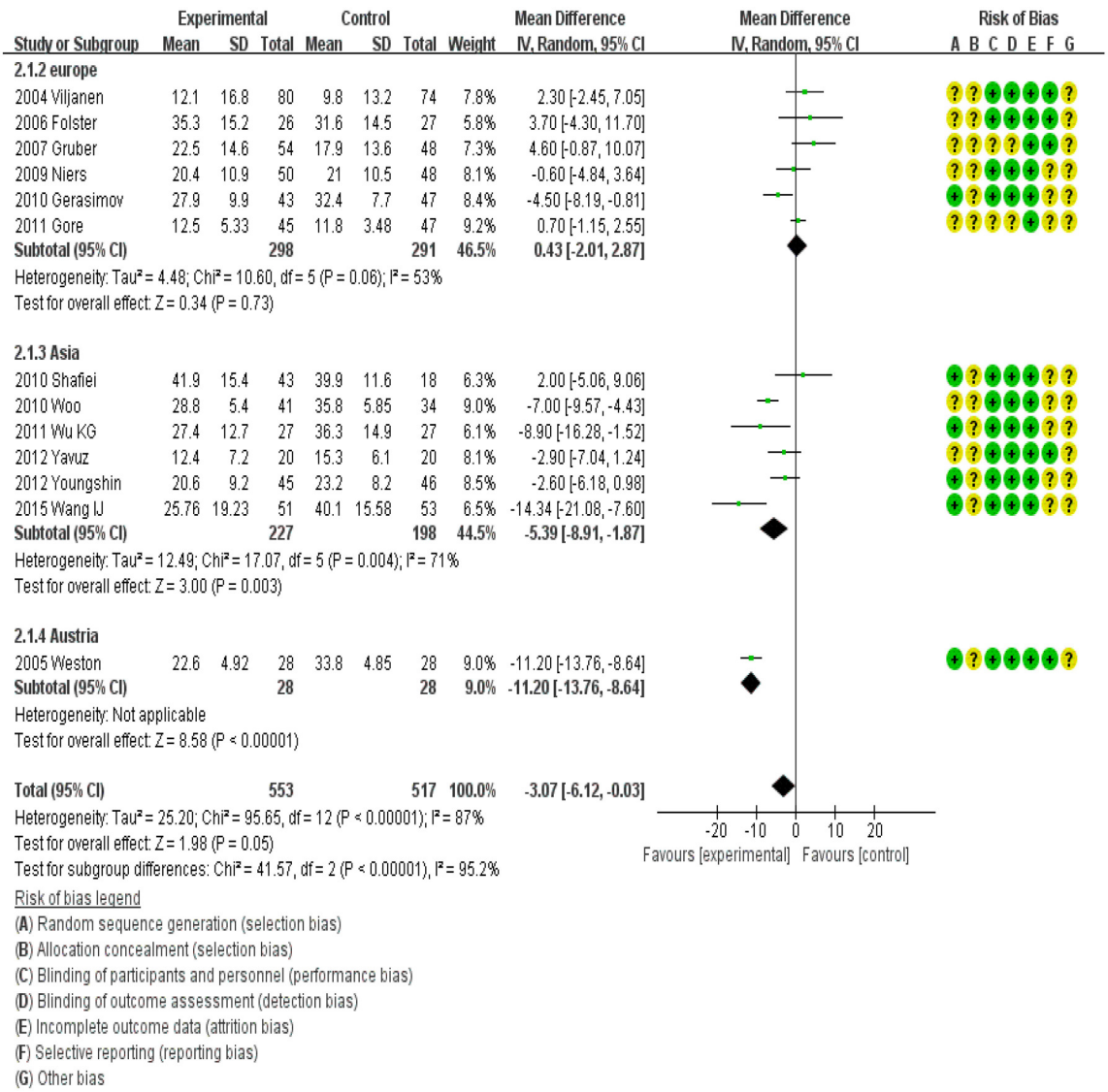

FIGURE 5 | MD scoring with probiotics treatment compared to control and placebo interventions by location.

used. Sistek et al. conducted a 12-week trial in the UK and found that a combination of *LR* and *Bifidobacteria lactis* (*BL*) improved AD symptoms in food-sensitive children (Sistek et al., 2006). At roughly the same time, a prospective German study by Folster-Holst et al. yielded insufficient evidence to make the conclusion that *LGG* is an effective treatment for moderate-to-severe AD in infants (Folster-Holst, 2010). Gruber et al. also found that *LGG* had no therapeutic effect in such patients (Gruber et al., 2007). Despite these discouraging findings, Gerasimov et al. reported that *Lactobacillus acidophilus DDS-1* and *Bifidobacterium lactis UABLA-12* afforded significant clinical improvements in children with moderate-to-severe AD (Gerasimov et al., 2010). Similarly, Wu et al. showed that *Lactobacillus salivarius* (*LS*) exerted short-term beneficial effects in patients with moderate-to-severe AD (Wu et al., 2012). Drago et al. suggested that such effects may be attributable to restoration of the altered intestinal microbiota (Drago et al., 2011). In contrast, Gore et al. found that *LS* exerted no beneficial effects on eczema when given as an adjunct to basic topical treatment (Gore et al., 2012). Several reports have examined the effects of other bacterial strains on AD in children. Supplementation with *LPCJLP 133*, *Lactobacillus paracasei*, and *LF* was reported to be effective. The discrepancies described above may be attributable to differences in the strains used, the study areas, and/or the ethnicities of the subjects. Several groups have performed meta-analyses to evaluate the effectiveness of probiotics on AD. Da Costa Baptista et al. reviewed all published trials and reported that the biological effects observed in most trials suggest that probiotic adjuvant treatments are of benefit for AD (da et al., 2013). The cited review, although comprehensive, did not report total MDs or 95%CIs. Chang performed a

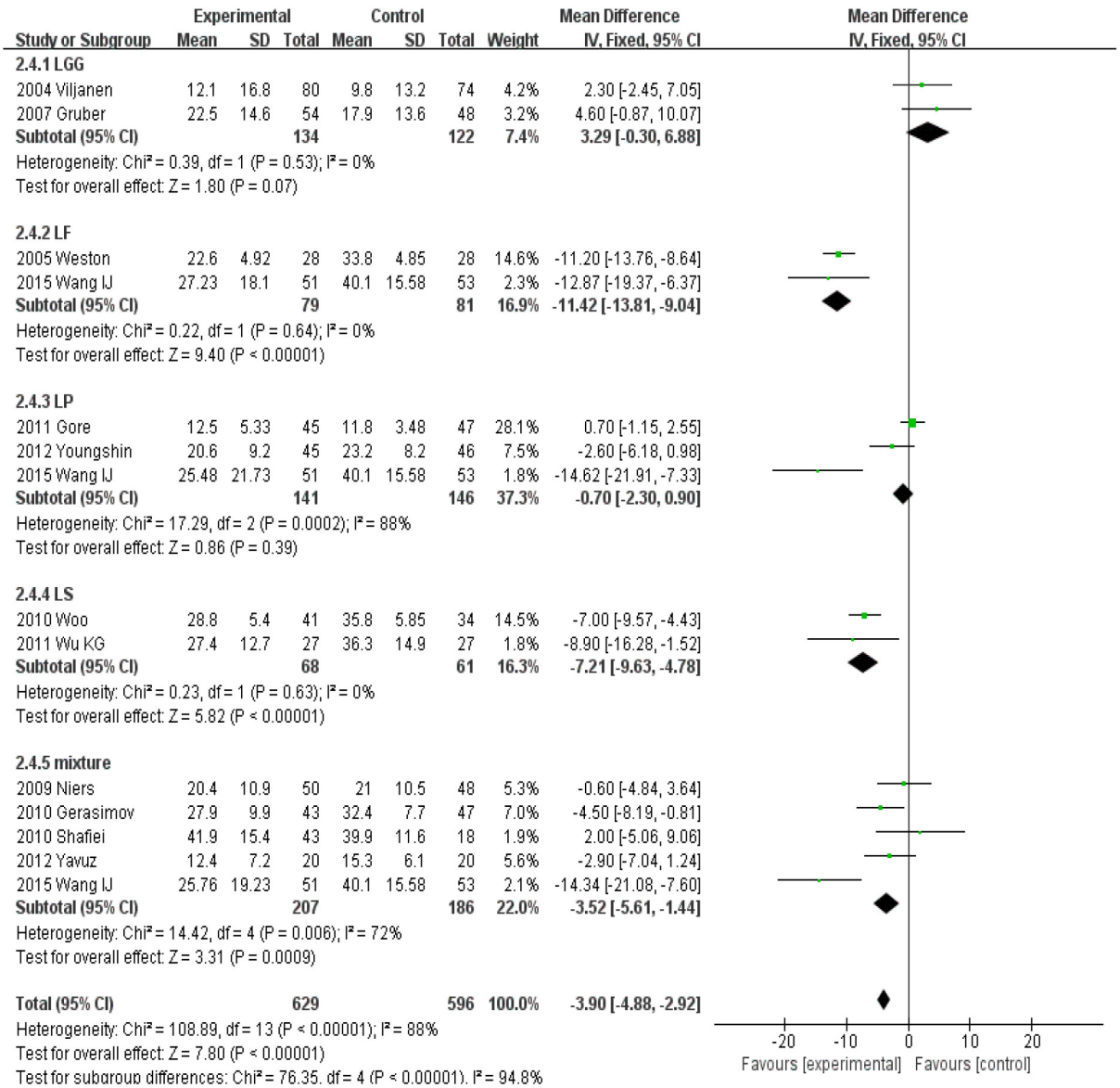

FIGURE 6 | MD scoring with probiotics treatment compared to control and placebo interventions by cultured organisms.

meta-analysis of studies in which either prebiotics or probiotics were given and reported that synbiotics may be useful to treat AD (Chang et al., 2017). However, the focus was on synbiotics rather than probiotics. Szajewska et al. stressed the need for data on individual probiotic strains rather than on probiotics in general (Szajewska and Mrukowicz, 2003; Szajewska et al., 2015). Ogden et al. suggested probiotics as a complementary approach to the treatment and prevention of pediatric AD (Ogden and Bielory, 2005). They concluded that probiotics should be an active area of investigation, considering the role of gut microbiota in altered immune responses in atopic patients. However, the authors did not perform a meta-analysis to obtain further details about the treatment effects of probiotics. Kim et al. reviewed 25 RCTs on the effects of probiotics in the treatment of AD in patients of all ages. They observed significant differences in SCORAD values favoring probiotics over the control group in children 1–18 years old and in adults, whereas no favorable effects were seen in infants <1 year old (Kim et al., 2014). We found that probiotics were efficacious in children aged 1–18 years (MD, −4.50; 95%CI, −7.45 to −1.54) and showed strong efficacy in Asia but not in Europe; furthermore, *LGG* had no effects on AD whereas *LS*, *LF*, *LP*, and a mixture of strains showed beneficial effects. Our findings are in agreement with those of Lee et al., who concluded that the evidence for probiotics as a useful treatment of AD in children is convincing. However, the cited authors reviewed only trials published before 2008, whereas we included later

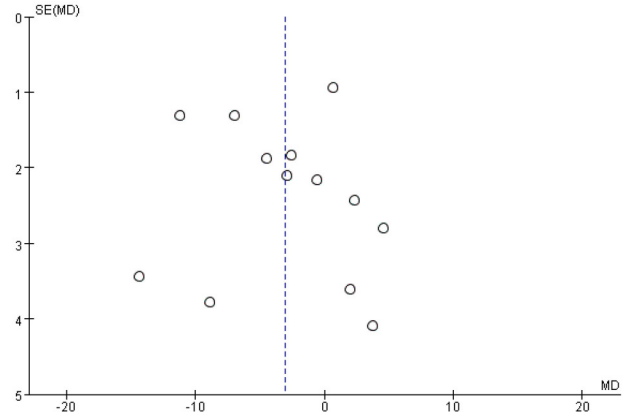

FIGURE 7 | Funnel plot: SD by mean difference and each dot represents 1 RCT.

trials to afford greater insight. The differences may be because we included only RCTs involving children under the age of 18 years and those that reported MDs. Some RCTs presented values other than MDs, including the study by Kim et al. (2010), and some presented the results as figures, rendering calculations impossible. We contacted the corresponding authors but did not receive useful replies. Thus, we excluded those studies. Third, some of the included studies had small sample sizes, which may affect the reliability and validity of the conclusions. Thus, our overall results are affected by these issues, and the data were highly heterogeneous. These topics require further attention. Also, in the subgroup analyses, children with AD may have different gut microbiota profiles from those of normal children. Thus, probiotics supplementation in children < 1 year old and 1–18 years old may promote a healthier gut microbiota profile, boosting their immune response. People from different areas have different dietary structures and gut bacterial compositions. Dehingia et al. compared gut bacterial diversity between Indian populations and worldwide data (Dehingia et al., 2015). Zhang et al. also suggested that a phylogenetically diverse gut microbiota at the genus level may be commonly shared by distinctive healthy populations, which may explain the diversity of the effects of probiotics across people from different countries (Zhang et al., 2015). The above discussion is of importance to physicians, dermatologists, and other public healthcare workers who deal with diverse ethnic populations.

To the best of our knowledge, there are no previous reports on the effects of different probiotic strains on AD in children. In our meta-analysis, all trials involving *LGG* and one trial involving *LP* showed no effects, while two studies confirmed the beneficial effects of *LP* on AD (MD, −0.70; 95%CI, −2.30 to 0.90; $P = 0.39$). This discrepancy may be associated with differences in dosages, the timing and duration of intervention, and sample sizes, and further trials are required to clarify this point.

Our meta-analysis had certain limitations. First, we attempted to minimize heterogeneity and publication bias, but significant heterogeneity among trials remained evident. Differences in study samples, study populations, and intervention methods contributed to the heterogeneity. For example, some of the included studies had small sample sizes, compromising the reliability and validity of the conclusions. In addition, the RCTs were performed in various countries, thus, the subjects differed among RCTs in terms of their genetic make-up and microbial exposure, which in turn are associated with varying responses to the same probiotic. Also, we excluded some RCTs from this meta-analysis, and fewer studies included will reduce the confidence associated with the data interpretation and increase heterogeneity and publication bias. Finally, we cannot draw robust conclusions as to which probiotic strain/mixture should be given to children with AD and which population(s) would receive maximum benefit from such treatment.

CONCLUSION

Our present work demonstrated that probiotics may have the potential to decrease SCORAD values in children with AD. However, the findings presented here must be generalized with caution because of heterogeneity. The results are a source of optimism with regard to the management of AD in children. More adequately powered RCTs using standardized measurements are necessary to assess which species of probiotics and dosages and what treatment periods are most efficacious for children with AD.

AUTHOR CONTRIBUTIONS

RH, MS, and XC proposed the idea of this study and designed the study; RH, HN, MS, and JL conducted data screening and performed quality assessment; RH and MS used RevMan software to assess the data and performed the statistical analysis and gave the explanations of the statistical results. RH drafted the initial manuscript. JL, JZ, and XC critically reviewed and revised the manuscript.

FUNDING

This work was supported by China's National Basic Work of Science and Technology (Grant# 2015FY111100).

REFERENCES

(1993). Severity scoring of atopic dermatitis: the SCORAD index. Consensus Report of the European Task Force on Atopic Dermatitis. *Dermatology* 186, 23–31. doi: 10.1159/000247298

Alexander, P. E., Bonner, A. J., Agarwal, A., Li, S. A., Hariharan, A. T., Izhar, Z., et al. (2016). Sensitivity subgroup analysis based on single-center vs. multi-center trial status when interpreting meta-analyses pooled estimates: the logical way forward. *J. Clin. Epidemiol.* 74, 80–92. doi: 10.1016/j.jclinepi.2015.08.027

Brouwer, M. L., Wolt-Plompen, S. A., Dubois, A. E., van der Heide, S., Jansen, D. F., Hoijer, M. A., et al. (2006). No effects of probiotics on atopic dermatitis in infancy: a randomized placebo-controlled trial. *Clin. Exp. Allergy.* 36, 899–906. doi: 10.1111/j.1365-2222.2006.02513.x

Chamlin, S. L., and Chren, M. M. (2010). Quality-of-life outcomes and measurement in childhood atopic dermatitis. *Immunol. Allergy Clin. North Am.* 30, 281–288. doi: 10.1016/j.iac.2010.05.004

Chang, H. Y., Chen, J. H., Chang, J. H., Lin, H. C., Lin, C. Y., and Peng, C. C. (2017). Multiple strains probiotics appear to be the most effective probiotics in the prevention of necrotizing enterocolitis and mortality: an updated meta-analysis. *PLoS ONE* 12:e171579. doi: 10.1371/journal.pone.0171579

Copas, J., and Shi, J. Q. (2000). Meta-analysis, funnel plots and sensitivity analysis. *Biostatistics* 1, 247–262. doi: 10.1093/biostatistics/1.3.247

da, C. B. I., Accioly, E., and de Carvalho, P. P. (2013). Effect of the use of probiotics in the treatment of children with atopic dermatitis; a literature review. *Nutr. Hosp.* 28, 16–26. doi: 10.3305/nh.2013.28.1.6207

Dehingia, M., Devi, K. T., Talukdar, N. C., Talukdar, R., Reddy, N., Mande, S. S., et al. (2015). Gut bacterial diversity of the tribes of India and comparison with the worldwide data. *Sci. Rep.* 5:18563. doi: 10.1038/srep18563

Drago, L., Iemoli, E., Rodighiero, V., Nicola, L., De Vecchi, E., and Piconi, S. (2011). Effects of *Lactobacillus salivarius* LS01 (DSM 22775) treatment on adult atopic dermatitis: a randomized placebo-controlled study. *Int. J. Immunopathol. Pharmacol.* 24, 1037–1048. doi: 10.1177/039463201102400421

Folster-Holst, R. (2010). Probiotics in the treatment and prevention of atopic dermatitis. *Ann. Nutr. Metab.* 57(Suppl.), 16–19. doi: 10.1159/000309054

Folster-Holst, R., Muller, F., Schnopp, N., Abeck, D., Kreiselmaier, I., Lenz, T., et al. (2006). Prospective, randomized controlled trial on *Lactobacillus rhamnosus* in infants with moderate to severe atopic dermatitis. *Br. J. Dermatol.* 155, 1256–1261. doi: 10.1111/j.1365-2133.2006.07558.x

Fuchs-Tarlovsky, V., Marquez-Barba, M. F., and Sriram, K. (2016). Probiotics in dermatologic practice. *Nutrition.* 32, 289–295. doi: 10.1016/j.nut.2015.09.001

Gerasimov, S. V., Vasjuta, V. V., Myhovych, O. O., and Bondarchuk, L. I. (2010). Probiotic supplement reduces atopic dermatitis in preschool children a randomized, double-blind, placebo-controlled, clinical trial. *Am. J. Clin. Dermatol.* 11, 351–361. doi: 10.2165/11531420-000000000-00000

Gordon, S. (2016). Elie metchnikoff, the man and the myth. *J. Innate Immun.* 8, 223–227. doi: 10.1159/000443331

Gore, C., Custovic, A., Tannock, G. W., Munro, K., Kerry, G., Johnson, K., et al. (2012). Treatment and secondary prevention effects of the probiotics *Lactobacillus paracasei* or *Bifidobacterium lactis* on early infant eczema: randomized controlled trial with follow-up until age 3 years. *Clin. Exp. Allergy* 42, 112–122. doi: 10.1111/j.1365-2222.2011.03885.x

Gruber, C., Wendt, M., Sulser, C., Lau, S., Kulig, M., Wahn, U., et al. (2007). Randomized, placebo-controlled trial of *Lactobacillus rhamnosus* GG as treatment of atopic dermatitis in infancy. *Allergy* 62, 1270–1276. doi: 10.1111/j.1398-9995.2007.01543.x

Han, Y., Kim, B., Ban, J., Lee, J., Kim, B. J., Choi, B. S., et al. (2012). A randomized trial of *Lactobacillus plantarum* CJLP133 for the treatment of atopic dermatitis. *Pediatr. Allergy Immunol.* 23, 667–673. doi: 10.1111/pai.12010

Hippocrates (2002). On the articulations. The genuine works of Hippocrates. *Clin. Orthop. Relat. Res.* 19–25.

Huang, R., and Hu, J. (2017). Positive effect of probiotics on constipation in children: a systematic review and meta-analysis of six randomized controlled trials. *Front. Cell. Infect. Microbiol.* 7:153. doi: 10.3389/fcimb.2017.00153

Huang, R., Wang, K., and Hu, J. (2016). Effect of probiotics on depression: a systematic review and meta-analysis of randomized controlled trials. *Nutrients.* 8:E483. doi: 10.3390/nu8080483

Kim, J. Y., Kwon, J. H., Ahn, S. H., Lee, S. I., Han, Y. S., Choi, Y. O., et al. (2010). Effect of probiotic mix (*Bifidobacterium bifidum*, *Bifidobacterium lactis*, *Lactobacillus acidophilus*) in the primary prevention of eczema: a double-blind, randomized, placebo-controlled trial. *Pediatr. Allergy Immunol.* 21, e386–e393. doi: 10.1111/j.1399-3038.2009.00958.x

Kim, S. O., Ah, Y. M., Yu, Y. M., Choi, K. H., Shin, W. G., and Lee, J. Y. (2014). Effects of probiotics for the treatment of atopic dermatitis: a meta-analysis of randomized controlled trials. *Ann. Allergy Asthma Immunol.* 113, 217–226. doi: 10.1016/j.anai.2014.05.021

Kirjavainen, P. V., Salminen, S. J., and Isolauri, E. (2003). Probiotic bacteria in the management of atopic disease: underscoring the importance of viability. *J. Pediatr. Gastroenterol. Nutr.* 36, 223–227. doi: 10.1097/00005176-200302000-00012

Licari, A., Marseglia, A., Castellazzi, A. M., Ricci, A., Tagliacarne, C., Valsecchi, C., et al. (2015). Atopic dermatitis: is there a role for probiotics? *J. Biol. Regul. Homeost. Agents.* 29, 18–24.

Machura, E., Karczewska, K., Findysz-Wylag, B., Mazur, B., and Lodwich, M. (2008). Influence of Staphylococcus aureus skin colonization on degree of sensitization in atopic dermatitis children. *Pol. Merkur. Lekarski.* 25, 51–56.

Margolis, D. J., and Mitra, N. (2017). Heterogeneity of data included in meta-analysis on persistence of atopic dermatitis changes interpretation. *J. Am. Acad. Dermatol.* 76:e181. doi: 10.1016/j.jaad.2016.11.068

Mizock, B. A. (2015). Probiotics. *Dis. Mon.* 61, 259–290. doi: 10.1016/j.disamonth.2015.03.011

Niers, L., Martin, R., Rijkers, G., Sengers, F., Timmerman, H., van Uden, N., et al. (2009). The effects of selected probiotic strains on the development of eczema (the PandA study). *Allergy* 64, 1349–1358. doi: 10.1111/j.1398-9995.2009.02021.x

Ogden, N. S., and Bielory, L. (2005). Probiotics: a complementary approach in the treatment and prevention of pediatric atopic disease. *Curr. Opin. Allergy Clin. Immunol.* 5, 179–184. doi: 10.1097/01.all.0000162312.64308.fc

Passeron, T., Lacour, J. P., Fontas, E., and Ortonne, J. P. (2006). Prebiotics and synbiotics: two promising approaches for the treatment of atopic dermatitis in children above 2 years. *Allergy* 61, 431–437. doi: 10.1111/j.1398-9995.2005.00956.x

Pessi, T., Sutas, Y., Hurme, M., and Isolauri, E. (2000). Interleukin-10 generation in atopic children following oral *Lactobacillus rhamnosus* GG. *Clin. Exp. Allergy* 30, 1804–1808. doi: 10.1046/j.1365-2222.2000.00948.x

Shafiei, A., Moin, M., Pourpak, Z., Gharagozlou, M., Aghamohammadi, A., Sajedi, V., et al. (2011). Synbiotics could not reduce the scoring of childhood atopic dermatitis (SCORAD): a randomized double blind placebo-controlled trial. *Iran. J. Allergy Asthma Immunol.* 10, 21–28.

Sidbury, R., and Khorsand, K. (2017). Evolving concepts in atopic dermatitis. *Curr. Allergy Asthma Rep.* 17, 42. doi: 10.1007/s11882-017-0710-5

Silverberg, N. B. (2016). A practical overview of pediatric atopic dermatitis, part 3: differential diagnosis, comorbidities, and measurement of disease burden. *Cutis* 97, 408–412.

Sistek, D., Kelly, R., Wickens, K., Stanley, T., Fitzharris, P., and Crane, J. (2006). Is the effect of probiotics on atopic dermatitis confined to food sensitized children? *Clin. Exp. Allergy* 36, 629–633. doi: 10.1111/j.1365-2222.2006.02485.x

Sung, M., Lee, K. S., Ha, E. G., Lee, S. J., Kim, M. A., Lee, S. W., et al. (2017). An association of periostin levels with the severity and chronicity of atopic dermatitis in children. *Pediatr Allergy Immunol.* doi: 10.1111/pai.12744. [Epub ahead of print].

Szajewska, H., and Mrukowicz, J. Z. (2003). Probiotics in prevention of antibiotic-associated diarrhea: meta-analysis. *J. Pediatr.* 142, 85.

Szajewska, H., Shamir, R., Turck, D., van Goudoever, J. B., Mihatsch, W. A., and Fewtrell, M. (2015). Recommendations on probiotics in allergy prevention should not be based on pooling data from different strains. *J. Allergy Clin. Immunol.* 136:1422. doi: 10.1016/j.jaci.2015.07.022

Totri, C. R., Eichenfield, L. F., Logan, K., Proudfoot, L., Schmitt, J., Lara-Corrales, I., et al. (2017). Prescribing practices for systemic agents in the treatment of severe pediatric atopic dermatitis in the US and Canada: The PeDRA TREAT survey. *J. Am. Acad. Dermatol.* 76, 281–285. doi: 10.1016/j.jaad.2016.09.021

Viljanen, M., Savilahti, E., Haahtela, T., Juntunen-Backman, K., Korpela, R., Poussa, T., et al. (2005). Probiotics in the treatment of atopic eczema/dermatitis syndrome in infants: a double-blind placebo-controlled trial. *Allergy* 60, 494–500. doi: 10.1111/j.1398-9995.2004.00514.x

Wang, I. J., and Wang, J. Y. (2015). Children with atopic dermatitis show clinical improvement after Lactobacillus exposure. *Clin. Exp. Allergy.* 45, 779–787. doi: 10.1111/cea.12489

Weidinger, S., and Novak, N. (2016). Atopic dermatitis. *Lancet.* 387, 1109–1122. doi: 10.1016/S0140-6736(15)00149-X

Weston, S., Halbert, A., Richmond, P., and Prescott, S. L. (2005). Effects of probiotics on atopic dermatitis: a randomised controlled trial. *Arch. Dis. Child.* 90, 892–897. doi: 10.1136/adc.2004.060673

Woo, S. I., Kim, J. Y., Lee, Y. J., Kim, N. S., and Hahn, Y. S. (2010). Effect of Lactobacillus sakei supplementation in children with atopic eczema-dermatitis syndrome. *Ann. Allergy Asthma Immunol.* 104, 343–348. doi: 10.1016/j.anai.2010.01.020

Wu, K. G., Li, T. H., and Peng, H. J. (2012). *Lactobacillus salivarius* plus fructo-oligosaccharide is superior to fructo-oligosaccharide alone for treating children with moderate to severe atopic dermatitis: a double-blind, randomized, clinical trial of efficacy and safety. *Br. J. Dermatol.* 166, 129–136. doi: 10.1111/j.1365-2133.2011.10596.x

Yesilova, Y., Calka, O., Akdeniz, N., and Berktas, M. (2012). Effect of probiotics on the treatment of children with atopic dermatitis. *Ann. Dermatol.* 24, 189–193. doi: 10.5021/ad.2012.24.2.189

Yoon, J. H., Nam, Y., Song, E. Y., Roh, E. Y., Yoon, H. S., and Shin, S. (2015). CCL28 cannot replace ige for severity by objective SCORAD index in atopic dermatitis in children. *Clin. Lab.* 61, 1577–1580. doi: 10.7754/Clin.Lab.2015.150311

Zhang, J., Guo, Z., Xue, Z., Sun, Z., Zhang, M., Wang, L., et al. (2015). A phylo-functional core of gut microbiota in healthy young Chinese cohorts across lifestyles, geography and ethnicities. *ISME J.* 9, 1979–1990. doi: 10.1038/ismej.2015.11

Zhang, Y. M., Chu, P., and Wang, W. J. (2017). PRISMA-combined alpha-blockers and antimuscarinics for ureteral stent-related symptoms: a meta-analysis. *Medicine* 96:e6098. doi: 10.1097/MD.0000000000006098

Conflict of Interest Statement: The authors declare that the research was conducted in the absence of any commercial or financial relationships that could be construed as a potential conflict of interest.

Copyright © 2017 Huang, Ning, Shen, Li, Zhang and Chen. This is an open-access article distributed under the terms of the Creative Commons Attribution License (CC BY). The use, distribution or reproduction in other forums is permitted, provided the original author(s) or licensor are credited and that the original publication in this journal is cited, in accordance with accepted academic practice. No use, distribution or reproduction is permitted which does not comply with these terms.

frontiers in Cellular and Infection Microbiology

REVIEW
published: 05 September 2017
doi: 10.3389/fcimb.2017.00387

Interactions of Intestinal Bacteria with Components of the Intestinal Mucus

*Jean-Félix Sicard[1], Guillaume Le Bihan[1], Philippe Vogeleer[1], Mario Jacques[2] and Josée Harel[1]**

[1] Centre de Recherche en Infectiologie Porcine et Aviaire, Faculté de Médecine Vétérinaire, Université de Montréal, Saint-Hyacinthe, QC, Canada, [2] Regroupement de Recherche Pour un Lait de Qualité Optimale (Op+Lait), Faculté de Médecine Vétérinaire, Université de Montréal, Saint-Hyacinthe, QC, Canada

The human gut is colonized by a variety of large amounts of microbes that are collectively called intestinal microbiota. Most of these microbial residents will grow within the mucus layer that overlies the gut epithelium and will act as the first line of defense against both commensal and invading microbes. This mucus is essentially formed by mucins, a family of highly glycosylated protein that are secreted by specialize cells in the gut. In this Review, we examine how commensal members of the microbiota and pathogenic bacteria use mucus to their advantage to promote their growth, develop biofilms and colonize the intestine. We also discuss how mucus-derived components act as nutrient and chemical cues for adaptation and pathogenesis of bacteria and how bacteria can influence the composition of the mucus layer.

Keywords: mucus, commensals, pathogens, biofilm, microbiota, microflora, goblet cells

INTRODUCTION

The gastrointestinal tract harbors a complex bacterial community called the intestinal microbiota that, in healthy conditions, maintains a commensal relationship with our body. Various mechanisms are used by the host to keep intestinal homeostasis and to prevent aberrant immune responses directed against the microbiota. One of these is the production of a mucus layer that covers the epithelial cells of the gut. This mucus is synthesized and secreted by host goblet cells and form an integral structural component of the mammal intestine. Its major function is to protect the intestinal epithelium from damage caused by food and digestive secretions (Deplancke and Gaskins, 2001). The mucus layer provides a niche for bacterial colonization because it contains attachment sites and is also a carbon source (Harel et al., 1993). Effectively, the mucus is a direct source of carbohydrates that are released in the lumen. Therefore, several bacterial species of the microbiota can use mucus glycan as a carbon source (Ouwerkerk et al., 2013). An alteration in glycan availability modifies the composition of the microbiota (Martens et al., 2008). The mucus layer also prevents pathogens from reaching and persisting on the intestinal epithelial surfaces and thereby is a major component of innate immunity. It is constantly renewed and acts as a trap for commensal residents, but also for pathogens, preventing their access to the epithelia (Johansson et al., 2008; Bertin et al., 2013). Although its composition and thickness vary along the gut, the mucus layer is mainly

Abbreviations: MLG, Mucus gel layer; A/E, Attaching and effacing; NAG, *N*-acetyl-D-glucosamine; NANA, *N*-acetylneuraminic acid; EHEC, Enterohemorrhagic *E. coli;* MUB, Mucus-binding proteins; LAB, Lactic acid bacteria; HBGA, Histoblood group antigen; SIgA, Secretory IgA; AIEC, Adherent invasive *E. coli;* LPB, LPS-binding protein; TLR, Toll-like receptor; VPI, *Vibrio* pathogenicity island.

OPEN ACCESS

Edited by:
Pascale Alard,
University of Louisville, United States

Reviewed by:
Valerio Iebba,
Sapienza Università di Roma, Italy
Bruce Vallance,
University of British Columbia, Canada

****Correspondence:***
Josée Harel
josee.harel@umontreal.ca

Received: *02 May 2017*
Accepted: *18 August 2017*
Published: *05 September 2017*

Citation:
Sicard J-F, Le Bihan G, Vogeleer P, Jacques M and Harel J (2017) Interactions of Intestinal Bacteria with Components of the Intestinal Mucus. Front. Cell. Infect. Microbiol. 7:387. doi: 10.3389/fcimb.2017.00387

formed of glycoproteins containing different glycans; nonspecific antimicrobial molecules, such as antimicrobial peptides (AMP); secreted antibodies targeting specific microbial antigens; and other intestinal proteins (McGuckin et al., 2011; Antoni et al., 2014). Interaction with the mucus layer is important for the colonization of gut commensals as well as some pathogens that have evolved to adhere to mucus and exploit it (Juge, 2012). Some pathogens also use mucus components as a cue to modulate the expression of virulence genes and thereby adapt to the host environment. In this Review, we describe the interactions between bacteria and components of the human mucus layer: their use as carbon sources, adhesion sites and their genetic adaptation (**Figure 1**).

THE GASTROINTESTINAL MUCUS

Mucus Composition

The intestinal mucus is composed mainly of mucins that are complex agglomerates of structural glycoproteins with specific O-linked glycans (O-glycans) produced by specialized cells of the host called goblet cells (Forstner, 1995). Mucins can either be secreted and form a gel, or be produced as membrane-bound glycoproteins that are part of the epithelial glycocalyx (Johansson et al., 2008, 2011; Jonckheere et al., 2013; Nilsson et al., 2014). These glycoproteins share a common structure made of tandem repeated amino acids rich in proline, threonine and serine and are call PTS domains. These sequences of amino acid provide sites for the covalent attachment of the polysaccharides and are widely *O*-glycosylated (Moran et al., 2011). Four different types of polysaccharide core structures are commonly found in mucin glycoproteins. These cores are formed by a combination of three polysaccharides, galactose, N-acetyl-galactosamine and N-acetyl-glucosamine (Larsson et al., 2009; Juge, 2012). Different chains of glycan will be attached to the core. The terminal monosaccharide is usually a fucose or a sialic acid (Larsson et al., 2009; Juge, 2012). Oligosaccharide chains are also sulfated, especially in colonic regions (Rho et al., 2005). The mucin proteins MUC1, MUC5AC, and MUC6 mainly form the mucus layer in the stomach, whereas MUC2 is the most abundant mucin in the small intestine and the colon (Johansson et al., 2009; Moran et al., 2011). The thickness of the mucus layer varies through the gut. The colon, which harbors the highest density of microorganisms, is covered by the thickest mucus layer (Gum et al., 1994). It is composed of an inner layer that is dense and firmly attached to the epithelium and an outer loose layer that is exposed to bacterial proteolytic activity. The numerous O-glycans of the outer layer can serve as adhesion sites and as nutrients for bacteria while the inner layer is less permissive to bacterial penetration in healthy individuals (Johansson et al., 2008, 2011). Most bacterial residents are present in the outer mucus layer and the competition for survival in this niche shapes the composition of the microbiota. The differential resource utilization of bacterial species participates to the establishment of distinct communities that includes non-mucolytic bacteria (Li et al., 2015).

Role of the Mucus Layer

The mucus barrier has an important role in regulating the severity of infectious diseases. It provides protection against many intestinal pathogens, including *Yersinia enterocolitica*, *Shigella flexneri*, *Salmonella*, and *Citrobacter rodentium* (Mantle and Rombough, 1993; Bergstrom et al., 2010; Arike and Hansson, 2016). MUC2 (Mouse, Muc2) plays a crucial role

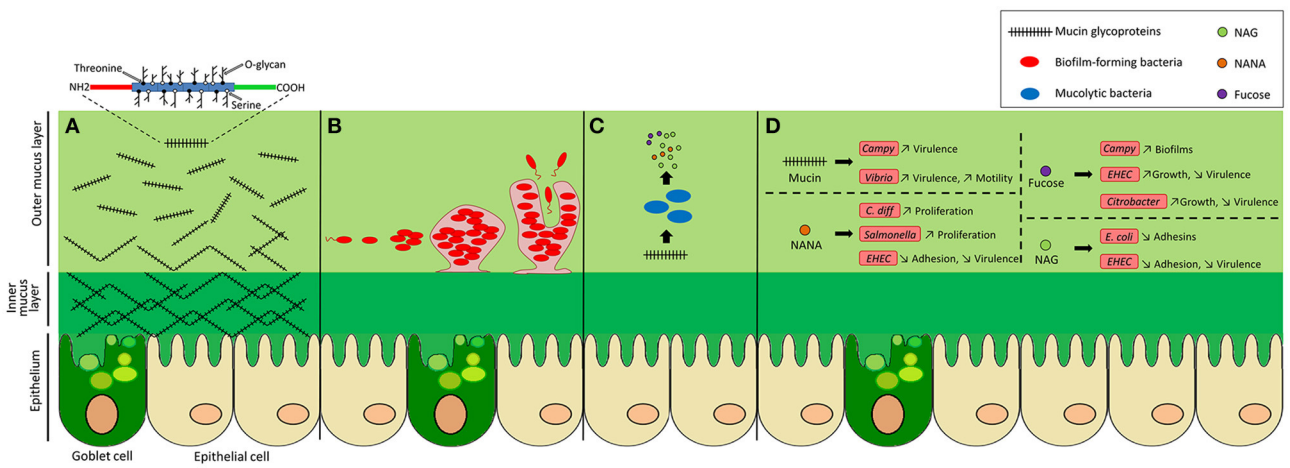

FIGURE 1 | Bacterial activities in the colonic mucus layer environment. The colonic epithelium is covered by a mucus gel layer formed of glycoproteins called mucins. **(A)** Mucins consist of a protein core and a high number of O-linked glycans. They are secreted by goblet cells and are assembled into a net-like structure that forms a dense inner layer, firmly attached to cells, that does not allow bacteria to penetrate. Further from the epithelium, the outer layer becomes loose and permissive, providing a niche for intestinal bacteria. **(B)** Mucus oligosaccharides can act as adhesion sites for bacteria, facilitating their colonization. Some bacteria are able to form microcolonies and biofilms. **(C)** Bacteria with mucolytic activity can release monosaccharides from mucin O-glycans and metabolize them. These sugars can also be utilized by nearby bacteria. **(D)** Mucus components can influence the behavior of pathogenic bacteria by increasing or decreasing their virulence expression, adhesion, motility, proliferation, or growth.

during infection. Using *Muc2*-deficient mice, it was shown that the glycoprotein is critical in controlling *Salmonella* infection (Zarepour et al., 2013). Moreover, $Muc2^{-/-}$ mice revealed higher susceptibility to attaching and effacing (A/E) *Citrobacter rodentium* infections (Bergstrom et al., 2010).

An alteration of mucosal integrity is generally associated with health problems, such as inflammatory bowel diseases, including ulcerative colitis and Crohn's disease (Trabucchi et al., 1986; Hanski et al., 1999). During ulcerative colitis, alteration of mucus integrity results in a thinner mucus layer due to goblet cell depletion (Pullan et al., 1994) and a reduced O-glycosylation and sulfation of mucins (Raouf et al., 1992; Larsson et al., 2011). During Crohn's disease, the mucus layer is essentially continuous and comparable to healthy mucosa (Strugala et al., 2008) although there is evidence of abnormal expression and glycosylation of the mucin (Buisine et al., 2001; Moehle et al., 2006; Dorofeyev et al., 2013). These changes in the mucosal environment could also be linked to dysbiosis, an abnormal change in the composition of the intestinal microbiota due to Crohn's disease. Once impaired, the mucus barrier becomes permeable to bacteria that are able to access the epithelium and therefore cause inflammation (Antoni et al., 2014; Johansson et al., 2014), which is why the integrity of the mucus layer is critical for the upkeep of a homeostatic relationship between the intestinal microbiota and its host.

MUCIN AS A GROWTH SUBSTRATE

Mucin proteins are highly glycosylated and therefore constitute a carbon and energy source for intestinal microbiota. A key nutritional aspect of the mucus layer for gut bacteria is its high polysaccharide content with up to 80% of the mucin biomass being composed of mostly O-linked glycans (Johansson et al., 2009, 2011; Marcobal et al., 2013).

Mucolytic Bacteria

A distinct subset of intestinal bacteria possesses the enzymatic activity, such as glycosidases, necessary for the degradation of mucin oligosaccharides, which can be further metabolized by resident microbiota (Koropatkin et al., 2012; Ouwerkerk et al., 2013). Indeed, various anaerobic bacteria species of gut microbiota, such as *Akkermansia muciniphila* (Derrien et al., 2004; Png et al., 2010), *Bacteroides thetaiotaomicron* (Xu et al., 2003; Sonnenburg et al., 2005), *Bifidobacterium bifidum* (Crociani et al., 1994; Png et al., 2010; Garrido et al., 2011), *Bacteroides fragilis* (Macfarlane and Gibson, 1991; Swidsinski et al., 2005a; Huang et al., 2011), *Ruminococcus gnavus* (Png et al., 2010; Crost et al., 2013), and *Ruminococcus torques* (Hoskins et al., 1985; Png et al., 2010) are now known as mucin-degrading specialists. These bacteria will use their specific enzymatic activities to release monosaccharides attached to the mucin glycoproteins. Some mucolytic bacteria, such as *B. thetaiotaomicron,* that possess an important variety of glycosidases, are better suited for the utilization of a wide range of glycans (Xu et al., 2003; Marcobal et al., 2013). To complete the degradation of mucins, a combination of enzymatic activity of several mucolytic bacteria is needed (Derrien et al., 2010; Marcobal et al., 2013). Therefore, MUC2 glycans act as nutritional sources for bacteria that can utilize the mucus-derived sugars, but lack the enzymes necessary for cleaving sugar linkages (Johansson et al., 2015; Arike and Hansson, 2016). Commonly, several bacteria collaborate in a community and it has been shown that the sulfatase activity of some commensal bacteria on sulfomucin allows glycosidases to access and act on mucins (Rho et al., 2005). Released saccharides, such as *N*-acetyl-D-glucosamine (GlcNAc also called NAG), *N*-acetylgalactosamine (GalNAc), galactose, fucose and sialic acid (*N*-acetylneuraminic acid also called NANA) can then be used by the degrader itself or by other resident bacteria (Bjursell et al., 2006; Martens et al., 2008; Sonnenburg et al., 2010). As example, commensal *E. coli* that are limited to growth on mono- or disaccharides, are unable to degrade the complex polysaccharides that constitute mucin (Hoskins et al., 1985) and therefore use such carbohydrate sources (Chang et al., 2004; Png et al., 2010; Bertin et al., 2013). Another example is vancomycin-resistant *Enterococcus* that can grow on mucin pre-digested with extracts from human stools, but not on purified mucin. This suggests that *Enterococcus* can benefit of the microbiota activity on mucin and uses released mucus-derived products (Pultz et al., 2006). In this way, mucolytic bacteria make mucus O-glycan derived products also available for other bacterial residents.

Use of Mucus-Derived Nutrients by Pathogens

Intestinal pathogens have developed strategies to compete with commensal microflora for nutrients, such as carbohydrates and these strategies have been reviewed in Conway and Cohen (2015), Vogt et al. (2015), and Baumler and Sperandio (2016). Pathogenic and commensal *E. coli* strains displayed considerable catabolic diversity when colonizing streptomycin-treated mice, indicating that nutrient availability can influence their colonization success and their niche adaptation (Maltby et al., 2013). For example, pathogenic *E. coli* such as enterohemorrhagic *E. coli* (EHEC) strain EDL933 efficiently utilizes some mucus-derived monosaccharides. This can provide competitive growth compared to that of commensal *E. coli* (Fabich et al., 2008). Moreover, the metabolic flexibility of some pathogenic strains to use both glycolytic and gluconeogenic nutrients may be advantageous (Bertin et al., 2013). The pathogen *Vibrio cholerae*'s preferential use of mucus-derived monosaccharides, such as GlcNAc and sialic acid confers an advantage in the infant mouse model of infection (Almagro-Moreno et al., 2015). *C. jejuni* also possess the ability to metabolize fucose. Its growth is enhanced in culture medium supplemented with it (Alemka et al., 2012). In addition, antibiotic treatment also perturbs the microbiota and therefore affects the availability of mucin carbohydrates. The concentration of free fucose and sialic acid reaching high levels during antibiotic treatment facilitates expansion of pathogens such as *Salmonella enterica* serotype Typhimurium and *Clostridium difficile* (Ng et al., 2013). In addition, *Salmonella* serotype Typhimurium is known both to bind glycoprotein containing sialic acids (Vimal et al., 2000) and to have the ability to release the carbohydrate using its sialidase (Hoyer et al.,

1992). Thereby, to colonize specific niches, many pathogens have evolved in a way to use mucus-derived sugars as a carbon source.

BACTERIAL ADHESION TO MUCINS

Mucins proteins are highly glycosylated. Their O-glycans are used as ligands for bacterial adhesins (Juge, 2012). It can be speculated that adhesion to mucins may initiate colonization of the intestine. The carbohydrate structures on mucins can provide initial attachment site to bacteria including specialized pathogens and could facilitate the invasion of epithelial cells (Derrien et al., 2010). As example, pathogenic microorganisms, such as *Campylobacter* and enterotoxinogenic *E. coli* (ETEC) are known to adhere to the glycoprotein MUC1 that is present in human breast milk. This interferes with colonization of these pathogens in the infant GI tract (Martin-Sosa et al., 2002; Ruiz-Palacios et al., 2003). Although no specific mucus-adherent microflora was identified (van der Waaij et al., 2005), there are evidence that bacteria can bind directly to mucins by expressing specific proteins, pili, fimbriae and flagella (**Table 1**).

Interactions between Mucin and Surface Proteins

To adhere to mucus, commensal and pathogenic bacteria use different strategies. First, they can produce proteins that specifically bind the mucus. Mucus-binding proteins (MUB) are cell-surface proteins mainly described in lactic acid bacteria (LAB) (Boekhorst et al., 2006), especially in *Lactobacillus reuteri* (Roos and Jonsson, 2002; MacKenzie et al., 2009). MUB contain domains that are similar to the model mucin-binding protein (MucBP) from the Pfam database (Boekhorst et al., 2006). The MucBP domain is found in a variety of bacterial proteins that are known for their capacity to adhere to mucus (Juge, 2012). MUB also share structural and functional homology with pathogenic Gram-positive adhesins that have specificity to sialylated mucin glycans (Etzold et al., 2014). For example, some surface proteins of *Listeria monocytogenes* contain a MucBP domain similar to those found in *Lactobacillus*, allowing them to adhere to mucin (Bierne et al., 2007; Mariscotti et al., 2014). The causative agent of cholera, *V. cholerae*, can also bind to mucin using surface protein called GbpA (chitin-binding protein) that binds specifically to N-acetyl D-glucosamine residues of intestinal mucins (Bhowmick et al., 2008). In addition, *C. jejuni* is well-known for its ability to interact with different human histoblood group antigens (HBGAs) expressed in mucosa (Naughton et al., 2013). The major outer membrane protein (MOMP) of *C. jejuni* is involved in these interactions (Mahdavi et al., 2014). This way, *C. jejuni* can interact with intestinal mucin MUC2 in the intestine (Tu et al., 2008). Furthermore, *Bifidobacterium* spp. is also known for its specific adhesion to mucus. For example, in a *B. bifidum* mucin-binding assay, the expression of an extracellular transaldolase correlated with a positive

TABLE 1 | Bacterial adhesion to mucin components.

Bacteria		Adhesin	Mucin glycoprotein	Mucin component	References
COMMENSAL BACTERIA					
Bacteroides fragilis					Huang et al., 2011
Bifidobacterium bifidum		Extracellular transaldolase			Marcobal et al., 2013
Bifidobacterium longum subsp. *infantis*		Family 1 of solute binding proteins		Mucin oligosaccharides	Garrido et al., 2011
Escherichia coli Nissle 1917		Flagellum			Troge et al., 2012
Lactic acid bacteria		MUB			Boekhorst et al., 2006
		Pili			Kankainen et al., 2009; Le et al., 2013
PATHOGENS					
Campylobacter jejuni		Carbohydrate-lectin, FlaA, MOMP	MUC2		Tu et al., 2008; Naughton et al., 2013; Mahdavi et al., 2014
Clostridium difficile		FliC		Cecal mucus	Tasteyre et al., 2001
		FliD			
Escherichia coli	UPEC CFT073	F9 fimbriae		Galβ1-3GlcNAc structures	Wurpel et al., 2014
	EPEC E2348/69	H6 flagella	MUC2	Mucin-type core 2 O-glycan	Erdem et al., 2007; Ye et al., 2015
	EHEC EDL933	H7 flagella	MUC2	Mucin-type core 2 O-glycan	Erdem et al., 2007; Ye et al., 2015
Listeria monocytogenes		LPXTG-internalin proteins (MucBP) LmiA			Bierne et al., 2007; Mariscotti et al., 2014
Salmonellae enterica serotype Typhimurium		Fimbrial adhesin (std operon)		Alpha1-2 fucosylated receptor(s)	Chessa et al., 2009
Vibrio cholerae		Vibrio polysaccharide (VPS)			Liu et al., 2015
		Chitin-binding protein (GbpA)		N-acetyl D-glucosamine	Bhowmick et al., 2008

mucin-binding phenotype (Gonzalez-Rodriguez et al., 2012). *B. longum* subsp. *infantis* is another species that binds specifically to mucin using family-1 solute binding proteins (Kankainen et al., 2009). Interestingly, a study using gnotobiotic mice colonized by *B. fragilis* and *E. coli* revealed that the commensal bacterium *B. fragilis* was found in the mucus layer while *E. coli* was only found in the lumen. Further analysis showed that *B. fragilis* specifically binds to highly purified mucins. This indicated that a direct bond with intestinal mucus could be a mechanism used by *B. fragilis* for gut colonization (Huang et al., 2011).

Interactions between Mucin and Pili/Fimbriae

In addition to produce specific mucus binding proteins, some bacteria can also use cell-surface appendix, such as pili or fimbriae to bind the mucus. For example, production of pili by LAB was shown to be implicated in mucus-binding activity (Douillard et al., 2013) and moreover, the SpaC pilus protein of *L. rhamnosus* GG was shown to strongly binds the human mucins (Kankainen et al., 2009). An *in vitro* study using mucus-secreting HT29-MTX intestinal epithelial cell model showed that the adhesion of *Salmonellae enterica* serotype Typhimurium to mucus-secreting intestinal epithelial cells was higher than in non- and low-mucus producing cells (Gagnon et al., 2013). Moreover, virulent strains seem to bind more efficiently to mucus than avirulent strains and the binding that preferentially targets the neutral mucin is mannose-dependant (Vimal et al., 2000). As with some uropathogenic *E. coli* (Wurpel et al., 2014), the adhesion of *S. enterica* serotype Typhimurium could be the result of interaction between fimbrial adhesin and mucin glycans, more specifically terminal fucose residues (Chessa et al., 2009). The *E. coli* K88 (F4) fimbriae is also able to bind mucus from the small intestines of 35-day-old piglets with a specificity to the glycolipid galactosylceramide (Blomberg et al., 1993). Hence, pili and fimbriae are involved in specific adhesion to mucus.

Interactions between Mucin and Flagella

Many enteric bacteria also produce flagellum. In addition to their role in motility, flagella are also involved in adhesion. As example, the *E. coli* probiotic strain Nissle 1917 was shown to be able to interact, via its flagella, with human and porcine mucus but not with murine mucus. Furthermore, the mucus component gluconate has been identified as one receptor for the adhesion of these flagella (Troge et al., 2012). Other studies have revealed the role of the flagella for the binding of mucin glycoproteins by *C. difficile* (Tasteyre et al., 2001) and pathogenic *E. coli* (Erdem et al., 2007). Indeed, a mutation of the flagellum element *fliC* prevents the adhesion of EPEC and EHEC to mucins (Erdem et al., 2007). More recently, the flagella of EPEC (O127:H6) and EHEC (O157:H7) were shown to adhere to mucin-type core 2 O-glycan in MUC2. *C. jejuni* is another pathogen that uses its flagella to bind mucin. It was showed that the major flagella subunit protein (FlaA) is also involved in the adhesion to HBGA in the mucus. Therefore, flagella can be used in attachment strategies by gut residents.

BACTERIAL BIOFILM AND MUCUS

There are more mucus-associated bacteria in the proximal region of the colon than in distal colonic sites. Among the complex microbial communities within the gut, some are believed to form mucosal biofilm, that is a complex and self-produced polymeric matrix where microorganisms can attach to each other and be attached to the mucosal surface (de Vos, 2015). The rapid growth of the intestinal mucus and the lack of effective preservation techniques complicated the study investigating biofilms in healthy individuals (Bollinger et al., 2007; de Vos, 2015). However, biofilms were observed in artificial mucin gels that simulate the proximal and distal colon (Macfarlane et al., 2005), and also by electron microscopy in uninflamed proximal large bowel of mice (Swidsinski et al., 2005a), rat, baboon, and humans (Palestrant et al., 2004). Some evidence, such as the rates of plasmids transfer and the expression of colonization factors by gut bacteria, plead for the presence of biofilms in the gut (Macfarlane et al., 1997; Licht et al., 1999; Hooper and Gordon, 2001). In addition, components of the mucus layer, such as secretory IgA (SIgA) and mucins are likely to play a role in biofilm formation as they have been shown to modulate biofilm production *in vitro* (Bollinger et al., 2003, 2006; Slizova et al., 2015). Moreover, adherence of bacteria to mucin proteins could lead to growth of microcolonies that could further develop into biofilms (Kleessen and Blaut, 2007). Biofilms could also be formed on the surface of intestinal or gastric epithelia and interact with the secreted or membrane-bound mucins.

Alteration of the mucus layer occurs in cases of inflammatory bowel diseases (Bodger et al., 2006; Baumgart et al., 2007; Sheng et al., 2012). The increased presence of *B. fragilis* group and *Enterobacteriaceae* and their ability to form biofilms could play a role in these diseases (Swidsinski et al., 2005b, 2009). Within the *Enterobacteriaceae* family, the adherent-invasive *E. coli* (AIEC) strains associated with Crohn's disease (Masseret et al., 2001; Darfeuille-Michaud et al., 2004; Eaves-Pyles et al., 2008; Martinez-Medina et al., 2009a), are shown to be higher biofilm producers than non-AIEC strains (Martinez-Medina et al., 2009b). As with inflammatory bowel diseases, impaired mucin production is related to colorectal cancer (Weiss et al., 1996; Kim and Ho, 2010) that is also linked to the presence of bacterial biofilms (Dejea et al., 2014). Altogether, these studies show that biofilms could play a key role in bacterial colonization of the healthy gut and in intestinal diseases.

ROLE OF MUCIN COMPONENTS IN MODULATION OF BACTERIAL VIRULENCE

In addition to acting as a carbon source or as receptors, mucin glycoprotein can influence the expression of different genes implicated in colonization and pathogenicity (Vogt et al., 2015). As example, MUC2 in the mucus layer can play a modulatory role in the pathogenesis of pathogens. Indeed, the ability of *S. enterica* serotype Typhimurium to cause cecal pathology in muc2$^{-/-}$ mice is more dependent on its *invA* gene, coding a *Salmonella* inner membrane protein component of the SPI-1 type

3 secretion system, than it is in wild-type mice (Zarepour et al., 2013). *C. jejuni* can also utilize mucin proteins as a signal to modulate the expression of its virulence factors. Many virulence genes of this pathogen are upregulated in the presence of MUC2 glycoprotein (Tu et al., 2008). Another example is the ability of *V. cholerae* to downregulate the expression of *vps*, coding for its polysaccharide, in response to mucosal signaling and inversely promoting motility in the mucus (Liu et al., 2015). Mucin also activates the two-component sensor histidine kinase ChiS in *V. cholera*. ChiS is the regulator of the chitinases and the chitin utilization pathway, but also plays a role in the virulence of the bacteria since the mutant strain is hypovirulent (Chourashi et al., 2016). Released monosaccharides from mucin O-glycans degradation can also act as a chemical cue to help pathogens to sense their environment and adapt accordingly. As such, sialic acid and GlcNAc are signals that regulate type 1 fimbriae gene expression and curli activity in *E. coli* (Barnhart et al., 2006; Konopka, 2012). GlcNAc and sialic acid also play roles in the virulence of EHEC. In aerobic condition, these mucin-derived sugars inhibit EHEC adhesion to epithelial cells. These amino sugars also repress the expression of genes of the locus of enterocyte effacement (LEE) via the transcriptional regulator NagC involved in the regulation of NAG catabolism (Le Bihan et al., 2017). In contrast, as the sole carbon sources under microaerobic conditions, sialic acid and NAG were shown to stimulate the production of EspB, an effector of the LEE (Carlson-Banning and Sperandio, 2016). EHEC and *C. rodentium* also sense fucose by a two-component system FusKR. It represses the expression of virulence genes while promoting growth (Pacheco et al., 2012; Keeney and Finlay, 2013). Moreover, it was also shown that fucose influences chemotaxis and biofilm formation of *C. jejuni* that are important during infection (Dwivedi et al., 2016). Thus, mucus and its derived sugars can play a role in the expression of virulence genes by pathogens.

MODULATION OF MUCIN COMPOSITION BY BACTERIA

Microbial molecular exchange with the host influences mucin composition. Several bacterial effectors can modulate the expression of mucin by mucus-producing cells (**Table 2**). Studies

TABLE 2 | Effects of bacterial effectors on mucin.

Bacteria		Effector	Target	Effect on mucin	References
Campylobacter jejuni			Distal colonic biopsies	Increased expression of MUC1	Linden et al., 2008
Clostridium difficile			Distal colonic biopsies	Increased expression of MUC1	Linden et al., 2008
		ToxA	HT-29 cells	Decrease of mucin exocytosis	Kelly et al., 1994; Branka et al., 1997
E. coli	EAEC	Secreted protein Pic	Hog gastric, bovine sub-maxillary and crude mouse large intestine mucin	Mucinase activity / Degradation	Henderson et al., 1999; Harrington et al., 2009
			Goblet cells	Secretagogue activity/Hypersecretion	Navarro-Garcia et al., 2010
	ETEC	Secreted EatA	Purified MUC2	Degradation of MUC2	Kumar et al., 2014
	AIEC (LF82)		T84 cells	Diminished expression of MUC2 and MUC5A	Elatrech et al., 2015
	EHEC (O157:H7)	Adhesion	HT-29 cells	Increased expression of MUC2	Xue et al., 2014
Lacto-bacillus	*plantarum* 299v		HT-29 cells	Increased MUC2 secretion	Mack et al., 1999
	rhamnosus GG		HT-29 cells	Increased MUC2 secretion	Mack et al., 1999
	casei GG		Caco-2 cells	Increased MUC2 secretion	Mattar et al., 2002
Listeria monocytogenes		Listeriolysin O (LLO)	HT29-MTX cells	Increased transcription of MUC3, MUC4 and MUC12 Increased secretion of MUC5A	Coconnier et al., 1998; Lievin-Le Moal et al., 2002, 2005
Salmonella St Paul			Distal colonic biopsies	Increased expression of MUC1	Linden et al., 2008
Shigella flexneri		SST3	Mucin-producing polarized human intestinal epithelial cells	Alteration of glycosylation/ Increased permeability	Sperandio et al., 2013
		Secreted protein Pic	Hog gastric, bovine sub-maxillary, crude mouse large-intestine mucin	Mucinase activity / Degradation	Henderson et al., 1999; Harrington et al., 2009
			Goblet cells	Secretagogue activity / Hypersecretion	Navarro-Garcia et al., 2010
Vibrio cholerae		Toxin CT	Goblet cells	Increased mucin secretion	Lencer et al., 1990; Epple et al., 1997
		Secreted TagA	LS174T goblet cell surface mucin	Cleaves mucin glycoproteins	Szabady et al., 2011
Yersinia enterocolitica		Virulence Plasmid	Rabbit small intestinal mucin	Degradation/Solubilisation	Mantle and Rombough, 1993

using germ-free rats revealed that the presence of microflora through the gastro intestinal tract has a strong and positive influence on the thickness and composition of the mucin (Szentkuti et al., 1990; Enss et al., 1992; Sharma et al., 1995). Different probiotic agents, such as *Lactobacillus* species, can stimulate the production of MUC2 and thereby the secretion of mucin in the intestine, improving pathogen resistance (Mack et al., 1999; Mattar et al., 2002; Caballero-Franco et al., 2007). Other commensal bacteria, such as *B. thetaiotaomicron* can increase the differentiation of goblet cells and their mucus-related gene expression (Wrzosek et al., 2013). Moreover, bacterial fermentation products, such as short-chain fatty acids (SCFAs) like butyrate and propionate enhance the production of MUC2 by the goblet cell in the gut (Barcelo et al., 2000; Burger-van Paassen et al., 2009). This could explain the therapeutic effect of butyrate in colitis where the mucin layer is altered (Finnie et al., 1995). Therefore, commensal residents are important in the maintenance of the mucus layer integrity.

Modulation of Mucin by Pathogens

Pathogens have also adapted mechanisms to modulate mucin secretion to enhance pathogenesis by acting on the mucin-secreting cells, altering or inhibiting mucin production (**Table 2**). One of them is *S. flexneri* that alters the mucus layer through a type III secretion system-dependent manner. This pathogen will act on different elements, such as gene expression, mucin glycosylation and secretion, leading to a less effective mucus barrier (Sperandio et al., 2013). *C. difficile* produces a toxin, ToxA that is responsible for barrier dysfunction and causes severe inflammatory enteritis. ToxA also decreases the mucin exocytosis of colonic mucus-producing cells (Kelly et al., 1994; Branka et al., 1997). The recognition of bacterial components by these cells can also lead to an increased production and secretion of mucin in order to harm the present pathogen. As example, the adhesion of the EHEC O157:H7 to human colon cells HT-29 leads to an increased expression of MUC2 (Xue et al., 2014). Moreover, the cholera toxin of *V. cholerae* and lysteriolysin O of *L. monocytogenes* enhance the secretion of mucin by goblet cells and HT29-MTX cells, respectively (Lencer et al., 1990; Epple et al., 1997; Coconnier et al., 1998; Lievin-Le Moal et al., 2002, 2005). Surprisingly, the Pic protein secreted by *S. flexneri* and enteroaggregative *E. coli* (Henderson et al., 1999; Harrington et al., 2009) is known for its mucolytic activity, but is also a potent mucus secretagogue that induced hypersecretion of mucus by goblet cells (Navarro-Garcia et al., 2010). These studies show how pathogens can affect the behavior of mucus-producing cells in their advantage.

Mucin Degradation by Pathogens

Pathogens also developed specific mechanisms to subvert and penetrate the mucus barrier. Some bacteria can directly act on the mucin through a mucinase activity. During enterotoxigenic *E. coli* infections, the autotransporter A (EatA) is involve in mucin degradation and this participate to the delivery of *E. coli* toxins to the cell surface (Kumar et al., 2014). Another example is the adherent and invasive *E. coli* strain LF82, associated with Crohn's disease. LF82 possesses a protease called Vat-AIEC that is implicated in the degradation of mucins and therefore decreases mucus viscosity (Gibold et al., 2016). The Pic autotransporter found in enteroaggregative *E. coli* and *Shigella flexneri* can also degrade various glycoproteins including mucins (Henderson et al., 1999; Harrington et al., 2009). Moreover, the plasmid-bearing *Yersinia enterocolitica*, which contain mucin-degrading enzyme(s), will increase the permeability of the mucus gel layer, allowing the bacteria to move more easily through the mucin (Mantle and Rombough, 1993). *V. cholerae* also produces a secreted protease called TagA that is encoded by the *Vibrio* pathogenicity island (VPI). TagA specifically cleaves mucin glycoproteins and may directly modify host cell surface molecules during *V. cholerae* infection (Szabady et al., 2011). Therefore, to facilitate their infection process, pathogens can directly modify the mucus.

Inflammation and Mucins

Pathogens associated molecular patterns, such as lipopolysaccharide (LPS) and peptidoglycan are also known to stimulate mucin production (Petersson et al., 2011). This stimulation can occur directly on secreting cells, but also be through proinflammatory cytokine production. Recognition of LPS by LPS-binding protein (LBP), CD14, and TLR4 (Toll-Like Receptor) leads to a strong pro-inflammatory response in mammalian cells. LPS has been shown to induce mucin gene expression by binding to TLR4 and LBP (Dohrman et al., 1998; Smirnova et al., 2003). LPS and flagellin from Gram-negative bacteria as well as lipoteichoic acid, a component of the cell wall of Gram-positive bacteria, induce mucin upregulation through the Ras pathway (McNamara and Basbaum, 2001; Theodoropoulos and Carraway, 2007). LPS also increases the production of IL-8 by goblet cells, which leads to secretion of mucin (Smirnova et al., 2003). In addition, pro-inflammatory cytokine IL-6 and TNF-α increase secretion of MUC2, MUC5A, MUC5B, and MUC6 by the intestinal cell line *LS180* despite a reduced glycosylation (Enss et al., 2000). Inflammation could be one of the aspects affecting the integrity of the mucus layer in inflammatory bowel diseases. Furthermore, the AIEC strain LF82 is able to alter the expression of the mucin gene and IL-8 of colonic cells T84 that could also lead to a defective mucus layer (Elatrech et al., 2015). Thus, pathogens can also alter the mucus production indirectly, through inflammation.

CONCLUSION

Intestinal bacteria have adapted to colonize the mucus layer by adhering to intestinal mucus components, using mucus-derived nutrients and sensing chemical cues for adaptation. In many ways, pathogenic bacteria have used these strategies for successful infection. There has been growing recognition of the important role played by the mucus barrier and microbiota and their interaction with the pathogens in regulating the severity of infectious diseases. But, the precise mechanisms by which enteric bacterial pathogens interact with mucus components in combination with the microbiota activity are being investigated. As the mucus layer acts as a first line of defense against enteric bacteria, further investigations are needed to understand the interactions between pathogens, microbiota and the mucus layer, in order to develop efficient therapeutic strategies. Identifying

and characterizing specific mucin signal(s) and corresponding regulatory adaptation and virulence responses could contribute to the development of new anti-infective strategies. In doing so, other weapons could be added to the arsenal against intestinal pathogens.

AUTHOR CONTRIBUTIONS

All authors listed have made a substantial, direct and intellectual contribution to the work, and approved it for publication. The manuscript was written by J-FS and JH and was duly revised by GLB, PV and MJ.

ACKNOWLEDGMENTS

We thank Judith Kashul for editing the manuscript. This research was supported by a Team grant from the Fonds de Recherche du Québec, Nature et Technologies (FRQNT PT165375), to JH and MJ and by the Discovery grant program of the Natural Sciences and Engineering Research Council of Canada (RGPIN-2015-05373 to JH and RGPIN-2016-04203 to MJ). J-FS is a recipient of a scholarship from the NSERC Collaborative Research and Training Experience Program in Milk Quality; and PV is a recipient of a scholarship from the FRQNT Québec Wallonie program.

REFERENCES

Alemka, A., Corcionivoschi, N., and Bourke, B. (2012). Defense and adaptation: the complex inter-relationship between *Campylobacter jejuni* and mucus. *Front. Cell Infect. Microbiol.* 2:15. doi: 10.3389/fcimb.2012.00015

Almagro-Moreno, S., Pruss, K., and Taylor, R. K. (2015). Intestinal colonization dynamics of *Vibrio cholerae*. *PLoS Pathog.* 11:e1004787. doi: 10.1371/journal.ppat.1004787

Antoni, L., Nuding, S., Wehkamp, J., and Stange, E. F. (2014). Intestinal barrier in inflammatory bowel disease. *World J. Gastroenterol.* 20, 1165–1179. doi: 10.3748/wjg.v20.i5.1165

Arike, L., and Hansson, G. C. (2016). The densely o-glycosylated MUC2 mucin protects the intestine and provides food for the commensal bacteria. *J. Mol. Biol.* 428, 3221–3229. doi: 10.1016/j.jmb.2016.02.010

Barcelo, A., Claustre, J., Moro, F., Chayvialle, J. A., Cuber, J. C., and Plaisancie, P. (2000). Mucin secretion is modulated by luminal factors in the isolated vascularly perfused rat colon. *Gut* 46, 218–224. doi: 10.1136/gut.46.2.218

Barnhart, M. M., Lynem, J., and Chapman, M. R. (2006). GlcNAc-6P levels modulate the expression of Curli fibers by *Escherichia coli*. *J. Bacteriol.* 188, 5212–5219. doi: 10.1128/JB.00234-06

Baumgart, M., Dogan, B., Rishniw, M., Weitzman, G., Bosworth, B., Yantiss, R., et al. (2007). Culture independent analysis of ileal mucosa reveals a selective increase in invasive *Escherichia coli* of novel phylogeny relative to depletion of *Clostridiales* in Crohn's disease involving the ileum. *ISME J.* 1, 403–418. doi: 10.1038/ismej.2007.52

Baumler, A. J., and Sperandio, V. (2016). Interactions between the microbiota and pathogenic bacteria in the gut. *Nature* 535, 85–93. doi: 10.1038/nature18849

Bergstrom, K. S., Kissoon-Singh, V., Gibson, D. L., Ma, C., Montero, M., Sham, H. P., et al. (2010). MUC2 protects against lethal infectious colitis by disassociating pathogenic and commensal bacteria from the colonic mucosa. *PLoS Pathog.* 6:e1000902. doi: 10.1371/journal.ppat.1000902

Bertin, Y., Chaucheyras-Durand, F., Robbe-Masselot, C., Durand, A., de la Foye, A., Harel, J., et al. (2013). Carbohydrate utilization by enterohaemorrhagic *Escherichia coli* O157:H7 in bovine intestinal content. *Environ. Microbiol.* 15, 610–622. doi: 10.1111/1462-2920.12019

Bhowmick, R., Ghosal, A., Das, B., Koley, H., Saha, D. R., Ganguly, S., et al. (2008). Intestinal adherence of *Vibrio cholerae* involves a coordinated interaction between colonization factor GbpA and mucin. *Infect. Immun.* 76, 4968–4977. doi: 10.1128/IAI.01615-07

Bierne, H., Sabet, C., Personnic, N., and Cossart, P. (2007). Internalins: a complex family of leucine-rich repeat-containing proteins in *Listeria* monocytogenes. *Microbes Infect.* 9, 1156–1166. doi: 10.1016/j.micinf.2007.05.003

Bjursell, M. K., Martens, E. C., and Gordon, J. I. (2006). Functional genomic and metabolic studies of the adaptations of a prominent adult human gut symbiont, *Bacteroides thetaiotaomicron*, to the suckling period. *J. Biol. Chem.* 281, 36269–36279. doi: 10.1074/jbc.M606509200

Blomberg, L., Krivan, H. C., Cohen, P. S., and Conway, P. L. (1993). Piglet ileal mucus contains protein and glycolipid (galactosylceramide) receptors specific for *Escherichia coli* K88 fimbriae. *Infect. Immun.* 61, 2526–2531.

Bodger, K., Halfvarson, J., Dodson, A. R., Campbell, F., Wilson, S., Lee, R., et al. (2006). Altered colonic glycoprotein expression in unaffected monozygotic twins of inflammatory bowel disease patients. *Gut* 55, 973–977. doi: 10.1136/gut.2005.086413

Boekhorst, J., Helmer, Q., Kleerebezem, M., and Siezen, R. J. (2006). Comparative analysis of proteins with a mucus-binding domain found exclusively in lactic acid bacteria. *Microbiology* 152(Pt 1), 273–280. doi: 10.1099/mic.0.28415-0

Bollinger, R. R., Barbas, A. S., Bush, E. L., Lin, S. S., and Parker, W. (2007). Biofilms in the normal human large bowel: fact rather than fiction. *Gut* 56, 1481–1482.

Bollinger, R. R., Everett, M. L., Palestrant, D., Love, S. D., Lin, S. S., and Parker, W. (2003). Human secretory immunoglobulin A may contribute to biofilm formation in the gut. *Immunology* 109, 580–587. doi: 10.1046/j.1365-2567.2003.01700.x

Bollinger, R. R., Everett, M. L., Wahl, S. D., Lee, Y. H., Orndorff, P. E., and Parker, W. (2006). Secretory IgA and mucin-mediated biofilm formation by environmental strains of *Escherichia coli*: role of type 1 pili. *Mol. Immunol.* 43, 378–387. doi: 10.1016/j.molimm.2005.02.013

Branka, J. E., Vallette, G., Jarry, A., Bou-Hanna, C., Lemarre, P., Van, P. N., et al. (1997). Early functional effects of *Clostridium* difficile toxin A on human colonocytes. *Gastroenterology* 112, 1887–1894. doi: 10.1053/gast.1997.v112.pm9178681

Buisine, M. P., Desreumaux, P., Leteurtre, E., Copin, M. C., Colombel, J. F., Porchet, N., et al. (2001). Mucin gene expression in intestinal epithelial cells in Crohn's disease. *Gut* 49, 544–551. doi: 10.1136/gut.49.4.544

Burger-van Paassen, N., Vincent, A., Puiman, P. J., van der Sluis, M., Bouma, J., Boehm, G., et al. (2009). The regulation of intestinal mucin MUC2 expression by short-chain fatty acids: implications for epithelial protection. *Biochem. J.* 420, 211–219. doi: 10.1042/BJ20082222

Caballero-Franco, C., Keller, K., De Simone, C., and Chadee, K. (2007). The VSL#3 probiotic formula induces mucin 554 gene expression and secretion in colonic epithelial cells. *Am. J. Physiol. Gastrointest. Liver Physiol.* 292, G315–G322. doi: 10.1152/ajpgi.00265.2006

Carlson-Banning, K. M., and Sperandio, V. (2016). Catabolite and oxygen regulation of enterohemorrhagic *Escherichia coli* virulence. *MBio* 7:e01852-16. doi: 10.1128/mBio.01852-16

Chang, D. E., Smalley, D. J., Tucker, D. L., Leatham, M. P., Norris, W. E., Stevenson, S. J., et al. (2004). Carbon nutrition of *Escherichia coli* in the mouse intestine. *Proc. Natl. Acad. Sci. U.S.A.* 101, 7427–7432. doi: 10.1073/pnas.0307888101

Chessa, D., Winter, M. G., Jakomin, M., and Baumler, A. J. (2009). *Salmonella enterica* serotype Typhimurium Std fimbriae bind terminal α(1,2)fucose residues in the cecal mucosa. *Mol. Microbiol.* 71, 864–875. doi: 10.1111/j.1365-2958.2008.06566.x

Chourashi, R., Mondal, M., Sinha, R., Debnath, A., Das, S., Koley, H., et al. (2016). Role of a sensor histidine kinase ChiS of *Vibrio cholerae* in pathogenesis. *Int. J. Med. Microbiol.* 306, 657–665. doi: 10.1016/j.ijmm.2016.09.003

Coconnier, M. H., Dlissi, E., Robard, M., Laboisse, C. L., Gaillard, J. L., and Servin, A. L. (1998). *Listeria* monocytogenes stimulates mucus exocytosis in cultured human polarized mucosecreting intestinal cells through action of listeriolysin O. *Infect. Immun.* 66, 3673–3681.

Conway, T., and Cohen, P. S. (2015). Commensal and pathogenic *Escherichia coli* metabolism in the gut. *Microbiol. Spectr.* 3, 343–362. doi: 10.1128/microbiolspec.MBP-0006-2014

Crociani, F., Alessandrini, A., Mucci, M. M., and Biavati, B. (1994). Degradation of complex carbohydrates by *Bifidobacterium* spp. *Int. J. Food Microbiol.* 24, 199–210. doi: 10.1016/0168-1605(94)90119-8

Crost, E. H., Tailford, L. E., Le Gall, G., Fons, M., Henrissat, B., and Juge, N. (2013). Utilisation of mucin glycans by the human gut symbiont Ruminococcus gnavus is strain-dependent. *PLoS ONE* 8:e76341. doi: 10.1371/journal.pone.0076341

Darfeuille-Michaud, A., Boudeau, J., Bulois, P., Neut, C., Glasser, A. L., Barnich, N., et al. (2004). High prevalence of adherent-invasive *Escherichia coli* associated with ileal mucosa in Crohn's disease. *Gastroenterology* 127, 412–421. doi: 10.1053/j.gastro.2004.04.061

Dejea, C. M., Wick, E. C., Hechenbleikner, E. M., White, J. R., Mark Welch, J. L., Rossetti, B. J., et al. (2014). Microbiota organization is a distinct feature of proximal colorectal cancers. *Proc. Natl. Acad. Sci. U.S.A.* 111, 18321–18326. doi: 10.1073/pnas.1406199111

Deplancke, B., and Gaskins, H. R. (2001). Microbial modulation of innate defense: goblet cells and the intestinal mucus layer. *Am. J. Clin. Nutr.* 73, 1131s–1141s.

Derrien, M., van Passel, M. W., van de Bovenkamp, J. H., Schipper, R. G., de Vos, W. M., and Dekker, J. (2010). Mucin-bacterial interactions in the human oral cavity and digestive tract. *Gut Microbes* 1, 254–268. doi: 10.4161/gmic.1.4.12778

Derrien, M., Vaughan, E. E., Plugge, C. M., and de Vos, W. M. (2004). *Akkermansia muciniphila* gen. nov., sp. nov., a human intestinal mucin-degrading bacterium. *Int. J. Syst. Evol. Microbiol.* 54(Pt 5), 1469–1476. doi: 10.1099/ijs.0.02873-0

de Vos, W. M. (2015). Microbial biofilms and the human intestinal microbiome. *NPJ Biofilms Microbiomes* 1:15005. doi: 10.1038/npjbiofilms.2015.5

Dohrman, A., Miyata, S., Gallup, M., Li, J. D., Chapelin, C., Coste, A., et al. (1998). Mucin gene (MUC 2 and MUC 5AC) upregulation by Gram-positive and Gram-negative bacteria. *Biochim. Biophys. Acta* 1406, 251–259. doi: 10.1016/S0925-4439(98)00010-6

Dorofeyev, A. E., Vasilenko, I. V., Rassokhina, O. A., and Kondratiuk, R. B. (2013). Mucosal barrier in ulcerative colitis and Crohn's disease. *Gastroenterol. Res. Pract.* 2013:431231. doi: 10.1155/2013/431231

Douillard, F. P., Ribbera, A., Jarvinen, H. M., Kant, R., Pietila, T. E., Randazzo, C., et al. (2013). Comparative genomic and functional analysis of *Lactobacillus casei* and *Lactobacillus rhamnosus* strains marketed as probiotics. *Appl. Environ. Microbiol.* 79, 1923–1933. doi: 10.1128/AEM.03467-12

Dwivedi, R., Nothaft, H., Garber, J., Xin Kin, L., Stahl, M., Flint, A., et al. (2016). L-fucose influences chemotaxis and biofilm formation in *Campylobacter jejuni*. *Mol. Microbiol.* 101, 575–589. doi: 10.1111/mmi.13409

Eaves-Pyles, T., Allen, C. A., Taormina, J., Swidsinski, A., Tutt, C. B., Jezek, G. E., et al. (2008). *Escherichia coli* isolated from a Crohn's disease patient adheres, invades, and induces inflammatory responses in polarized intestinal epithelial cells. *Int. J. Med. Microbiol.* 298, 397–409. doi: 10.1016/j.ijmm.2007.05.011

Elatrech, I., Marzaioli, V., Boukemara, H., Bournier, O., Neut, C., Darfeuille-Michaud, A., et al. (2015). *Escherichia coli* LF82 differentially regulates ROS production and mucin expression in intestinal epithelial T84 cells: implication of NOX1. *Inflamm. Bowel Dis.* 21, 1018–1026. doi: 10.1097/MIB.0000000000000365

Enss, M. L., Cornberg, M., Wagner, S., Gebert, A., Henrichs, M., Eisenblatter, R., et al. (2000). Proinflammatory cytokines trigger MUC gene expression and mucin release in the intestinal cancer cell line LS180. *Inflamm. Res.* 49, 162–169. doi: 10.1007/s000110050576

Enss, M. L., Grosse-Siestrup, H., Schmidt-Wittig, U., and Gartner, K. (1992). Changes in colonic mucins of germfree rats in response to the introduction of a "normal" rat microbial flora. Rat colonic mucin. *J. Exp. Anim. Sci.* 35, 110–119.

Epple, H. J., Kreusel, K. M., Hanski, C., Schulzke, J. D., Riecken, E. O., and Fromm, M. (1997). Differential stimulation of intestinal mucin secretion by cholera toxin and carbachol. *Pflugers Arch.* 433, 638–647.

Erdem, A. L., Avelino, F., Xicohtencatl-Cortes, J., and Giron, J. A. (2007). Host protein binding and adhesive properties of H6 and H7 flagella of attaching and effacing *Escherichia coli*. *J. Bacteriol.* 189, 7426–7435. doi: 10.1128/JB.00464-07

Etzold, S., Kober, O. I., Mackenzie, D. A., Tailford, L. E., Gunning, A. P., Walshaw, J., et al. (2014). Structural basis for adaptation of lactobacilli to gastrointestinal mucus. *Environ. Microbiol.* 16, 888–903. doi: 10.1111/1462-2920.12377

Fabich, A. J., Jones, S. A., Chowdhury, F. Z., Cernosek, A., Anderson, A., Smalley, D., et al. (2008). Comparison of carbon nutrition for pathogenic and commensal *Escherichia coli* strains in the mouse intestine. *Infect. Immun.* 76, 1143–1152. doi: 10.1128/IAI.01386-07

Finnie, I. A., Dwarakanath, A. D., Taylor, B. A., and Rhodes, J. M. (1995). Colonic mucin synthesis is increased by sodium butyrate. *Gut* 36, 93–99.

Forstner, G. (1995). Signal transduction, packaging and secretion of mucins. *Annu. Rev. Physiol.* 57, 585–605.

Gagnon, M., Zihler Berner, A., Chervet, N., Chassard, C., and Lacroix, C. (2013). Comparison of the Caco-2, HT-29 and the mucus-secreting HT29-MTX intestinal cell models to investigate *Salmonella* adhesion and invasion. *J. Microbiol. Methods* 94, 274–279. doi: 10.1016/j.mimet.2013.06.027

Garrido, D., Kim, J. H., German, J. B., Raybould, H. E., and Mills, D. A. (2011). Oligosaccharide binding proteins from *Bifidobacterium longum* subsp. infantis reveal a preference for host glycans. *PLoS ONE* 6:e17315. doi: 10.1371/journal.pone.0017315

Gibold, L., Garenaux, E., Dalmasso, G., Gallucci, C., Cia, D., Mottet-Auselo, B., et al. (2016). The Vat-AIEC protease promotes crossing of the intestinal mucus layer by Crohn's disease-associated *Escherichia coli*. *Cell. Microbiol.* 18, 617–631. doi: 10.1111/cmi.12539

Gonzalez-Rodriguez, I., Sanchez, B., Ruiz, L., Turroni, F., Ventura, M., Ruas-Madiedo, P., et al. (2012). Role of extracellular transaldolase from *Bifidobacterium bifidum* in mucin adhesion and aggregation. *Appl. Environ. Microbiol.* 78, 3992–3998. doi: 10.1128/AEM.08024-11

Gum, J. R. Jr., Hicks, J. W., Toribara, N. W., Siddiki, B., and Kim, Y. S. (1994). Molecular cloning of human intestinal mucin (MUC2) cDNA. Identification of the amino terminus and overall sequence similarity to prepro-von Willebrand factor. *J. Biol. Chem.* 269, 2440–2446.

Hanski, C., Born, M., Foss, H. D., Marowski, B., Mansmann, U., Arasteh, K., et al. (1999). Defective post-transcriptional processing of MUC2 mucin in ulcerative colitis and in Crohn's disease increases detectability of the MUC2 protein core. *J. Pathol.* 188, 304–311.

Harel, J., Fairbrother, J., Forget, C., Desautels, C., and Moore, J. (1993). Virulence factors associated with F165-positive *Escherichia coli* strains isolated from piglets and calves. *Vet. Microbiol.* 38, 139–155.

Harrington, S. M., Sheikh, J., Henderson, I. R., Ruiz-Perez, F., Cohen, P. S., and Nataro, J. P. (2009). The pic protease of enteroaggregative *Escherichia coli* promotes intestinal colonization and growth in the presence of mucin. *Infect. Immun.* 77, 2465–2473. doi: 10.1128/IAI.01494-08

Henderson, I. R., Czeczulin, J., Eslava, C., Noriega, F., and Nataro, J. P. (1999). Characterization of pic, a secreted protease of *Shigella flexneri* and enteroaggregative *Escherichia coli*. *Infect. Immun.* 67, 5587–5596.

Hooper, L. V., and Gordon, J. I. (2001). Commensal host-bacterial relationships in the gut. *Science* 292, 1115–1118. doi: 10.1126/science.1058709

Hoskins, L. C., Agustines, M., McKee, W. B., Boulding, E. T., Kriaris, M., and Niedermeyer, G. (1985). Mucin degradation in human colon ecosystems. Isolation and properties of fecal strains that degrade ABH blood group antigens and oligosaccharides from mucin glycoproteins. *J. Clin. Invest.* 75, 944–953.

Hoyer, L. L., Hamilton, A. C., Steenbergen, S. M., and Vimr, E. R. (1992). Cloning, sequencing and distribution of the *Salmonella typhimurium* LT2 sialidase gene, nanH, provides evidence for interspecies gene transfer. *Mol. Microbiol.* 6, 873–884.

Huang, J. Y., Lee, S. M., and Mazmanian, S. K. (2011). The human commensal *Bacteroides fragilis* binds intestinal mucin. *Anaerobe* 17, 137–141. doi: 10.1016/j.anaerobe.2011.05.017

Johansson, M. E., Gustafsson, J. K., Holmen-Larsson, J., Jabbar, K. S., Xia, L., Xu, H., et al. (2014). Bacteria penetrate the normally impenetrable inner colon mucus layer in both murine colitis models and patients with ulcerative colitis. *Gut* 63, 281–291. doi: 10.1136/gutjnl-2012-303207

Johansson, M. E., Jakobsson, H. E., Holmen-Larsson, J., Schutte, A., Ermund, A., Rodriguez-Pineiro, A. M., et al. (2015). Normalization of host intestinal mucus layers requires long-term microbial colonization. *Cell Host Microbe* 18, 582–592. doi: 10.1016/j.chom.2015.10.007

Johansson, M. E., Larsson, J. M., and Hansson, G. C. (2011). The two mucus layers of colon are organized by the MUC2 mucin, whereas the outer layer is a legislator of host-microbial interactions. *Proc. Natl. Acad. Sci. U.S.A.* 108(Suppl. 1), 4659–4665. doi: 10.1073/pnas.1006451107

Johansson, M. E., Phillipson, M., Petersson, J., Velcich, A., Holm, L., and Hansson, G. C. (2008). The inner of the two Muc2 mucin-dependent mucus layers in colon is devoid of bacteria. *Proc. Natl. Acad. Sci. U.S.A.* 105, 15064–15069. doi: 10.1073/pnas.0803124105

Johansson, M. E., Thomsson, K. A., and Hansson, G. C. (2009). Proteomic analyses of the two mucus layers of the colon barrier reveal that their main component, the Muc2 mucin, is strongly bound to the Fcgbp protein. *J. Proteome Res.* 8, 3549–3557. doi: 10.1021/pr9002504

Jonckheere, N., Skrypek, N., Frenois, F., and Van Seuningen, I. (2013). Membrane-bound mucin modular domains: from structure to function. *Biochimie* 95, 1077–1086. doi: 10.1016/j.biochi.2012.11.005

Juge, N. (2012). Microbial adhesins to gastrointestinal mucus. *Trends Microbiol.* 20, 30–39. doi: 10.1016/j.tim.2011.10.001

Kankainen, M., Paulin, L., Tynkkynen, S., von Ossowski, I., Reunanen, J., Partanen, P., et al. (2009). Comparative genomic analysis of *Lactobacillus rhamnosus* GG reveals pili containing a human- mucus binding protein. *Proc. Natl. Acad. Sci. U.S.A.* 106, 17193–17198. doi: 10.1073/pnas.0908876106

Keeney, K. M., and Finlay, B. B. (2013). Microbiology: EHEC downregulates virulence in response to intestinal fucose. *Curr. Biol.* 23, R108–R110. doi: 10.1016/j.cub.2012.12.027

Kelly, C. P., Becker, S., Linevsky, J. K., Joshi, M. A., O'Keane, J. C., Dickey, B. F., et al. (1994). Neutrophil recruitment in *Clostridium* difficile toxin A enteritis in the rabbit. *J. Clin. Invest.* 93, 1257–1265. doi: 10.1172/JCI117080

Kim, Y. S., and Ho, S. B. (2010). Intestinal goblet cells and mucins in health and disease: recent insights and progress. *Curr. Gastroenterol. Rep.* 12, 319–330. doi: 10.1007/s11894-010-0131-2

Kleessen, B., and Blaut, M. (2007). Modulation of gut mucosal biofilms. *Br. J. Nutr.* 93, S35–S40. doi: 10.1079/BJN20041346

Konopka, J. B. (2012). N-acetylglucosamine (GlcNAc) functions in cell signaling. *Scientifica (Cairo)* 2012:489208. doi: 10.6064/2012/489208

Koropatkin, N. M., Cameron, E. A., and Martens, E. C. (2012). How glycan metabolism shapes the human gut microbiota. *Nat. Rev. Microbiol.* 10, 323–335. doi: 10.1038/nrmicro2746

Kumar, P., Luo, Q., Vickers, T. J., Sheikh, A., Lewis, W. G., and Fleckenstein, J. M. (2014). EatA, an immunogenic protective antigen of enterotoxigenic *Escherichia coli*, degrades intestinal mucin. *Infect. Immun.* 82, 500–508. doi: 10.1128/IAI.01078-13

Larsson, J. M., Karlsson, H., Crespo, J. G., Johansson, M. E., Eklund, L., Sjovall, H., et al. (2011). Altered O-glycosylation profile of MUC2 mucin occurs in active ulcerative colitis and is associated with increased inflammation. *Inflamm. Bowel Dis.* 17, 2299–2307. doi: 10.1002/ibd.21625

Larsson, J. M., Karlsson, H., Sjovall, H., and Hansson, G. C. (2009). A complex, but uniform O-glycosylation of the human MUC2 mucin from colonic biopsies analyzed by nanoLC/MSn. *Glycobiology* 19, 756–766. doi: 10.1093/glycob/cwp048

Le, D. T., Tran, T. L., Duviau, M. P., Meyrand, M., Guerardel, Y., Castelain, M., et al. (2013). Unraveling the role of surface mucus-binding protein and pili in muco-adhesion of *Lactococcus lactis*. *PLoS ONE* 8:e79850. doi: 10.1371/journal.pone.0079850

Le Bihan, G., Sicard, J. F., Garneau, P., Bernalier-Donadille, A., Gobert, A. P., Garrivier, A., et al. (2017). The NAG sensor NagC regulates LEE gene expression and contributes to gut colonization by *Escherichia coli* O157:H7. *Front. Cell. Infect. Microbiol.* 7:134. doi: 10.3389/fcimb.2017.00134

Lencer, W. I., Reinhart, F. D., and Neutra, M. R. (1990). Interaction of cholera toxin with cloned human goblet cells in monolayer culture. *Am. J. Physiol.* 258(1 Pt 1), G96–G102.

Li, H., Limenitakis, J. P., Fuhrer, T., Geuking, M. B., Lawson, M. A., Wyss, M., et al. (2015). The outer mucus layer hosts a distinct intestinal microbial niche. *Nat. Commun.* 6:8292. doi: 10.1038/ncomms9292

Licht, T. R., Christensen, B. B., Krogfelt, K. A., and Molin, S. (1999). Plasmid transfer in the animal intestine and other dynamic bacterial populations: the role of community structure and environment. *Microbiology* 145(Pt 9), 2615–2622. doi: 10.1099/00221287-145-9-2615

Lievin-Le Moal, V., Huet, G., Aubert, J. P., Bara, J., Forgue-Lafitte, M. E., Servin, A. L., et al. (2002). Activation of mucin exocytosis and upregulation of MUC genes in polarized human intestinal mucin-secreting cells by the thiol-activated exotoxin listeriolysin O. *Cell. Microbiol.* 4, 515–529. doi: 10.1046/j.1462-5822.2002.00210.x

Lievin-Le Moal, V., Servin, A. L., and Coconnier-Polter, M. H. (2005). The increase in mucin exocytosis and the upregulation of MUC genes encoding for membrane-bound mucins induced by the thiol-activated exotoxin listeriolysin O is a host cell defence response that inhibits the cell-entry of *Listeria monocytogenes*. *Cell. Microbiol.* 7, 1035–1048. doi: 10.1111/j.1462-5822.2005.00532.x

Linden, S. K., Florin, T. H., and McGuckin, M. A. (2008). Mucin dynamics in intestinal bacterial infection. *PLoS ONE* 3:e3952. doi: 10.1371/journal.pone.0003952

Liu, Z., Wang, Y., Liu, S., Sheng, Y., Rueggeberg, K. G., Wang, H. et al. (2015). *Vibrio cholerae* represses polysaccharide synthesis to promote motility in mucosa. *Infect. Immun.* 83, 1114–1121. doi: 10.1128/IAI.02841-14

Macfarlane, G. T., and Gibson, G. R. (1991). Formation of glycoprotein degrading enzymes by *Bacteroides fragilis*. *FEMS Microbiol. Lett.* 61, 289–293. doi: 10.1111/j.1574-6968.1991.tb04363.x

Macfarlane, S., McBain, A. J., and Macfarlane, G. T. (1997). Consequences of biofilm and sessile growth in the large intestine. *Adv. Dent. Res.* 11, 59–68. doi: 10.1177/08959374970110011801

Macfarlane, S., Woodmansey, E. J., and Macfarlane, G. T. (2005). Colonization of mucin by human intestinal bacteria and establishment of biofilm communities in a two-stage continuous culture system. *Appl. Environ. Microbiol.* 71, 7483–7492. doi: 10.1128/AEM.71.11.7483-7492.2005

Mack, D. R., Michail, S., Wei, S., McDougall, L., and Hollingsworth, M. A. (1999). Probiotics inhibit enteropathogenic *E. coli* adherence *in vitro* by inducing intestinal mucin gene expression. *Am. J. Physiol.* 276(4 Pt 1), G941–G950.

MacKenzie, D. A., Tailford, L. E., Hemmings, A. M., and Juge, N. (2009). Crystal structure of a mucus-binding protein repeat reveals an unexpected functional immunoglobulin binding activity. *J. Biol. Chem.* 284, 32444–32453. doi: 10.1074/jbc.M109.040907

Mahdavi, J., Pirinccioglu, N., Oldfield, N. J., Carlsohn, E., Stoof, J., Aslam, A., et al. (2014). A novel O-linked glycan modulates Campylobacter jejuni major outer membrane protein-mediated adhesion to human histo-blood group antigens and chicken colonization. *Open Biol.* 4:130202. doi: 10.1098/rsob.130202

Maltby, R., Leatham-Jensen, M. P., Gibson, T., Cohen, P. S., and Conway, T. (2013). Nutritional basis for colonization resistance by human commensal *Escherichia coli* strains HS and Nissle 1917 against *E. coli* O157:H7 in the mouse intestine. *PLoS ONE* 8:e53957. doi: 10.1371/journal.pone.0053957

Mantle, M., and Rombough, C. (1993). Growth in and breakdown of purified rabbit small intestinal mucin by *Yersinia enterocolitica*. *Infect. Immun.* 61, 4131–4138.

Marcobal, A., Southwick, A. M., Earle, K. A. and Sonnenburg, J. L. (2013). A refined palate: bacterial consumption of host glycans in the gut. *Glycobiology* 23, 1038–1046. doi: 10.1093/glycob/cwt040

Mariscotti, J. F., Quereda, J. J., Garcia-Del Portillo, F., and Pucciarelli, M. G. (2014). The *Listeria* monocytogenes LPXTG surface protein Lmo1413 is an invasin with capacity to bind mucin. *Int. J. Med. Microbiol.* 304, 393–404. doi: 10.1016/j.ijmm.2014.01.003

Martens, E. C., Chiang, H. C., and Gordon, J. I. (2008). Mucosal glycan foraging enhances fitness and transmission of a saccharolytic human gut bacterial symbiont. *Cell Host Microbe* 4, 447–457. doi: 10.1016/j.chom.2008.09.007

Martinez-Medina, M., Aldeguer, X., Lopez-Siles, M., Gonzalez-Huix, F., Lopez-Oliu, C., Dahbi, G., et al. (2009a). Molecular diversity of *Escherichia coli* in the human gut: new ecological evidence supporting the role of adherent-invasive *E. coli* (AIEC) in Crohn's disease. *Inflamm Bowel Dis.* 15, 872–882. doi: 10.1002/ibd.20860

Martinez-Medina, M., Naves, P., Blanco, J., Aldeguer, X., Blanco, J. E., Blanco, M., et al. (2009b). Biofilm formation as a novel phenotypic feature of adherent-invasive *Escherichia coli* (AIEC). *BMC Microbiol.* 9:202. doi: 10.1186/1471-2180-9-202

Martin-Sosa, S., Martin, M. J., and Hueso, P. (2002). The sialylated fraction of milk oligosaccharides is partially responsible for binding to enterotoxigenic and uropathogenic *Escherichia coli* human strains. *J. Nutr.* 132, 3067–3072.

Masseret, E., Boudeau, J., Colombel, J. F., Neut, C., Desreumaux, P., Joly, B., et al. (2001). Genetically related *Escherichia coli* strains associated with Crohn's disease. *Gut* 48, 320–325. doi: 10.1136/gut.48.3.320

Mattar, A. F., Teitelbaum, D. H., Drongowski, R. A., Yongyi, F., Harmon, C. M., and Coran, A. G. (2002). Probiotics up-regulate MUC-2 mucin gene expression in a Caco-2 cell-culture model. *Pediatr. Surg. Int.* 18, 586–590. doi: 10.1007/s00383-002-0855-7

McGuckin, M. A., Linden, S. K., Sutton, P., and Florin, T. H. (2011). Mucin dynamics and enteric pathogens. *Nat. Rev. Microbiol.* 9, 265–278. doi: 10.1038/nrmicro2538

McNamara, N., and Basbaum, C. (2001). Signaling networks controlling mucin production in response to Gram-positive and Gram-negative bacteria. *Glycoconj. J.* 18, 715–722. doi: 10.1023/A:1020875423678

Moehle, C., Ackermann, N., Langmann, T., Aslanidis, C., Kel, A., Kel-Margoulis, O., et al. (2006). Aberrant intestinal expression and allelic variants of mucin genes associated with inflammatory bowel disease. *J. Mol. Med.* 84, 1055–1066. doi: 10.1007/s00109-006-0100-2

Moran, A. P., Gupta, A., and Joshi, L. (2011). Sweet-talk: role of host glycosylation in bacterial pathogenesis of the gastrointestinal tract. *Gut* 60, 1412–1425. doi: 10.1136/gut.2010.212704

Naughton, J. A., Marino, K., Dolan, B., Reid, C., Gough, R., Gallagher, M. E., et al. (2013). Divergent mechanisms of interaction of *Helicobacter pylori* and *Campylobacter jejuni* with mucus and mucins. *Infect. Immun.* 81, 2838–2850. doi: 10.1128/IAI.00415-13

Navarro-Garcia, F., Gutierrez-Jimenez, J., Garcia-Tovar, C., Castro, L. A., Salazar-Gonzalez, H., and Cordova, V. (2010). Pic, an autotransporter protein secreted by different pathogens in the *Enterobacteriaceae* family, is a potent mucus secretagogue. *Infect. Immun.* 78, 4101–4109. doi: 10.1128/IAI.00523-10

Ng, K. M., Ferreyra, J. A., Higginbottom, S. K., Lynch, J. B., Kashyap, P. C., Gopinath, S., et al. (2013). Microbiota-liberated host sugars facilitate post-antibiotic expansion of enteric pathogens. *Nature* 502, 96–99. doi: 10.1038/nature12503

Nilsson, H. E., Ambort, D., Backstrom, M., Thomsson, E., Koeck, P. J., Hansson, G. C., et al. (2014). Intestinal MUC2 mucin supramolecular topology by packing and release resting on D3 domain assembly. *J. Mol. Biol.* 426, 2567–2579. doi: 10.1016/j.jmb.2014.04.027

Ouwerkerk, J. P., de Vos, W. M., and Belzer, C. (2013). Glycobiome: bacteria and mucus at the epithelial interface. *Best Pract. Res. Clin. Gastroenterol.* 27, 25–38. doi: 10.1016/j.bpg.2013.03.001

Pacheco, A. R., Curtis, M. M., Ritchie, J. M., Munera, D., Waldor, M. K., Moreira, C. G., et al. (2012). Fucose sensing regulates bacterial intestinal colonization. *Nature* 492, 113–117. doi: 10.1038/nature11623

Palestrant, D., Holzknecht, Z. E., Collins, B. H., Parker, W., Miller, S. E., and Bollinger, R. R. (2004). Microbial biofilms in the gut: visualization by electron microscopy and by acridine orange staining. *Ultrastruct. Pathol.* 28, 23–27. doi: 10.1080/01913120490275196

Petersson, J., Schreiber, O., Hansson, G. C., Gendler, S. J., Velcich, A., Lundberg, J. O., et al. (2011). Importance and regulation of the colonic mucus barrier in a mouse model of colitis. *Am. J. Physiol. Gastrointest. Liver Physiol.* 300, G327–G333. doi: 10.1152/ajpgi.00422.2010

Png, C. W., Linden, S. K., Gilshenan, K. S., Zoetendal, E. G., McSweeney, C. S., Sly, L. I., et al. (2010). Mucolytic bacteria with increased prevalence in IBD mucosa augment *in vitro* utilization of mucin by other bacteria. *Am. J. Gastroenterol.* 105, 2420–2428. doi: 10.1038/ajg.2010.281

Pullan, R. D., Thomas, G. A., Rhodes, M., Newcombe, R. G., Williams, G. T., Allen, A., et al. (1994). Thickness of adherent mucus gel on colonic mucosa in humans and its relevance to colitis. *Gut* 35, 353–359. doi: 10.1136/gut.35.3.353

Pultz, N. J., Hoskins, L. C., and Donskey, C. J. (2006). Vancomycin-resistant *Enterococci* may obtain nutritional support by scavenging carbohydrate fragments generated during mucin degradation by the anaerobic microbiota of the colon. *Microb. Drug Resist.* 12, 63–67. doi: 10.1089/mdr.2006.12.63

Raouf, A. H., Tsai, H. H., Parker, N., Hoffman, J., Walker, R. J., and Rhodes, J. M. (1992). Sulphation of colonic and rectal mucin in inflammatory bowel disease: reduced sulphation of rectal mucus in ulcerative colitis. *Clin. Sci.* 83, 623–626. doi: 10.1042/cs0830623

Rho, J. H., Wright, D. P., Christie, D. L., Clinch, K., Furneaux, R. H., and Roberton, A. M. (2005). A novel mechanism for desulfation of mucin: identification and cloning of a mucin-desulfating glycosidase (sulfoglycosidase) from Prevotella strain RS2. *J. Bacteriol.* 187, 1543–1551. doi: 10.1128/JB.187.5.1543-1551.2005

Roos, S., and Jonsson, H. (2002). A high-molecular-mass cell-surface protein from *Lactobacillus reuteri* 1063 adheres to mucus components. *Microbiology* 148(Pt 2), 433–442. doi: 10.1099/00221287-148-2-433

Ruiz-Palacios, G. M., Cervantes, L. E., Ramos, P., Chavez-Munguia, B., and Newburg, D. S. (2003). *Campylobacter jejuni* binds intestinal H(O) antigen (Fuc α1, 2Gal β1, 4GlcNAc), and fucosyloligosaccharides of human milk inhibit its binding and infection. *J. Biol. Chem.* 278, 14112–14120. doi: 10.1074/jbc.M207744200

Sharma, R., Schumacher, U., Ronaasen, V., and Coates, M. (1995). Rat intestinal mucosal responses to a microbial flora and different diets. *Gut* 36, 209–214. doi: 10.1136/gut.36.2.209

Sheng, Y. H., Hasnain, S. Z., Florin, T. H., and McGuckin, M. A. (2012). Mucins in inflammatory bowel diseases and colorectal cancer. *J. Gastroenterol. Hepatol.* 27, 28–38. doi: 10.1111/j.1440-1746.2011.06909.x

Slizova, M., Nemcova, R., Mad'ar, M., Hadryova, J., Gancarcikova, S., Popper, M., et al. (2015). Analysis of biofilm formation by intestinal *lactobacilli*. *Can. J. Microbiol.* 61, 437–446. doi: 10.1139/cjm-2015-0007

Smirnova, M. G., Guo, L., Birchall, J. P., and Pearson, J. P. (2003). LPS up-regulates mucin and cytokine mRNA expression and stimulates mucin and cytokine secretion in goblet cells. *Cell. Immunol.* 221, 42–49. doi: 10.1016/S0008-8749(03)00059-5

Sonnenburg, E. D., Zheng, H., Joglekar, P., Higginbottom, S. K., Firbank, S. J., Bolam, D. N., et al. (2010). Specificity of polysaccharide use in intestinal bacteroides species determines diet-induced microbiota alterations. *Cell* 141, 1241–1252. doi: 10.1016/j.cell.2010.05.005

Sonnenburg, J. L., Xu, J., Leip, D. D., Chen, C. H., Westover, B. P., Weatherford, J., et al. (2005). Glycan foraging *in vivo* by an intestine-adapted bacterial symbiont. *Science* 307, 1955–1959. doi: 10.1126/science.1109051

Sperandio, B., Fischer, N., Joncquel Chevalier-Curt, M., Rossez, Y., Roux, P., Robbe Masselot, C., et al. (2013). Virulent *Shigella flexneri* affects secretion, expression, and glycosylation of gel-forming mucins in mucus-producing cells. *Infect. Immun.* 81, 3632–3643. doi: 10.1128/IAI.00551-13

Strugala, V., Dettmar, P. W., and Pearson, J. P. (2008). Thickness and continuity of the adherent colonic mucus barrier in active and quiescent ulcerative colitis and Crohn's disease. *Int. J. Clin. Pract.* 62, 762–769. doi: 10.1111/j.1742-1241.2007.01665.x

Swidsinski, A., Loening-Baucke, V., and Herber, A. (2009). Mucosal flora in Crohn's disease and ulcerative colitis-an overview. *J. Physiol. Pharmacol.* 60(Suppl. 6), 61–71.

Swidsinski, A., Loening-Baucke, V., Lochs, H., and Hale, L. P. (2005a). Spatial organization of bacterial flora in normal and inflamed intestine: a fluorescence *in situ* hybridization study in mice. *World J. Gastroenterol.* 11, 1131–1140. doi: 10.3748/wjg.v11.i8.1131

Swidsinski, A., Weber, J., Loening-Baucke, V., Hale, L. P., and Lochs, H. (2005b). Spatial organization and composition of the mucosal flora in patients with inflammatory bowel disease. *J. Clin. Microbiol.* 43, 3380–3389. doi: 10.1128/JCM.43.7.3380-3389.2005

Szabady, R. L., Yanta, J. H., Halladin, D. K., Schofield, M. J., and Welch, R. A. (2011). TagA is a secreted protease of *Vibrio cholerae* that specifically cleaves mucin glycoproteins. *Microbiology* 157(Pt 2), 516–525. doi: 10.1099/mic.0.044529-0

Szentkuti, L., Riedesel, H., Enss, M. L., Gaertner, K., and Von Engelhardt, W. (1990). Pre-epithelial mucus layer in the colon of conventional and germ-free rats. *Histochem. J.* 22, 491–497. doi: 10.1007/BF01007234

Tasteyre, A., Barc, M. C., Collignon, A., Boureau, H., and Karjalainen, T. (2001). Role of FliC and FliD flagellar proteins of *Clostridium difficile* in adherence and gut colonization. *Infect. Immun.* 69, 7937–7940. doi: 10.1128/IAI.69.12.7937-7940.2001

Theodoropoulos, G., and Carraway, K. L. (2007). Molecular signaling in the regulation of mucins. *J. Cell. Biochem.* 102, 1103–1116. doi: 10.1002/jcb.21539

Trabucchi, E., Mukenge, S., Baratti, C., Colombo, R., Fregoni, F., and Montorsi, W. (1986). Differential diagnosis of Crohn's disease of the colon from ulcerative colitis: ultrastructure study with the scanning electron microscope. *Int. J. Tissue React.* 8, 79–84.

Troge, A., Scheppach, W., Schroeder, B. O., Rund, S. A., Heuner, K., Wehkamp, J., et al. (2012). More than a marine propeller–the flagellum of the probiotic *Escherichia coli* strain Nissle 1917 is the major adhesin mediating binding to human mucus. *Int. J. Med. Microbiol.* 302, 304–314. doi: 10.1016/j.ijmm.2012.09.004

Tu, Q. V., McGuckin, M. A., and Mendz, G. L. (2008). *Campylobacter jejuni* response to human mucin MUC2: modulation of colonization and pathogenicity determinants. *J. Med. Microbiol.* 57(Pt 7), 795–802. doi: 10.1099/jmm.0.47752-0

van der Waaij, L. A., Harmsen, H. J., Madjipour, M., Kroese, F. G., Zwiers, M., van Dullemen, H. M., et al. (2005). Bacterial population analysis of human colon and terminal ileum biopsies with 16S rRNA-based fluorescent probes: commensal bacteria live in suspension and have no direct contact with epithelial cells. *Inflamm. Bowel Dis.* 11, 865–871. doi: 10.1097/01.mib.0000179212.80778.d3

Vimal, D. B., Khullar, M., Gupta, S., and Ganguly, N. K. (2000). Intestinal mucins: the binding sites for *Salmonella typhimurium*. *Mol. Cell. Biochem.* 204, 107–117. doi: 10.1023/A:1007015312036

Vogt, S. L., Pena-Diaz, J., and Finlay, B. B. (2015). Chemical communication in the gut: effects of microbiota-generated metabolites on gastrointestinal bacterial pathogens. *Anaerobe* 34, 106–115. doi: 10.1016/j.anaerobe.2015.05.002

Weiss, A. A., Babyatsky, M. W., Ogata, S., Chen, A., and Itzkowitz, S. H. (1996). Expression of MUC2 and MUC3 mRNA in human normal, malignant, and inflammatory intestinal tissues. *J. Histochem. Cytochem.* 44, 1161–1166. doi: 10.1177/44.10.8813081

Wrzosek, L., Miquel, S., Noordine, M. L., Bouet, S., Joncquel Chevalier-Curt, M., Robert, V., et al. (2013). *Bacteroides thetaiotaomicron* and *Faecalibacterium prausnitzii* influence the production of mucus glycans and the development of goblet cells in the colonic epithelium of a gnotobiotic model rodent. *BMC Biol.* 11:61. doi: 10.1186/1741-7007-11-61

Wurpel, D. J., Totsika, M., Allsopp, L. P., Hartley-Tassell, L. E., Day, C. J., Peters, K. M., et al. (2014). F9 fimbriae of uropathogenic *Escherichia coli* are expressed at low temperature and recognise Galbeta1-3GlcNAc-containing glycans. *PLoS ONE* 9:e93177. doi: 10.1371/journal.pone.0093177

Xu, J., Bjursell, M. K., Himrod, J., Deng, S., Carmichael, L. K., Chiang, H. C., et al. (2003). A genomic view of the human-*Bacteroides thetaiotaomicron* symbiosis. *Science* 299, 2074–2076. doi: 10.1126/science.1080029

Xue, Y., Zhang, H., Wang, H., Hu, J., Du, M., and Zhu, M. J. (2014). Host inflammatory response inhibits *Escherichia coli* O157:H7 adhesion to gut epithelium through augmentation of mucin expression. *Infect. Immun.* 82, 1921–1930. doi: 10.1128/IAI.01589-13

Ye, J., Song, L., Liu, Y., Pan, Q., Zhong, X., Li, S., et al. (2015). Core 2 Mucin-Type O-Glycan is related to EPEC and EHEC O157:H7 adherence to human colon carcinoma HT-29 epithelial cells. *Dig. Dis. Sci.* 60, 1977–1990. doi: 10.1007/s10620-015-3548-5

Zarepour, M., Bhullar, K., Montero, M., Ma, C., Huang, T., Velcich, A., et al. (2013). The mucin Muc2 limits pathogen burdens and epithelial barrier dysfunction during *Salmonella enterica* serovar Typhimurium colitis. *Infect. Immun.* 81, 3672–3683. doi: 10.1128/IAI.00854-13

Conflict of Interest Statement: The authors declare that the research was conducted in the absence of any commercial or financial relationships that could be construed as a potential conflict of interest.

Copyright © 2017 Sicard, Le Bihan, Vogeleer, Jacques and Harel. This is an open-access article distributed under the terms of the Creative Commons Attribution License (CC BY). The use, distribution or reproduction in other forums is permitted, provided the original author(s) or licensor are credited and that the original publication in this journal is cited, in accordance with accepted academic practice. No use, distribution or reproduction is permitted which does not comply with these terms.

frontiers in Cellular and Infection Microbiology

ORIGINAL RESEARCH
published: 24 August 2017
doi: 10.3389/fcimb.2017.00381

Alterations of the Gut Microbiome in Hypertension

Qiulong Yan[1,2], Yifang Gu[3], Xiangchun Li[4], Wei Yang[5], Liqiu Jia[1], Changming Chen[1], Xiuyan Han[1], Yukun Huang[1], Lizhe Zhao[1], Peng Li[3], Zhiwei Fang[3], Junpeng Zhou[3], Xiuru Guan[5], Yanchun Ding[6], Shaopeng Wang[7], Muhammad Khan[8], Yi Xin[9], Shenghui Li[3] and Yufang Ma[1]**

[1] Department of Biochemistry and Molecular Biology, Dalian Medical University, Dalian, China, [2] Department of Microbiology, Dalian Medical University, Dalian, China, [3] Shenzhen Puensum Genetech Institute, Shenzhen, China, [4] Beijing Genomics Institute, Shenzhen, China, [5] Department of Laboratory Diagnostics, The First Affiliated Hospital of Harbin Medical University, Harbin, China, [6] Department of Cardiology V, The Second Affiliated Hospital of Dalian Medical University, Dalian, China, [7] Department of Cardiology, The First Affiliated Hospital of Dalian Medical University, Dalian, China, [8] College of Basic Medical Sciences, Dalian Medical University, Dalian, China, [9] Department of Biotechnology, Dalian Medical University, Dalian, China

Introduction: Human gut microbiota is believed to be directly or indirectly involved in cardiovascular diseases and hypertension. However, the identification and functional status of the hypertension-related gut microbe(s) have not yet been surveyed in a comprehensive manner.

Methods: Here we characterized the gut microbiome in hypertension status by comparing fecal samples of 60 patients with primary hypertension and 60 gender-, age-, and body weight-matched healthy controls based on whole-metagenome shotgun sequencing.

Results: Hypertension implicated a remarkable gut dysbiosis with significant reduction in within-sample diversity and shift in microbial composition. Metagenome-wide association study (MGWAS) revealed 53,953 microbial genes that differ in distribution between the patients and healthy controls (false discovery rate, 0.05) and can be grouped into 68 clusters representing bacterial species. Opportunistic pathogenic taxa, such as, *Klebsiella* spp., *Streptococcus* spp., and *Parabacteroides merdae* were frequently distributed in hypertensive gut microbiome, whereas the short-chain fatty acid producer, such as, *Roseburia* spp. and *Faecalibacterium prausnitzii*, were higher in controls. The number of hypertension-associated species also showed stronger correlation to the severity of disease. Functionally, the hypertensive gut microbiome exhibited higher membrane transport, lipopolysaccharide biosynthesis and steroid degradation, while in controls the metabolism of amino acid, cofactors and vitamins was found to be higher. We further provided the microbial markers for disease discrimination and achieved an area under the receiver operator characteristic curve (AUC) of 0.78, demonstrating the potential of gut microbiota in prediction of hypertension.

Conclusion: These findings represent specific alterations in microbial diversity, genes, species and functions of the hypertensive gut microbiome. Further studies on the causality relationship between hypertension and gut microbiota will offer new prospects for treating and preventing the hypertension and its associated diseases.

Keywords: hypertension, gut microbiome, microbial dysbiosis, metagenome-wide association study

OPEN ACCESS

Edited by:
Venkatakrishna Rao Jala, University of Louisville, United States

Reviewed by:
Bina Joe, University of Toledo, United States
Morgan Langille, Dalhousie University, Canada

Correspondence:
Shenghui Li
lishenghui@puensum.com
Yufang Ma
yufang_ma@hotmail.com

Received: *16 May 2017*
Accepted: *09 August 2017*
Published: *24 August 2017*

Citation:
Yan Q, Gu Y, Li X, Yang W, Jia L, Chen C, Han X, Huang Y, Zhao L, Li P, Fang Z, Zhou J, Guan X, Ding Y, Wang S, Khan M, Xin Y, Li S and Ma Y (2017) Alterations of the Gut Microbiome in Hypertension. Front. Cell. Infect. Microbiol. 7:381. doi: 10.3389/fcimb.2017.00381

INTRODUCTION

Hypertension is a global public health problem. In 2010, about 31% of the world's population has been estimated to suffer from hypertension and over 1 billon of this population is living in low- and middle- income countries(Mittal and Singh, 2010; Mills et al., 2016). Hypertension is one of the major risk factors for cardiovascular diseases, such as, stroke and heart failure (Lim et al., 2012; Faraco and Iadecola, 2013). Moreover, it is believed to be one of the most common comorbidities associated with chronic renal disease (Lash et al., 2009), obesity and type 2 diabetes (Landsberg and Molitch, 2004; Kotchen, 2010). Presently, genome-wide association studies (GWAS) have identified a series of genetic loci and pathways associated with blood pressure (Xu et al., 2015; Liu et al., 2016).The environmental factors, such as, dietary salt intake, alcohol consumption and lack of exercise, are also linked to the occurrence of hypertension (Fuchs et al., 2001; Karppanen and Mervaala, 2006). Recent practice of metabolomics also identified new pathogenic pathways involved in blood pressure regulation (Menni et al., 2015; Galla et al., 2017). Nevertheless, due to the complexity and heterogeneity of hypertension, identification of the causes of this disease is still challenging.

Recent studies have demonstrated that the gut microflora plays an essential role in development of cardiovascular diseases, via metabolizing dietary choline, phosphatidylcholine and L-carnitine to produce trimethylamine (TMA), which is further oxidized into TMA N-oxide (TMAO, a metabolite that enhances atherosclerosis; Wang et al., 2011; Koeth et al., 2013; Tang et al., 2013). Even though the direct link between hypertension and TMAO has not been established currently, TMAO's role to prolong the hypertensive effect of angiotensin II were reported (Ufnal et al., 2014). Inhibition of gut microbiota-mediated TMAO production may serve as a potential therapeutic approach for the treatment of cardiometabolic diseases (Wang Z. et al., 2015). These findings suggest an intricate and predictable correlation between hypertension and gut microbiota. To validate this, a recent study based on metagenomic analyses of the fecal samples of 41 healthy controls, 56 pre-hypertension subjects, and 99 hypertension individuals described a novel causal role of aberrant gut microbiota in contributing to the pathogenesis of hypertension, and emphasized the significance of early intervention for pre-hypertension (Li et al., 2017). Moreover, rat experiments have linked gut microbial dysbiosis with hypertension (Mell et al., 2015; Yang et al., 2015; Adnan et al., 2017; Santisteban et al., 2017). The causal role of gut microbiome in obstructive sleep apnea-induced hypertension have been reported (Durgan et al., 2016). Here, to investigate the alteration of the human gut microbiome underlying hypertension, we compared the microbial composition of fecal samples obtained from 60 patients with primary hypertension and 60 healthy counterparts of Chinese origin. We used quantitative metagenomic analysis to identify genic, microbial, and functional characteristics underlying hypertension.

METHODS

Subjects and Sample Collection

Sixty primary hypertensive patients (current blood pressure ≥140/90 mm Hg) and sixty gender-, age-, and body weight-matched healthy controls (current blood pressure ≤ 120/80 mm Hg) were recruited for this study. Other than systolic blood pressure (SBP) and diastolic blood pressure (DBP), the other clinical parameters have no significant differences in the two groups of populations, except for triglyceride (TG). The characteristics of the subjects are summarized in **Table 1**, and detailed information is given in Table S1. Subjects were excluded if they had symptoms of respiratory infection or digestive tract disease, or if they were treated with antibiotics or anti-inflammatory agents in recent 2 months before sampling. Subjects with hypertension or severe cardiovascular diseases (such as, coronary artery disease or stroke) history in previous 5 years were also excluded from healthy controls. Fresh fecal samples were collected from each subject and were stored at a −80°C freezer immediately.

Ethics Statement

This study received approval from the ethics committee of The First Affiliated Hospital of Harbin Medical University, and written informed consent was obtained from each participant. The methods were carried out in accordance with the approved guidelines.

DNA Preparation and Sequencing

Genomic DNA was extracted from all samples according to a modified protocol provided in the QIAamp DNA mini kit (Qiagen, Manchester, UK; Yan et al., 2016). Briefly, ASL buffer (1.4 ml) was added to 220 mg of fecal sample and the pellets were homogenized in a 2 ml screw cap tubes

TABLE 1 | Characteristics of subjects.

	Case (n = 60)	Control (n = 60)	P-value
Gender (F/M)	25/35	28/32	0.713
Age, y	57.0 ± 9.6	56.0 ± 8.6	0.523
BMI, kg/m^2	23.5 ± 2.9	23.4 ± 2.6	0.854
SBP, mm Hg	165 ± 20	111 ± 6	<0.001
DBP, mm Hg	101 ± 11	71 ± 7	<0.001
FGB, mmol/L	6.37 ± 2.39	6.19 ± 2.09	0.649
HDL, mmol/L	1.15 ± 0.24	1.23 ± 0.29	0.112
LDL, mmol/L	3.08 ± 0.76	3.04 ± 0.71	0.752
TG, mmol/L	1.87 ± 0.85	1.52 ± 0.69	<0.05
TC, mmol/L	5.02 ± 0.97	5.07 ± 0.97	0.791
Smoke	31.7%	40.0%	0.447

The data for age, BMI, SBP, DBP, FGB, HDL, LDL, TG, and TC were presented as mean ± SD. P-values for gender and smoke were calculated by Fisher's exact test. P-values for age, BMI, SBP, DBP, FGB, HDL, LDL, TG, and TC were calculated using Student's t-test. BMI, body mass index; SBP, systolic blood pressure; DBP, diastolic blood pressure; HDL, high density lipoprotein; LDL, low density lipoprotein; TG, total triglyceride; and TG, total cholesterol.

(Axygen) by vortex. The suspension was incubated at 95°C for 5 min to lyse bacterial cells. After centrifugation (13,000 × g, 1 min) and incubation with an InhibitEx tablet, the supernatant was treated with 15 μl proteinase K and 200 μl Buffer AL at 70°C for 10 min. The extracted DNA was dissolved in 100 μl sterile water. Paired-end DNA libraries (insert size 350 bp, read length 150 bp) were constructed according to the manufacturer's instructions (Illumina, USA). Whole-metagenome shotgun sequencing was performed on the Illumina HiSeq3000 platform. Further methodological detail is available in the Supplementary Methods.

Bioinformatic Analysis

Quantification of Metagenomic Genes and Species

High-quality reads from each sample were aligned to the integrated non-redundant human gut gene catalog (IGC; Li et al., 2014) using SOAP2 (Li et al., 2009; >90% similarity). The relative abundance of a gene in a sample was estimated by dividing the number of reads uniquely mapped to that gene by the length of gene region and by the total number of reads from the sample. We also aligned the sequencing reads against the available microbial genomes (bacteria, archaea, and virus) from the National Center for Biotechnology Information (NCBI) database and generated the taxonomic compositions (i.e., phylum and genus composition) for all samples.

Alpha Diversity

The gene count (Le Chatelier et al., 2013) of a metagenomic sample were calculated based on their mapped reads number on the gene catalog (to eliminate the influence of sequencing amount fluctuation, 10 million reads were randomly extracted from each sample for mapping). The Shannon index (within-sample diversity) was calculated based on the gene relative abundance profiles, using the method described previously (Qin et al., 2012).

Functional Annotation and Profiling

The Kyoto Encyclopedia of Genes and Genomes (KEGG, downloaded Jan-2016) database (Kanehisa et al., 2014) was used for functional annotation of genes. Amino acid sequences were searched against the databases using USEARCH v8.1 (Edgar, 2010) with a minimum similarity of 30%. Each gene was assigned a KEGG ortholog (KO) based on the best hit protein. The abundance profiles of KO were calculated by summing the relative abundance of its genes. The choline-trimethylamine lyase (*cutC*, KO: K20038; Craciun and Balskus, 2012) was used to evaluate the gut microbiota-mediated TMA production in subjects, and the short-chain fatty acid (SCFA)-producing enzymes were represented by acetyl-CoA decarbonylase/synthase (K00193, K00194, K00197, K14138, which are key enzymes of the acetate biosynthesis pathways: KEGG modules M00377 and M00422; Koh et al., 2016), propionyl-CoA:succinate-CoA transferase (Reichardt et al., 2014), butyryl-CoA:acetate CoA-transferase (K01034, K01035), and butyrate kinase (K00929) (Pryde et al., 2002; Louis et al., 2010).

Metagenome-Wide Association Study

We used the metagenome-wide association study (MGWAS) method to identify gene markers that showed significant abundance differences between hypertensive patients and control subjects. The MGWAS was performed using the methodology developed by Qin et al. (2012). Co-abundance genes were clustered into metagenomic linkage groups (MLGs) based on the previous methods (Qin et al., 2012). Taxonomic assignment and abundance profiling of the MLGs were performed according to the taxonomy and the relative abundance of their constituent genes (see Supplementary Methods for detail). MLGs were considered to be interacted if absolute value of Spearman's correlation coefficient between them is greater than 0.4, and the co-occurrence network of MLGs was visualized by Cytoscape (Shannon et al., 2003).

Statistical Analyses

Statistical analyses were implemented using the R platform. Distance-based redundancy analysis (dbRDA) was performed on normalized taxa abundance matrices with R *vegan* package (Dixon, 2003) according to Bray-Curtis distance, then visualized with R *ggplot2* package. Random forest models were trained with R *randomForest* package (10,000 trees) to predict hypertension status according to MLG abundance profiles. The performance of the predictive model was evaluated with cross-validation error. Receiver operator characteristic (ROC) analysis was performed using R *pROC* package. P-value < 0.05 was considered statistical significance, and the q-value was calculated to evaluate the false discovery rate (FDR) for correction of multiple comparisons.

Data Availability

The raw whole-metagenomic shotgun sequencing data acquired in this study have been deposited to the European Bioinformatics Institute (EBI) database under the accession code ERP023883.

RESULTS

Comparison of the Gut Microbiota between Hypertensive Patients and Controls

To investigate the gut microbial composition of 60 hypertensive patients and 60 healthy controls, we obtained 652.9 Gbp high-quality data (5.4 ± 1.1 Gbp per sample) via whole-metagenome shotgun sequencing on their fecal samples. When we quantified the microbial (alpha) diversity within each subject, the patients showed significantly lower gene count and Shannon index compared with the controls (**Figure 1A**). Multivariate analysis based on Bray-Curtis distance between microbial genera revealed remarkable differences between patients and controls (**Figure 1B**). At the phylum level, patients had higher levels of Proteobacteria ($p < 0.01$), but fewer Actinobacteria ($p = 0.02$). At the genus level, *Klebsiella*, *Clostridium*, *Streptococcus*, *Parabacteroides*, *Eggerthella,* and *Salmonella* were frequently distributed in hypertensive gut compared to normal controls while *Faecalibacterium*, *Roseburia,* and *Synergistetes* were found to be higher in control group compared to hypertensive patients (**Figure 1C**). These findings demonstrated considerable gut microbial dysbiosis in hypertensive patients.

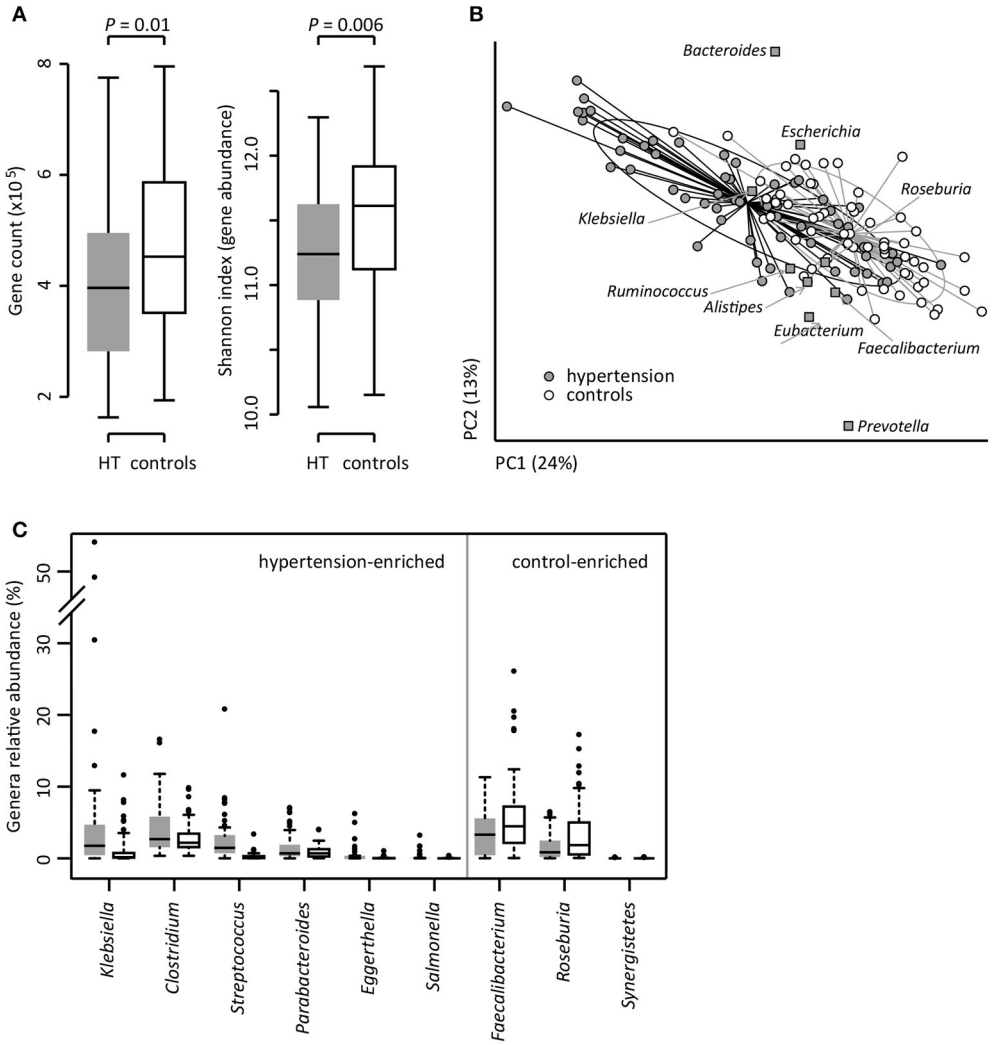

FIGURE 1 | Difference of gut microbial community between hypertensive patients and controls. **(A)**, Difference of alpha diversity between hypertensive (HT) patients and controls. **(B)**, dbRDA based on the Bray-Curtis distances between microbial genera, revealing a hypertensive microbial dysbiosis which overlaps only in part with taxonomic composition in patients and controls. The first two principle components and the ratio of variance contributed is shown. Genera (square) as the main contributors are plotted by their loadings in these two components. Lines connect samples in the same group, and circles cover samples near the center of gravity for each group. **(C)**, Boxplot shows the significantly different genera between patients and controls. Genera with $q < 0.05$ (Mann-Whitney *U*-test corrected by FDR) are shown. Only the genera with average relative abundances greater than 0.05% of total abundance in all samples are shown for clarity. Gray and white boxes represent the patients and controls, respectively. For A and C, the boxes represent the interquartile range (IQR) between first and third quartiles and the line inside represents the median. The whiskers denote the lowest and highest values within 1.5 times IQR from the first and third quartiles, respectively. The dots represent outliers beyond the whiskers.

Identification of Hypertension-Associated Markers from Gut Microbiome

To explore signatures of the gut microbiome in hypertensive patients and controls, we integrated the sequencing data into an existing gut microbial reference gene catalog to obtain a set of 5.3 million genes, which allowed for saturation mapping of the reads (80.3%). Using the MGWAS methods, we identified 53,953 genes that showed a significant difference between two groups (FDR corrected $q < 0.05$). Approximately, 69% of these genes were clustered into 68 metagenome linkage groups (MLGs, Table S2), that allowed to species level description for the microbiome differences. Thirty-one MLGs were higher in patients while 37 in controls. Consistent with the genus level observations, MLGs of *Klebsiella* (mainly consisting of *K. pneumoniae* and *K. variicola*), *Streptococcus* (*S. infantarius*, *S. pasteurianus* and *S. salivarius*), and *Parabacteroides merdae* were found to be higher in hypertensive samples, whereas MLGs of *Roseburia* (mainly consisting of *R. intestinalis* and *R. hominis*) and *Faecalibacterium prausnitzii* were higher in controls. Moreover, the MLGs enriched in hypertensive patients also contain several *Bacteroides* spp. (including *B. eggerthii* and *B. cellulosilyticus*), *Sutterella wadsworthensis* and *Pyramidobacter piscolens*, and the

MLGs enriched in controls include several other *Bacteroides* spp. (including *B. uniformis*, *B. nordii* and *B. dorei*), *Megasphaera* spp. (*M. micronuciformis*), and *Aeromicrobium massiliense*. A co-occurrence network on these MLGs revealed a large number of interconnections within hypertension-enriched and control-enriched MLGs (**Figure 2A**), as well as some MLGs derived from two groups negatively correlated. This result suggested that the MLGs did not occur independently and interacted with the taxa in its environment.

We next found that the gross abundances of hypertension- and control-enriched MLGs are correlated to the severity of hypertension (**Figure 2B**), suggesting that the bacterial relative abundance of these MLGs could be related to the development and disease progress of hypertension.

Functional Characterization of Gut Microbiota

Based on the KEGG pathway comparison, we revealed that the hypertensive gut microbiomes were more abundant in membrane transport, lipopolysaccharide (LPS) biosynthesis, and steroid degradation (**Figure 3A** and Table S3), while the controls were enriched in metabolism of "other amino acids," cofactors and vitamins (including folate biosynthesis and metabolism, riboflavin metabolism, and ubiquinone biosynthesis). In addition, the gut microbial enzymes involved in TMA production were enriched in the hypertensive patients compared to controls, whereas the SCFA-producing enzymes were depleted (**Figure 3B**).

Gut Microbiota-Based Classification of Hypertension

We evaluated the performance of gut microbiota composition to identify hypertension status in the MLG profiles using the Random Forest model, and obtained the discriminatory power of the area under the ROC curve (AUC) of 0.78 (95% CI 0.73–0.82; **Figure 4A**). Several control-enriched MLGs (including *Clostridiales*, *Blautia hansenii*, *Megasphaera*) and two hypertension-enriched members of *Streptococcus* (*S. salivarius* and *S. infantarius*) featured the highest score for the discrimination of hypertensive patients and healthy controls (**Figure 4B**).

DISCUSSION

To identify and analyze the differences of the gut microbiota in hypertension, we characterized the genic, microbial, and functional repertoire of the microbiomes of 60 hypertensive patients and 60 gender-, age-, and body weight-matched controls. Our study strengthened previous metagenomic study on gut microbiome of hypertension (Li et al., 2017) by adding more information. Furthermore, we observed significant differences in microbial community dysbiosis, taxonomic shifts, and functional changes between hypertensive- and control-gut microbiome.

Previous studies showed that the gut microbes participate in choline and phosphatidylcholine metabolism to form circulating and urinary TMAO, while high levels of plasma TMAO promote accelerated atherosclerosis and increase the risk of cardiovascular disorders (Tang et al., 2013; Wang Z. et al., 2015). The choline utilization (*cutC*) gene, a critical gene that coverts the choline to trimethylamine, was identified in a variety of human gut commensals belonging to Firmicutes, Proteobacteria, and Actinobacteria (Craciun and Balskus, 2012). Notably, several genera such as, *Klebsiella*, *Clostridium,* and *Streptococcus*, which are highly distributed in hypertensive patients are choline degraders (Hakenbeck et al., 2009; Craciun and Balskus, 2012; Kalnins et al., 2015). Functional analysis also showed that the abundance of *cutC* gene was enriched in the gut microbiota of the hypertensive patients. These findings suggested that the dietary choline intake and TMAO production via gut microflora would be a probable pathway for hypertensive pathogenesis.

Klebsiella, is a pathogen routinely found in human gut that causes pneumonia, diarrhea, and urinary tract infection. The distribution of *Klebsiella* was found to be significantly higher in hypertensive patients compared to healthy controls as evident from **Figure 1C**. Overgrowth of *Klebsiella* usually foreshadows gut flora dysbiosis, which leads to a variety of serious chronic disease, such as, colitis (Garrett et al., 2010), Crohn's disease and ankylosing spondylitis (Ebringer et al., 2007).The present study demonstrates that *Klebsiella* species which are highly distributed in hypertensive patients are *K. pneumoniae* (the main component of *Klebsiella* that associated with nosocomial infection and multiple diseases), *K. variicola* [a human and animal opportunistic pathogen that is associated with bovine mastitis (Brisse and Duijkeren, 2005)], and four unclassified MLGs. Based on these information, however, the potential correlation between *Klebsiella* and hypertension is still unclear.

Streptococcus, the dominant species of human oral microbiome (Wade, 2013) that causes upper respiratory tract infection, were also found highly distributed in gut microbiota of hypertensive patients as compared to the controls. Gut streptococci is also associated with diseases, such as, inflammatory bowel disease (Conte et al., 2006) and liver cirrhosis (Qin et al., 2014). It has been reported previously that oral cavity and/or gut might be the source of streptococci found in the majority of atherosclerotic plaque microbiota (Koren et al., 2011). These findings suggest that possible correlation of gut streptococci in hypertension.

F. prausnitzii and *Roseburia* spp., which were abundantly distributed in controls compared to hypertensive patients, were also distributed abundantly in the healthy control microbiomes of many chronic diseases, including type 2 diabetes (Qin et al., 2012), liver cirrhosis (Qin et al., 2014), Crohn's disease (Gevers et al., 2014), and ulcerative colitis (Machiels et al., 2014). *F. prausnitzii* and *Roseburia* (both *R. intestinalis* and *R. hominis*) are the major SCFA producer in human colon (Shoaie et al., 2015), which might explain the depletion of SCFA-producing enzymes in hypertensive gut microbiome. Functionally, SCFAs modulates the gut inflammation and metabolism via functioning as important colonocytes energy source and signaling molecules (Donohoe et al., 2011), suggesting that low level of SCFA production in gut microbiota may be a considerable risk factor of multiple metabolic syndromes and hypertension.

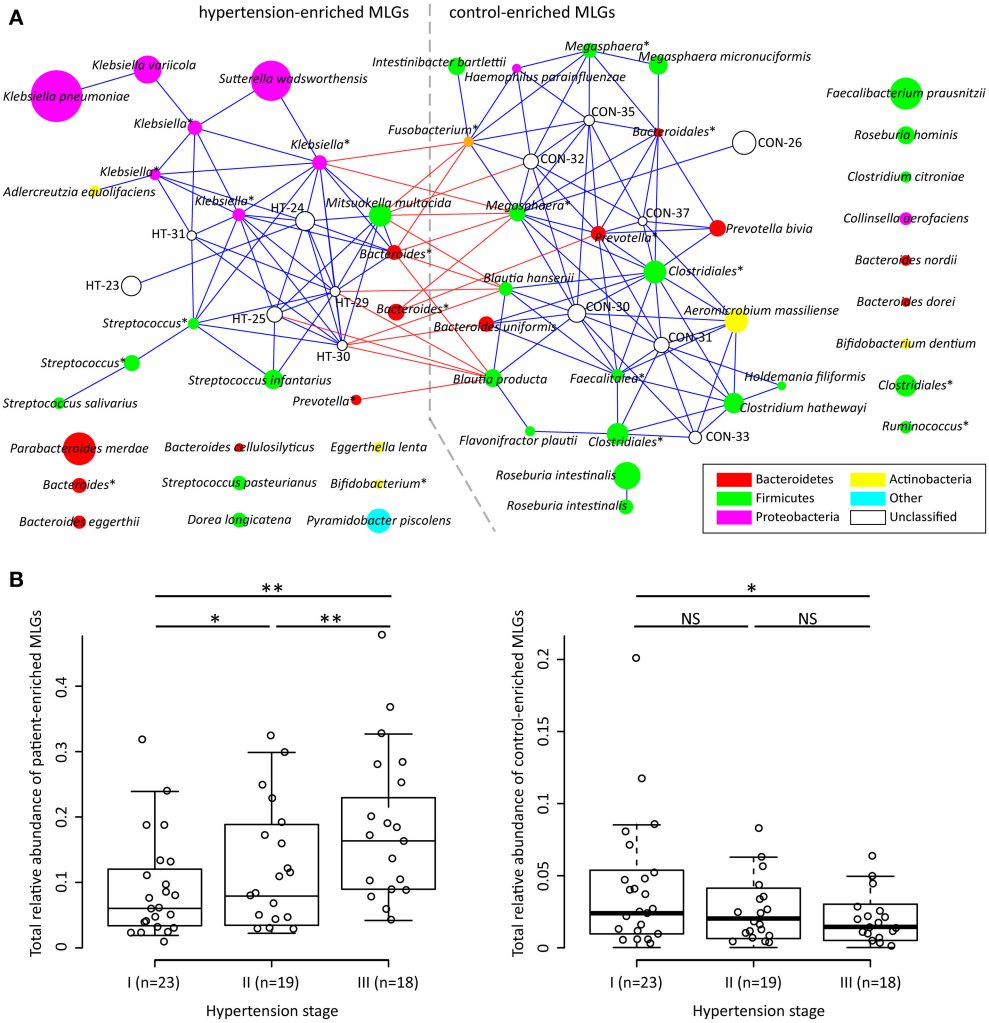

FIGURE 2 | Characterization and interconnection of hypertension-associated MLGs. **(A)** Co-occurrence network shows the interconnection of the hypertension- and control-enriched MLGs. Nodes depict MLGs with their ID or taxonomic assignment (unclassified MLGs under genus or higher taxonomy rank are marked by "*") displayed in the center. The size of the nodes indicates the number of gene within the MLG. Connecting lines represent Spearman correlation coefficient $\rho > 0.40$ (represented by blue line) or < -0.40 (represented by red line). **(B)**, Correlation of gross abundance of hypertension- and control-enriched MLGs with hypertension stage. NS, not significant; *, $q < 0.05$; **, $q < 0.01$; Mann-Whitney *U*-test corrected by FDR.

Several other bacteria also played important function in human gut and showed potential function in hypertension, such as, the patient-enriched *Bacteroides* (including *B. eggerthii*, *B. cellulosilyticus,* and 3 unclassified *Bacteroides* MLGs) and *Parabacteroides* (*P. merdae*) which are generally opportunistic pathogens in infectious diseases and are able to develop antimicrobial drug resistance (Boente et al., 2010), and the control-enriched *Megasphaera* spp. (*M. micronuciformis* and two unclassified MLGs) which are producer of SCFAs, vitamins and essential amino acids (Shetty et al., 2013). In addition, co-abundance analysis (**Figure 2A**) generated a striking number of positive correlations within the patient/control-enriched MLGs and negative correlations between the two groups, revealing that a comprehensive bacterial synergism and antagonism existed in the human gut. In this case, the microbial dysbiosis of hypertensive gut microbiome would not be determined by independent pathogens (e.g., the patient-enriched MLGs), but more likely to be caused by a series of risk factors (e.g., improper diet or lifestyle that inhibit the growth of beneficial bacterium) that change the balance of ecosystem. Intriguingly, the severity of hypertension was positively correlated with the total abundance of patient-enriched MLGs and negatively correlated with those of control-enriched MLGs (**Figure 2B**), suggesting that the bacterial relative abundance may also be a potential risk factor of hypertension development. Such a "dose response" was also found in the gut microbiome of liver cirrhosis (Qin et al., 2014) and colorectal adenoma-carcinoma patients (Feng et al., 2015).

Our study further provided the microbial markers for hypertension discrimination, and achieved an AUC of 0.78 for identifying disease status based on 68 species-level MLGs. This discriminatory power was higher than that from the prediction models based on genomic markers identified by GWAS (Evans

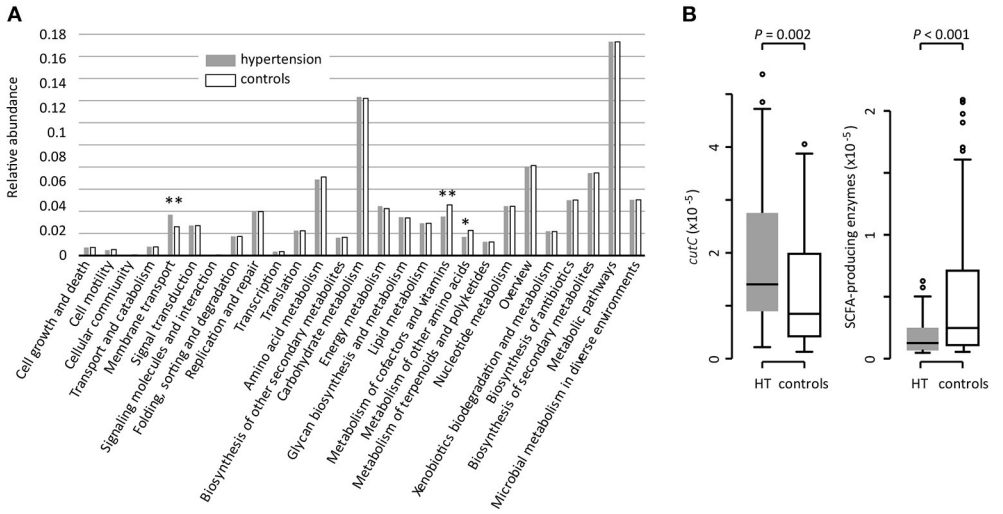

FIGURE 3 | Functional comparison of the gut microbiomes between hypertensive patients and healthy controls. **(A)**, Distributions of relative abundances of KEGG pathway categories in hypertensive patients and controls. *, $q < 0.05$; **, $q < 0.01$; Mann-Whitney *U*-test corrected by FDR. **(B)**, Difference of the relative abundance of *cutC* (TMA-producing) and SCFA-producing enzymes between hypertensive (HT) patients and controls.

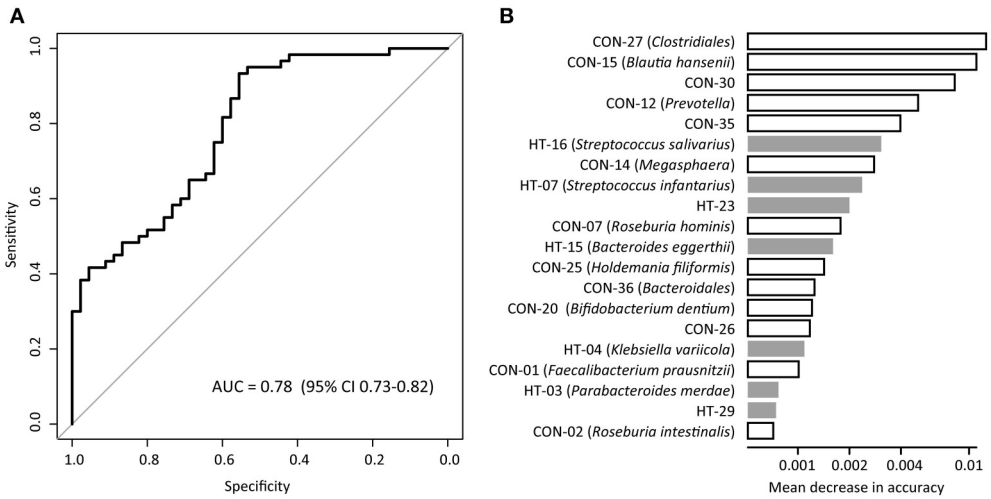

FIGURE 4 | Classification of hypertension status by the abundances of MLGs. **(A)**, ROC analysis for classification of hypertensive status by MLGs, assessed by AUC. **(B)**, The 20 most discriminant MLGs in the model classifying hypertensive patients and healthy controls. The bar lengths indicate the importance of the variable, and colors represent enrichment in patients (black) or controls (white).

et al., 2009; Fava et al., 2013), and was almost at same level with the phenotype-based models (AUC 0.71-0.81) (Echouffo-Tcheugui et al., 2013; Wang A. et al., 2015). Thus, the fecal microbiota showed a good potential on prediction and early diagnosis of hypertension, however, systematic investigations of key species and gene markers identified here might be helpful in the future.

Drug-induced gut microbiome shifts were observed during the treatment of multiple diseases, such as, the metformin therapy in type 2 diabetes (Forslund et al., 2015) and antirheumatic drugs therapy in rheumatoid arthritis (Zhang et al., 2015). In this study, a part of patients (∼35%) had taken antihypertensive drugs or specific nutritious supplementary, however, the relationship between drug treatment and gut microbiota is still unclear. Another significant limitation of this study is that the gut microbial community would be sensitive to environmental factors, such as, host race, geography, life and diet style, and so on. Although our samples were age-, gender-, BMI-matched, some phenotype differences were still unobservable. To avoid this, larger cohort containing multi-types of hypertensive patients are needed for further investigation. Generally, hypertension is a highly complex and heterogeneous disease, it is still infeasible at this moment to draw any conclusions about causal relationships of gut microbiota and

hypertension, and direct experimental studies (e.g., the animal model studies) are needed to show causality of proposed microbes or pathways.

In summary, our finding extends previous knowledge of correlation between gut microbiota and hypertension in animal models (Yang et al., 2015; Durgan et al., 2016) and provides a range of signatures in metagenomic diversity, genes, species, and functions of the hypertensive gut microbiome. Further studies on the causality relationship between hypertension and gut microbiota will lead to a better understanding of the mutual interaction.

AUTHOR CONTRIBUTIONS

YM, SL, and QY designed experiments; QY, LJ, CC, XH, YH, LZ, PL, and MK carried out experiments; QY, WY, YD, SW, and YX analyzed experimental results. SL, YG, XL, ZF, and JZ analyzed sequencing data. WY, XG, YD, and SW collected the samples. YM, SL, and QY wrote the manuscript.

FUNDING

This study was supported by grants from the National Naturel Science Foundation of China (81573469) and the National Basic Research Program of China (2012CB518803).

SUPPLEMENTARY MATERIAL

The Supplementary Material for this article can be found online at: http://journal.frontiersin.org/article/10.3389/fcimb.2017.00381/full#supplementary-material

REFERENCES

Adnan, S., Nelson, J. W., Ajami, N. J., Venna, V. R., Petrosino, J. F., Bryan, R. M. Jr., et al. (2017). Alterations in the gut microbiota can elicit hypertension in rats. *Physiol. Genomics* 49, 96–104. doi: 10.1152/physiolgenomics.00081.2016

Boente, R. F., Ferreira, L. Q., Falcao, L. S., Miranda, K. R., Guimaraes, P. L., Domingues, R. M., et al. (2010). Detection of resistance genes and susceptibility patterns in Bacteroides and Parabacteroides strains. *Anaerobe* 16, 190–194. doi: 10.1016/j.anaerobe.2010.02.003

Brisse, S., and Duijkeren, E. (2005). Identification and antimicrobial susceptibility of 100 Klebsiella animal clinical isolates. *Vet. Microbiol.* 105, 307–312. doi: 10.1016/j.vetmic.2004.11.010

Conte, M. P., Schippa, S., Zamboni, I., Penta, M., Chiarini, F., Cucchiara, S., et al. (2006). Gut-associated bacterial microbiota in paediatric patients with inflammatory bowel disease. *Gut* 55, 1760–1767. doi: 10.1136/gut.2005.078824

Craciun, S., and Balskus, E. P. (2012). Microbial conversion of choline to trimethylamine requires a glycyl radical enzyme. *Proc. Natl. Acad. Sci. U.S.A.* 109, 21307–21312. doi: 10.1073/pnas.1215689109

Dixon, P. (2003). VEGAN, a package of R functions for community ecology. *J. Veg. Sci.* 14, 927–930. doi: 10.1111/j.1654-1103.2003.tb02228.x

Donohoe, D. R., Garge, N., Zhang, X., Sun, W., O'Connell, T. M., Bultman, S. J., et al. (2011). The microbiome and butyrate regulate energy metabolism and autophagy in the mammalian colon. *Cell Metab.* 13, 517–526. doi: 10.1016/j.cmet.2011.02.018

Durgan, D. J., Ganesh, B. P., Cope, J. L., Ajami, N. J., Phillips, S. C., Petrosino, J. F., et al. (2016). Role of the gut microbiome in obstructive sleep apnea-induced hypertension. *Hypertension* 67, 469–474. doi: 10.1161/HYPERTENSIONAHA.115.06672

Ebringer, A., Rashid, T., Tiwana, H., and Wilson, C. (2007). A possible link between Crohn's disease and ankylosing spondylitis via Klebsiella infections. *Clin. Rheumatol.* 26, 289–297. doi: 10.1007/s10067-006-0391-2

Echouffo-Tcheugui, J. B., Batty, G. D., Kivimaki, M., and Kengne, A. P. (2013). Risk models to predict hypertension: a systematic review. *PLoS ONE* 8:e67370. doi: 10.1371/journal.pone.0067370

Edgar, R. C. (2010). Search and clustering orders of magnitude faster than BLAST. *Bioinformatics* 26, 2460–2461. doi: 10.1093/bioinformatics/btq461

Evans, D. M., Visscher, P. M., and Wray, N. R. (2009). Harnessing the information contained within genome-wide association studies to improve individual prediction of complex disease risk. *Hum. Mol. Genet.* 18, 3525–3531. doi: 10.1093/hmg/ddp295

Faraco, G., and Iadecola, C. (2013). Hypertension: a harbinger of stroke and dementia. *Hypertension* 62, 810–887. doi: 10.1161/HYPERTENSIONAHA.113.01063

Fava, C., Sjogren, M., Montagnana, M., Danese, E., Almgren, P., Engstrom, G., et al. (2013). Prediction of blood pressure changes over time and incidence of hypertension by a genetic risk score in Swedes. *Hypertension* 61, 319–326. doi: 10.1161/HYPERTENSIONAHA.112.202655

Feng, Q., Liang, S., Jia, H., Stadlmayr, A., Tang, L., Lan, Z., et al. (2015). Gut microbiome development along the colorectal adenoma-carcinoma sequence. *Nat. Commun.* 6:6528. doi: 10.1038/ncomms7528

Forslund, K., Hildebrand, F., Nielsen, T., Falony, G., Le Chatelier, E., Sunagawa, S., et al. (2015). Disentangling type 2 diabetes and metformin treatment signatures in the human gut microbiota. *Nature* 528, 262–266. doi: 10.1038/nature15766

Fuchs, F. D., Chambless, L. E., Whelton, P. K., Nieto, F. J., and Heiss, G. (2001). Alcohol consumption and the incidence of hypertension: the atherosclerosis risk in communities study. *Hypertension* 37, 1242–1250. doi: 10.1161/01.HYP.37.5.1242

Galla, S., Chakraborty, S., Mell, B., Vijay-Kumar, M., and Joe, B. (2017). Microbiotal-host interactions and hypertension. *Physiology* 32, 224–233. doi: 10.1152/physiol.00003.2017

Garrett, W. S., Gallini, C. A., Yatsunenko, T., Michaud, M., DuBois, A., Glimcher, L. H., et al. (2010). Enterobacteriaceae act in concert with the gut microbiota to induce spontaneous and maternally transmitted colitis. *Cell Host Microbe* 8, 292–300. doi: 10.1016/j.chom.2010.08.004

Gevers, D., Kugathasan, S., Denson, L. A., Vazquez-Baeza, Y., Van Treuren, W., Xavier, R. J., et al. (2014). The treatment-naive microbiome in new-onset Crohn's disease. *Cell Host Microbe* 15, 382–392. doi: 10.1016/j.chom.2014.02.005

Hakenbeck, R., Madhour, A., Denapaite, D., and Bruckner, R. (2009). Versatility of choline metabolism and choline-binding proteins in *Streptococcus pneumoniae* and commensal streptococci. *FEMS Microbiol. Rev.* 33, 572–586. doi: 10.1111/j.1574-6976.2009.00172.x

Kalnins, G., Kuka, J., Grinberga, S., Makrecka-Kuka, M., Liepinsh, E., Dambrova, M., et al. (2015). Structure and function of CutC Choline Lyase from human microbiota bacterium *Klebsiella pneumoniae*. *J. Biol. Chem.* 290, 21732–21740. doi: 10.1074/jbc.M115.670471

Kanehisa, M., Goto, S., Sato, Y., Kawashima, M., Furumichi, M., and Tanabe, M. (2014). Data, information, knowledge and principle: back to metabolism in KEGG. *Nucleic Acids Res.* 42, D199–D205. doi: 10.1093/nar/gkt1076

Karppanen, H., and Mervaala, E. (2006). Sodium intake and hypertension. *Prog. Cardiovasc. Dis.* 49, 59–75. doi: 10.1016/j.pcad.2006.07.001

Koeth, R. A., Wang, Z., Levison, B. S., Buffa, J. A., Org, E., Hazen, S. L., et al. (2013). Intestinal microbiota metabolism of L-carnitine, a nutrient in red meat, promotes atherosclerosis. *Nat. Med.* 19, 576–585. doi: 10.1038/nm.3145

Koh, A., De Vadder, F., Kovatcheva-Datchary, P., and Backhed, F. (2016). From dietary fiber to host physiology: short-chain fatty acids as key bacterial metabolites. *Cell* 165, 1332–1345. doi: 10.1016/j.cell.2016.05.041

Koren, O., Spor, A., Felin, J., Fak, F., Stombaugh, J., Tremaroli, V., et al. (2011). Human oral, gut, and plaque microbiota in patients with atherosclerosis. *Proc. Natl. Acad. Sci. U.S.A.* 108(Suppl. 1), 4592–4598. doi: 10.1073/pnas.1011383107

Kotchen, T. A. (2010). Obesity-related hypertension: epidemiology, pathophysiology, and clinical management. *Am. J. Hypertens.* 23, 1170–1178. doi: 10.1038/ajh.2010.172

Landsberg, L., and Molitch, M. (2004). Diabetes and hypertension: pathogenesis, prevention and treatment. *Clin. Exp. Hypertens.* 26, 621–628. doi: 10.1081/CEH-200031945

Lash, J. P., Go, A. S., Appel, L. J., He, J., Ojo, A., Chronic Renal Insufficiency Cohort Study, G., et al. (2009). Chronic Renal Insufficiency Cohort (CRIC) study: baseline characteristics and associations with kidney function. *Clin. J. Am. Soc. Nephrol.* 4, 1302–1311. doi: 10.2215/CJN.00070109

Le Chatelier, E., Nielsen, T., Qin, J., Prifti, E., Hildebrand, F., Falony, G., et al. (2013). Richness of human gut microbiome correlates with metabolic markers. *Nature* 500, 541–546. doi: 10.1038/nature12506

Li, J., Jia, H., Cai, X., Zhong, H., Feng, Q., Sunagawa, S., et al. (2014). An integrated catalog of reference genes in the human gut microbiome. *Nat. Biotechnol.* 32, 834–841. doi: 10.1038/nbt.2942

Li, J., Zhao, F., Wang, Y., Chen, J., Tao, J., Tian, G., et al. (2017). Gut microbiota dysbiosis contributes to the development of hypertension. *Microbiome* 5:14. doi: 10.1186/s40168-016-0222-x

Li, R., Yu, C., Li, Y., Lam, T. W., Yiu, S. M., Wang, J., et al. (2009). SOAP2: an improved ultrafast tool for short read alignment. *Bioinformatics* 25, 1966–1967. doi: 10.1093/bioinformatics/btp336

Lim, S. S., Vos, T., Flaxman, A. D., Danaei, G., Shibuya, K., Memish, Z. A., et al. (2012). A comparative risk assessment of burden of disease and injury attributable to 67 risk factors and risk factor clusters in 21 regions, 1990-2010: a systematic analysis for the global burden of disease study 2010. *Lancet* 380, 2224–2260. doi: 10.1016/S0140-6736(12)61766-8

Liu, C., Kraja, A. T., Smith, J. A., Brody, J. A., Franceschini, N., Chasman, D. I., et al. (2016). Meta-analysis identifies common and rare variants influencing blood pressure and overlapping with metabolic trait loci. *Nat. Genet.* 48, 1162–1170. doi: 10.1038/ng.3660

Louis, P., Young, P., Holtrop, G., and Flint, H. J. (2010). Diversity of human colonic butyrate-producing bacteria revealed by analysis of the butyryl-CoA:acetate CoA-transferase gene. *Environ. Microbiol.* 12, 304–314. doi: 10.1111/j.1462-2920.2009.02066.x

Machiels, K., Joossens, M., Sabino, J., De Preter, V., Arijs, I., Eeckhaut, V., et al. (2014). A decrease of the butyrate-producing species *Roseburia hominis* and *Faecalibacterium prausnitzii* defines dysbiosis in patients with ulcerative colitis. *Gut* 63, 1275–1283. doi: 10.1136/gutjnl-2013-304833

Mell, B., Jala, V. R., Mathew, A. V., Byun, J., Waghulde, H., Joe, B., et al. (2015). Evidence for a link between gut microbiota and hypertension in the Dahl rat. *Physiol. Genomics* 47, 187–197. doi: 10.1152/physiolgenomics.00136.2014

Menni, C., Graham, D., Kastenmuller, G., Alharbi, N. H., Alsanosi, S., M., Valdes, A. M., et al. (2015). Metabolomic identification of a novel pathway of blood pressure regulation involving hexadecanedioate. *Hypertension* 66, 422–429. doi: 10.1161/HYPERTENSIONAHA.115.05544

Mills, K. T., Bundy, J. D., Kelly, T. N., Reed, J. E., Kearney, P. M., He, J., et al. (2016). Global disparities of hypertension prevalence and control: a systematic analysis of population-based studies from 90 countries. *Circulation* 134, 441–450. doi: 10.1161/CIRCULATIONAHA.115.018912

Mittal, B. V., and Singh, A. K. (2010). Hypertension in the developing world: challenges and opportunities. *Am. J. Kidney Dis.* 55, 590–598. doi: 10.1053/j.ajkd.2009.06.044

Pryde, S. E., Duncan, S. H., Hold, G. L., Stewart, C. S., and Flint, H. J. (2002). The microbiology of butyrate formation in the human colon. *FEMS Microbiol. Lett.* 217, 133–139. doi: 10.1111/j.1574-6968.2002.tb11467.x

Qin, J., Li, Y., Cai, Z., Li, S., Zhu, J., Zhang, F., et al. and Wang, J. (2012). A metagenome-wide association study of gut microbiota in type 2 diabetes. *Nature* 490, 55–60. doi: 10.1038/nature11450

Qin, N., Yang, F., Li, A., Prifti, E., Chen, Y., Shao, L., et al. (2014). Alterations of the human gut microbiome in liver cirrhosis. *Nature* 513, 59–64. doi: 10.1038/nature13568

Reichardt, N., Duncan, S. H., Young, P., Belenguer, A. C., McWilliam Leitch,C., Scott, K., et al. (2014). Phylogenetic distribution of three pathways for propionate production within the human gut microbiota. *ISME J.* 8, 1323–1335. doi: 10.1038/ismej.2014.14

Santisteban, M. M., Qi, Y., Zubcevic, J., Kim, S., Yang, T., Raizada, M. K., et al. (2017). Hypertension-linked pathophysiological alterations in the gut. *Circ. Res.* 120, 312–323. doi: 10.1161/CIRCRESAHA.116.309006

Shannon, P., Markiel, A., Ozier, O., Baliga, N. S., Wang, J. T., Ideker, T., et al. (2003). Cytoscape: a software environment for integrated models of biomolecular interaction networks. *Genome Res.* 13, 2498–2504. doi: 10.1101/gr.1239303

Shetty, S. A., Marathe, N. P., Lanjekar, V., Ranade, D., and Shouche, Y. S. (2013). Comparative genome analysis of *Megasphaera* sp. reveals niche specialization and its potential role in the human gut. *PLoS ONE* 8:e79353. doi: 10.1371/journal.pone.0079353

Shoaie, S., Ghaffari, P., Kovatcheva-Datchary, P., Mardinoglu, A., Sen, P., Pujos-Guillot, E., et al. (2015). Quantifying diet-induced metabolic changes of the human gut microbiome. *Cell Metab.* 22, 320–331. doi: 10.1016/j.cmet.2015.07.001

Tang, W. H., Wang, Z., Levison, B. S., Koeth, R. A., Britt, E. B., Hazen, S. L., et al. (2013). Intestinal microbial metabolism of phosphatidylcholine and cardiovascular risk. *N. Engl. J. Med.* 368, 1575–1584. doi: 10.1056/NEJMoa1109400

Ufnal, M., Jazwiec, R., Dadlez, M., Drapala, A., Sikora, M., and Skrzypecki, J. (2014). Trimethylamine-N-oxide: a carnitine-derived metabolite that prolongs the hypertensive effect of angiotensin II in rats. *Can. J. Cardiol.* 30, 1700–1705. doi: 10.1016/j.cjca.2014.09.010

Wade, W. G. (2013). The oral microbiome in health and disease. *Pharmacol. Res.* 69, 137–143. doi: 10.1016/j.phrs.2012.11.006

Wang, A., An, N., Chen, G., Li, L., and Alterovitz, G. (2015). Predicting hypertension without measurement: a non-invasive, questionnaire-based approach. *Expert Syst. Appl.* 42, 7601–7609. doi: 10.1016/j.eswa.2015.06.012

Wang, Z., Klipfell, E., Bennett, B. J., Koeth, R., Levison, B. S., Hazen, S. L., et al. (2011). Gut flora metabolism of phosphatidylcholine promotes cardiovascular disease. *Nature* 472, 57–63. doi: 10.1038/nature09922

Wang, Z., Roberts, A. B., Buffa, J. A., Levison, B. S., Zhu, W., Hazen, S. L., et al. (2015). Non-lethal inhibition of gut microbial trimethylamine production for the treatment of atherosclerosis. *Cell* 163, 1585–1595. doi: 10.1016/j.cell.2015.11.055

Xu, K., Ma, L., Li, Y., Wang, F., Zheng, G. Y., Tian, X. L., et al. (2015). Genetic and functional evidence supports LPAR1 as a susceptibility gene for hypertension. *Hypertension* 66, 641–646. doi: 10.1161/HYPERTENSIONAHA.115.05515

Yan, Q., Cui, S., Chen, C., Li, S., Sha, S., Wan, X., et al. (2016). Metagenomic analysis of sputum microbiome as a tool toward culture-independent pathogen detection of patients with ventilator-associated pneumonia. *Am. J. Respir. Crit. Care Med.* 194, 636–639. doi: 10.1164/rccm.201601-0034LE

Yang, T., Santisteban, M. M., Rodriguez, V., Li, E., Ahmari, N., Mohamadzadeh, M., et al. (2015). Gut dysbiosis is linked to hypertension. *Hypertension* 65, 1331–1340. doi: 10.1161/HYPERTENSIONAHA.115.05315

Zhang, X., Zhang, D., Jia, H., Feng, Q., Wang, D., Liang, D., et al. (2015). The oral and gut microbiomes are perturbed in rheumatoid arthritis and partly normalized after treatment. *Nat. Med.* 21, 895–905. doi: 10.1038/nm.3914

Conflict of Interest Statement: The authors declare that the research was conducted in the absence of any commercial or financial relationships that could be construed as a potential conflict of interest.

Copyright © 2017 Yan, Gu, Li, Yang, Jia, Chen, Han, Huang, Zhao, Li, Fang, Zhou, Guan, Ding, Wang, Khan, Xin, Li and Ma. This is an open-access article distributed under the terms of the Creative Commons Attribution License (CC BY). The use, distribution or reproduction in other forums is permitted, provided the original author(s) or licensor are credited and that the original publication in this journal is cited, in accordance with accepted academic practice. No use, distribution or reproduction is permitted which does not comply with these terms.

frontiers in Cellular and Infection Microbiology

PERSPECTIVE
published: 11 July 2017
doi: 10.3389/fcimb.2017.00318

Secretory Products of the Human GI Tract Microbiome and Their Potential Impact on Alzheimer's Disease (AD): Detection of Lipopolysaccharide (LPS) in AD Hippocampus

Yuhai Zhao[1,2], *Vivian Jaber*[1] *and Walter J. Lukiw*[1,3,4]*

[1] LSU Neuroscience Center, Louisiana State University Health Science Center, New Orleans, LA, United States, [2] Department of Anatomy and Cell Biology, Louisiana State University Health Science Center, New Orleans, LA, United States, [3] Department of Ophthalmology, Louisiana State University Health Science Center, New Orleans, LA, United States, [4] Department of Neurology, Louisiana State University Health Science Center, New Orleans, LA, United States

Although the potential contribution of the human gastrointestinal (GI) tract microbiome to human health, aging, and disease is becoming increasingly acknowledged, the molecular mechanics and signaling pathways of just how this is accomplished is not well-understood. Major bacterial species of the GI tract, such as the abundant Gram-negative bacilli *Bacteroides fragilis* (*B. fragilis*) and *Escherichia coli* (*E. coli*), secrete a remarkably complex array of pro-inflammatory neurotoxins which, when released from the confines of the healthy GI tract, are pathogenic and highly detrimental to the homeostatic function of neurons in the central nervous system (CNS). For the first time here we report the presence of bacterial lipopolysaccharide (LPS) in brain lysates from the hippocampus and superior temporal lobe neocortex of Alzheimer's disease (AD) brains. Mean LPS levels varied from two-fold increases in the neocortex to three-fold increases in the hippocampus, AD over age-matched controls, however some samples from advanced AD hippocampal cases exhibited up to a 26-fold increase in LPS over age-matched controls. This "Perspectives" paper will further highlight some very recent research on GI tract microbiome signaling to the human CNS, and will update current findings that implicate GI tract microbiome-derived LPS as an important internal contributor to inflammatory degeneration in the CNS.

Keywords: 42 amino acid amyloid-beta (Aβ42) peptide, Alzheimer's disease (AD), *Bacteriodetes fragilis* (*B. fragilis*), *Escherichia coli* (*E. coli*), lipopolysaccharide (LPS), microbiome, small non-coding RNAs (sncRNAs), thanatomicrobiome

OPEN ACCESS

Edited by:
Michele Marie Kosiewicz, University of Louisville, United States

Reviewed by:
Rebecca Drummond, National Institutes of Health, United States
Valerio Iebba, Sapienza Università di Roma, Italy

***Correspondence:**
Walter J. Lukiw
wlukiw@lsuhsc.edu

Received: *24 March 2017*
Accepted: *27 June 2017*
Published: *11 July 2017*

Citation:
Zhao Y, Jaber V and Lukiw WJ (2017) Secretory Products of the Human GI Tract Microbiome and Their Potential Impact on Alzheimer's Disease (AD): Detection of Lipopolysaccharide (LPS) in AD Hippocampus. Front. Cell. Infect. Microbiol. 7:318. doi: 10.3389/fcimb.2017.00318

INTRODUCTION: THE HUMAN GI TRACT MICROBIOME

The human GI tract is fundamentally a highly vascularized and extensively innervated, columnar epithelial-cell lined tube about 9 m (30 feet) in length that consists of the stomach, small intestine (duodenum, jejunum, and ileum) and large intestine (cecum, colon, rectum, and anal canal; Reinus and Simon, 2014). Each anatomical region of this tubular structure harbors a complex and dynamic microbiome, containing ~1,000 different species of anaerobic or facultative anaerobic

bacteria that appear to be characteristic for that GI tract segment. Indeed, the dynamism of the GI tract microbiome along its length is in part reflected by the abundance, speciation, complexity and stoichiometry of individual resident bacterial species. In addition to the major bacterial component of the GI tract are microbial eukaryotes, archaea, fungi, protozoa, viruses, and other commensal microorganisms which make up the remainder. Together with host cells these jointly comprise the complete metaorganism: (i) whose symbiotic associations and interactions are indispensable for homeostatic physiological functions in human health; and (ii) which exhibit alterations in composition in response to dietary factors, developmental stage, GI tract disturbances, aging, and neurological disorders, including AD (Bhattacharjee and Lukiw, 2013; Hill et al., 2014; Perez et al., 2014; Potgieter et al., 2015; Zhao and Lukiw, 2015; Alkasir et al., 2016; Ghaisas et al., 2016; Hu et al., 2016; Lukiw, 2016; Pistollato et al., 2016; Scheperjans, 2016).

GI TRACT BACTERIAL MICROBIOME—EXUDATES AND SECRETORY PRODUCTS

Two large prokaryotic classes of Bacteria (*or "Eubacteria"*) and Archaea (or "*Archaeobacteria*") have been recently reclassified (as of 10/2016) into 35 phyla (http://www.bacterio.net/-classifphyla.html) or major bacterial divisions. Interestingly the GI tract microbiome of *Homo sapiens* has co-evolved with just two major phyla: *Bacteriodetes*, which make up ∼20% of all GI tract bacteria, and *Firmicutes,* which make up ∼80% of all GI tract bacteria; with *Actinobacteria* (∼3%), *Proteobacteria* (∼1%), and *Verrumicrobia* (∼0.1%) making up significantly smaller fractions. These five bacterial groups appear to constitute the essential "*core*" of the human GI tract microbiome (http://www.bacterio.net/-classifphyla.html; Zhao et al., 2015; Hug et al., 2016; Lloyd-Price et al., 2016; Sender et al., 2016). The vast proportion of all GI tract microbiota consists of anaerobic or facultative anaerobic bacteria (Bhattacharjee and Lukiw, 2013; Heintz and Mair, 2014; Köhler et al., 2016; Lloyd-Price et al., 2016). For example, although variable, the obligate anaerobe *Bacteroides fragilis* (*B. fragilis*; phyla *Bacteroidetes)* and the facultative anaerobe *Escherichia coli* (*E. coli*; phyla Proteobacteria): (i) together constitute ∼35–40 percent of all GI tract bacteria; (ii) are the most abundant Gram-negative bacilli of the middle and lower colon, respectively, of the human GI tract; and (iii) constitute about ∼30–50 percent of the dry weight of fecal matter. *B. fragilis* or *E. coli* require about 20 min to divide under optimal conditions of commensal bacterial growth, and unless special biophysical processes of growth dynamics are in operation (such as dormancy, hibernation, spore formation, etc.) have a life span of up to several hours (Choi and Cho, 2016; Pinti et al., 2016; Todar, 2016). Interestingly, species of the obligate anaerobe *Bacteroides* such as *B. fragilis* display remarkably diverse antibiotic resistance mechanisms and exhibit the highest resistance rates of any anaerobic pathogen. This includes an inherent high-level resistance to penicillin through their ability to produce beta-lactamase enzymes which endow them with multiple resistance to β-lactam antibiotics such as penicillin and cephamycin (Ayala et al., 2005; Bush and Bradford, 2016; Hu et al., 2016). Specific species of *Bacteroidetes* such as *Bacteroides fragilis* (*B. fragilis*), normally an abundant commensal microorganism of the middle GI tract, are known to be generally beneficial to human health through their ability to digest dietary fiber and related dietary fiber precursors containing substances such as cellulose, lignin, and pectin, which are normally resistant to the action of host digestive enzymes.

Dietary fibers are catabolized into digestible short-chain fatty acids (SCFAs), volatile fatty acids and polysaccharides in part through the biosynthetic capability of this GI tract abundant bacillus (Keenan et al., 2016; Scheperjans, 2016). When *B. fragilis* escapes the highly compartmentalized microbe-dense environment of the GI tract (10^{11} microbes per gram of fecal matter), they can induce substantial systemic inflammatory pathology with significant sickness, morbidity and mortality (Choi et al., 2016; Fathi and Wu, 2016; Cattaneo et al., 2017; Shivaji, 2017). Enterotoxigenic strains of *B. fragilis* have been associated with bacteremia, colitis, diarrhea, sepsis, systemic infection, and the development of GI tract cancers and neurological disorders, including AD, that have an increased incidence with aging (Choi et al., 2016; Fathi and Wu, 2016; Keenan et al., 2016; Scheperjans, 2016). Interestingly, certain species of Bacteroidetes have been recently shown to propagate in animal models fed high fat-cholesterol (HFC) diets deprived of sufficient intake of dietary fiber; this suggests that sufficient dietary fiber may have a significant role in regulating the abundance, complexity and stoichiometry of certain species in the GI tract microbiome, including *B. fragilis* (Heinritz et al., 2016; Köhler et al., 2016; Pistollato et al., 2016; unpublished observations). In addition to these positive health benefits however, these vast numbers of human GI tract resident Gram-negative bacilli when stressed secrete prodigious quantities of endotoxins, exotoxins, endotoxins, exotoxins, lipooligosacahrides (LOSs) and lipopolysaccharides (LPSs), amyloids, and small non-coding RNAs (sncRNAs; see below and **Figure 1**).

ENDOTOXINS AND EXOTOXINS

Generally, microbiome-derived endotoxins are heat-stable polypeptides associated with the outer membranes of the cell wall of Gram-negative bacteria. They may be composed in part by the Lipid A component of LPS, and once they diffuse into the local environment induce irritation of the GI tract epithelia, capillaries and blood vessels inducing hemorrhage and various pro-inflammatory effects. Endotoxins also induce fever, hemorrhagic shock, diarrhea, altered resistance to bacterial infection, leukopenia followed by leukocytosis, and numerous other systemic effects (Choi et al., 2016; Seong et al., 2016; Zhan and Davies, 2016). For example, in addition to their prodigious LPS generation (see below), *B. fragilis* endotoxins are a leading cause of anaerobic bacteremia, sepsis and systemic inflammatory distress through their generation of the highly pro-inflammatory zinc metalloproteinase fragilysin, also known as *B. fragilis* toxin

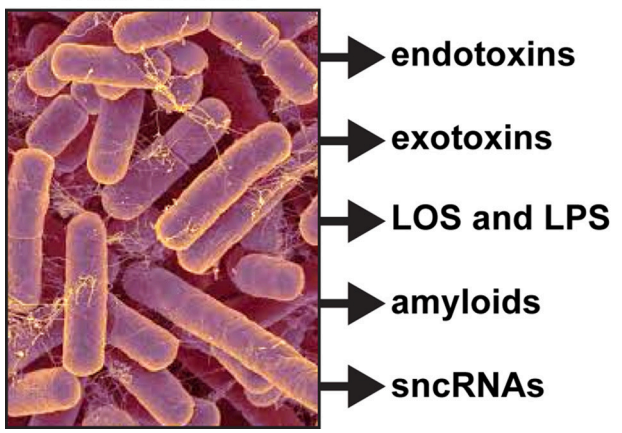

FIGURE 1 | Like other Gram-negative bacilli, the gastrointestinal (GI) tract abundant *Bacteroides fragilis* (micrograph of *B. fragilis* shown; original photo courtesy of Rosa Rubicondior; (http://rosarubicondior.blogspot.com/2014/11/evolving-cooperation-but-for-who-or-what.html) is capable, when stressed, of releasing a broad spectrum of highly neurotoxic, pro-inflammatory and potentially pathogenic molecules; these comprise five major classes of secreted molecules and include endotoxins, exotoxins, lipooligosacahride (LOS) and lipopolysaccharide (LPS), amyloids, and small non-coding RNAs (sncRNA). For example, the human GI tract-abundant *B. fragilis* secretes the endotoxin fragilysin and *B. fragilis* LPS (BF-LPS) both of which have been shown recently to be strongly pro-inflammatory and extremely neurotoxic toward human CNS neurons in primary culture (Li et al., 2016; Lukiw, 2016). While the phyla *Bacteriodetes* (∼20% of all GI tract bacteria), *Firmicutes* (∼80% of all GI tract bacteria), *Actinobacteria, Proteobacteria,* and *Verrumicrobia* (together, typically ∼4% of all GI tract bacteria), are the most common microbes in the human GI tract microbiome it should be kept in mind that other microbes including fungus, protozoa, viruses, and other commensal microorganisms may also contribute neurotoxic exudates which are highly toxic and detrimental to the homeostasis of CNS neurons.

or BFT (Zhao and Lukiw, 2015; Choi et al., 2016; Fathi and Wu, 2016). BFT has recently been shown to effectively disrupt epithelial cells of GI tract barriers via cleavage of the synaptic type-1 transmembrane zonula adhesion calcium-dependent adhesion protein E-cadherin (Choi et al., 2016; Seong et al., 2016; Zhan and Davies, 2016). It is currently not understood if GI tract- or BBB-disrupting proteolytic endotoxins such as BFT are able to propagate their pathogenic activities via the systemic circulation to further disrupt the GI tract or BBB at distant sites, to ultimately transfer endotoxins, exotoxins, LPSs, amyloids and/or sncRNAs into the cerebrovascular circulation to target brain cells within the CNS. *B. fragilis* has been suggested to contribute to neurodevelopmental pathology in autism spectrum disorder (ASD; Hsiao et al., 2013; Hofer, 2014; Keaney and Campbell, 2015). It has also recently been reported that along with BFTs amyloid peptide-dependent changes in synaptic adhesion affect both the function and integrity of synapses, suggesting that the observed failure of synaptic adhesion in AD play key roles in the progressive disruption of functional signaling throughout neuronal networks, as is observed in AD brain (Lin et al., 2014; Seong et al., 2015; Leshchyns'ka and Sytnyk, 2016).

Exotoxins are generally complex soluble polypeptides produced on the inside of pathogenic bacteria as part of their normal growth and metabolism, and these are typically excreted by living cells or released during bacterial cell lysis into the surrounding medium. The relatively short lifespan of GI tract bacteria (see above) and their subsequent lysis indicate that lysed bacteria contents may be a relatively persistent source of exotoxins which may need to be either efficiently neutralized or eliminated by the GI tract. Interestingly, under some conditions in rodents certain endotoxins are so toxic that they may be lethal to the host before the innate immune system has a chance to mount immune defenses to promote their neutralization (Bhattacharjee and Lukiw, 2013; Asti and Gioglio, 2014; Hill et al., 2014; Hill and Lukiw, 2015).

LIPOOLIGOSACAHRIDE (LOS) AND LIPOPOLYSACCHARIDE (LPS)

As an abundant Gram negative bacilli of the human GI tract microbiome both *B. fragilis* and *E. coli* secrete lipooligosacahrides (LOS) and lipopolysaccharides (LPS) that are strongly immunogenic and highly pro-inflammatory toward human neurons (Bian et al., 2011; Alkasir et al., 2016; Fathi and Wu, 2016; Foster et al., 2016; Ghaisas et al., 2016; Hug et al., 2016; Lukiw, 2016; Rogers and Aronoff, 2016; Sender et al., 2016; Sharon et al., 2016). LPSs, as characteristic components of the outer leaflet of the outer membrane of Gram-negative bacteria shed into the extracellular space, play key roles in host-pathogen interactions and the innate-immune system (Hill and Lukiw, 2015; Zhao et al., 2015; Maldonado et al., 2016). While LPSs contain large and hypervariable oligosaccharide/polysaccharide regions, the relatively conserved lipid region (lipid A) is the endotoxic and biologically active moiety that is largely responsible for septic shock (Jiang et al., 2016; Maldonado et al., 2016). A canonic LPS structure is represented by that of *E. coli* LPS, one of the most potent neurotoxic lipid A species known, consisting of a 1,4′-biphosphorylated glucosamine disaccharide bearing six fatty acids which are unbranched chains 12–14 methyl(ene) units in length. Other "lipid A" species show variability in the number, length, and composition of the attached fatty acids, as well as variability in the degree of phosphorylation and number and types of substituted phosphate ligands. For instance, BF-LPS lipid A is penta-acylated and mono-phosphorylated, and contains branched fatty acids 15–17 methyl(ene) units in length; deviations from the canonical lipid A structure are known to have a profound impact on innate-immune responses. Gram-negative bacterial exudates such as BF-LPSs are hypervariable in composition, and different *Bacteroidetes* species appear to generate unique temporal patterns of LPS production. These exhibit rapid and remarkably adaptive changes in LPS structure and alterations in *damage- or pathogen-associated molecular patterns* (DAMP/PAMP) as strategies for host immune evasion (Friedland, 2015; Land, 2015; Maldonado et al., 2016; Richards et al., 2016). Here, for

the first time, we provide evidence that *E. coli* LPS is abundant in neocortical and hippocampal extracts from AD brain, regions of the human limbic system targeted by intense neuro-inflammation characteristic of the AD process (see **Figure 1** and legend). Similarly the pathological actions of LPS on the induction of pro-inflammatory signaling in primary human neurons have recently been demonstrated, and additional studies are in progress (Lukiw, 2016).

AMYLOIDS

Atypical amyloid generation, aggregation, folding, and impaired clearance are characteristic pathological features of human neuro-inflammatory and neurodegenerative disorders of the CNS that include AD (Calsolaro and Edison, 2016; Andreeva et al., 2017). What is generally not appreciated is that a major secretory product of the GI tract microbiome is amyloid, and that the life-long contribution of microbial amyloid to CNS pathophysiology can be very substantial. "Amyloid" is a generic term for any aggregated, insoluble, lipoprotein-enriched deposit that exhibits β-pleated sheet structures oriented perpendicular to the fibrillar axis (Lukiw, 2012; Clark and Vissel, 2015; Lim et al., 2015; Andreeva et al., 2017; Bolós et al., 2017). The potential for amyloid formation is surprisingly high in almost all proteins; a major factor for amyloid formation is the presence within proteins of primary amino acid sequences that can form a tight, self-complementary interface with an identical segment, thus permitting the cooperative formation of a steric zipper. Two self-complementary beta-sheets form the backbone of the amyloid fibril (Goldschmidt et al., 2010; Buxbaum and Linke, 2012; Andreeva et al., 2017). The characterization of the "amylome," a categorization of amino acid sequences that possess self-complementary interfaces and high fiber-forming propensity has improved our understanding of the capability of different proteins to generate amyloid (Goldschmidt et al., 2010; Lukiw, 2012; Andreeva et al., 2017). The progressive generation and aggregation of amyloids contribute to "dense-deposit" disease; the pathogenesis of diseases that accumulate amyloid, including AD, all involve prominent inflammatory responses at sites of amyloid deposition—these accumulations are often mediated by microglial cells, the "resident immune cells" of the CNS. Interestingly, most microbial species, including fungi and bacteria, secrete self-associating and strongly amyloidogenic lipoproteins (Hill et al., 2014; Syed and Boles, 2014; Schwartz et al., 2016). For instance, amyloids are associated with fungal surface-structures and the recent observation of amyloidogenic fungal proteins and diffuse mycoses in the blood of AD patients suggest that chronic fungal infection over the course of aging may increase AD risk (Alonso et al., 2014; Hill et al., 2014). Of further relevance is that: (i) Aβ42 peptide monomers, dimers, oligomers and fibrils each induce patterns of pro-inflammatory gene signaling typical of the classical microglial-mediated innate-immune and inflammatory response induced by infectious agents such as bacterial LPS (Ferrera et al., 2014; Calsolaro and Edison, 2016; Lukiw, 2016; Andreeva et al., 2017); (ii) the presence of bacterial LPS or endotoxin/exotoxin-mediated inflammatory signaling strongly contributes to amyloid neurotoxicity (Lee et al., 2008; Asti and Gioglio, 2014; Zhao and Lukiw, 2015; Zhao et al., 2016); (iii) AD amyloids, like prion amyloids, once formed, may induce a self-perpetuating process leading to amplification, aggregation, and spreading of pathological aggregates (Le et al., 2014); and (iv) recently it has been shown that Aβ42 peptide fibrillogenesis is strongly potentiated by soluble bacterial exudates and viruses such as HSV-1, suggesting the contribution of microbial-sourced factors and/or infectious events to amyloidogenesis, a distinguishing feature of the AD neuropathology (Hill et al., 2014; Stilling et al., 2014; Zhao et al., 2015; Russo et al., 2017).

SMALL NON-CODING RNA (sncRNA)

While the secretion of proteins, lipids, and nucleic acids (both RNA and DNA) from neural cells into the extracellular space is a commonly recognized phenomenon in neurobiology, the secretion of small non-coding RNA (sncRNA) from microbial cells into the GI tract has only been very recently characterized (Ghosal et al., 2015; Lukiw, 2016; Ghosal, 2017). Employing multi-component secretion systems, sncRNAs may be exuded from bacteria as separate entities, or more commonly, contained within lipid spheres or outer membrane vesicles (OMVs; Ghosal et al., 2015; unpublished observations). A major fraction of all secreted extracellular RNAs are sncRNAs in the size range of 15–40 nucleotides derived from specific intracellular bacterial RNAs. These sncRNAs have been speculated to be involved in immune-evasion, intra-species communication, in inter-kingdom genetic exchanges, pathogenicity and/or microbiome-host signaling; indeed protein-, lipid-, and nucleic acid-containing OMVs released by GI tract Gram-negative bacteria can be intensely pro-inflammatory, pathogenic or even lethal to the host (Zhao and Lukiw, 2015; Ghosal, 2017; Lukiw and Rogaev, 2017; unpublished observations). Several important questions remain to be answered: (i) do secreted sncRNAs play any role in microbiome survival, immune evasion and/or antibiotic resistance? (ii) how do GI tract microbes promote and organize the regulation of sncRNA trafficking (iii) how are bacterial sncRNAs transported across bacterial membranes and subsequently released into the extracellular space? (iv) how are the sncRNAs selected and packaged for export? and (v) are there differences in secreted sncRNA profiles between pathogenic and non-pathogenic bacteria and/or between healthy and diseased states of the host? Further investigations in the field of extracellular bacterial sncRNAs are clearly needed to shed light on their potential role as mediators of microbiome-host signaling and intercellular communication. By studying bacterial secreted sncRNA patterns, we may be able to further advance our understanding of the complex interactions that exist between humans and their GI tract microbiome and design, perhaps through dietary manipulation, highly effective intervention strategies that could improve and optimize human neurological health.

THANATOMICROBIOME

Evidence for the immense biophysiological efforts in keeping the GI tract microbiome contained within GI tract compartments

and from expansion beyond its normal niche, comes from analysis of the human microbiome at the time of death. Very little data are available concerning what happens to the microbiome when a human host dies—in a healthy adult, most internal organs such as the spleen, liver, heart, and brain are generally devoid of microbes because the innate-immune system or other microbial components keeps them in check. After death, however, the generation of ATP ceases, the innate-immune system falters and microbes proliferate throughout the body; this has recently been shown to begin in the ileocecal area of the GI tract, spreading to the liver and spleen, and continuing to the heart and brain (Alan and Sarah, 2012; Can et al., 2014; Clement et al., 2016; Javan et al., 2016). Still evolving concepts of what happens to GI tract microbiome speciation and complexity at the time of death are currently being researched. Indeed the thanatomicrobiome (thanatos, Greek for death) is a relatively new designation defined as the composition and organization of the GI tract microbiome and other microbial communities following cessation of all life activities (Clement et al., 2016; Javan et al., 2016). Recent studies so far underscore the fact that in the GI tract microbiome there is a constant struggle to contain GI tract microbiome integrity and regulate specific bacterial abundance and complexity (Clement et al., 2016; Javan et al., 2016). Ongoing work from temporal studies on the thanatomicrobiome across defined post-mortem intervals (PMI) further indicate (i) that the majority of the microbes within the human body and those which propagate most rapidly at the time of death are the obligate anaerobes that begin to non-randomly proliferate from the GI tract continuing throughout the human organs over the PMI (Javan et al., 2016); and (ii) that comprehensive knowledge of the number and abundance of each organ's microbial signature could be useful to forensic microbiologists as a new source of data for estimating PMI. These data combined with nucleic acid sequencing and bioinformatics would also be invaluable in aiding researchers who use post-mortem tissues in their research work and in forensic criminology, microbial speciation and the study of microbiome-host genetics in the later stages of life.

CONCLUDING REMARKS

In summary, the human GI tract constitutes the largest repository of the human microbiome, and its impact on human neurological aging, health and disease is becoming increasingly appreciated. Consisting of about $\sim 4 \times 10^{13}$ microorganisms, the human GI tract microbiome forms a highly complex, symbiotic and dynamic ecosystem within the host and dietary factors and host genetics appear to have a strong influence on microbial abundance, speciation and complexity, and their ability to influence CNS functions (Foster et al., 2016; Li et al., 2016; Richards et al., 2016; Brandscheid et al., 2017; Tremlett et al., 2017). We sincerely hope that this "Perspectives" article has effectively highlighted recent findings on microbial-derived endotoxins, exotoxins, LOSs and LPSs, amyloids and sncRNAs and has stimulated interest in the potential contribution of these neurotoxic and pro-inflammatory microbial exudates to age-related inflammatory neurodegeneration, amyloidogenesis, and AD-relevant pathology (**Figure 1**). Taken together, these current observations and recent data advance at least seven areas in our understanding of the role of the GI tract microbiome in age-related neurological diseases associated with progressive, inflammatory neurodegeneration of the human brain: (i) that the GI tract microbiome are a potent source of neurotoxic species that are abundantly secreted by multiple Gram-negative bacilli in the gut (*B. fragilis, E. coli,* and others); (ii) that bacterial LPS are readily detectable in the neocortex and hippocampus of the AD brain, and at significantly higher abundance in AD than controls, indicating that LPS may be able to transit physiological barriers to access CNS compartments (**Figure 2**); (iii) that the transit of highly pro-inflammatory neurotoxins such as LPS across compromised GI tract and blood-brain barriers underscore the critical roles of cellular adhesion structures in allowing passage of noxious molecules from the GI tract into the systemic circulation and CNS (Montagne et al., 2016; Soenen et al., 2016; van de Haar et al., 2016); (iv) that extremely complex mixtures of neurotoxins may be generated by either single microbes or by combinations of bacilli that constitute the GI tract microbiome (**Figure 1**); (v) that biophysical, gastrointestinal, and neurobiological barriers that may become more "leaky" with aging again underscore the important role of intact membrane barriers in moderating systemic and CNS inflammation and immune-mediated inflammatory disease (Hill and Lukiw, 2015; Keaney and Campbell, 2015; Montagne et al., 2015; Choi et al., 2016; Köhler et al., 2016; Minter et al., 2016a; Richards et al., 2016; van de Haar et al., 2016; Zhan and Davies, 2016; Varatharaj and Galea, 2017); (vi) that bacterial complexity, neurotoxin abundance, speciation, and complexity in the CSF, blood serum or in brain tissues may be useful for the diagnosis of AD (Zhao et al., 2015; Soenen et al., 2016); and (vii) that studies on the thanatomicrobiome should be useful for a clearer understanding of the neuro- and micro-biological processes in operation over the PMI that should be useful in scientific research that utilizes post-mortem tissues in basic research, in forensic applications, in criminology and in the more accurate diagnosis of neurological disease (Clement et al., 2016; Javan et al., 2016). While one other recent investigation reported the detection of LPS in gray matter (temporal lobe) and white matter (frontal lobe) in AD (Zhan et al., 2016), here for the first time we report the detection of bacterial LPS in brain lysates from AD hippocampus, an anatomical region of the AD brain that develops the earliest and most profound neuropathology. Some advanced AD hippocampal patients exhibited up to a 26-fold increase in LPS over age-matched controls. Lastly, more research into the intriguing field of human GI tract microbiome-host interaction and its potential contributory role to human aging, neurological health and disease is clearly needed. The study of these symbiotic prokaryotic and eukaryotic divisions, their evolution and their intriguing interrelationships, genetic interactions and associations in future work should be useful in expanding our understanding of microbiome-host interplay and control in the initiation, development, propagation, and diagnosis of human neurological disorders in which microbial involvement appears to play some contributory or even deterministic role.

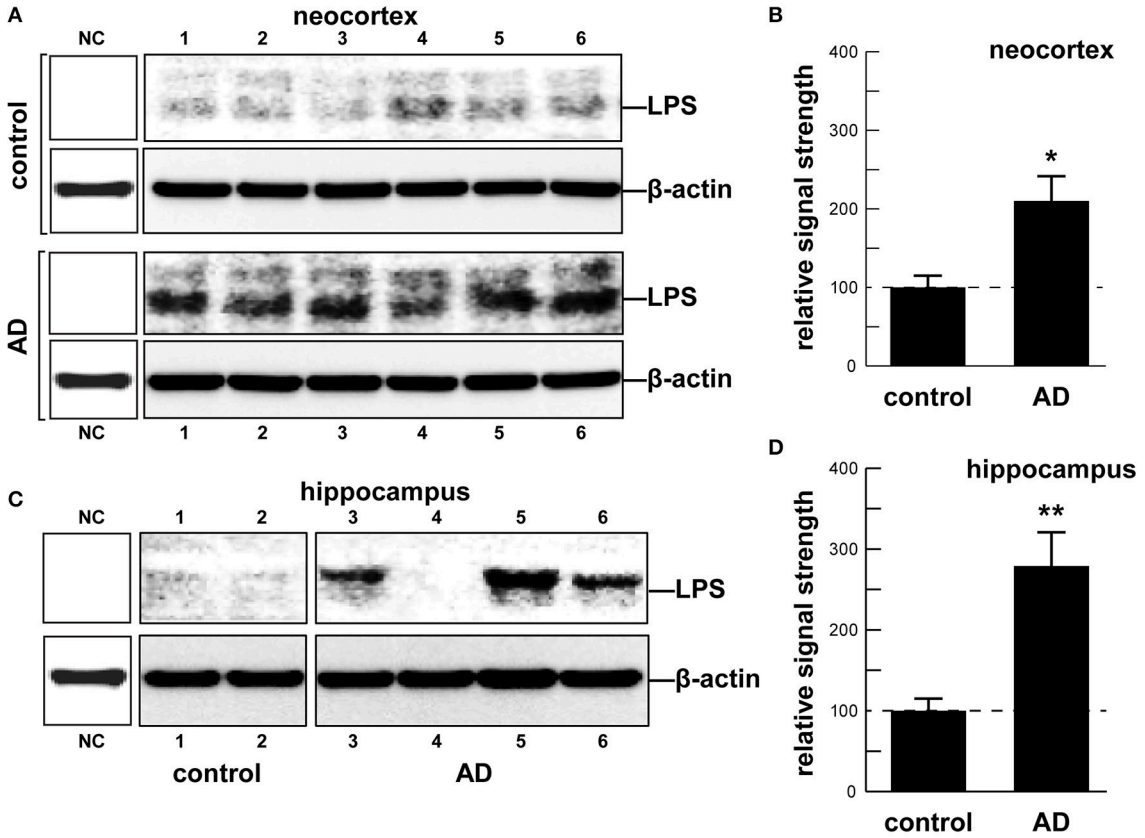

FIGURE 2 | (A) human brain temporal lobe neocortex [$N = 6$ control and 6 sporadic AD cases; quantified in **(B)**]; and **(C)** hippocampus ($N = 2$ control and $N = 4$ AD cases; quantified in **(D)**] were analyzed for LPS against β-actin abundance in the same sample (using anti-*E. coli* LPS; cat # ab35654 from Abcam, Cambridge UK and anti-β-actin cat # 3700 from Cell Signaling, Danvers MA, USA) using Western analysis as previously described by our group (Bhattacharjee et al., 2016; Zhao et al., 2016); all AD and control tissues were analyzed in a RNA-analysis clean room facility; all control and AD tissues were age- and gender-matched; there were no significant differences between the age (control 72.9 ± 8.1 years, AD 74.2 ± 9.1 years), gender (all female), PMI (all tissues 3.5 h post-mortem or less), RNA quality or RNA yield between each of the two groups; LPS abundance was found to be on average over two-fold as abundant in AD when compared to age-, gender, and PMI-matched control neocortex in 6 of 6 cases; LPS was found to be on average three-fold as abundant in AD when compared to age-, gender, and PMI-matched control hippocampus in 3 of 4 cases; some advanced AD hippocampal samples exhibited up to a 26-fold increase in LPS over age-matched controls (**C**, LPS in control lane 2 vs. AD lane 5); because one major source of LPS are Gram-negative bacteria of the human GI tract (predominantly *B. fragilis* and *E. coli*), this suggests that *in vivo* intensely pro-inflammatory LPS species may be able to "leak" through at least two major biophysiological barriers—the GI tract barrier and the BBB—to access brain compartments (see Devier et al., 2015; Halmer et al., 2015; Choi et al., 2016; Minter et al., 2016b; Montagne et al., 2016; Richards et al., 2016; Soenen et al., 2016; van de Haar et al., 2016; Zhan and Davies, 2016; Zhao et al., 2016; Varatharaj and Galea, 2017). Unpublished work from this laboratory further indicates the positive detection of LPS in 36 of 36 AD tissues sampled from the superior temporal lobe neocortex in aged individuals (age range 66–79 yr; see Table 1 in Cui et al., 2010). Another recent investigation reports the finding of LPS in gray matter (temporal lobe) and white matter (frontal lobe) of the AD brain (Zhan et al., 2016). Together these data also suggest that neurotoxic cocktails secreted by multiple GI tract microbes or other microbial species (**Figure 1**) may have considerable potential to support intense pro-inflammatory signaling within the CNS especially over the course of aging when barriers become more "leaky" (Hill and Lukiw, 2015; Keaney and Campbell, 2015; Montagne et al., 2015; Choi et al., 2016; Köhler et al., 2016; Minter et al., 2016a,b; Richards et al., 2016; van de Haar et al., 2016; Zhan and Davies, 2016; Varatharaj and Galea, 2017); **(B)** and **(D)** represent the mean plus one standard deviation of that mean; $^{*}p < 0.05$, $^{**}p < 0.01$ ANOVA; NC, negative control using a control murine brain extract (strain C57BL/6J); in **(B)** and **(D)** a dashed horizontal line at 100 is included for ease of comparison.

AUTHOR CONTRIBUTIONS

YZ and VJ analyzed brains for LPS content; WL compiled and analyzed the data and wrote the paper.

ACKNOWLEDGMENTS

This research work was presented in part at the Society for Neuroscience (SFN) Annual Meeting 12–16 November 2016, San Diego CA, USA and at the Alzheimer Association International Congress 2016 (AAIC 2016) Annual conference 21–27 July 2016 in Toronto, Canada. These studies utilized total nucleic acid and/or cytoplasmic fractions extracted from primary human neuronal-glial (HNG) co-cultures; sincere thanks are extended to Drs. P. N. Alexandrov, J. G. Cui, F. Culicchia, W. Poon, K. Navel, C. Hebel, and C. Eicken for short PMI human brain tissues or extracts, unpublished Western data and immunochemistry, HNG tissue culture and NF-kB-DNA binding assay, initial bioinformatics and data interpretation, and to D. Guillot and A. I. Pogue for expert technical assistance and medical

artwork. All human tissues were used in strict accordance with ethical compliance procedures and protocols followed by donor institutions; thanks are also extended to the Institute for Memory Impairments and Neurological Disorders (MIND), to the University of California at Irvine (UCI) and to the many neuropathologists, physicians and researchers of the US, Canada and Europe who have provided high quality, short PMI human CNS or extracted tissue fractions for scientific study. Research on the human microbiome, pro-inflammatory and pathogenic signaling in the Lukiw laboratory involving the innate-immune response, neuroinflammation and amyloidogenesis in AD and in other neurological diseases was supported through an unrestricted grant to the LSU Eye Center from Research to Prevent Blindness (RPB); the Louisiana Biotechnology Research Network (LBRN) and NIH grants NEI EY006311, NIA AG18031 and NIA AG038834.

REFERENCES

Alan, G., and Sarah, J. P. (2012). Microbes as forensic indicators. *Trop. Biomed.* 29, 311–330.

Alkasir, R., Li, J., Li, X., Jin, M., and Zhu, B. (2016). Human gut microbiota: the links with dementia development. *Protein Cell* 8, 90–102. doi: 10.1007/s13238-016-0338-6

Alonso, R., Pisa, D., Marina, A. I., Morato, E., Rábano, A., and Carrasco, L. (2014). Fungal infection in patients with Alzheimer's disease. *J. Alzheimers Dis.* 41, 301–311. doi: 10.3233/JAD-132681

Andreeva, T. V., Lukiw, W. J., and Rogaev, E. I. (2017). Biological basis for amyloidogenesis in Alzheimer's disease. *Biochemistry* 82, 122–139. doi: 10.1134/S0006297917020043

Asti, A., and Gioglio, L. (2014). Can a bacterial endotoxin be a key factor in the kinetics of amyloid fibril formation? *J. Alzheimers Dis.* 39, 169–179. doi: 10.3233/JAD-131394

Ayala, J., Quesada, A., Vadillo, S., Criado, J., and Píriz, S. (2005). Penicillin-binding proteins of *Bacteroides fragilis* and their role in the resistance to imipenem of clinical isolates. *J. Med. Microbiol.* 54, 1055–1064. doi: 10.1099/jmm.0.45930-0

Bhattacharjee, S., and Lukiw, W. J. (2013). Alzheimer's disease and the microbiome. *Front. Cell. Neurosci.* 7:153. doi: 10.3389/fncel.2013.00153

Bhattacharjee, S., Zhao, Y., Dua, P., Rogaev, E. I., and Lukiw, W. J. (2016). miRNA-34a-mediated down-regulation of the microglial-enriched triggering receptor and phagocytosis-sensor TREM2 in age-related macular degeneration. *PLoS ONE* 11:e0150211. doi: 10.1371/journal.pone.0150211

Bian, Z. M., Elner, S. G., Khanna, H., Murga-Zamalloa, C. A., Patil, S., and Elner, V. M. (2011). Expression and functional roles of caspase-5 in inflammatory responses of human retinal pigment epithelial cells. *Invest. Ophthalmol. Vis. Sci.* 52, 8646–8656. doi: 10.1167/iovs.11-7570

Bolós, M., Perea, J. R., and Avila, J. (2017). Alzheimer's disease as an inflammatory disease. *Biomol. Concepts* 8, 37–43. doi: 10.1515/bmc-2016-0029

Brandscheid, C., Schuck, F., Reinhardt, S., Schäfer, K. H., Pietrzik, C. U., and Grimm, M., et al. (2017). Altered gut microbiome composition and tryptic activity of the 5xFAD Alzheimer's mouse model. *J. Alzheimers Dis.* 56, 775–788. doi: 10.3233/JAD-160926

Bush, K., and Bradford, P. A. (2016). β-Lactams and β-Lactamase inhibitors: an overview. *Cold Spring Harb. Perspect. Med.* 6:a025247. doi: 10.1101/cshperspect.a025247

Buxbaum, J. N., and Linke, R. P. (2012). A molecular history of the amyloidoses. *J. Mol. Biol.* 421, 142–159. doi: 10.1016/j.jmb.2012.01.024

Calsolaro, V., and Edison, P. (2016). Neuroinflammation in Alzheimer's disease: Current evidence and future directions. *Alzheimers Dement.* 12, 719–732. doi: 10.1016/j.jalz.2016.02.010

Can, I., Javan, G. T., Pozhitkov, A. E., and Noble, P. A. (2014). Distinctive thanatomicrobiome signatures found in the blood and internal organs of humans. *J. Microbiol. Methods* 106, 1–7. doi: 10.1016/j.mimet.2014.07.026

Cattaneo, A., Cattane, N., Galluzzi, S., Provasi, S., Lopizzo, N., Festari, C., et al. (2017). Association of brain amyloidosis with pro-inflammatory gut bacterial taxa and peripheral inflammation markers in cognitively impaired elderly. *Neurobiol. Aging.* 49, 60–68. doi: 10.1016/j.neurobiolaging.2016.08.019

Choi, H. H., and Cho, Y. S. (2016). Fecal microbiota transplantation: current applications, effectiveness, and future perspectives. *Clin. Endosc.* 49, 257–265. doi: 10.5946/ce.2015.117

Choi, V. M., Herrou, J., Hecht, A. L., Teoh, W. P., Turner, J. R., Crosson, S., et al. (2016). Activation of *Bacteroides fragilis* toxin by a novel bacterial protease contributes to anaerobic sepsis in mice. *Nat. Med.* 22, 563–567. doi: 10.1038/nm.4077

Clark, I. A., and Vissel, B. (2015). Amyloid β: one of three danger-associated molecules that are secondary inducers of the proinflammatory cytokines that mediate Alzheimer's disease. *Br. J. Pharmacol.* 172, 3714–3727. doi: 10.1111/bph.13181

Clement, C., Hill, J. M., Dua, P., Culicchia, F., and Lukiw, W. J. (2016). Analysis of RNA from Alzheimer's disease post-mortem brain tissues. *Mol. Neurobiol.* 53, 1322–1328. doi: 10.1007/s12035-015-9105-6

Cui, J. G., Li, Y. Y., Zhao, Y., Bhattacharjee, S., and Lukiw, W. J. (2010). Differential regulation of interleukin-1 receptor-associated kinase-1 (IRAK-1) and IRAK-2 by microRNA-146a and NF-kB in stressed human astroglial cells and in Alzheimer disease. *J. Biol. Chem.* 285, 38951–38960. doi: 10.1074/jbc.M110.178848

Devier, D. J., Lovera, J. F., and Lukiw, W. J. (2015). Increase in NF-κB-sensitive miRNA-146a and miRNA-155 in multiple sclerosis (MS) and pro-inflammatory neurodegeneration. *Front. Mol. Neurosci.* 8:5. doi: 10.3389/fnmol.2015.00005

Fathi, P., and Wu, S. (2016). Isolation, detection and characterization of enterotoxigenic *Bacteroides fragilis* in clinical samples. *Open Microbiol. J.* 10, 57–63. doi: 10.2174/1874285801610010057

Ferrera, D., Mazzaro, N., Canale, C., and Gasparini, L. (2014). Resting microglia react to Aβ42 fibrils but do not detect oligomers or oligomer-induced neuronal damage. *Neurobiol. Aging.* 35, 2444–2457. doi: 10.1016/j.neurobiolaging.2014.05.023

Foster, J. A., Lyte, M., Meyer, E., and Cryan, J. F. (2016). Gut microbiota and brain function: an evolving field in neuroscience. *Int. J. Neuropsychopharmacol.* 19:pyv114. doi: 10.1093/ijnp/pyv114

Friedland, R. P. (2015). Mechanisms of molecular mimicry involving the microbiota in neurodegeneration. *J. Alzheimers Dis.* 45, 349–362. doi: 10.3233/JAD-142841

Ghaisas, S., Maher, J., and Kanthasamy, A. (2016). Gut microbiome in health and disease: Linking the microbiome-gut-brain axis and environmental factors in the pathogenesis of systemic and neurodegenerative diseases. *Pharmacol Ther.* 158, 52–62. doi: 10.1016/j.pharmthera.2015.11.012

Ghosal, A. (2017). Importance of secreted bacterial RNA in bacterial-host interactions in the gut. *Microb. Pathog.* 104, 161–163. doi: 10.1016/j.micpath.2017.01.032

Ghosal, A., Upadhyaya, B. B., Fritz, J. V., Heintz-Buschart, A., Desai, M. S., Yusuf, D., et al. (2015). The extracellular RNA complement of *Escherichia coli*. *Microbiologyopen* 4, 252–266. doi: 10.1002/mbo3.235

Goldschmidt, L., Teng, P. K., Riek, R., and Eisenberg, D. (2010). Identifying the amylome, proteins capable of forming amyloid-like fibrils. *Proc. Natl. Acad. Sci. U.S.A.* 107, 3487–3492. doi: 10.1073/pnas.0915166107

Halmer, R., Davies, L., Liu, Y., Fassbender, K., and Walter, S. (2015). The innate immune receptor CD14 mediates lymphocyte migration in EAE. *Cell. Physiol. Biochem.* 37, 269–275. doi: 10.1159/000430351

Heinritz, S. N., Weiss, E., Eklund, M., Aumiller, T., Heyer, C. M., Messner, S., et al. (2016). Impact of a high-fat or high-fiber diet on intestinal microbiota and metabolic markers in a pig model. *Nutrients* 8:E317. doi: 10.3390/nu8050317

Heintz, C., and Mair, W. (2014). You are what you host: microbiome modulation of the aging process. *Cell* 156, 408–411. doi: 10.1016/j.cell.2014.01.025

Hill, J. M., and Lukiw, W. J. (2015). Microbial-generated amyloids and Alzheimer's disease (AD). *Front. Aging Neurosci.* 7:9. doi: 10.3389/fnagi.2015.00009

Hill, J. M., Clement, C., Pogue, A. I., Bhattacharjee, S., Zhao, Y., and Lukiw, W J. (2014). Pathogenic microbes, the microbiome, and Alzheimer's disease (AD). *Front. Aging Neurosci.* 6:127. doi: 10.3389/fnagi.2014.00127

Hofer, U. (2014). Microbiome: *B. fragilis* and the brain. *Nat. Rev. Microbiol.* 12, 76–77. doi: 10.1038/nrmicro3197

Hsiao, E. Y., McBride, S. W., Hsien, S., Sharon, G., Hyde, E. R., McCue, T., et al. (2013). Microbiota modulate behavioral and physiological abnormalities associated with neurodevelopmental disorders. *Cell* 155, 1451–1463. doi: 10.1016/j.cell.2013.11.024

Hu, X., Wang, T., and Jin, F. (2016). Alzheimer's disease and gut microbiota. *Sci. China Life Sci.* 59, 1006–1023. doi: 10.1007/s11427-016-5083-9

Hug, L. A., Baker, B. J., Anantharaman, K., Brown, C. T., Probst, A. J., Castelle, C. J., et al. (2016). A new view of the tree of life. *Nat. Microbiol.* 1:16048. doi: 10.1038/nmicrobiol.2016.48

Javan, G. T., Finley, S. J., Abidin, Z., and Mulle, J. G. (2016). The thanatomicrobiome: a missing piece of the microbial puzzle of death. *Front. Microbiol.* 7:225. doi: 10.3389/fmicb.2016.00225

Jiang, Q., Jin, S., Jiang, Y., Liao, M., Feng, R., Zhang, L., et al. (2016). Alzheimer's disease variants with the genome-wide significance are significantly enriched in immune pathways and active in immune cells. *Mol. Neurobiol.* 54, 594–600. doi: 10.1007/s12035-015-9670-8

Keaney, J., and Campbell, M. (2015). The dynamic blood-brain barrier. *FEBS J.* 282, 4067–4079. doi: 10.1111/febs.13412

Keenan, J. I., Aitchison, A., Purcell, R. V., Greenlees, R., Pearson, J. F., and Frizelle, F. A. (2016). Screening for enterotoxigenic *Bacteroides fragilis* in stool samples. *Anaerobe* 40, 50–53. doi: 10.1016/j.anaerobe.2016.05.004

Köhler, C. A., Maes, M., Slyepchenko, A., Berk, M., Solmi, M., Lanctôt, K. L., et al. (2016). The gut-brain axis, including the microbiome, leaky gut and bacterial translocation: mechanisms and pathophysiological role in Alzheimer's disease. *Curr. Pharm. Des.* 22, 6152–6166. doi: 10.2174/1381612822666160907093807

Land, W. G. (2015). The role of damage-associated molecular patterns (DAMPs) in human diseases: part II: DAMPs as diagnostics, prognostics and therapeutics in clinical medicine. *Sultan Qaboos Univ. Med. J.* 15, e157–e170.

Le, N. T., Narkiewicz, J., Aulić, S., Salzano, G., Tran, H. T., Scaini, D., et al. (2014). Synthetic prions and other human neurodegenerative proteinopathies. *Virus Res.* 207, 25–37. doi: 10.1016/j.virusres.2014.10.020

Lee, J. W., Lee, Y. K., Yuk, D. Y., Choi, D. Y., Ban, S. B., Oh, K. W., et al. (2008). Neuro-inflammation induced by lipopolysaccharide causes cognitive impairment through enhancement of beta-amyloid generation. *J. Neuroinflammation* 5:37. doi: 10.1186/1742-2094-5-37

Leshchyns'ka, I., and Sytnyk, V. (2016). Synaptic cell adhesion molecules in Alzheimer's disease. *Neural Plast.* 2016:6427537. doi: 10.1155/2016/6427537

Li, C. Q., Zheng, Q., Wang, Q., and Zeng, Q. P. (2016). Biotic/abiotic stress-driven Alzheimer's disease. *Front. Cell Neurosci.* 10:269. doi: 10.3389/fncel.2016.00269

Lim, S. L., Rodriguez-Ortiz, C. J., and Kitazawa, M. (2015). Infection, systemic inflammation, and Alzheimer's disease. *Microbes Infect.* 17, 549–556. doi: 10.1016/j.micinf.2015.04.004

Lin, C. S., Chang, C. J., Lu, C. C., Martel, J., Ojcius, D. M., Ko, Y. F., et al. (2014). Impact of the gut microbiota, prebiotics, and probiotics on human health and disease. *Biomed. J.* 37, 259–268. doi: 10.4103/2319-4170.138314

Lloyd-Price, J., Abu-Ali, G., and Huttenhower, C. (2016). The healthy human microbiome. *Genome Med.* 8:51. doi: 10.1186/s13073-016-0307-y

Lukiw, W. J. (2012). NF-κB-regulated micro RNAs (miRNAs) in primary human brain cells. *Exp. Neurol.* 235, 484–490. doi: 10.1016/j.expneurol.2011.11.022

Lukiw, W. J. (2016). *Bacteroides fragilis* lipopolysaccharide and inflammatory signaling in Alzheimer's disease. *Front. Microbiol.* 7:1544. doi: 10.3389/fmicb.2016.01544

Lukiw, W. J., and Rogaev, E. I. (2017). Genetics of Aggression in Alzheimer's Disease (AD). *Front. Aging Neurosci.* 9:87. doi: 10.3389/fnagi.2017.00087

Maldonado, R. F., Sá-Correia, I., and Valvano, M. A. (2016). Lipopolysaccharide modification in Gram-negative bacteria during chronic infection. *FEMS Microbiol. Rev.* 40, 480–493. doi: 10.1093/femsre/fuw007

Minter, M. R., Taylor, J. M., and Crack, P. J. (2016a). The contribution of neuroinflammation to amyloid toxicity in Alzheimer's disease. *J. Neurochem.* 136, 457–474.

Minter, M. R., Zhang, C., Leone, V., Ringus, D. L., Zhang, X., Oyler-Castrillo, P., et al. (2016b). Antibiotic-induced perturbations in gut microbial diversity influences neuro-inflammation and amyloidosis in a murine model of Alzheimer's disease. *Sci Rep.* 6:30028. doi: 10.1038/srep30028

Montagne, A., Barnes, S. R., Sweeney, M. D., Halliday, M. R., Sagare, A. P., Zhao, Z., et al. (2015). Blood-brain barrier breakdown in the aging human hippocampus. *Neuron* 85 296–302. doi: 10.1016/j.neuron.2014.12.032

Montagne, A., Toga, A. W., and Zlokovic, B. V. (2016). Blood-Brain Barrier Permeability and Gadolinium: Benefits and Potential Pitfalls in Research. *JAMA Neurol.* 73, 13–14. doi: 10.1001/jamaneurol.2015.2960

Perez, H. J., Menezes, M. E., and d'Acâmpora, A. J. (2014). [Intestinal microbiota]. *Acta Gastroenterol. Latinoam.* 44, 265–272.

Pinti, M., Appay, V., Campisi, J., Frasca, D., Fülöp, T., Sauce, D., et al. (2016). Aging of the immune system: focus on inflammation and vaccination. *Eur. J. Immunol.* 46, 2286–2301. doi: 10.1002/eji.201546178

Pistollato, F., Sumalla Cano, S., Elio, I., Masias Vergara, M., Giampieri, F., and Battino, M. (2016). Role of gut microbiota and nutrients in amyloid formation and pathogenesis of Alzheimer disease. *Nutr. Rev.* 74, 624–634. doi: 10.1093/nutrit/nuw023

Potgieter, M., Bester, J., Kell, D. B., and Pretorius, E. (2015). The dormant blood microbiome in chronic, inflammatory diseases. *FEMS Microbiol. Rev.* 39, 567–591. doi: 10.1093/femsre/fuv013

Reinus, J. F., and Simon, D. (2014). *Gastrointestinal Anatomy and Physiology: The Essentials*. New York, NY: Wiley-Blackwell Publishers.

Richards, R. I., Robertson, S. A., O'Keefe, L. V., Fornarino, D., Scott, A., Lardelli, M., et al. (2016). The enemy within: innate surveillance-mediated cell death, the common mechanism of neurodegenerative disease. *Front. Neurosci.* 10:193. doi: 10.3389/fnins.2016.00193

Rogers, M. A., and Aronoff, D. M. (2016). The influence of non-steroidal anti-inflammatory drugs on the gut microbiome. *Clin. Microbiol. Infect.* 22, 178.e1–178.e9. doi: 10.1016/j.cmi.2015.10.003

Russo, R., Cristiano, C., Avagliano, C., De Caro, C., La Rana, G., Raso, G. M., et al. (2017). Gut-brain axis: Role of lipids in the regulation of inflammation, pain and CNS diseases. *Curr. Med. Chem.* doi: 10.2174/0929867324666170216113756. [Epub ahead of print].

Scheperjans, F. (2016). Can microbiota research change our understanding of neurodegenerative diseases? *Neurodegener. Dis. Manag.* 6, 81–85. doi: 10.2217/nmt-2015-0012

Schwartz, K., Ganesan, M., Payne, D. E., Solomon, M. J., and Boles, B. R. (2016). Extracellular DNA facilitates the formation of functional amyloids in *Staphylococcus aureus* biofilms. *Mol. Microbiol.* 99, 123–134. doi: 10.1111/mmi.13219

Sender, R., Fuchs, S., and Milo, R. (2016). Are we really vastly outnumbered? Revisiting the ratio of bacterial to host cells in humans. *Cell* 164, 337–340. doi: 10.1016/j.cell.2016.01.013

Seong, E., Yuan, L., and Arikkath, J. (2015). Cadherins and catenins in dendrite and synapse morphogenesis. *Cell Adh. Migr.* 9, 202–213. doi: 10.4161/19336918.2014.994919

Seong, K. J., Lee, H. G., Kook, M. S., Ko, H. M., Jung, J. Y., Kim, W. J. (2016). Epigallocatechin-3-gallate rescues LPS-impaired adult hippocampal neurogenesis through suppressing the TLR4-NF-κB signaling pathway in mice. *Korean J. Physiol. Pharmacol.* 20, 41–51. doi: 10.4196/kjpp.2016.20.1.41

Sharon, G., Sampson, T. R., Geschwind, D. H., and Mazmanian, S. K. (2016). The central nervous system and the gut microbiome. *Cell* 167, 915–932. doi: 10.1016/j.cell.2016.10.027

Shivaji, S. (2017). We are not alone: a case for the human microbiome in extra intestinal diseases. *Gut Pathog.* 9, 13. doi: 10.1186/s13099-017-0163-3

Soenen, S., Rayner, C. K., Jones, K. L., and Horowitz, M. (2016). The ageing gastrointestinal tract. *Curr. Opin. Clin. Nutr. Metab. Care* 19, 12–18. doi: 10.1097/MCO.0000000000000238

Stilling, R. M., Dinan, T. G., and Cryan, J. F. (2014). Microbial genes, brain and behaviour - epigenetic regulation of the gut-brain axis. *Genes Brain Behav.* 13, 69–86. doi: 10.1111/gbb.12109

Syed, A. K., and Boles, B. R. (2014). Fold modulating function: bacterial toxins to functional amyloids. *Front. Microbiol.* 5:401. doi: 10.3389/fmicb.2014.00401

Todar, K. (2016). *Textbook of Bacteriology*. Available online at: http://textbookofbacteriology.net/growth_3.html

Tremlett, H., Bauer, K. C., Appel-Cresswell, S., Finlay, B. B., and Waubant, E. (2017). The gut microbiome in human neurological disease: a review. *Ann. Neurol.* 81, 369–382. doi: 10.1002/ana.24901

van de Haar, H. J., Burgmans, S., Jansen, J. F., van Osch, M. J., van Buchem, M. A., Muller, M., et al. (2016). Blood-brain barrier leakage in patients with early Alzheimer disease. *Radiology* 281, 527–535. doi: 10.1148/radiol.2016152244

Varatharaj, A., and Galea, I. (2017). The blood-brain barrier in systemic inflammation. *Brain Behav. Immun.* 60, 1–12. doi: 10.1016/j.bbi.2016.03.010

Zhan, L. S., and Davies, S. S. (2016). Microbial metabolism of dietary components to bioactive metabolites: opportunities for new therapeutic interventions. *Genome Med.* 8:46. doi: 10.1186/s13073-016-0296-x

Zhan, X., Stamova, B., Jin, L. W., DeCarli, C., Phinney, B., and Sharp, F. R. (2016). Gram-negative bacterial molecules associate with Alzheimer disease pathology. *Neurology* 87, 2324–2332. doi: 10.1212/WNL.0000000000003391

Zhao, Y., and Lukiw, W. J. (2015). Microbiome-generated amyloid and potential impact on amyloidogenesis in Alzheimer's disease (AD). *J. Nat. Sci.* 1:e138.

Zhao, Y., Dua, P., and Lukiw, W. J. (2015). Microbial sources of amyloid and relevance to amyloidogenesis and Alzheimer's disease (AD). *J. Alzheimers Dis. Parkinsonism* 5:177. doi: 10.4172/2161-0460.1000177

Zhao, Y., Jaber, V., and Lukiw, W. J. (2016). Over-expressed pathogenic miRNAs in Alzheimer's disease (AD) and prion disease (PrD) drive deficits in TREM2-mediated Aβ42 peptide clearance. *Front. Aging Neurosci.* 8:140. doi: 10.3389/fnagi.2016.00140

Conflict of Interest Statement: The authors declare that the research was conducted in the absence of any commercial or financial relationships that could be construed as a potential conflict of interest.

Copyright © 2017 Zhao, Jaber and Lukiw. This is an open-access article distributed under the terms of the Creative Commons Attribution License (CC BY). The use, distribution or reproduction in other forums is permitted, provided the original author(s) or licensor are credited and that the original publication in this journal is cited, in accordance with accepted academic practice. No use, distribution or reproduction is permitted which does not comply with these terms.

frontiers in Cellular and Infection Microbiology

ORIGINAL RESEARCH
published: 06 July 2017
doi: 10.3389/fcimb.2017.00302

Molecular Characterization of the Human Stomach Microbiota in Gastric Cancer Patients

Guoqin Yu[1], Javier Torres[2], Nan Hu[3], Rafael Medrano-Guzman[4], Roberto Herrera-Goepfert[5], Michael S. Humphrys[6], Lemin Wang[3], Chaoyu Wang[3], Ti Ding[7], Jacques Ravel[6], Philip R. Taylor[3], Christian C. Abnet[3] and Alisa M. Goldstein[8]**

[1] Integrative Tumor Epidemiology Branch, Division of Cancer Epidemiology and Genetics, National Cancer Institute, National Institutes of Health, Bethesda, MD, United States, [2] Unidad de Investigacion en Enfermedades Infecciosas, Unidad Medica de Alta Especialidad Pediatria, Centro Medico Nacional SXXI, Instituto Mexicano del Seguro Social, Mexico City, Mexico, [3] Metabolic Epidemiology Branch, Division of Cancer Epidemiology and Genetics, National Cancer Institute, National Institutes of Health, Bethesda, MD, United States, [4] Unidad Medica de Alta Especialidad Oncología, Centro Medico Nacional SXXI, Instituto Mexicano del Seguro Social, Mexico City, Mexico, [5] Instituto Nacional de Cancerología, Secretaria de Salúd, Mexico City, Mexico, [6] Institute for Genome Sciences, University of Maryland School of Medicine, Baltimore, MD, United States, [7] Shanxi Cancer Hospital, Taiyuan, China, [8] Clinical Genetics Branch, Division of Cancer Epidemiology and Genetics, National Cancer Institute, National Institutes of Health, Bethesda, MD, United States

Helicobacter pylori (*Hp*) is the primary cause of gastric cancer but we know little of its relative abundance and other microbes in the stomach, especially at the time of gastric cancer diagnosis. Here we characterized the taxonomic and derived functional profiles of gastric microbiota in two different sets of gastric cancer patients, and compared them with microbial profiles in other body sites. Paired non-malignant and tumor tissues were sampled from 160 gastric cancer patients with 80 from China and 80 from Mexico. The 16S rRNA gene V3–V4 region was sequenced using MiSeq platform for taxonomic profiles. PICRUSt was used to predict functional profiles. Human Microbiome Project was used for comparison. We showed that *Hp* is the most abundant member of gastric microbiota in both Chinese and Mexican samples (51 and 24%, respectively), followed by oral-associated bacteria. Taxonomic (phylum-level) profiles of stomach microbiota resembled oral microbiota, especially when the *Helicobacter* reads were removed. The functional profiles of stomach microbiota, however, were distinct from those found in other body sites and had higher inter-subject dissimilarity. Gastric microbiota composition did not differ by *Hp* colonization status or stomach anatomic sites, but did differ between paired non-malignant and tumor tissues in either Chinese or Mexican samples. Our study showed that *Hp* is the dominant member of the non-malignant gastric tissue microbiota in many gastric cancer patients. Our results provide insights on the gastric microbiota composition and function in gastric cancer patients, which may have important clinical implications.

Keywords: *Helicobacter pylori*, 16S rRNA, KEGG modules, microbiome, gastric cancer

OPEN ACCESS

Edited by:
Lorenza Putignani, Bambino Gesù Ospedale Pediatrico (IRCCS), Italy

Reviewed by:
Jeong-Heon Cha, Yonsei University, South Korea
Valerio Iebba, Sapienza Università di Roma, Italy

****Correspondence:***
Guoqin Yu
yug3@mail.nih.gov
Alisa M. Goldstein
goldstea@mail.nih.gov

Received: *15 March 2017*
Accepted: *20 June 2017*
Published: *06 July 2017*

Citation:
Yu G, Torres J, Hu N, Medrano-Guzman R, Herrera-Goepfert R, Humphrys MS, Wang L, Wang C, Ding T, Ravel J, Taylor PR, Abnet CC and Goldstein AM (2017) Molecular Characterization of the Human Stomach Microbiota in Gastric Cancer Patients. Front. Cell. Infect. Microbiol. 7:302. doi: 10.3389/fcimb.2017.00302

Abbreviations: GC, Gastric Cancer; *Hp*, *Helicobacter pylori*; HMP, Human Microbiome Project; NCI, National Cancer Institute; OTUs, Operational Taxonomy Units; QIIME, Quantitative Insights into Microbial Ecology; PD_whole_tree, Phylogenetic diversity; PICRUSt, Phylogenetic Investigation of Communities by Reconstruction of Unobserved States; PERMANOVA, Permutational Multivariate Analysis of Variance.

BACKGROUND

Gastric cancer (GC) is the fifth most common cancer in the world and the third leading cause of cancer death (Ferlay et al., 2013). GC incidence varies widely with high rates in Asia, Eastern Europe, and Central and South America, and low rates in North America and Africa (Carneiro, 2014). GC may arise in cardia or in non-cardia (the fundus, body, or pylorus section). Chronic colonization of *Helicobacter pylori (Hp)* is known to increase the risk of non-cardia cancer (Cavaleiro-Pinto et al., 2011). The association between *Hp* colonization and gastric cardia cancer varies by populations. The studies in Western countries tend to show a neutral or even negative association while in Eastern populations namely China, Japan, and Korea, there is strong evidence of a higher risk of cardia cancer among subjects with *Hp* colonization (Cavaleiro-Pinto et al., 2011).

Chronic inflammation of the stomach may progress through a series of steps including atrophic gastritis, intestinal metaplasia, dysplasia, and gastric adenocarcinoma (Correa, 2013). Atrophic gastritis, the loss of specialized glandular tissue with impaired acid secretion and differentiation of gastric progenitor cells, results in hypochlorhydria in the stomach. It is generally believed that *Hp* prefers a healthy gastric mucosa and that as the steps to GC progress, *Hp* is also gradually fading, until it disappears. Therefore, the stomachs of patients with GC should facilitate the colonization of the gastric mucosa by bacteria other than *Hp* (Sheh and Fox, 2013). Studies of gastric microbiota are sparse. Previous studies were often small, not in GC patients or used biopsy samples collected during endoscopy, which may have led to contamination from the oral cavity (see Supplementary Table 1 for summary of previous studies). Therefore, gastric microbiota in GC patients remains largely unknown.

Chronic colonization of *Hp* is the major risk factor for GC in both Chinese and Mexican populations (Kamangar et al., 2007; Ayala et al., 2011). However, GC occurs mainly at the cardia of the stomach in Shanxi, China, but in the non-cardia of the stomach in Mexico. In this study, we profiled the taxonomic and functional profiles in non-malignant gastric tissue from two collections of GC patients separately, one from China (cardia cancer cases) and the second from Mexico (non-cardia cancer cases). We compared gastric non-malignant tissue with paired tumor tissues and with other body sites including oral, nasal cavity, stool, vagina, and skin using data from the Human Microbiome Project (HMP) (Human Microbiome Project Consortium, 2012). We also evaluated differences in the gastric microbiota by *Hp* colonization status, anatomical sites within the stomach for the non-cardia cancer samples, and tissue type (non-malignant and tumor) separately for the two sample populations.

MATERIALS AND METHODS

Study Subjects and Sample Collection

The Chinese gastric tissue samples were from 80 gastric cardia cancer patients recruited at the Shanxi Cancer Hospital in Taiyuan, Shanxi Province, China, between 1998 and 2001. This study was approved by the Institutional Review Boards of the Shanxi Cancer Hospital and the National Cancer Institute (NCI). All subjects provided written informed consent prior to participation. Cases were histologically confirmed as adenocarcinomas by pathologists at both the Shanxi Cancer Hospital and the NCI. Clinical data was collected by review of medical records. Patients who were <18 years old, with cancer other than GC or with previous treatment for GC were excluded. Tumor tissues and matched non-malignant tissues distant to the tumor were obtained from surgical resections, snap frozen in liquid nitrogen, and stored at −130°C until used. H&E slides were used to determine the percentage of tumor cells in the tissues. Total DNA was extracted using the Allprep RNA/DNA/Protein mini kit (QIAGEN) following the protocol provided by the manufacturer.

The Mexican gastric tissue samples were from 80 gastric non-cardia cancer patients recruited at the Oncology Hospital, Centro Médico Nacional Siglo XXI, Instituto Mexicano del Seguro Social, and the Instituto Nacional de Cancerología, Secretaria de Salud in Mexico City, Mexico, between 2008 and 2013. The study was approved by the ethics committee of each hospital and written informed consent was obtained from all patients prior to enrollment in the study. Cases were histologically confirmed by the pathologist. The clinical and pathological data were recorded in questionnaires. Patients who were <18 years old, with any autoimmune disease, diabetes, or cancer other than GC, and with a previous treatment for GC were excluded from the study. Tumor tissue and matched non-malignant tissue distant to the tumor were obtained from surgical resection specimens, placed immediately in microfuge tubes and submerged in a container with liquid nitrogen, and stored at −70°C until tested. H&E slides were used to determine the percentage of tumor cells in the tissues. Total DNA was extracted by QIAamp DNA mini kit (QIAGEN) using the protocol provided by the manufacturer.

All the non-malignant tissue samples were verified with absence of tumor cells. Tumor tissue samples without tumor cells were excluded from all analyses. The percentage of tumor cells were 70–80% in the Chinese tumor samples and 30–50% in Mexican tumor samples. Examples of H& E slides are shown in Supplementary Figure 1.

16S rRNA Gene Sequence Analysis

The V3–V4 region of the 16S rRNA gene was amplified and sequenced on the Illumina MiSeq platform using the 300 paired-end protocol at the Institute of Genome Sciences, University of Maryland School of Medicine as described previously (Fadrosh et al., 2014).

Sequence reads were processed to remove low quality, short, or chimera reads (Yu et al., 2015). We removed low quality reads (reads with average quality <20 over 30 bp window based on Phred algorithm; paired reads which have at least one read with length <75% of its original length) and chimera reads (by UCHIME). The remaining reads with at least 97% sequence identity were clustered into species-level Operational Taxonomy Units (OTUs) in the software package Quantitative Insights into Microbial Ecology (QIIME 1.8.0) (Caporaso et al., 2010) by using command pick_open_reference_otus.py with usearch61

clustering algorithm and other default settings. The OTUs were assigned to taxa (e.g., genus, family, phylum) using the Greengenes database as reference (version 13_8; DeSantis et al., 2006). OTUs with only one read were excluded from analysis. Samples with <1,000 reads were excluded from analysis. The sequence data were submitted to BioProject database (accession number of 310127) at the National Center for Biotechnology Information website.

Alpha diversity was estimated as number of OTUs, Shannon's Index (Shannon, 1997), and Phylogenetic diversity (PD_whole_tree) (Faith and Baker, 2006) by averaging over 20 rarefied tables of 1,000 reads/sample. Alpha diversity was used to measure the species diversity of each sample. The number of OTUs, also known as richness, is a measure of diversity that does not consider the frequency of OTUs. Shannon's index is estimated by both the number and frequency of the OTUs. PD_whole_tree further takes account of the phylogenetic relationship of OTUs. The phylogenetic tree of OTUs used for PD_whole-tree estimates was prepared in QIIME based on neighbor-joining method. The alpha diversity increased with number of sequence reads sampled (Supplementary Figure 2). The alpha diversity showed differences by sample groups with 1,000 reads/sample; the order of sample groups based on alpha diversity did not change by number of sequence reads.

Beta diversity was measured as unweighted (presence/absence of taxa) and weighted (using taxa relative abundance information) UniFrac distance (Lozupone et al., 2011). Beta diversity measures dissimilarities of two samples in microbial profiles. We calculated both alpha and beta diversity based on rarefied tables of 1,000 reads/sample.

The relative abundance of taxa at different levels (phylum, class, order, family, and genus) was calculated based on the unrarefied table. The taxa relative abundance was estimated as the proportion of OTUs assigned to a taxon.

The Human Microbiome Project (HMP) 16S rRNA V3–V5 data were downloaded for comparison (http://hmpdacc.org/HMQCP/; Human Microbiome Project Consortium, 2012). The HMP sequence reads were processed in the same manner as described above. A total of 2,579 samples from 5 body sites (including oral, nasal cavity, stool, vagina, and skin) of 242 healthy US adults in HMP phase 1 were used for comparison (Aagaard et al., 2013). The study by Lozupone et al. (2013) showed that the difference in population or technologies used should not affect the comparison by body sites. In addition, we limited the comparison of HMP and stomach microbiota data to the highest and least variable taxonomic (phylum)/functional (module) level so that the population/technology differences between these two studies would have limited effect on the comparisons.

Metagenomic Prediction

We used Phylogenetic Investigation of Communities by Reconstruction of Unobserved States (PICRUSt)1.0.0 (Langille et al., 2013) to predict virtual metagenomes for each sample from the 16S rRNA gene sequence data and used the KEGG database as a reference (Kanehisa et al., 2014) to determine the relative abundance of metabolic pathways and modules within the virtual metagenomes. PICRUSt requires the use of Greengenes reference, version 13_5 to cluster reads into OTUs (DeSantis et al., 2006). Therefore, we re-clustered all the sequence data (including HMP) in QIIME with the command parallel_pick_otus_usearch61_ref.py and the Greengenes reference version 13_5.

Statistical Analysis

The Wilcoxon rank-sum test was used to examine gastric microbiota alpha diversity and taxa relative abundance differences between antrum and corpus in Mexican samples or between *Hp*+ and *Hp*− samples. Wilcoxon signed-rank test was used for the differences between non-malignant and matched tumor samples in each population. When examining taxa relative abundance, Bonferroni correction was used to adjust for tests of multiple taxa. Permutational Multivariate Analysis of Variance (PERMANOVA, adonis) was used to compare sample groups by unweighted/weighted UniFrac distance matrix. $P < 0.05$ were considered significant after adjustment for multiple tests.

In order to compare gastric microbiota with the oral, nasal, stool, skin, and vagina microbiota from the HMP study, we calculated Euclidean/Bray-Curtis distances and generated a matrix from the phylum-level/KEGG module profiles, performed principal coordinate analysis (PCoA) on the Euclidean/Bray-Curtis distance matrix, and then plotted the figure based on the first three principal coordinates to visualize the similarities and differences among different body sites. All statistical analyses were performed in R. Bray-Curtis and Euclidean distance showed similar results, therefore only Bray-Curtis distance is shown.

Quality Control

To address the concerns about possible contamination, we included 2 blank samples as negative controls. We also included 1 vaginal and 1 stool sample as positive controls to evaluate the performance of DNA amplification and sequencing. The two positive controls generated 2,703 and 58,201 reads, respectively, suggesting good performance of DNA amplification and sequencing. The blanks had extremely low number of reads (41 and 43 reads/sample, respectively). Furthermore, the OTUs found in both blanks were extremely rare in the gastric samples with accumulated relative abundance range of 0–0.006. Therefore, our results were unlikely to have been affected by contamination.

The conventional DNA extraction method for microbiome studies often includes an extra cell lysis step (bead-beating) to break the hard-to-break cell membranes of some species. To examine whether some taxa were missed due to the lack of a bead-beating step in our DNA extraction protocols, we evaluated 2 Chinese tissue samples using two different DNA extraction methods: a DNA extraction method with a bead-beating step and commonly used for microbiome study (Flores et al., 2012) and the method used for our Chinese samples in the current study. We found 14 genus-level taxa discovered by the extraction method with the bead-beating step that were not discovered by our DNA extraction method (Supplementary Table 2). However, these taxa were extremely rare with total cumulated relative

abundance of 0.007 and 0.038 for two samples, respectively. Therefore, the DNA extraction method should not have adversely affected our findings, although we cannot exclude missing some rare taxa.

RESULTS

Characteristics of the Study Subjects

After excluding samples with <1,000 reads per sample, 77 non-malignant gastric tissue samples from China and 80 from Mexico were included for analysis and the median (interquartile range) was 10,460 (5,454–19,980) reads per sample. The raw and qualified number of reads for each sample group are shown in Supplementary Table 3. The average age of these Chinese cases was 60.8 years old, 83% were male, and all were diagnosed with gastric cardia adenocarcinoma. The average age of Mexican cases was 64.5 years old, 54% were male, and all tumors were located in the non-cardia regions of the stomach (21 antrum, 24 corpus, 35 unspecified). In addition, 80 tumor samples from China and 54 from Mexico were also included for comparison [median (interquartile range): 9,406 (4,228–15,330) reads/sample] after excluding samples with <1,000 reads per sample or no tumor cells.

Taxonomic and Functional Profiles of Non-malignant Gastric Microbiota

The taxonomic and functional profiles are shown in **Figure 1** for non-malignant tissue samples. According to the non-malignant gastric tissues, the gastric microbiota for both sample sets was mainly composed of *Proteobacteria*, followed by *Bacteroidetes* in Chinese samples or *Firmicutes* in Mexican samples (**Figure 1A**). The majority of samples from China (78%) and Mexico (50%) were dominated by *Proteobacteria* (relative abundance >50%). Nineteen Mexican samples were dominated by *Firmicutes* and one Chinese sample was dominated by *Bacteroidetes*. The remaining samples did not have a dominant phylum.

The most abundant genus in the non-malignant microbiota of both Chinese and Mexican gastric cancer patients was *Helicobacter* (**Figure 1B**), and 99% of the *Helicobacter* reads [median (interquartile range): 98.8% (98.7–99.3%)] were classified as *Hp*. As shown in **Table 1**, the majority of GC patients' stomachs (94% Chinese and 55% Mexican) were colonized by *Hp*, and 53% Chinese and 28% Mexican gastric microbiota were dominated by *Hp* (*Hp* relative abundance >50%).

The virtual reconstructed functional profiles (KEGG modules) of non-malignant gastric tissue samples predicted by PICRUSt are shown in **Figure 1C**. The most abundant module functions in gastric microbiota were membrane transport, amino acid metabolism, carbohydrate metabolism, replication and repair, and energy metabolism in both Chinese and Mexican samples. Compared to the variation in taxonomic profiles, the variation in functional profiles among non-malignant gastric tissue samples was more limited (**Figure 1A** vs. **Figure 1C**).

Neither Chinese nor Mexican samples showed an association between gastric microbial features and age or gender (data not shown). Within Mexican samples, no significant difference in microbial alpha diversity, beta diversity and taxa relative abundance for the antrum and corpus non-malignant samples was observed (Supplementary Table 4).

Comparison of Non-malignant Gastric Tissue to Matched Tumor Tissue

After excluding samples with <1,000 reads, 80 tumor tissue samples from China and 54 from Mexico remained for comparison with their matched non-malignant tissues. The taxonomic and functional profiles for these samples are shown in Supplementary Figure 3. The average profiles for both non-malignant and tumor sample groups are shown in **Figure 2**. Similar to the profiles in non-malignant tissues, the tumor gastric microbiota for both sample sets was also mainly composed of *Proteobacteria*, followed by *Bacteroidetes* in Chinese tumor samples or *Firmicutes* in Mexican tumor samples (Supplementary Figure 3A vs. **Figure 2A**). The genus with the most abundance in both tumor sample sets was *Helicobacter* (Supplementary Figure 3B vs. **Figure 2B**) with average relative abundance of 21% in Chinese samples and 18% in Mexican samples. Compared to non-malignant tissues, tumor tissue had less *Proteobacteria*, and higher *Bacteriodetes*, *Firmicutes*, *Fusobacteria,* and *Spirochaetes* in Chinese samples. There was no significant change in Mexican samples in phylum-level taxa (Supplementary Table 5). At the genus level, tumor tissue had lower *Helicobacter* abundance relative to non-malignant tissue in both Chinese and Mexican samples. Chinese samples showed substantial differences in alpha diversity as well as several other genus taxa. Mexican samples showed differences in *Clostridia* relative abundance, but did not display differences in alpha diversity measures (Supplementary Table 5). *Hp* relative abundance was also lower in tumor tissues compared to matched non-malignant tissues in both sample sets (Supplementary Table 5). However, the majority of tumor tissues (94% Chinese and 56% Mexican) were colonized by *Hp*, and many tumor samples (20% Chinese and 17% Mexican) were dominated by *Hp* (*Hp* relative abundance >50%; **Table 1**).

The most abundant module functions in tumor tissues were membrane transport, amino acid metabolism, carbohydrate metabolism, replication and repair, translation, and energy metabolism in both Chinese and Mexican samples (Supplementary Figure 3C, **Figure 2C**). In both Chinese and Mexican samples, the functional module of infectious disease was higher in non-malignant than in tumor tissues (Supplementary Table 6). Chinese samples showed substantial differences in other functional modules after Bonferroni correction for multiple comparisons (Supplementary Table 6). Mexican samples did not display differences in relative abundance for other functional modules between tumors and non-malignant tissues (Supplementary Table 6). Functional and taxonomic profiles were correlated (Supplementary Figure 4). For example, high infectious disease function was mainly contributed by *Helicobacter* as these factors were positively correlated in relative abundance.

We made PCoA plots based on both unweighted or weighted UniFrac distance matrix to visualize similarities and differences among gastric samples. Both plots suggested that gastric samples

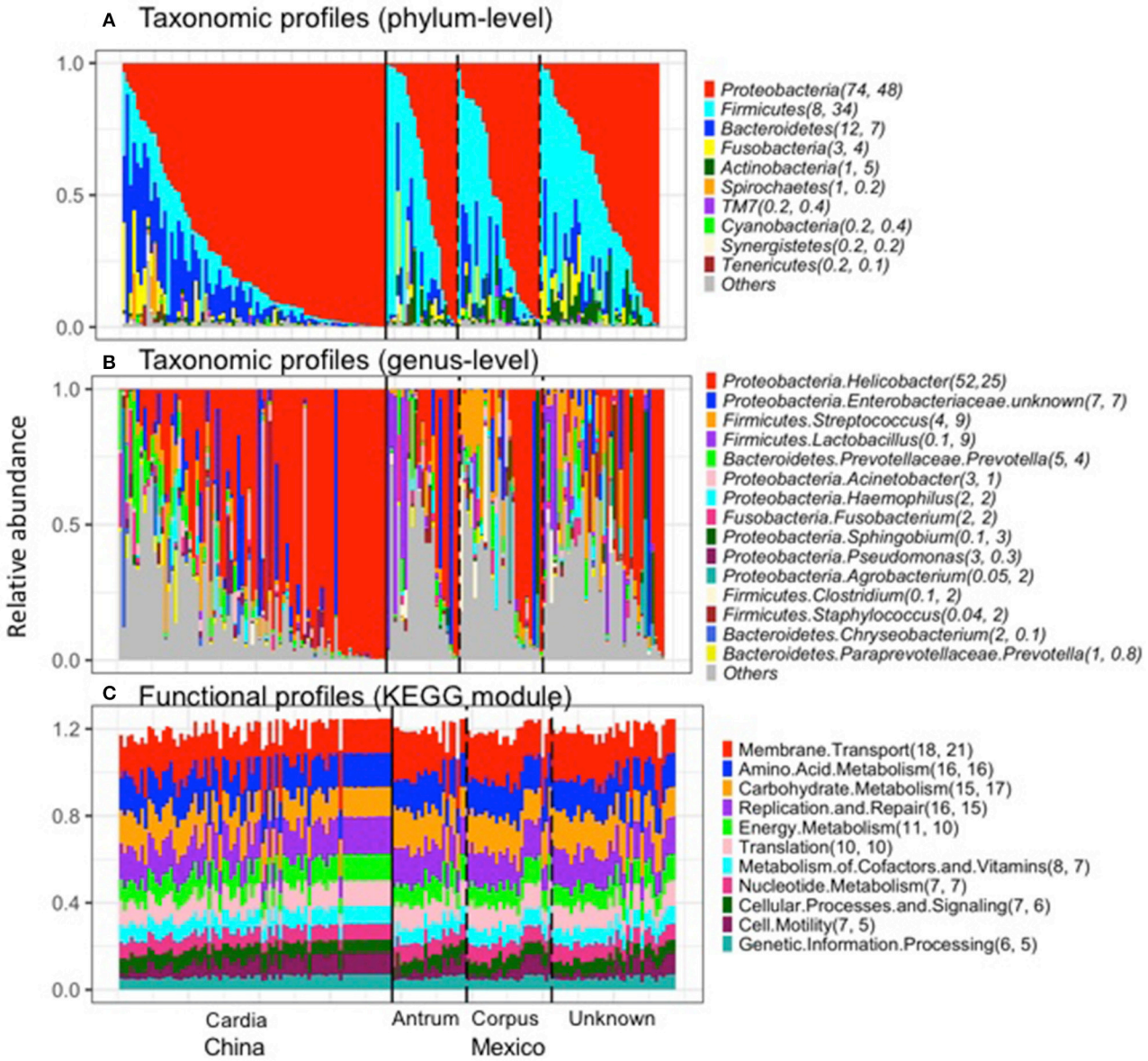

FIGURE 1 | Taxonomic profiles (**A**, Phylum-level; **B**, genus-level) and functional profiles **(C)** of gastric non-malignant tissue microbiota. Each vertical bar represents a unique sample. The numbers in the parenthesis after each phylum/genus/module are the mean relative abundance (%) for Chinese and Mexican samples, respectively. On average, 99% of *Helicobacter* sequence reads were classified as *Hp*. Only the most abundant phyla/genera/modules in Chinese or Mexican samples are shown. All the samples from **(A–C)** are in the same order. The anatomical location and source of the samples are shown at the bottom of the figure.

were primarily clustered by geographic location, rather than by tissue types (**Figure 3**).

Comparison of Non-malignant Gastric Tissue to the Other Body Sites

The average relative abundance of the top abundant genera by body sites are shown in **Table 2**. The top abundant genera are the genera with average relative abundance >0.05 in at least one body site. The top abundant genera in stomach includes *Helicobacter* and an unknown *Enterobacteriaceae* genus in either Chinese or Mexico samples, and two additional genera *Streptococcus and Lactobacillus* in Mexico samples. The top abundant genera in other body sites included *Streptococcus, Prevotella, Haemophilus, Veillonella,* and *Neisseria* in oral cavity, *Lactobacillus* in vagina, *Bacteroides, Faecalibacterium,* and *Alistipes* in stool, *Staphylococcus, Corynebacterium,* and *Propionibacterium* in both skin and nasal cavity. These top genera in each body site were considered as the genera associated with their corresponding body site (e.g., vagina_associated genus refers to *Lactobacillus*). We found that the stomach microbiota was enriched with the genera associated with the oral cavity (combined relative

abundance of 17.6 and 11.6% in Mexico and China samples, respectively).

Similarities and differences of taxonomic/functional profiles by body sites are shown in **Figure 4**. The principal coordinates plots based on taxonomic profiles (phylum-level) demonstrated the primary clustering of samples by body sites (**Figures 4A,B**). The stomach samples, Chinse or Mexico, largely overlapping with oral sample cluster, which was clearer when *Helicobacter* reads were removed (**Figures 4A,B**). Compared to the principal coordinates plots based on taxonomic profiles, the plots based on functional profiles (KEGG modules) showed a much clearer pattern of clustering by body sites (**Figure 4A** vs. **Figure 4C**, **Figure 4B** vs. **Figure 4D**). The stomach samples, with or without *Helicobacter* reads removed, either Mexico or Chinese samples, did not cluster with the other body sites, but they also did not cluster with each other as closely as the samples in the other body sites. It suggested higher inter-subject dissimilarity in stomach samples than in the other body sites in functional profiles. The inter-subject dissimilarity by body sites based on Bray-Curtis distance of phylum/KEGG module profiles were then evaluated (Supplementary Figure 5). Mexican stomach samples had the highest inter-subject dissimilarity in phylum profiles. The Chinese samples, however, had inter-subject dissimilarity higher than the other body sites only when *Helicobacter* reads were removed (Supplementary Figure 5A). This might be due to the fact that almost all Chinese samples (94%) had *Helicobacter*. The inter-subject dissimilarity in functional profiles was much higher in the stomachs of both sample sets than in other body sites (Supplementary Figure 5B).

TABLE 1 | *Hp* in GC patients for both nonmalignant and tumor gastric tissue microbiota.

	China		Mexico	
	Non-malignant (*n* = 77)	**Tumor (*n* = 80)**	**Non-malignant (*n* = 80)**	**Tumor (*n* = 54)**
Samples with *Hp* colonization, n (%)	72 (94%)	75 (94%)	44 (55%)	30 (56%)
Samples with relative *Hp* >50%, n (%)	41 (53%)	16 (20%)	22 (28%)	9 (17%)
***HP* RELATIVE ABUNDANCE (%)**				
Average	51%	20%	24%	18%
Median (interquartile range)	56% (14–89%)	4% (1–36%)	4% (0–58%)	0 (0–25%)
Maximum	99%	87%	97%	98%

Comparison of Gastric Tissue Microbiota Features by *Hp* Colonization Status

To further evaluate the gastric tissue microbiota by *Hp* colonization status, we removed the *Helicobacter* reads from the *Hp*+ samples (with *Hp*) and then compared them to the

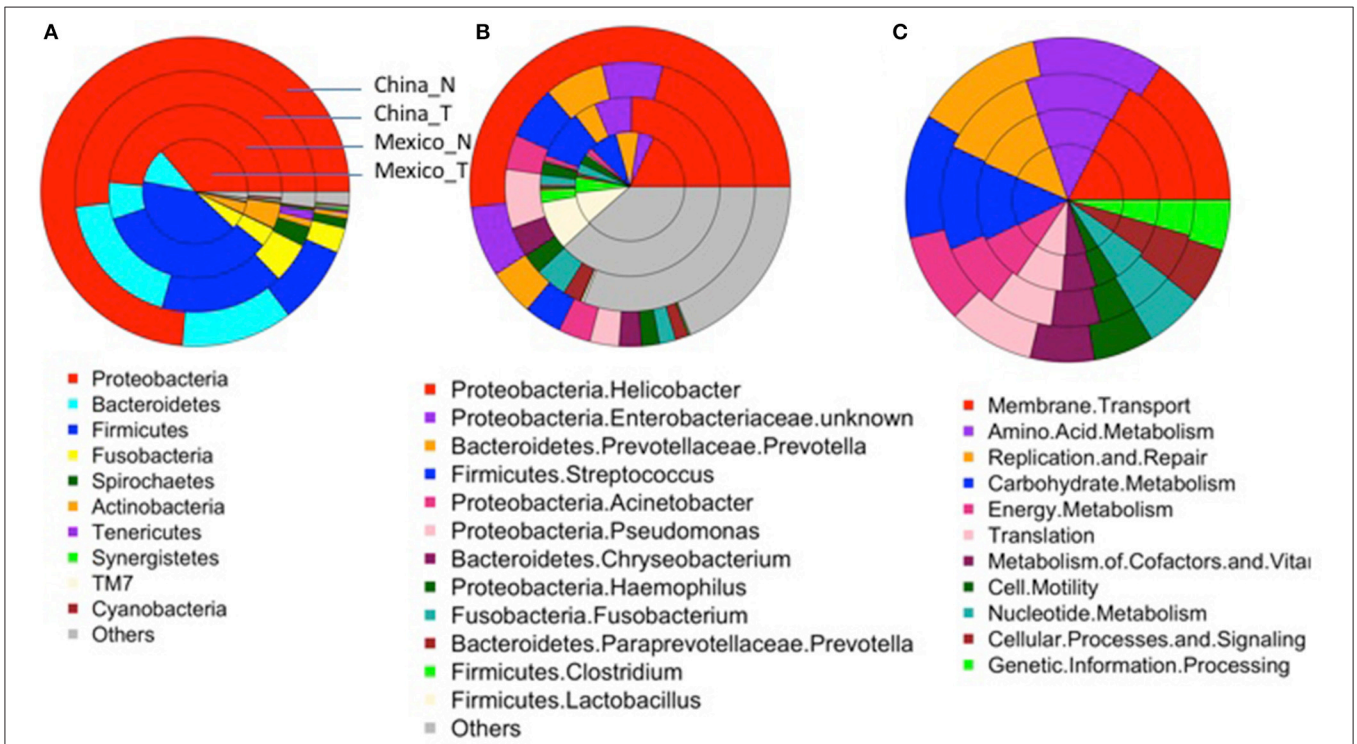

FIGURE 2 | Average taxonomic (**A**, Phylum-level; **B**, genus-level) and functional profiles **(C)** of gastric microbiota in the non-malignant (China_N, Mexico_N) or tumor (China_T, Mexico_T) tissue group. As shown in **(A)**, each donut includes a single sample group. The colors represent different taxonomical/functional groups as shown at the bottom of each figure. The proportion of the color in each donut represents the average relative abundance in each sample group.

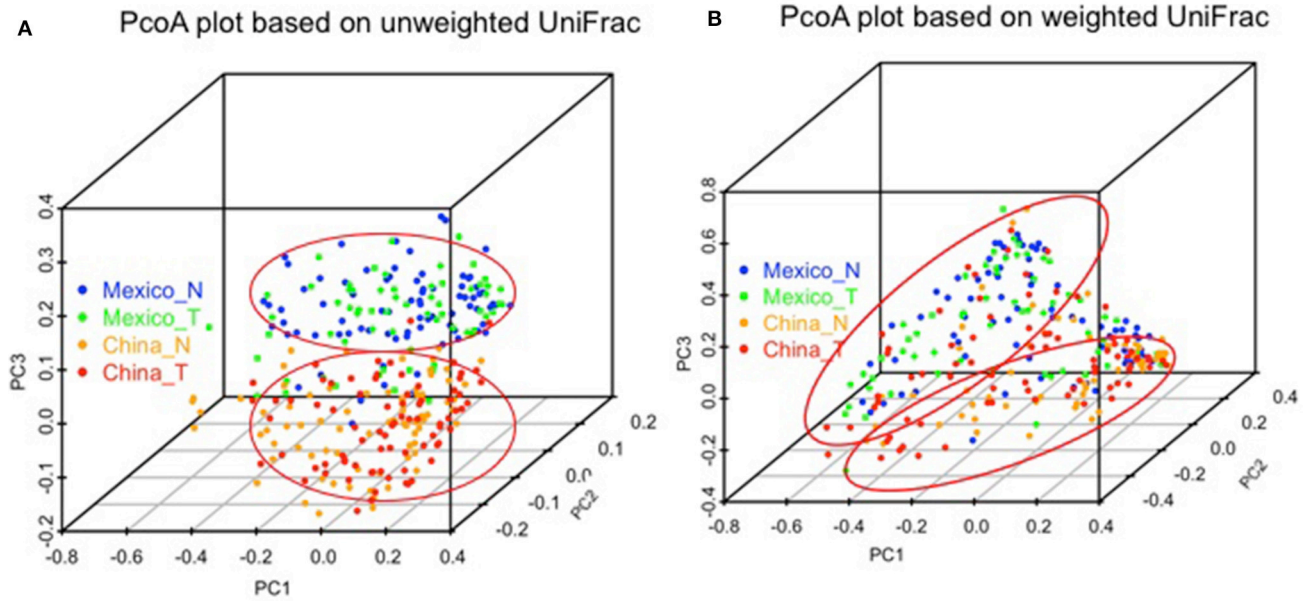

FIGURE 3 | Comparison of gastric microbiota among different sample groups by PCoA plots based on unweighted **(A)** and weighted UniFrac distance **(B)**. The color represents different sample groups as shown in the legend (non-malignant, China_N, Mexico_N; and tumor, China_T, Mexico_T).

TABLE 2 | The average relative abundance of top abundant genera by body sites and their comparison.

	Stomach_mexico	Stomach_china	Oral	Vagina	Stool	Skin	Nasal
Helicobacter	**0.247**	**0.521**	0.000	0.000	0.000	0.003	0.002
Enterobacteriaceae.unknown	**0.067**	**0.072**	0.000	0.000	0.000	0.000	0.000
Lactobacillus	**0.089**	0.001	0.000	**0.850**	0.000	0.002	0.002
Streptococcus	**0.089**	0.038	**0.294**	0.003	0.000	0.015	0.017
Prevotella	0.040	0.047	**0.097**	0.027	0.032	0.005	0.004
Haemophilus	0.022	0.018	**0.100**	0.000	0.001	0.002	0.006
Veillonella	0.015	0.005	**0.069**	0.000	0.000	0.002	0.002
Neisseria	0.010	0.008	**0.054**	0.000	0.000	0.002	0.002
Bacteroides	0.003	0.003	0.001	0.001	**0.482**	0.007	0.005
Faecalibacterium	0.000	0.000	0.000	0.000	**0.051**	0.002	0.001
Alistipes	0.000	0.000	0.000	0.000	**0.054**	0.001	0.000
Staphylococcus	0.023	0.000	0.000	0.000	0.000	**0.150**	**0.192**
Corynebacterium	0.009	0.001	0.020	0.001	0.000	**0.051**	**0.338**
Propionibacterium	0.000	0.000	0.002	0.000	0.000	**0.602**	**0.235**
COMBINED RELATIVE ABUNDANCE OF THE TOP GENERA IN OTHER BODY SITES							
Oral_associated	**0.176**	**0.116**					
Nasal_associated	0.032	0.001					
Skin_associated	0.032	0.001					
Stool_associated	0.003	0.003					
Vagina_associated	0.089	0.001					

The stomach microbiota in this table were based on non-malignant tissue samples only. Top abundant genera refer to genera with relative abundance >0.05 in at least one body site (bolded and highlighted). These top genera in each body site were considered as genera associated with their corresponding body site. For example, oral_associated genera include Streptococcus, Prevotella, Haemophilus, Veillonella, and Neisseria, and their combined relative abundance in stomach samples is the relative abundance of oral_associated genera in the stomach.

Hp− samples (without *Hp*) for alpha diversity, beta diversity, and taxa relative abundance separately for non-malignant and tumor samples. No significant differences were observed among Mexican samples (Supplementary Table 7). A similar comparison could not be performed in the Chinese samples because too few samples were *Hp*− ($n = 5$).

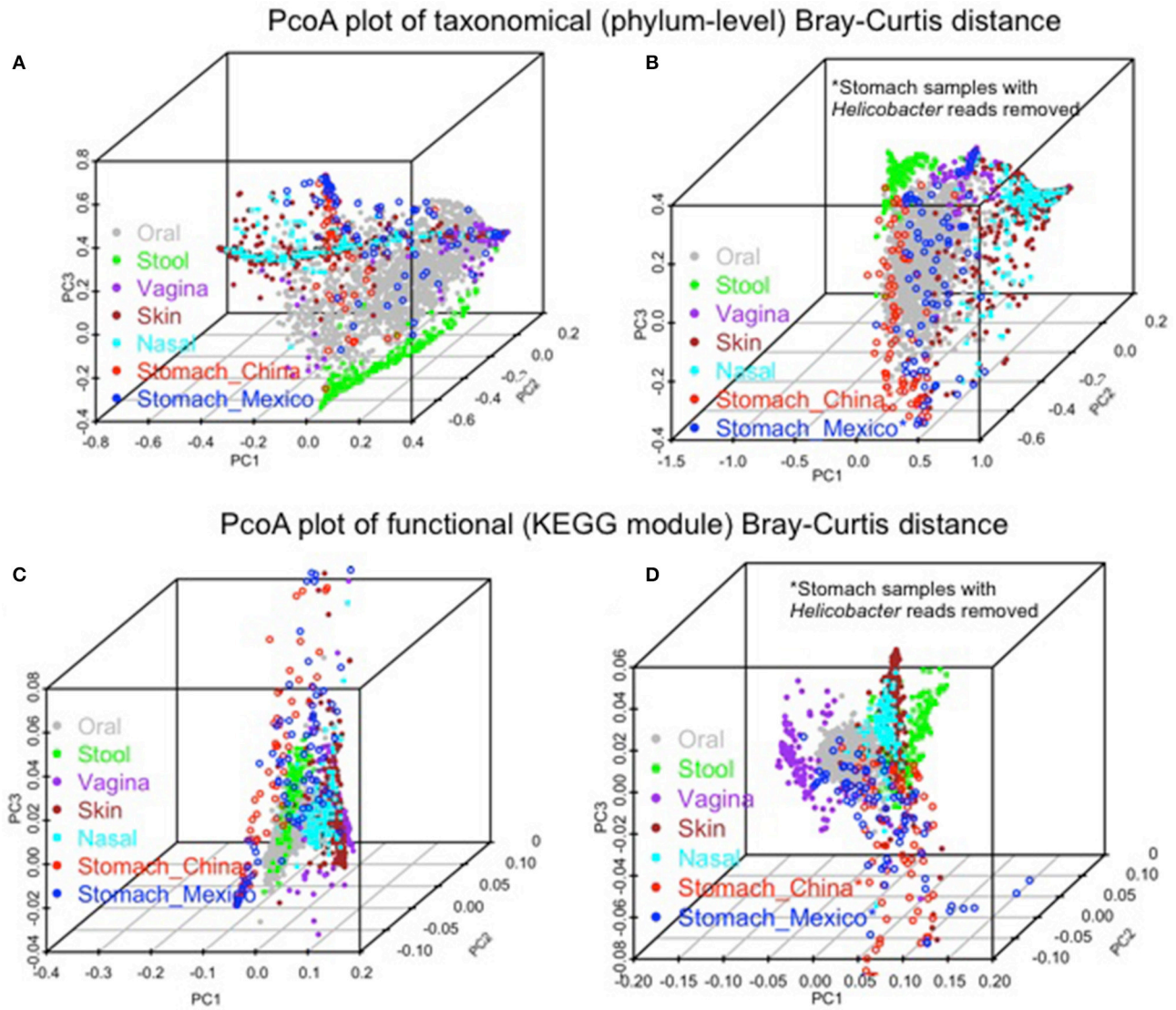

FIGURE 4 | Comparison of the gastric microbiota of the non-malignant tissues with microbiota in the other human body sites (HMP 16S V3–V5 phase 1 data). **(A,B)** PCoA plots of Bray-Curtis distance of phylum-level taxonomic profiles with *Helicobacter* **(A)** or without *Helicobacter* reads **(B)** in stomach samples. **(C,D)** PCoA plots of Bray-Curtis distance of KEGG module profiles with *Helicobacter* **(C)** or without *Helicobacter* reads **(D)** in stomach samples. The color represents different body sites or sample groups as shown in the legend.

DISCUSSION

In the largest study of gastric tissue to date, we investigated the gastric microbiota in sets of patients from Mexico and China. In both sets, we showed that *Hp* is the most abundant member of the stomach microbiota, followed by the genera that are commonly seen in the oral microbiota. The principal coordinates plots of Bray–Curtis distance matrix based on phylum-level taxonomic profiles suggested that stomach samples largely overlapped with oral samples. The principal coordinates plots based on functional profiles, however, suggested that stomach microbiota was distinct from the microbiota of other body sites, and had higher inter-subject dissimilarity. We found no differences in microbiota composition by anatomic site or *Hp* status, although we had only limited sample size to detect differences. We did find that the relative abundance of *Hp* was higher in non-malignant than in tumor tissues for both Chinese and Mexican samples.

Gastric microbiota was dominated by phyla *Proteobacteria* in Chinese samples, and by *Proteobacteria* and *Firmicutes* in Mexican samples. This result is consistent with most previous studies based on gastric biopsy, fluid, or tissue in either healthy or cancer cases (Supplementary Table 1). Overall, in cases with high *Hp* relative abundance, the most abundant gastric phylum is *Proteobacteria*, otherwise it is *Firmicutes*.

GC patients, both non-cardia and cardia in Asian populations have been proposed to have chronic gastritis that leads to

hypochlorhydria in the stomach (Cavaleiro-Pinto et al., 2011; Sheh and Fox, 2013). Therefore, GC patients have been hypothesized to have diminished or no colonization of *Hp* in the stomach (Sheh and Fox, 2013). Previous studies of gastric microbiota in GC patients were limited, small, and found inconsistent results (summarized in Supplementary Table 1). Studies from Sweden (Eun et al., 2014) and Mexico (Aviles-Jimenez et al., 2014) did not identify *Hp* as the dominant species in any of the samples evaluated, while four other studies in Korea, Taiwan and USA showed results consistent with our finding with *Hp* as the dominant species in GC samples (Dicksved et al., 2009; Eun et al., 2014; Zhang et al., 2015; Tseng et al., 2016). This difference between studies might be due to *Hp* prevalence heterogeneity across study samples. A recent study of 212 chronic gastritis and 103 GC patients in China that used quantitative PCR showed that the bacteria load in the gastric mucosa was increased in cancer patients compared to gastritis patients, and the bacterial load was positively correlated with *Hp* quantity ($R = 0.38$, $P < 0.001$), suggesting *Hp* colonization in GC patients (Wang et al., 2016). In the current study, we found that many Chinese and Mexican GC patients had stomachs dominated by *Hp*. This finding may be relevant to the decision-making of GC treatment. Endoscopic resection has been considered the first line of treatment for early GC in Korea and Japan because it is minimally invasive and effective (Chung et al., 2009; Isomoto et al., 2009). Several studies have shown a benefit for *Hp* eradication in reducing metachronous tumors after resection for early gastric cancer (Fukase et al., 2008; Bang et al., 2015). Our data suggest that the majority of patients diagnosed with GC in these populations have current *Hp* colonization and this may explain why eradication therapy at time of diagnosis may be beneficial.

Our study of gastric microbiota showed less between-sample variation in the functional profiles than in the taxonomic profiles, which is similar to a previous study in other body sites (Human Microbiome Project Consortium, 2012). This finding of less variation in function than in taxa is consistent with functional redundancy across taxa and suggests that taxonomically distinct microbes may have similar functions. Therefore, analysis of functional modules appears to provide insights that analysis of phyla alone may not be able to identify. For example, we showed that stomach microbiota was distinct from microbiotas in other body sites in functional profiles, but not in taxonomical profiles. In addition, inter-subject dissimilarity in functional profiles is much higher in stomach than in other body sites. However, it is important to note that the functional profiles were based on prediction only. Therefore, it is possible that prediction-based biases toward well-documented microbial genomes resulted from exclusion of unknown or poorly documented taxa. Further studies are needed to validate these findings.

Consistent with a study in a United States population (Bik et al., 2006), we did not observe differences in the microbiota between the antrum and corpus in the Mexican GC samples. In contrast, a Chinese study reported that gastritis patients without *Hp* infection had decreased *Prevotella* in the antrum compared to the corpus (Li et al., 2009). Larger studies in subjects without GC are needed to further compare the gastric microbiota by different anatomical sites and also control for population and health conditions.

Hp colonization may impact gastric microbiota by induction of host antimicrobial peptides (Hornsby et al., 2008), by directly killing other bacteria through the activity of its own cecropin-like peptide (Putsep et al., 1999), or by inducing physiological changes in host stomach such as pH alteration (Smolka and Backert, 2012), epithelial surface (Wroblewski et al., 2016), gastric hormones and immunologic state (Blaser and Atherton, 2004). However, the difference in the gastric microbiota by host *Hp* colonization status is not fully understood. Consistent with our findings, a study in the United States showed that the relative abundance of non-*Hp* bacteria in *Hp*+ subjects was not altered compared to *Hp*− subjects when *Hp* sequences were eliminated from the analysis (Bik et al., 2006). A study in China however suggested that the major influence of *Hp* on microbiota is the increased bacterial load in the stomach, not the relative abundance of non-*Hp* bacteria groups (Wang et al., 2015). In contrast, a small study of 10 Amerindians and 2 non-Amerindians using the PhyloChip reported marked differences in relative abundance of non-*Hp* bacteria by *Hp* status (Maldonado-Contreras et al., 2011). Our study examined cancer patients, and thus *Hp*− GC patients may have a prior history of *Hp* colonization. Larger studies in subjects without GC using advanced sequencing technology are needed.

As has been previously shown for tumor and matched non-malignant samples from colorectal cancer patients (Burns et al., 2015), we also found taxonomical and functional composition differences between non-malignant and tumor tissues in both Chinese and Mexican cases. This observation might suggest the change of local environment in tumor (e.g., reduction of acid secretion) compared to non-malignant tissues, which leads to *Hp* diminution and corresponding microbial functional changes in tumor. Whether these changes contribute to gastric carcinogenesis or tumor progression require further investigation. Our recent study of the Chinese sample set suggested that the changes in the gastric microbiota including *Hp* relative abundance in non-malignant tissue were associated with cancer risk factors and clinical outcomes including family history of upper gastrointestinal cancer and tumor grades (Yu et al., 2017). Similar associations were, however, not found in the tumor tissues or in the Mexican sample set (data not shown).

While this study includes noteworthy strengths, it also includes limitations. Although, it is the largest study of the gastric non-malignant tissue microbiota from GC patients to date, it includes samples from two different populations with different rates and types of GC. The non-malignant tissue samples were obtained distant but unmeasured from the tumor lesion under sterile conditions and were frozen immediately. Also, unlike most studies of gastric microbiota, we analyzed not only the taxonomic profiles and *Hp* relative abundance, but also virtual reconstructed functional profiles. We compared our gastric tissue data to the HMP data, which included different populations, DNA extraction techniques, and sequencing platforms. We

tried to minimize the effects of these differences by restricting our comparisons to the highest and least variable taxonomic level (phylum-level) and functional entity (KEGG module). In addition, a meta-analysis of microbiota studies suggested that differences in microbial populations across body sites are larger than those driven by the experimental protocols, age, geography, and other population characteristics (Lozupone et al., 2013). Another limitation was the use of a DNA extraction method without a bead-beating step. However, we showed that although we may have missed certain bacteria with potentially hard-to-break cell membranes, these bacteria were rare and should not have adversely affected our conclusions. Finally, our study was restricted to cancer patients and we did not have gastric samples from subjects without GC for comparison. Therefore, we cannot evaluate whether results found in GC patients generalize to subjects without GC.

CONCLUSIONS

By analyzing the gastric tissues of two different populations with different types of GC separately, we showed that *Hp* was the dominant taxa in the stomach of many subjects with GC, followed by oral-associated bacteria. Comparison with other body sites suggested that stomach microbiota resembled oral microbiota in phylum-level taxonomical profiles, but not in functional profiles. Our study provided insights of gastric microbiota composition and function in GC patients.

AUTHOR CONTRIBUTIONS

GY designed the study, analyzed the data and wrote the initial manuscript. JT, NH, RM, RH, MH, LW, CW, TD, PT, and AG performed sample collection and laboratory experiments. GY, JT, JR, PT, CA, and AG contributed to the data interpretation and manuscript revision.

FUNDING

This work was supported by Intramural Research Program of Division of Cancer Epidemiology and Genetics, National Cancer Institute, National Institutes of Health. Work in Mexico was supported by Coordinacion de Investigacion, Instituto Mexicano del Seguro Social. (Grant number FIS/IMSS/PRIOR/PROT/13/027).

ACKNOWLEDGMENTS

We thank all the study participants. We thank B. Ma from Ravel lab for delivering the sequence data to us.

SUPPLEMENTARY MATERIAL

The Supplementary Material for this article can be found online at: http://journal.frontiersin.org/article/10.3389/fcimb.2017.00302/full#supplementary-material

REFERENCES

Aagaard, K., Petrosino, J., Keitel, W., Watson, M., Katancik, J., Garcia, N., et al. (2013). The Human Microbiome Project strategy for comprehensive sampling of the human microbiome and why it matters. *FASEB J.* 27, 1012–1022. doi: 10.1096/fj.12-220806

Aviles-Jimenez, F., Vazquez-Jimenez, F., Medrano-Guzman, R., Mantilla, A., and Torres, J. (2014). Stomach microbiota composition varies between patients with non-atrophic gastritis and patients with intestinal type of gastric cancer. *Sci. Rep.* 4:4202. doi: 10.1038/srep04202

Ayala, G., Flores-Luna, L., Hernandez-Amaro, D., Mendoza-Hernandez, G., Chihu-Amparan, L., Bernal-Sahagun, F., et al. (2011). Association of circulating VacA-neutralizing antibodies with gastric cancer and duodenal ulcer. *Cancer Causes Control* 22, 1425–1434. doi: 10.1007/s10552-011-9817-5

Bang, C. S., Baik, G. H., Shin, I. S., Kim, J. B., Suk, K. T., Yoon, J. H., et al. (2015). *Helicobacter pylori* eradication for prevention of metachronous recurrence after endoscopic resection of early gastric cancer. *J. Korean Med. Sci.* 30, 749–756. doi: 10.3346/jkms.2015.30.6.749

Bik, E. M., Eckburg, P. B., Gill, S. R., Nelson, K. E., Purdom, E. A., Francois, F., et al. (2006). Molecular analysis of the bacterial microbiota in the human stomach. *Proc. Natl. Acad. Sci. U.S.A.* 103, 732–737. doi: 10.1073/pnas.0506655103

Blaser, M., and Atherton, J. (2004). *Helicobacter pylori* persistence: biology and disease. *J. Clin. Invest.* 113, 321–333. doi: 10.1172/JCI20925

Burns, M. B., Lynch, J., Starr, T. K., Knights, D., and Blekhman, R. (2015). Virulence genes are a signature of the microbiome in the colorectal tumor microenvironment. *Genome Med.* 7:55. doi: 10.1186/s13073-015-0177-8

Caporaso, J. G., Kuczynski, J., Stombaugh, J., Bittinger, K., Bushman, F. D., Costello, E. K., et al. (2010). QIIME allows analysis of high-throughput community sequencing data. *Nat. Methods* 7, 335–336. doi: 10.1038/nmeth.f.303

Carneiro, F. (2014). "Stomach cancer," in *World Cancer Report*, eds B. Steward and C. P. Wild (Lyon: International Agency for Research on Cancer), 383–391.

Cavaleiro-Pinto, M., Peleteiro, B., Lunet, N., and Barros, H. (2011). *Helicobacter pylori* infection and gastric cardia cancer: systematic review and meta-analysis. *Cancer Causes Control* 22, 375–387. doi: 10.1007/s10552-010-9707-2

Chung, I. K., Lee, J. H., Lee, S. H., Kim, S. J., Cho, J. Y., Cho, W. Y., et al. (2009). Therapeutic outcomes in 1000 cases of endoscopic submucosal dissection for early gastric neoplasms: korean ESD Study Group multicenter study. *Gastrointest. Endosc.* 69, 1228–1235. doi: 10.1016/j.gie.2008.09.027

Correa, P. (2013). Gastric cancer: overview. *Gastroenterol. Clin. North Am.* 42, 211–217. doi: 10.1016/j.gtc.2013.01.002

DeSantis, T. Z., Hugenholtz, P., Larsen, N., Rojas, M., Brodie, E. L., Keller, K., et al. (2006). Greengenes, a chimera-checked 16S rRNA gene database and workbench compatible with ARB. *Appl. Environ. Microbiol.* 72, 5069–5072. doi: 10.1128/AEM.03006-05

Dicksved, J., Lindberg, M., Rosenquist, M., Enroth, H., Jansson, J. K., and Engstrand, L. (2009). Molecular characterization of the stomach microbiota in patients with gastric cancer and in controls. *J. Med. Microbiol.* 58(Pt 4), 509–516. doi: 10.1099/jmm.0.007302-0

Eun, C. S., Kim, B. K., Han, D. S., Kim, S. Y., Kim, K. M., Choi, B. Y., et al. (2014). Differences in gastric mucosal microbiota profiling in patients with chronic gastritis, intestinal metaplasia, and gastric cancer using pyrosequencing methods. *Helicobacter* 19, 407–416. doi: 10.1111/hel.12145

Fadrosh, D. W., Ma, B., Gajer, P., Sengamalay, N., Ott, S., Brotman, R. M., et al. (2014). An improved dual-indexing approach for multiplexed 16S rRNA gene sequencing on the Illumina MiSeq platform. *Microbiome* 2:6. doi: 10.1186/2049-2618-2-6

Faith, D. P., and Baker, A. M. (2006). Phylogenetic diversity (PD) and biodiversity conservation: some bioinformatics challenges. *Evol. Bioinform. Online* 2, 121–128. doi: 10.4137/ebo.s0

Ferlay, J., S. I., Ervik, M., Dikshit, R., Eser, S., Mathers, C., Rebelo, M., et al. (2013). *GLOBOCAN 2012 v1.0, Cancer Incidence and Mortality Worldwide: IARC CancerBase No. 11 [Online]*. Lyon: International Agency for Research on Cancer. Available online at: http://globocan.iarc.fr/ (Accessed 2013).

Flores, R., Shi, J., Fuhrman, B., Xu, X., Veenstra, T. D., Gail, M. H., et al. (2012). Fecal microbial determinants of fecal and systemic estrogens and estrogen metabolites: a cross-sectional study. *J. Transl. Med.* 10:253. doi: 10.1186/1479-5876-10-253

Fukase, K., Kato, M., Kikuchi, S., Inoue, K., Uemura, N., Okamoto, S., et al. (2008). Effect of eradication of *Helicobacter pylori* on incidence of metachronous gastric carcinoma after endoscopic resection of early gastric cancer: an open-label, randomised controlled trial. *Lancet* 372, 392–397. doi: 10.1016/S.0140-6736(08)61159-9

Hornsby, M. J., Huff, J. L., Kays, R. J., Canfield, D. R., Bevins, C. L., and Solnick, J. V. (2008). *Helicobacter pylori* induces an antimicrobial response in rhesus Macaques in a cag pathogenicity island-dependent manner. *Gastroenterology* 134, 1049–1057. doi: 10.1053/j.gastro.2008.01.018

Human Microbiome Project Consortium (2012). Structure, function and diversity of the healthy human microbiome. *Nature* 486, 207–214. doi: 10.1038/nature11234

Isomoto, H., Shikuwa, S., Yamaguchi, N., Fukuda, E., Ikeda, K., Nishiyama, H., et al. (2009). Endoscopic submucosal dissection for early gastric cancer: a large-scale feasibility study. *Gut* 58, 331–336. doi: 10.1136/gut.2008.165381

Kamangar, F., Qiao, Y. L., Blaser, M. J., Sun, X. D., Katki, H., Fan, J. H., et al. (2007). *Helicobacter pylori* and oesophageal and gastric cancers in a prospective study in China. *Br. J. Cancer* 96, 172–176. doi: 10.1038/sj.bjc.6603517

Kanehisa, M., Goto, S., Sato, Y., Kawashima, M., Furumichi, M., and Tanabe, M. (2014). Data, information, knowledge and principle: back to metabolism in KEGG. *Nucleic Acids Res.* 42, D199–D205. doi: 10.1093/nar/gkt1076

Langille, M. G. I., Zaneveld, J., Caporaso, J. G., McDonald, D., Knights, D., Reyes, J. A., et al. (2013). Predictive functional profiling of microbial communities using 16S rRNA marker gene sequences. *Nat. Biotechnol.* 31, 814–821. doi: 10.1038/nbt.2676

Li, X. X., Wong, G. L. H., To, K. F., Wong, V. W. S., Lai, L. H., Chow, D. K. L., et al. (2009). Bacterial microbiota profiling in gastritis without *Helicobacter pylori* infection or non-steroidal anti-inflammatory drug use. *PLoS ONE* 4:e7985. doi: 10.1371/journal.pone.0007985

Lozupone, C., Lladser, M. E., Knights, D., Stombaugh, J., and Knight, R. (2011). UniFrac: an effective distance metric for microbial community comparison. *ISME J.* 5, 169–172. doi: 10.1038/ismej.2010.133

Lozupone, C. A., Stombaugh, J., Gonzalez, A., Ackermann, G., Wendel, D., Vazquez-Baeza, Y., et al. (2013). Meta-analyses of studies of the human microbiota. *Genome Res.* 23, 1704–1714. doi: 10.1101/gr.151803.112

Maldonado-Contreras, A., Goldfarb, K. C., Godoy-Vitorino, F., Karaoz, U., Contreras, M., Blaser, M. J., et al. (2011). Structure of the human gastric bacterial community in relation to *Helicobacter pylori* status. *ISME J.* 5, 574–579. doi: 10.1038/ismej.2010.149

Putsep, K., Normark, S., and Boman, H. G. (1999). The origin of cecropins; implications from synthetic peptides derived from ribosomal protein L1. *FEBS Lett.* 451, 249–252. doi: 10.1016/S0014-5793(99)00582-7

Shannon, C. E. (1997). The mathematical theory of communication. 1963. *MD. Comput.* 14, 306–317.

Sheh, A., and Fox, J. G. (2013). The role of the gastrointestinal microbiome in *Helicobacter pylori* pathogenesis. *Gut Microbes* 4, 505–531. doi: 10.4161/gmic.26205

Smolka, A. J., and Backert, S. (2012). How *Helicobacter pylori* infection controls gastric acid secretion. *J. Gastroenterol.* 47, 609–618. doi: 10.1007/s00535-012-0592-1

Tseng, C. H., Lin, J. T., Ho, H. J., Lai, Z. L., Wang, C. B., Tang, S. L., et al. (2016). Gastric microbiota and predicted gene functions are altered after subtotal gastrectomy in patients with gastric cancer. *Sci. Rep.* 6:20701. doi: 10.1038/srep20701

Wang, L., Zhou, J., Xin, Y., Geng, C., Tian, Z., Yu, X., et al. (2015). Bacterial overgrowth and diversification of microbiota in gastric cancer. *Eur. J. Gastroenterol. Hepatol.* 28, 261–266. doi: 10.1097/MEG.0000000000000542

Wang, L. L., Zhou, J. H., Xin, Y. N., Geng, C. X., Tian, Z. B., Yu, X. J., et al. (2016). Bacterial overgrowth and diversification of microbiota in gastric cancer. *Eur. J. Gastroenterol. Hepatol.* 28, 261–266. doi: 10.1097/MEG.0000000000000542

Wroblewski, L. E., Peek, R. M., and Coburn, L. A. (2016). The role of the microbiome in gastrointestinal cancer. *Gastroenterol. Clin. North Am.* 45, 543–556. doi: 10.1016/j.gtc.2016.04.010

Yu, G., Fadrosh, D., Goedert, J. J., Ravel, J., and Goldstein, A. M. (2015). Nested PCR biases in interpreting microbial community structure in 16S rRNA gene sequence datasets. *PLoS ONE* 10:e0132253. doi: 10.1371/journal.pone.0132253

Yu, G., Hu, N., Wang, L., Wang, C., Han, X. Y., Humphry, M., et al. (2017). Gastric microbiota features associated with cancer risk factors and clinical outcomes: a pilot study in gastric cardia cancer patients from Shanxi, China. *Int. J. Cancer* 141, 45–51. doi: 10.1002/ijc.30700

Zhang, C., Cleveland, K., Schnoll-Sussman, F., McClure, B., Bigg, M., Thakkar, P., et al. (2015). Identification of low abundance microbiome in clinical samples using whole genome sequencing. *Genome Biol.* 16, 265. doi: 10.1186/s13059-015-0821-z

Conflict of Interest Statement: The authors declare that the research was conducted in the absence of any commercial or financial relationships that could be construed as a potential conflict of interest.

Copyright © 2017 Yu, Torres, Hu, Medrano-Guzman, Herrera-Goepfert, Humphrys, Wang, Wang, Ding, Ravel, Taylor, Abnet and Goldstein. This is an open-access article distributed under the terms of the Creative Commons Attribution License (CC BY). The use, distribution or reproduction in other forums is permitted, provided the original author(s) or licensor are credited and that the original publication in this journal is cited, in accordance with accepted academic practice. No use, distribution or reproduction is permitted which does not comply with these terms.

frontiers in Cellular and Infection Microbiology

ORIGINAL RESEARCH
published: 06 June 2017
doi: 10.3389/fcimb.2017.00237

Reducing Viability Bias in Analysis of Gut Microbiota in Preterm Infants at Risk of NEC and Sepsis

Gregory R. Young[1], Darren L. Smith[1], Nicholas D. Embleton[2], Janet E. Berrington[2], Edward C. Schwalbe[1], Stephen P. Cummings[3], Christopher J. van der Gast[4] and Clare Lanyon[1]**

[1] Faculty of Health and Life Sciences, University of Northumbria, Newcastle upon Tyne, United Kingdom, [2] Newcastle Neonatal Service, Newcastle upon Tyne Hospitals NHS Foundation Trust, Newcastle upon Tyne, United Kingdom, [3] School of Science and Engineering, Teesside University, Middlesbrough, United Kingdom, [4] School of Healthcare Science, Manchester Metropolitan University, Manchester, United Kingdom

Necrotising enterocolitis (NEC) and sepsis are serious diseases of preterm infants that can result in feeding intolerance, the need for bowel resection, impaired physiological and neurological development, and high mortality rates. Neonatal healthcare improvements have allowed greater survival rates in preterm infants leading to increased numbers at risk of developing NEC and sepsis. Gut bacteria play a role in protection from or propensity to these conditions and have therefore, been studied extensively using targeted 16S rRNA gene sequencing methods. However, exact epidemiology of these conditions remain unknown and the role of the gut microbiota in NEC remains enigmatic. Many studies have confounding variables such as differing clinical intervention strategies or major methodological issues such as the inability of 16S rRNA gene sequencing methods to determine viable from non-viable taxa. Identification of viable community members is important to identify links between the microbiota and disease in the highly unstable preterm infant gut. This is especially important as remnant DNA is robust and persists in the sampling environment following cell death. Chelation of such DNA prevents downstream amplification and inclusion in microbiota characterisation. This study validates use of propidium monoazide (PMA), a DNA chelating agent that is excluded by an undamaged bacterial membrane, to reduce bias associated with 16S rRNA gene analysis of clinical stool samples. We aim to improve identification of the viable microbiota in order to increase the accuracy of clinical inferences made regarding the impact of the preterm gut microbiota on health and disease. Gut microbiota analysis was completed on stools from matched twins ($n = 16$) that received probiotics. Samples were treated with PMA, prior to bacterial DNA extraction. Meta-analysis highlighted a significant reduction in bacterial diversity in 68.8% of PMA treated samples as well as significantly reduced overall rare taxa abundance. Importantly, overall abundances of genera associated with protection from and propensity to NEC and sepsis such as: *Bifidobacterium; Clostridium,* and *Staphylococcus* sp. were significantly different following PMA-treatment. These results suggest non-viable cell exclusion by PMA-treatment reduces bias in gut microbiota analysis from which clinical inferences regarding patient susceptibility to NEC and sepsis are made.

Keywords: preterm, neonate, stool, microbiota, viability, propidium monoazide

OPEN ACCESS

Edited by:
Nathan W. Schmidt,
University of Louisville, United States

Reviewed by:
Valerio Iebba,
Sapienza Università di Roma, Italy
Renate Lux,
UCLA School of Dentistry,
United States

****Correspondence:***
Gregory R. Young
greg.young@northumbria.ac.uk
Clare Lanyon
clare.lanyon@northumbria.ac.uk

Received: *17 March 2017*
Accepted: *22 May 2017*
Published: *06 June 2017*

Citation:
Young GR, Smith DL, Embleton ND, Berrington JE, Schwalbe EC, Cummings SP, van der Gast CJ and Lanyon C (2017) Reducing Viability Bias in Analysis of Gut Microbiota in Preterm Infants at Risk of NEC and Sepsis. Front. Cell. Infect. Microbiol. 7:237. doi: 10.3389/fcimb.2017.00237

INTRODUCTION

Severely preterm infants (<32 weeks) have immature immune systems (Levy, 2007; Strunk et al., 2011), improperly formed intestinal lumen (Halpern and Denning, 2015), and often feeding intolerance (Fanaro, 2013). All such characteristics increase the risk of onset of nosocomial infection, necrotising enterocolitis (NEC), and sepsis (Gregory et al., 2011). Outbreaks of NEC within the neonatal intensive care unit (NICU) (Boccia et al., 2001) and the absence of such diseases prior to bacterial colonization at birth suggest a key role of gut bacterial dysbiosis in these conditions. True causation is, however, very difficult to identify and compacted by complex to understand, highly turbulent community characteristics in the gut, probably in part affected by "routine" interventions of neonatal intensive care (antibiotic administration, feeding strategies, etc.) (Stoll et al., 1996; Hoy et al., 2000).

Targeted 16S rRNA gene sequencing technologies are used to produce microbial metadata for entire populations of a biotope with superior depth, specificity and, most importantly, in significantly less time than previous culture-based or molecular methods (Weinstock, 2012). In addition, the price of sequencing continues to decline (Caporaso et al., 2012), providing further incentives for microbiologists to employ this technique. However, 16S rRNA gene sequencing does introduce inherent biases (von Wintzingerode et al., 1997), including enrichment of particular bacterial groups before storage (Rochelle et al., 1994), insufficient or preferential disruption of certain bacterial cells (Leff et al., 1995; Schneegurt et al., 2003), introduction of sequencing artefacts such as chimeras (Wang and Wang, 1996) and inability to exclude DNA from non-viable sources (Nocker et al., 2006; Nocker and Camper, 2009; Rogers et al., 2013). Persistence of non-viable DNA is due to the stability of the molecule, which enables DNA to remain in an environment long after the originating organism has died. DNA from non-viable bacterial cells (NVBCs) can persist in the lumen of the GI tract, resulting in identification during targeted 16S rRNA gene sequencing analyses. Such bias is especially important whilst studying the highly unstable (Koenig et al., 2011; Bergstrom et al., 2014), low diversity (Tuddenham and Sears, 2015) gut bacterial communities of severely preterm infants. A technique to enable non-viable cell exclusion (NVCE), from such analyses is, therefore, an important and necessary requirement in order to reduce bias and improve the current understanding of bacterial taxa associated with NEC and sepsis.

PMA is a DNA chelating compound that cannot translocate across a viable cellular membrane (Nocker et al., 2007). Nocker et al. (2006), developed the use of Propidium Monoazide (PMA), for differentiation between viable and non-viable bacterial cells during targeted 16S rRNA gene sequencing microbiota analyses (Nocker et al., 2006; Nocker and Camper, 2009; Rogers et al., 2013). This process has been applied in microbial ecology studies of other environments, including wastewater samples (Nocker et al., 2007, 2010), human oral cavities (Sanchez et al., 2013), human adult faeces (Bae and Wuertz, 2009; Fujimoto and Watanabe, 2013), the cystic fibrosis lung (Rogers et al., 2010; Nguyen et al., 2016), and other lower lung respiratory infections (Rogers et al., 2013). The technique, however, has not yet been validated for use in the unique biotope of preterm infant stool despite vast quantities of research being published regarding this microbiota (Mshvildadze et al., 2010; Mai et al., 2011; Torrazza et al., 2013; McMurty et al., 2015). Furthermore, no studies so far have validated combining PMA treatment of this sample type in conjunction with the Schloss method for paired end targeted 16S rRNA gene sequencing (Kozich et al., 2013).

This study aims to identify and alleviate the bias associated with non-viable bacterial DNA inclusion in studies of the gut microbiota of significantly preterm infants at risk of NEC and sepsis. In doing so we hope to increase the accuracy of microbiota characterization in patients at risk of NEC and sepsis, therefore improving the quality of clinical inferences made in relation to the conditions.

The effects of PMA treatment were assessed by comparing bacterial richness, diversity, and community structure as well as individual taxa abundances within PMA-treated and untreated frozen stool samples ($n = 16$) when assessed using targeted paired end sequencing of the 16S rRNA gene.

MATERIALS AND METHODS

Faecal samples were collected when available from day of life 43–81 from a set of significantly preterm twins born 25(+2) weeks gestation and at ≤710 g, enrolled on the SERVIS study at the Royal Victoria Infirmary NICU, Newcastle upon Tyne, England, with ethical permission (NRES Committee North East—Newcastle & North Tyneside 2). Both patients were administered Infloran® (Laboratorio Farmaceutico SIT, Mede, PV, ITA) probiotic supplements throughout the course of the sampling period (*Bifidobacterium bifidum, Lactobacillus acidophilus*). Stool was collected in sterile glass pots with sealed lids and frozen immediately on the ward. Batch collection and transportation to freezers at Northumbria University followed. Samples were stored at −80°C until PMA treatment and DNA extraction for analysis.

PMA Treatment and DNA Extraction

PMA was supplied by Biotium (Hayward, CA, USA), and dissolved in dimethyl sulfoxide to a stock concentration of 20 mM. Faecal samples were homogenised in 2.5 ml PBS per 0.1 g of stool (≤0.5 g), and centrifuged. The centrifuged pellet was resusupended in 2 ml PBS and split evenly to facilitate PMA-treated and untreated conditions per sample. PMA stock solution was added to a final concentration of 50 μM in treated samples and the equivalent volume of PBS was added to untreated samples. PMA cross-linking was initiated by 30 min incubation on ice, in the dark with occasional mixing. Following this, samples were exposed to blue LED light at 464 nm during 30-s intervals for a total of 2 min. After light exposure, samples were centrifuged at 10,000 × g for 5 min. The supernatant was discarded and DNA extracted from the cellular pellet using MoBio PowerLyzer PowerSoil DNA Isolation Kit (Carlsbad, CA, USA), as per manufacturer's instructions.

Nested PCR Protocol and MiSeq Analysis

Prior to paired end targeted 16S rRNA gene analysis, extracted viable DNA was amplified by PCR. Nested PCR was employed in this scenario not to increase copy number prior to sequencing but to increase impact of PMA-intercalation of DNA by blocking amplification of the whole 16S rRNA gene sequence prior to targeted sequencing of the shorter V4 region. Banihashemi et al. (2012) showed that amplification of a 200 bp fragment failed to omit dead cell signals fully from DNA based community analyses. Universal bacterial 16S rRNA gene specific primers 27f (Lane, 1991), and 1,492r (Turner et al., 1999) were used under the following conditions: initial denaturation at 95°C for 5 min then 25 cycles of 30 s denaturation at 95°C; primer annealing at 44.5°C for 30 s; elongation at 72°C for 30 s then a final elongation at 72°C for 10 min.

PCR products were serially diluted 1:10 and paired end targeted analysis of V4 regions of the 16S rRNA gene was performed as described by Kozich et al. (2013), on the Illumina MiSeq using primers described by Caporaso et al. (2011). MiSeq 250 × 2 chemistry was used to perform the targeted 16S rRNA sequencing.

Analysis

Sequence reads with phred-score ≥Q30 were trimmed, merged and processed in Mothur (Schloss et al., 2009), following the MiSeq SOP. Number of sequences passing Q30 in each sample are illustrated in Figure S1. Reads with phred-score <Q30 were not included in analysis. Uncorrected pairwise distances were calculated before clustering sequences in to OTUs using average neighbor joining, as recommended by Schloss and Westcott (2011). The same sequence reads were also submitted to the EBI ENA database for analysis (study accession PRJEB10326; http://www.ebi.ac.uk/ena/data/view/PRJEB10326).

Singletons were not removed from analysis to allow identification of PMA-treatment on all rare taxa identified by targeted sequencing. Normalization was not performed by rarefaction or subsampling due to the nature of the investigation. Instead relative abundances of individual taxa per sample were calculated. This is because the impact of PMA NVCE was assessed by omission of sequence reads from the community, therefore the absence of any sequence read was as informative as the presence of the same.

Per sample richness and beta-diversity was calculated using R statistical software (R_Core_Team., 2014) and the vegan package for community ecology (Oksanen et al., 2015). Meta-analysis (Borenstein et al., 2009) was used to compare results by treatment condition. Meta-analysis has previously been used to quantify the effect of PMA-treatment on bacterial communities of expectorated CF sputum samples (Rogers et al., 2013), allowing direct comparison of the effect of PMA-treatment between paired and unpaired samples by comparing effect size, rather than comparing means of highly variable individual samples by *t*-test. Each microbiota was randomly sub-sampled with bootstrapping $n = 1{,}000$ times. Standard error was reported.

SIMPER comparison of individual taxa relative abundance per treatment condition was performed using PAST (Hammer et al., 2001). Significance of results was calculated and plotted using R statistical software.

Comparison of non-frozen and frozen stool microbiotas was performed using ANOSIM and unconstrained Morisita–Horn cluster analysis.

RESULTS

Stool samples from a set of significantly preterm twins (25+2 weeks gestation) ($n = 16$) receiving Infloran® probiotic supplements were subjected to PMA-treatment for comparison to an untreated control of each sample. 16S rRNA gene sequencing identified a total of 161 individual taxa producing 4.72×10^6 total reads from 16 × 2 samples.

Identification of Common and Rare Taxa

To identify differences between common and rare taxa in PMA-treated and untreated conditions distribution abundance relationship plots were produced (**Figure 1**).

Significant positive distribution abundance relationships were observed between taxa abundance and persistence of taxa across samples in both treatment conditions (untreated: $r^2 = 0.58$, $n = 120$, $P = <0.001$; PMA-treated: $r^2 = 0.72$, $n = 97$, $P = <0.001$). Using this relationship, taxa in the upper quartile of occupancy (≥75% samples), in each treatment condition were classified as common, the remaining taxa were classified as rare.

Distribution of taxa appeared more even in the PMA-treated condition: fewer ubiquitous taxa dominate the communities in the PMA-treated condition (2 taxa); compared to the untreated condition (6 taxa).

In untreated sample conditions 6 taxa were identified as common, all of which were observed in every sample. *Bifidobacterium, Enterococcus,* 2 *Clostridia* spp., a *Veillonella* and an unclassified Enterobacteriaceae accounted for 77.9% of the total community member sequences. In PMA-treated samples, 8 common taxa were identified, comprising 82.2% of total community member sequences however of these, only 2 (*Bifidobacterium* and *Enterococcus*) were found in all samples. *Anaerococcus* and *Finegoldia* sp. were identified as common in PMA-treated samples but not in untreated samples.

Effect of PMA Treatment on Bacterial Richness and Diversity

Due to the large coverage variability between the stool sample communities ($m = 1.47 \times 10^5$, $SD = 1.26 \times 10^5$), meta-analysis was used to identify the effect size of PMA-treatment on microbiota composition by bacterial OTU richness (O∗); Shannon diversity index (H′); and Inverse Simpson's diversity index (1/D).

Bacterial OTU richness was variable between stool samples of the same treatment condition (untreated $m = 9.1 \pm 2.7$, PMA-treated $m = 8.8 \pm 1.9$). The effect of PMA-treatment on O∗ was only once greater than the significance threshold (0.2), and showed no directional consistency (**Figure 2**).

Like richness, bacterial diversity also varied between individual stool samples in the same treatment condition (**Table 1**).

Meta-analysis showed negative effect sizes of PMA-treatment on bacterial diversity in 71.9% of samples, of which 73.9% were highly significant (>0.8) (**Figures 3**, **4**). Significant negative mean

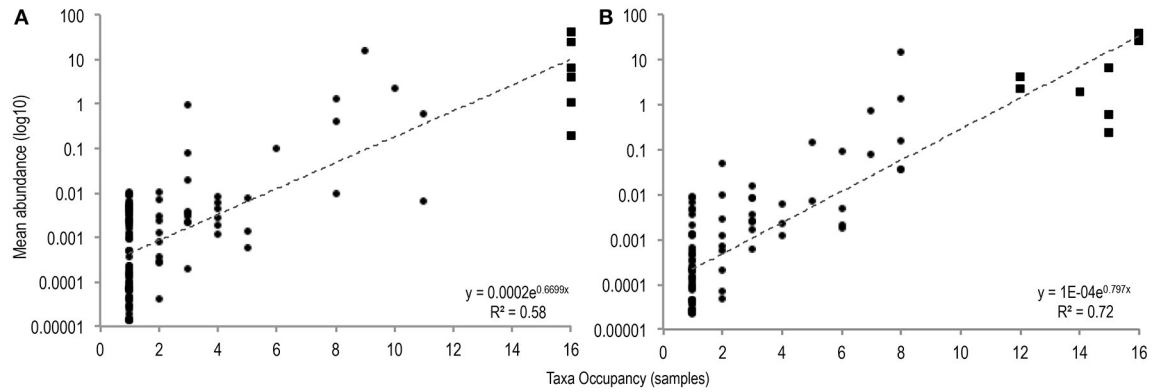

FIGURE 1 | The number of samples in which taxa were observed plotted against mean taxa abundance (log10 scale) in untreated sample **(A)**, and PMA-treated sample **(B)**, conditions [(**A**: $r^2 = 0.58$; $P = <0.001$), (**B**: $r^2 = 0.72$; $P = < 0.001$)]. Common taxa (>75% sample occupancy) are plotted square, rare samples (<75% sample occupancy) are plotted circle.

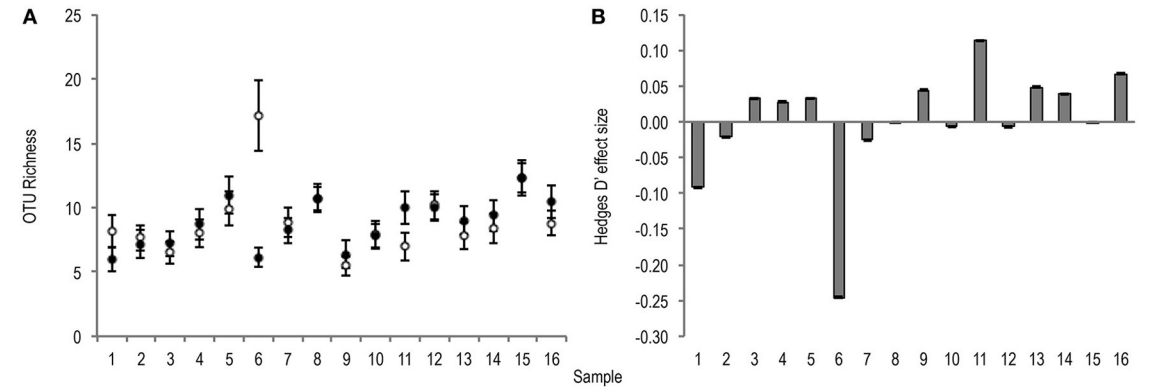

FIGURE 2 | (A) Bootstrapped ($n = 1{,}000$) O* values for untreated (hollow points), and PMA-treated (solid points) conditions of all samples (1–16). Error bars are included. **(B)** Hedges' d effect size of PMA-treatment on O* of all samples (1–16). Positive effect was observed in 50% of samples. Sample 6 was the only observed effect size >0.2 (small effect).

TABLE 1 | Mean and standard deviation for Shannon and inverse Simpson diversity indices for PMA-treated and untreated conditions.

	Diversity index			
	Shannon (H')		Inverse Simpson (1/D)	
	Mean	*SD*	Mean	*SD*
PMA-treated	1.13	0.32	2.64	0.95
Non-PMA-treated	1.30	0.16	2.99	0.50
P-value	<0.05		>0.05	

overall effect sizes on both measures of diversity were observed following PMA-treatment (m: $H' = -0.95$; $1/D = -1.23$).

Effect of PMA-Treatment on Individual Bacterial Taxa Abundance

To investigate the effect of PMA-treatment on observable abundance values of individual taxa relative sequence abundance was calculated. Initial analysis of the PMA-treatment effect on individual taxa abundance within the bacterial communities of stools was performed by SIMPER (**Table 2**). SIMPER provides an insight in to the variance, expressed as a percentage, between abundance of taxa from the untreated group and the PMA-treated group.

Table 2 illustrates which taxa contributed greatest to dissimilarity of common and rare community structures between untreated and PMA-treated conditions.

Greater average dissimilarity is observed in rare (83.21%), than common (42.87), taxa. The taxon labelled *Escherichia_shigella* by the *SILVA* database (Quast et al., 2013) appears to contribute to the average dissimilarity between non-PMA and PMA treated conditions most (63.45%), in spite of a mean abundance difference of only 1.3%. This contrasts with other taxa such as *Bifidobacterium* and *Enterococcus,* for which lower average dissimilarities of 15.20 and 12.25 are observed, however much greater mean abundance differences of 14.6 and 14.8 are found, respectively. This incongruence could be explained by variation in abundance of individual taxa between samples within the same condition. The SD of *Escherichia*

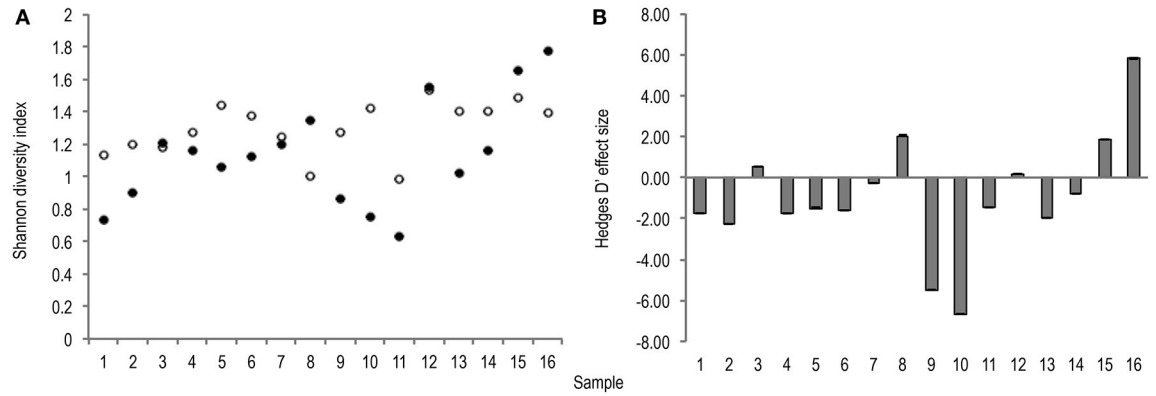

FIGURE 3 | (A) Bootstrapped (n = 1,000) Shannon diversity index values for untreated (hollow points), and PMA-treated (solid points), conditions for all samples (1–16). Standard error bars are included. **(B)** Hedges' d effect size of PMA-treatment on Shannon diversity index values of all samples (1–16). Seventy-five percentage of samples exhibit significant (>0.8) effect size, 75% of which are negative.

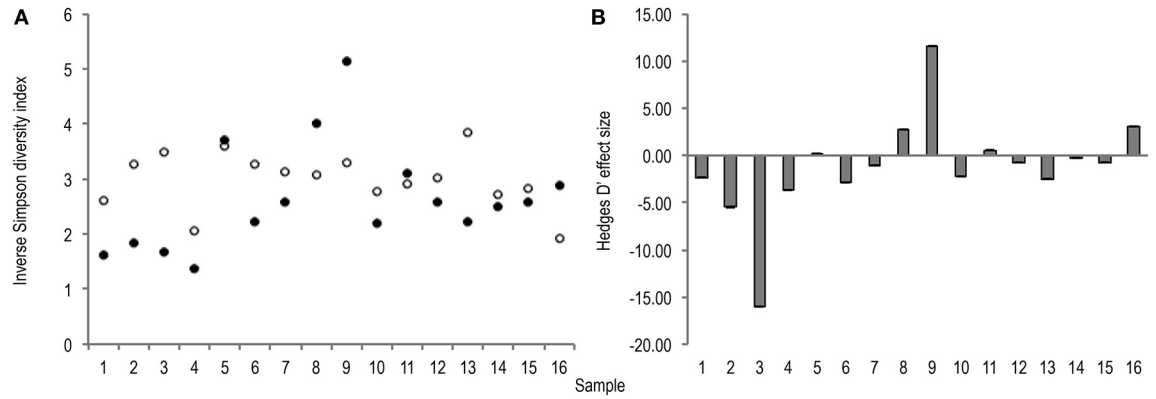

FIGURE 4 | (A) Bootstrapped (n = 1,000), inverse Simpson diversity index values for untreated (hollow points), and PMA-treated (solid points), conditions for all samples (1–16). Standard error bars are included but error is too insignificant to be visible. **(B)** Hedges' d effect size of PMA-treatment on inverse Simpson diversity index values of all samples (1–16). 68.8% samples exhibit significant (>0.8) effect size. 72.3% of which are negative rare **(B)** taxa.

abundance is much greater (untreated: $m = 16.2$, $SD = 18.2$; PMA-treated: $m = 14.9$, $SD = 24.3$), than that of *Bifidobacterium* (untreated: $m = 41.1$, $SD = 15.2$; PMA-treated: $m = 26.5$, $SD = 19.5$), or *Enterococcus* (untreated: $m = 25.0$, $SD = 10.2$; PMA-treated: $m = 39.8$, $SD = 14.0$).

To normalise for this variance Wilcoxon rank sum tests were performed to assess the similarities of mean abundance for each taxon in both conditions as identified by SIMPER analysis. The same means were used to calculate a fold change in taxa abundance between the two conditions and both parameters were plotted on a volcano plot (**Figure 5**).

The majority of taxa showed substantial fold changes in abundance following PMA-treatment; however only 6 of these fold changes pass the significance threshold ($P < 0.05$): *Bifidobacterium*; Enterobacteriaceae; *Enterococcus; Clostridium; Actinomyces;* and *Peptoniphilus* sp.

In untreated conditions *Bifidobacterium* and *Enterobacteriaceae* sp. abundances are significantly greater while *Enterococcus*, *Clostridium, Peptoniphilus,* and *Actinomyces* sp. abundances are significantly lower. This suggests that the presence of non-viable DNA originating from highly abundant species such as *Bifidobacteria* and *Enterobacteriaceae* could potentially mask that of less abundant species such as *Enterococcus, Clostridium, Peptoniphilus,* and *Actinomyces* sp.

As volcano plots (**Figure 5**) only represent fold change in abundance for taxa present in both sample conditions, rank abundance plots (**Figure 6**) were generated to illustrate abundance of taxa identifiable in only one treatment condition.

Fewer taxa were observed PMA-treated than untreated sample conditions. Of 111 total taxa present in only one condition 68 (61.3%), were present in untreated samples while only 43 (38.7%), were present in PMA-treated samples, representing a 22.6% reduction in presence of taxa measurable in only one condition. Levels of 2 rare taxa (*Staphylococcus* and *Phenylobacterium*), were observable at levels > 0.09% sequence abundance (almost 10 fold more than all other taxa observable in only one treatment condition), following PMA-treatment. These taxa were completely masked in the untreated condition. All other

TABLE 2 | SIMPER analysis of common **(A)** and rare **(B)** taxa.

Average dissimilarity between conditions = 42.87				**Non-PMA-treated**	**PMA-treated**
Taxon	**Av. dissim**	**Contrib. %**	**Cumulative %**	**Mean abund. 1**	**Mean abund. 2**
(A)					
Bifidobacterium	15.20	35.44	35.44	41.1	26.5
Enterococcus	12.23	28.52	63.96	25.0	39.8
Clostridium 1	4.60	10.74	74.70	4.0	6.6
Enterobacteriaceae; unclassified	4.03	9.41	84.11	6.6	0.6
*Anaerococcus**	3.25	7.58	91.68	2.2	4.2
*Finegoldia**	1.75	4.08	95.76	1.3	2.3
Clostridium 2	1.08	2.51	98.27	0.2	1.9
Veillonella	0.74	1.73	100.00	1.1	0.2
Average dissimilarity between conditions = 83.21				**Non-PMA-treated**	**PMA-treated**
(B)					
Escherichia_Shigella	52.81	63.46	63.46	16.2	14.9
Peptoniphilus	11.07	13.3	76.76	0.576	1.41
Actinomyces	6.88	8.267	85.03	0.389	0.75
Streptococcus	4.087	4.911	89.94	0.986	0.0157
Staphylococcus	1.378	1.656	91.59	0	0.15
Phenylobacterium	1.333	1.602	93.2	0	0.0939

Cut-off value set at taxa contributing <1% to dissimilarity between treatment conditions.
**Denotes taxa only attributed common status in PMA-treated condition.*
Cut-off set at taxa contributing <1% to dissimilarity between treatment conditions.

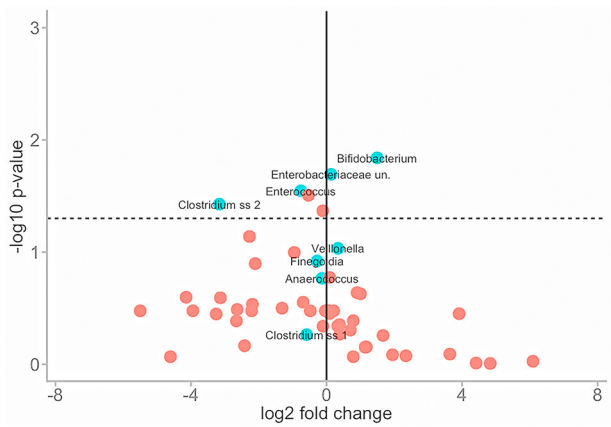

FIGURE 5 | Illustrates the effect of PMA-treatment on individual taxa abundances. Fold change in abundance is plotted (*x*) against the *P*-value of that same fold change (*y*) for each taxon. The solid vertical line represents no fold-change. Travelling in either direction from this line the fold change increases. The dotted horizontal line represents significance cut-off (.05). Core taxa are blue and labelled. Rare taxa are red.

taxa abundances were reduced to <0.009% following PMA-treatment. A significant difference between mean abundances of rare taxa presence between untreated ($m = 0.0052$), and PMA-treated ($m = 0.0012$), sample conditions ($P = <0.001$), was observed. This suggests that performing gut microbiota analysis of frozen stool by paired end targeted 16S rRNA gene sequencing without PMA-treatment could fail to identify presence of rare community members due to significant background sequence noise orignating from non-living taxa. This could explain the significant overall reduction in mean bacterial diversity following PMA-treatment observed in meta-analysis (**Figures 3**, **4**). Principle coordinate analysis of sample communities was also performed based on Bray-Curtis dissimilarity of taxa abundances (Figure S2).

To confirm the differences observed were due to genuine viable differences in the sample microbiota rather than bacterial cell death during freezing (−80°C) one further stool sample was split ($n = 10$). The microbiota of frozen and non-frozen samples in untreated and PMA-treated conditions were compared. Overall 4.04×10^6 reads were recorded from 10×2 samples ($m = 2.02 \times 10^5$). Sample storage had an insignificant effect on observed Bray–Curtis community similarity between treatment conditions (**Table 3**), and no separation by PMA-treatment within storage groups was observed (Figure S3). This data further supports Shaw et al. (2016), findings suggesting freeze storage of severely preterm stool samples does not significantly impact the gut microbiota observed with or without PMA-treatment.

DISCUSSION

The gut microbiota of significantly preterm infants held within the neonatal intensive care unit has been previously identified to be extremely changeable (Koenig et al., 2011; Bergstrom et al., 2014). Microbial communities colonising this biotope are challenged by frequent antibiotic intervention (Craft et al., 2000), administration of probiotics (AlFaleh and Anabrees, 2014),

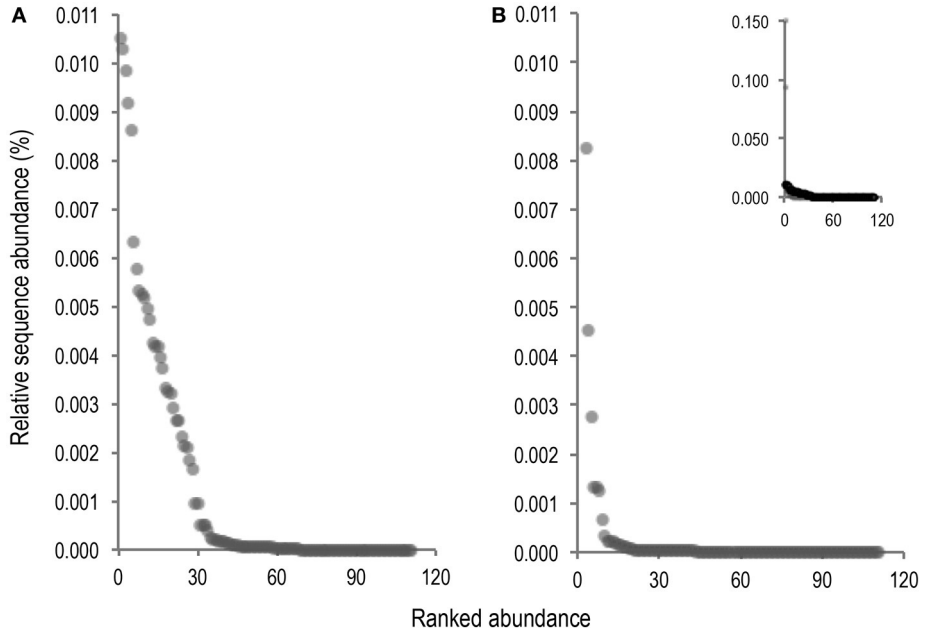

FIGURE 6 | Rank abundance plots of taxa for which abundance was only measurable in either the untreated **(A)**, or PMA-treated **(B)**, sample condition. Ranked abundance of the untreated condition including *Staphylococcus* and *Phenylobacterium* is inset at top right corner of PMA-treated condition plot **(B)**.

TABLE 3 | *P*-values associated with ANOSIM analysis comparing Bray Curtis dissimilarity between frozen and non-frozen samples in control and PMA-treated sample conditions.

	ANOSIM × groups (Bray-Curtis)			
	Frozen CTRL	**Frozen PMA**	**Non-frozen CTRL**	**Non-frozen PMA**
Frozen CTRL		>0.1	<0.01	<0.01
Frozen PMA	>0.1		<0.01	<0.01
Non-frozen CTRL	<0.01	<0.01		>0.5
Non-frozen PMA	<0.01	<0.01	>0.5	

fluctuating pH due to the use of proton pump inhibitors (Omari et al., 2007, 2009), and gut lumen and immune system maturation (Israel, 1994; Levy, 2007; Strunk et al., 2011). All of these factors complex the first months of a newborn infant's life, thereby it is considered the most unstable with respect to microbiota composition. In order for clinicians to accurately assess the requirement for, and effect of, intervention strategies on infant microbial populations the analysis techniques used must be able to reliably quantify unbiased and viable microbiotas.

Currently techniques either cannot provide results within a short turnaround time at a sufficient phylogenetic resolution to assess the diversity in the gut (bacterial culture), or fail to differentiate viable from non-viable community members (Q-PCR). While RNA sequencing enables exclusive identification of genes actively transcribed by viable cells there are downstream issues regarding storage and contaminating RNAses (Zheng et al., 1996) RNA samples require collection in an RNA preservative (Mutter et al., 2004) which is not always possible in the clinic. Furthermore, use of DNA in combination with PMA eliminates the need for reverse transcription of sequences prior to analysis.

Nocker and Camper (2009), have previously shown PMA-treatment excludes DNA from non-viable cells. This study builds on those results by illustrating PMA-treatment of frozen preterm infant stool alters observable microbiota structure and diversity following paired end targeted 16S rRNA gene sequencing. This would suggest inclusion of non-viable community members during preterm infant stool microbiota analysis introduces a bias. Additionally, DNA from non-viable cells can have significant impact on individual taxa quantification. We propose it may be necessary to employ the use of PMA as a tool for NVCE in 16S rRNA gene sequencing based microbiota analysis. Effects of PMA NVCE should not be attributed to cell death during storage as no difference in PMA effect was observed between frozen and fresh stool samples. It is probable that the changes in abundance illustrated by PMA NVCE are caused by antibiotic, probiotic, or other clinical interventions however further study is required to confirm this.

Importantly, this study illustrates that the presence of particular, clinically relevant taxa may be either over-represented (*Bifidobacterium*), or under-represented (*Clostridium, Staphylococcus*), in the absence of PMA-treatment. This is most probably due to the suppression of DNA sequence reads from rare taxa by dominant taxa as illustrated by the reduced bacterial diversity and presence of rare taxa observed in PMA-treated samples.

These findings are of particular relevance in the gut microbiota of the preterm infants analysed in this study due to administration of probiotic supplements. While *Bifidobacterium* remained ubiquitous and abundant across samples in both

treatment conditions it has been shown in several studies (Alander et al., 2001; Charbonneau et al., 2013; Rattanaprasert et al., 2014) that administered probiotic strains often fail to engraft long-term. This would make PMA treatment extremely important for analysis of future intervention trials of this manner. Maldonado-Gómez María et al. (2016), showed that presence of phylogenetically or functionally similar keystone species can prevent engraftment of probiotic strains. The results of this study suggest *Bifidobacteria* within the probiotics may not maintain viability throughout the entire GI tract; a further possible reason for this failed engraftment. We demonstrate persistent DNA from non-viable *Bifidobacteria* may conceal the presence of less abundant, transient colonisers with the potential to confound clinical inferences drawn from 16S rRNA gene sequencing data. Further work should compare the functional profiles of the probiotic *Bifidobacterium* strain in Infloran® and the bacterial metagenomes of patients administered the supplement as well as investigating the community engraftment potential of the specific probiotic strains administered to patients enrolled in this study.

This study has deliberately selected a pair of twins with good longitudinal sampling to evaluate the effect of PMA treatment on observable microbiota members, however the number of actual samples ($n = 16$), is relatively small and recruitment purely convenience based. In lieu of the individual taxa for which significant changes in abundance are observed in this study may not be replicated in repeated studies, dependant on viable and non-viable taxa abundances. Specifically, *Bifidobacterium* may not necessarily be observed at significantly altered abundances in microbiota of patients not receiving probiotics or in patients with a greater engraftment potential. Given the key role of *Bifidobacteria* in preterm gut health, this requires further exploration. We stress that use of PMA need not be limited to that of preterm infant stool but could be applied to any unstable environment where clinical microbiota intervention is employed or in which abundance of community members may be regularly changeable. Further studies may wish to explore the use of such techniques in these environments.

Consideration should be granted that the use of a nested PCR technique represents a potential source of amplification bias in populations of low bacterial load (Yu et al., 2015). In contrast, Fan et al. (2009), have demonstrated that use of a 25 cycle nested PCR does not significantly affect observable bacterial communities. Moreover, nested PCR was employed in this study to increase the inhibitory capacity of PMA on chelated DNA, rather than increase identifiable sequences.

One possible reason for the widespread disregard of PMA use for NVCE could be the specification of non-viable cells solely as membrane-compromised cells using this method. Contreras et al. (2011), describe membrane integrity as a "conservative parameter" for viability identification, explaining inability to culture bacteria occurs sooner than membrane denaturation in heat-killed cells. We propose conservative NVCE is more appealing in this clinical context than nihil NVCE, in which non-viable DNA persists and can bias results or exaggerated NVCE, where community members may be excluded from analysis while still viable.

This study represents the first time PMA-treatment has been combined with paired end targeted 16S rRNA gene sequence analysis of a gut microbiota using the methods described by Kozich et al. (2013). Future research should focus on validation of this method of analysis in a larger sample cohort to include greater inter-sample microbiota variation. Analysis of probiotic and commensal bacterial viability throughout the preterm infant GI tract would be another logical progression from this work.

ETHICS STATEMENT

This study was carried out in accordance with the recommendations of "NRES Committee North East – Newcastle & North Tyneside 2" with written informed consent from all subjects. All subjects gave written informed consent in accordance with the Declaration of Helsinki. The protocol was approved by the "NRES Committee North East – Newcastle & North Tyneside 2."

AUTHOR CONTRIBUTIONS

GY, Cv, and CL conceived the study. NE and JB collected samples and clinical data. GY designed the study and performed the experiments. DS ran the sequencing. GY, Cv, ES, and SC analysed the data. GY, DS, and Cv wrote the paper. All authors proof read and approved the paper prior to submission.

FUNDING

This work was supported by Northumbria University [grant number 10031605/2 awarded to GY].

ACKNOWLEDGMENTS

The authors would like to acknowledge the work of the clinical staff of the neonatal intensive care unit at the Royal Victoria Infirmary, Newcastle for collection and storage of samples. Particular thanks go to Julie Groombridge, the research nurse at the RVI NICU for organisation and sample labelling. Further personal acknowledgement must be given to Dr. Andrew Nelson, Northumbria University, for being a great antagonist: challenging and questioning the findings; to help improve the validity of the research. Sequencing of the 16S rRNA gene was performed by the NUOMICS sequencing service.

SUPPLEMENTARY MATERIAL

The Supplementary Material for this article can be found online at: http://journal.frontiersin.org/article/10.3389/fcimb.2017.00237/full#supplementary-material

REFERENCES

Alander, M., Matto, J., Kneifel, W., Johansson, M., Kogler, B., Crittenden, R., et al. (2001). Effect of galacto-oligosaccharide supplementation on human faecal microflora and on survival and persistence of *Bifidobacterium lactis* Bb-12 in the gastrointestinal tract. *Int. Dairy J.* 11, 817–825. doi: 10.1016/S0958-6946(01)00100-5

AlFaleh, K., and Anabrees, J. (2014). Probiotics for prevention of necrotizing enterocolitis in preterm infants. *Cochrane Database Syst. Rev.* 4, 16:CD005496. doi: 10.1002/14651858.CD005496

Bae, S. W., and Wuertz, S. (2009). Discrimination of viable and dead fecal bacteroidales bacteria by quantitative PCR with propidium monoazide. *Appl. Environ. Microbiol.* 75, 2940–2944. doi: 10.1128/AEM.01333-08

Banihashemi, A., Van Dyke, M. I., and Huck, P. M. (2012). Long-amplicon propidium monoazide-PCR enumeration assay to detect viable Campylobacter and Salmonella. *J. Appl. Microbiol.* 113, 863–873. doi: 10.1111/j.1365-2672.2012.05382.x

Bergstrom, A., Skov, T. H., Bahl, M. I., Roager, H. M., Christensen, L. B., Ejlerskov, K. T., et al. (2014). Establishment of intestinal microbiota during early life: a longitudinal, explorative study of a large cohort of danish infants. *Appl. Environ. Microbiol.* 80, 2889–2900. doi: 10.1128/AEM.00342-14

Boccia, D., Stolfi, I., Lana, S., and Moro, M. L. (2001). Nosocomial necrotising enterocolitis outbreaks: epidemiology and control measures. *Eur. J. Pediatr.* 160, 385–391. doi: 10.1007/s004310100749

Borenstein, M., Hedges, L. V., Higgins, J. P. T., and Rothstein, H. R. (2009). *How a Meta-Analysis Works*. Chichester: John Wiley & Sons, Ltd.

Caporaso, J. G., Lauber, C. L., Walters, W. A., Berg-Lyons, D., Huntley, J., Fierer, N., et al. (2012). Ultra-high-throughput microbial community analysis on the Illumina HiSeq and MiSeq platforms. *ISME J.* 6, 1621–1624. doi: 10.1038/ismej.2012.8

Caporaso, J. G., Lauber, C. L., Walters, W. A., Berg-Lyons, D., Lozupone, C. A., Turnbaugh, P. J., et al. (2011). Global patterns of 16S rRNA diversity at a depth of millions of sequences per sample. *Proc. Natl. Acad. Sci. U.S.A.* 108, 4516–4522. doi: 10.1073/pnas.1000080107

Charbonneau, D., Gibb, R. D., and Quigley, E. M. (2013). Fecal excretion of *Bifidobacterium infantis* 35624 and changes in fecal microbiota after eight weeks of oral supplementation with encapsulated probiotic. *Gut. Microbes* 4, 201–211. doi: 10.4161/gmic.24196

Contreras, P. J., Urrutia, H., Sossa, K., and Nocker, A. (2011). Effect of PCR amplicon length on suppressing signals from membrane-compromised cells by propidium monoazide treatment. *J. Microbiol. Methods* 87, 89–95. doi: 10.1016/j.mimet.2011.07.016

Craft, A. P., Finer, N. N., and Barrington, K. J. (2000). Vancomycin for prophylaxis against sepsis in preterm neonates. *Cochrane Database Syst. Rev.* 2:CD001971. doi: 10.1002/14651858.CD001971

Fan, Z.-Y., Li, X.-R., Mao, D.-P., Zhu, G.-F., Wang, S.-Y., and Quan, Z.-X. (2009). Could nested PCR be applicable for the study of microbial diversity? *World J. Microbiol. Biotechnol.* 25, 1447–1452. doi: 10.1007/s11274-009-0033-3

Fanaro, S. (2013). Feeding intolerance in the preterm infant. *Early Hum. Dev.* 89(Suppl. 2), S13–S20. doi: 10.1016/j.earlhumdev.2013.07.013

Fujimoto, J., and Watanabe, K. (2013). Quantitative detection of viable *Bifidobacterium bifidum* BF-1 Cells in human feces by using propidium monoazide and strain-specific primers. *Appl. Environ. Microbiol.* 79, 2182–2188. doi: 10.1128/AEM.03294-12

Gregory, K. E., Deforge, C. E., Natale, K. M., Phillips, M., and Van Marter, L. J. (2011). Necrotizing enterocolitis in the premature infant: neonatal nursing assessment, disease pathogenesis, and clinical presentation. *Adv. Neonatal Care* 11, 155–164. doi: 10.1097/ANC.0b013e31821baaf4

Halpern, M. D., and Denning, P. W. (2015). The role of intestinal epithelial barrier function in the development of NEC. *Tissue Barriers* 3:e1000707. doi: 10.1080/21688370.2014.1000707

Hammer, Ø., Harper, D. A. T., and Ryan, P. D. (2001). "Past: Paleontological Statistics Software Package for education and data analysis," in *Palaeontologia Electronica*, Vol. 4, 9. Available online at: http://palaeo-electronica.org/2001_1/past/issue1_01.htm

Hoy, C. M., Wood, C. M., Hawkey, P. M., and Puntis, J. W. L. (2000). Duodenal microflora in very-low-birth weight neonates and relation to necrotizing enterocolitis. *J. Clin. Microbiol.* 38, 4539–4547. Available online at: https://www.scopus.com/record/display.uri?eid=2-s2.0-0034460430&origin=inward&txGid=A4A23F490D36796B4CB5E0ED1D87F2CE.wsnAw8kcdt7IPYLO0V48gA%3a1

Israel, E. J. (1994). Neonatal necrotizing enterocolitis, a disease of the immature intestinal Mucosal Barrier. *Acta Paediatr.* 83, 27–32. doi: 10.1111/j.1651-2227.1994.tb13238.x

Koenig, J. E., Spor, A., Scalfone, N., Fricker, A. D., Stombaugh, J., Knight, R., et al. (2011). Succession of microbial consortia in the developing infant gut microbiome. *Proc. Natl. Acad. Sci. U.S.A.* 108, 4578–4585. doi: 10.1073/pnas.1000081107

Kozich, J. J., Westcott, S. L., Baxter, N. T., Highlander, S. K., and Schloss, P. D. (2013). Development of a dual-index sequencing strategy and curation pipeline for analyzing amplicon sequence data on the MiSeq illumina sequencing platform. *Appl. Environ. Microbiol.* 79, 5112–5120. doi: 10.1128/AEM.01043-13

Lane, D. J. (1991). "16S/23S rRNA sequencing," in *Nucleic Acid Techniques in Bacterial Systematics,* eds E. Stackebrandt and M Goodfellow (Chichester, UK: John Wiley & Sons), 115–175.

Leff, L. G., Dana, J. R., McArthur, J. V., and Shimkets, L. J. (1995). Comparison of methods of DNA extraction from stream sediments. *Appl. Environ. Microbiol.* 61, 1141–1143.

Levy, O. (2007). Innate immunity of the newborn: basic mechanisms and clinical correlates. *Nat. Rev. Immunol.* 7, 379–390. doi: 10.1038/nri2075

Mai, V., Young, C. M., Ukhanova, M., Wang, X. Y., Sun, Y. J., Casella, G., et al. (2011). Fecal microbiota in premature infants prior to necrotizing Enterocolitis. *PLoS ONE* 6:e20647. doi: 10.1371/journal.pone.0020647

Maldonado-Gómez María, X., Martínez, I., Bottacini, F., O'Callaghan, A., Ventura, M., van Sinderen, D., et al. (2016). Stable engraftment of *Bifidobacterium longum* AH1206 in the human gut depends on individualized features of the resident microbiome. *Cell Host Microbe* 4, 515–526. doi: 10.1016/j.chom.2016.09.001

McMurty, V. E., Gupta, R. W., Tran, L., Blanchard, E. E., Penn, D., Taylor, C. M., et al. (2015). Bacterial diversity and Clostridia abundance decrease with increasing severity of necrotizing enterocolitis. *Microbiome* 3, 11. doi: 10.1186/s40168-015-0075-8

Mshvildadze, M., Neu, J., Shuster, J., Theriaque, D., Li, N., and Mai, V. (2010). Intestinal microbial ecology in premature infants assessed with non–culture-based techniques. *J. Pediatr.* 156, 20–25. doi: 10.1016/j.jpeds.2009.06.063

Mutter, G. L., Zahrieh, D., Liu, C., Neuberg, D., Finkelstein, D., Baker, H. E., et al. (2004). Comparison of frozen and RNALater solid tissue storage methods for use in RNA expression microarrays. *BMC Gen.* 5:88. doi: 10.1186/1471-2164-5-88

Nguyen, L. D. N., Deschaght, P., Merlin, S., Loywick, A., Audebert, C., Van Daele, S., et al. (2016). Effects of Propidium Monoazide (PMA) treatment on mycobiome and bacteriome analysis of cystic fibrosis airways during exacerbation. *PLoS ONE* 11:e0168860. doi: 10.1371/journal.pone.0168860

Nocker, A., and Camper, A. K. (2009). Novel approaches toward preferential detection of viable cells using nucleic acid amplification techniques. *FEMS Microbiol. Lett.* 291, 137–142. doi: 10.1111/j.1574-6968.2008.01429.x

Nocker, A., Cheung, C. Y., and Camper, A. K. (2006). Comparison of propidium monoazide with ethidium monoazide for differentiation of live vs. dead bacteria by selective removal of DNA from dead cells. *J. Microbiol. Methods* 67, 310–320. doi: 10.1016/j.mimet.2006.04.015

Nocker, A., Richter-Heitmann, T., Montijn, R., Schuren, F., and Kort, R. (2010). Discrimination between live and dead cells in bacterial communities from environmental water samples analyzed by 454 pyrosequencing. *Int. Microbiol.* 13, 59–65. doi: 10.2436/20.1501.01.111

Nocker, A., Sossa-Fernandez, P., Burr, M. D., and Camper, A. K. (2007). Use of propidium monoazide for live/dead distinction in microbial ecology. *Appl. Environ. Microbiol.* 73, 5111–5117. doi: 10.1128/AEM.02987-06

Oksanen, J., Guillaume Blanchet, F., Kindt, R., Legendre, P., Minchin, P. R., O'Hara, R. B., et al. (2015). *vegan: Community Ecology Package*.

Omari, T. I., Haslam, R. R., Lundborg, P., and Davidson, G. P. (2007). Effect of omeprazole on acid gastroesophageal reflux and gastric acidity in preterm

infants with pathological acid reflux. *J. Pediatr. Gastroenterol. Nutr.* 44, 41–44. doi: 10.1097/01.mpg.0000252190.97545.07

Omari, T., Lundborg, P., Sandstrom, M., Bondarov, P., Fjellman, M., Haslam, R., et al. (2009). Pharmacodynamics and systemic exposure of esomeprazole in preterm infants and term neonates with gastroesophageal reflux disease. *J. Pediatr.* 155, 222–228. doi: 10.1016/j.jpeds.2009.02.025

Quast, C., Pruesse, E., Yilmaz, P., Gerken, J., Schweer, T., Yarza, P., et al. (2013). The SILVA ribosomal RNA gene database project: improved data processing and web-based tools. *Nucl. Acids Res.* 41, D590–D596. doi: 10.1093/nar/gks1219

R_Core_Team. (2014). *R: A Language and Environment for Statistical Computing*. R Foundation for Statistical Computing. Available online at: http://www.R-project.org/

Rattanaprasert, M., Roos, S., Hutkins, R. W., and Walter, J. (2014). Quantitative evaluation of synbiotic strategies to improve persistence and metabolic activity of *Lactobacillus reuteri* DSM 17938 in the human gastrointestinal tract. *J. Funct. Foods* 10, 85–94. doi: 10.1016/j.jff.2014.05.017

Rochelle, P. A., Cragg, B. A., Fry, J. C., Parkes, R. J., and Weightman, A. J. (1994). Effect of sample handling on estimation of bacterial diversity in marine sediments by 16S rRNA gene sequence analysis. *FEMS Microbiol. Ecol.* 15, 215–225. doi: 10.1111/j.1574-6941.1994.tb00245.x

Rogers, G. B., Cuthbertson, L., Hoffman, L. R., Wing, P. A. C., Pope, C., Hooftman, D. A. P., et al. (2013). Reducing bias in bacterial community analysis of lower respiratory infections. *ISME J.* 7, 697–706. doi: 10.1038/ismej.2012.145

Rogers, G. B., Marsh, P., Stressmann, A. F., Allen, C. E., Daniels, T. V. W., Carroll, M. P., et al. (2010). The exclusion of dead bacterial cells is essential for accurate molecular analysis of clinical samples. *Clin. Microbiol. Infect.* 16, 1656–1658. doi: 10.1111/j.1469-0691.2010.03189.x

Sanchez, M. C., Marin, M. J., Figuero, E., Llama-Palacios, A., Herrera, D., and Sanz, M. (2013). Analysis of viable vs. dead Aggregatibacter actinomycetemcomitans and *Porphyromonas gingivalis* using selective quantitative real-time PCR with propidium monoazide. *J. Periodontal Res.* 48, 213–220. doi: 10.1111/j.1600-0765.2012.01522.x

Schloss, P. D., and Westcott, S. L. (2011). Assessing and Improving methods used in operational taxonomic unit-based approaches for 16S rRNA gene sequence analysis. *Appl. Environ. Microbiol.* 77, 3219–3226. doi: 10.1128/AEM.02810-10

Schloss, P. D., Westcott, S. L., Ryabin, T., Hall, J. R., Hartmann, M., Hollister, E. B., et al. (2009). Introducing mothur: open-source, platform-independent, community-supported software for describing and comparing microbial communities. *Appl. Environ. Microbiol.* 75, 7537–7541. doi: 10.1128/AEM.01541-09

Schneegurt, M. A., Dore, S. Y., and Kulpa, C. F. Jr. (2003). Direct extraction of DNA from soils for studies in microbial ecology. *Curr. Issues Mol. Biol.* 5, 1–8.

Shaw, A. G., Sim, K., Powell, E., Cornwell, E., Cramer, T., McClure, Z. E., et al. (2016). Latitude in sample handling and storage for infant faecal microbiota studies: the elephant in the room? *Microbiome* 4, 1–14. doi: 10.1186/s40168-016-0186-x

Stoll, B. J., Gordon, T., Korones, S. B., Shankaran, S., Tyson, J. E., Bauer, C. R., et al. (1996). Early-onset sepsis in very low birth weight neonates. A report from the National Institute of Child Health and Human Development Neonatal Research Network. *J. Pediatr.* 129, 72–80. doi: 10.1016/S0022-3476(96)70192-0

Strunk, T., Currie, A., Richmond, P., Simmer, K., and Burgner, D. (2011). Innate immunity in human newborn infants: prematurity means more than immaturity. *J. Matern. Fetal Neonatal Med.* 24, 25–31. doi: 10.3109/14767058.2010.482605

Torrazza, R. M., Ukhanova, M., Wang, X. Y., Sharma, R., Hudak, M. L., Neu, J., et al. (2013). Intestinal Microbial ecology and environmental factors affecting necrotizing Enterocolitis. *PLoS ONE* 8:e83304. doi: 10.1371/journal.pone.0083304

Tuddenham, S., and Sears, C. L. (2015). The intestinal microbiome and health. *Curr. Opin. Infect. Dis.* 28, 464–470. doi: 10.1097/QCO.0000000000000196

Turner, S., Pryer, K. M., Miao, V. P. W., and Palmer, J. D. (1999). Investigating deep phylogenetic relationships among cyanobacteria and plastids by small subunit rRNA sequence analysis1. *J. Eukaryot. Microbiol.* 46, 327–338. doi: 10.1111/j.1550-7408.1999.tb04612.x

von Wintzingerode, F., Gobel, U. B., and Stackebrandt, E. (1997). Determination of microbial diversity in environmental samples: pitfalls of PCR-based rRNA analysis. *FEMS Microbiol. Rev.* 21, 213–229. doi: 10.1111/j.1574-6976.1997.tb00351.x

Wang, G. C. Y., and Wang, Y. (1996). The frequency of chimeric molecules as a consequence of PCR co amplification of 16S rRNA genes from different bacterial species. *Microbiology* 142, 1107–1114. doi: 10.1099/13500872-142-5-1107

Weinstock, G. M. (2012). Genomic approaches to studying the human microbiota. *Nature* 489, 250–256. doi: 10.1038/nature11553

Yu, G., Fadrosh, D., Goedert, J. J., Ravel, J., and Goldstein, A. M. (2015). Nested PCR Biases in interpreting microbial community structure in 16S rRNA gene sequence datasets. *PLoS ONE* 10:e0132253. doi: 10.1371/journal.pone.0132253

Zheng, D., Alm, E. W., Stahl, D. A., and Raskin, L. (1996). Characterization of universal small-subunit rRNA hybridization probes for quantitative molecular microbial ecology studies. *Appl. Environ. Microbiol.* 62, 4504–4513.

Conflict of Interest Statement: The authors declare that the research was conducted in the absence of any commercial or financial relationships that could be construed as a potential conflict of interest.

Copyright © 2017 Young, Smith, Embleton, Berrington, Schwalbe, Cummings, van der Gast and Lanyon. This is an open-access article distributed under the terms of the Creative Commons Attribution License (CC BY). The use, distribution or reproduction in other forums is permitted, provided the original author(s) or licensor are credited and that the original publication in this journal is cited, in accordance with accepted academic practice. No use, distribution or reproduction is permitted which does not comply with these terms.

frontiers in Cellular and Infection Microbiology

ORIGINAL RESEARCH
published: 24 April 2017
doi: 10.3389/fcimb.2017.00134

The NAG Sensor NagC Regulates LEE Gene Expression and Contributes to Gut Colonization by *Escherichia coli* O157:H7

Guillaume Le Bihan[1], Jean-Félix Sicard[1], Philippe Garneau[1], Annick Bernalier-Donadille[2], Alain P. Gobert[2], Annie Garrivier[2], Christine Martin[2], Anthony G. Hay[3], Francis Beaudry[4], Josée Harel[1] and Grégory Jubelin[2]**

[1] Faculté de Médecine Vétérinaire, Centre de Recherche en Infectiologie Porcine et Aviaire, Université de Montréal, Saint-Hyacinthe, QC, Canada, [2] INRA, Université Clermont Auvergne, MEDIS, Clermont-Ferrand, France, [3] Department of Microbiology, Cornell University, Ithaca, NY, USA, [4] Groupe de Recherche en Pharmacologie Animal du Québec, Département de Biomédecine Vétérinaire, Faculté de Médecine Vétérinaire, Université de Montréal, Saint-Hyacinthe, QC, Canada

Enterohemorrhagic *Escherichia coli* (EHEC) O157:H7 are human pathogens responsible for bloody diarrhea and renal failures. EHEC employ a type 3 secretion system to attach directly to the human colonic epithelium. This structure is encoded by the locus of enterocyte effacement (LEE) whose expression is regulated in response to specific nutrients. In this study, we show that the mucin-derived sugars N-acetylglucosamine (NAG) and N-acetylneuraminic acid (NANA) inhibit EHEC adhesion to epithelial cells through down-regulation of LEE expression. The effect of NAG and NANA is dependent on NagC, a transcriptional repressor of the NAG catabolism in *E. coli*. We show that NagC is an activator of the LEE1 operon and a critical regulator for the colonization of mice intestine by EHEC. Finally, we demonstrate that NAG and NANA as well as the metabolic activity of *Bacteroides thetaiotaomicron* affect the *in vivo* fitness of EHEC in a NagC-dependent manner. This study highlights the role of NagC in coordinating metabolism and LEE expression in EHEC and in promoting EHEC colonization *in vivo*.

Keywords: NagC, LEE, EHEC, N-acetylglucosamine (or eventually NAG), N-acetylneuraminic acid (or eventually NANA)

OPEN ACCESS

Edited by:
Pascale Alard, University of Louisville, USA

Reviewed by:
Fernando Navarro-Garcia, Center for Advanced Research, The National Polytechnic Institute, Cinvestav-IPN, Mexico
Mauricio J. Farfan, Universidad de Chile, Chile

***Correspondence:**
Josée Harel
josee.harel@umontreal.ca
Grégory Jubelin
gregory.jubelin@inra.fr

Received: *27 January 2017*
Accepted: *31 March 2017*
Published: *24 April 2017*

Citation:
Le Bihan G, Sicard J-F, Garneau P, Bernalier-Donadille A, Gobert AP, Garrivier A, Martin C, Hay AG, Beaudry F, Harel J and Jubelin G (2017) The NAG Sensor NagC Regulates LEE Gene Expression and Contributes to Gut Colonization by Escherichia coli O157:H7. Front. Cell. Infect. Microbiol. 7:134. doi: 10.3389/fcimb.2017.00134

INTRODUCTION

Escherichia coli O157:H7 are human foodborne pathogens responsible for outbreaks mostly in developed countries. Infections by EHEC occur following ingestion of contaminated food and provoke symptoms ranging from watery or bloody diarrhea to hemolytic and uremic syndrome (HUS). A range of virulence factors are involved in EHEC O157:H7 pathogenicity including the Shiga-toxin which is associated with development of HUS, and the T3SS which enables the pathogen to attach to the intestinal epithelium and cause diarrhea (Kaper et al., 2004).

T3SS-encoding genes are gathered into the locus of enterocyte effacement (LEE) that is composed of five operons (LEE1 to LEE5) which encode for structural proteins, regulators, chaperones and effectors that are secreted into the host cells (Kaper et al., 2004). The first gene of the LEE, *ler*, encodes an activator that regulates the five major LEE operons. Expression of

ler is controlled by several regulators in response to intestinal metabolites, such as bacterial waste products (Nakanishi et al., 2009), quorum-sensing molecules (Sircili et al., 2004), hormones (Walters and Sperandio, 2006), biotin (Yang et al., 2015), fucose (Pacheco et al., 2012), and ethanolamine (Kendall et al., 2012).

During its infectious cycle, EHEC O157:H7 encounters a large amount of mucin-derived sugars (Fabich et al., 2008; Bertin et al., 2013). Mucin is part of the mucous layer covering the intestinal epithelium and is heavily O-glycosylated. The mucous layer is a physical barrier that limits contact between bacteria and host epithelial cells (McGuckin et al., 2011). By producing specific glycosidases, several species of the gut microbiota release sugars from O-glycans into the intestinal lumen (Bertin et al., 2013; Ng et al., 2013; Elhenawy et al., 2014). Released mucin sugars, including N-acetylglucosamine (NAG), N-acetylneuraminic acid (NANA), galactose, fucose, mannose and N-acetylgalactosamine, represent an important reservoir of nutrients that promotes the growth of commensal and pathogenic bacteria including *E. coli* (Fabich et al., 2008; Bertin et al., 2013; Conway and Cohen, 2015). *Escherichia coli* and more particularly EHEC O157:H7 are able to concomitantly metabolize *in vitro* up to nine mucin sugars at a time, and preferentially use NAG and galactose (Fabich et al., 2008; Bertin et al., 2013; Conway and Cohen, 2015).

Genes involved in the catabolism of sugars are often regulated by proteins responding to the presence of their cognate sugar. For example, the regulator NagC, known as a repressor of NAG and galactose catabolism, is a NAG-6 phosphate (NAG-6P) sensing protein, NAG-6P being produced during the catabolism of NAG and NANA (Plumbridge, 1991; El Qaidi et al., 2009). When NAG-6P concentrations are low, NagC acts as a DNA binding protein, an activity that is lost with high intracellular NAG-6P concentration (Plumbridge and Kolb, 1991; Sohanpal et al., 2004). In addition to the role they play as nutrients, some mucin sugars can act as regulatory signals that influence bacterial colonization and adherence to cells (Sohanpal et al., 2004; Barnhart et al., 2006; Pacheco et al., 2012).

Previously, we have shown that EHEC O157:H7 respond to the metabolic activity of the human gut microbiota by activating the expression of genes required for NANA utilization and by down-regulating the expression of the LEE genes (Le Bihan et al., 2015). In this study, the effect of NANA and NAG on the adhesion phenotype of EHEC O157:H7 was examined. We found that NANA and NAG are inhibitors of EHEC O157:H7 adhesion to epithelial cells. We demonstrated that NANA and NAG reduce the expression of the five LEE operons in a NagC-dependent way. Mutation in *nagC* diminished the expression of LEE genes. In addition, NagC was shown to bind directly to the LEE1 promoter region, thereby could influence expression of *ler* gene, which encodes the LEE master regulator. We also show that NagC promotes EHEC colonization of mouse intestine. Further, we demonstrate that exogenous addition of NAG into the intestine or gavage with the mucin degrading commensal *Bacteroides thetaiotaomicron* modulates the fitness of EHEC *in vivo* in a NagC-dependent manner. Taken together, our data indicate that NagC coordinates the catabolism of mucus-derived sugars and T3SS production, and promotes EHEC intestinal colonization.

MATERIALS AND METHODS

Bacteria, Mutagenesis, and Growth Conditions

Strains and plasmids are listed in Table EV1. The EHEC O157:H7 strain EDL933 (O'Brien et al., 1983) was used in this study. *B. thetaiotamicron* strain VPI-5482 was grown anaerobically at 37°C in a complex medium containing clarified rumen fluid (Leedle and Hespell, 1980). The medium was prepared, dispensed and inoculated by using strictly anaerobic techniques in Balch tubes. The EDL933 Δ*nagC* and Δ*nanR* mutants were generated by allelic exchange using a suicide vector as described in EV Methods. When required, the growth medium was supplemented with kanamycin (25 mg/ml), ampicillin (50 mg/ml), NANA (0.1 mM or 1 mM), or NAG (0.1 mM or 1 mM) (Sigma Aldrich).

Beta-Galactosidase Assays

The entire intergenic region between *ler* (LEE1) and *espG* (bp −1,225 to +19) containing two *ler* promoters (Sperandio et al., 2002; Porter et al., 2005) was inserted upstream of *lacZ* in pRS551 (see EV Methods). The resulting plasmid pGLB was introduced into EDL933 or its isogenic mutants. After growth in DMEM with or without NANA or NAG until OD_{600} of 0.6, β-galactosidase assays were performed as described previously (Miller, 1972). Student *t*-tests were performed to determine statistical significance.

Quantitative Real Time PCR (qRT-PCR)

Bacteria were harvested at OD_{600} of 0.6 and RNA was extracted as previously described (Le Bihan et al., 2015). cDNAs were synthesized from 10 μg RNA using reverse transcriptase. The concentration of cDNA samples was then adjusted to 25 ng/μL. A standard curve was performed for genes of interest to determine the copy number of targeted transcripts in 50 ng of cDNA. Primers used in this study are listed in Table EV2. Results are presented as the ratios between the cDNA copy number of the gene of interest and the cDNA copy number of the housekeeping gene. Student *t*-tests were performed to calculate *p*-values.

Western Blotting

Western blot analyses were performed with slight modifications to those previously described (Chekabab et al., 2014). Culture supernatants (8 ml) were harvested and supplemented with 1 μg Bovine Serum Albumin (BSA). Proteins were precipitated overnight at 4°C using 10% trichloroacetic acid and sodium deoxycholate, pelleted by centrifugation, washed with acetone, resuspended in SDS sample buffer and boiled. Proteins were then run on 14% SDS-PAGE gels and transferred to nitrocellulose membranes. Protein transfer including BSA was assessed using Ponceau S dye. The EspB protein was revealed using a rabbit EspB specific polyclonal antiserum (1:2,000) and a goat anti-rabbit HRP-linked secondary antibody (Bio-Rad Laboratories, Hercules, CA).

Cell Culture and Bacterial Infections

Epithelial cell lines HeLa, HCT-8, and HCT-116 were maintained in MEM with 10% FBS, 100 U/mL penicillin and 100 mg/mL

streptomycin at 37°C under 5% CO_2(Branchu et al., 2014). Cells were seeded into 6-well plates (5×10^5 cells/well) and grown for 24 h without antibiotics. Bacteria were pre-grown in DMEM in the presence or absence of NANA or NAG before the infection assays. Cells were then washed and infected with bacteria with an MOI of 10 for 90 min, in the presence or absence of NANA or NAG. Following infection, cells were washed 3 times with DPBS, trypsinized for 5 min at 37°C, pelleted by a low-speed centrifugation (100 *g*; 3 min). The pellet was washed once to ensure the plating of adherent bacteria only. Results are presented as the percentage of adherent bacteria as compared to the wild-type strain incubated without NANA or NAG. The EDL933 Δ*escN* strain that does not produce the T3SS (Deng et al., 2004) was used as a negative control. Student *t*-tests were performed to determine the significance.

Electrophoretic Mobility Shift Assays (EMSA)

The EMSA was adapted from previous report (Chekabab et al., 2014). The EMSA reaction mix consisted of purified NagC at the desired concentration (0.5–2.5 μM), 50 nM of 5′ 6-FAM labeled pLEE1 probe, 0.1 mg/mL calf thymus DNA and 0.1 mg/mL BSA in EMSA buffer (50 mM NaCl, 20 mM Tris, pH 7.4, 0.02% v/v sodium azide). Reactions were incubated for 30 min at 25°C, and then loaded onto a 12% native polyacrylamide gel running at 120 V in 1x TBE buffer. The forward primer contained a 5′ 6-FAM fluorescein tag. Competitive EMSA assay was done with 50 nM of 6-FAM labeled pLEE1 probe and unlabeled probes corresponding to P_{LEE1}, P_{kan} (negative control) or $P_{nagB-nagE}$ (positive control). The ratio "cold probe/labeled probe" was 10/1.

DNAse Footprinting

DNase I footprinting of free DNA and DNA–protein complexes was performed as described (El Qaidi et al., 2009; Graveline et al., 2011). The DNA fragment corresponding to the *ler* regulatory region (259 bp) was amplified using primers listed in Table EV2, alternately end labeled with ^{32}P (140,000 cpm, 0.6 nM). Each end-labeled amplicon was subsequently incubated in a total volume of 80 μl in binding buffer (25 mM Hepes (pH 8.0), 100 mM K glutamate (pH 8.0), 0.5 mg/ml BSA). After incubation with purified NagC for 10 min at room temperature, 2 μl of DNase I (1.3 U/ml; New England BioLabs) containing 5 mM $CaCl_2$ and 25 mM $MgCl_2$ was added for 5 min. The reaction was stopped by the addition of 150 μL of phenol/chloroform/isoamyl alcohol and 350 μl of stop buffer (0.5 M Na acetate pH 5.0, 2.5 mM EDTA, 10 μg/ml Salmon sperm DNA) to each sample. DNA fragments were precipitated in ethanol, and amounts with equivalent cpm (5.10^4) from each reaction were loaded onto 6% polyacrylamide–7 M urea gels. Maxam-Gilbert A+G reactions were carried out on the appropriate 32 P-labeled DNA fragments, and the products loaded alongside the DNase I footprinting reaction mixtures. The gels were dried and analyzed by autoradiography. A control footprinting experiment realized with *nagE-nagB* regulatory region and with NagC (Figure EV5).

Mice Infection

BALB/c mice were purchased from Janvier Labs (Le-Genest-St-Isle, France). Sets of 5 mice aged 5 weeks were given drinking water containing streptomycin sulfate (5 g/l) throughout the experiment. On day 1 following the addition of streptomycin, each mouse was infected intragastrically with 100 μl of a mix containing 10^7 each of EDL933 Sm^R and EDL933 Sm^R Δ*nagC* strains. Mice treated with *B. thetaiotaomicron* were gavaged daily with 5×10^9 cells of *B. thetaiotaomicron* strain VPI-5482, starting from day 1 before EHEC infection to day 7. At indicated time points, fecal or tissue samples were collected, homogenized in PBS and subsequently diluted before plating on LB-streptomycin agar plates and LB-streptomycin-kanamycin agar plates. Output ratios were calculated for each time point and competitive indices were obtained by dividing the output ratio by the input ratio. A One-way ANOVA was performed to determine the significance. For NANA and NAG quantification in intestinal contents, see EV Methods.

Ethics Statement

All animal experiments were reviewed and approved by the Auvergne Committee for Animal Experimentation (C2E2A). All procedures were carried out according to the European directives for the protection of animals used for scientific purposes, 2010/63/EU, and to the guidelines of the local ethics committee.

RESULTS

NANA and NAG Inhibit EHEC O157:H7 Adhesion to Epithelial Cells by Repressing LEE Genes

The effect of NANA and NAG on EHEC adhesion was examined by measuring the ability of the EHEC O157:H7 EDL933 strain to adhere to cultured epithelial cells in the presence or absence of NANA or NAG. Our data showed that EDL933 adhesion to HeLa cells was significantly decreased by 40 ± 21 or 23 ± 11% in presence of 1 mM NAG or NANA, respectively (**Figure 1A**; Figure EV1). At 0.1 mM, only NAG significantly decreased the number of cell-attached bacteria (53 ± 22%).

The adhesion of EHEC O157:H7 to HeLa cells is mainly driven by the production of a T3SS, as previously demonstrated (Branchu et al., 2014) and as verified using the Δ*escN* strain which is defective in the production of the T3SS (Figure EV1). Thus, we investigated the effect of NANA and NAG on LEE gene expression. As a first step, strain EDL933 carrying a P_{LEE1}:*lacZ* fusion was cultured in the presence of different concentrations of the sugars. The expression of LEE1 was significantly repressed in the presence of either 1 mM NANA or 0.1 and 1 mM NAG (**Figure 1B**), but not at 0.01 mM of either sugar. Next, we examined the expression of genes from the five LEE operons and observed that expression of *ler* (LEE1), *sepZ* (LEE2), *escV* (LEE3), *espB* (LEE4), *tir*, and *eae* (LEE5) was significantly lower in presence of 1 mM NANA or NAG (**Figure 1C**). Consistent with the decreased expression of the LEE4 gene, the secretion of the effector EspB, encoded by the LEE4, was dose dependently reduced when EDL933 was incubated with 0.1 and 1 mM of

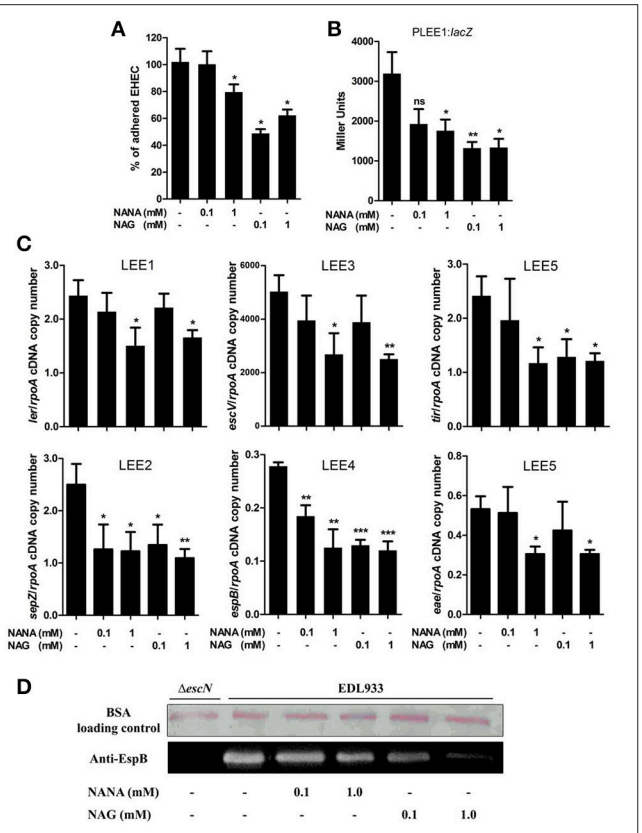

FIGURE 1 | NANA and NAG regulate EDL933 adhesion and LEE expression. (A) HeLa cells were co-incubated with EDL933 in DMEM with or without NANA or NAG for 90 min. Bacteria adhered to HeLa cells were harvested and counted on agar plates. Results are presented as the percentage of adhesion as compared to the wild type strain incubated without NANA or NAG. **(B)** β-galactosidase assays using the P_{LEE1}:*lacZ* transcriptional fusion integrated into EDL933. EDL933 was grown in DMEM with or without NANA or NAG 0.1 or 1 mM and cells were harvested at OD_{600} = 0.6. Results are presented as Miller Units. **(C)** qRT-PCR measurement of LEE gene expression in DMEM with or without NANA or NAG. Results are shown as the ratio copy number of the LEE transcripts/copy number of *rpoA* transcripts. **(D)** Western blot analysis of the EspB secretion by EDL933 grown in DMEM with or without NANA or NAG. BSA was used as a loading control. $n \geq 3$, ns for non-significant, $^{*}p < 0.05$, $^{**}p < 0.01$, and $^{***}p < 0.001$.

either sugar (**Figure 1D**). Taken together, these data indicate that NANA and NAG inhibit the adhesion of EDL933 to epithelial cells and repress T3SS encoding genes. In addition no significant difference was observed upon addition of other mucin sugars, such as mannose, galactose, N-acetylgalactosamine and glucuronate on the expression of *ler* (Figure EV2).

Repression of LEE Gene Transcription by NANA and NAG Is NagC-Dependent

Activation of the metabolic pathways required for the catabolism of NANA and NAG influence the activity of two transcriptional regulators, NanR and NagC (**Figure 2A**). Intracellular NANA inactivates NanR while NAG-6P derived from the catabolic conversion of both NANA and NAG inactivates NagC. To evaluate the role of NanR and NagC on LEE1 promoter activity, the P_{LEE1}:*lacZ* fusion was introduced into Δ*nanR* and Δ*nagC* mutants. The *nagC* deletion led to a significant decrease of the activity of P_{LEE1} whereas the deletion of *nanR* had no significant effect (**Figure 2B**). Moreover, the addition of NANA or NAG still repressed the activity of P_{LEE1} in the Δ*nanR* mutant whereas it did not in the Δ*nagC* mutant. These results indicate that LEE1 repression by NANA and NAG was NagC-dependent but NanR-independent. We further demonstrated that a *nagC* deletion also impairs the expression of *escV*, *sepZ*, *espB*, *tir,* and *eae* genes with a fold change ranging from −2.9 to −5.5 (**Figure 2C**), as well as secretion of EspB (**Figure 2D**). Consequently, the Δ*nagC* mutant adhered less to epithelial cells, using HeLa and the two human intestinal cell lines HCT-8 and HCT-116 (**Figure 2E**; Figures EV1, EV3). Importantly, LEE gene expression, EspB secretion and adhesion levels were restored to a wild-type status in a Δ*nagC*-complemented strain. Additionally, we assessed the potential involvement of NagC in the transcription of other genes encoding adhesins in EDL933. Neither *fliC* (flagellin), *ycbQ* (fimbriae) (Samadder et al., 2009), *hcpA* (hemorrhagic coli pilus), *espP* (autotransporter), *lpfA* (long polar fimbriae), *csgA* (curli) nor *pgaB* (poly-β-1,6-N-acetyl-D-glucosamine) were differentially expressed between wild type and Δ*nagC* strains (Supplementary Figure EV4). Since NagC does not affect the synthesis of these adhesins, it suggests that the defect in cell adhesion observed with the *nagC* mutant is mainly driven by a reduced production of the T3SS.

NagC Interacts with LEE1 Promoter Region *In vitro*

Using a NagC consensus DNA binding site generated from seven NagC binding sequences, we identified a single putative NagC binding site in the LEE1 promoter region (5′-GTATTTTACACATTAGAAAAAAG-3′) located at a position that overlaps the −10 box of the distal promoter (**Figure 3A**). The binding of NagC to the LEE1 promoter was first investigated by EMSA that showed that NagC forms a specific low-mobility complex with the LEE1 promoter as previously observed with NagC interacting with type 1 fimbriae *fim* intergenic region upstream of the *fimB* promoter (Sohanpal et al., 2004). Competition EMSA using an unrelated probe (P_{kan}) demonstrated that NagC binding to the LEE1 promoter is specific (**Figure 3B**). Further, DNase footprinting experiments confirmed that NagC bound to the predicted NagC binding site (**Figure 3C**). Consistent with the expected specificity, a single base substitution at position 18 of the putative NagC binding site prevented DNAse protection by NagC (**Figure 3D**). An additional DNase footprinting control experiment using *nagBE* intergenic region as expected showed clear protection zones indicating the functional activity of NagC (Figure EV5). These findings demonstrate that NagC interacts with the LEE1 promoter region in a sequence specific manner. Interestingly, the NagC-binding sequence in the promoter of *ler* is conserved among other EHEC O157:H7 strains and this is correlated with ler repression in the presence of 1 mM of NAG (Figure EV6). EHEC, EPEC,

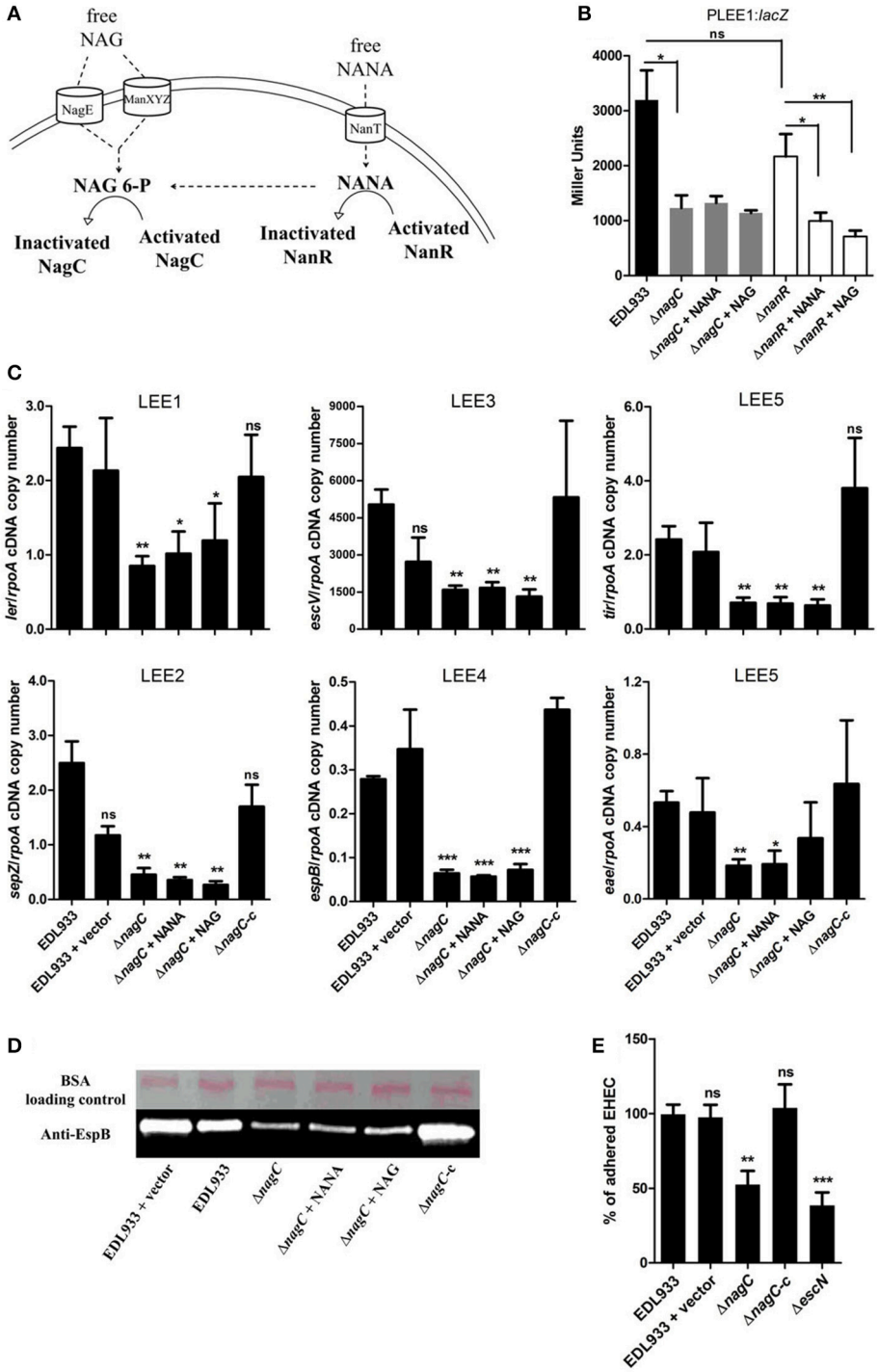

FIGURE 2 | NagC is a transcriptional activator of the LEE genes. (A) Schematic representation of the influence of NANA and NAG on the activity of the transcriptional regulators NagC and NanR. **(B)** β-galactosidase assays using the P_{LEE1}*:lacZ* transcriptional fusion integrated into EDL933 or the isogenic mutants Δ*nagC* and Δ*nanR*. The strains were grown in DMEM with or without NANA or NAG at 1 mM and harvested at $OD_{600} = 0.6$. Results are presented as Miller Units. **(C)** qRT-PCR measurement of LEE gene expression. EDL933, the isogenic mutant Δ*nagC* and the complemented strain Δ*nagC*-c were grown in DMEM with or without NANA or NAG at 1 mM. Results are shown as the ratio copy number of the LEE transcripts/copy number of *rpoA* transcripts. **(D)** Western blot analysis of the EspB secretion by EDL933, the isogenic mutant Δ*nagC* and the complement grown in DMEM with or without NANA or NAG at 1 mM. BSA was used as a loading control. **(E)** HeLa cells were co-incubated for 90 min with either the wild type EDL933 strain, Δ*nagC* mutant, the Δ*nagC* complemented strain or the Δ*escN* mutant. Adhered bacteria were harvested and counted on agar plates. Results are presented as the percentage of adhered cells compared to the wild type strain EDL933. $n \geq 3$, ns for non-significant, $^{*}p < 0.05$, $^{**}p < 0.01$, and $^{***}p < 0.001$.

or *C. rodentium* strains with degenerated NagC binding site in the LEE1 promoter region were insensitive to NAG exposure.

Mucin-Derived Sugars Sensing by NagC Is Important for Successful Colonization in Mice

To assess if NagC regulates the gut colonization process, we co-infected mice with an equal mixture of wild-type EDL933 and the Δ*nagC* mutant and followed the outcome of each strain overtime. We observed a marked increase in the wild-type strain over the Δ*nagC* mutant in the feces at days 6 and 8 post-infection (competitive index (CI) of 13 ± 5 and 20 ± 6, respectively), as well as in the cecal content at day 8 (CI of 270 ± 76) (**Figures 4A,B**). The competitive advantage of the wild-type strain was also recorded for bacteria adhering to cecal and colonic mucosa (Figure EV7). These data demonstrate that the deletion of *nagC* greatly impaired the ability of EDL933 to colonize the intestinal tract of mice.

We next sought to determine if the concentrations of NANA and NAG may alter EDL933 fitness *in vivo* through the modulation of NagC activity. For that, the drinking water of WT/Δ*nagC*-infected mice was supplemented with purified NANA or NAG. Supplementation led to increased sugar concentrations in the cecal content of uninfected mice but not in the cecal content of infected mice (**Figure 4C**). Interestingly, NANA and NAG concentrations also significantly decreased in supplemented mice upon infection, with fold-change of 4.9- and 1.9, respectively, suggesting that EDL933 consumes NANA and NAG in the intestine of mice. In these conditions, NAG supplementation significantly decreased the competitive advantage of the wild-type strain over the Δ*nagC* mutant by a factor 7.1 (**Figure 4B**). Co-infected mice were also subjected to a daily gavage with *B. thetaiotaomicron* to see if the behavior of EHEC is modulated by the population level of a mucin degrading bacterium. Gavage of mice did not change NANA concentration in the gut of infected mice but led to a 1.9-fold increase of NAG concentration (**Figure 5**). Importantly, we observed that the competitive index between the wild-type strain and the Δ*nagC* mutant significantly dropped from 297 in control mice to 54 in *B. thetaiotaomicron*–treated animals (**Figure 5**). Overall, our findings indicate that NAG concentration in the intestine, derived notably from activity of mucin degrading commensals, such as *B. thetaiotaomicron*, affects the fitness of EHEC *in vivo* in a NagC-dependent manner.

DISCUSSION

This work demonstrates that the host mucin-derived sugars NAG and NANA inhibit the expression level of LEE genes in EHEC O157:H7 strain EDL933 and, consequently, inhibit the ability of the pathogen to adhere to epithelial cells *in vitro*. NAG and NANA are known to be used as carbon sources by commensal *E. coli* and EHEC O157:H7 in the gut (Fabich et al., 2008; Bertin et al., 2013, 2014; Conway and Cohen, 2015). Their catabolism induces transcriptional responses mediated by NanR and/or NagC regulatory proteins with NanR controlling NANA catabolism and NagC controlling both NAG and galactose catabolism (Plumbridge, 1991; El Qaidi et al., 2009). The role of NagC as a repressor of the expression of *nagE*, *nagB* and *galP* encoding the NAG PTS permease, the glucosamine-6-P deaminase, and the major galactose transporter respectively, was confirmed in EDL933 (Figure EV8). We also demonstrated that NagC controls the expression level of LEE genes in EDL933 through a direct activation of LEE1 gene transcription. NagC has been shown to modulate the expression of distinct adhesins in other *E. coli* strains. Indeed, NagC, together with NanR, activates the expression of *fimB* encoding for a recombinase required for the expression of the type I fimbriae in K-12 strain MG1655 (McClain et al., 1991; Sohanpal et al., 2004). This is not the case in EDL933 since this strain does not produce type 1 fimbriae due to a 16-bp deletion in the regulatory switch region of *fimA* (Vogeleer et al., 2015). While we observed no change in EDL933, a deletion of *nagC* has been shown to decrease expression of *csgAB* and *csgDEFG* genes and curli production in strain C600, though the mechanism remains unknown (Barnhart et al., 2006). Overall these observations suggest that NagC has served a common role as a regulator of adhesin expression during the evolution of several *E. coli* strains.

Most operons known to be controlled by NagC require two sites for NagC to function (*nagE-B, chb, glmU, fimB*) so that cooperative binding to two sites through DNA looping is necessary for regulation (Plumbridge, 1996; Sohanpal et al., 2004; El Qaidi et al., 2009; Brechemier-Baey et al., 2015). However, like the *galP* promoter, another target of NagC (El Qaidi et al., 2009), only one potential NagC operator is found in LEE1 promoter region of EHEC strain EDL933. Interestingly, this NagC sequence was conserved in other O157:H7 strains but not in other LEE encoding pathogens, such as EPEC E2348/69 or *C. rodentium* ICC168. Yet it is not clear how NagC activates the LEE1 promoter. As proposed by authors working on *fimB* and *galP*, NagC could contact RNA polymerase directly (or another regulatory protein bound closer to the LEE1 promoter region) to enhance transcription activation, or that the nucleoprotein complex that includes NagC and other regulators alters the DNA structure nearer the promoter in such a way as to facilitate transcription initiation (Sohanpal et al., 2004, 2007; El Qaidi and Plumbridge, 2008; El Qaidi et al., 2009).

By regulating genes involved in sugar catabolism and genes involved in T3SS production, NagC is likely to influence the behavior of EHEC during an infection. Indeed, we demonstrated by co-infection experiments that deletion of *nagC* strongly affect the fitness of EHEC in the digestive tract of infected mice. Moreover, the addition of NAG in the drinking water of infected mice reduced the competitive advantage of the wild type strain over the Δ*nagC* mutant. This suggests that intestinal concentration of NAG modulates NagC activation and therefore expression level of NagC-dependent genes, affecting the fitness of EHEC *in vivo*. In the gut, some commensal species expressing mucinolytic enzymes can degrade mucins from the outer layer of mucus and release free carbohydrates into the intestinal lumen (Xu et al., 2003; Elhenawy et al., 2014; Tailford et al., 2015). These sugars can then be consumed by members of the gut

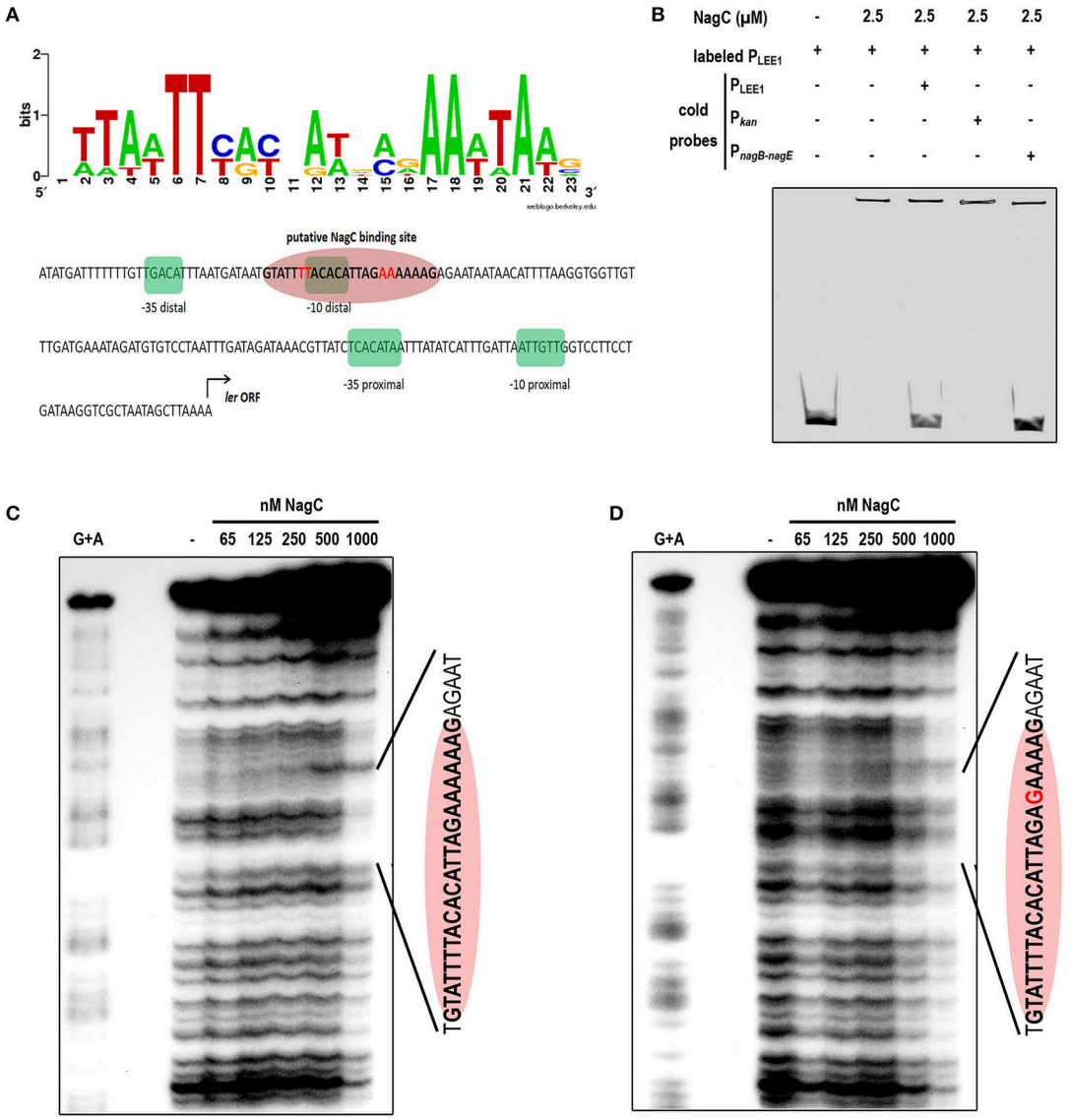

FIGURE 3 | NagC binds *in vitro* to the promoter of LEE1. (A) Predicted binding site generated by Weblogo from seven known NagC binding sequences and schematic representation of the regulatory region of LEE1. The −35 and −10 boxes of the proximal and the distal promoters are highlighted in green and the putative NagC binding site in red. **(B)** Competitive EMSA assays were performed using purified NagC (2.5 μM) and a 6-FAM labeled P_{LEE1} probe (50 nM) and unlabeled probes corresponding to P_{LEE1}, P_{kan} (negative control) or $P_{nagB-nagE}$ (positive control). **(C)** Footprinting experiment was performed with end-labeled PCR product of the native LEE1 regulatory region and purified NagC. The DNA sequence of the protected region is indicated and includes the NagC putative binding sequence (red ellipse). **(D)** Footprinting experiment was performed with end-labeled PCR product of the mutated LEE1 regulatory region. The base substitution (A → G) is indicated in red.

microbiota (Derrien et al., 2010). By affecting the concentration of free NAG and NANA available in the digestive tract, gut bacterial species expressing sialidase or N-acetylglucosaminidase might therefore affect the fitness of EHEC through a modulation of NagC activity. Indeed, we showed that the metabolic activity of the mucin degrader *B. thetaiotaomicron* when gavaged to co-infected mice increased the concentration of NAG and reduced the competitive advantage of the wild-type strain over the *nagC* mutant. To our knowledge, no information is available on NAG and NANA concentration in human intestine. However, its concentration probably fluctuates within the gastrointestinal tract since there is high variations in terms of (i) abundance and types of mucins; (ii) patterns of O-glycosylation and (iii) bioavailability of carbohydrates (free or mucin-linked forms). In **Figures 4**, **5**, the concentration of NANA and NAG in the cecal content of uninfected mouse was 0.27 mM (500 nmol/g) and 0.12 mM (225 nmol/g), respectively. In another study, NANA and NAG were quantified in the bovine small intestine content to be 0.1 and 0.45 mM (Bertin et al., 2013). Altogether, it gives information on physiological NAG and NANA concentrations in

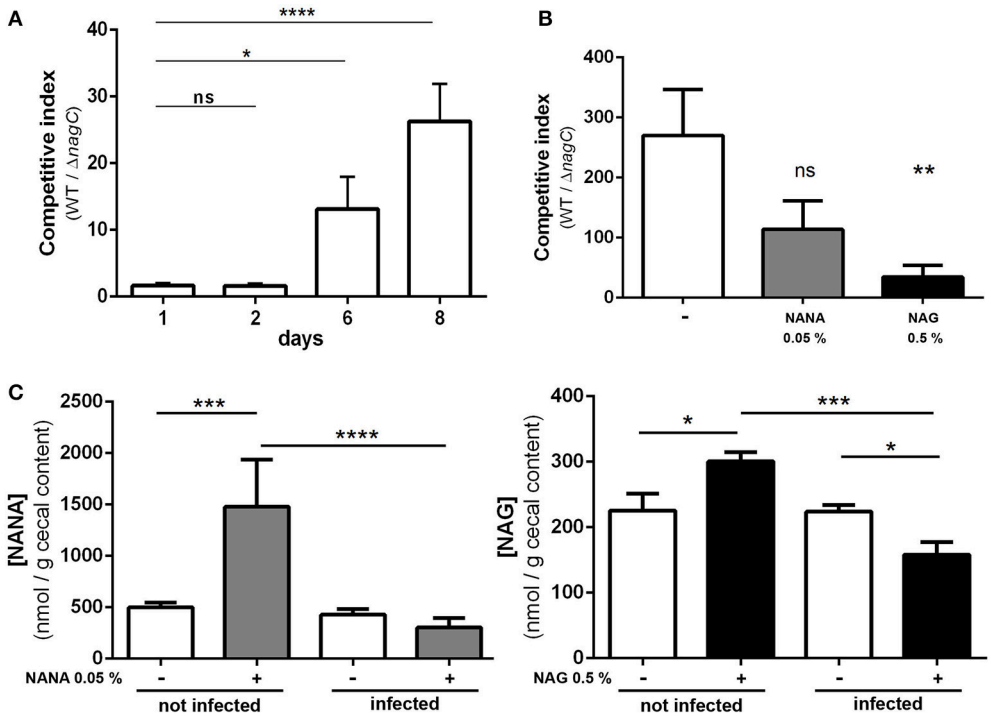

FIGURE 4 | The Δ*nagC* mutant is outcompeted by the wild type strain during mice infection. Streptomycin-treated BALBc mice were infected with a 1:1 mixture of wild type and Δ*nagC* EDL933 strains. **(A)** Wild type and Δ*nagC* strains were numerated from feces and competitive indices WT/Δ*nagC* were calculated at indicated time points. **(B)** Competitive indices WT/Δ*nagC* obtained at day 8 in the cecal contents of mice provided with water with or without NANA 0.05% or NAG 0.5%. **(C)** Concentration of NANA and NAG in the cecal contents of non-infected mice or EHEC-infected mice provided with or without either NANA 0.05% or NAG 0.5%. $^{*}p < 0.05$, $^{**}p < 0.01$, $^{***}p < 0.001$, and $^{****}p < 0.0001$.

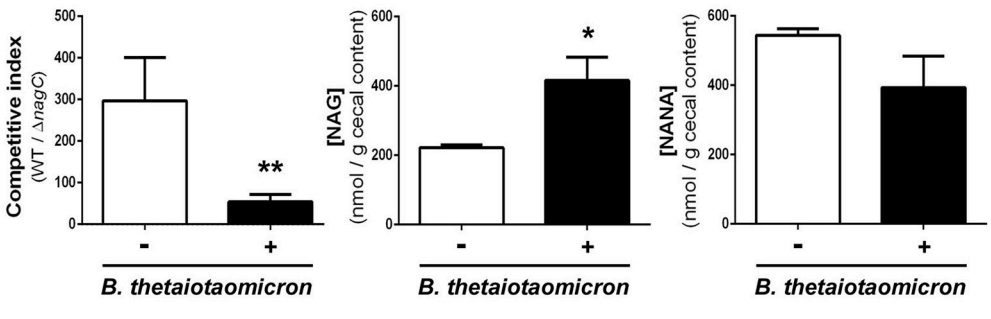

FIGURE 5 | *Bacteroides thetaiotaomicron* influences the outcome of wild type and Δ*nagC* strains in co-infected mice. Streptomycin-treated BALBc were infected with a 1:1 mixture of wild type and Δ*nagC* EDL933 strains. Mice were gavaged or not daily with 5×10^9 *B. thetaiotaomicron* cells starting 1 day before EHEC infection. Competitive indices WT/Δ*nagC* and concentrations of NAG and NANA obtained at day 8 post-infection in the cecal contents of mice treated or not with *B. thetaiotaomicron* are shown. $^{*}p < 0.05$ and $^{**}p < 0.01$.

digestive tracts and indicates that concentrations used in our *in vitro* studies were relevant.

If we determined that NagC is essential for the fitness of EHEC in the digestive tract of mice, we have no information about the NagC-regulated genes involved in fitness alteration. Fabich et al. demonstrated that a mutation in gene *nagE* encoding the NAG transporter, causes a colonization defect for EDL933 in infected mice, indicating that NAG is utilized by the pathogen in the digestive tract of mice. In contrast, a mutation in *nanAT* where *nanT* encodes the NANA transporter, has no impact on colonization efficiency (Fabich et al., 2008), indicating that NANA catabolism is not essential for a good colonization of mice gut. In contrast to *nagE* and *nanAT* mutants that are unable to internalize NAG and NANA respectively, *nagC* mutant is still able to uptake and catabolize both sugars since gene deletion leads to an upregulation of *nagE* and *nagBACD* gene expression (Figure EV8). In addition to sugar catabolism and T3SS related genes, NagC also probably controls the expression of other genes in EHEC, that might be involved in EHEC fitness. One example is the gene z2210 (Figure EV9), which encodes a putative sulfatase

that might be involved in mucus degradation since secreted mucins are heavily sulfated (Nieuw Amerongen et al., 1998). NagC of *Vibrio fischeri* was shown to facilitate colonization of the light organ of the squid Euprymna scolopes (Miyashiro et al., 2011). Sun Y et al. proposed that in *V. fischeri* NagC ability to regulate gene expression contributes to its overall fitness in environments that vary in levels of GlcNAc (Sun et al., 2015).

In many pathogens, relationship between metabolism and virulence has been determined (Wilharm and Heider, 2014). We propose that NagC is part of the regulatory circuit controlling the infectious process of EHEC by coordinating mucin-derived sugar metabolism and T3SS production (Figure EV10). At the level of the colonic intestine within the mucus there is a gradient of NANA and NAG due to their release from the intestinal mucin by mucinolytic bacteria, such as *B. thetaiotaomicron* (Derrien et al., 2010). When the concentration of NANA and/or NAG is high, their catabolism by *E. coli* O157:H7 produces high amount of intracellular NAG-6P which inactivates the transcriptional regulator NagC. In such case, the expression of NAG catabolic genes is induced while that of the LEE genes is reduced and thus adherence is prevented. This suggestion is supported by our observation that expression of LEE operons decreased after EDL933 growth in cecal content of gnotobiotic rats inoculated with human cecal content (Le Bihan et al., 2015). In reaching deeper mucus layer toward the intestinal epithelium, NANA and NAG are less found as free forms in the inner layer of mucus but are rather complexed to mucins (Derrien et al., 2010). In consequence, the amount of intracellular NAG-6P is low and the protein NagC is active allowing the repression of *nagB*, *nagE* and *galP* and activation of the LEE genes and thus adherence is promoted. Such a mechanism could contribute to the relocation of the pathogen from the intestinal lumen to the surface of intestinal epithelial cells, as previously suggested by others (Kamada et al., 2012; Pacheco et al., 2012; Cameron and Sperandio, 2015).

In this study, we described a novel mechanism by which EHEC O157:H7 regulate the expression of its T3SS-encoding genes in response to sugars derived from intestinal mucin. The NAG-6P sensor NagC was shown to promote the adherence of EHEC O157:H7 to intestinal cells *in vitro* through a direct regulation of *ler* and to be an important regulator for the fitness of EHEC *in vivo*. This work sheds further light on the link between the nutrient availability and EHEC O157:H7 adaptation and virulence gene expression.

AUTHOR CONTRIBUTIONS

Conceived and designed the experiments: GL, CM, JH, and GJ. Performed the experiments: GL, JS, PG, AG, FB, and GJ. Analyzed the data: GL, AB, APG, CM, JH, and GJ. Wrote the paper: GL, CM, JH, and GJ.

FUNDING

GL was supported by a scholarship from the Institut de recherche en santé publique de l'Université de Montréal-Fonds de recherche du Québec-santé (Project 40148). This work was also supported in part by the 61st Session de la Commission permanente de coopération franco-québécoise (Project 61. 116 to CM and JH), by the Natural Sciences and Engineering Research Council of Canada (NSERC) (Strategic and Discovery Grants to JH, RGPIN STP 307430 and RGPIN-2015-05373, respectively) and by EADGENE, N FOOD-CT-2004-506416, Network of Excellence under the 6th Research Framework Program of the European Union (CM).

ACKNOWLEDGMENTS

We thank C. Del'Homme, E. Delmas, G. Lopes and J. Daniel for excellent technical assistance. We are grateful to Dr. J. Plumbridge (Institut de Biologie Physico-Chimique, Paris) her helpful comments and sharing information on NagC and help in identifying putative NagC binding DNA sequences and to Judith Kashul, for editing the manuscript.

SUPPLEMENTARY MATERIAL

The Supplementary Material for this article can be found online at: http://journal.frontiersin.org/article/10.3389/fcimb.2017.00134/full#supplementary-material

REFERENCES

Barnhart, M. M., Lynem, J., and Chapman, M. R. (2006). GlcNAc-6P levels modulate the expression of Curli fibers by *Escherichia coli*. *J. Bacteriol.* 188, 5212–5219. doi: 10.1128/JB.00234-06

Bertin, Y., Chaucheyras-Durand, F., Robbe-Masselot, C., Durand, A., de la Foye, A., Harel, J., et al. (2013). Carbohydrate utilization by enterohaemorrhagic *Escherichia coli* O157:H7 in bovine intestinal content. *Environ. Microbiol.* 15, 610–622. doi: 10.1111/1462-2920.12019

Bertin, Y., Deval, C., de la Foye, A., Masson, L., Gannon, V., Harel, J., et al. (2014). The gluconeogenesis pathway is involved in maintenance of enterohaemorrhagic *Escherichia coli* O157:H7 in bovine intestinal content. *PLoS ONE* 9:e98367. doi: 10.1371/journal.pone.0098367

Branchu, P., Matrat, S., Vareille, M., Garrivier, A., Durand, A., Crepin, S., et al. (2014). NsrR, GadE, and GadX interplay in repressing expression of the *Escherichia coli* O157:H7 LEE pathogenicity island in response to nitric oxide. *PLoS Pathog.* 10:e1003874. doi: 10.1371/journal.ppat.1003874

Brechemier-Baey, D., Dominguez-Ramirez, L., Oberto, J., and Plumbridge, J. (2015). Operator recognition by the ROK transcription factor family members, NagC and Mlc. *Nucleic Acids Res.* 43, 361–372. doi: 10.1093/nar/gku1265

Cameron, E. A., and Sperandio, V. (2015). Frenemies: signaling and nutritional integration in pathogen-microbiota-host interactions. *Cell Host Microb.* 18, 275–284. doi: 10.1016/j.chom.2015.08.007

Chekabab, S. M., Jubelin, G., Dozois, C. M., and Harel, J. (2014). PhoB activates *Escherichia coli* O157:H7 virulence factors in response to inorganic phosphate limitation. *PLoS ONE* 9:e94285. doi: 10.1371/journal.pone.0094285

Conway, T., and Cohen, P. S. (2015). Commensal and pathogenic *Escherichia coli* metabolism in the gut. *Microb. Spectr.* 3:MBP-0006-2014. doi: 10.1128/microbiolspec.MBP-0006-2014

Deng, W., Puente, J. L., Gruenheid, S., Li, Y., Vallance, B. A., Vazquez, A., et al. (2004). Dissecting virulence: systematic and functional analyses of a pathogenicity island. *Proc. Natl. Acad. Sci. U.S.A.* 101, 3597–3602. doi: 10.1073/pnas.0400326101

Derrien, M., van Passel, M. W., van de Bovenkamp, J. H., Schipper, R. G., de Vos, W. M., and Dekker, J. (2010). Mucin-bacterial interactions in the human oral cavity and digestive tract. *Gut. Microb.* 1, 254–268. doi: 10.4161/gmic.1.4.12778

Elhenawy, W., Debelyy, M. O., and Feldman, M. F. (2014). Preferential packing of acidic glycosidases and proteases into *Bacteroides* outer membrane vesicles. *mBio* 5, e00909–14. doi: 10.1128/mBio.00909-14

El Qaidi, S., Allemand, F., Oberto, J., and Plumbridge, J. (2009). Repression of *galP*, the galactose transporter in *Escherichia coli*, requires the specific regulator of N-acetylglucosamine metabolism. *Mol. Microbiol.* 71, 146–157. doi: 10.1111/j.1365-2958.2008.06515.x

El Qaidi, S., and Plumbridge, J. (2008). Switching control of expression of *ptsG* from the Mlc regulon to the NagC regulon. *J. Bacteriol.* 190, 4677–4686. doi: 10.1128/JB.00315-08

Fabich, A. J., Jones, S. A., Chowdhury, F. Z., Cernosek, A., Anderson, A., Smalley, D., et al. (2008). Comparison of carbon nutrition for pathogenic and commensal *Escherichia coli* strains in the mouse intestine. *Infect. Immun.* 76, 1143–1152. doi: 10.1128/IAI.01386-07

Graveline, R., Mourez, M., Hancock, M. A., Martin, C., Boisclair, S., and Harel, J. (2011). Lrp-DNA complex stability determines the level of ON cells in type P fimbriae phase variation. *Mol. Microbiol.* 81, 1286–1299. doi: 10.1111/j.1365-2958.2011.07761.x

Kamada, N., Kim, Y. G., Sham, H. P., Vallance, B. A., Puente, J. L., Martens, E. C., et al. (2012). Regulated virulence controls the ability of a pathogen to compete with the gut microbiota. *Science* 336, 1325–1329. doi: 10.1126/science.1222195

Kaper, J. B., Nataro, J. P., and Mobley, H. L. (2004). Pathogenic *Escherichia coli*. *Nat. Rev. Microbiol.* 2, 123–140. doi: 10.1038/nrmicro818

Kendall, M. M., Gruber, C. C., Parker, C. T., and Sperandio, V. (2012). Ethanolamine controls expression of genes encoding components involved in interkingdom signaling and virulence in enterohemorrhagic *Escherichia coli* O157:H7. *mBio* 3:e00050-12. doi: 10.1128/mBio.00050-12

Le Bihan, G., Jubelin, G., Garneau, P., Bernalier-Donadille, A., Martin, C., Beaudry, F., et al. (2015). Transcriptome analysis of *Escherichia coli* O157:H7 grown *in vitro* in the sterile-filtrated cecal content of human gut microbiota associated rats reveals an adaptive expression of metabolic and virulence genes. *Microb. Infect.* 17, 23–33. doi: 10.1016/j.micinf.2014.09.008

Leedle, J. A., and Hespell, R. B. (1980). Differential carbohydrate media and anaerobic replica plating techniques in delineating carbohydrate-utilizing subgroups in rumen bacterial populations. *Appl. Environ. Microbiol.* 39, 709–719.

McClain, M. S., Blomfield, I. C., and Eisenstein, B. I. (1991). Roles of *fimB* and *fimE* in site-specific DNA inversion associated with phase variation of type 1 fimbriae in *Escherichia coli*. *J. Bacteriol.* 173, 5308–5314.

McGuckin, M. A., Linden, S. K., Sutton, P., and Florin, T. H. (2011). Mucin dynamics and enteric pathogens. *Nat. Rev. Microbiol.* 9, 265–278. doi: 10.1038/nrmicro2538

Miller, J. H. (1972). *Experiments in Molecular Genetics*. Cold Spring Harbor, NY: Cold Spring Harbor Laboratory.

Miyashiro, T., Klein, W., Oehlert, D., Cao, X., Schwartzman, J., and Ruby, E. G. (2011). The N-acetyl-D-glucosamine repressor NagC of *Vibrio fischeri* facilitates colonization of Euprymna scolopes. *Mol. Microbiol.* 82, 894–903. doi: 10.1111/j.1365-2958.2011.07858.x

Nakanishi, N., Tashiro, K., Kuhara, S., Hayashi, T., Sugimoto, N., and Tobe, T. (2009). Regulation of virulence by butyrate sensing in enterohaemorrhagic *Escherichia coli*. *Microbiology* 155, 521–530. doi: 10.1099/mic.0.023499-0

Ng, K. M., Ferreyra, J. A., Higginbottom, S. K., Lynch, J. B., Kashyap, P. C., Gopinath, S., et al. (2013). Microbiota-liberated host sugars facilitate post-antibiotic expansion of enteric pathogens. *Nature* 502, 96–99. doi: 10.1038/nature12503

Nieuw Amerongen, A. V., Bolscher, J. G., Bloemena, E., and Veerman, E. C. (1998). Sulfomucins in the human body. *Biol. Chem.* 379, 1–18.

O'Brien, A. O., Lively, T. A., Chen, M. E., Rothman, S. W., and Formal, S. B. (1983). *Escherichia coli* O157:H7 strains associated with haemorrhagic colitis in the United States produce a *Shigella dysenteriae* 1 (SHIGA) like cytotoxin. *Lancet* 1, 702.

Pacheco, A. R., Curtis, M. M., Ritchie, J. M., Munera, D., Waldor, M. K., Moreira, C. G., et al. (2012). Fucose sensing regulates bacterial intestinal colonization. *Nature* 492, 113–117. doi: 10.1038/nature11623

Plumbridge, J. (1996). How to achieve constitutive expression of a gene within an inducible operon: the example of the nagC gene of *Escherichia coli*. *J. Bacteriol.* 178, 2629–2636.

Plumbridge, J. A. (1991). Repression and induction of the *nag* regulon of *Escherichia coli* K-12: the roles of *nagC* and *nagA* in maintenance of the uninduced state. *Mol. Microbiol.* 5, 2053–2062.

Plumbridge, J., and Kolb, A. (1991). CAP and Nag repressor binding to the regulatory regions of the nagE-B and manX genes of *Escherichia coli*. *J. Mol. Biol.* 217, 661–679.

Porter, M. E., Mitchell, P., Free, A., Smith, D. G., and Gally, D. L. (2005). The LEE1 promoters from both enteropathogenic and enterohemorrhagic *Escherichia coli* can be activated by PerC-like proteins from either organism. *J. Bacteriol.* 187, 458–472. doi: 10.1128/Jb.187.2.458-472.2005

Samadder, P., Xicohtencatl-Cortes, J., Saldana, Z., Jordan, D., Tarr, P. I., Kaper, J. B., et al. (2009). The *Escherichia coli ycbQRST* operon encodes fimbriae with laminin-binding and epithelial cell adherence properties in Shiga-toxigenic *E. coli* O157:H7. *Environ. Microbiol.* 11, 1815–1826. doi: 10.1111/j.1462-2920.2009.01906.x

Sircili, M. P., Walters, M., Trabulsi, L. R., and Sperandio, V. (2004). Modulation of enteropathogenic *Escherichia coli* virulence by quorum sensing. *Infect. Immun.* 72, 2329–2337. doi: 10.1128/IAI.72.4.2329-2337.2004

Sohanpal, B. K., El-Labany, S., Lahooti, M., Plumbridge, J. A., and Blomfield, I. C. (2004). Integrated regulatory responses of *fimB* to N-acetylneuraminic (sialic) acid and GlcNAc in *Escherichia coli* K-12. *Proc. Natl. Acad. Sci. U.S.A.* 101, 16322–16327. doi: 10.1073/pnas.0405821101

Sohanpal, B. K., Friar, S., Roobol, J., Plumbridge, J. A., and Blomfield, I. C. (2007). Multiple co-regulatory elements and IHF are necessary for the control of fimB expression in response to sialic acid and N-acetylglucosamine in *Escherichia coli* K-12. *Mol. Microbiol.* 63, 1223–1236. doi: 10.1111/j.1365-2958.2006.05583.x

Sperandio, V., Li, C. C., and Kaper, J. B. (2002). Quorum-sensing *Escherichia coli* regulator A: a regulator of the LysR family involved in the regulation of the locus of enterocyte effacement pathogenicity island in enterohemorrhagic *E. coli*. *Infect. Immun.* 70, 3085–3093. doi: 10.1128/IAI.70.6.3085-3093.2002

Sun, Y., Verma, S. C., Bogale, H., and Miyashiro, T. (2015). NagC represses N-acetyl-glucosamine utilization genes in *Vibrio fischeri* within the light organ of *Euprymna scolopes*. *Front. Microbiol.* 6:741. doi: 10.3389/fmicb.2015.00741

Tailford, L. E., Crost, E. H., Kavanaugh, D., and Juge, N. (2015). Mucin glycan foraging in the human gut microbiome. *Front. Genet.* 6:81. doi: 10.3389/fgene.2015.00081

Vogeleer, P., Tremblay, Y. D., Jubelin, G., Jacques, M., and Harel, J. (2015). Biofilm-forming abilities of Shiga toxin-producing *Escherichia coli* isolates associated with human infections. *Appl. Environ. Microbiol.* 82, 1448–1458. doi: 10.1128/aem.02983-15

Walters, M., and Sperandio, V. (2006). Autoinducer 3 and epinephrine signaling in the kinetics of locus of enterocyte effacement gene expression in enterohemorrhagic *Escherichia coli*. *Infect. Immun.* 74, 5445–5455. doi: 10.1128/IAI.00099-06

Wilharm, G., and Heider, C. (2014). Interrelationship between type three secretion system and metabolism in pathogenic bacteria. *Front. Cell. Infect. Microbiol.* 4:150. doi: 10.3389/fcimb.2014.00150

Xu, J., Bjursell, M. K., Himrod, J., Deng, S., Carmichael, L. K., Chiang, H. C., et al. (2003). A genomic view of the human-*Bacteroides thetaiotaomicron* symbiosis. *Science* 299, 2074–2076. doi: 10.1126/science.1080029

Yang, B., Feng, L., Wang, F., and Wang, L. (2015). Enterohemorrhagic *Escherichia coli* senses low biotin status in the large intestine for colonization and infection. *Nat. Commun.* 6, 6592. doi: 10.1038/ncomms7592

Conflict of Interest Statement: The authors declare that the research was conducted in the absence of any commercial or financial relationships that could be construed as a potential conflict of interest.

Copyright © 2017 Le Bihan, Sicard, Garneau, Bernalier-Donadille, Gobert, Garrivier, Martin, Hay, Beaudry, Harel and Jubelin. This is an open-access article distributed under the terms of the Creative Commons Attribution License (CC BY). The use, distribution or reproduction in other forums is permitted, provided the original author(s) or licensor are credited and that the original publication in this journal is cited, in accordance with accepted academic practice. No use, distribution or reproduction is permitted which does not comply with these terms.

frontiers in Cellular and Infection Microbiology

REVIEW
published: 24 February 2017
doi: 10.3389/fcimb.2017.00051

Sampling Strategies for Three-Dimensional Spatial Community Structures in IBD Microbiota Research

Shaocun Zhang[1,2,3†], *Xiaocang Cao*[4†] *and He Huang*[1,2,3*]

[1] Department of Biochemical Engineering, School of Chemical Engineering and Technology, Tianjin University, Tianjin, China, [2] Key Laboratory of Systems Bioengineering, Ministry of Education, Tianjin University, Tianjin, China, [3] Collaborative Innovation Center of Chemical Science and Engineering, Tianjin, China, [4] Department of Gastroenterology and Hepatology, Tianjin Medical University General Hospital; Tianjin Medical University, Tianjin, China

Identifying intestinal microbiota is arguably an important task that is performed to determine the pathogenesis of inflammatory bowel diseases (IBD); thus, it is crucial to collect and analyze intestinally-associated microbiota. Analyzing a single niche to categorize individuals does not enable researchers to comprehensively study the spatial variations of the microbiota. Therefore, characterizing the spatial community structures of the inflammatory bowel disease microbiome is critical for advancing our understanding of the inflammatory landscape of IBD. However, at present there is no universally accepted consensus regarding the use of specific sampling strategies in different biogeographic locations. In this review, we discuss the spatial distribution when screening sample collections in IBD microbiota research. Here, we propose a novel model, a three-dimensional spatial community structure, which encompasses the x-, y-, and z-axis distributions; it can be used in some sampling sites, such as feces, colonoscopic biopsy, the mucus gel layer, and oral cavity. On the basis of this spatial model, this article also summarizes various sampling and processing strategies prior to and after DNA extraction and recommends guidelines for practical application in future research.

Keywords: sampling strategies, community structure, IBD microbiota research, feces, colonoscopic biopsy, mucus gel layer, oral cavity

OPEN ACCESS

Edited by:
Nathan W. Schmidt,
University of Louisville, USA

Reviewed by:
Thomas Thurnheer,
University of Zurich, Switzerland
Venkatakrishna Rao Jala,
University of Louisville, USA

***Correspondence:**
He Huang
huang@tju.edu.cn

[†] *These authors have contributed equally to this work.*

Received: *25 November 2016*
Accepted: *10 February 2017*
Published: *24 February 2017*

Citation:
Zhang S, Cao X and Huang H (2017) Sampling Strategies for Three-Dimensional Spatial Community Structures in IBD Microbiota Research. Front. Cell. Infect. Microbiol. 7:51. doi: 10.3389/fcimb.2017.00051

INTRODUCTION

Inflammatory bowel diseases (IBDs), including Crohn's disease (CD) and ulcerative colitis (UC), are emerging as a part of a worldwide epidemic. CD was first diagnosed by Dr Burril B. Crohn (Crohn et al., 1932), in New York, in 1932, and UC was first described by White (1888), in Europe, in 1888. The former condition can cause inflammation in any digestive tracts, while the latter

Abbreviations: IBD, Inflammatory bowel disease; CD, Crohn's disease; UC, Ulcerative colitis; NGS, Next-generation sequencing technologiesl; HMP, International Human Microbiome Project; IBS, Irritable bowel syndrome; FMT, Fecal microbiota transplantation; VOC, Volatile organic compound; SOP, Standard operating procedures; IHMS, International Human Microbiome Standards; OUT, Operational taxonomic units; PBS, Phosphate buffered saline; ADD, Abundance–distance dispersion; MGL, Mucus gel layer; MUP, Mucus-binding protein; PCR, Polymerase chain reaction; PSB, Protected specimen brush; LCM, Laser capture microdissection; ANOVA, Analysis of variance; DSS, Dextran sulfate sodium.

invariably affects the mucosa of the large intestine and rectum. Previous studies revealed that the prevalence of IBDs were greatly related to time (Molodecky et al., 2012), regions (Reinberg, 2015), age (Choi et al., 2015; Connelly et al., 2015), genes (Sharp et al., 2015; Wang and Achkar, 2015; Yang et al., 2015), stress (Gray et al., 2015), diet (Vagianos et al., 2016), etc., Some of these factors, including diet, were thought to be crucially connected to the genetic imbalance of the intestinal microbiota (Kosiewicz et al., 2011; Manichanh et al., 2012; Gevers et al., 2014; Kostic et al., 2014; Munyaka et al., 2016). Several studies have shown dysbiosis of the gut microbiome between patients with IBD and healthy individuals (Sokol et al., 2006; Andoh et al., 2012; Ottman et al., 2012). Owing to the decreasing cost and rapid development of next-generation sequencing (NGS) technologies (Zoetendal et al., 2008; Sheridan, 2014), the advancement of bioinformatics tools (Schloss et al., 2009; Caporaso et al., 2010; Glass et al., 2010), and the updating of online databases (DeSantis et al., 2006; Quast et al., 2013), 16S rRNA gene amplicon sequencing (Minamoto et al., 2015; Scher et al., 2015) and metagenomics analysis (Pérezcobas et al., 2014; Wang et al., 2015) have opened new frontiers to identify the variability of IBD microbiota research, which simultaneously characterizes multiple samples; it can also enable subsequent studies of microbial communities, both structurally, and functionally, while determining their interactions with the habitats they occupy.

Besides IBD, intestinal dysbiosis also plays a profound role in multiple chronic and metabolic diseases, including diabetes (Heintz-Buschart et al., 2016), obesity (Greenhill, 2015), irritable bowel syndrome (IBS) (Bennet et al., 2015), and so forth. Similar to IBD research; many studies conducted on the intestinal microbiota in relation to diabetes mellitus have predominantly used feces samples (Qin et al., 2012; Heintz-Buschart et al., 2016; Knip and Siljander, 2016). Additionally, in view of the connections between the periodontitis and diabetes mellitus, some studies have explored the diversity of subgingival microbiota between healthy controls and diabetics (Demmer et al., 2016). When investigating the relationship between intestinal microbiota and obesity, plenty of studies targeted the fecal microbiota for the reason that it is easily obtainable (Aguirre and Venema, 2015). Even though the small intestine is much more difficult to acquire than feces specimens, some researchers believed that sampling site should focus on the small intestinal microbiota, because it is where the calories are absorbed (Angelakis and Lagier, 2016). Moreover, a recent work showed that the obesity affected the subgingival microbial composition (Maciel et al., 2016). In IBS studies, the prevalently obtainable materials when sampling intestinal microbiota are feces and mucosal biopsies (Rangel et al., 2015; Parthasarathy et al., 2016). Accordingly, each disease has suitable sampling methods depending on pathophysiology and feasibility of the operation. Compared with other diseases, spatial ecological patterns are evident in common diseases of the colon, including the distribution of UC, and CD, which make the sampling sources diversified in IBD research (Lavelle et al., 2015). Meanwhile, understanding how the potentially complex pathogenesis of IBD occurs requires the integration of tools from spatial ecology with comprehensive sampling sources to define microbial dysbiosis in various niches (Lavelle et al., 2013).

The human body is composed of many niches. Biogeography studies the patterns of biological diversity in different niches, varying in both time and space (Fierer, 2008). The selection pressures of biology and the environment, elucidated by biogeography, are thought to be responsible for shaping the various habitats in the body (Lavelle et al., 2016). The community structure of microbiota across spatial niches might be disturbed to different degrees and in association with various disease states. Without cooperation among the other dimensions of microbial ecology, it may be difficult to investigate subjective signals from disturbances in a single niche (Jeffery et al., 2012; Lozupone et al., 2012). The International Human Microbiome Project (HMP)[1], with its sum total funding of $115 million, has showcased the distinct variations of the human microbiota in different community structures (Group et al., 2009). Other studies of the human microbiome have also characterized the bacterial biogeography of different habitats (Costello et al., 2009; Grice et al., 2009; Zhou et al., 2013). Numerous research initiatives have shown interpersonal variation in human-associated microbiota in IBD (Lavelle et al., 2015, 2016). Likewise, intrapersonal variability has been discovered between different niches. Currently, the bacterial diversity in IBD research is determined by analyzing different community structures, and following the various aspects of feces (Kolho et al., 2015; Norman et al., 2015), colonoscopic biopsy samples (De Cruz et al., 2015; Rossen et al., 2015), and the mucus gel layer (MGL) (Johansson, 2014; Johansson et al., 2014). To obtain the MGL, researchers often use rectal swabs (Araújopérez et al., 2012), microbiological protected specimen brushes (PSBs) (Lavelle et al., 2013), and laser capture microdissection (LCM) (Lavelle et al., 2015). Recent research studies have indicated that oral microbiota will be used in clinical and diagnostic utilities (Yoshizawa et al., 2013; Said et al., 2014). Despite very promising prospects in the future, there is still no clear guidance identifying those methodologies that can be accurately used to systematically collect and process the samples. Some highly complex biological samples are often difficult to process, which can introduce much bias. These drawbacks can potentially influence the final result; yet, to comprehensively study the microbial diversity in IBDs, more information is indispensable in the design of spatial sampling strategies.

In this review, we focus on discussing the different sampling strategies used in IBD microbiota research from the perspective of three planes. Y-axis distribution includes the oral cavity and feces. X-axis gradients are distributed in intestinal biopsies, with sampling levels varying in the ileum, colon (ascending colon, transverse colon, and descending colon), rectum, and caecum. Z-axis distribution involves collecting luminal, mucosal, and mucous communities in a specific and regional manner, and it includes the feces, colonoscopy biopsy samples, and the MGL. Starting with a description of the y-axis distribution, we discuss the classic sampling sites—feces and the oral cavity. We

[1]International Human Microbiome Standards (IHMS) project http://www.microbiome-standards.org/ [Online]. [Accessed].

then describe the x-axis distributions of colonoscopy biopsy. Ultimately, we will concentrate on the different sampling methods used for the MGLs, which are located on the z-axis. We herein provide an overview of the most crucial sampling strategies to help researchers make informed decisions.

SAMPLING SITES DISTRIBUTED ALONG THE Y-AXIS

Feces

In the 1680s, Leeuwenhoek first described fecal bacteria using homemade microscopes (Egerton, 2006). With the rapidly evolving research on IBD in the nineteenth century, fecal flora was frequently used to represent intestinal microflora, as it was easily collected in patients. *Firmicutes* and *Bacteroidetes* phyla constitute the majority of dominant fecal microbiota using 16S rRNA amplicon sequencing, and with *Bacteroides* being the most abundant (Arumugam et al., 2011). Some work suggested that fecal bacterial communities could be divided into three enterotypes (*Bacteroides*, *Prevotella*, and *Ruminococcus*; Arumugam et al., 2011; Wu et al., 2011). Nowadays, fecal microbiota transplantation (FMT) has been widely used in the treatment of patients with IBD, which was found to be an effective therapy for some recipients (Kelly et al., 2015; Ince et al., 2016; Vermeire et al., 2016); thus, it was concluded that there should be some close connections between fecal microbiota and IBD. Probert et al. (2014) compared IBD patients and animal models of colitis with healthy individuals, and they found that the volatile organic compound (VOC) in feces held a potential role in identifying a novel diagnostic method for IBD. With a high sensitivity to inflammatory states, bacterial biomarkers in stool may therefore constitute a promising non-invasive source to diagnose IBD (Berry et al., 2015). In IBDs, the pH progressively increases along the duodenum to the terminal ileum; it decreases in the caecum, and then slowly rises from the colon to the rectum (Nugent et al., 2001). Such changes in colonic physiology are possibly reflected in the microbiota. Additionally, important factors such as diet (Lee et al., 2016), physical exercise (Queipoortuño et al., 2013), smoking habits (Biedermann et al., 2013), and antibiotic use (Pérezcobas et al., 2013) should exert subtle differences on fecal microbiota composition; of these, antibiotic use has a strong impact on one's initial microbiota composition (Macfarlane, 2014; Zhang et al., 2015b). Consequently, all of these issues shall be considered prior to sampling.

Sampling Operating Procedures

In view of the importance of the fecal sampling method, the study of the standard operating procedures (SOP) used to collect the fecal specimens has been, and still is, crucial for identifying pathogens. In the early stages, Moore (Moore and Holdeman, 1974) pointed out that some unique problems may arise with respect to the isolation and identification of intestinal bacteria in fecal flora studies, including collection, shipping, and isolation. Some experiments confirmed that the collection procedures and storage conditions did influence the diversity and integrity of the microbial flora (Cardona et al., 2012; Gorzelak et al., 2015; Boers et al., 2016; Nishimoto et al., 2016). It has been suggested that stool consistency is strongly associated with gut microbiota diversity (Vandeputte et al., 2016).

Swidsinski et al. (2008a,b) developed a new method using a punched-out freshstool cylinder; they demonstrated that the fecal flora were highly structured and spatially organized. The homogenization step in this procedure significantly reduced the intra-individual variation in the detected bacteria (Hsieh et al., 2016). Specifically, the results indicated that the relative abundance of *Firmicutes* to *Bacteroidetes* was significantly higher when snap-freezing fecal samples were compared with fresh samples (Bahl et al., 2012). Meanwhile, a study recommended that stool should be frozen within 15 min of being defecated, and it should be stored in a domestic, frost-free freezer for $<$3 days before DNA extraction (Carroll et al., 2012). During storage and processing, freeze–thaw cycles were detrimental to microbial cell integrity (Cardona et al., 2012). Conventionally, samples can be stored at -80°C in the long term until DNA extraction (for no longer than 6 months; Carroll et al., 2012). Based on the above, the ideal storing procedure might be as follows: homogenizing prior to sampling, sampling aliquot fresh stool to avoid subsampling; and then freezing at 80°C as soon as possible. If the laboratory has difficulty snap freezing, some researchers believe that RNAlater® (Life Technologies) might be selected to maintain DNA stabilization at $+4^{\circ}$C, or even at room temperature, for several days without affecting the 16S rRNA repertoire (for specific treatments, see **Figure 1**). However, a new study suggested that RNAlater should be avoided due to its ability to degrade the yield of DNA and bacterial taxa (Gorzelak et al., 2015). Otherwise, a guanidine thiocyanate solution might ensure the high stability of fecal microbiota at room temperature (Nishimoto et al., 2016). Despite this, there are still no universally accepted standards in the field of feces sampling.

Sample Extraction

According to the instructions and manual operation, 100 or 200 mg were the most frequently used dosages. One study showed that a 200 mg starting weight produced significantly higher DNA yields than 100 mg (Claassen et al., 2013); however, there was no similarity with respect to DNA purity. Conversely, Ariefdjohan (Ariefdjohan et al., 2010) tested 10–50 mg fecal samples and found that these weights, and not 100 mg or 200 mg, could result in maximum DNA yields. The phenol: chloroform-based DNA isolation method was illustrated to effectively obtain the requisite DNA yield (Mackenzie et al., 2015); however, this method is not suitable for clinical or large-scale studies. Owing to the bead-beating step, hot phenol with bead beating resulted in a proportional increase in *Firmicutes* (Wu et al., 2010; Mackenzie et al., 2015).

With respect to DNA extraction kits, those associated with the HMP view the MoBio PowerSoil® DNA Isolation Kit as the most effective microbial DNA extraction method. Moreover, some researchers involved in the International Human Microbiome Standards (IHMS; http://www.microbiome.standard.org/) prefer to use the QIAamp DNA Stool Mini Kit. Some researchers have conducted several studies on different extraction methods. As a result, the combination of mechanical cell disruption by

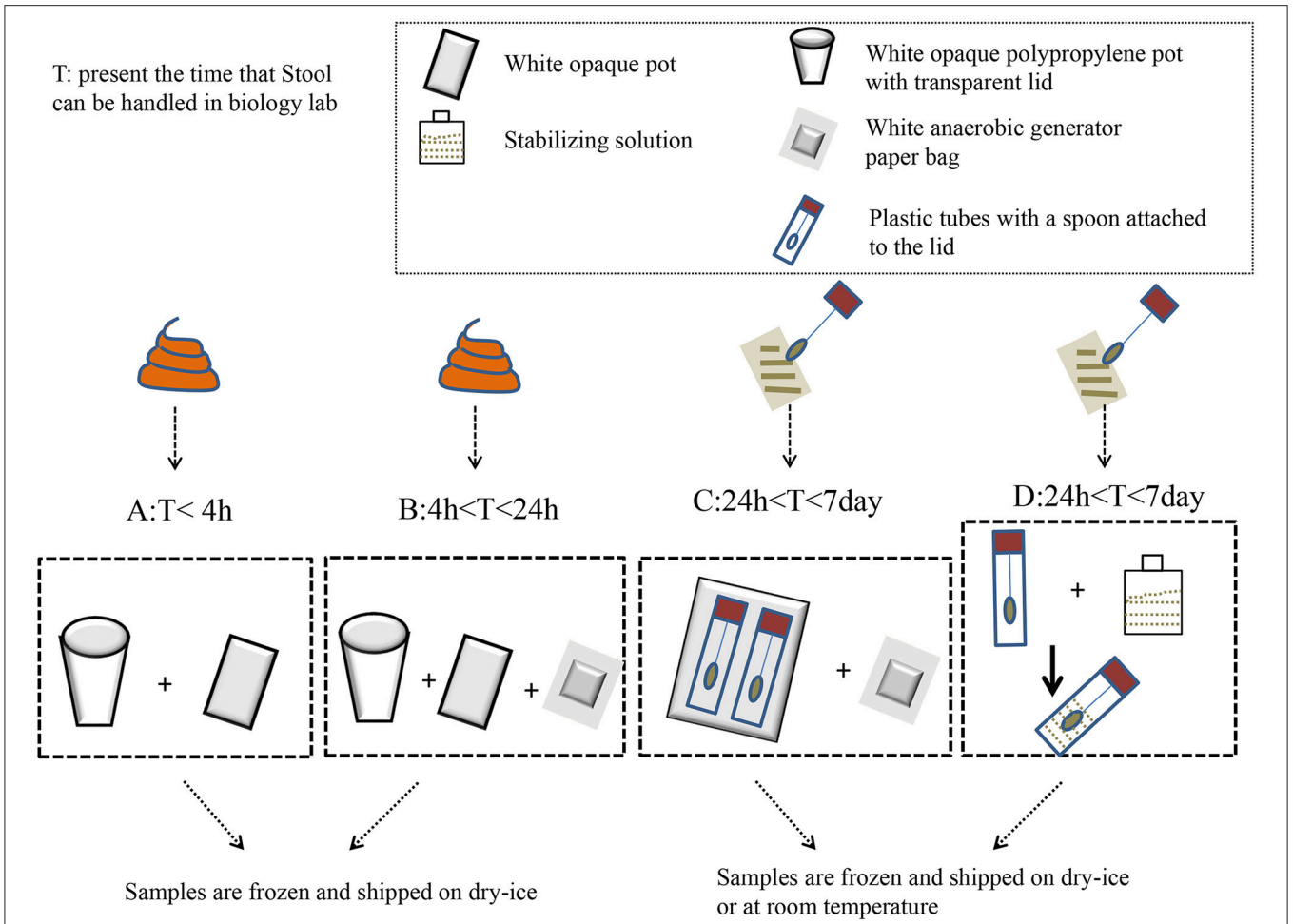

FIGURE 1 | The impact of methods that can be used to collect feces before laboratory handling. When the fecal samples are transported to a biology lab within 4 h, they only need to be placed in a white opaque polypropylene pot with a transparent lid and a white opaque pot to hold the bag. Then, the samples are frozen and shipped on dry–ice to the lab **(A)**. When the samples can be brought to the laboratory within 4–24 h, tools should be used to add a white anaerobic generator paper bag on the basis of A to maintain a anaerobic atmosphere **(B)**. The plastic tubes, which have a spoon attached to their lids, are used to collect feces when the transit time is longer than 1 day. Fill up to two-thirds of the spoon with feces, and do not overfill. Then, the spoon and anaerobic generator paper bag are inserted in the opaque plastic bag **(C)**. Plastic tubes containing the stabilizing solution can keep the fecal DNA stable at room temperature for a few days (**D**).

repeated bead-beating (Yu and Morrison first described the repeated bead-beating and column purification method, Yu and Morrison, 2004) for 6 min, (Salonen et al., 2010) and with a 95°C heating step, showed greater bacterial diversity; it resulted in the significantly improved DNA extraction abundance of archaea and some bacteria, especially for bacteria in the phylum *Firmicutes*, including *Clostridium cluster IV* (Salonen et al., 2010; Thomas et al., 2015). However, bead-beating for long periods of time had a negative effect on DNA yield, and zirconium–silica beads were considered to be the best choice (Salonen et al., 2010). Due to the aromatic acids that exist in stool, some inhibition removal technology or substances were utilized to prevent interference—such as the inhibitEX tablets in the QIAamp DNA Stool Mini Kit (Thomas et al., 2015). Additionally, the size of the spin columns may also influence filter efficiency; for instance, sizes smaller than 0.45 μm would hold back some larger fragments (Thomas et al., 2015).

Several studies have compared various DNA extraction kits and methods to assess the bacterial diversity in stool samples (Wu et al., 2010; Claassen et al., 2013; Kennedy et al., 2014; Mackenzie et al., 2015; see **Table 1**). It was found that finding a protocol to extract DNA without bias is a challenging task.

Sample Sequencing

Two methods are frequently used for taxonomic classification of organisms that are found in microbiomes: 16S rRNA gene amplicon sequencing and metagenomic sequencing. 16S rRNA gene amplicon sequencing is increasingly being used to provide information about the compositions and the relative abundance of microorganisms and classify microbial communities based on amplification of 16S rRNA gene, both taxonomically and phylogenetically (Clarridge, 2004). To analyze 16S rRNA gene sequences from microbial communities, QIIME, Mothur, and

TABLE 1 | Overview of different processing methods or commercial DNA extraction kits that were compared in some studies to extract DNA from stool samples for further bioinformatics analysis.

序号	Kit/method	Sample store condition	Sample homogenization	Extra Lysis type	Inhibitor removal	Sequencing methods	DNA analysis	DNA yield	DNA purity	Bacterial diversity
1 Wu et al., 2010	Hot phenol with bead beating+ QIAamp® DNA Stool Mini Kit	Immediately frozen (−80°C)	NO	Mechanical + Heat + Chemical + Enzymatic	YES	454 GS FLX and 454 Titanium	16V1–V2 ,V1–V3,V3–V5, V6–V9	B	–	The largest proportion of *Firmicutes*
	QIAamp® DNA Stool Mini Kit	Immediately frozen (−80°C)	NO	Mechanical + Heat + Chemical + Enzymatic	YES	454 GS FLX and 454 Titanium	16V1–V2 ,V1–V3,V3–V5, V6–V9	B	–	Similar to PowerSoil DNA Isolation Kit
	Stratec® PSP Spin Stool DNA Kit	PSP for 48 h, then frozen (−80°C)	NO	Mechanical + Heat + Enzymatic	YES	454 GS FLX and 454 Titanium	16V1–V2 ,V1–V3,V3–V5, V6–V9	A	–	With higher proportion of *Firmicutes*
	MoBio® PowerSoil DNA Isolation Kit	Immediately frozen (−80°C)	NO	Mechanical + Heat +	YES	454 GS FLX and 454 Titanium	16V1–V2 ,V1–V3,V3–V5, V6–V9	C	–	Similar to QIAamp DNA Stool Mini Kit
2 Mackenzie et al., 2015	Phenol: chloroform-based DNA isolation	Immediately frozen (−80°C)	YES	Mechanical	NO	Illumina MiSeq	16V4	A	B	With higher proportion of *Parabacteroides distasonis*
	QIAamp® DNA Stool Mini Kit	Immediately frozen (−80°C)	YES	Mechanical + Heat + Chemical + Enzymatic	YES	Illumina MiSeq	16V4	B	A	The largest proportion of *Bacteroidetes*
	MoBio® PowerSoil DNA Isolation Kit	Immediately frozen (−80°C)	YES	Mechanical	YES	Illumina MiSeq	16V4	A	B	With higher proportion of *Bifidobacterium adolescentis*
	ZR Fecal DNA Mini Prep TM Kit	Immediately frozen (−80°C)	YES	Mechanical	NO	Illumina MiSeq	16V4	B	C	The highest proportion of *Firmicutes*
	HMP Extraction Method	Pre-processed supernatant + 65°C 10 min, 95°C 10 min, then frozen at −80°C	YES	Mechanical + Heat	YES	Illumina MiSeq	16V4	C	B	The lowest proportion of *Firmicutes*, the highest proportions of *Cyanobacteria* and *Proteobacteria*
3 Kennedy et al., 2014	MoBio® PowerSoil DNA Isolation Kit	65°C 10 min, 95°C 10 min, then frozen at −80°C	YES	Mechanical	YES	Roche 454 Titanium	16V3–V5	B	–	With higher proportion of *Bacteroidaceae*, *Ruminococcaceae* and *Porphyromonadaceae*
	FastDNA® SPIN Kit for Soil	65°C 10 min, 95°C 10 min, then frozen at −80°C	YES	Mechanical	NO	Roche 454 Titanium	16V3–V5	A	–	With higher proportion of *Enterobacteriaceae*, *Lachnospiraceae*, *Clostridiaceae* and *Erysipelotrichaceae*

A–C stands for the performance rank: A (best performance) to C (worst performance)

LotuS have been widely used to process data from high-throughput sequencing (Schloss et al., 2009; Kuczynski et al., 2011; Hildebrand et al., 2014). Additionally, PICRUSt (http://picrust.github.com/) has been developed to predict metabolic pathways based on 16S data and a reference genome database (Langille et al., 2013). Although this approach is unable to outperform metagenomic sequencing, it can predict and compare probable functions across a large amount of samples from different niches. Meanwhile, it can reproduce functional information that shows highly similar to the metagenomic sequencing in the HMP and other data sets (Anonymous, 2013). Compared with 16S rRNA gene amplicon sequencing, metagenomic approach is able to identify some of the distinctive functional attributes encoded in intestinal microbiota and comprehensively characterize metabolic capabilities of the microorganisms (Gill et al., 2006). Several tools have been developed to process the metagenomic data, such as MetaPhlAn (Segata et al., 2012), HUMAnN (Abubucker et al., 2012), and TruSPADES (Hildebrand et al., 2014). All approaches have merits and drawbacks. 16S rRNA gene sequencing is more cost-effective and less time consuming than metagenomic sequencing. However, metagenome approaches enable the analyses of all kingdoms as well as viral sequences. The 16S rRNA gene captures broader range of microbiome diversity, but with a lower resolution and sensitivity compared with metagenomic (Poretsky et al., 2014). Limitations withstanding, 16S rRNA is limited by the biases inherent to PCR amplification, which results from the lack of truly universal primers and different copy numbers of 16S rRNA gene (Vallescolomer et al., 2016). As for metagenomic sequencing, it could be less efficient at detecting rare species in a microbial community compared with 16S rRNA. Metagenomic sequencing also requires advanced bioinformatics skills to process and analyze the data (Shakya et al., 2013).

Theoretically, the best analysis method currently available is metagenomics; however, its associated costly budget is not suitable for clinic settings or large cohorts, and it faces some limitations with respect to environmental interactions. As a result, it was found that until recently, 16S rRNA gene amplicon sequencing is often used as an exploratory step before metagenomic research. With respect to the sequencing, the 16S rRNA database only includes bacteria and archaea; yet, the absence of viruses and eukaryotes misses many pathogenic factors, which may bias the analysis. The smallest units of operational taxonomic units (OTUs) are species, so the strains resulting in antibiotic resistance, as well as mobile elements cannot be identified (Thomas et al., 2015). Besides, *Bifidobacteriaceae* are not well represented in some 16S V1–V3 analyses (Jumpstart Consortium Human Microbiome Project Data Generation Working, 2012). According to some investigations, the optimal choice for the variable regions in the 16S rRNA approach were V1–V3 and V3–V5, as the choice of a V6–V9 primer did not appear to efficiently cover the V6–V9 regions (Wu et al., 2010; Jumpstart Consortium Human Microbiome Project Data Generation Working, 2012). Otherwise, the amount of chimera increased and amplified the polymerase chain reaction (PCR) bias (Schloss et al., 2011). To reduce the bias of the PCR methods, and to minimize the errors introduced during sequencing, some researchers developed a method known as Low-Error Amplicon Sequencing (LEA-Seq) (Faith et al., 2013), which has been applied to QIIME. Next, for high-throughput sequencing, both 454 GS FLX and 454 Titanium sequencing methods can be used, depending on convenience (Wu et al., 2010). With read lengths of currently up to 2 × 300 bp and low sequencing costs, Illumina's MiSeq (Solexa) is increasingly becoming one of the most potential sequencing platforms worldly used in IBD research (Quince et al., 2015; Chung et al., 2016). It gathers the integration of cluster generation, sequencing, and data analysis in a single instrument and can analyze data within 24 h (as few as 8 h; Liu et al., 2012). For sequencing technology, instead of pyrosequencing technology applied to 454 sequencer, MiSeq leverages sequencing by synthesis. Compared with 454 platforms, the MiSeq has a higher throughput per run and a lower error rate but a shorter reads (Liu et al., 2012; Loman et al., 2012). At the start of the IHMS project, the SOPs of fecal sample self-collection, conservation practice, and formulated sequencing standards are crucial for better understanding the fecal microbiome and for optimizing data comparisons in clinical settings.

Oral Cavity

While feces are frequently used in IBD research, there are certain limitations associated with outpatient distaste for handling these samples. Yet, researchers seek a simpler, more efficient, and more acceptable method. Oral samples are an important option. The oral cavity is a complex environment that includes the saliva, the tongue, teeth, tonsils, the buccal mucosa, and gingival sulci, which are colonized by a number of molecular and microbial analytes and bacteria (Human Microbiome Project, 2012). The microbiota in the oral cavity has a multitude of opportunities to reach the gut (Rochet et al., 2007). Pittock et al. (2001) reported oral lesion in nearly half of children that were newly diagnosed with CD. Similarly, one prospective study found that more than 30% of children with CD had involvement of the mouth (Harty et al., 2005). Another study noted a significant decrease in the overall diversity in the oral microbiota of pediatric CD patients (Docktor et al., 2012). Some bacteria in the oral cavity have recently been investigated for their association with IBD (Yoneda et al., 2016); these bacteria can be analyzed as microbial biomarkers for evaluating pathologies of the oral cavity, such as *Campylobacter concisus* (Ismail et al., 2012) and *Fusobacterium nucleatum* (Swidsinski et al., 2009). Thus, using oral microbial diagnostics is not a novel concept. Nowadays, scientists pursue a timely, accurate, cost-effective, and non-invasive diagnostic method to detect IBD. In view of these, further research on the oral microbiota in IBD might hold potential clinical and diagnostic utility in the future (Docktor et al., 2012). In this review, two frequently used sampling origins are primarily discussed: saliva and subgingival plaques.

Saliva

The average adult produces more than 1,000 mL of saliva per day, which always flows into the gastrointestinal tract. Thus, it can be stated that the salivary microbiota affects the development of gut microbiota in some respects. The

composition of salivary microbiota was found to be different between CD patients, UC patients, and healthy controls (Said et al., 2014). Furthermore, when analyzing the composition of the tongue, buccal mucosa, saliva, and stool microbiota in colitis patients, the saliva microbiota exhibited the most alterations in terms of abundance (Rautava et al., 2015). The dominant genera, *Veillonella* and *Haemophilus* were recommended to largely contribute to dysbiosis of salivary microbiota in IBD patients (Said et al., 2014). At the species level, *C. concisus* (Ismail et al., 2012; Mahendran et al., 2013) and *Mycobacterium avium Paratuberculosis* (Bruno and Isabelle, 2015) have been investigated for its role in saliva dysbiosis of IBD patients.

For sample processing, DNA yield and quality, as well as 16S rRNA/DNA products and representations of the microbial community from oral wash samples, were investigated by six commonly used commercial DNA extraction kits, utilizing either mechanical bead-beating or enzymatic methods for cell lysis (Wu et al., 2014). Researchers discovered that mechanical bead-beating extraction kits produced less total DNA when compared with the enzymatic methods. On the other hand, microbial diversity showed no difference by either mechanical bead-beating or enzymatic extraction methods. As non-invasive and informative as saliva sampling is, but now there are currently no universally accepted techniques for sample collection. Prior to sampling the saliva, one must clean the oral cavity by rinsing it with water; this is imperative to avoid the presence of contaminants (Yoshizawa et al., 2013).

Subgingival Plaques

As a human microbiome community, dental plaques were initially observed by Leeuwenhoek (Dobell, 1932) over 300 years ago. Using combinatorial labeling and spectral imaging fluorescent *in situ* hybridization (FISH) to differentiate up to 15 fluorescent probes, Welch and colleagues (Mark Welch et al., 2016) showed, for the first time, the informative value of the oral microbiota biogeography at the micron scale. The fantastic color images that they created showed that the oral cavity acted as a "coaggregation." Similar to the role of canopies in hedgehog structures, *Corynebacterium* primarily gathered in subgingival plaques and supragingival dental plaques. Zhang et al. (2015a) first combined subgingival plaques and feces to analyze the microbiota perturbed in disease, and they partly normalized after treatment; at the same time, the researchers strongly confirmed the overlap in the abundance and function of species at different body sites. This will lead to potential ways to use the supragingival microbiota community for diagnosis and prognosis. Several recent studies have demonstrated connections between the composition of IBD and periodontitis (Kelsen et al., 2013; Elburki, 2015; Agossa et al., 2016). Meanwhile, additional studies have illustrated the associations between the composition of the subgingival microbiota and IBD (Brito et al., 2013; Kelsen et al., 2015). By analyzing inflamed subgingival sites, which depends on the checkerboard DNA–DNA hybridization technique, researchers found that the levels of *Prevotella melaninogenica*, *Staphylococcus aureus*, *Streptococcus anginosus*, and *Streptococcus mutans* are higher in CD patients than in controls. Furthermore, UC patients harbored a greater abundance of *Staphylococcus aureus* and *Peptostreptococcus anaerobius* than controls (Brito et al., 2013).

Thus, it is essential to study and collect subgingival plaques. To do so, place cotton balls in such a way that they can clean out residual supragingival plaques, prior to the collection of subgingival samples. Collect the subgingival plaque in a tube with buffer, using a sterile Gracey curette to gather the targeted teeth of the mesio-buccal surface. Then, firmly close the cap on the tube and shake the tube for 5 s to entirely homogenize the sample distribution in the buffer. Finally, place the sample on ice and send it to the biology lab within 4 h (McInnes and Cutting, 2010). The HMP method uses the MoBio PowerSoil® DNA Isolation Kit; other researchers have used the MasterPure DNA Extraction Kit (Moutsopoulos et al., 2015), the FastDNA spin Kit (Kuehbacher et al., 2008), the PSP Spin Stool DNA Plus Kit (Kelsen et al., 2015), and others. Optimal methods for DNA extraction are still under development.

SAMPLING SITES DISTRIBUTED ALONG THE X-AXIS

Colonoscopy Biopsy

Accordingly, luminal microbiota and mucosa-associated microbiota have been reported to be different in IBD (Lepage et al., 2005; Morgan et al., 2012; Gevers et al., 2014). Fecal microbiota might not adequately represent bacterial communities at the epithelial interface. Colonoscopy biopsy is the most common sampling technique used to assess microbial niches associated with the intestinal mucosa; it was shown to play a crucial role in diagnosis, and it can distinguish between disease types in IBD (Salvatori et al., 2012). Mucosal biopsies sample multiple amounts of the submucosa, epithelium, and MGL. The most comprehensive method to analyze the mucosa-associated microbiota may be proctocolectomy. In fact, Chiodini et al. (2013) were the first to examine the microbial populations of submucosal tissues using proctocolectomy during active disease; they also discussed the submucosal microbiota and biotypes within CD. Some other works also elected to use tissue sections of the terminal ileum and colon, obtained during surgery, for this process (Kleessen et al., 2002; Neut et al., 2002). As accurate as proctocolectomy is, this method cannot be applied to most of IBDs, except on rare occasions. Therefore, a more suitable method to obtain the tissue should be colonoscopy.

Sampling Spatial Distribution and Processing

It has been said that diverse bacteria distribute heterogeneously along the small bowel to the colon (Eckburg et al., 2005). Biopsy specimens can be taken from different gut locations, such as the ileum, colon (ascending colon, transverse colon, and descending colon), rectum, and caecum. In addition, the intestinal tract contains a variety of distinct microbial communities along the ileum (around 155 cm from the anus), caecum (around 150 cm from the anus), ascending colon (around 142 cm from the anus), transverse colon (around 109 cm from the anus), descending colon (around 64 cm from the anus), and rectum (around 10 cm from the anus; Zhang et al., 2014), and the difference between longitudinal regions in the intestinal tract should be

positioned to select the target regions for sampling (**Figure 2A**). Comparing the microbial diversity of samples obtained with sheathed forceps with those obtained with standard unsheathed forceps, biopsies from the specific sites were not contaminated with the work channel (Dave et al., 2011). Additionally, a novel biopsy technique (Brisbane Aseptic Biopsy Device) has been developed to prevent cross-contamination from intestinal luminal contents (Shanahan et al., 2016). To avoid the influence of biopsy specimen sizes of colonoscopic tissue, researchers quantified tissue cell numbers using primers of the β-globin gene to determine the total amount of mucosa-associated microbiota in the biopsy specimens (Wang et al., 2014b). Previous studies revealed that bowel preparation (PEG electrolyte solution) before endoscopy affected the composition and diversity of the tissue and stool samples (Harrell et al., 2012; Jalanka et al., 2015; Shobar et al., 2016). Dividing a single dose into two separate dosages may introduce fewer alterations to the intestinal microbiota, which is preferred in clinical practice (Jalanka et al., 2015). Still, bowel preparation may have little effect on the next sampling procedure, as it has a short-term effect on the composition of the intestinal microbiota (O'Brien et al., 2013). Once taken, some works suggested that biopsy samples were placed in a cryovial with a lid, immediately snap-frozen in liquid nitrogen, and then stored at −80°C until further analysis (van den Heuvel et al., 2015; Hedin et al., 2016; Munyaka et al., 2016). However, other mucosal biopsy specimens were harvested and then washed twice in 500 mL of phosphate buffered saline (PBS; pH 7–8) to ensure that there was no fecal contamination prior to being snap–frozen in liquid nitrogen (Shen et al., 2010; Sanapareddy et al., 2012; Budding et al., 2014; Berry et al., 2015). Considering the actual process, a protective solution can maintain the sample at −20°C for a few weeks, or at 4°C for 24 h (Zoetendal et al., 2006). Despite this, it is recommended that biopsy samples be processed as soon as possible to avoid the lysis of microbial cells.

Sample Extraction and Analysis

Quantities of bacterial cells in biopsy samples are 1% less than in feces samples (Lyra et al., 2012). DNA extraction procedures should be more carefully conducted in order to better represent the microbial community. A study that compared some DNA extraction methods, drew the conclusion that the bead-beating and column method, as well as high molecular weight methods, were likely to result in the increased production of DNA yield, which primarily included the *Firmicutes* bacteria (Ó Cuív et al., 2011). Nowadays, a large number of studies have preferred to use the QIAamp DNA Mini Kit for IBD biopsy DNA extraction (Hansen et al., 2013; Chen et al., 2014; Wang et al., 2014a; Lavelle et al., 2015). The positive effect of bead-beating on mechanical cell lysis has been discussed for fecal samples, which are sometimes also used in DNA isolation from biopsy samples (Chen et al., 2014). However, it appears that bead-beating may not require efficient microbial DNA extraction from biopsy specimens due to the fact that mechanical cell lysis of the biopsy specimens might increase the concentration of eukaryotic DNA,

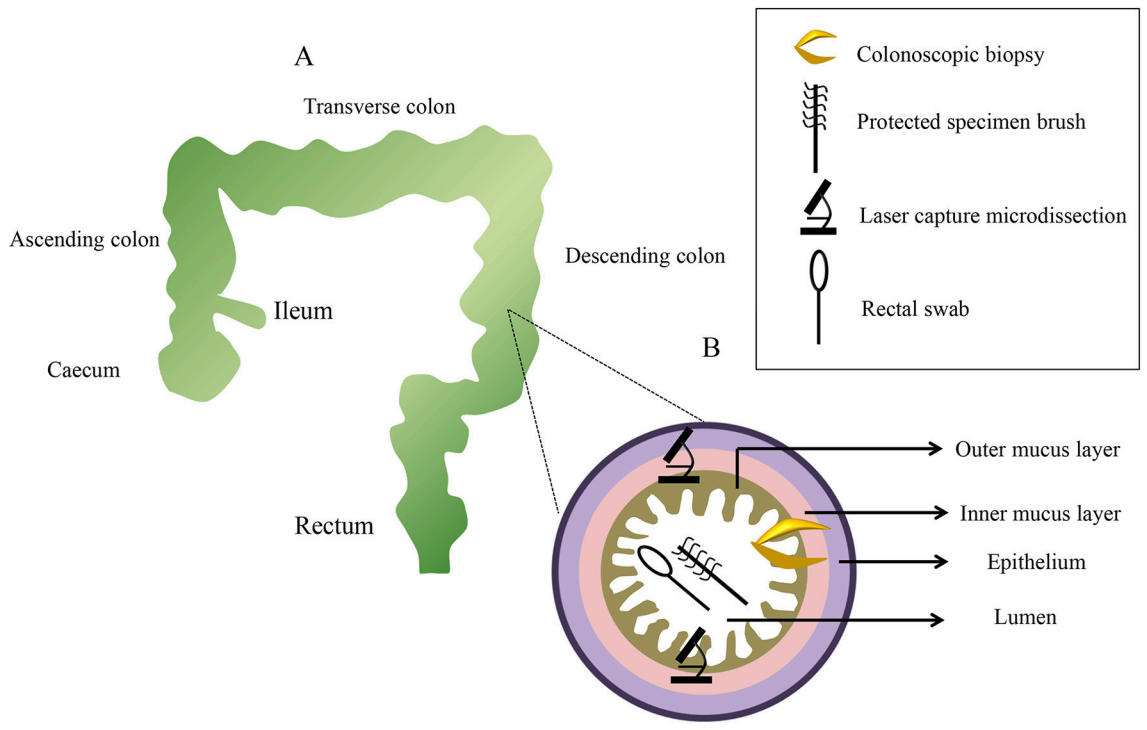

FIGURE 2 | A diagram of sampling sites distributed along the x-axis and z-axis with representative pictures from each sampling method. Colonoscopic biopsy samples are collect from six levels: the ileum, ascending colon, transverse colon, descending colon, rectum, and caecum **(A)**. Samplings of the mucus gel layer occur at six sections using three methods **(B)**.

which may bias 16S rRNA gene sequencing analysis (Carbonero et al., 2011). A microbiome DNA enrichment method might potentially yield a higher fraction of microbial production, which methylated the human genomic DNA to selectively separate from microbial DNA (Yigit et al., 2016).

As for the spatial community structures (ileum, ascending colon, transverse colon, descending colon, and rectum) of human mucosal-associated intestinal microbiota, spatial variations of mucosa-associated microbiota have not provided feasible explanations to account for the observed longitudinal variations along the intestine, despite the previously observed spatial heterogeneity of mucosa microbiota (Aguirre de Carcer et al., 2011; Hong et al., 2011). Single-species abundance–distance dispersion (ADD) modeling results indicated that it was impossible to use conventional multivariate analysis methods to describe spatial heterogeneity and co-relationships across the multiple loci of microbial communities. The co-occurrence network analysis (Barberan et al., 2012) revealed a huge specialization among vertical and lateral gradients, and it addressed how interpersonal variation was a significant constituent of variance, particularly in light of the fact that the microbiota remains stable (Faust et al., 2012; Zhang et al., 2014). To reveal the longitudinal gradients in the microbiota along the x-axis distribution, studies may need to develop suitable statistical models and bioinformatics software.

SAMPLING SITES DISTRIBUTED ALONG THE Z-AXIS

Mucus Gel Layer

Secreted by goblet cells that reside in intestinal crypts, the colonic MGL partially or entirely covers the epithelium and creates a boundary between the lumen and the host mucosa. Mucus is subsequently secreted and the layers fall off, generating a "district" that is carried into the fecal stream (Swidsinski et al., 2008b). The mucus is continuously secreted and can be divided into two layers: an outer, loosely adherent layer that can be removed by suction or gentle scraping; and an inner, firmly stratified layer that adheres to the epithelial cells (Atuma et al., 2001). In mouse models, the thickness of both MGL layers is appropriately estimated at 150 μm, with the outer layer measured at 100 μm and the inner layer at 50 μm (Johansson et al., 2008). The thickness of the human MGL is thought to be between 107 and 155 μm, depending on the loci (Pullan et al., 1994). Both layers are made up of MUC2-type mucin (Johansson et al., 2008). In healthy individuals, the inner layer is devoid of bacteria, while the outer layer serves as a habitat for the commensal microbiota (Hansson and Johansson, 2010; Johansson et al., 2011). The architecture of MGL exhibits a diverse range of polymers, including the mucus-binding protein (MUP), which offers numerous binding locations for both pathogenic and commensal bacteria (MacKenzie et al., 2009; Alemka et al., 2012). Some commensal bacteria are able to bind to and degrade the MUP, and they can be utilized as a barrier to pathogen binding. Mucin degradation of the MLG provides nutrients for some commensals, and it may initiate the initiation of pathogen invasion (Lennon et al., 2014b). As a result, the MGL plays a double role, providing a mutually beneficial environment for the host cells and resident microbiota, while serving as the first line of defense against pathogen bacteria translocating into the mucosa (see **Figure 3**). In IBD, bacteria are allowed to penetrate the inner MGL and reach the epithelium, triggering an inflammatory response; this suggests that the barriers of MUC2, with the absence of the MUC2 mucin polymer constituent, are disturbed, resulting in inflammatory responses (Schultsz et al., 1999; Swidsinski et al., 2007; Johansson et al., 2014).

On the basis of the aforementioned biological mechanism, identification of the mucus-degrading bacteria in the MGL is crucial. Conventionally, the MGL isolated from the precise fixation of intestinal biopsies or tissues, where dehydrating aldehyde fixatives are used, can result in loss and detachment of the mucus. Matsuo (Matsuo et al., 1997) demonstrated that using Carnoy's solution can preserve the integrity of surface mucus in paraffin sections of human colon specimens. Recent developments in overcoming this experimental limitation have achieved great success. Here, we describe three main sampling methods: rectal swab, the microbiologically protected specimen brush, and LCM. The vivid cross-sectional organization of each sampling method can be seen in **Figure 2B**.

Rectal Swab

As a simple, standardized, non-invasive, and inexpensive method, rectal swab represents an important contribution when the patient does not wish to handle feces or undergo the discomfort and inconvenience of colonoscopy. A swab-sucked microbiota is reproducible, and the procedure can be performed by either the patient at home or by medical professionals in clinical settings; thus, this method may be suitable for clinical diagnostic purposes and clinical studies (Budding et al., 2014). Rectal swabs aim at collecting the colorectal mucus (Braun et al., 2009). Rectal swab specimens can be easily handled and stored immediately without perturbation of the microbiota. Swab specimens are obtained about 1–2 cm from the anal verge and collected by inserting a sterile cotton-tipped swab. This pioneering work suggested that swab sampling, without previous bowel preparation, harvested undisturbed microbiota (Budding et al., 2014). The swab was inserted into sterile PBS shaken for at least 2 min to ensure the sufficient release of microbiota, and the samples were then stored at −80°C until DNA isolation (Araújopérez et al., 2012); conversely, the samples could also be placed in tubes containing 500 mL of Reduced Transport Fluid buffer and maintained at room temperature for 2 h prior to storage at −20°C until DNA isolation (Syed and Loesche, 1972; Budding et al., 2014). For DNA isolation, the bead-beating step may have a negative effect on the estimated abundance of *Bacteroidetes* (Budding et al., 2014). DNA extraction kits can use the QIAamp DNA Mini Kit (Qiagen, Hilden, Germany) or Qiagen's DNeasy Blood and Tissue Kit (Araújopérez et al., 2012; Budding et al., 2014).

Previous work that has analyzed T-RFLP profiles and quantitative PCR (qPCR) has highlighted the differences in community diversity between samples obtained by biopsy or swab, and it was found that a higher abundance of *Lactobacillus*

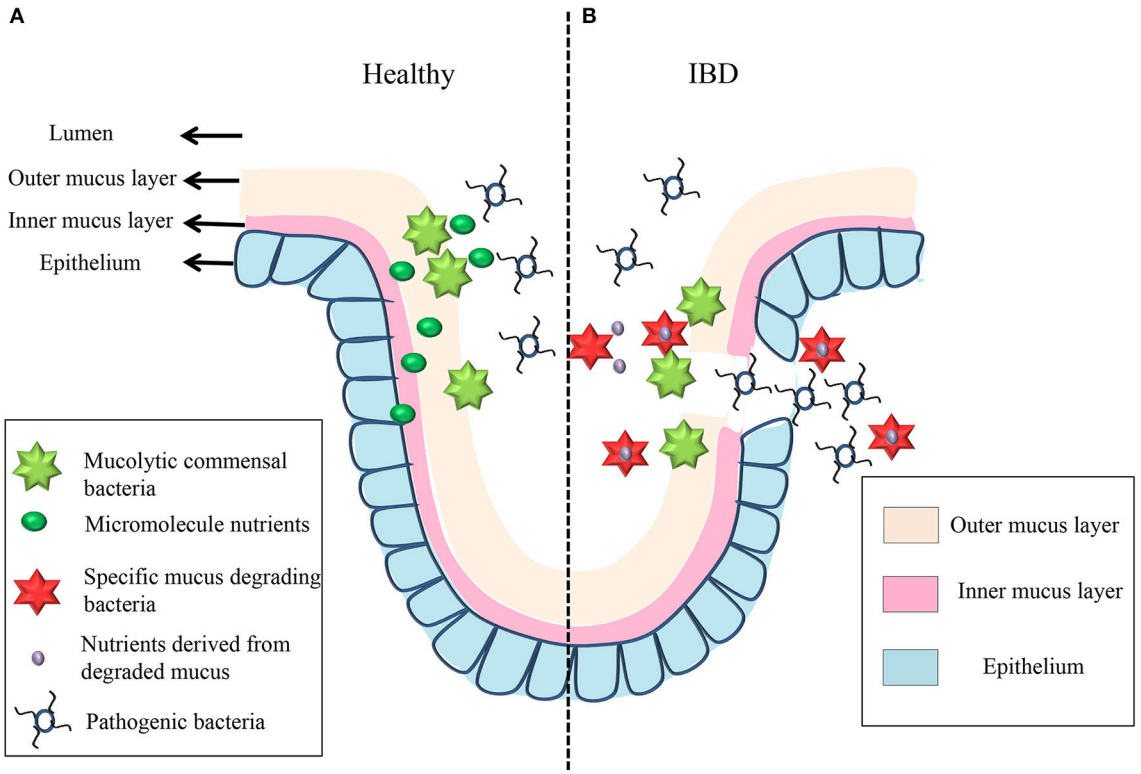

FIGURE 3 | The mechanism underlying mucin degradation in healthy individual and IBD patient. In healthy individual, some commensal bacteria can bind to the outer mucus gel layer and act as a defensive barrier to resist pathogenic bacteria. At the same time, some short-chain fatty acids get through the mucus gel layers and epithelium to provide energy for mucus degradation, which is the first barrier between the lumen and the mucosa **(A)**. When inflammation occurs in IBD patient, some oligosaccharides derived from the degraded mucus offer energy to the mucus-degrading bacteria (like *Rumminococcus gnavus* and *Rumminococcus torques*); then, the invading bacteria change the mucus gel layer's structure, and pathogenic bacteria are now able to bind to and degrade the structure of the layers and invade the epithelium **(B)**.

and *Eubacteria* were present in the swab specimens when compared with biopsies (Araújopérez et al., 2012). It was also previously demonstrated that *Staphylococcus aureus*, a dominant skin bacteria, could be used to assess the level of skin contamination between swabs and biopsies (Araújopérez et al., 2012). With respect to spatial organization, the fecal samples and swabs seemed to harbor more or less distinct diversity (Budding et al., 2014). One study revealed that the microbiota obtained by rectal biopsy and swab showed a greater similarity to one another than to feces (Glover et al., 2013). The diagnoses that are usually based on culture or NAAT on rectal swabs are widely utilized to distinguish between *Chlamydia* proctitis and CD (Hoentjen and Rubin, 2012). To prevent disturbances, from occurring, harvesting samples through a sheathed swab might lower the level of contamination by the skin and luminal microbiota in further studies.

Microbiological Protected Specimen Brush

In recent research, a specimen brush was often applied to sample the human lung microbiota (Dickson et al., 2015; Schmidlin et al., 2015; Hogan et al., 2016; Sibila et al., 2016). Inspired by these investigations, Lavelle and colleagues (Lavelle et al., 2013) developed a novel sampling technique using the microbiological PSB for spatial microbial assessment; they targeted the superficial MGL from the luminal side, as it can fold over the light mucosa and avoid pools of fluid. Structurally, when compared with rectal swabs, this brush also targets an outer, colonized mucus layer that becomes separated from the epithelium via a dense layer of removable mucus. As a sterile, single–use sampling method, the brush is covered with a sheath, which consists of a distal plug at the tip to seal the brush when introducing and retracting the brush through the colonoscopy channel. After collecting the specimen, a sterile wire cutter is used to separate the tip of the wire and the plug, and the sample is then placed in a sterile, nuclease–free container until DNA extraction. The Qiagen DNA Mini Kit is frequently employed to extract DNA. The qPCR confirmed that the increased proportion of microbial DNA is sampled in the brush when compared with biopsy samples. Based on the 16S rRNA gene, the analysis of similarity analyses illustrated that there was a similar and highly significant difference between the PSB and biopsy samples, as well as between the Shannon Diversity Index values for reduced diversity in brush samples when compared to the biopsy samples (Lavelle et al., 2013).

Laser Capture Microdissection

Developed at the National Institutes of Health (Emmert-Buck et al., 1996), LCM is a systemic technique whereby individual DNA, RNA, and proteins can be sampled from the gut tissue by fixing targeted cells to an adhesive film with a laser beam; they are then observed under the microscope (Zhang et al., 2016b). LCM is a powerful method used to directly isolate pure sections from complex tissues with greater rapidity, specificity, and precision. This method does not require specific markers for identification, either prior to or after isolation, which is in contrast to rectal swabs and the microbiological PSB. To get at the MGL, researchers used LCM in healthy subjects undergoing a clinical routine colonoscopy, as well as in UC patients undergoing proctocolectomy for sampling (Lavelle et al., 2015), as based on the PALM MicroBeam system (Rowan et al., 2010a). Specifically, some researchers combined LCM and PCR to isolate and count the total amount of some mucosa-adherent bacteria, such as *Desulfovibrio* copies in the mucous gel of UC patients (Rowan et al., 2010a; Lennon et al., 2014a), as well as adherent–invasive *E. coli* from the macrophages of CD patients (Elliott et al., 2015). Given that *Mycobacterium avium subsp paratuberculosis* micro-organisms are few in number when present in CD patients, LCM was used to overcome this issue by accurately isolating subepithelial tissue, thus preventing contamination from the lumen (Ryan et al., 2002). Significant variations were observed between the colonic crypts and the central luminal compartment in mouse models, which used LCM to specifically profile the composition of the microbial communities in a discontinuous locus (Nava et al., 2011; Pedron et al., 2012). As a result, the study of colonic crypt mucus in UC patients, using LCM-harvested specimens, found that these patients had a lower abundance of crypt-associated bacteria than controls (Rowan et al., 2010b). Studies using LCM have placed standard and systemic histological sections of stained tissue under a microscope, and subsequently visualized the MGL of interest (Lennon et al., 2014a; Lavelle et al., 2015). Using a joystick to navigate around the image, researchers simply pushed a button to transfer the desired pure cells of the heterogeneous tissue to each slide to yield an average sample area of 175 mm^2. Then, the LCM-harvested productions were catapulted onto an inverted opaque AdhesiveCap. As a targeted and specific quantified sampling method, LCM is suitable for research in precision medicine.

CONCLUSION

As is well-known, suitable sampling strategies play an important role when studying the full landscape of intestinal microbiota. Here, this review highlighted the biogeographically stratified sampling strategies used in IBD, and it simultaneously proposed a novel three-dimensional spatial model of different community structures. Across these sampling sites, the non-invasive nature of fecal sampling can be implemented on a large scale as a screening or follow-up tool. However, feces are comprised of a mixture of products from all intestinal regions, which may not reflect the true nature of host–bacterial interactions in different biogeographic locations (Swidsinski et al., 2008b). Compared with fecal sampling, standard colonoscopy biopsy sample is sufficient to assess mucosal microbiota, which might affect mucosal and epithelial function to a greater degree than fecal sampling, as mucosal microbiota has a closer contact with immune cells and epithelial cells (Sartor, 2015). Furthermore, biopsy samples can be captured from specific regions ranging from the caecum to the rectum. These deep strengths notwithstanding, biopsy collection requires streamlining the logistics for sampling with nurses, physicians, and endoscopy technicians in advance to decrease the patients' time under sedation (Tong et al., 2014). The microbial profiles have indicated that at the early stage of disease, assessing rectal biopsy microbiota offered particular potential for convenient and early diagnosis of CD (Gevers et al., 2014). Particularly, in mouse studies, both tissue and feces sampling allowed targeted analyses of microbial under tractable and reproducible conditions. Fecal samplings could timely process feces to study the diversity of intestinal microbiota, varying in time (Zackular et al., 2013; Zhang et al., 2016a). Meanwhile, fecal pellets could also be collected from sacrificed mouse across different anatomical sites which often utilized caecal and colon contents (Bibiloni et al., 2005; Gaudier et al., 2005; Mishiro et al., 2013). Sometimes, the luminal content were flushed together by injecting PBS and then collected (Berry et al., 2012). The mucosa-associated microbiome is sampled by washing with PBS to remove the fecal contents then releasing epithelial cells (containing mucosal microbes) from the intestine tissue with mechanical means (Nagalingam et al., 2011; Tong et al., 2014). Specifically, LCM could specifically sample microbes that were located in the particular parts of mucosa (Nava et al., 2011). Evaluation of microbial community composition revealed striking differences between feces and tissues. The comparison between dextran sulfate sodium (DSS)-colitis mouse and controls showed that the 16S rDNA content (bacterial) was significantly decreased in feces but increased in mucosa, exhibiting the same trend as 18S rDNA (fungal; Qiu et al., 2015).

Coupled with the luminal microbiota, researchers have demonstrated that when using the MGL and entire mucosal biopsies, there is spatial variation in the intestinal microbiota, particularly among different community niches in UC patients (Lavelle et al., 2015). Moreover, human swab and colon biopsy samples have revealed that the mucosal diversity is prominent and enriched, particularly among the species from the phyla *Proteobacteria* and *Actinobacteria*, and when compared with the fecal microbiota (Albenberg et al., 2014). Zhou (Zhou et al., 2013) characterized the microbial variation between different community niches using a Dirichlet–Multinomial Distribution model, which concluded that feces and oral samples had the lowest interpersonal variability across the studied body sites studied in terms of community structure. To further illustrate this point, it has been reported that the numbers of bacteria in the *Clostridium coccoides* group remained stable in both feces and saliva over time (Singhal et al., 2011). Stearns et al. (2011) sampled species across the human digestive tract, including from feces, the stomach, colon, duodenum, and oral cavity, and illustrated that the oral cavity harbored the greatest phylogenetic

diversity. Predictably, the oral microbiota holds great potential with respect to clinical and diagnostic utility.

Specific to mucosal biopsies and the MGL, there should be heterogeneity in the mucosal species that exist along cross-sectional and longitudinal axes of the bowel within specific individuals. However, due to the masking of a high level of individual variation, significant differences across longitudinal variations were not discovered by analysis of variance (ANOVA) (Zhang et al., 2014). Employing a multidisciplinary approach (such as by investigating ecological relationships and performing co-occurrence network analysis) may lift this mask of spatial variation to uncover the truth in prospective studies (Zhang et al., 2014). Specific to our study, we are devoted to developing statistical models to show the informative value of microbial biogeography in IBD research.

Traditional protocols are currently limited by the present difficulties associated with comprehensively evaluating the microbiota in IBD research. Such difficulties include fastidious experimental requirements and sampling errors. Therefore, it is critical that risk-free, standardized, simpler, and inexpensive sampling strategies be formulated in the future. To study potential contributions of the microbiota in IBD research, we should standardize the SOPs and reach a consensus that better facilitates our understanding of these methods in subsequent studies. Moreover, data should be exchanged and further studies should be designed in which we evaluate the microbiota within those individuals at the early stages of IBD. To construct a full picture of the microbial diversity in IBD research, synergistic profiles, combined with a co-culture consortium that can study bacteria, will be necessary. Comprehensively, it should be stated that a mutually beneficial cooperative effort can be achieved, but only if data on these methods are shared all over the world.

AUTHOR CONTRIBUTIONS

SZ wrote the paper; XC and HH performed the collected the data. All authors listed, have made substantial, direct and intellectual contribution to the work, and approved it for publication.

ACKNOWLEDGMENTS

This work was supported by National High Technology Research and Development Program of China, No. 2015AA020701 and National Natural Science Foundation of China, No. 31470967. China Alliance of Inflammatory Bowel Disease, Wu Jie Ping Medical Foundation, No. 2017001.

REFERENCES

Abubucker, S., Segata, N., Goll, J., Schubert, A. M., Izard, J., Cantarel, B. L., et al. (2012). Metabolic reconstruction for metagenomic data and its application to the human microbiome. *PLoS Comput. Biol.* 8:e1002358. doi: 10.1371/journal.pcbi.1002358

Agossa, K., Dendooven, A., Dubuquoy, L., Gower-Rousseau, C., Delcourt-Debruyne, E., and Capron, M. (2016). Periodontal manifestations of inflammatory bowel disease: emerging epidemiologic and biologic evidence. *J. Periodont. Res.* doi: 10.1111/jre.12422. [Epub ahead of print].

Aguirre, M., and Venema, K. (2015). The use of fecal samples for studying human obesity. *Eur. J. Epidemiol.* 30, 1067–1069. doi: 10.1007/s10654-015-0048-z

Aguirre de Carcer, D., Cuiv, P. O., Wang, T., Kang, S., Worthley, D., Whitehall, V., et al. (2011). Numerical ecology validates a biogeographical distribution and gender-based effect on mucosa-associated bacteria along the human colon. *ISME J.* 5, 801–809. doi: 10.1038/ismej.2010.177

Albenberg, L., Esipova, T. V., Judge, C. P., Bittinger, K., Chen, J., Laughlin, A., et al. (2014). Correlation between intraluminal oxygen gradient and radial partitioning of intestinal microbiota. *Gastroenterology* 147, 1055–1063.e8. doi: 10.1053/j.gastro.2014.07.020

Alemka, A., Corcionivoschi, N., and Bourke, B. (2012). Defense and adaptation: the complex inter-relationship between *Campylobacter jejuni and mucus*. *Front. Cell. Infect. Microbiol.* 2:15. doi: 10.3389/fcimb.2012.00015

Andoh, A., Kuzuoka, H., Tsujikawa, T., Nakamura, S., Hirai, F., Suzuki, Y., et al. (2012). Multicenter analysis of fecal microbiota profiles in Japanese patients with Crohn's disease. *J. Gastroenterol.* 47, 1298–1307. doi: 10.1007/s00535-012-0605-0

Angelakis, E., and Lagier, J. C. (2016). Samples and techniques highlighting the links between obesity and microbiota. *Microb. Pathog.* doi: 10.1016/j.micpath.2016.01.024. [Epub ahead of print].

Anonymous (2013). Microbiology: extracting microbial function from phylogeny. *Nat. Meth.* 10, 934. doi: 10.1038/nmeth.2670

Araújopérez, F., McCoy, A. N., Okechukwu, C., Carroll, I. M., Smith, K. M., Jeremiah, K., et al. (2012). Differences in microbial signatures between rectal mucosal biopsies and rectal swabs. *Gut Microbes* 3, 530–535. doi: 10.4161/gmic.22157

Ariefdjohan, M. W., Savaiano, D. A., and Nakatsu, C. H. (2010). Comparison of DNA extraction kits for PCR-DGGE analysis of human intestinal microbial communities from fecal specimens. *Nutr. J.* 9:23. doi: 10.1186/1475-2891-9-23

Arumugam, M., Raes, J., Pelletier, E., Le Paslier, D., Yamada, T., Mende, D. R., et al. (2011). Enterotypes of the human gut microbiome. *Nature* 473, 174–180. doi: 10.1038/nature09944

Atuma, C., Strugala, V., Allen, A., and Holm, L. (2001). The adherent gastrointestinal mucus gel layer: thickness and physical state *in vivo*. *Am. J. Physiol. Gastrointest. Liver Physiol.* 280, G922–G929.

Bahl, M. I., Bergstrom, A., and Licht, T. R. (2012). Freezing fecal samples prior to DNA extraction affects the Firmicutes to Bacteroidetes ratio determined by downstream quantitative PCR analysis. *FEMS Microbiol. Lett.* 329, 193–197. doi: 10.1111/j.1574-6968.2012.02523.x

Barberan, A., Bates, S. T., Casamayor, E. O., and Fierer, N. (2012). Using network analysis to explore co-occurrence patterns in soil microbial communities. *ISME J.* 6, 343–351. doi: 10.1038/ismej.2011.119

Bennet, S. M., Ohman, L., and Simren, M. (2015). Gut microbiota as potential orchestrators of irritable bowel syndrome. *Gut Liver* 9, 318–331. doi: 10.5009/gnl14344

Berry, D., Kuzyk, O., Rauch, I., Heider, S., Schwab, C., Hainzl, E., et al. (2015). Intestinal microbiota signatures associated with inflammation history in mice experiencing recurring colitis. *Front. Microbiol.* 6:1408. doi: 10.3389/fmicb.2015.01408

Berry, D., Schwab, C., Milinovich, G., Reichert, J., Ben Mahfoudh, K., Decker, T., et al. (2012). Phylotype-level 16S rRNA analysis reveals new bacterial indicators of health state in acute murine colitis. *ISME J.* 6, 2091–2106. doi: 10.1038/ismej.2012.39

Bibiloni, R., Simon, M. A., Albright, C., Sartor, B., and Tannock, G. W. (2005). Analysis of the large bowel microbiota of colitic mice using PCR/DGGE. *Lett. Appl. Microbiol.* 41, 45–51. doi: 10.1111/j.1472-765X.2005.01720.x

Biedermann, L., Zeitz, J., Mwinyi, J., Sutter-Minder, E., Rehman, A., Ott, S. J., et al. (2013). Smoking cessation induces profound changes in the composition of the intestinal microbiota in humans. *PLoS ONE* 8:e59260. doi: 10.1371/journal.pone.0059260

Boers, S. A., Jansen, R., and Hays, J. P. (2016). Suddenly everyone is a microbiota specialist! *Clin. Microbiol. Infect.* 227, 581–582. doi: 10.1016/j.cmi.2016.05.002

Braun, A., Treede, I., Gotthardt, D., Tietje, A., Zahn, A., Ruhwald, R., et al. (2009). Alterations of phospholipid concentration and species composition of the intestinal mucus barrier in ulcerative colitis: a clue to pathogenesis. *Inflamm. Bowel Dis.* 15, 1705–1720. doi: 10.1002/ibd.20993

Brito, F., Zaltman, C., Carvalho, A. T., Fischer, R. G., Persson, R., Gustafsson, A., et al. (2013). Subgingival microflora in inflammatory bowel disease patients

with untreated periodontitis. *Eur. J. Gastroenterol. Hepatol.* 25, 239–245. doi: 10.1097/MEG.0b013e32835a2b70

Bruno, D., and Isabelle, L. B. (2015). *Mycobacterium avium Paratuberculosis* (MAP) and Cytomegalovirus (CMV) are frequently detected in the saliva of patients recently diagnosed with Crohn Disease (CD) Whereas Oral Propionibacterium Acnes (PA) or Methylacetate (MA) in their breath is rare. *J. Biosci. Med.* 03, 13–18. doi: 10.4236/jbm.2015.312003

Budding, A. E., Grasman, M. E., Eck, A., Bogaards, J. A., Vandenbroucke-Grauls, C. M., van Bodegraven, A. A., et al. (2014). Rectal swabs for analysis of the intestinal microbiota. *PLoS ONE* 9:e101344. doi: 10.1371/journal.pone.0101344

Caporaso, J. G., Kuczynski, J., Stombaugh, J., Bittinger, K., Bushman, F. D., Costello, E. K., et al. (2010). QIIME allows analysis of highthroughput community sequencing data. *Nat. Methods* 7, 335–336. doi: 10.1038/nmeth.f.303

Carbonero, F., Nava, G. M., Benefiel, A. C., Greenberg, E., and Gaskins, H. R. (2011). Microbial DNA extraction from intestinal biopsies is improved by avoiding mechanical cell disruption. *J. Microbiol. Methods* 87, 125–127. doi: 10.1016/j.mimet.2011.07.014

Cardona, S., Eck, A., Cassellas, M., Gallart, M., Alastrue, C., Dore, J., et al. (2012). Storage conditions of intestinal microbiota matter in metagenomic analysis. *BMC Microbiol.* 12:158. doi: 10.1186/1471-2180-12-158

Carroll, I. M., Ringel-Kulka, T., Siddle, J. P., Klaenhammer, T. R., and Ringel, Y. (2012). Characterization of the fecal microbiota using high-throughput sequencing reveals a stable microbial community during storage. *PLoS ONE* 7:e46953. doi: 10.1371/journal.pone.0046953

Chen, L., Wang, W., Zhou, R., Ng, S. C., Li, J., Huang, M., et al. (2014). Characteristics of fecal and mucosa-associated microbiota in Chinese patients with inflammatory bowel disease. *Medicine* 93:e51. doi: 10.1097/MD.0000000000000051

Chiodini, R. J., Dowd, S. E., Davis, B., Galandiuk, S., Chamberlin, W. M., Kuenstner, J. T., et al. (2013). Crohn's disease may be differentiated into 2 distinct biotypes based on the detection of bacterial genomic sequences and virulence genes within submucosal tissues. *J. Clin. Gastroenterol.* 47, 612–620. doi: 10.1097/MCG.0b013e31827b4f94

Choi, J. H., Kim, E. S., Cho, K. B., Park, K. S., Lee, Y. J., Lee, S. M., et al. (2015). Old age at diagnosis is associated with favorable outcomes in korean patients with inflammatory bowel disease. *Intest. Res.* 13, 60–67. doi: 10.5217/ir.2015.13.1.60

Chung, H. K., Tay, A., Octavia, S., Chen, J., Liu, F., Ma, R., et al. (2016). Genome analysis of *Campylobacter concisus* strains from patients with inflammatory bowel disease and gastroenteritis provides new insights into pathogenicity. *Sci. Rep.* 6:38442. doi: 10.1038/srep38442

Claassen, S., du Toit, E., Kaba, M., Moodley, C., Zar, H. J., and Nicol, M. P. (2013). A comparison of the efficiency of five different commercial DNA extraction kits for extraction of DNA from faecal samples. *J. Microbiol. Methods* 94, 103–110. doi: 10.1016/j.mimet.2013.05.008

Clarridge, J. E. (2004). Impact of 16S rRNA gene sequence analysis for identification of bacteria on clinical microbiology and infectious diseases. *Clin. Microbiol. Rev.* 17, 840–862. doi: 10.1128/CMR.17.4.840-862.2004

Connelly, T. M., Berg, A. S., Harris, L. III, Brinton, D., Deiling, S., and Koltun, W. A. (2015). Genetic determinants associated with early age of diagnosis of IBD. *Dis. Colon Rectum* 58, 321–327. doi: 10.1097/DCR.0000000000000274

Costello, E. K., Lauber, C. L., Hamady, M., Fierer, N., Gordon, J. I., and Knight, R. (2009). Bacterial community variation in human body habitats across space and time. *Science* 326, 1694–1697. doi: 10.1126/science.1177486

Crohn, B. B., Ginzburg, L., and Oppenheimer, G. D. (1932). Regional ileitis: a pathologic and clinical entity. *J. Am. Med. Assoc.* 99, 1323–1329. doi: 10.1001/jama.1932.02740680019005

Dave, M., Johnson, L. A., Walk, S. T., Young, V. B., Stidham, R. W., Chaudhary, M. N., et al. (2011). A randomised trial of sheathed versus standard forceps for obtaining uncontaminated biopsy specimens of microbiota from the terminal ileum. *Gut* 60, 1043–1049. doi: 10.1136/gut.2010.224337

De Cruz, P., Kang, S., Wagner, J., Buckley, M., Sim, W. H., Prideaux, L., et al. (2015). Association between specific mucosa-associated microbiota in Crohn's disease at the time of resection and subsequent disease recurrence: a pilot study. *J. Gastroenterol. Hepatol.* 30, 268–278. doi: 10.1111/jgh.12694

Demmer, R. T., Breskin, A., Rosenbaum, M., Zuk, A., LeDuc, C., Leibel, R., et al. (2016). The subgingival microbiome, systemic inflammation and insulin resistance: the oral infections, glucose intolerance and insulin resistance study. *J. Clin. Periodontol.* doi: 10.1111/jcpe.12664.[Epub ahead of print].

DeSantis, T. Z., Hugenholtz, P., Larsen, N., Rojas, M., Brodie, E. L., Keller, K., et al. (2006). Greengenes, a chimera-checked 16S rRNA gene database and workbench compatible with ARB. *Appl. Environ. Microbiol.* 72, 5069–5072. doi: 10.1128/AEM.03006-05

Dickson, R. P., Erb-Downward, J. R., Freeman, C. M., McCloskey, L., Beck, J. M., Huffnagle, G. B., et al. (2015). Spatial variation in the healthy human lung microbiome and the adapted island model of lung biogeography. *Ann. Am. Thorac. Soc.* 12, 821–830. doi: 10.1513/AnnalsATS.201501-029OC

Dobell, C. (1932). *Antony van Leeuwenhoek and his" Little Animals." Being Some Account of the Father of Protozoology and Bacteriology and his Multifarious Discoveries in these Disciplines. Collected, Translated, and Edited, from his Printed Works, Unpublished Manuscripts, and Contemporary Records.* Published on the 300th Anniversary of his Birth.

Docktor, M. J., Paster, B. J., Abramowicz, S., Ingram, J., Wang, Y. E., Correll, M., et al. (2012). Alterations in diversity of the oral microbiome in pediatric inflammatory bowel disease. *Inflamm. Bowel Dis.* 18, 935–942. doi: 10.1002/ibd.21874

Eckburg, P. B., Bik, E. M., Bernstein, C. N., Purdom, E., Dethlefsen, L., Sargent, M., et al. (2005). Diversity of the human intestinal microbial flora. *Science* 308, 1635–1638. doi: 10.1126/science.1110591

Egerton, F. N. (2006). A history of the ecological sciences part 19: leeuwenhoek's microscopic natural history. *Bull. Ecol. Soc. Am.* 88, 47–58. doi: 10.1890/0012-9623(2006)87[47:AHOTES]2.0.CO;2

Elburki, M. S. (2015). Periodontal disease and potential association with systemic diseases and conditions (Mini-review). *Appl. Clin. Res. Clin. Trials Regul. Aff.* 2, 73–79. doi: 10.2174/2213476X03666151116174402

Elliott, T. R., Rayment, N. B., Hudspith, B. N., Hands, R. E., Taylor, K., Parkes, G. C., et al. (2015). Lamina propria macrophage phenotypes in relation to *Escherichia coli* in Crohn's disease. *BMC Gastroenterol.* 15:75. doi: 10.1186/s12876-015-0305-3

Emmert-Buck, M. R., Bonner, R. F., Smith, P. D., Chuaqui, R. F., Zhuang, Z., Goldstein, S. R., et al. (1996). Laser capture microdissection. *Science* 274, 998–1001. doi: 10.1126/science.274.5289.998

Faith, J. J., Guruge, J. L., Charbonneau, M., Subramanian, S., Seedorf, H., Goodman, A. L., et al. (2013). The long-term stability of the human gut microbiota. *Science* 341:1237439. doi: 10.1126/science.1237439

Faust, K., Sathirapongsasuti, J. F., Izard, J., Segata, N., Gevers, D., Raes, J., et al. (2012). Microbial co-occurrence relationships in the human microbiome. *PLoS Comput. Biol.* 8:e1002606. doi: 10.1371/journal.pcbi.1002606

Gaudier, E., Michel, C., Segain, J. P., Cherbut, C., and Hoebler, C. (2005). The VSL 3 probiotic mixture modifies microflora but does not heal chronic dextran-sodium sulfate-induced colitis or reinforce the mucus barrier in mice. *J. Nutr.* 135, 2753–2761.

Fierer, N. (2008). "Microbial biogeography: patterns in microbial diversity across space and time," in *Accessing Uncultivated Microorganisms: From the Environment to Organisms and Genomes and Back*, ed K. Zengler (Washington, DC: ASM Press), 95–115. doi: 10.1128/9781555815509.ch6

Gevers, D., Kugathasan, S., Denson, L. A., Vazquez-Baeza, Y., Van Treuren, W., Ren, B., et al. (2014). The treatment-naive microbiome in new-onset Crohn's disease. *Cell Host Microbe* 15, 382–392. doi: 10.1016/j.chom.2014.02.005

Gill, S. R., Pop, M., Deboy, R. T., Eckburg, P. B., Turnbaugh, P. J., Samuel, B. S., et al. (2006). Metagenomic analysis of the human distal gut microbiome. *Science* 312, 1355–1359. doi: 10.1126/science.1124234

Glass, E. M., Wilkening, J., Wilke, A., Antonopoulos, D., and Meyer, F. (2010). Using the metagenomics RAST server (MG-RAST) for analyzing shotgun metagenomes. *Cold Spring Harb. Protoc.* 2010:pdb prot5368. doi: 10.1101/pdb.prot5368

Glover, L., Saeedi, B., Kelly, C., Campbell, E., Bayless, A., and Kominsky, D. (2013). O-017 HIF-mediated autophagy contributes to intestinal epithelial cell-intrinsic innate immune response against invasive bacteria. *Inflamm. Bowel Dis.* 19, S12. doi: 10.1097/01.MIB.0000438568.18012.49

Gorzelak, M. A., Gill, S. K., Tasnim, N., Ahmadi-Vand, Z., Jay, M., and Gibson, D. L. (2015). Methods for improving human gut microbiome data by reducing variability through sample processing and storage of stool. *PLoS ONE* 10:e0134802. doi: 10.1371/journal.pone.0134802

Gray, W. N., Boyle, S. L., Graef, D. M., Janicke, D. M., Jolley, C. D., Denson, L. A., et al. (2015). Health-related quality of life in youth with Crohn disease: role of disease activity and parenting stress. *J. Pediatr. Gastroenterol. Nutr.* 60, 749–753. doi: 10.1097/MPG.0000000000000696

Greenhill, C. (2015). Obesity: gut microbiota, host genetics and diet interact to affect the risk of developing obesity and the metabolic syndrome. *Nat. Rev. Endocrinol.* 11, 630. doi: 10.1038/nrendo.2015.152

Grice, E. A., Kong, H. H., Conlan, S., Deming, C. B., Davis, J., Young, A. C., et al. (2009). Topographical and temporal diversity of the human skin microbiome. *Science* 324, 1190–1192. doi: 10.1126/science.1171700

Group, N. H., Peterson, J., Garges, S., Giovanni, M., McInnes, P., Wang, L., et al. (2009). The NIH human microbiome project. *Genome Res.* 19, 2317–2323. doi: 10.1101/gr.096651.109

Hansen, R., Berry, S. H., Mukhopadhya, I., Thomson, J. M., Saunders, K. A., Nicholl, C. E., et al. (2013). The microaerophilic microbiota of de-novo paediatric inflammatory bowel disease: the BISCUIT study. *PLoS ONE* 8:e58825. doi: 10.1371/journal.pone.0058825

Hansson, G. C., and Johansson, M. E. (2010). The inner of the two Muc2 mucin-dependent mucus layers in colon is devoid of bacteria. *Gut Microbes* 1, 51–54. doi: 10.4161/gmic.1.1.10470

Harrell, L., Wang, Y., Antonopoulos, D., Young, V., Lichtenstein, L., Huang, Y., et al. (2012). Standard colonic lavage alters the natural state of mucosal-associated microbiota in the human colon. *PLoS ONE* 7:e32545. doi: 10.1371/journal.pone.0032545

Harty, S., Fleming, P., Rowland, M., Crushell, E., McDermott, M., Drumm, B., et al. (2005). A prospective study of the oral manifestations of Crohn's disease. *Clin. Gastroenterol. Hepatol.* 3, 886–891. doi: 10.1016/S1542-3565(05)00424-6

Hedin, C., van der Gast, C. J., Rogers, G. B., Cuthbertson, L., McCartney, S., Stagg, A. J., et al. (2016). Siblings of patients with Crohn's disease exhibit a biologically relevant dysbiosis in mucosal microbial metacommunities. *Gut* 65, 944–953. doi: 10.1136/gutjnl-2014-308896

Heintz-Buschart, A., May, P., Laczny, C. C., Lebrun, L. A., Bellora, C., Krishna, A., et al. (2016). Integrated multi-omics of the human gut microbiome in a case study of familial type 1 diabetes. *Nat. Microbiol.* 2:16180. doi: 10.1038/nmicrobiol.2016.180

Hildebrand, F., Tadeo, R., Voigt, A. Y., Bork, P., and Raes, J. (2014). LotuS: an efficient and user-friendly OTU processing pipeline. *Microbiome* 2:30. doi: 10.1186/2049-2618-2-30

Hoentjen, F., and Rubin, D. T. (2012). Infectious proctitis: when to suspect it is not inflammatory bowel disease. *Dig. Dis. Sci.* 57, 269–273. doi: 10.1007/s10620-011-1935-0

Hogan, D. A., Willger, S. D., Dolben, E. L., Hampton, T. H., Stanton, B. A., Morrison, H. G., et al. (2016). Analysis of lung microbiota in bronchoalveolar lavage, protected brush and sputum samples from subjects with mild-to-moderate cystic fibrosis lung disease. *PLoS ONE* 11:e0149998. doi: 10.1371/journal.pone.0149998

Hong, P. Y., Croix, J. A., Greenberg, E., Gaskins, H. R., and Mackie, R. I. (2011). Pyrosequencing-based analysis of the mucosal microbiota in healthy individuals reveals ubiquitous bacterial groups and micro-heterogeneity. *PLoS ONE* 6:e25042. doi: 10.1371/journal.pone.0025042

Hsieh, Y. H., Peterson, C. M., Raggio, A., Keenan, M. J., Martin, R. J., Ravussin, E., et al. (2016). Impact of different fecal processing methods on assessments of bacterial diversity in the human intestine. *Front. Microbiol.* 7:1643. doi: 10.3389/fmicb.2016.01643

Human Microbiome Project, C. (2012). Structure, function and diversity of the healthy human microbiome. *Nature* 486, 207–214. doi: 10.1038/nature11234

Ince, M. N., Blazar, B. R., Edmond, M. B., Tricot, G., and Wannemuehler, M. J. (2016). Understanding Luminal Microorganisms and Their Potential Effectiveness in Treating Intestinal Inflammation. *Inflamm. Bowel Dis.* 22, 194–201. doi: 10.1097/MIB.0000000000000599

Ismail, Y., Mahendran, V., Octavia, S., Day, A. S., Riordan, S. M., Grimm, M. C., et al. (2012). Investigation of the enteric pathogenic potential of oral *Campylobacter concisus* strains isolated from patients with inflammatory bowel disease. *PLoS ONE* 7:e38217. doi: 10.1371/journal.pone.0038217

Jalanka, J., Salonen, A., Salojarvi, J., Ritari, J., Immonen, O., Marciani, L., et al. (2015). Effects of bowel cleansing on the intestinal microbiota. *Gut* 64, 1562–1568. doi: 10.1136/gutjnl-2014-307240

Jeffery, I. B., Claesson, M. J., O'Toole, P. W., and Shanahan, F. (2012). Categorization of the gut microbiota: enterotypes or gradients? *Nat. Rev. Microbiol.* 10, 591–592. doi: 10.1038/nrmicro2859

Johansson, M. E. (2014). Mucus layers in inflammatory bowel disease. *Inflamm. Bowel Dis.* 20, 2124–2131. doi: 10.1097/MIB.0000000000000117

Johansson, M. E., Gustafsson, J. K., Holmen-Larsson, J., Jabbar, K. S., Xia, L., Xu, H., et al. (2014). Bacteria penetrate the normally impenetrable inner colon mucus layer in both murine colitis models and patients with ulcerative colitis. *Gut* 63, 281–291. doi: 10.1136/gutjnl-2012-303207

Johansson, M. E., Larsson, J. M., and Hansson, G. C. (2011). The two mucus layers of colon are organized by the MUC2 mucin, whereas the outer layer is a legislator of host-microbial interactions. *Proc. Natl. Acad .Sci. U.S.A.* 108(Suppl. 1), 4659–4665. doi: 10.1073/pnas.1006451107

Johansson, M. E., Phillipson, M., Petersson, J., Velcich, A., Holm, L., and Hansson, G. C. (2008). The inner of the two Muc2 mucin-dependent mucus layers in colon is devoid of bacteria. *Proc. Natl. Acad. Sci. U.S.A.* 105, 15064–15069. doi: 10.1073/pnas.0803124105

Jumpstart Consortium Human Microbiome Project Data Generation Working, G. (2012). Evaluation of 16S rDNA-based community profiling for human microbiome research. *PLoS ONE* 7:e39315. doi: 10.1371/journal.pone.0039315

Kelly, C. R., Kahn, S., Kashyap, P., Laine, L., Rubin, D., Atreja, A., et al. (2015). Update on fecal microbiota transplantation 2015: indications, methodologies, mechanisms, and outlook. *Gastroenterology* 149, 223–237. doi: 10.1053/j.gastro.2015.05.008

Kelsen, J., Bittinger, K., Pauly-Hubbard, H., Posivak, L., Grunberg, S., Baldassano, R., et al. (2015). Alterations of the subgingival microbiota in pediatric crohn's disease studied longitudinally in discovery and validation cohorts. *Inflamm. Bowel Dis.* 21, 2797–2805. doi: 10.1097/MIB.0000000000000557

Kelsen, J., Pauly-Hubbard, H., Posivak, L., Grunberg, S., Baldassano, R., Bittinger, K., et al. (2013). P-234 pediatric crohn's disease intrinsic associations with the subgingival microbiota revealed by a prospective longitudinal cohort study. *Inflamm. Bowel Dis.* 19, S118. doi: 10.1097/01.MIB.0000439032.28768.21

Kennedy, N. A., Walker, A. W., Berry, S. H., Duncan, S. H., Farquarson, F. M., Louis, P., et al. (2014). The impact of different DNA extraction kits and laboratories upon the assessment of human gut microbiota composition by 16S rRNA gene sequencing. *PLoS ONE* 9:e88982. doi: 10.1371/journal.pone.0088982

Kleessen, B., Kroesen, A. J., Buhr, H. J., and Blaut, M. (2002). Mucosal and invading bacteria in patients with inflammatory bowel disease compared with controls. *Scand. J. Gastroenterol.* 37, 1034–1041. doi: 10.1080/003655202320378220

Knip, M., and Siljander, H. (2016). The role of the intestinal microbiota in type 1 diabetes mellitus. *Nat. Rev. Endocrinol.* 12, 154–167. doi: 10.1038/nrendo.2015.218

Kolho, K. L., Korpela, K., Jaakkola, T., Pichai, M. V., Zoetendal, E. G., Salonen, A., et al. (2015). Fecal microbiota in pediatric inflammatory bowel disease and its relation to inflammation. *Am. J. Gastroenterol.* 110, 921–930. doi: 10.1038/ajg.2015.149

Kosiewicz, M. M., Zirnheld, A. L., and Alard, P. (2011). Gut microbiota, immunity, and disease: a complex relationship. *Front. Microbiol.* 2:180. doi: 10.3389/fmicb.2011.00180

Kostic, A. D., Xavier, R. J., and Gevers, D. (2014). The microbiome in inflammatory bowel disease: current status and the future ahead. *Gastroenterology* 146, 1489–1499. doi: 10.1053/j.gastro.2014.02.009

Kuczynski, J., Stombaugh, J., Walters, W. A., Gonzalez, A., Caporaso, J. G., and Knight, R. (2011). Using QIIME to analyze 16S rRNA gene sequences from microbial communities. *Curr. Protoc. Bioinformatics* Chapter 10, Unit 10 17. doi: 10.1002/0471250953.bi1007s36

Kuehbacher, T., Rehman, A., Lepage, P., Hellmig, S., Folsch, U. R., Schreiber, S., et al. (2008). Intestinal TM7 bacterial phylogenies in active inflammatory bowel disease. *J. Med. Microbiol.* 57(Pt. 12), 1569–1576. doi: 10.1099/jmm.0.47719-0

Langille, M. G., Zaneveld, J., Caporaso, J. G., McDonald, D., Knights, D., Reyes, J. A., et al. (2013). Predictive functional profiling of microbial communities using 16S rRNA marker gene sequences. *Nat. Biotechnol.* 31, 814–821. doi: 10.1038/nbt.2676

Lavelle, A., Lennon, G., Docherty, N., Balfe, A., Mulcahy, H. E., Doherty, G., et al. (2013). Depth-dependent differences in community structure of the human colonic microbiota in health. *PLoS ONE* 8:e78835. doi: 10.1371/journal.pone.0078835

Lavelle, A., Lennon, G., O'Sullivan, O., Docherty, N., Balfe, A., Maguire, A., et al. (2015). Spatial variation of the colonic microbiota in patients with ulcerative colitis and control volunteers. *Gut* 64, 1553–1561. doi: 10.1136/gutjnl-2014-307873

Lavelle, A., Lennon, G., Winter, D. C., and O'Connell, P. R. (2016). Colonic biogeography in health and ulcerative colitis. *Gut Microbes* 7, 435–442. doi: 10.1080/19490976.2016.1216748

Lee, T., Clavel, T., Smirnov, K., Schmidt, A., Lagkouvardos, I., Walker, A., et al. (2016). Oral versus intravenous iron replacement therapy distinctly alters the gut microbiota and metabolome in patients with IBD. *Gut*. doi: 10.1136/gutjnl-2015-309940. [Epub ahead of print].

Lennon, G., Balfe, A., Bambury, N., Lavelle, A., Maguire, A., Docherty, N. G., et al. (2014a). Correlations between colonic crypt mucin chemotype, inflammatory grade and Desulfovibrio species in ulcerative colitis. *Colorectal Dis.* 16, O161–O169. doi: 10.1111/codi.12503

Lennon, G., Balfe, A., Earley, H., Devane, L. A., Lavelle, A., Winter, D. C., et al. (2014b). Influences of the colonic microbiome on the mucous gel layer in ulcerative colitis. *Gut Microbes* 5, 277–285. doi: 10.4161/gmic.28793

Lepage, P., Seksik, P., Sutren, M., de la Cochetiere, M. F., Jian, R., Marteau, P., et al. (2005). Biodiversity of the mucosa-associated microbiota is stable along the distal digestive tract in healthy individuals and patients with IBD. *Inflamm. Bowel Dis.* 11, 473–480. doi: 10.1097/01.MIB.0000159662.62651.06

Liu, L., Li, Y., Li, S., Hu, N., He, Y., Pong, R., et al. (2012). Comparison of next-generation sequencing systems. *J. Biomed. Biotechnol.* 2012:251364. doi: 10.1155/2012/251364

Loman, N. J., Misra, R. V., Dallman, T. J., Constantinidou, C., Gharbia, S. E., Wain, J., et al. (2012). Performance comparison of benchtop high-throughput sequencing platforms. *Nat. Biotechnol.* 30, 434–439. doi: 10.1038/nbt.2198

Lozupone, C. A., Stombaugh, J. I., Gordon, J. I., Jansson, J. K., and Knight, R. (2012). Diversity, stability and resilience of the human gut microbiota. *Nature* 489, 220–230. doi: 10.1038/nature11550

Lyra, A., Forssten, S., Rolny, P., Wettergren, Y., Lahtinen, S. J., Salli, K., et al. (2012). Comparison of bacterial quantities in left and right colon biopsies and faeces. *World J. Gastroenterol.* 18, 4404–4411. doi: 10.3748/wjg.v18.i32.4404

Macfarlane, S. (2014). Antibiotic treatments and microbes in the gut. *Environ. Microbiol.* 16, 919–924. doi: 10.1111/1462-2920.12399

Maciel, S. S., Feres, M., Goncalves, T. E., Zimmermann, G. S., da Silva, H. D., Figueiredo, L. C., et al. (2016). Does obesity influence the subgingival microbiota composition in periodontal health and disease? *J. Clin. Periodontol.* 43, 1003–1012. doi: 10.1111/jcpe.12634

Mackenzie, B. W., Waite, D. W., and Taylor, M. W. (2015). Evaluating variation in human gut microbiota profiles due to DNA extraction method and inter-subject differences. *Front. Microbiol.* 6, 130. doi: 10.3389/fmicb.2015.00130

MacKenzie, D. A., Tailford, L. E., Hemmings, A. M., and Juge, N. (2009). Crystal structure of a mucus-binding protein repeat reveals an unexpected functional immunoglobulin binding activity. *J. Biol. Chem.* 284, 32444–32453. doi: 10.1074/jbc.M109.040907

Mahendran, V., Tan, Y. S., Riordan, S. M., Grimm, M. C., Day, A. S., Lemberg, D. A., et al. (2013). The prevalence and polymorphisms of zonula occluden toxin gene in multiple *Campylobacter concisus* strains isolated from saliva of patients with inflammatory bowel disease and controls. *PLoS ONE* 8:e75525. doi: 10.1371/journal.pone.0075525

Manichanh, C., Borruel, N., Casellas, F., and Guarner, F. (2012). The gut microbiota in IBD. *Nat. Rev. Gastroenterol. Hepatol.* 9, 599–608. doi: 10.1038/nrgastro.2012.152

Mark Welch, J. L., Rossetti, B. J., Rieken, C. W., Dewhirst, F. E., and Borisy, G. G. (2016). Biogeography of a human oral microbiome at the micron scale. *Proc. Natl. Acad. Sci. U.S.A.* 113, 201522149. doi: 10.1073/pnas.1522149113

Matsuo, K., Ota, H., Akamatsu, T., Sugiyama, A., and Katsuyama, T. (1997). Histochemistry of the surface mucous gel layer of the human colon. *Gut* 40, 782–789. doi: 10.1136/gut.40.6.782

McInnes, P., and Cutting, M. (2010). *Manual of Procedures for Human Microbiome Project: Core Microbiome Sampling, Protocol A, HMP Protocol no. 07–001, version 11. 2010*, Bethesda, MD.

Minamoto, Y., Otoni, C. C., Steelman, S. M., Buyukleblebici, O., Steiner, J. M., Jergens, A. E., et al. (2015). Alteration of the fecal microbiota and serum metabolite profiles in dogs with idiopathic inflammatory bowel disease. *Gut Microbes* 6, 33–47. doi: 10.1080/19490976.2014.997612

Mishiro, T., Kusunoki, R., Otani, A., Ansary, M. M., Tongu, M., Harashima, N., et al. (2013). Butyric acid attenuates intestinal inflammation in murine DSS-induced colitis model via milk fat globule-EGF factor 8. *Lab. Invest.* 93, 834–843. doi: 10.1038/labinvest.2013.70

Molodecky, N. A., Soon, I. S., Rabi, D. M., Ghali, W. A., Ferris, M., Chernoff, G., et al. (2012). Increasing incidence and prevalence of the inflammatory bowel diseases with time, based on systematic review. *Gastroenterology* 142, 46–54 e42; quiz e30. doi: 10.1053/j.gastro.2011.10.001

Moore, W. E., and Holdeman, L. V. (1974). Special problems associated with the isolation and identification of intestinal bacteria in fecal flora studies. *Am. J. Clin. Nutr.* 27, 1450–1455.

Morgan, X. C., Tickle, T. L., Sokol, H., Gevers, D., Devaney, K. L., Ward, D. V., et al. (2012). Dysfunction of the intestinal microbiome in inflammatory bowel disease and treatment. *Genome Biol.* 13:R79. doi: 10.1186/gb-2012-13-9-r79

Moutsopoulos, N. M., Chalmers, N. I., Barb, J. J., Abusleme, L., Greenwell-Wild, T., Dutzan, N., et al. (2015). Subgingival microbial communities in Leukocyte Adhesion Deficiency and their relationship with local immunopathology. *PLoS Pathog.* 11:e1004698. doi: 10.1371/journal.ppat.1004698

Munyaka, P. M., Sepehri, S., Ghia, J. E., and Khafipour, E. (2016). Carrageenan gum and adherent invasive *Escherichia coli* in a piglet model of inflammatory bowel disease: impact on intestinal mucosa-associated microbiota. *Front. Microbiol.* 7:462. doi: 10.3389/fmicb.2016.00462

Nagalingam, N. A., Kao, J. Y., and Young, V. B. (2011). Microbial ecology of the murine gut associated with the development of dextran sodium sulfate-induced colitis. *Inflam. Bowel Dis.* 17, 917–926. doi: 10.1002/ibd.21462

Nava, G. M., Friedrichsen, H. J., and Stappenbeck, T. S. (2011). Spatial organization of intestinal microbiota in the mouse ascending colon. *ISME J.* 5, 627–638. doi: 10.1038/ismej.2010.161

Neut, C., Bulois, P., Desreumaux, P., Membreé, J.-M., Lederman, E., Gambiez, L., et al. (2002). Changes in the bacterial flora of the neoterminal ileum after ileocolonic resection for Crohn's disease. *Am. J. Gastroenterol.* 97, 939–946. doi: 10.1111/j.1572-0241.2002.05613.x

Nishimoto, Y., Mizutani, S., Nakajima, T., Hosoda, F., Watanabe, H., Saito, Y., et al. (2016). High stability of faecal microbiome composition in guanidine thiocyanate solution at room temperature and robustness during colonoscopy. *Gut* 0, 1–2. doi: 10.1136/gutjnl-2016-311937

Norman, J. M., Handley, S. A., Baldridge, M. T., Droit, L., Liu, C. Y., Keller, B. C., et al. (2015). Disease-specific alterations in the enteric virome in inflammatory bowel disease. *Cell* 160, 447–460. doi: 10.1016/j.cell.2015.01.002

Nugent, S. G., Kumar, D., Rampton, D. S., and Evans, D. F. (2001). Intestinal luminal pH in inflammatory bowel disease: possible determinants and implications for therapy with aminosalicylates and other drugs. *Gut* 48, 571–577. doi: 10.1136/gut.48.4.571

O'Brien, C. L., Allison, G. E., Grimpen, F., and Pavli, P. (2013). Impact of colonoscopy bowel preparation on intestinal microbiota. *PLoS ONE* 8:e62815. doi: 10.1371/journal.pone.0062815

Ó Cuív, P., Aguirre de Carcer, D., Jones, M., Klaassens, E. S., Worthley, D. L., Whitehall, V. L., et al. (2011). The effects from DNA extraction methods on the evaluation of microbial diversity associated with human colonic tissue. *Microb. Ecol.* 61, 353–362. doi: 10.1007/s00248-010-9771-x

Ottman, N., Smidt, H., de Vos, W. M., and Belzer, C. (2012). The function of our microbiota: who is out there and what do they do? *Front. Cell. Infect. Microbiol.* 2:104. doi: 10.3389/fcimb.2012.00104

Parthasarathy, G., Chen, J., Chen, X., Chia, N., O'Connor, H. M., Wolf, P. G., et al. (2016). Relationship between microbiota of the colonic mucosa vs feces and symptoms, colonic transit, and methane production in female patients with chronic constipation. *Gastroenterology* 150, 367–379 e361. doi: 10.1053/j.gastro.2015.10.005

Pedron, T., Mulet, C., Dauga, C., Frangeul, L., Chervaux, C., Grompone, G., et al. (2012). A crypt-specific core microbiota resides in the mouse colon. *MBio* 3, 2153–2154. doi: 10.1128/mBio.00116-12

Pérezcobas, A. E., Artacho, A., Ott, S. J., Moya, A., Gosalbes, M. J., and Latorre, A. (2014). Structural and functional changes in the gut microbiota associated to Clostridium difficile infection. *Front. Microbiol.* 5:335. doi: 10.3389/fmicb.2014.00335

Pérezcobas, A. E., Gosalbes, M. J., Friedrichs, A., Knecht, H., Artacho, A., Eismann, K., et al. (2013). Gut microbiota disturbance during antibiotic therapy: a

multi-omic approach. *Gut Microbes* 62, 1591–1601. doi: 10.1136/gutjnl-2012-303184

Pittock, S., Drumm, B., Fleming, P., McDermott, M., Imrie, C., Flint, S., et al. (2001). The oral cavity in Crohn's disease. *J. Pediatr.* 138, 767–771. doi: 10.1067/mpd.2001.113008

Poretsky, R., Rodriguez, R. L., Luo, C., Tsementzi, D., and Konstantinidis, K. T. (2014). Strengths and limitations of 16S rRNA gene amplicon sequencing in revealing temporal microbial community dynamics. *PLoS ONE* 9:e93827. doi: 10.1371/journal.pone.0093827

Probert, C. S., Reade, S., and Ahmed, I. (2014). Fecal volatile organic compounds: a novel, cheaper method of diagnosing inflammatory bowel disease? *Expert Rev. Clin. Immunol.* 10, 1129–1131. doi: 10.1586/1744666X.2014.943664

Pullan, R. D., Thomas, G. A., Rhodes, M., Newcombe, R. G., Williams, G. T., Allen, A., et al. (1994). Thickness of adherent mucus gel on colonic mucosa in humans and its relevance to colitis. *Gut* 35, 353–359. doi: 10.1136/gut.35.3.353

Qin, J., Li, Y., Cai, Z., Li, S., Zhu, J., Zhang, F., et al. (2012). A metagenome-wide association study of gut microbiota in type 2 diabetes. *Nature* 490, 55–60. doi: 10.1038/nature11450

Qiu, X., Zhang, F., Yang, X., Wu, N., Jiang, W., Li, X., et al. (2015). Changes in the composition of intestinal fungi and their role in mice with dextran sulfate sodium-induced colitis. *Sci. Rep.* 5:10416. doi: 10.1038/srep10416

Quast, C., Pruesse, E., Yilmaz, P., Gerken, J., Schweer, T., Yarza, P., et al. (2013). The SILVA ribosomal RNA gene database project: improved data processing and web-based tools. *Nucleic Acids Res.* 41(Database issue), D590–D596. doi: 10.1093/nar/gks1219

Queipoortuño, M. I., Seoane, L. M., Murri, M., Pardo, M., Gomezzumaquero, J. M., Cardona, F., et al. (2013). Gut microbiota composition in male rat models under different nutritional status and physical activity and its association with serum leptin and ghrelin levels. *PLoS ONE* 8:e65465. doi: 10.1371/journal.pone.0065465

Quince, C., Ijaz, U. Z., Loman, N., Eren, A. M., Saulnier, D., Russell, J., et al. (2015). Extensive modulation of the fecal metagenome in children with crohn's disease during exclusive enteral nutrition. *Am. J. Gastroenterol.* 110, 1718–1729; quiz 1730. doi: 10.1038/ajg.2015.357

Rangel, I., Sundin, J., Fuentes, S., Repsilber, D., de Vos, W. M., and Brummer, R. J. (2015). The relationship between faecal-associated and mucosal-associated microbiota in irritable bowel syndrome patients and healthy subjects. *Aliment. Pharmacol. Ther.* 42, 1211–1221. doi: 10.1111/apt.13399

Rautava, J., Pinnell, L. J., Vong, L., Akseer, N., Assa, A., and Sherman, P. M. (2015). Oral microbiome composition changes in mouse models of colitis. *J. Gastroenterol. Hepatol.* 30, 521–527. doi: 10.1111/jgh.12713

Reinberg, A. (2015). Geographical patterns of the standing and active human gut microbiome in health and IBD. *Gut* 15, 349–356. doi: 10.1136/gutjnl-2014-308341

Rochet, V., Rigottier-Gois, L., Sutren, M., Krementscki, M.-N., Andrieux, C., Furet, J.-P., et al. (2007). Effects of orally administered Lactobacillus casei DN-114 001 on the composition or activities of the dominant faecal microbiota in healthy humans. *Br. J. Nutr.* 95, 421. doi: 10.1079/BJN20051625

Rossen, N. G., Fuentes, S., Boonstra, K., D'Haens, G. R., Heilig, H. G., Zoetendal, E. G., et al. (2015). The mucosa-associated microbiota of PSC patients is characterized by low diversity and low abundance of uncultured Clostridiales II. *J. Crohns. Colitis* 9, 342–348. doi: 10.1093/ecco-jcc/jju023

Rowan, F., Docherty, N. G., Murphy, M., Murphy, B., Calvin Coffey, J., and O'Connell, P. R. (2010a). Desulfovibrio bacterial species are increased in ulcerative colitis. *Dis. Colon Rectum* 53, 1530–1536. doi: 10.1007/DCR.0b013e3181f1e620

Rowan, F., Docherty, N. G., Murphy, M., Murphy, T. B., Coffey, J. C., and O'Connell, P. R. (2010b). Bacterial colonization of colonic crypt mucous gel and disease activity in ulcerative colitis. *Ann. Surg.* 252, 869–875. doi: 10.1097/SLA.0b013e3181fdc54c

Ryan, P., Bennett, M. W., Aarons, S., Lee, G., Collins, J. K., O'Sullivan, G. C., et al. (2002). PCR detection of *Mycobacterium paratuberculosis* in Crohn's disease granulomas isolated by laser capture microdissection. *Gut* 51, 665–670.

Said, H. S., Suda, W., Nakagome, S., Chinen, H., Oshima, K., Kim, S., et al. (2014). Dysbiosis of salivary microbiota in inflammatory bowel disease and its association with oral immunological biomarkers. *DNA Res.* 21, 15–25. doi: 10.1093/dnares/dst037

Salonen, A., Nikkila, J., Jalanka-Tuovinen, J., Immonen, O., Rajilic-Stojanovic, M., Kekkonen, R. A., et al. (2010). Comparative analysis of fecal DNA extraction methods with phylogenetic microarray: effective recovery of bacterial and archaeal DNA using mechanical cell lysis. *J. Microbiol. Methods* 81, 127–134. doi: 10.1016/j.mimet.2010.02.007

Salvatori, F., Siciliano, S., Maione, F., Esposito, D., Masone, S., Persico, M., et al. (2012). Confocal laser endomicroscopy in the study of colonic mucosa in IBD patients: a review. *Gastroenterol. Res. Pract.* 2012:525098. doi: 10.1155/2012/525098

Sanapareddy, N., Legge, R. M., Jovov, B., McCoy, A., Burcal, L., Araujo-Perez, F., et al. (2012). Increased rectal microbial richness is associated with the presence of colorectal adenomas in humans. *ISME J.* 6, 1858–1868. doi: 10.1038/ismej.2012.43

Sartor, R. B. (2015). Gut microbiota: optimal sampling of the intestinal microbiota for research. *Nat. Rev. Gastroenterol. Hepatol.* 12, 253–254. doi: 10.1038/nrgastro.2015.46

Scher, J. U., Ubeda, C., Artacho, A., Attur, M., Isaac, S., Reddy, S. M., et al. (2015). Decreased bacterial diversity characterizes the altered gut microbiota in patients with psoriatic arthritis, resembling dysbiosis in inflammatory bowel disease. *Arth. Rheumatol.* 67, 128–139. doi: 10.1002/art.38892

Schloss, P. D., Gevers, D., and Westcott, S. L. (2011). Reducing the effects of PCR amplification and sequencing artifacts on 16S rRNA-based studies. *PLoS ONE* 6:e27310. doi: 10.1371/journal.pone.0027310

Schloss, P. D., Westcott, S. L., Ryabin, T., Hall, J. R., Hartmann, M., Hollister, E. B., et al. (2009). Introducing mothur: open-source, platform-independent, community-supported software for describing and comparing microbial communities. *Appl. Environ. Microbiol.* 75, 7537–7541. doi: 10.1128/AEM.01541-09

Schmidlin, P. R., Fachinger, P., Tini, G., Graber, S., Seifert, B., Dombrowa, S., et al. (2015). Shared microbiome in gums and the lung in an outpatient population. *J. Infect.* 70, 255–263. doi: 10.1016/j.jinf.2014.10.005

Schultsz, C., Van Den Berg, F. M., Ten Kate, F. W., Tytgat, G. N., and Dankert, J. (1999). The intestinal mucus layer from patients with inflammatory bowel disease harbors high numbers of bacteria compared with controls. *Gastroenterology* 117, 1089–1097. doi: 10.1016/S0016-5085(99)70393-8

Segata, N., Waldron, L., Ballarini, A., Narasimhan, V., Jousson, O., and Huttenhower, C. (2012). Metagenomic microbial community profiling using unique clade-specific marker genes. *Nat. Methods* 9, 811–814. doi: 10.1038/nmeth.2066

Shakya, M., Quince, C., Campbell, J. H., Yang, Z. K., Schadt, C. W., and Podar, M. (2013). Comparative metagenomic and rRNA microbial diversity characterization using archaeal and bacterial synthetic communities. *Environ. Microbiol.* 15, 1882–1899. doi: 10.1111/1462-2920.12086

Shanahan, E. R., Zhong, L., Talley, N. J., Morrison, M., and Holtmann, G. (2016). Characterisation of the gastrointestinal mucosa-associated microbiota: a novel technique to prevent cross-contamination during endoscopic procedures. *Aliment. Pharmacol. Ther.* 43, 1186–1196. doi: 10.1111/apt.13622

Sharp, R. C., Abdulrahim, M., Naser, E. S., and Naser, S. A. (2015). Genetic variations of PTPN2 and PTPN22: role in the pathogenesis of Type 1 diabetes and crohn's disease. *Front. Cell. Infect. Microbiol.* 5:95. doi: 10.3389/fcimb.2015.00095

Shen, X. J., Rawls, J. F., Randall, T., Burcal, L., Mpande, C. N., Jenkins, N., et al. (2010). Molecular characterization of mucosal adherent bacteria and associations with colorectal adenomas. *Gut Microbes* 1, 138–147. doi: 10.4161/gmic.1.3.12360

Sheridan, C. (2014). Milestone approval lifts Illumina's NGS from research into clinic. *Nat. Biotechnol.* 32, 111–112. doi: 10.1038/nbt0214-111

Shobar, R. M., Velineni, S., Keshavarzian, A., Swanson, G., DeMeo, M. T., Melson, J. E., et al. (2016). The effects of bowel preparation on microbiota-related metrics differ in health and in inflammatory bowel disease and for the mucosal and luminal microbiota compartments. *Clin. Transl. Gastroenterol.* 7, e143. doi: 10.1038/ctg.2015.54

Sibila, O., Garcia-Bellmunt, L., Giner, J., Rodrigo-Troyano, A., Suarez-Cuartin, G., Torrego, A., et al. (2016). Airway MUC2 is decreased in severe COPD patients with bacterial colonization. *Ann. Am. Thorac. Soc.* 13, 636–642. doi: 10.1513/AnnalsATS.201512-797OC

Singhal, S., Dian, D., Keshavarzian, A., Fogg, L., Fields, J. Z., and Farhadi, A. (2011). The role of oral hygiene in inflammatory bowel disease. *Dig. Dis. Sci.* 56, 170–175. doi: 10.1007/s10620-010-1263-9

Sokol, H., Seksik, P., Rigottier-Gois, L., Lay, C., Lepage, P., Podglajen, I., et al. (2006). Specificities of the fecal microbiota in inflammatory bowel disease. *Inflamm. Bowel Dis.* 12, 106–111. doi: 10.1097/01.MIB.0000200323.38139.c6

Stearns, J. C., Lynch, M. D., Senadheera, D. B., Tenenbaum, H. C., Goldberg, M. B., Cvitkovitch, D. G., et al. (2011). Bacterial biogeography of the human digestive tract. *Sci. Rep.* 1:170. doi: 10.1038/srep00170

Swidsinski, A., Dörffel, Y., Loening-Baucke, V., Theissig, F., Rückert, J. C., Ismail, M., et al. (2009). Acute appendicitis is characterized by local invasion with *Fusobacterium nucleatum/necrophorum*. *Gut.* 2009:191320. doi: 10.1136/gut.2009.191320

Swidsinski, A., Loening-Baucke, V., Theissig, F., Engelhardt, H., Bengmark, S., Koch, S., et al. (2007). Comparative study of the intestinal mucus barrier in normal and inflamed colon. *Gut* 56, 343–350. doi: 10.1136/gut.2006.098160

Swidsinski, A., Loening-Baucke, V., Vaneechoutte, M., and Doerffel, Y. (2008a). Active Crohn's disease and ulcerative colitis can be specifically diagnosed and monitored based on the biostructure of the fecal flora. *Inflamm. Bowel Dis.* 14, 147–161. doi: 10.1002/ibd.20330

Swidsinski, A., Loening-Baucke, V., Verstraelen, H., Osowska, S., and Doerffel, Y. (2008b). Biostructure of fecal microbiota in healthy subjects and patients with chronic idiopathic diarrhea. *Gastroenterology* 135, 568–579. doi: 10.1053/j.gastro.2008.04.017

Syed, S. A. and Loesche, W. J. (1972). Survival of human dental plaque flora in various transport media. *Appl. Microbiol.* 24, 638–644.

Thomas, V., Clark, J., and Dore, J. (2015). Fecal microbiota analysis: an overview of sample collection methods and sequencing strategies. *Future Microbiol.* 10, 1485–1504. doi: 10.2217/fmb.15.87

Tong, M., Jacobs, J. P., McHardy, I. H., and Braun, J. (2014). Sampling of intestinal microbiota and targeted amplification of bacterial 16S rRNA genes for microbial ecologic analysis. *Curr. Protoc. Immunol.* 107, 41.41–11. doi: 10.1002/0471142735.im0741s107

Vagianos, K., Clara, I., Carr, R., Graff, L. A., Walker, J. R., Targownik, L. E., et al. (2016). What are adults with inflammatory bowel disease (IBD) eating? A closer look at the dietary habits of a population-based canadian IBD Cohort. JPEN *J. Parenter Enteral. Nutr.* 40, 405–411. doi: 10.1177/0148607114549254

Vallescolomer, M., Darzi, Y., Vieira-Silva, S., Falony, G., Raes, J., and Joossens, M. (2016). Meta-omics in IBD research: applications, challenges and guidelines. *Int. J. Epidemiol.* 10, 735–746. doi: 10.1093/ecco-jcc/jjw024

van den Heuvel, T. R., Jonkers, D. M., Jeuring, S. F., Romberg-Camps, M. J., Oostenbrug, L. E., Zeegers, M. P., et al. (2015). Cohort Profile: The Inflammatory Bowel Disease South Limburg Cohort (IBDSL). *Int. J. Epidemiol.* doi: 10.1093/ije/dyv088. [Epub ahead of print].

Vandeputte, D., Falony, G., Vieira-Silva, S., Tito, R. Y., Joossens, M., and Raes, J. (2016). Stool consistency is strongly associated with gut microbiota richness and composition, enterotypes and bacterial growth rates. *Gut* 65, 57–62. doi: 10.1136/gutjnl-2015-309618

Vermeire, S., Joossens, M., Verbeke, K., Wang, J., Machiels, K., Sabino, J., et al. (2016). Donor species richness determines faecal microbiota transplantation success in inflammatory bowel disease. *J. Crohns. Colitis* 10, 387–394. doi: 10.1093/ecco-jcc/jjv203

Wang, M. H., and Achkar, J. P. (2015). Gene-environment interactions in inflammatory bowel disease pathogenesis. *Curr. Opin. Gastroenterol.* 31, 277–282. doi: 10.1097/MOG.0000000000000188

Wang, W., Chen, L., Zhou, R., Wang, X., Song, L., Huang, S., et al. (2014a). Increased proportions of Bifidobacterium and the Lactobacillus group and loss of butyrate-producing bacteria in inflammatory bowel disease. *J. Clin. Microbiol.* 52, 398–406. doi: 10.1128/JCM.01500-13

Wang, W., Chen, L., Zhou, R., Wang, X., Song, L., Huang, S., et al. (2014b). Increased proportions of Bifidobacterium and the Lactobacillus group and loss of butyrate-producing bacteria in inflammatory bowel disease. *J. Clin. Microbiol.* 52, 398–406. doi: 10.1128/JCM.01500-13

Wang, W., Jovel, J., Halloran, B., Wine, E., Patterson, J., Ford, G., et al. (2015). Metagenomic analysis of microbiome in colon tissue from subjects with inflammatory bowel diseases reveals interplay of viruses and bacteria. *Inflamm. Bowel Dis.* 21, 1419–1427. doi: 10.1097/mib.0000000000000344

White, W. H. (1888). On simple ulcerative colitis and other rare intestinal ulcers. *Guy's Hosp. Rep.* 45, 131–162.

Wu, G. D., Chen, J., Hoffmann, C., Bittinger, K., Chen, Y. Y., Keilbaugh, S. A., et al. (2011). Linking long-term dietary patterns with gut microbial enterotypes. *Science* 334, 105–108. doi: 10.1126/science.1208344

Wu, G. D., Lewis, J. D., Hoffmann, C., Chen, Y. Y., Knight, R., Bittinger, K., et al. (2010). Sampling and pyrosequencing methods for characterizing bacterial communities in the human gut using 16S sequence tags. *BMC Microbiol.* 10:206. doi: 10.1186/1471-2180-10-206

Wu, J., Lin, I. H., Hayes, R. B., and Ahn, J. Y. (2014). Comparison of DNA extraction methods for human oral microbiome research. *Br. J. Med. Med. Res.* 4, 1980–1991. doi: 10.9734/BJMMR/2014/5333

Yang, Q. F., Chen, B. L., Zhang, Q. S., Zhu, Z. H., Hu, B., He, Y., et al. (2015). Contribution of MDR1 gene polymorphisms on IBD predisposition and response to glucocorticoids in IBD in a Chinese population. *J. Dig. Dis.* 16, 22–30. doi: 10.1111/1751-2980.12205

Yigit, E., Feehery, G. R., Langhorst, B. W., Stewart, F. J., Dimalanta, E. T., Pradhan, S., et al. (2016). A microbiome DNA enrichment method for next-generation sequencing sample preparation. *Curr. Protoc. Mol. Biol.* 115, 7.26.1–7.26.14. doi: 10.1002/cpmb.12

Yoneda, M., Suzuki, N., Morita, H., and Hirofuji, T. (2016). Oral bacteria and bowel diseases – mini review. *J. Gastrointest. Dig. Syst.* 6:404. doi: 10.4172/2161-069X.1000404

Yoshizawa, J. M., Schafer, C. A., Schafer, J. J., Farrell, J. J., Paster, B. J., and Wong, D. T. (2013). Salivary biomarkers: toward future clinical and diagnostic utilities. *Clin. Microbiol. Rev.* 26, 781–791. doi: 10.1128/CMR.00021-13

Yu, Z., and Morrison, M. (2004). Improved extraction of PCR-quality community DNA from digesta and fecal samples. *BioTechniques* 36, 808–813.

Zackular, J. P., Baxter, N. T., Iverson, K. D., Sadler, W. D., Petrosino, J. F., Chen, G. Y., et al. (2013). The gut microbiome modulates colon tumorigenesis. *MBio* 4, e00692–e00613. doi: 10.1128/mBio.00692-13

Zhang, Q., Wu, Y., Wang, J., Wu, G., Long, W., Xue, Z., et al. (2016a). Accelerated dysbiosis of gut microbiota during aggravation of DSS-induced colitis by a butyrate-producing bacterium. *Sci. Rep.* 6:27572. doi: 10.1038/srep27572

Zhang, X., Zhang, D., Jia, H., Feng, Q., Wang, D., Liang, D., et al. (2015a). The oral and gut microbiomes are perturbed in rheumatoid arthritis and partly normalized after treatment. *Nat. Med.* 21, 895–905. doi: 10.1038/nm.3914

Zhang, Y. J., Li, S., Gan, R. Y., Zhou, T., Xu, D. P., and Li, H. B. (2015b). Impacts of gut bacteria on human health and diseases. *Int. J. Mol. Sci.* 16, 7493–7519. doi: 10.3390/ijms16047493

Zhang, Y., Teichert, I., Kück, U., and Fischer, R. (2016b). Laser capture microdissection to identify septum-associated proteins in *Aspergillus nidulans*. *Mycologia* 108, 15–218. doi: 10.3852/15-218

Zhang, Z., Geng, J., Tang, X., Fan, H., Xu, J., Wen, X., et al. (2014). Spatial heterogeneity and co-occurrence patterns of human mucosal-associated intestinal microbiota. *ISME J.* 8, 881–893. doi: 10.1038/ismej.2013.185

Zhou, Y., Gao, H., Mihindukulasuriya, K. A., La Rosa, P. S., Wylie, K. M., Vishnivetskaya, T., et al. (2013). Biogeography of the ecosystems of the healthy human body. *Genome Biol.* 14:R1. doi: 10.1186/gb-2013-14-1-r1

Zoetendal, E. G., Heilig, H. G., Klaassens, E. S., Booijink, C. C., Kleerebezem, M., Smidt, H., et al. (2006). Isolation of DNA from bacterial samples of the human gastrointestinal tract. *Nat. Protoc.* 1, 870–873. doi: 10.1038/nprot.2006.142

Zoetendal, E. G., Rajilic-Stojanovic, M., and de Vos, W. M. (2008). High-throughput diversity and functionality analysis of the gastrointestinal tract microbiota. *Gut* 57, 1605–1615. doi: 10.1136/gut.2007.133603

Conflict of Interest Statement: The authors declare that the research was conducted in the absence of any commercial or financial relationships that could be construed as a potential conflict of interest.

The reviewer VJ and handling Editor declared their shared affiliation and the handling Editor states that the process nevertheless met the standards of a fair and objective review.

Copyright © 2017 Zhang, Cao and Huang. This is an open-access article distributed under the terms of the Creative Commons Attribution License (CC BY). The use, distribution or reproduction in other forums is permitted, provided the original author(s) or licensor are credited and that the original publication in this journal is cited, in accordance with accepted academic practice. No use, distribution or reproduction is permitted which does not comply with these terms.

frontiers in Cellular and Infection Microbiology

ORIGINAL RESEARCH
published: 23 February 2017
doi: 10.3389/fcimb.2017.00047

Enterotype May Drive the Dietary-Associated Cardiometabolic Risk Factors

*Ana C. F. de Moraes[1], Gabriel R. Fernandes[2], Isis T. da Silva[1], Bianca Almeida-Pititto[3], Everton P. Gomes[4], Alexandre da Costa Pereira[4] and Sandra R. G. Ferreira[1]**

[1] Department of Epidemiology, School of Public Health, University of São Paulo, São Paulo, Brazil, [2] René Rachou Research Center, Oswaldo Cruz Foundation, Belo Horizonte, Brazil, [3] Department of Preventive Medicine, Federal University of São Paulo, São Paulo, Brazil, [4] Laboratory of Genetics and Molecular Cardiology, Heart Institute (Incor), University of São Paulo Medical School, São Paulo, Brazil

Analyses of typical bacterial clusters in humans named enterotypes may facilitate understanding the host differences in the cardiometabolic profile. It stills unknown whether the three previously described enterotypes were present in populations living below the equator. We examined how the identification of enterotypes could be useful to explain the dietary associations with cardiometabolic risk factors in Brazilian subjects. In this cross-sectional study, a convenience sample of 268 adults (54.2% women) reported their dietary habits and had clinical and biological samples collected. In this study, we analyzed biochemical data and metagenomics of fecal microbiota (16SrRNA sequencing, V4 region). Continuous variables were compared using ANOVA, and categorical variables using chi-square test. Vsearch clustered the operational taxonomic units, and Silva Database provided the taxonomic signatures. Spearman coefficient was used to verify the correlation between bacteria abundances within each enterotype. One hundred subjects were classified as omnivore, 102 lacto-ovo-vegetarians, and 66 strict vegetarians. We found the same structure as the three previously described enterotypes: 111 participants were assigned to *Bacteroides*, 55 to *Prevotella,* and 102 to *Ruminococcaceae* enterotype. The *Prevotella* cluster contained higher amount of strict vegetarians individuals than the other enterotypes (40.0 vs. 20.7 and 20.6, $p = 0.04$). Subjects in this enterotype had a similar anthropometric profile but a lower mean LDL-c concentration than the *Bacteroides* enterotype (96 ± 23 vs. 109 ± 32 mg/dL, $p = 0.04$). We observed significant correlations between bacterial abundances and cardiometabolic risk factors, but coefficients differed depending on the enterotype. In *Prevotella* enterotype, *Eubacterium ventriosum* (r BMI $= -0.33$, $p = 0.03$, and r HDL-c $= 0.33$, $p = 0.04$), *Akkermansia* (r 2h glucose $= -0.35$, $p = 0.02$), *Roseburia* (r BMI $= -0.36$, $p = 0.02$ and r waist $= -0.36$, $p = 0.02$), and *Faecalibacterium* (r insulin $= -0.35$, $p = 0.02$) abundances were associated to better cardiometabolic profile. The three enterotypes previously described are present in Brazilians, supporting that those bacterial clusters are not population-specific. Diet-independent lower LDL-c levels in

OPEN ACCESS

Edited by:
Michele Marie Kosiewicz, University of Louisville, USA

Reviewed by:
Valerio Iebba, Sapienza University of Rome, Italy
Gena D. Tribble, University of Texas Health Science Center at Houston, USA

***Correspondence:**
Sandra R. G. Ferreira
sandrafv@usp.br

Received: *30 October 2016*
Accepted: *07 February 2017*
Published: *23 February 2017*

Citation:
de Moraes ACF, Fernandes GR, da Silva IT, Almeida-Pititto B, Gomes EP, Pereira AdC and Ferreira SRG (2017) Enterotype May Drive the Dietary-Associated Cardiometabolic Risk Factors. Front. Cell. Infect. Microbiol. 7:47. doi: 10.3389/fcimb.2017.00047

subjects from *Prevotella* than in other enterotypes suggest that a protective bacterial cluster in the former should be driving this association. Enterotypes seem to be useful to understand the impact of daily diet exposure on cardiometabolic risk factors. Prospective studies are needed to confirm their utility for predicting phenotypes in humans.

Keywords: gut microbiota, enterotype, cardiometabolic risk, diet, lipid profile

INTRODUCTION

Cardiometabolic diseases are among the leading causes of mortality, and an unhealthy diet plays a significant etiopathogenetic role (World Health Organization, 2011; Laslett et al., 2012). Pieces of evidence indicate that the gut microbiota mediates the relationship between dietary habits and cardiometabolic abnormalities (Koeth et al., 2013; Yin et al., 2015). The vast number of intestinal bacteria, and the large intra- and inter-individual variability has limited the understanding of such relationship. The observation of bacterial clusters in human gut has represented a way to reduce the complexity of these analyses. Arumugam et al. (2011) found three bacteria groups in humans, driven by high proportions of one of three taxa: *Bacteroides* (enterotype 1), *Prevotella* (enterotype 2), and *Ruminococcus* (enterotype 3). The bacterial communities play an important role driving diverse pathophysiological processes (Arumugam et al., 2011). Another study discussed the associations of dietary habits with two enterotypes, distinct from this seminal study since the *Bacteroides* enterotype was fused with the less distinct *Ruminococcus* enterotype (Wu et al., 2011). Animal protein and fat intake were associated with *Bacteroides* cluster, while *Prevotella* with a carbohydrate-enriched diet.

Populations are exposed to different dietary habits, and it is unknown how the enterotypes are distributed worldwide. Most studies that describe the enterotypes involves European, North American, and Asian (Arumugam et al., 2011; Wu et al., 2011; Lim et al., 2014; Roager et al., 2014) populations. Only a few scientific publications analyzed the clusters in South American or African individuals (Yatsunenko et al., 2012; Ou et al., 2013). The knowledge on the distribution of enterotypes, in populations with different genetic backgrounds and lifestyle, could be useful to understand underlying mechanisms linking dietary habits with the risk of cardiometabolic diseases (Zupancic et al., 2012; Koeth et al., 2013; Kelder et al., 2014).

Brazilian population offers an opportunity to investigate the presence of enterotypes in a high-food variety environment, and to deepen knowledge on the role of the gut microbiota mediating the impact of diet on metabolic disturbances. We hypothesized that enterotypes might participate in underlying mechanisms linking dietary habits to cardiometabolic diseases. We investigated whether enterotypes could be identified in a sample of Brazilians and examined the impact of this categorization of the gut microbiota on the association with the cardiometabolic profile.

MATERIALS AND METHODS

Subjects

In this cross-sectional analysis, we included a convenience sample of 268 participants from the major study named ADVENTO—Analysis of Diet and Lifestyle for Cardiovascular Prevention in Seventh-Day Adventists (http://www.estudoadvento.org). The ethical committee of the School of Public Health, Univesity of São Paulo, approved this study; all individuals provided written consent. Inclusion criteria were age from 35 to 65 years and body mass index (BMI) <40 kg/m2. Diabetes mellitus, history of inflammatory bowel diseases, persistent diarrhea, and use of antibiotics or probiotic or prebiotic supplements within the 2 months before the data collection were exclusion criteria. Dietary data was obtained using a validated food frequency questionnaire from the ADVENTO. Subjects were classified according to the dietary habit adopted for at least 12 months, in strict vegetarian (no consumption of animal products), lacto-ovo-vegetarian (consumption of dairy products and/or eggs), and omnivore (consumption of animal products more than once a month; Tonstad et al., 2009).

Clinical Data

Weight was measured using a digital scale with 200 kg capacity, height using a fixed stadiometer and BMI was calculated as weight in kilograms divided by height in meters squared. Blood pressure (BP) was measured with a standard oscillometric device (Omron HEM 705CPINT, Omron Health Care, Lake Forest, IL, USA). Blood samples were taken after an overnight fasting. Plasma glucose was measured by the hexokinase method (ADVIA Chemistry; Siemens, Deerfield, IL, USA). Measurements of total cholesterol, triglyceride, and high-density lipoprotein (HDL-c) were assessed by enzymatic methods. Low-density lipoprotein cholesterol (LDL-c) was calculated by the Friedewald equation.

Gut Microbiota

The analysis of the 16S rRNA gene (V4 region) was performed by Illumina® MiSeq platform using 200 mg of fecal samples maintained under refrigeration (6°C) within a maximum of 24 h after collection, and the aliquots stored at −80°C until analysis. The Maxwell® 16 DNA purification kit was used to extract DNA, and the manufacturer's instruction was used to carry out the protocol in the Maxwell® 16 Instrument (Promega, Madison, WI, USA). The DNA was amplified by a PCR assay using the 515F and 806R primers, as described by Caporaso et al. (2012), and sequenced in Illumina Miseq platform generating paired reads of

250 bp. 16S ribosomal DNA sequences are available under study accession PRJEB19103.

The paired reads were trimmed to remove bases with Phred score lower than five at the 5′ and 3′ extremities. These procedures also trimmed sequences with an average quality <15 in a sliding window of 4 bases. The software Trimmomatic (Bolger et al., 2014) performed this quality filter. Paired reads were merged using the FLASh tool (Magoč and Salzberg, 2011), requiring a minimum overlap of 20 nucleotides.

The redundancy among the sequences was removed using the dereplication step from Vsearch (Rognes et al., 2016), and filtered to remove the unique entries. The dereplicated reads with 97% identity were clustered, using the same tool, to create the OTUs. Taxonomical assignment to the OTUs was performed by the assign_taxonomy script from Qiime (Caporaso et al., 2010) and Silva database, version 123 (Quast et al., 2013).

Enterotype Clustering

The enterotypes were identified by the methods previously described (Arumugam et al., 2011, 2014) and available in http://enterotype.embl.de/enterotypes.html. The Calinski-Harabasz (CH) index suggested the optimal number of clusters. A silhouette analysis and elbow plot evaluated the groups' robustness (Supplementary Figure S1).

Statistical Analysis

The descriptive statistical analysis calculated means, standard deviations, medians, and interquartile ranges. Variables with skewed distributions were log-transformed before analysis to achieve normality. ANOVA with Bonferroni *post-hoc* test was used to compare variables according to enterotypes and diet. Chi-square test was employed to compare proportions. The Spearman correlation coefficient pointed associations between metadata and most common genera or species (present in at least 80% of subjects). The most abundant genera were shown in the figures. Statistical analyses were performed using Statistical Package for the Social Sciences (SPSS), version 23 (IBM, Armonk, NY, USA), and R for enterotype analyses (cluster package). Beta diversity comparisons were computed as Principal Coordinate Analyses generated from Jensen-Shannon divergence matrices. A $p < 0.05$ was considered to identify important correlations.

RESULTS

The mean age of participants was 49.4 ± 8.4 years, 54.2% were women and 41.4% and had increased BMI (≥25 kg/m2). Sixty-six subjects were considered strict vegetarians, 102 lacto-ovo-vegetarians, and 100 omnivores. Strict and lacto-ovo-vegetarians had lower BMI (23.1 ± 4.1 and 24.4 ± 3.9 vs. 26.4 ± 4.7 kg/m2, respectively, $p < 0.001$) and LDL-c values (99 ± 31 and 101 ± 27 vs. 112 ± 29 mg/dL, respectively, $p = 0.005$) than omnivores (Supplementary Table S1).

Taxonomical distribution of fecal samples showed the predominance of *Firmicutes* and *Bacteroidetes* (**Figure 1**). The 10 most abundant phyla and 20 genera according to enterotypes and dietary habits were depicted in Supplementary Figure S2.

Three bacterial clusters were identified; 111 participants were assigned to *Bacteroides*, 55 to *Prevotella,* and 102 to *Ruminococcaceae* enterotype (**Figure 2A**). Relative abundances in each enterotype confirmed the expected predominance of genera *Bacteroides*, *Prevotella,* and *Ruminococcaceae*, respectively (**Figure 2B**). Subjects in each enterotype did not differ according to sex distribution, mean age, and BMI. The frequency of strict vegetarians was greater in *Prevotella* than in the *Bacteroides* and *Ruminococacceae* enterotypes (40.0 vs. 20.7 and 20.6%, $p = 0.04$, respectively), but frequencies of lacto-ovo-vegetarians and omnivores did not differ (Supplementary Figure S3).

Comparisons of clinical variables among enterotypes showed lower mean LDL-c values in *Prevotella* compared to *Bacteroides* (96 ± 23 vs. 109 ± 32 mg/dL, $p = 0.04$), despite similar measurements of body adiposity (**Table 1**). When a sub-stratification of Supplementary Table S1 comparing enterotypes according to dietary habits (Supplementary Table S2), the lowest LDL-c levels were invariably observed in the *Prevotella* enterotype independently of the dietary pattern. Within the *Prevotella* enterotype, the strict vegetarian and lacto-ovo-vegetarian showed mean LDL-c values significantly lower than omnivores (92 ± 23 and 88 ± 18 vs. 107 ± 25 mg/dL, respectively, $p = 0.04$). Strict vegetarians belonging to the *Ruminococcaceae* cluster had the greatest mean value of HDL-c that was significantly higher than subjects from the same enterotype but consumers of other dietary habits (59 ± 1 and 47 ± 1 vs. 51 ± 1 mg/dL, respectively, $p = 0.004$).

Correlations of clinical variables to bacteria abundances considering the entire sample ranged from −0.23 to 0.21. When stratified by enterotypes (**Figure 3**), the coefficients changed. In *Bacteroides* cluster, the abundance of *Streptococcus* was correlated to body adiposity (r BMI = 0.25, $p = 0.02$) and *Blautia* to systolic ($r = 0.22$, $p = 0.04$) and diastolic BP ($r = 0.26$, $p = 0.01$), while abundances of *Desulfovibrio* were inversely correlated to BMI ($r = -0.22$, $p = 0.04$) and *Haemophilus* to triglyceride levels ($r = -0.22$, $p = 0.04$).

The strongest correlations coefficients to cardiometabolic risk factors were detected in the *Prevotella* enterotype. *Blautia* (r BMI = −0.34, $p = 0.03$ and r waist = −0.37, $p = 0.02$), *Coprococcus* (r BMI = −0.45, $p < 0.01$; r waist = −0.41, $p < 0.01$; r glucose = −0.37, $p = 0.02$; r insulin = −0.31, $p = 0.04$, and r triglyceride = −0.37, $p = 0.02$), *Roseburia* (r BMI = −0.36, $p = 0.02$ and r waist = −0.36, $p = 0.02$), *Faecalibacterium* (r insulin = −0.35, $p = 0.02$), *Eubacterium ventriosum* (r BMI = −0.33, $p = 0.03$ and r HDL-c = 0.33, $p = 0.04$), and *Akkermansia* (r 2h glucose = −0.35, $p = 0.02$) abundances were correlated to a better cardiometabolic profile, while *Streptococcus* (r systolic BP = 0.44, $p = 0.004$, r diastolic BP = 0.51, $p < 0.001$, r insulin = 0.33, $p = 0.04$, and r LDL-c = 0.40, $p = 0.009$) and *Desulfovibrio* (r BMI = 0.42, $p = 0.006$, r diastolic BP = 0.37, $p = 0.02$, r insulin = 0.32, $p = 0.04$, and r LDL-c = 0.40, $p = 0.01$) abundances to a worse profile.

In *Ruminococcaceae* enterotype, *Blautia* abundance was directly correlated to systolic ($r = 0.20$, $p = 0.02$) and diastolic BP ($r = 0.22$, $p = 0.008$) and inversely to HDL-c levels ($r = -0.20$, $p = 0.02$). *Roseburia* was correlated to unfavorable lipid profile (r LDL-c = 0.24, $p < 0.01$ and r HDL-c = −0.28,

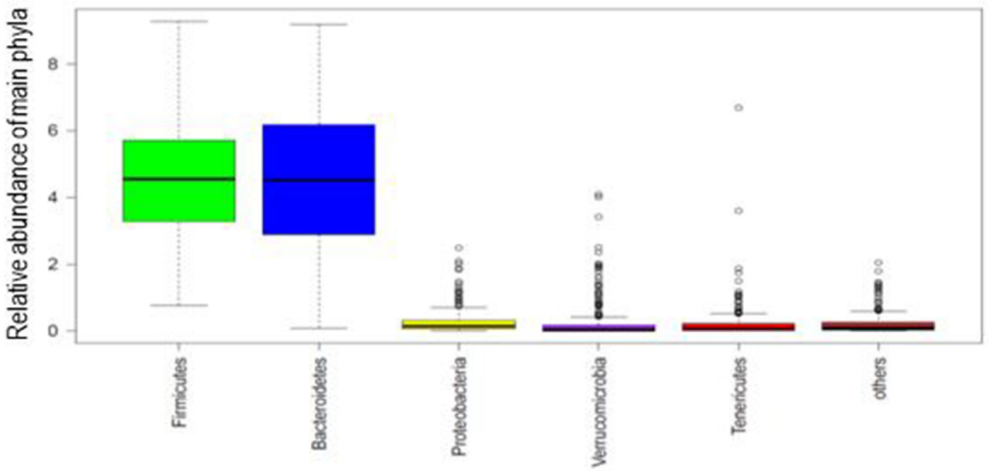

FIGURE 1 | Box plot of the phylogenetic profile of the fecal microbiota of 268 participants according to phyla abundance. The five most abundant phyla are shown and the rest as others. Boxes represent the interquartile range and the line inside represents the median.

$p < 0.001$) and *Eubacterium hallii* to BMI ($r = 0.21$, $p = 0.02$), while *Bifidobacterium* (r total cholesterol $= -0.21$, $p = 0.01$) and *Haemophilus* (r diastolic BP $= -0.23$, $p < 0.01$) to better cardiometabolic parameters.

DISCUSSION

The three enterotypes, described in populations from the North hemisphere, were found in the Brazilian population in a similar structure as previously described. Our observation of increased proportion of strict vegetarians in the *Prevotella* enterotype supports that dietary habits are important determinants of commensal bacteria clustering. Additionally, vegetarian diet associated with lower LDL-c levels suggest that the presence of a protective bacterial cluster in this enterotype could be driving this association. Such consistency of findings in the *Prevotella* cluster was not seen in the other enterotypes, in which we observed different correlations between bacterial abundances and cardiometabolic parameters. A broader variety of the dietary components of the subjects from the *Bacteroides* and *Ruminococcaceae* enterotypes could have limited identifying the relationship between bacteria and risk factors.

The main phyla, *Firmicutes* and *Bacteroidetes*, as well as the most common commensal genera that usually dominate the human gut microbiota, were observed in our sample. Cluster analyses clearly identified the three bacterial groups previously described (Arumugam et al., 2011). Other studies conducted in American, Korean, and Danish populations failed to demonstrate them (Wu et al., 2011; Lim et al., 2014; Roager et al., 2014), which may be attributed, in parts, to differences in methodological approaches to clustering data (Koren et al., 2013).

An opportunist characteristic of our sample was the diversity of dietary patterns, which allowed investigating how the participants were distributed among the bacterial clusters. The diversity facilitated our interpretation of possible physiological roles of bacteria present in the enterotypes. Our findings suggest that different diet-dependent combinations of bacteria should result in different effects on the cardiometabolic profile. Apparently, the importance of genetic factors, breastfeeding, and other early life events for the cardiometabolic risk cannot be neglected.

Lower LDL-c levels were found in subjects belonging to *Prevotella* enterotype, which is consonant with the greater number of strict vegetarians in this enterotype. We speculated that the absence of animal food-derived saturated fatty acids could account for this result (Bradbury et al., 2014; Le and Sabaté, 2014), although our methods are unable to confirm such assumption. Participants classified in this enterotype were not leaner or had lower plasma glucose levels, as previously reported in subjects consuming plant-based diet (Le and Sabaté, 2014; Sabaté and Wien, 2015). Few studies examined the association of enterotypes with cardiometabolic risk factors (Zupancic et al., 2012; Lim et al., 2014); one conducted in Koreans reported increased uric acid concentration in *Bacteroides* cluster compared to the other enterotypes (Lim et al., 2014). As far as we know, this is the first study that detects differences in lipid metabolism using bacterial clustering. Furthermore, when consumers of diverse diets were stratified according to enterotypes, the lowest LDL-c values seen in *Prevotella* enterotype seems to be independent of the dietary habit. This finding suggests that bacteria associated with *Prevotella* may be important drivers of the effect in lipid metabolism.

We tested the correlations of bacteria with cardiometabolic variables within each enterotype to clarify the pathophysiological relationship. We found diverging relationships between a given genus and metabolic parameter when compared one enterotype to another. *Blautia* abundance was favorably correlated to anthropometric measurement in *Prevotella* cluster, but in *Bacteroides* and *Ruminococcaceae* enterotypes showed an unfavorable relationship with cardiometabolic parameters.

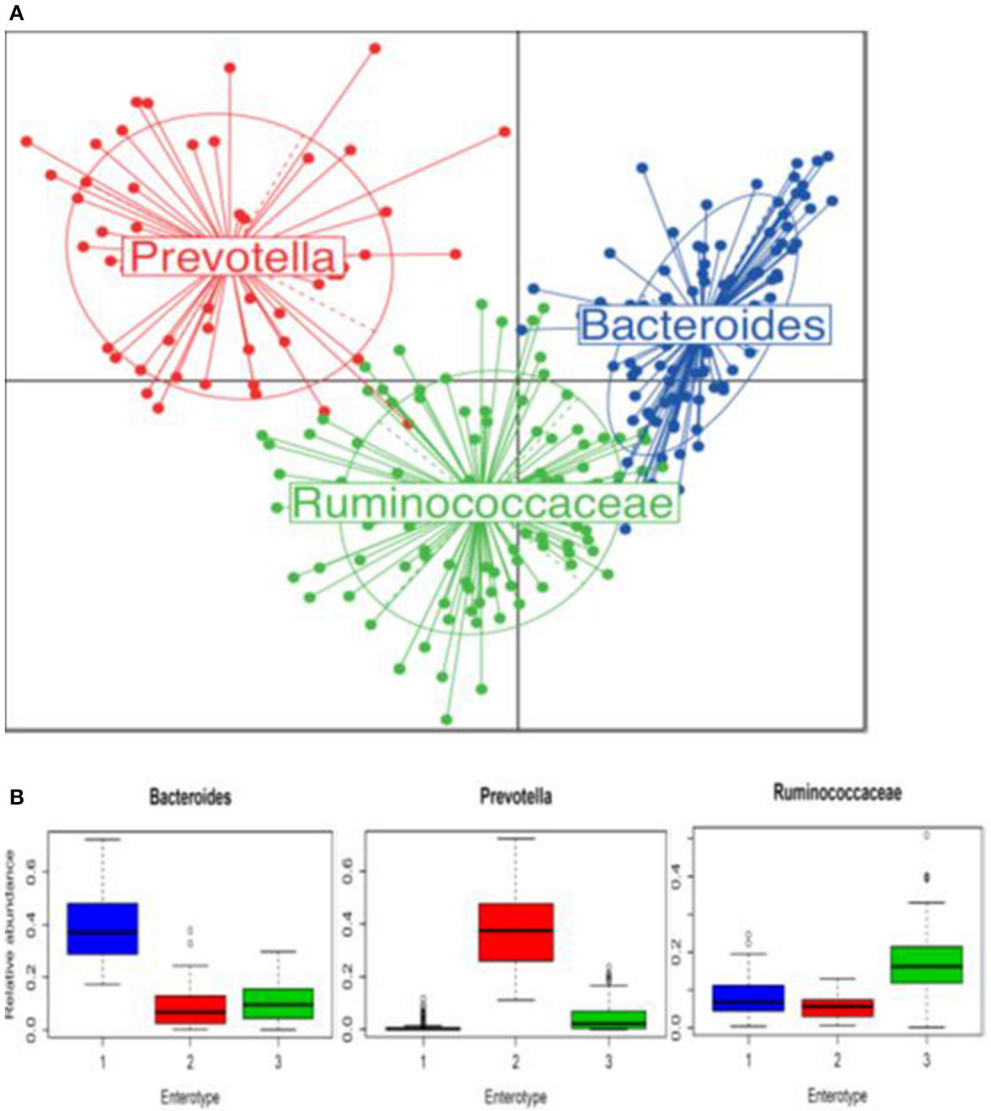

FIGURE 2 | Enterotypes identified in 268 participants using Principal Coordinate Analysis. (A) Samples colored by the enterotype they belong to: blue is enterotype 1 (*Bacteroides*), red is enterotype 2 (*Prevotella*) and green is enterotype 3 (*Ruminococcaceae*). **(B)** Relative abundances of *Bacteroides*, *Prevotella*, and *Ruminococcaceae* in each enterotype. Boxes represent the interquartile range and the line inside represents the median.

This genus belonging to *Lachnospiraceae* family was more commonly found in animals consuming herbivore diet and is known due to its capacity to degrade complex polysaccharides to short-chain fatty acids, such as butyrate, acetate, and propionate (Furet et al., 2009; Biddle et al., 2013; Eren et al., 2015). Several fermentation-dependent metabolic benefits have been described. Butyrate stimulates enteroendocrine cells to secrete incretins (Kasubuchi et al., 2015; Woting and Blaut, 2016), inhibits of pro-inflammatory cytokines production (Miquel et al., 2013; Hippe et al., 2016) and enhances expression of tight-junction proteins (Cani et al., 2009; Peng et al., 2009) that improve gut barrier and reduce metabolic endotoxemia. Such effects have a protective impact on obesity and insulin resistance (Cani et al., 2009; Brahe et al., 2015; Kasubuchi et al., 2015; Hippe et al., 2016). Our findings suggest that this could be occurring in subjects belonging to the *Prevotella* enterotype. Since a high number of vegetarians was present in this enterotype, we suggest that butyrate-producing bacteria should contribute inducing several metabolic benefits.

Only in *Prevotella* enterotype, abundances of other butyrate-producing bacteria, *E. ventriosum*, *Roseburia*, *Coprococcus,* and *Faecalibacterium* (Barcenilla et al., 2000; Pryde et al., 2002; Brahe et al., 2015), showed correlations that are suggestive of a protective role of increased body adiposity and metabolic disturbances. Interestingly, the positive relationship between *E. ventriosum* abundance and HDL-c had not been described. This correlation was not an unexpected finding since another butyrate property is the capacity of activating the GPR109A, which in turn

TABLE 1 | Mean values (±standard deviation) of clinical and biochemical data of 268 participants according to their enterotypes.

	Bacteroides $n = 111$	*Prevotella* $n = 55$	*Ruminococcaceae* $n = 102$	*P*-value
Body mass index (kg/m^2)	25.1 ± 4.6	24.5 ± 4.2	24.8 ± 4.5	0.743
Waist circumference (cm)	83.2 ± 12.0	83.4 ± 10.8	82.5 ± 12.5	0.886
Systolic BP (mmHg)	115 ± 15	120 ± 12	116 ± 14	0.060
Diastolic BP (mmHg)	72 ± 10	75 ± 8	72 ± 10	0.184
Plasma glucose (mg/dL)	93 ± 8	94 ± 12	92 ± 7	0.337
Fasting insulin$^{\#}$ (μUI /mL)	8.4 ± 1.7	7.3 ± 1.9	7.5 ± 1.7	0.205
Total cholesterol (mg/dL)	181 ± 40	169 ± 25	179 ± 35	0.093
LDL-cholesterol (mg/dL)	109 ± 32	96 ± 23$^{\Omega}$	105 ± 29	0.036
HDL-cholesterol$^{\#}$ (mg/dL)	50 ± 1	49 ± 1	51 ± 1	0.648
Triglycerides$^{\#}$ (mg/dL)	93 ± 2	100 ± 1	91 ± 2	0.458

BP, blood pressure.$^{\#}$*Log-transformed values for analysis and were back-transformed to return to the natural scale. ANOVA followed by Bonferroni post hoc test.* $^{\Omega}$ *vs. Bacteroides.*

regulates lipid homeostasis (Elangovan et al., 2014). Also, this effect is coherent with lower LDL-c levels observed in participants belonging to *Prevotella* enterotype. *Coprococcus* was previously associated with adequate bacterial richness in healthy lean adults (Furet et al., 2010) and high abundance of *Faecalibacterium* in subjects consuming fiber-enriched diets (Canani et al., 2011; Matijašić et al., 2014) and low in those with obesity and type 2 diabetes (Furet et al., 2010; Zhang et al., 2013). Our findings are in agreement with the majority of investigators who suggested that these genera abundances are markers of gut health (Miquel et al., 2013; Martín et al., 2015; Hippe et al., 2016), but not all (Balamurugan et al., 2010; Feng et al., 2014). Additionally, the correlation of *Akkermansia* abundance and plasma glucose is consistent with previously reported benefits of this genus in inflammatory status and glucose metabolism (Everard et al., 2013; Schneeberger et al., 2015; Greer et al., 2016).

We speculate that the enterotype-mediated risk pattern is dependent of the local microenvironment, and the combination of abundant bacteria in each enterotype would drive the pathophysiological outcomes. The fiber-rich diet of vegetarians included in the *Prevotella* enterotype could have triggered beneficial effects at the intestinal and systemic levels. Therefore, our findings are consistent reports of favorable cardiometabolic risk profile in subjects consuming diets rich in fruits and vegetables like the Adventists (Pettersen et al., 2012; Sabaté and Wien, 2015).

Interestingly, in *Ruminococcaceae* enterotype, *Eubacterium hallii,* and *Roseburia* were unfavorably associated with metabolic parameters, while *Desulfovibrio* and *Haemophilus*, from the *Proteobacteria* phylum, with a protective relationship. It is well-known that the latter are gram-negative bacteria with lipopolysaccharide on its surface. This endotoxin is an important ligand for toll-like receptor 4 that activates the innate immune system, which could result in a pro-inflammatory condition (Cani et al., 2009; Velloso et al., 2015). Considering that *Proteobacteria* preferentially metabolize proteins (Ferrocino et al., 2015), higher abundance of bacteria from this phylum could be expected in *Bacteroides* and *Ruminococcaceae* enterotypes, in which lacto-ovo-vegetarians and omnivores were more commonly present. This agrees with a report of high abundance of *Proteobacteria* in children consuming a protein-fat based diet (De Filippo et al., 2010). However, some inverse correlations with cardiometabolic factors were unexpectedly detected in both enterotypes. Only in the *Prevotella* enterotype, *Desulfovibrio* abundance was directly correlated to BMI, BP, insulin, and LDL-c, in line with previous animal and human studies. In db/db mice (Geurts et al., 2011) and humans with cardiovascular diseases (Yin et al., 2015) compared to respective controls, *Proteobacteria* was more abundant. Such results may reinforce that the resulting balance of a great variety of bacteria present in gut drives metabolic processes in the host. Therefore, different diet-dependent combinations of bacteria would be related to distinct cardiometabolic risk profile. Comparisons of clinical data of subjects within each diet stratified by enterotype reinforced our assumption that enterotype may be driving the dietary lipid-associated risk since the LDL-c values were invariably lower in the subsets of participants from the *Prevotella* enterotype.

In all enterotypes, the abundance of *Streptococcus* was correlated to unfavorable cardiometabolic risk profile (increased adiposity, BP, and lipids), although correlation coefficients in the *Ruminococcaceae* enterotype were weak (data not shown). This genus belongs to *Firmicutes* phylum, which was originally described as the predominant in animal obesity (Ley et al., 2005; Turnbaugh et al., 2006). We have reported a greater abundance of *Streptococcus alactolyticus* in obese animals compared to hypertensive and Winstar rat (Petriz et al., 2014). Our correlations might be in part due to its proinflammatory role previously described (Al-Jashamy et al., 2010; Jiang et al., 2015).

Our study has limitations. Regarding the dietary intake assessment, raw data were not available impeding to establish associations of nutrients and the microbiota. Determination of fecal supernatants would be desirable to support the assumption of a lower content of fat among strict vegetarian subjects. Fecal consistency was not systematically obtained and was not considered as a confounder in our analyses. Recently, the influence of fecal consistency with gut microbiota richness and composition and bacterial growth rates has been raised (Vandeputte et al., 2016). Our sample from the ADVENTO study is not representative of the general population living in Brazil. As a matter of fact, smoking and drinking habits are known to be less frequent among Adventists. On the other hand, such characteristics should have contributed to minimizing confounders in our analyses.

In conclusion, the three enterotypes previously described are present in Brazilians, supporting that those bacterial clusters are not population-specific. Diet-independent lower LDL-c levels in subjects from *Prevotella* than in other enterotypes suggest that a

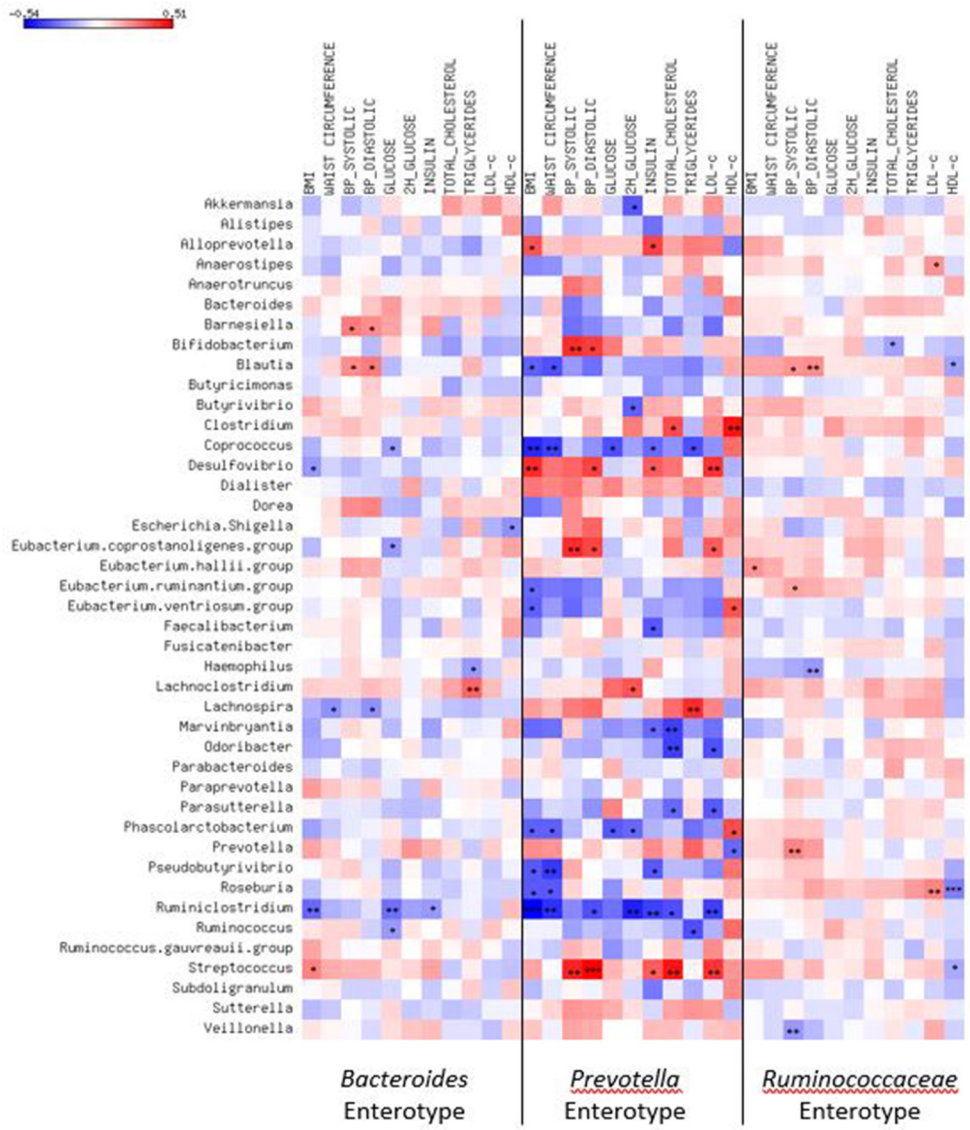

FIGURE 3 | Heatmap of correlations of most common genera or species and cardiometabolic risk factors according to enterotypes. Spearman correlation test used. *$p < 0.05$; **$p < 0.01$; ***$p < 0.001$; BMI, body mass index; BP, blood pressure.

protective bacterial group in the former should be driving this association. Enterotypes seem to be useful to understand the impact of daily diet exposure on cardiometabolic risk factors. Prospective studies are needed to confirm their utility for predicting phenotypes in humans.

AUTHOR CONTRIBUTIONS

Ad, BA, SF had substantial contributions to the conception and design of the work. Ad, EG, AP, SF to the acquisition of data. Ad, GF, Id, SF to the analysis and interpretation of data for the work. Ad, Id, SF drafted the work and GF, BP, EG, AP revised it critically for important intellectual content. Ad, GF, Id, BP, EG, AP, SF participated of the final approval of the version to be published. Ad, GF, Id, BP, EG, AP, SF agreed to be accountable for all aspects of the work in ensuring that questions related to the accuracy or integrity of any part of the work are appropriately investigated and resolved.

FUNDING

The present study was supported by FAPESP (2012/12626-9 and 2012/03880-9).

ACKNOWLEDGMENTS

Authors thank the FAPESP, Advento Study Group* and participants. *Members of the Advento Study Group: I. J. M. Bensenor, P. A. Lotufo, K. R. M. Gomes, L. C. B. Soares, V. Kunz,

N. V. Silva, L. A. Portes, D. T. Kanno, L. F. Sella, R. França, M. C. Teixeira, S. Gasparini, E. O. L. Ferreira, B. Bonifácio, T. C. Souza, F. M. Diaz, S. C. C. Dammann, I.R. Pinheiro, W. F. S. Costa, D. M. S. Larchert, D. F. Nunes, J. S. Amorim, E. M. Reis, I. P. Manfrim, N. V. Ferreira, J. L. V. Passos, E. Barreto.

SUPPLEMENTARY MATERIAL

The Supplementary Material for this article can be found online at: http://journal.frontiersin.org/article/10.3389/fcimb.2017.00047/full#supplementary-material

REFERENCES

Al-Jashamy, K., Murad, A., Zeehaida, M., Rohaini, M., and Hasnan, J. (2010). Prevalence of colorectal cancer associated with *Streptococcus bovis* among inflammatory bowel and chronic gastrointestinal tract disease patients. *Asian Pac. J. Cancer Prev.* 11, 1765–1768.

Arumugam, M., Raes, J., Pelletier, E., Le Paslier, D., Yamada, T., Mende, D. R., et al. (2011). Enterotypes of the human gut microbiome. *Nature* 473, 174–180. doi: 10.1038/nature09944

Arumugam, M., Raes, J., Pelletier, E., Le Paslier, D., Yamada, T., Mende, D. R., et al. (2014). Addendum: enterotypes of the human gut microbiome. *Nature* 506, 516. doi: 10.1038/nature13075

Balamurugan, R., George, G., Kabeerdoss, J., Hepsiba, J., Chandragunasekaran, A. M., and Ramakrishna, B. S. (2010). Quantitative differences in intestinal *Faecalibacterium prausnitzii* in obese Indian children. *Br. J. Nutr.* 103, 335–338. doi: 10.1017/S0007114509992182

Barcenilla, A., Pryde, S. E., Martin, J. C., Duncan, S. H., Stewart, C. S., Henderson, C., et al. (2000). Phylogenetic relationships of butyrate-producing bacteria from the human gut. *Appl. Environ. Microbiol.* 66, 1654–1661. doi: 10.1128/AEM.66.4.1654-1661.2000

Biddle, A., Stewart, L., Blanchard, J., and Leschine, S. (2013). Untangling the genetic basis of fibrolytic specialization by *Lachnospiraceae* and *Ruminococcaceae* in diverse gut communities. *Diversity* 5, 627–640. doi: 10.3390/d5030627

Bolger, A. M., Lohse, M., and Usadel, B. (2014). Trimmomatic: a flexible trimmer for Illumina sequence data. *Bioinformatics* 30, 2114–2120. doi: 10.1093/bioinformatics/btu170

Bradbury, K. E., Crowe, F. L., Appleby, P. N., Schmidt, J. A., Travis, R. C., and Key, T. J. (2014). Serum concentrations of cholesterol, apolipoprotein A-I and apolipoprotein B in a total of 1694 meat-eaters, fish-eaters, vegetarians and vegans. *Eur. J. Clin. Nutr.* 68, 178–183. doi: 10.1038/ejcn.2013.248

Brahe, L. K., Le Chatelier, E., Prifti, E., Pons, N., Kennedy, S., Hansen, T., et al. (2015). Specific gut microbiota features and metabolic markers in postmenopausal women with obesity. *Nutr. Diabetes* 5:e159. doi: 10.1038/nutd.2015.9

Canani, R. B., Costanzo, M. D., Leone, L., Pedata, M., Meli, R., and Calignano, A. (2011). Potential beneficial effects of butyrate in intestinal and extraintestinal diseases. *World J. Gastroenterol.* 17, 1519–1528. doi: 10.3748/wjg.v17.i12.1519

Cani, P. D., Possemiers, S., Van de Wiele, T., Guiot, Y., Everard, A., Rottier, O., et al. (2009). Changes in gut microbiota control inflammation in obese mice through a mechanism involving GLP-2-driven improvement of gut permeability. *Gut* 58, 1091–1103. doi: 10.1136/gut.2008.165886

Caporaso, J. G., Kuczynski, J., Stombaugh, J., Bittinger, K., Bushman, F. D., Costello, E. K., et al. (2010). QIIME allows analysis of high-throughput community sequencing data. *Nat. Methods* 7, 335–336. doi: 10.1038/nmeth.f.303

Caporaso, J. G., Lauber, C. L., Walters, W. A., Berg-Lyons, D., Huntley, J., Fierer, N., et al. (2012). Ultra-high-throughput microbial community analysis on the Illumina HiSeq and MiSeq platforms. *ISME J.* 6, 1621–1624. doi: 10.1038/ismej.2012.8

De Filippo, C., Cavalieri, D., Di Paola, M., Ramazzotti, M., Poullet, J. B., Massart, S., et al. (2010). Impact of diet in shaping gut microbiota revealed by a comparative study in children from Europe and rural Africa. *Proc. Natl. Acad. Sci. U.S.A.* 107, 14691–14696. doi: 10.1073/pnas.1005963107

Elangovan, S., Pathania, R., Ramachandran, S., Ananth, S., Padia, R. N., Lan, L., et al. (2014). The niacin/butyrate receptor GPR109A suppresses mammary tumorigenesis by inhibiting cell survival. *Cancer Res.* 74, 1166–1178. doi: 10.1158/0008-5472.CAN-13-1451

Eren, A. M., Sogin, M. L., Morrison, H. G., Vineis, J. H., Fisher, J. C., Newton, R. J., et al. (2015). A single genus in the gut microbiome reflects host preference and specificity. *ISME J.* 9, 90–100. doi: 10.1038/ismej.2014.97

Everard, A., Belzer, C., Geurts, L., Ouwerkerk, J. P., Druart, C., Bindels, L. B., et al. (2013). Cross-talk between *Akkermansia muciniphila* and intestinal epithelium controls diet-induced obesity. *Proc. Natl. Acad. Sci. U.S.A.* 110, 9066–9071. doi: 10.1073/pnas.1219451110

Feng, J., Tang, H., Li, M., Pang, X., Wang, L., Zhang, M., et al. (2014). The abundance of fecal *Faecalibacterium prausnitzii* in relation to obesity and gender in Chinese adults. *Arch. Microbiol.* 196, 73–77. doi: 10.1007/s00203-013-0942-2

Ferrocino, I., Di Cagno, R., De Angelis, M., Turroni, S., Vannini, L., Bancalari, E., et al. (2015). Fecal microbiota in healthy subjects following omnivore, vegetarian and vegan diets: culturable populations and rRNA DGGE profiling. *PLoS ONE* 10:e0128669. doi: 10.1371/journal.pone.0128669

Furet, J. P., Kong, L. C., Tap, J., Poitou, C., Basdevant, A., Bouillot, J. L., et al. (2010). Differential adaptation of human gut microbiota to bariatric surgery-induced weight loss. *Diabetes* 59, 3049–3057. doi: 10.2337/db10-0253

Furet, J.-P., Firmesse, O., Gourmelon, M., Bridonneau, C., Tap, J., Mondot, S., et al. (2009). Comparative assessment of human and farm animal faecal microbiota using real-time quantitative PCR. *FEMS Microbiol. Ecol.* 68, 351–362. doi: 10.1111/j.1574-6941.2009.00671.x

Geurts, L., Lazarevic, V., Derrien, M., Everard, A., Van Roye, M., Knauf, C., et al. (2011). Altered gut microbiota and endocannabinoid system tone in obese and diabetic leptin-resistant mice: impact on apelin regulation in adipose tissue. *Front. Microbiol.* 2:149. doi: 10.3389/fmicb.2011.00149

Greer, R. L., Dong, X., Moraes, A. C., Zielke, R. A., Fernandes, G. R., Peremyslova, E., et al. (2016). Akkermansia muciniphila mediates negative effects of IFNγ on glucose metabolism. *Nat. Commun.* 7:13329. doi: 10.1038/ncomms13329

Hippe, B., Remely, M., Aumueller, E., Pointner, A., Magnet, U., and Haslberger, A. G. (2016). *Faecalibacterium prausnitzii* phylotypes in type two diabetic, obese, and lean control subjects. *Benef Microbes* 7, 511–517. doi: 10.3920/BM2015.0075

Jiang, W., Wu, N., Wang, X., Chi, Y., Zhang, Y., Qiu, X., et al. (2015). Dysbiosis gut microbiota associated with inflammation and impaired mucosal immune function in intestine of humans with non-alcoholic fatty liver disease. *Sci. Rep.* 5:8096. doi: 10.1038/srep08096

Kasubuchi, M., Hasegawa, S., Hiramatsu, T., Ichimura, A., and Kimura, I. (2015). Dietary gut microbial metabolites, short-chain fatty acids, and host metabolic regulation. *Nutrients* 7, 2839–2849. doi: 10.3390/nu7042839

Kelder, T., Stroeve, J. H., Bijlsma, S., Radonjic, M., and Roeselers, G. (2014). Correlation network analysis reveals relationships between diet-induced changes in human gut microbiota and metabolic health. *Nutr. Diab.* 4:e122. doi: 10.1038/nutd.2014.18

Koeth, R. A., Wang, Z., Levison, B. S., Buffa, J. A., Org, E., Sheehy, B. T., et al. (2013). Intestinal microbiota metabolism of l-carnitine, a nutrient in red meat, promotes atherosclerosis. *Nat. Med.* 19, 576–585. doi: 10.1038/nm.3145

Koren, O., Knights, D., Gonzalez, A., Waldron, L., Segata, N., Knight, R., et al. (2013). A guide to enterotypes across the human body: meta-analysis of microbial community structures in human microbiome datasets. *PLoS Comput. Biol.* 9:e1002863. doi: 10.1371/journal.pcbi.1002863

Laslett, L. J., Alagona, P. Jr., Clark, B. A. III, Drozda, J. P. Jr., Saldivar, F., Wilson, S. R., et al. (2012). The worldwide environment of cardiovascular disease: prevalence, diagnosis, therapy, and policy issues: a report from the American College of Cardiology. *J. Am. Coll. Cardiol.* 60, S1–S49. doi: 10.1016/j.jacc.2012.11.002

Le, L. T., and Sabaté, J. (2014). Beyond meatless, the health effects of vegan diets: findings from the adventist cohorts. *Nutrients* 6, 2131–2147. doi: 10.3390/nu6062131

Ley, R. E., Bäcked, F., Turnbaugh, P., Lozupone, C. A., Knight, R. D., and Gordon, J. I. (2005). Obesity alters gut microbial ecology. *Proc. Natl. Acad. Sci. U.S.A.* 102, 11070–11075. doi: 10.1073/pnas.0504978102

Lim, M. Y., Rho, M., Song, Y.-M., Lee, K., Sung, J., and Ko, G. (2014). Stability of gut enterotypes in Korean monozygotic twins and their association with biomarkers and diet. *Sci. Rep.* 4:7348. doi: 10.1038/srep07348

Magoč, T., and Salzberg, S. L. (2011). FLASH: fast length adjustment of short reads to improve genome assemblies. *Bioinformatics* 27, 2957–2963. doi: 10.1093/bioinformatics/btr507

Martín, R., Miquel, S., Chain, F., Natividad, J. M., Jury, J., Lu, J., et al. (2015). *Faecalibacterium prausnitzii* prevents physiological damages in a chronic low-grade inflammation murine model. *BMC Microbiol.* 15:67. doi: 10.1186/s12866-015-0400-1

Matijašić, B. B., Obermajer, T., Lipoglavšek, L., Grabnar, I., Avguštin, G., and Rogelj, I. (2014). Association of dietary type with fecal microbiota in vegetarians and omnivores in Slovenia. *Eur. J. Nutr.* 53, 1051–1064. doi: 10.1007/s00394-013-0607-6

Miquel, S., Martín, R., Rossi, O., Bermúdez-Humarán, L. G., Chatel, J. M., Sokol, H., et al. (2013). *Faecalibacterium prausnitzii* and human intestinal health. *Curr. Opin. Microbiol.* 16, 255–261. doi: 10.1016/j.mib.2013.06.003

Ou, J., Carbonero, F., Zoetendal, E. G., DeLany, J. P., Wang, M., Newton, K., et al. (2013). Diet, microbiota, and microbial metabolites in colon cancer risk in rural Africans and African Americans. *Am. J. Clin. Nutr.* 98, 111–120. doi: 10.3945/ajcn.112.056689

Peng, L., Li, Z. R., Green, R. S., Holzman, I. R., and Lin, J. (2009). Butyrate enhances the intestinal barrier by facilitating tight junction assembly via activation of AMP-activated protein kinase in Caco-2 cell monolayers. *J. Nutr.* 139, 1619–1625. doi: 10.3945/jn.109.104638

Petriz, B. A., Castro, A. P., Almeida, J. A., Gomes, C. P., Fernandes, G. R., Kruger, R. H., et al. (2014). Exercise induction of gut microbiota modifications in obese, non-obese and hypertensive rats. *BMC Genomics* 15:511. doi: 10.1186/1471-2164-15-511

Pettersen, B. J., Anousheh, R., Fan, J., Jaceldo-Siegl, K., and Fraser, G. E. (2012). Vegetarian diets and blood pressure among white subjects: results from the adventist health Study-2 (AHS-2). *Public Health Nutr.* 15, 1909–1916. doi: 10.1017/S1368980011003454

Pryde, S. E., Duncan, S. H., Hold, G. L., Stewart, C. S., and Flint, H. J. (2002). The microbiology of butyrate formation in the human colon. *FEMS Microbiol. Lett.* 217, 133–139. doi: 10.1111/j.1574-6968.2002.tb11467.x

Quast, C., Pruesse, E., Yilmaz, P., Gerken, J., Schweer, T., Yarza, P., et al. (2013). The SILVA ribosomal RNA gene database project: improved data processing and web-based tools. *Nucleic Acids Res.* 41, D590–D596. doi: 10.1093/nar/gks1219

Roager, H. M., Licht, T. R., Poulsen, S. K., Larsen, T. M., and Bahl, M. I. (2014). Microbial enterotypes, inferred by the Prevotella-to-Bacteroides ratio, remained stable during a 6-month randomized controlled diet intervention with the new nordic diet. *Appl. Environ. Microbiol.* 80, 1142–1149. doi: 10.1128/AEM.03549-13

Rognes, T., Flouri, T., Nichols, B., Quince, C., and Mahé, F. (2016). VSEARCH: a versatile open source tool for metagenomics. *Peer J.* 4:e2584. doi: 10.7717/peerj.2584

Sabaté, J., and Wien, M. (2015). A perspective on vegetarian dietary patterns and risk of metabolic syndrome. *Br. J. Nutr.* 113, S136–S143. doi: 10.1017/S0007114514004139

Schneeberger, M., Everard, A., Gómez-Valadés, A. G., Matamoros, S., Ramírez, S., Delzenne, N. M., et al. (2015). *Akkermansia muciniphila* inversely correlates with the onset of inflammation, altered adipose tissue metabolism and metabolic disorders during obesity in mice. *Sci. Rep.* 5:16643. doi: 10.1038/srep16643

Tonstad, S., Butler, T., Yan, R., and Fraser, G. E. (2009). Type of vegetarian diet, body weight, and prevalence of type 2 diabetes. *Diabetes Care* 32, 791–796. doi: 10.2337/dc08-1886

Turnbaugh, P. J., Ley, R. E., Mahowald, M. A., Magrini, V., Mardis, E. R., and Gordon, J. I. (2006). An obesity-associated gut microbiome with increased capacity for energy harvest. *Nature* 444, 1027–1031. doi: 10.1038/nature05414

Vandeputte, D., Falony, G., Vieira-Silva, S., Tito, R. Y., Joossens, M., and Raes, J. (2016). Stool consistency is strongly associated with gut microbiota richness and composition, enterotypes and bacterial growth rates. *Gut* 65, 57–62. doi: 10.1136/gutjnl-2015-309618

Velloso, L. A., Folli, F., and Saad, M. J. (2015). TLR4 at the crossroads of nutrients, gut microbiota and metabolic inflammation. *Endocr. Rev.* 36, 245–271. doi: 10.1210/er.2014-1100

World Health Organization (2011). *Global Atlas on Cardiovascular Disease Prevention and Control*. Geneva: WHO.

Woting, A., and Blaut, M. (2016). The intestinal microbiota in metabolic disease. *Nutrients* 8:202. doi: 10.3390/nu8040202

Wu, G. D., Chen, J., Hoffmann, C., Bittinger, K., Chen, Y. Y., Sue, A., et al. (2011). Linking long-term dietary patterns with gut microbial enterotypes. *Science* 334, 105–108. doi: 10.1126/science.1208344

Yatsunenko, T., Contreras, M., Magris, M., Hidalgo, G., Robert, N., Anokhin, A. P., et al. (2012). Human gut microbiome viewed across age and geography. *Nature* 486, 222–227. doi: 10.1038/nature11053

Yin, J., Liao, S.-X., He, Y., Wang, S., Xia, G.-H., Liu, F.-T., et al. (2015). Dysbiosis of gut microbiota with reduced trimethylamine-N-oxide level in patients with large-artery atherosclerotic stroke or transient ischemic attack. *J. Am. Heart Assoc.* 4, 1–13. doi: 10.1161/JAHA.115.002699

Zhang, X., Shen, D., Fang, Z., Jie, Z., Qiu, X., Zhang, C., et al. (2013). Human gut microbiota changes reveal the progression of glucose intolerance. *PLoS ONE* 8:e71108. doi: 10.1371/journal.pone.0071108

Zupancic, M. L., Cantarel, B. L., Liu, Z., Drabek, E. F., Ryan, K. A., Cirimotich, S., et al. (2012). Analysis of the gut microbiota in the old order amish and its relation to the metabolic syndrome. *PLoS ONE* 7:e43052. doi: 10.1371/journal.pone.0043052

Conflict of Interest Statement: The authors declare that the research was conducted in the absence of any commercial or financial relationships that could be construed as a potential conflict of interest.

Copyright © 2017 de Moraes, Fernandes, da Silva, Almeida-Pititto, Gomes, Pereira and Ferreira. This is an open-access article distributed under the terms of the Creative Commons Attribution License (CC BY). The use, distribution or reproduction in other forums is permitted, provided the original author(s) or licensor are credited and that the original publication in this journal is cited, in accordance with accepted academic practice. No use, distribution or reproduction is permitted which does not comply with these terms.

frontiers in Cellular and Infection Microbiology

ORIGINAL RESEARCH
published: 08 February 2017
doi: 10.3389/fcimb.2017.00029

Human Enterovirus 68 Interferes with the Host Cell Cycle to Facilitate Viral Production

Zeng-yan Wang[1], Ting Zhong[2], Yue Wang[3], Feng-mei Song[4], Xiao-feng Yu[5], Li-ping Xing[1], Wen-yan Zhang[5], Jing-hua Yu[5], Shu-cheng Hua[1]* and Xiao-fang Yu[5]**

[1] Department of Internal Medicine, The First Hospital of Jilin University, Jilin University, Changchun, China, [2] Medicinal Chemistry, College of Pharmacy, Changchun University of Chinese Medicine, Changchun, China, [3] Chemistry of Traditional Chinese Medicine, College of Pharmacy, Changchun University of Chinese Medicine, Changchun, China, [4] Department of Experimental Pharmacology and Toxicology, School of Pharmacy, Jilin Univrsity, Changchun, China, [5] Institute of Virology and AIDS Research, The First Hospital of Jilin University, Jilin University, Changchun, China

Enterovirus D68 (EV-D68) is an emerging pathogen that recently caused a large outbreak of severe respiratory disease in the United States and other countries. Little is known about the relationship between EV-D68 virus and host cells. In this study, we assessed the effect of the host cell cycle on EV-D68 viral production, as well as the ability of EV-D68 to manipulate host cell cycle progression. The results suggest that synchronization in G0/G1 phase, but not S phase, promotes viral production, while synchronization in G2/M inhibits viral production. Both an early EV-D68 isolate and currently circulating strains of EV-D68 can manipulate the host cell cycle to arrest cells in the G0/G1 phase, thus providing favorable conditions for virus production. Cell cycle regulation by EV-D68 was associated with corresponding effects on the expression of cyclins and CDKs, which were observed at the level of the protein and/or mRNA. Furthermore, the viral non-structural protein 3D of EV-D68 prevents progression from G0/G1 to S. Interestingly, another member of the *Picornaviridae* family, EV-A71, differs from EV-D68 in that G0/G1 synchronization inhibits, rather than promotes, EV-A71 viral replication. However, these viruses are similar in that G2/M synchronization inhibits the production and activity of both viruses, which is suggestive of a common therapeutic target for both types of enterovirus. These results further clarify the pathogenic mechanisms of enteroviruses and provide a potential strategy for the treatment and prevention of EV-D68-related disease.

Keywords: enterovirus 68 (EV-D68), cell cycle, G0/G1 arrest, viral replication, host-pathogen interaction

OPEN ACCESS

Edited by:
Chioma M. Okeoma, University of Iowa, USA

Reviewed by:
Jingwen Wang, Yale University, USA
Xin Zhao, Institute of Microbiology (CAS), China

***Correspondence:**
Jing-hua Yu
yjh-0-2002@163.com
Shu-cheng Hua
shuchenghua@eyou.com
Xiao-fang Yu
yuxiaofang@jlu.edu.cn

Received: *08 October 2016*
Accepted: *20 January 2017*
Published: *08 February 2017*

Citation:
Wang Z-y, Zhong T, Wang Y, Song F-m, Yu X-f, Xing L-p, Zhang W-y, Yu J-h, Hua S-c and Yu X-f (2017) Human Enterovirus 68 Interferes with the Host Cell Cycle to Facilitate Viral Production. Front. Cell. Infect. Microbiol. 7:29. doi: 10.3389/fcimb.2017.00029

INTRODUCTION

Human enterovirus 68 (EV-D68) is an emerging pathogen that can cause severe respiratory disease and is associated with cases of paralysis, especially among children. It was first isolated from samples obtained in California in 1962 from four children with pneumonia and bronchiolitis (Schieble et al., 1967). Over the past 10 years, EV-D68 infection outbreaks have been reported in Italy, the United States, Germany, China, and several other countries (Esposito et al., 2015; Farrell et al., 2015; Reiche et al., 2015; Zhang et al., 2015), with a record number of confirmed cases in 2014 (http://www.cdc.gov/non-polio-enterovirus/about/ev-d68.html). Unfortunately, no vaccines for prevention or medicines for treatment are currently available for future outbreaks, mainly due to the fact that information on host factors required for EV-D68 replication is scarce.

EV-D68 belong to enterovirus (family *Picornaviridae*, genus *Enterovirus*), which are non-enveloped, positive-sense single-strand RNA viruses of approximately 7500 nt and contain a large open reading frame that encodes a polyprotein that is cleaved to yield corresponding viral proteins. Based on the molecular and biological characteristics, four human enterovirus (HEV) species are currently designated as HEV-A, -B, -C, and -D (Oberste et al., 1999a,b). The representative of HEV-A serotype is human enterovirus 71 (EV-A71), which is a primary causative agent for Hand, foot, and mouth disease (HFMD) that is associated with the recent outbreaks in Asia (Liu et al., 2011; Wang et al., 2012). EV-D68 is assigned to HEV-D serotype, but EV-D68 is unlike other enteroviruses in that it is acid labile and biologically more similar to human rhinoviruses that are associated with respiratory diseases (Smura et al., 2010).

As a feature of their pathogenic mechanism, many viruses facilitate their own replication by interacting with host factors that regulate cell cycle progression. Examples can be discovered in DNA viruses, retroviruses and RNA viruses. DNA viruses, which replicate in the nucleus, have been extensively investigated in regard to control the cell cycle of host cells. For example, some small DNA viruses including simian virus 40 (DeCaprio et al., 1988), adenovirus (Howe et al., 1990; Eckner et al., 1994), and human papillomavirus (Werness et al., 1990), which lack their own polymerases, use the host polymerase to promote the entry of cells into S phase from G0/G1 phase. For other large DNA viruses, for example, herpesviruses can induce G0/G1 arrest in order to avoid competing for cellular DNA replication resources (Flemington, 2001). Cell cycle regulation also has been observed for retroviruses, which, like DNA viruses, replicate in the nucleus. The Vpr protein of human immunodeficiency virus type 1 is responsible for eliciting cell cycle arrest in G2/M phase (He et al., 1995; Goh et al., 1998). Furthermore, RNA viruses, whose primary site of replication is normally the cytoplasm, have also been demonstrated to interfere with the host cell cycle. Infectious bronchitis virus (IBV) induces an S and G2/M-phase arrest to favor viral replication (Dove et al., 2006; Li et al., 2007), and mouse hepatitis virus (MHV) (Chen and Makino, 2004) and some severe acute respiratory syndrome coronavirus (SARS-CoV) proteins induce cell cycle arrest in G0/G1 phase (Yuan et al., 2005, 2006). In a previous study, we found that human EV-A71 and Coxsackievirus A16, manipulate the host cell cycle at S phase in order to promote their own viral replication (Yu et al., 2015); however, the potential manipulation of the host cell cycle by EV-D68, which is associated with higher lethality in recent large-scale outbreaks, has not been previously characterized.

In the current study, we examined the effects of the cell cycle status on EV-D68 viral replication, as well as the impact of EV-D68 virus on the host cell cycle. Our data show that EV-D68 replication is integrally associated with the host cell cycle, though the pattern of regulation differs distinctly from that of EV-A71. These results further increase the understanding of the pathogenic mechanisms of enteroviruses and provide a potential target for the treatment and prevention of enterovirus-related diseases.

MATERIALS AND METHODS

Viruses and Cells

The Fermon (ATCC, VR-1826), US/KY/14-18953 (ATCC, VR-1825D), and US/MO/14-18947 (ATCC, VR-1823D) strains of EV-D68; and the Changchun077 strain of EV-A71 have been reported previously (Wang et al., 2012). Viruses were propagated in human rhabdomyosarcoma RD cells (No CCL-136), and the supernatants were harvested and stored at −80°C. Human embryonic kidney cells (HEK 293T cells) (No CRL-11268) and RD cells were purchased from the ATCC (Manassas, VA, USA) and used according to a previous study (Wang et al., 2015). Cells were maintained in Dulbecco's modified Eagle's medium (DMEM) (Hyclone, Logan, UT, USA) supplemented with 10% fetal bovine serum (FBS) (GIBCO BRL, Grand Island, NY, USA).

Viral Titer Determination

The viral titers were determined by measuring the 50% tissue culture infective dose (TCID50) in a microtitration assay using RD cells, as described (Gay et al., 2006). RD cells were seeded and incubated at 37°C for 24 h in 96-well plates. Virus-containing supernatant was serially diluted 10-fold, and 100 μl of diluent virus was added per well in octuplicate. Until the experimental endpoint was reached the cytopathic effect was observed once per day. According to the Reed-Muench method (Reed, 1983) the viral titers of the TCID50 were determined, based on the assumption that material with 1×10^5 TCID50/ml will produce 0.7×10^5 plaque forming units/ml (www.protocol-online.org/biology-forums/posts/1664.html).

Infection

Cells were mock-infected or infected with EV-D68 or EV-A71 at a multiplicity of infection (MOI) of 0.8. After 2 h of virus adsorption, cells were washed with phosphate-buffered saline (PBS) one time, then added fresh culture medium.

Cell Cycle Release

Subconfluent cultures of RD cells were synchronized in G0/G1 phase by serum deprivation (He et al., 2010). Approximately 5×10^5 cells were plated in a 6-well plate and maintained in serum-free medium for 24 h. After EV-D68 virus infection, fresh 10% DMEM was added to release the cells from G0/G1.

Synchronization of Cells

In order to observe the effects of the cell cycle on virus growth, subconfluent cultures of RD cells were synchronized in G0/G1 phase by serum deprivation for 24 h (He et al., 2010). For S-phase synchronization, a final concentration of 0.85 mM thymidine (Sigma) were added (Helt and Harris, 2005; Yu et al., 2015) for 24 h. For G2/M synchronization, 25 ng/ml of nocodazole (Sigma) was added (He et al., 1995; Yu et al., 2015) for 24 h. For sustained S and G2/M cell-cycle arrest after virus infection, cells were treated with fresh 0.85 mM thymidine and 25 ng/ml nocodazole for the indicated times.

Cell Cycle Analysis by Flow Cytometry

Propidium iodide (PI) staining was used to measure the nuclear DNA content according to previous study (Yu et al.,

2015). Firstly, the cells were collected and fixed with 1 ml of cold 70% ethanol at 4°C overnight and then re-suspended in PI staining buffer (50 μg/ml PI (Sigma), 20 μg/ml RNase in PBS) for 2 h at 4°C. Fluorescence-activated cell sorting (FACScan; BD) were used to analyze the PI-stained cells, and at least 10,000 cells were counted for each sample. ModFit LT, version 2.0 (Verity Software House) was performed for data analysis.

Western Blot Analysis

Virus-infected or mock-infected cells were collected at various times after EV-D68 infection and washed once with PBS as previously described (Yu et al.). The following antibodies were used in Western blot analyses: anti-CDK2 (Cell Signal), anti-cyclinE1 (Proteintech), anti-CDK4 (Cell Signal), anti-CDK6 (Cell Signal), anti-cyclinD (Cell Signal), anti-CDK1 (Boster), anti-cyclinB1 (Santa Cruz), and anti-histone (GenScript). Secondary antibodies from mouse or rabbit were obtained from Jackson Immuno Research.

Quantitative Real-Time PCR

All work was carried out in a designated PCR-clean area as previously described (Yu et al.). RNA was extracted from infected and uninfected cells using Trizol reagent (Gibco-BRL, Rockville, Md.) and isolated as specified by the manufacturer. The RNA was DNAse-treated (DNase I-RNase-Free, Ambion) to remove any contaminating DNA; 200 ng of total RNA was reverse-transcribed with oligo dT primers using the High Capacity cDNA RT Kit (Applied Biosystems) in a 20 μl cDNA reaction, as specified by the manufacturer. For quantitative PCR, the template cDNA was added to a 20 μl reaction with SYBR GREEN PCR Master Mix (Applied Biosystems) and 0.2 μM of primer (**Table 1**). The amplification was carried out using an ABI Prism 7000 for 40 cycles under the following conditions: initial denaturation at 95°C for 10 min; 40 cycles of 95°C for 15 s and 60°C for 1 min. The fold changes were calculated relative to GAPDH using the ΔΔCt method.

Enzyme-Linked Immunosorbent Assays

The cell lysates were examined for CDK4, CDK6, cyclinD1, CDK2, cyclinE1, CDK1, cyclinB1 and histone with ELISA kits (Meiyan, Shanghai, China) according to the manufacturer's instructions. The microplate was quantified using a microplate reader (Bio-Rad, Hercules, CA, USA). Target protein expression was normalized to the histone expression.

Statistical Analyses

Statistical differences were analyzed using the Student's *t*-test for all analysis, except of 3C and 3D dose-dependent test in **Figures 4B,D** with Pearson correlation coefficient. Data are presented as means and standard deviations (SD). $^*P$-values of < 0.05 were considered statistically significant.

TABLE 1 | The primer for real time PCR and plasmid construct.

Primer pair	Role	Forward sequence5′–3′ (restriction enzyme)	Reverse sequence5′–3′ (restriction enzyme)
EV-D68 VP1 (Fermon)	Real time	CACCATACTCACAACTGTGGC	AATGAAATGAATCCTGCTCCT
EV-D68 VP1 (US/KY/14-18953)	Real time	GCCCTTACTCCAGAAAAACA	CAAAACCATCATAGAAAACT
EV-D68 VP1 (US/MO/14-18947)	Real time	CGTGGGTCTTCCTGACTTGA	GGGGGGTCGGAGATTTTAAA
EV-A71 VP1	Real time	AGCACCCACAGGCCAGAACACAC	ATCCCGCCCTACTGAAGAAACTA
CyclinE	Real time	TCAGGGTATCAGTGGTGCGA	CAAATCCAAGCTGTCTCTGTG
CDK2	Real time	CTCCTGGGCTCGAAATATTATTCCACAG	CCGGAAGAGCTGGTCAATCTCAGA
CDK4	Real time	AAGCCGACCAGTTGGGCAAAAT	GCTCCACGGGGCAGGGATACAT
CDK6	Real time	GGTCAGGTTGTTTGATGTGTGC	TATCCTTTATGGTTTCAGTGGG
CylcinD	Real time	CTACTACCGCCTCACACGCTTC	TCCTCCTCCTCTTCCTCCTCCT
CDK1	Real time	TCAAGTGGTAGCCATGAAAAAA	TAACCTGGAATCCTGCATAAGC
CyclinB1	Real time	TGGCCTCACAAAGCACATGA	GCTGTGCCAGCGTGCTAATC
GAPDH	Real time	GCAAATTCCATGGCACCGT	TCGCCCCACTTGATTTTGG
3D	Plasmid construct	AACTGCAGACCATGTACCCTTACGACGTCCCAGATTACGCGGGTGAGATAGTTAGCAATGAGA (PST1)	CGGGATCCCTAAAACGAATCTAACCATTTCCG (BamH1)
3C	Plasmid construct	AACTGCAGACCATGTACCCTTACGACGTCCCAGATTACGCGGGACCAGGATTTGATTTT (PST1)	CGGGATCCCTATTGTGTATCAGTAAAGTAAGAGT (BamH1)

3D and 3C forward primer with hemagglutinin (HA) sequence: (TACCCTTACGACGTCCCAGATTACGCG).

RESULTS

Synchronization at Different Cell Cycle Stages Has Profound Effects on EV-D68 Production

Viral replication often is integrally associated with the cell cycle status of host cells (Feuer et al., 2002). To explore the possible benefits of different cell cycle phases for EV-D68 viral replication, we synchronized cells in different phases and then assessed viral replication and virulence. First, we assessed the effects of G0/G1 synchronization by serum deprivation (Darzynkiewicz et al., 1980). RD cells were cultured in either serum medium (control) or serum-free medium (G0/G1 synchronization) for 24 h. Then the cells were infected with the same titer of 0.8 MOI of EV-D68 (Fermon strain) or were mock-infected for 2 h, and either serum medium or serum-free medium was added for another 24 h (**Figure 1A**). As previously reported (He et al., 2010), serum deprivation induced obvious G0/G1 arrest as assessed by flow cytometry ($P < 0.001$; **Figure 1B**). At 2 h post-infection (viral entry stage), the EV-D68 genomic RNA levels were not significantly different in the control and serum-starved cells (**Figure 1M**); however, at 18 h post infection (viral replication stage) 13.55 times more viral RNA was detected in the serum-starved cells than in the control cells ($P < 0.01$; **Figure 1C**). Furthermore, at 24 h (viral production stage) the TCID50/mL of infectious EV-D68 particles was 348.84 times higher for supernatant from G0/G1 phase-synchronized cells ($202.17 \pm 42.60 \times 10^5$) than for supernatant from control cells ($0.59 \pm 0.08 \times 10^5$) ($P < 0.01$; **Figure 1D**). These results suggest that G0/G1-phase arrest does not affect viral entry, but promotes EV-D68 viral replication and production.

To determine whether viral replication and production also is elevated at other phases of the cell cycle, the effect of S phase synchronization was assessed. The cells were cultured in medium or were synchronized in S phase by culture with 0.85 mM thymidine for 24 h. Then, the cells were mock infected or were infected with 0.8 MOI of EV-D68 for 2 h, and fresh culture medium or 0.85 mM thymidine was added for another 24 h (**Figure 1E**). Thymidine induced obvious S phase arrest ($P < 0.001$; **Figure 1F**). The genomic RNA level remained similar in S phase-synchronized cells and control non-synchronized cells at 2 h post-infection (**Figure 1M**) and at 24 h post-infection ($P > 0.05$; **Figure 1G**). Furthermore, the TCID50/mL values at 24 h post-infection were equivalent for the S phase-synchronized cell supernatant ($2.59 \pm 1.37 \times 10^5$) and the control cell supernatant ($3.28 \pm 1.80 \times 10^5$) ($P > 0.05$; **Figure 1H**). These results suggest that S-phase arrest does not affect EV-D68 viral entry, replication or production.

To assess the effects of G2/M phase synchronization, cells were cultured in medium or were treated with 25 ng/ml nocodazole for 24 h; then, the cells were mock infected or were infected with EV-D68 at 0.8 MOI for 2 h, and cultured in fresh medium or 25 ng/ml nocodazole for another 24 h (**Figure 1I**). Nododazole induced obvious G2/M arrest ($P < 0.001$; **Figure 1J**). At 2 h post-infection, there was no significant difference in the genomic RNA level in the control and G2/M phase-synchronized cells (**Figure 1M**); however, at 24 h post-infection the genomic level was lower in the synchronized cells than in the control cells ($P < 0.05$; **Figure 1K**). Furthermore, at 24 h post-infection the TCID50/mL for supernatant from the G2/M phase-synchronized cells ($0.46 \pm 0.29 \times 10^5$) was obviously lower than that from the control cells ($1.40 \pm 0.16 \times 10^5$) ($P < 0.01$; **Figure 1L**). Therefore, these results suggest that G2/M synchronization does not affect viral entry, but inhibits EV-D68 viral replication and production.

EV-D68 Infection Manipulates the Host Cell Cycle and Arrests Cells at G0/G1

Given that EV-D68 replication and production is dependent on the cell cycle, we next asked whether EV-D68 might have the ability to manipulate the host cell cycle to facilitate its own production. RD cells were infected with EV-D68 Fermon stain at an MOI of 0.8, and the cells were collected for cell cycle distribution analysis after 24 h. An obvious increase in the percentage of cells in G0/G1 was observed in EV-D68-infected cells ($45.20 \pm 0.14\%$) as compared to mock-infected cells ($36.50 \pm 0.76\%$) (23.84% increase; $P < 0.01$; **Figure 2A**). Therefore, EV-D68 itself can manipulate the host cell to accumulate preferentially at G0/G1 phase rather than at G2/M, which favors viral production.

Though the latter experiments were performed using the Fermon strain of EV-D68, which was isolated from 4 children with pneumonia and bronchiolitis in the United States in 1962 (Schieble et al., 1967; Zhang et al., 2015), several more recent strains of the virus have been isolated. The currently circulating EV-D68 US/MO/14-18947 and US/KY/14-18953 strains are similar to the Fermon strain in clinical characteristics and genome structure, but it is not known whether they are similar in virulence and ability to manipulate the cell cycle. Therefore, we compared the US/MO/14-18947 and US/KY/14-18953 strains to the Fermon strain. Under normal culture conditions, RD cells were infected with three strains virus at an MOI of 0.8 for 24 h, respectively, the TCID50/mL of the US/MO/14-18947 strain ($43.07 \pm 10.22 \times 10^5$) was 29.76 times higher and the TCID50/mL of the US/KY/14-18953 ($195.00 \pm 54.03 \times 10^5$) was 138.29 higher than the TCID50/mL of the Fermon strain ($1.40 \pm 0.16 \times 10^5$) (**Figure 2B**). These results suggest that the EV-D68 virulence has increased over time, which could explain the recent rise in the incidence of Enterovirus-related disease (Esposito et al., 2015; Farrell et al., 2015; Reiche et al., 2015; Zhang et al., 2015).

Next, we assessed the cell cycle distribution after RD cells were infected with the currently circulating strains of EV-D68 at an MOI of 0.8 for 24 h. An obvious increase in the percentage of cells in G0/G1 phase was observed for both US/MO/14-18947 (25.83% increase; $P < 0.01$) (**Figure 2C**) and US/KY/14-18953 (10.85% increase; $P < 0.01$) (**Figure 2D**). These strains also caused a corresponding increase in the ratio of cells in G0/G1–G2/M (53.54% increase for US/MO/14-18947; 85.91% increase US/KY/14-18953; $P < 0.001$; **Figures 2C,D**). Therefore, the currently circulating strains possess increased virulence and a similar ability as the Fermon strain to skew the cell cycle toward the G0/G1 phase, which facilitates viral production.

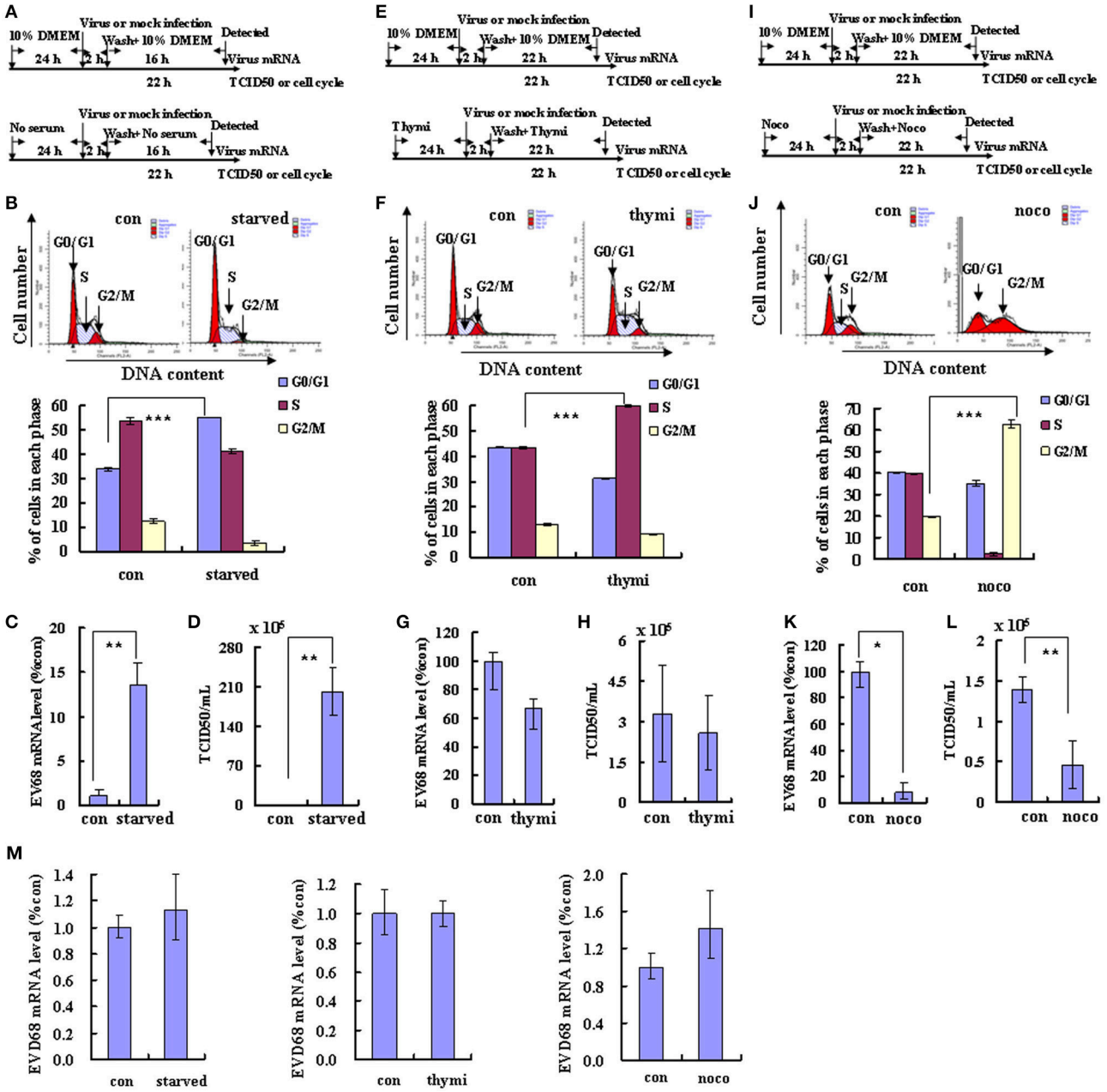

FIGURE 1 | Different cell cycle stages have profound effects on EV-D68 replication. The effects of cell cycle synchronization on EV-D68 are shown for G0/G1 arrest **(A–D)**, S phase arrest **(E–H)**, and G2/M arrest **(I–L)**. **(A,E,I)** Flow diagram of how RD cells were treated with serum starvation (starved) for G0/G1 synchronization **(A)**, with thymidine (thymi) for S synchronization **(E)**, or with nocodazole (noco) for G2/M synchronization **(I)**. The top diagram in each panel shows the strategy for the control group, and the bottom panel shows the strategy for cell cycle synchronization. **(B,F,J)** Cell-cycle profiles were determined by flow cytometry after G0/G1, S, and G2/M synchronization with serum starvation, thymidine, and nocodazole treatment, respectively. Histograms below show the percentage of cells in each phase of the cell cycle as analyzed by the ModFit LT program. **(C,G,K)** Levels of intracellular EV-D68 Fermon strain RNA were detected in RD cells after cell cycle synchronization by quantitative real-time PCR. The results were standardized to GAPDH mRNA expression and normalized to 1.0 in mock-infected cells. **(D,H,I)** Progeny viruses in the supernatants were titrated using RD cells. A relative quantitative analysis of the TCID50/mL is shown. **(M)** Intracellular EV-D68 Fermon strain RNA levels were detected in RD cells with different cell cycle synchronization treatment by quantitative real-time PCR at post-infection 2 h. The results were standardized using GAPDH mRNA as a control and normalized to 1.0 in mock-infected cells. The results represent the mean ± S.D of three independent experiments. $^{*}P < 0.05$, $^{**}P < 0.01$, and $^{***}P < 0.001$.

EV-D68 Infection Inhibits G0/G1 Exit

To further understand the mechanism of EV-D68 manipulation of the host cell cycle, we assessed whether EV-D68 could regulate cell cycle exit from G0/G1 into S phase. RD cells were synchronized in G0/G1 by serum starvation for 24 h, and then mock-infected or infected with EV-D68 Fermon strain for

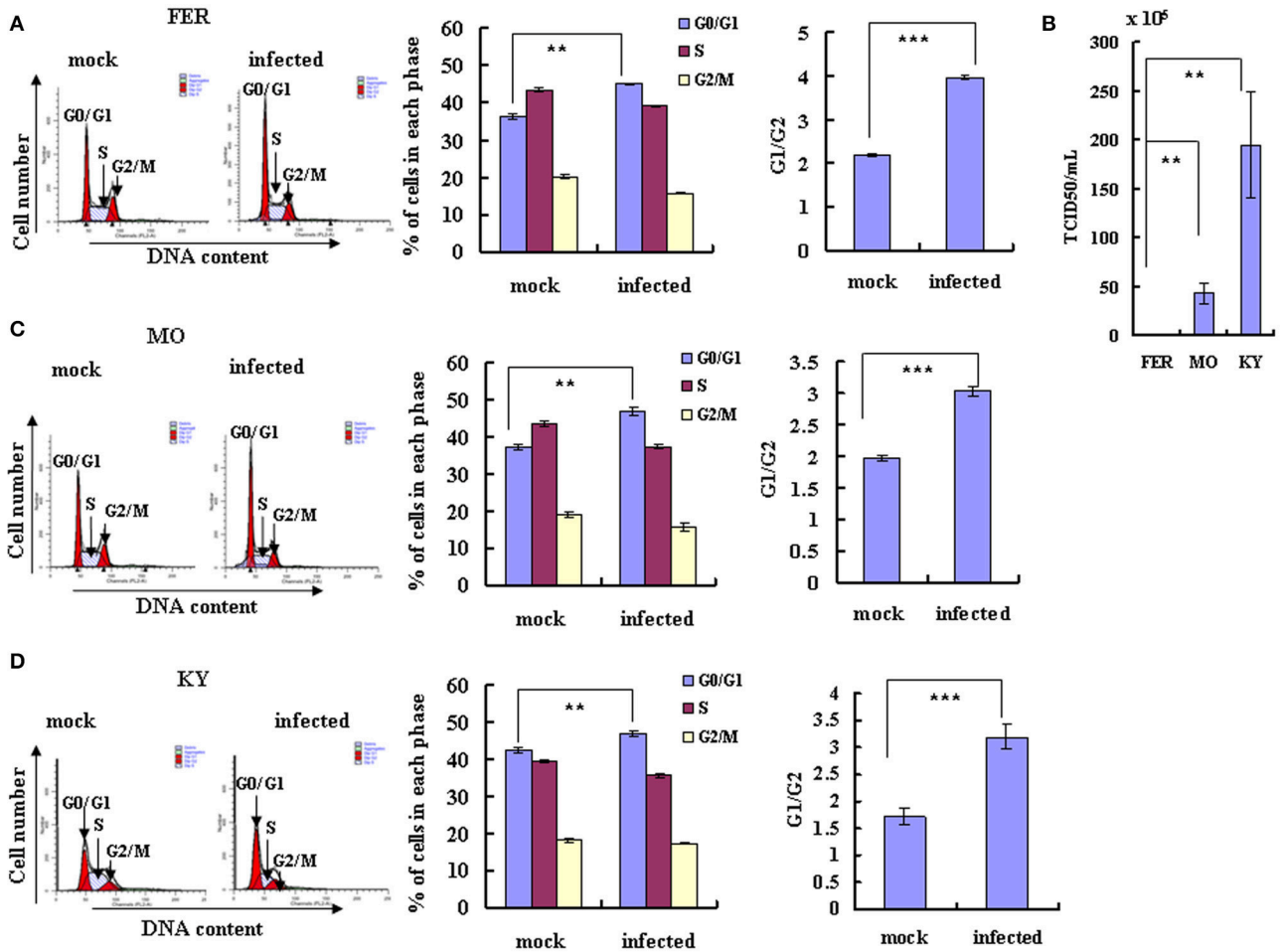

FIGURE 2 | EV-D68 infection induces G0/G1 arrest. (A,C,D) RD cells were infected with EV-D68 Fermon **(A)**, US/MO/14-18947 **(C)** or US/KY/14-18953 **(D)** at an MOI of 0.8 or mock for 24 h for analysis of cell cycle status. Left: Cell-cycle profiles were determined by flow cytometry. Middle: The histograms show the percentage of cells in each phase of the cell cycle in mock-infected and EV-D68-infected cells. Right: The ratio of G0/G1 to G2/M is shown. **(B)** The virulence of Fermon, US/KY/14-18953 and US/MO/14-18947strains in infected RD cells was assessed 24 h post-infection with virus at MOI 0.8. Values are expressed as the TCID50/mL of the progeny viruses in the supernatant. The results represent the mean ± S.D of three independent experiments. $^{**}P < 0.01$ and $^{***}P < 0.001$.

2 h. The cells were then stimulated with 10% FBS in order to trigger cell cycle re-entry into S phase from G0/G1. At 24 h of mitogenic stimulation with serum, the mock-infected cells progressed synchronously from G0/G1 into S phase. In contrast, the majority of the EV-D68-infected RD cells remained in G0/G1 phase over the 24 h time period without S entry ($P < 0.001$; **Figure 3A**). Therefore, these results support a model in which EV-D68 infection regulates the cell cycle by preventing entry into the S phase.

Cyclin/CDK complexes are known to regulate cell cycle progression (Sherr, 1994). To identify the key molecules and signaling pathways that may mediate the inhibition of cell entry into S phase by EV-D68, we examined the protein expression profiles of host G0/G1-phase and S-phase proteins by Western blotting of RD cells at 0, 16, 20, 24, and 28 h post-infection. Among the molecules CDK4, CDK6, and cyclinD (which mediate cell cycle progression in G0/G1; Massagué, 2004) and CDK2 and cyclinE1 (which mediate cell cycle transition from G0/G1 to S phase; Hinds et al., 1992), the expression of CDK6 was not changed, and the expression of cyclinE1 was increased at 24 h post-infecion (**Figure 3B**), while all of them were significantly decreased in virus-infected cells as compared to mock-infected cells at 28 h post-infection (**Figures 3B,G**). Furthermore, the CDK2 mRNA level was decreased by EV-D68 infection; however, there were no significant differences between the virus and mock-infected groups in CDK4, CDK6, cyclinD or cyclinE1 mRNA levels (**Figure 3C**). Therefore, EV-D68 infection inhibits host expression of several cell cycle proteins, which is consistent with its ability to inhibit G0/G1 to S phase entry, and the modulation is likely to occur transcriptionally for CDK2 and post-transcriptionally for CDK4, CDK6, cyclinD, and cyclinE1.

EV-D68 Infection Promotes G0/G1 Entry

To further examine the potential effect of virus infection on cell cycle transition from G2/M phase into G0/G1, RD cells were treated with 25 ng/ml nocodazole or medium for 24 h for G2/M

phase synchronization and then the cells were mock infected or infected with EV-D68 at 0.8 MOI for 2 h. Next, the cells were treated for an additional 24 h with 25 ng/ml nocodazole or fresh medium. Nocodazole induced obvious G2/M cell cycle arrest (35.91 ± 1.44 vs. $18.77 \pm 0.20\%$; $P < 0.01$); however, after EV-D68 infection for 24 h, the percentage of cells in G2/M was decreased (21.82 ± 1.07 vs. 35.91 ± 1.44; $P < 0.001$), and the percentage of cells in G0/G1 was increased (48.59 ± 1.22 vs. 32.51 ± 0.21; $P < 0.01$) (**Figure 3D**). Therefore, EV-D68 infection also regulates the cell cycle by promoting exit from G2/M phase. Consistent with these findings, the expression of cyclinB1 and CDK1 (which mediate G2/M progression; Coverley et al., 2002; Yam et al., 2002) was down regulated by EV-D68 infection (**Figures 3E,G**). CDK1 was decreased at the mRNA level upon EV-D68 infection (*transition from*$P < 0.01$), but cyclinB1 mRNA expression was not significantly regulated (**Figure 3F**). Therefore, EV-D68 virus promotes cell cycle exit from G2/M and entry into G0/G1 by modifying the pathway of G0/G1 entry at the transcriptional level for CDK1 and at the post-translational level for cyclinB1.

The Non-structural Proteins 3D and 3C of EV-D68 Mediate Cell Cycle Alterations

A previous study concluded that exogenous expression of EV-A71 viral non-structural 3D protein, an RNA-dependent RNA polymerase, mediates cell cycle arrest at S phase (Yu et al.). Given this finding, we examined whether non-structural 3D protein of EV-D68 had the same ability to mediate cell cycle alteration. Transfection of 3D expression vector (2 μg) induced G0/G1 arrest, with an increase in the percentage of G0/G1 cells from $39.37 \pm 0.52\%$ to $44.76 \pm 1.29\%$ (13.69% increase; $P < 0.01$) and a corresponding increase in the G0/G1–G2/M ratio from 2.02 ± 0.04 to 2.62 ± 0.18 (29.70% increase; $P < 0.01$) (**Figure 4A**). Furthermore, the extent of the increase in the percentage of G0/G1 cells was dependent on the dose of 3D vector (0, 0.5, 1, 2 μg; $R = 0.932$; $P < 0.001$), and the G0/G1 to G2/M ratio also depended on the dose of 3D vector ($R = 0.827$; $P < 0.001$; **Figure 4B**). These results suggest that the non-structural protein 3D of EV-D68 contributes to G0/G1 arrest.

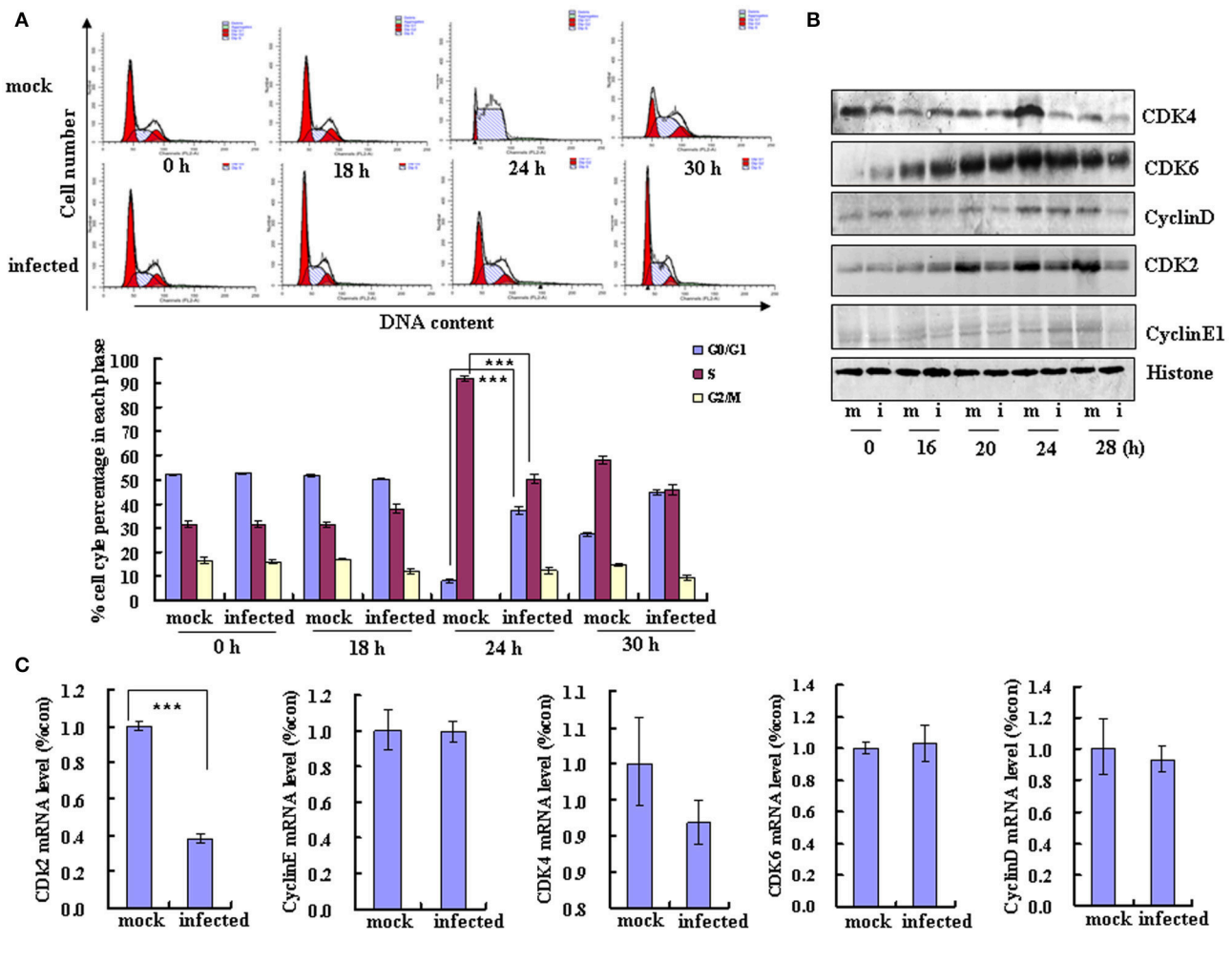

FIGURE 3 | Continued

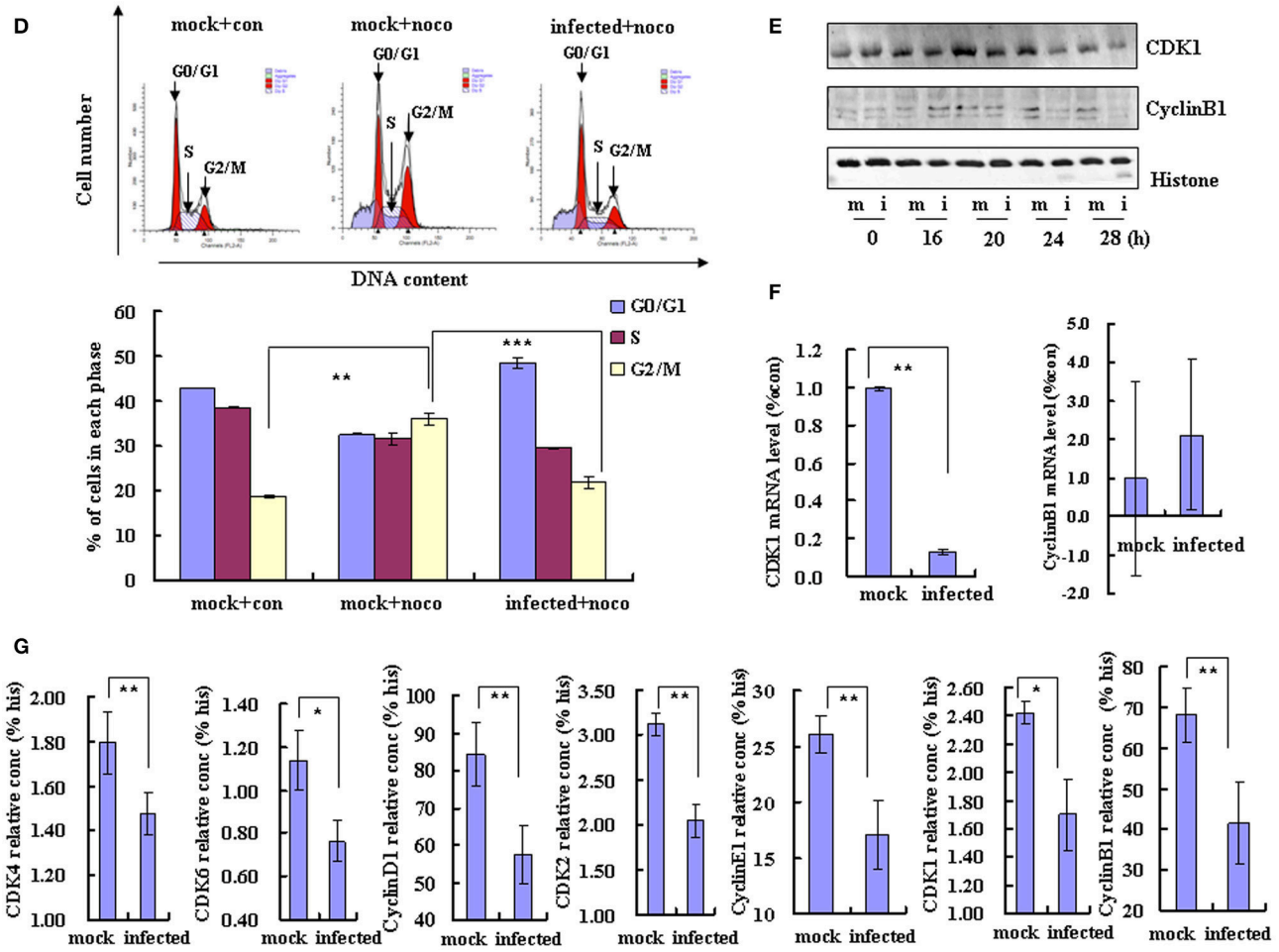

FIGURE 3 | EV-D68 infection prevents cell exit from G0/G1 into S phase and promotes G2/M to G0/G1 transition. (A) RD cells were serum-starved for 24 h and then mock-infected (mock) or infected with EV-D68 Fermon strain (infected) at an MOI of 0.8. After 2 h of virus adsorption, the cells were treated with medium without FBS for 18 h, followed by medium containing 10% FBS. Top panel: The cell cycle profiles were determined by flow cytometry at 0, 18, 24, and 30 h post-infection. Bottom panel: The histograms show the percentage of cells in each phase of the cell cycle. **(B)** G0/G1 and S phase-related cell cycle proteins were analyzed by western blot analysis. RD cells were mock-infected (m) or infected with EV-D68 Fermon strain at an MOI of 0.8 (i) for 0, 16, 20, 24, and 28 h. Histone is shown as a loading control. Results are representative of three independent experiments. **(C)** At 24 h post-infection, mRNA levels of CDK2, cyclinE1, CDK4, CDK6, and cyclinD were evaluated in mock infected (mock) and EV-D68 infected (infected) cells by quantitative real-time PCR. The results are standardized to GAPDH and normalized to 1.0 in mock-infected cells. **(D)** RD cells were treated with 25 ng/mL nocodazole or control medium for 24 h, infected with EV-D68 Fermon strain at an MOI of 0.8 or mock for 2 h and then re-treated with 25 ng/mL nocodazole for synchronization. Top panel: Cell-cycle profiles were determined by flow cytometry. Low panel: The histograms show the percentage of cells in each phase of the cell cycle. **(E)** G2/M phase-related proteins were detected by western blot analysis. Results are representative of three independent experiments. **(F)** At 24 h post-infection, mRNA levels of CDK1 and cyclinB1 were assessed in mock-infected (mock) and EV-D68 infected (infected) cells by quantitative real-time PCR. The results are standardized to GAPDH mRNA and normalized to 1.0 in mock-infected cells. **(G)** At 28 h post-infection, the protein concentration of CDK4, CDK6, cyclinD1, CDK2, cyclinE1, CDK1, cyclinB1, and histone were assessed in mock-infected (mock) and EV-D68 infected (infected) cells by Elisa kit. The results are standardized to Histone (his). The results indicate the mean ± S.D of three independent experiments. $^{*}P < 0.05$, $^{**}P < 0.01$, and $^{***}P < 0.001$.

We also examined the potential role of non-structural protein 3C in cell cycle regulation by EV-D68. Transfection of high dose 3C expression vector (2μg) decreased the percentage of cells in G2/M phase from 19.53 ± 0.26% to 13.19 ± 0.48% (32.46% decrease) and increased in the ratio of cells in G0/G1 to G2/M from 2.01 ± 0.04 to 2.75 ± 0.17 (36.82% increase; $P < 0.01$) (**Figure 4C**). High dose 3C transfection also increased the percentage of cells in S phase (from 41.10 ± 0.48% to 50.53 ± 0.73%). Although the change in the cell cycle profile was not dose-dependent, the G0/G1 to G2/M ratio was dose-dependent ($R = 0.951$; $P < 0.001$; **Figure 4D**). These results suggest that the non-structural protein 3C may contribute to the enhanced cell cycle exit from G2/M phase after EV-D68 infection.

To verify these findings and to evaluate the mechanism of cell cycle regulation after 3D and 3C transfection, we performed Western blotting assays to examine their effect on the

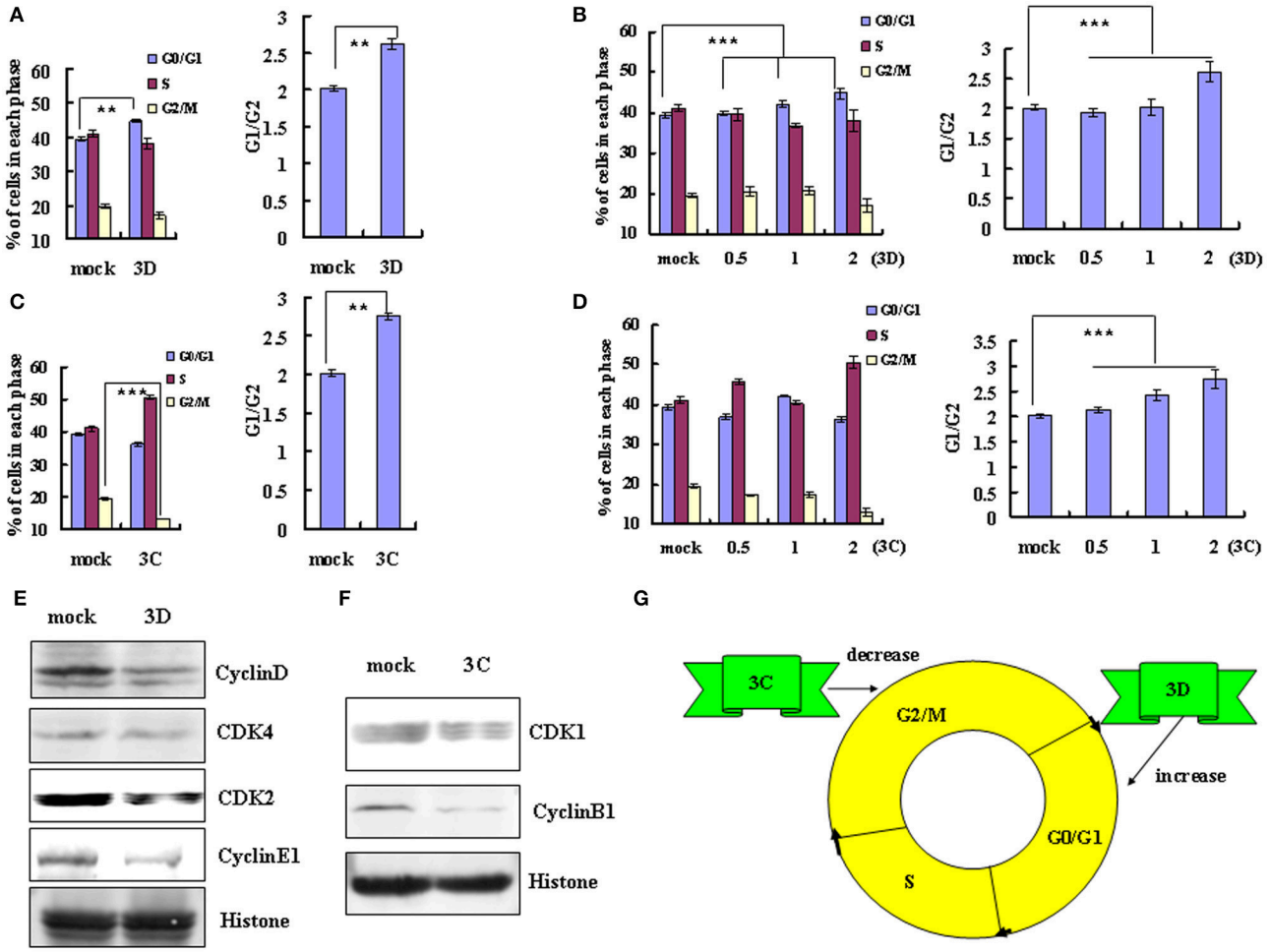

FIGURE 4 | The non-structural protein 3D and 3C of EV-D68 mediates cell cycle alterations. (A,C) Effect of 3D and 3C on cell cycle progression. Left panel: The distribution of cell cycle in 293T cells was analyzed at 36 h after transfection with 2 μg of VR1012-3D-HA (3D), VR1012-3C-HA (3C) or the corresponding control vector VR1012 (mock). Right panel: The ratio of cells in G0/G1 to G2/M at 36 h after transfection with 2 μg of VR1012-3D-HA (3D), VR1012-3C-HA (3C) or the corresponding control vector VR1012 (mock). **(B,D)** The cell cycle distribution in 293T cells was analyzed at 36 h after transfection with 0, 0.5, 1, or 2 μg plasmid as indicated. Left panel: The histograms show the percentage of each phase in the cell cycle. Right panel: The ratios of cells in G0/G1 to G2/M. **(E,F)** The expression of cell cycle-related proteins after transfection of 293T cells with 3D, 3C or corresponding vector (mock) was assessed by Western blot analysis at 36 h. Histone is shown as a loading control. **(G)** Model for the distinct effects of the non-structural proteins 3D and 3C in cell cycle arrest caused by EV-D68. The results indicate the mean ± S.D of three independent experiments. $^{**}P < 0.01$ and $^{***}P < 0.001$.

expression of cycle-related proteins. Consistent with the cell cycle analyses, 3D down-regulated the expression of cyclinD, CDK4, CDK2, and cyclinE1 (**Figure 4E**), while 3C down-regulated the expression of CDK1 and cyclinB1 (**Figure 4F**). Therefore the non-structural protein 3C facilitates exit from G2/M and the non-structural protein 3D mediates arrest in G0/G1 (**Figure 4G**).

G0/G1-Phase Synchronization Has Distinct Effects on EV-D68 and EV-A71 Viral Replication

EV-D68 (serotype HEV-D) and EV-A71 (serotype HEV-A) are both enteroviruses. We have demonstrated that G0/G1 synchronization promotes EV-D68 viral replication (**Figures 1A–D**). However, in our previous study, we determined that G0/G1 synchronization inhibits EV-A71 viral replication. To exclude experimental variation as an explanation for the disparate responses of these viruses to G0/G1 synchronization, we performed a side-by-side comparison of the two enteroviruses. Our results confirm that no serum treatment induces G0/G1 synchronization (**Figures 5A,B**) and G0/G1 synchronization has opposite effects for the two viruses (**Figure 5**). After 18 h infection with EV-D68, the viral genomic mRNA level was 13.55 times higher in serum-starved cells than in control cells ($P < 0.01$; **Figure 5C**); however, after 18 h infection with EV-A71, the viral genomic mRNA level was 3.12 times lower in serum-starved cells ($P < 0.05$; **Figure 5D**). Furthermore, after 24 h infection, the TCID50/mL for EVD68 was 341.66 times higher for G0/G1 phase-synchronized cells

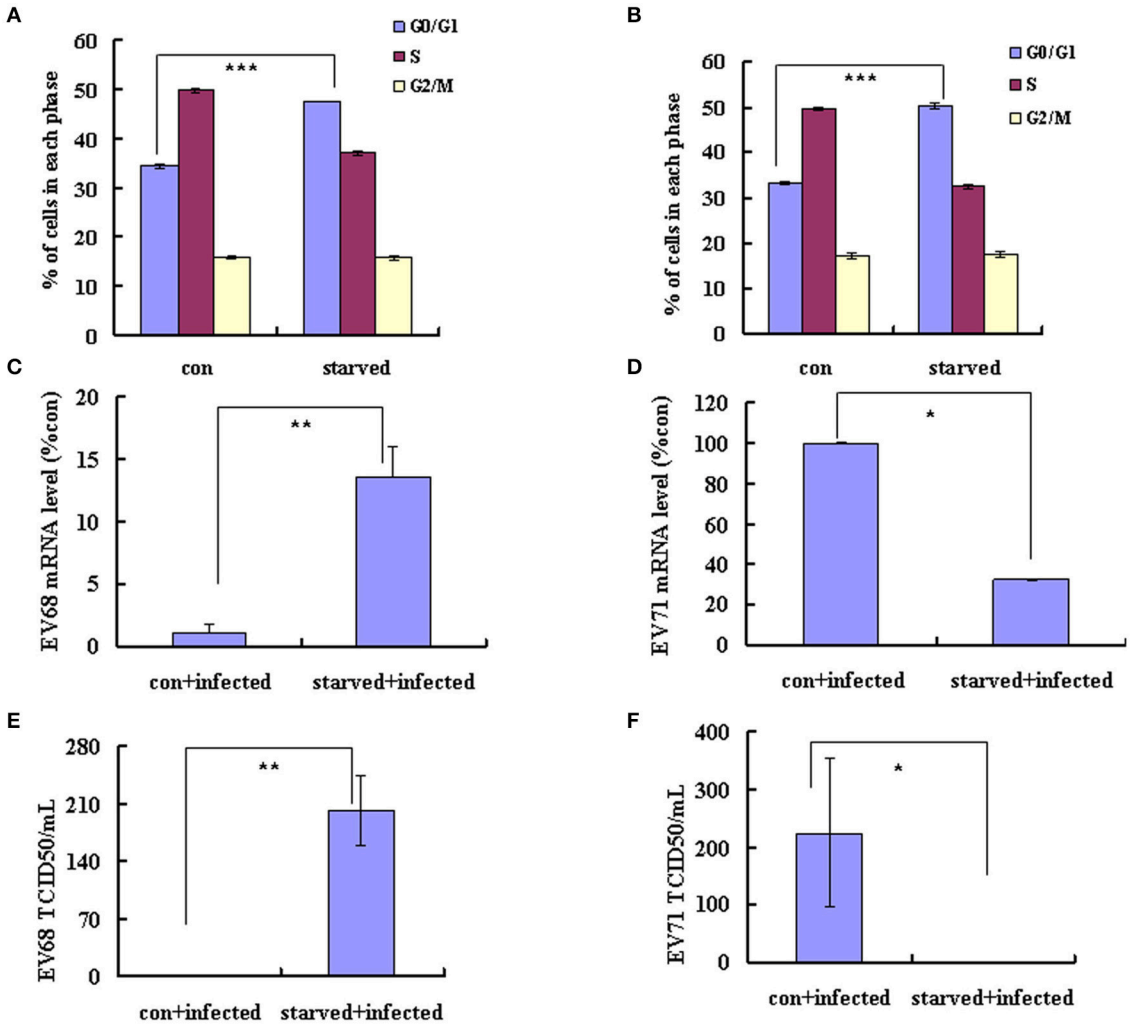

FIGURE 5 | G0/G1-phase synchronization has different effect on the replication of EV-A71 and EV-D68. RD cells infected with EV-D68 Fermon strain **(A,C,E)** or EV-A71 **(B,D,F)** at an MOI of 0.8 and the effects of synchronization by starvation were assessed. **(A,B)** RD cells were serum-starved for 48 h to synchronize cells in G0/G1 phase. The cell-cycle distribution was then detected by flow cytometry. The histograms showed the percentage of each phase in the cell cycle. **(C,D)** At 18 h post-infection, intracellular EV-D68 and EV-A71 RNA levels were assessed in control medium (con+infected)-treated or no serum (starved+infected)-treated RD cells by quantitative real-time PCR. The results were standardized using GAPDH mRNA as a control and normalized to 1.0 in mock-infected cells. **(E,F)** At 24 h post-infection, The TCID50/mL was shown through titrating the progeny viruses of EV-D68 or EV-A71 in the supernatants with RD cells. The results represent the mean ± S.D of three independent experiments. $^{*}P < 0.05$, $^{**}P < 0.01$, and $^{***}P < 0.001$.

than for control cells ($202.17 \pm 42.60 \times 10^5$ vs. $0.59 \pm 0.08 \times 10^5$; $P < 0.01$; **Figure 5E**), while the TCID50/mL for EV-A71 was 489.37 times lower for G0/G1 phase-synchronized cells than for control cells ($0.46 \pm 0.15 \times 10^5$ vs. $225.11 \pm 129.36 \times 10^5$; $P < 0.05$; **Figure 5F**). These results confirm that G0/G1-phase arrest has different effects for the two enteroviruses.

G2/M-Phase Synchronization Has Similar Effects on Different Strains of EV-D68 and EV-A71

G2/M synchronization with nocodazole has been shown to inhibit both the EV-D68 Fermon strain in this study (**Figures 1I–L**) and EV-A71 in our previous study (Yu et al., 2015). To determine whether similar effects of G2/M-phase synchronization are observed for the currently circulating strains of EV-D68, cells were treated with 25 ng/ml nocodazole or medium for 24 h, and were then infected at 0.8 MOI for 2 h and treated with 25 ng/ml nocodazole or fresh medium for another 24 h. Our results demonstrate that nocodazole treatment decreased the genomic RNA levels (**Figure 6A**) and the TCID50/ml value (**Figure 6B**) of Fermon, US/KY/14-18953 and US/MO/14-18947, which suggests that the virus inhibition upon G2/M synchronization may be similar for all enteroviruses.

To confirm that G2/M synchronization inhibits EV-D68 and EV-A71, we assessed the effects of an alternate agent that can exert G2/M arrest *in vitro*, pseudolaric acid B (PAB), which

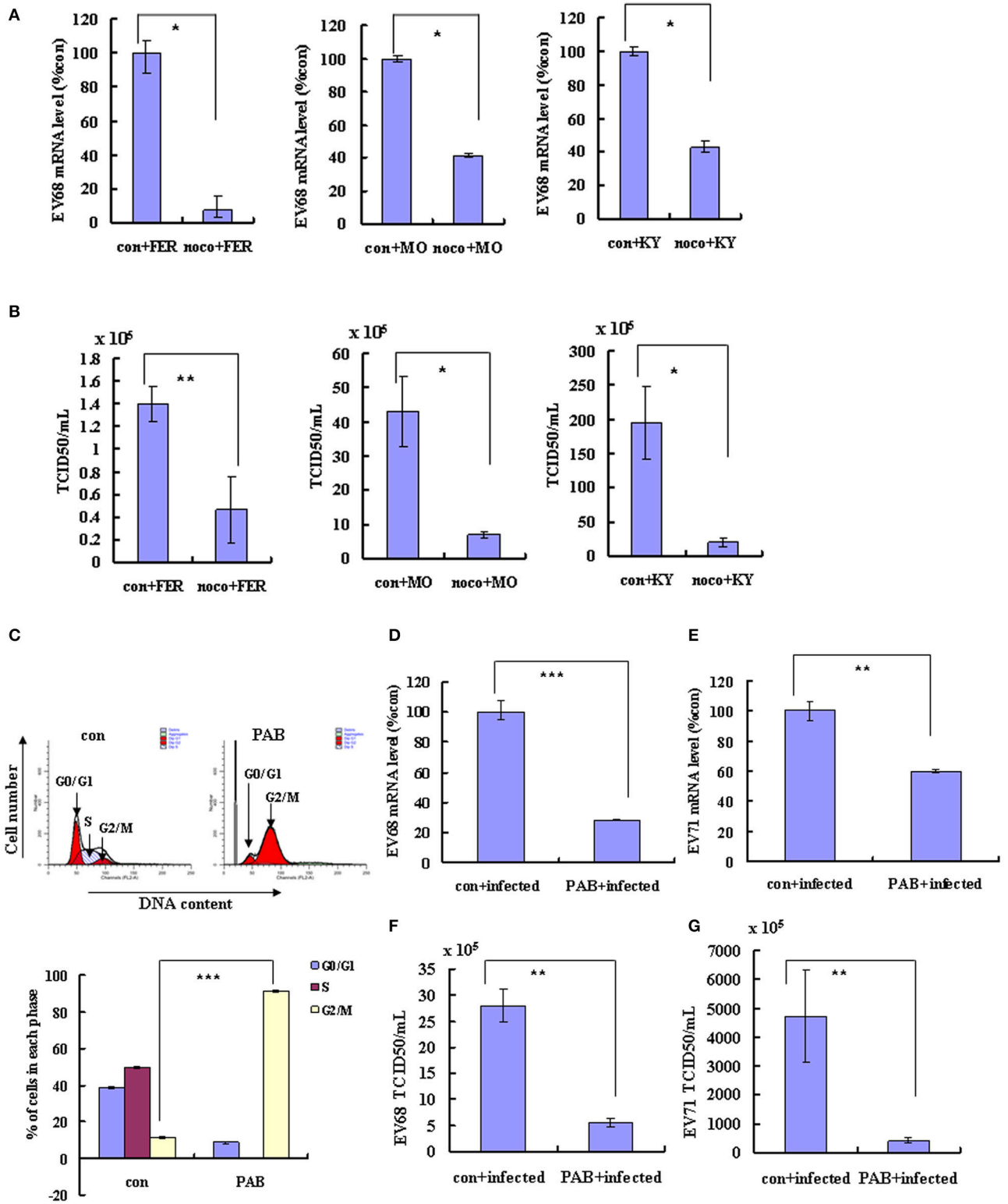

FIGURE 6 | Synchronization in the G2/M phase inhibits the replication of EV-D68 and SV-A71. (A–C) RD cells were treated with or without 25 ng/mL nocodazole (noco) for 24 h, infected with EV-D68 Fermon (FER), US/MO/14-18947 (MO) or US/KY/14-18953 (KY) strains at an MOI of 0.8 for 2 h, and then treated again with or without 25 ng/mL nocodazole for synchronization. **(A)** At 24 h post-infection, intracellular EV-D68 RNA levels were detected by quantitative real-time PCR. The results were standardized using GAPDH mRNA as a control and normalized to 1.0 in mock-infected cells. **(B)** At 24 h post-infection, the TCID50/ml of the

(Continued)

FIGURE 6 | Continued
progeny viruses was determined. **(C–G)** RD cells were infected with EV-D68 strains US/KY/14-18953 or EV-A71 at an MOI of 0.8 for 2 h, and then treated with 2 μM Pseudolaric acid B (PAB) for 24 h for G2/M synchronization. **(C)** RD cells were treated with 2 μM Pseudolaric acid B (PAB) for 24 h for G2/M synchronization. Top panel: Cell-cycle profiles were determined by flow cytometry. Bottom panel: The histograms show the percentage of cells in each phase of the cell cycle. **(D,E)** Intracellular EV-D68 or EV-A71 RNA levels were assessed in control medium (con+infected) or PAB containing medium (PAB+infected)-treated RD cells by real-time quantitative PCR. The results are standardized by GAPDH mRNA as a control and normalized to 1.0 in control-infected cells. **(F,G)** The progeny viruses of EV-D68 or EV-A71 in the supernatant were titrated using RD cells, and the TCID50/mL was shown. The results indicate the mean ± S.D of three independent experiments. $^{*}P < 0.05$, $^{**}P < 0.01$, and $^{***}P < 0.001$.

is a diterpene acid isolated from the root and trunk bark of *Pseudolarix kaempferi Grord (Pinaceae)* (Yu et al., 2007, 2013). PAB was confirmed to promote G2/M arrest after 24 h (**Figure 6C**). To assess the effects of PAB on viral RNA and virulence, RD cells were infected with EV-D68 US/KY/14-18953 strain or EV-A71 at an MOI of 0.8 for 2 h and then treated with 2 μM PAB for 24 h. PAB decreased the genomic RNA levels of both EV-D68 (28.32% of control; $P < 0.001$; **Figure 6D**) and EV-A71 (59.87% of control; $P < 0.001$; **Figure 6E**). Furthermore, PAB decreased the TCID50/ml value of both EV-D68 (80.31% decrease; $P < 0.01$; **Figure 6F**) and EV-A71 (91.27% decrease; $P < 0.01$; **Figure 6G**). These results confirm that G2/M arrest inhibits both the EV-D68 and EV-A71 strains, which suggest a common approach for therapeutic intervention that might potentially target a broader range of enteroviruses.

DISCUSSION

Enterovirus 68 (EV-D68) usually causes mild to severe respiratory illness, including runny nose, sneezing, cough, body and muscle ache, wheezing, difficulty breathing, and in the cases of some infants, children and teens, death. Although EV-D68 was first identified in California in 1962, the number of people in one breakout in 2014 with confirmed EV-D68 infection was much greater than the number reported in previous years (http://www.cdc.gov/non-polio-enterovirus/about/ev-d68.html). It is hard to predict whether EV-D68 will emerge again in future outbreaks, but the value of resolving the pathogenic mechanism of EV-D68 is obvious. In this study, we investigated the pathogenic mechanism of EV-D68 to reveal the relationship between virus infection and the host cell cycle.

To assess the possibility that the cell cycle status affects EV-D68 viral replication, we first synchronized cells in G0/G1. Our results demonstrate that G0/G1 arrest promotes EV-D68 replication and increases viral virulence without affecting virus entry. We also assessed the effects of S phase and G2/M phase synchronization on viral production. Our results suggest that S phase synchronization does not affect viral entry, replication or production compared to the control treatment, while G2/M synchronization inhibits viral replication and decreases viral virulence, but does not affect virus entry. These results indicate that G0/G1 phase is most favorable for EV-D68 replication, that S phase can support some viral production, and that G2/M phase is inhibitory for host viral production.

Given that G0/G1 phase supports EV-D68 production, it would be advantageous for the virus to manipulate the host cell cycle to increase viral production. Indeed, the EV-D68 Fermon strain displayed significant ability to increase the percentage of cells in G0/G1 phase. The EV-D68 Fermon strain was isolated in the United States in 1962 (Schieble et al., 1967), but currently circulating strains, including EV-D68 US/MO/14-18947 and US/KY/14-18953, may be more relevant to current human health. Therefore, we examined whether these two currently circulating strains had similar ability to manipulate the cell cycle. Our results confirmed that the circulating EV-D68 strains manipulate the cell cycle in a similar manner as does the Fermon strain, though the current strains have higher virulence than Fermon. Therefore, after more than 50 years' evolution, EV-D68 still possesses the ability to arrest cells at G0/G1 phase but EV-D68 virulence has increased.

To pinpoint the cause for G0/G1 accumulation upon EV-D68 infection, we analyzed the transitions from G0/G1 into S and from G2/M into G0/G1. After cell cycle release from G0/G1, mock-infected cells entered S phase, while EV-D68-infected cells still accumulated at G0/G1 phase, thus demonstrating that EV-D68 infection prevents S phase entry from G0/G1 phase. Furthermore, after G2/M synchronization, EV-D68 infection promoted cell cycle transition from G2/M into G0/G1 phase. Therefore, EV-D68 infection regulates G0/G1 cell cycle arrest both by promoting G0/G1 phase entry and by inhibiting G0/G1 phase departure. To further analyze the mechanism of host cell cycle manipulation by EV-D68, we assessed the expression of cyclins and CDKs that are known to form complexes to regulate cell cycle progression (Oosthuysen et al., 2015). For example: cyclinD/CDK4 and cyclinD/CDK6 regulate G0/G1 progression (Massagué, 2004); cyclinE/CDK2 regulates S-phase entry from G1 (Hinds et al., 1992); cyclinA/CDK2 regulates S-phase progression by replacing cyclinE (Coverley et al., 2002; Yam et al., 2002); and cyclinB1/CDK1 prevents cell cycle transition from G2/M into G0/G1 (Yu et al., 2013; Adeyemi and Pintel, 2014). We demonstrated that cyclinD, CDK4, CDK6, cyclinE1 and CDK2 are down-regulated after EV-D68 infection, which could explain the ability of EV-D68 to inhibit the transition from G0/G1 to S phase. Furthermore, the expression of cyclinB1 and CDK1 was down-regulated after EV-D68 infection, which is consistent with the ability of EV-D68 to promoting the transition from G2/M to G0/G1. Therefore, expression of cell cycle-related proteins further supports our results suggesting that EV-D68 induces G0/G1 arrest by regulating G0/G1 phase entry and exit. We also analyzed whether the regulation of protein expression occurred at the mRNA level and found that CDK2 and CDK1 were down-regulated by EV-D68, but that the other cell cycle

proteins were not. This indicates that the regulation of cellular factors related to the cell cycle by EV-D68 occurs partly at the transcriptional level, but mostly occurs at the post-translational level.

Viral non-structural proteins are often essential for viral replication, so we also evaluated whether EV-D68 might exert its host cell cycle regulatory function via its viral non-structural proteins. Our results confirmed that the non-structural protein 3D increases the percentage of cells in G0/G1 phase by decreasing the expression of the G0/G1 and S phase related-cell cycle proteins cyclinD, CDK4 and cyclinE1, while 3C decreases the percentage of cells in G2/M phase by decreasing the expression of G2/M-related proteins CDK1 and cyclinB1. These findings raise the possibility that the non-structural proteins 3D and 3C may function coordinately in the context of an EV-D68 infection to enhance the percentage of cells in G0/G1 and increase the G0/G1 to G2/M ratio. It is noted that non-structural 3D protein of EV-A71 mediates cell cycle arrest at S phase, while 3D of EV-D68 mediated cell cycle at G0/G1, although until now the detailed reason of the difference is not clear, it is speculated that 290 of same amino acid sequence might bind with a same target which is responsible for the function of cell cycle arrest, while 172 of different amino acid sequence might bind other different factors which is responsible for different ability of cell cycle regulation, and this part will be investigated in the future.

In the current study, we demonstrated that G0/G1 phase arrest was required by EV-D68 production; however, in a previous study, EV-A71 was shown to have the opposite effect (Yu et al., 2015). This difference is surprising given that both EV-A71 and EV-D68 belong to the *Picornaviridae* family. To further confirm the different activities between the two viruses, we analyzed them side by side, and our results confirm that G0/G1 synchronization promotes EV-D68 viral production but inhibits EV-A71 viral production. Therefore, EV-D68 an EV-A71 can both manipulate the host cell cycle, but the process and outcomes of cell cycle manipulation are entirely different, which could explain why EV-D68 and EV-A71 have varying characteristics, such as the epidemic region (Europe and Asia), the clinical symptoms, and the epidemic size. Meanwhile, these results serve as a reminder that different enteroviruses may require different therapeutic treatments targeting a different set of host factors. Unfortunately, the reason of the difference between them is not clear, but it is speculated that some a host factor(s) generated or kept high level in G0/G1 phase was required by EV-D68 production, while EV-A71 required some a host factor(s) generated or kept high level in S phase so that their non-structural 3D were obligated by two viruses to regulate host cell cycle for their own replication.

The main goal of analyzing the mechanism of EV-D68 pathogenesis was to identify new strategies for preventing and treating the disease, so we did additional experiments to further explore G2/M synchronization as an approach to inhibit the replication of different EV-D68 strains. Our results demonstrate that in addition to its effects on the EV-D68 Fermon strain, G2/M synchronization by nocodazole inhibited the replication and virulence of US/KY/14-18953 and US/MO/14-18947. Additionally, PAB, which is another agent that can induce G2/M arrest, also significantly inhibited the production of EV-D68 and EV-A71. Because nocodazole also has been shown to be effective in inhibiting the production of EV-A71 (Yu et al., 2015), medicines that induce G2/M arrest might be considered as a common approach for inhibiting different types of anti-enterovirus infection, which provides a new direction for anti-enterovirus drug development.

ETHICS STATEMENT

This study has obtained ethics approval from the ethics committee at the First Hospital of Jilin University.

AUTHOR CONTRIBUTIONS

JY, X-fangY, and SH designed the experiments and wrote the paper, ZW and JY conducted the experiments, TZ and YW analyzed cell culture, FS, X-fengY and WZ prepared the virus, LX prepared the reagents.

ACKNOWLEDGMENTS

This work was supported by the National Natural Science Foundation of China (81301416) to JY, Postdoctoral Science Foundation of China (2014M561302, 2015T80299) to JY, Norman Bethune Program of Jilin University (2015202) to JY, the Jilin Provincial Science and Technology Department (20140204004YY, 20160414025GH) to JY, and the Department of Human Resources and Social Security of Jilin Province (2016014) to JY. It was also supported by funding from the Chinese Ministry of Science and Technology (2012CB911100 and 2013ZX10001005) to X-fang Y.

REFERENCES

Adeyemi, R. O., and Pintel, D. J. (2014). Parvovirus-induced depletion of cyclin B1 prevents mitotic entry of infected cells. *PLoS Pathog.* 10:e1003891. doi: 10.1371/journal.ppat.1003891

Chen, C. J., and Makino, S. (2004). Murine coronavirus replication induces cell cycle arrest in G0/G1 phase. *J. Virol.* 78, 5658–5669. doi: 10.1128/JVI.78.11.5658-5669.2004

Coverley, D., Laman, H., and Laskey, R. A. (2002). Distinct roles for cyclins E and A during DNA replication complex assembly and activation. *Nat. Cell Biol.* 4, 523–528. doi: 10.1038/ncb813

Darzynkiewicz, Z., Sharpless, T., Staiano-Coico, L., and Melamed, M. R. (1980). Subcompartments of the G1 phase of cell cycle detected by flow cytometry. *Proc. Natl. Acad. Sci. U.S.A.* 77, 6696–6699. doi: 10.1073/pnas.77.11.6696

DeCaprio, J. A., Ludlow, J. W., Figge, J., Shew, J. Y., Huang, C. M., Lee, W. H., et al. (1988). SV40 large tumor antigen forms a specific complex with the product of the retinoblastoma susceptibility gene. *Cell* 54, 275–283. doi: 10.1016/0092-8674(88)90559-4

Dove, B., Brooks, G., Bicknell, K., Wurm, T., and Hiscox, J. A. (2006). Cell cycle perturbations induced by infection with the coronavirus infectious bronchitis virus and their effect on virus replication. *J. Virol.* 80, 4147–4156. doi: 10.1128/JVI.80.8.4147-4156.2006

Eckner, R., Ewen, M. E., Newsome, D., Gerdes, M., DeCaprio, J. A., Lawrence, J. B., et al. (1994). Molecular cloning and functional analysis of the adenovirus E1A-associated 300-kD protein (p300) reveals a protein with properties of a transcriptional adaptor. *Genes Dev.* 8, 869–884. doi: 10.1101/gad.8.8.869

Esposito, S., Zampiero, A., Ruggiero, L., Madini, B., Niesters, H., and Principi, N. (2015). Enterovirus D68-associated community-acquired pneumonia in children living in Milan, Italy. *J. Clin. Virol.* 68, 94–96. doi: 10.1016/j.jcv.2015.05.017

Farrell, J. J., Ikladios, O., Wylie, K. M., O'Rourke, L. M., Lowery, K. S., Cromwell, J. S., et al. (2015). Enterovirus D68-associated acute respiratory distress syndrome in adult, United States, 2014. *Emerging Infect. Dis.* 21, 914–916. doi: 10.3201/eid2105.142033

Feuer, R., Mena, I., Pagarigan, R., Slifka, M. K., and Whitton, J. L. (2002). Cell cycle status affects coxsackievirus replication, persistence, and reactivation *in vitro*. *J. Virol.* 76, 4430–4440. doi: 10.1128/JVI.76.9.4430-4440.2002

Flemington, E. K. (2001). Herpesvirus lytic replication and the cell cycle: arresting new developments. *J. Virol.* 75, 4475–4481. doi: 10.1128/JVI.75.10.4475-4481.2001

Gay, R. T., Belisle, S., Beck, M. A., and Meydani, S. N. (2006). An aged host promotes the evolution of avirulent coxsackievirus into a virulent strain. *Proc. Natl. Acad. Sci. U.S.A.* 103, 13825–13830. doi: 10.1073/pnas.0605507103

Goh, W. C., Rogel, M. E., Kinsey, C. M., Michael, S. F., Fultz, P. N., Nowak, M. A., et al. (1998). HIV-1 Vpr increases viral expression by manipulation of the cell cycle: a mechanism for selection of Vpr *in vivo*. *Nat. Med.* 4, 65–71. doi: 10.1038/nm0198-065

He, J., Choe, S., Walker, R., Di Marzio, P., Morgan, D. O., and Landau, N. R. (1995). Human immunodeficiency virus type 1 viral protein R (Vpr) arrests cells in the G2 phase of the cell cycle by inhibiting p34cdc2 activity. *J. Virol.* 69, 6705–6711.

He, Y., Xu, K., Keiner, B., Zhou, J., Czudai, V., Li, T., et al. (2010). Influenza A virus replication induces cell cycle arrest in G0/G1 phase. *J. Virol.* 84, 12832–12840. doi: 10.1128/JVI.01216-10

Helt, A. M., and Harris, E. (2005). S-phase-dependent enhancement of dengue virus 2 replication in mosquito cells, but not in human cells. *J. Virol.* 79, 13218–13230. doi: 10.1128/JVI.79.21.13218-13230.2005

Hinds, P. W., Mittnacht, S., Dulic, V., Arnold, A., Reed, S. I., and Weinberg, R. A. (1992). Regulation of retinoblastoma protein functions by ectopic expression of human cyclins. *Cell* 70, 993–1006. doi: 10.1016/0092-8674(92)90249-C

Howe, J. A., Mymryk, J. S., Egan, C., Branton, P. E., and Bayley, S. T. (1990). Retinoblastoma growth suppressor and a 300-kDa protein appear to regulate cellular DNA synthesis. *Proc. Natl. Acad. Sci. U.S.A.* 87, 5883–5887. doi: 10.1073/pnas.87.15.5883

Li, F. Q., Tam, J. P., and Liu, D. X. (2007). Cell cycle arrest and apoptosis induced by the coronavirus infectious bronchitis virus in the absence of p53. *Virology* 365, 435–445. doi: 10.1016/j.virol.2007.04.015

Liu, M. Y., Liu, W., Luo, J., Liu, Y., Zhu, Y., Berman, H., et al. (2011). Characterization of an outbreak of hand, foot, and mouth disease in Nanchang, China in 2010. *PLoS ONE* 6:e25287. doi: 10.1371/journal.pone.0025287

Massagué, J. (2004). G1 cell-cycle control and cancer. *Nature* 432, 298–306. doi: 10.1038/nature03094

Oberste, M. S., Maher, K., Kilpatrick, D. R., Flemister, M. R., Brown, B. A., and Pallansch, M. A. (1999a). Typing of human enteroviruses by partial sequencing of VP1. *J. Clin. Microbiol.* 37, 1288–1293.

Oberste, M. S., Maher, K., Kilpatrick, D. R., and Pallansch, M. A. (1999b). Molecular evolution of the human enteroviruses: correlation of serotype with VP1 sequence and application to picornavirus classification. *J. Virol.* 73, 1941–1948.

Oosthuysen, W. F., Mueller, T., Dittrich, M. T., and Schubert-Unkmeir, A. (2015). *Neisseria meningitidis* causes cell cycle arrest of human brain microvascular endothelial cells at S phase via p21 and cyclin G2. *Cell. Microbiol.* 18, 46–65. doi: 10.1111/cmi.12482

Reed, L. J., M. L. (1983). A simple method of estimating fifty percent endpoints. *Am. J. Hyg.* 27, 493–497.

Reiche, J., Bottcher, S., Diedrich, S., Buchholz, U., Buda, S., Haas, W., et al. (2015). Low-level circulation of enterovirus D68-associated acute respiratory infections, Germany, 2014. *Emerging Infect. Dis.* 21, 837–841. doi: 10.3201/eid2105.141900

Schieble, J. H., Fox, V. L., and Lennette, E. H. (1967). A probable new human picornavirus associated with respiratory diseases. *Am. J. Epidemiol.* 85, 297–310.

Sherr, C. J. (1994). G1 phase progression: cycling on cue. *Cell* 79, 551–555. doi: 10.1016/0092-8674(94)90540-1

Smura, T., Ylipaasto, P., Klemola, P., Kaijalainen, S., Kyllönen, L., Sordi, V., et al. (2010). Cellular tropism of human enterovirus D species serotypes EV-94, EV-70, and EV-68 in vitro: implications for pathogenesis. *J. Med. Virol.* 82, 1940–1949. doi: 10.1002/jmv.21894

Wang, X., Zhu, C., Bao, W., Zhao, K., Niu, J., Yu, X. F., et al. (2012). Characterization of full-length enterovirus 71 strains from severe and mild disease patients in northeastern China. *PLoS ONE* 7:e32405. doi: 10.1371/journal.pone.0032405

Wang, Y., Yang, B., Zhai, Y., Yin, Z., Sun, Y., and Rao, Z. (2015). Peptidyl aldehyde NK-1.8k suppresses enterovirus 71 and enterovirus 68 infection by targeting protease 3C. *Antimicrob. Agents Chemother.* 59, 2636–2646. doi: 10.1128/AAC.00049-15

Werness, B. A., Levine, A. J., and Howley, P. M. (1990). Association of human papillomavirus types 16 and 18 E6 proteins with p53. *Science* 248, 76–79. doi: 10.1126/science.2157286

Yam, C. H., Fung, T. K., and Poon, R. Y. (2002). Cyclin A in cell cycle control and cancer. *Cell. Mol. Life Sci.* 59, 1317–1326. doi: 10.1007/s00018-002-8510-y

Yu, J. H., Cui, Q., Jiang, Y. Y., Yang, W., Tashiro, S., Onodera, S., et al. (2007). Pseudolaric acid B induces apoptosis, senescence, and mitotic arrest in human breast cancer MCF-7. *Acta Pharmacol. Sin.* 28, 1975–1983. doi: 10.1111/j.1745-7254.2007.00706.x

Yu, J. H., Liu, C. Y., Zheng, G. B., Zhang, L. Y., Yan, M. H., Zhang, W., et al. (2013). Pseudolaric acid B induced cell cycle arrest, autophagy and senescence in murine fibrosarcoma l929 cell. *Int. J. Med. Sci.* 10, 707–718. doi: 10.7150/ijms.5726

Yu, J., Zhang, L., Ren, P., Zhong, T., Li, Z., Wang, Z., et al. (2015). Enterovirus 71 mediates cell cycle arrest in S phase through non-structural protein 3D. *Cell Cycle* 14, 425–436. doi: 10.4161/15384101.2014.980631

Yuan, X., Shan, Y., Zhao, Z., Chen, J., and Cong, Y. (2005). G0/G1 arrest and apoptosis induced by SARS-CoV 3b protein in transfected cells. *Virol. J.* 2, 66. doi: 10.1186/1743-422X-2-66

Yuan, X., Wu, J., Shan, Y., Yao, Z., Dong, B., Chen, B., et al. (2006). SARS coronavirus 7a protein blocks cell cycle progression at G0/G1 phase via the cyclin D3/pRb pathway. *Virology* 346, 74–85. doi: 10.1016/j.virol.2005.10.015

Zhang, T., Ren, L., Luo, M., Li, A., Gong, C., Chen, M., et al. (2015). Enterovirus D68-associated severe Pneumonia, China, 2014. *Emerging Infect. Dis.* 21, 916–918. doi: 10.3201/eid2105.150036

Conflict of Interest Statement: The authors declare that the research was conducted in the absence of any commercial or financial relationships that could be construed as a potential conflict of interest.

Copyright © 2017 Wang, Zhong, Wang, Song, Yu, Xing, Zhang, Yu, Hua and Yu. This is an open-access article distributed under the terms of the Creative Commons Attribution License (CC BY). The use, distribution or reproduction in other forums is permitted, provided the original author(s) or licensor are credited and that the original publication in this journal is cited, in accordance with accepted academic practice. No use, distribution or reproduction is permitted which does not comply with these terms.

frontiers in Cellular and Infection Microbiology

ORIGINAL RESEARCH
published: 25 January 2017
doi: 10.3389/fcimb.2017.00011

Oral Multiple Sclerosis Drugs Inhibit the *In vitro* Growth of Epsilon Toxin Producing Gut Bacterium, *Clostridium perfringens*

Kareem R. Rumah[1]*, *Timothy K. Vartanian*[2] *and Vincent A. Fischetti*[1]

[1] *Laboratory of Bacterial Pathogenesis and Immunology, Rockefeller University, New York, NY, USA,* [2] *The Brain and Mind Research Institute and Department of Neurology, Weill Cornell Medical College, New York, NY, USA*

There are currently three oral medications approved for the treatment of multiple sclerosis (MS). Two of these medications, Fingolimod, and Teriflunomide, are considered to be anti-inflammatory agents, while dimethyl fumarate (DMF) is thought to trigger a robust antioxidant response, protecting vulnerable cells during an MS attack. We previously proposed that epsilon toxin from the gut bacterium, *Clostridium perfringens*, may initiate newly forming MS lesions due to its tropism for blood-brain barrier (BBB) vasculature and central nervous system myelin. Because gut microbiota will be exposed to these oral therapies prior to systemic absorption, we sought to determine if these compounds affect *C. perfringens* growth *in vitro*. Here we show that Fingolimod, Teriflunomide, and DMF indeed inhibit *C. perfringens* growth. Furthermore, several compounds similar to DMF in chemical structure, namely α, β unsaturated carbonyls, also known as Michael acceptors, inhibit *C. perfringens*. Sphingosine, a Fingolimod homolog with known antibacterial properties, proved to be a potent *C. perfringens* inhibitor with a Minimal Inhibitory Concentration similar to that of Fingolimod. These findings suggest that currently approved oral MS therapies and structurally related compounds possess antibacterial properties that may alter the gut microbiota. Moreover, inhibition of *C. perfringens* growth and resulting blockade of epsilon toxin production may contribute to the clinical efficacy of these disease-modifying drugs.

Keywords: multiple sclerosis, oral therapies, anti-bacterial agents, *Clostridium perfringens*, microbiome

OPEN ACCESS

Edited by:
Venkatakrishna Rao Jala, University of Louisville, USA

Reviewed by:
Michael L. Vasil, University of Colorado Denver School of Medicine, USA
Caitlin S. L. Parello, Biomodels, LLC, USA

***Correspondence:**
Kareem R. Rumah
rrumah@rockefeller.edu

Received: *09 September 2016*
Accepted: *06 January 2017*
Published: *25 January 2017*

Citation:
Rumah KR, Vartanian TK and Fischetti VA (2017) Oral Multiple Sclerosis Drugs Inhibit the In vitro Growth of Epsilon Toxin Producing Gut Bacterium, Clostridium perfringens. Front. Cell. Infect. Microbiol. 7:11. doi: 10.3389/fcimb.2017.00011

INTRODUCTION

Multiple sclerosis (MS) is the most common non-traumatic neurological disease of young adults in Western Europe and North America (Conway and Cohen, 2010). Although traditionally considered an autoimmune disease that specifically targets central nervous system myelin (Frohman et al., 2006), increasingly, investigators have been pursuing the idea that host-pathogen interactions may play a role in the MS disease process (Collins et al., 2012). Indeed, investigations into how the gut microbiota may trigger or modulate MS relapses are currently under way. With the advent of the first oral treatments for MS, Fingolimod, Teriflunomide, and dimethyl fumarate (DMF), a reasonable question arises. Do these oral medications possess antibacterial properties, and if so, could modulation of gut bacteria contribute to protection against MS relapse?

We have previously proposed that a bacterial neurotoxin, epsilon toxin, from the anaerobic gut bacterium, *Clostridium perfringens*, may play a pivotal role in triggering newly forming MS lesions (Rumah et al., 2013, 2015; Linden et al., 2015). Epsilon toxin (ETX) is a rational candidate MS trigger due to its tropism for the blood-brain barrier (BBB) and for the myelin sheath; both of which are specifically damaged during each MS relapse (Dorca-Arévalo et al., 2008; Rumah et al., 2013; Linden et al., 2015). Remarkably, newly forming MS lesions display evidence of BBB breakdown, oligodendrocyte cell death and early microglial activation in the absence of a peripheral inflammatory infiltrate (Barnett and Prineas, 2004). While the triggering agent of these early pathologic changes remains unknown, *C. perfringens* epsilon toxin serves as a provocative candidate due to its tissue specificity and resultant mechanistic plausibility (Rumah et al., 2013, 2015; Linden et al., 2015).

C. perfringens is an anaerobic, spore forming, gram-positive bacillus that is sub-classified into five distinct toxinotypes based on differential exotoxin production (**Table 1**). *C. perfringens* type A typically colonizes the human gut with a prevalence of 63% among healthy individuals (Carman et al., 2008), while *C. perfringens* types B and D, the producers of ETX, are commonly found in the intestines of ruminant animals such as sheep, goats, and cattle but not humans (Popoff, 2011). ETX toxin is a potent neurotoxin secreted as a 33 kDa inactive precursor during the logarithmic growth phase of *C. perfringens* in the mammalian intestine. This poorly active precursor is cleaved by gut trypsin, chymotrypsin and/or an additional clostridial exotoxin, lamda toxin. The 28.6 kDa enzymatic cleavage product permeablizes the gut epithelium, enters the blood stream and binds to receptors on the luminal surface of brain endothelial cells. Once bound to brain microvessels, ETX oligomerizes and forms a heptameric pore in the endothelial cell plasma membrane. Brain endothelial cell damage leads to breakdown of the BBB (Popoff, 2011). In addition to its known effects on BBB vasculature, ETX has been found to specifically bind to and damage myelin when incubated with mammalian brain slices (Dorca-Arévalo et al., 2008; Linden et al., 2015; Wioland et al., 2015). This unique ability to interact specifically with the tissues that are damaged in MS, the BBB, and CNS myelin, makes it a promising candidate as an environmental MS trigger.

Fingolimod was the first oral therapy to be approved for the treatment of MS. It was rationally engineered from the antifungal molecule Myriocin, which was later shown to possess immunosuppressive properties. Fingolimod and Myriocin are both structurally homologous to sphingosine, a lipid that is a necessary component of cell membrane sphingolipids (Strader et al., 2011). Similar to Myriocin, sphingosine is also known to possess antimicrobial properties. However, while Myriocin is antifungal in nature, sphingosine is antibacterial (Fischer et al., 2012). Interestingly, Fingolimod has been shown to mimic sphingosine's antibacterial properties by protecting the cystic fibrosis transmembrane conductance regulator (CFTR) knockout mouse from luminal airway infection by *Pseudomonas auerginosa* (Pewzner-Jung et al., 2014).

In the context of MS, Fingolimod is phosphorylated in the bloodstream and subsequently binds to the lymphocyte sphingosine-1-phosphate receptor 1 (S1PR1), causing rapid internalization of S1PR1. In the absence of surface S1PR1, lymphocytes are unable to egress from lymphoid tissues and cannot traffic to target tissues such as the brain; thus the rationale that Fingolimod may reduce the risk of MS relapse and the severity of attacks through immune modulation (Strader et al., 2011).

TABLE 1 | *Clostridium perfringens* toxinotypes, genotypes, and associated diseases.

A	α	Humans: Gangrene, toxic enteritis, food poisoning, sporadic diarrhea, some cases of SIDS. Fowl: Necrotic enteritis. Foals, pigs: Diarrhea.
B	α, β, ε	Newborn Lambs: Dysentery. Newborn Calves and Foals: Hemorrhagic enteritis. Sheep and Goats: Enterotoxemia. Focal symmetric encephalomalacia.
C	α, β	Humans: Necrotic enteritis (Pigbel). Piglets, Lambs, Calves and Foals: Necrotic enteritis. Sheep: Enterotoxemia.
D	α, ε	Lambs, Sheep, Calves and Goats: Enterotoxemia. Focal symmetric encephalomalacia.
E	α, ι	Calves: Enterotoxemia.

Teriflunomide is the active metabolite of the immunosuppressant Lenflunomide, which is currently approved for the treatment of rheumatoid arthritis (Munier-Lehmann et al., 2013). Teriflunomide inhibits *de novo* pyrimidine synthesis in rapidly dividing cells such as clonally expanding lymphocytes, potentially mitigating an autoimmune attack against myelin. More specifically, Teriflunomide non-competitively inhibits dihydroorotate dehydrogenase, an enzyme involved in the first step of de novo pyrimidine synthesis. Memory B cells and T cells remain unaffected by Teriflunomide as they divide more slowly and can synthesize DNA by utilizing the pyrimidine salvage pathway (Bar-Or et al., 2014). Interestingly, dihydroorotate dehydrogenase inhibitors have been shown to arrest the growth of unicellular organisms such as plasmodium falciparum presumably by inhibiting *de novo* pyrimidine synthesis (Pavadai et al., 2016).

DMF is a fumaric acid ester, which was originally investigated for use as an antimicrobial preservative[1]. It was first used therapeutically to treat psoriasis based on a hypothesis that psoriasis is caused by a defect in fumarate mediated carbohydrate metabolism in the skin. In the early 2000s, a German neurologist noticed that MS patients taking DMF for concurrent psoriasis showed stabilization of their MS symptoms and a reduction in relapse rates (Phillips and Fox, 2013).

DMF has been shown to react with thiol-containing molecules such as the cellular antioxidant, glutathione, and the cysteine residues of proteins via a chemical reaction called the Michael

[1]Pest control. Patent Publication Number: US2218181 A.

addition (Brennan et al., 2015). Although DMF initially depletes mammalian cells of glutathione, its proposed protective action in MS stems from its ability to alkylate key cysteine residues in the redox sensitive protein Kelch-Like ECH-Associated Protein 1 (Keap1). Keap1 normally inhibits Nuclear factor (erythroid-derived 2)-like 2 (Nrf2) from translocating to the nucleus and activating antioxidant gene expression. When the cysteine residues of Keap1 are oxidized by reactive oxygen species (ROS) or organic electrophiles such as DMF, Keap1 dissociates from Nrf-2, allowing nuclear translocation to occur. This elicits a robust antioxidant cellular response. The initial decrease in cellular glutathione after DMF treatment is followed by a sharp glutathione increase via the Nrf-2 pathway, which may protect vulnerable cells in MS (Phillips and Fox, 2013).

Although Fingolimod, Teriflunomide, and DMF have proposed mechanisms for how they protect the central nervous system from MS mediated damage, one unexplored possibility is that these orally administered agents may inhibit the growth of neurotoxin-secreting gut bacteria. Because, during log-phase growth, *C. perfringens* secretes ETX, a toxin that specifically targets the BBB and the myelin sheath, we chose to investigate the effect of these oral MS therapies on *C. perfringens* growth *in vitro*.

METHODS

Drugs and Compounds

All drugs and compounds used in this study were purchased from Sigma Aldrich.

Bacterial Strains and Growth Conditions

C. perfringens ATCC 13124 (type A), ATCC 3626 (type B), ATCC 51880 (type C), ATCC 3631 (type D), ATCC 27324 (type E), and two type A clinical isolates provided by New York Presbyterian Hospital were used for the initial screen while the "type strain," ATCC 13124, was used for all subsequent experiments. Bacteria were cultured anaerobically at 37°C overnight using the GasPak 100 system (BD). Anaerobiosis was achieved by pre-reducing the culture media using an anaerobic jar containing a GasPak EZ Anaerobe System sachet for a minimum of 6 h before inoculation. After inoculation, the GasPak sachet was replaced for the overnight culture.

Experimental Procedures

The compounds used for the initial growth inhibition screen were diluted to a final concentration of 500 μg/ml in Mueller Hinton broth (BD) and media was inoculated with 5×10^6 colony-forming units (CFUs) of different *C. perfringens* strains. Minimal Inhibitory Concentration values (≥95% growth inhibition, MIC_{95}) were determined for inhibitory compounds using cation adjusted Mueller Hinton II broth (BD). Inhibitory compounds were diluted serially from 512 μg/ml down to 0.5 μg/ml, inoculated with 5×10^5 CFUs of *C. perfringens* and then anaerobically cultured at 37°C overnight as previously described. Culture conditions for each compound were performed in triplicate and bacterial growth was determined by measuring OD_{600}-values from 1 ml of re-suspended bacteria.

Statistical Analysis

Results are representative of data obtained from repeated independent experiments. Each value represents the mean ± *SD* for three replicates. Statistical analysis was performed using the two-tailed Student *t*-test (GraphPad Software, San Diego, CA, USA).

RESULTS

With renewed interest in gut bacteria and their potential involvement in the pathogenesis of MS (Bhargava and Mowry, 2014), we wished to determine if oral disease-modifying drugs (DMDs) have the ability to modulate growth of *C. perfringens* since type B and D strains secrete ETX during log-phase growth. Therefore, we tested if oral DMDs affected the growth of *C. perfringens* toxinotypes A–E. We compared the growth inhibitory effects of Fingolimod, DMF, and Teriflunomide to that of oral symptom management drugs (SMDs) Baclofen, Bupropion, and Gabapentin; drugs not thought to alter the disease course of MS. We exposed *C. perfringens* cultures to 500 μg/ml of each compound, allowed for overnight anaerobic growth, and determined the optical density (OD_{600}) the following day. We found that each oral DMD significantly inhibited all *C. perfringens* toxinotypes and strains tested, while the oral SMDs did not (**Figure 1A**). We then plotted the minimal inhibitory concentration (MIC) values for each inhibitory compound and found that Fingolimod was the most potent inhibitor at 4 μg/ml (**Figure 1B**).

Because Fingolimod is a homolog of D-sphingosine and Myriocin, both of which have been shown to possess antimicrobial properties (Fischer et al., 2012), we compared the inhibitory activity of Fingolimod to these related sphingoid molecules. We exposed the type strain, *C. perfringens* ATCC 13124 (type A), to Fingolimod, D-sphingosine, and Myriocin and identified that, like Fingolimod, D-sphingosine also displayed inhibitory activity. Myriocin failed to inhibit *C. perfringens*, but instead, enhanced bacterial growth (**Figure 2A**). We then plotted and compared MICs for Fingolimod and D-sphingosine and determined that D-sphingosine displayed a similar inhibitory potency to that of Fingolimod with an MIC_{95} of 4 μg/ml (**Figure 2B**).

Although an antioxidant mechanism has been proposed for how DMF protects cells against MS mediated damage, DMF was originally investigated for use as an antimicrobial compound[1]. Interestingly, DMF was also found to inhibit the growth of *Clostridium botulinum* (Dymicky et al., 1987), a bacterial species closely related to *C. perfringens*. DMF is known to be a Michael acceptor and its ability to affect the redox status of cells stems from its electrophilic nature. Michael acceptors accept electrons during the Michael reaction, while nucleophilic thiols (Michael donors) donate electrons. The Michael reaction results in covalent alkylation of the sulfhydryl group. This covalent linkage permanently inactivates thiol-containing molecules if the thiol is necessary for the molecule's function, as is the case for glutathione and its antioxidant properties (Brennan et al., 2015).

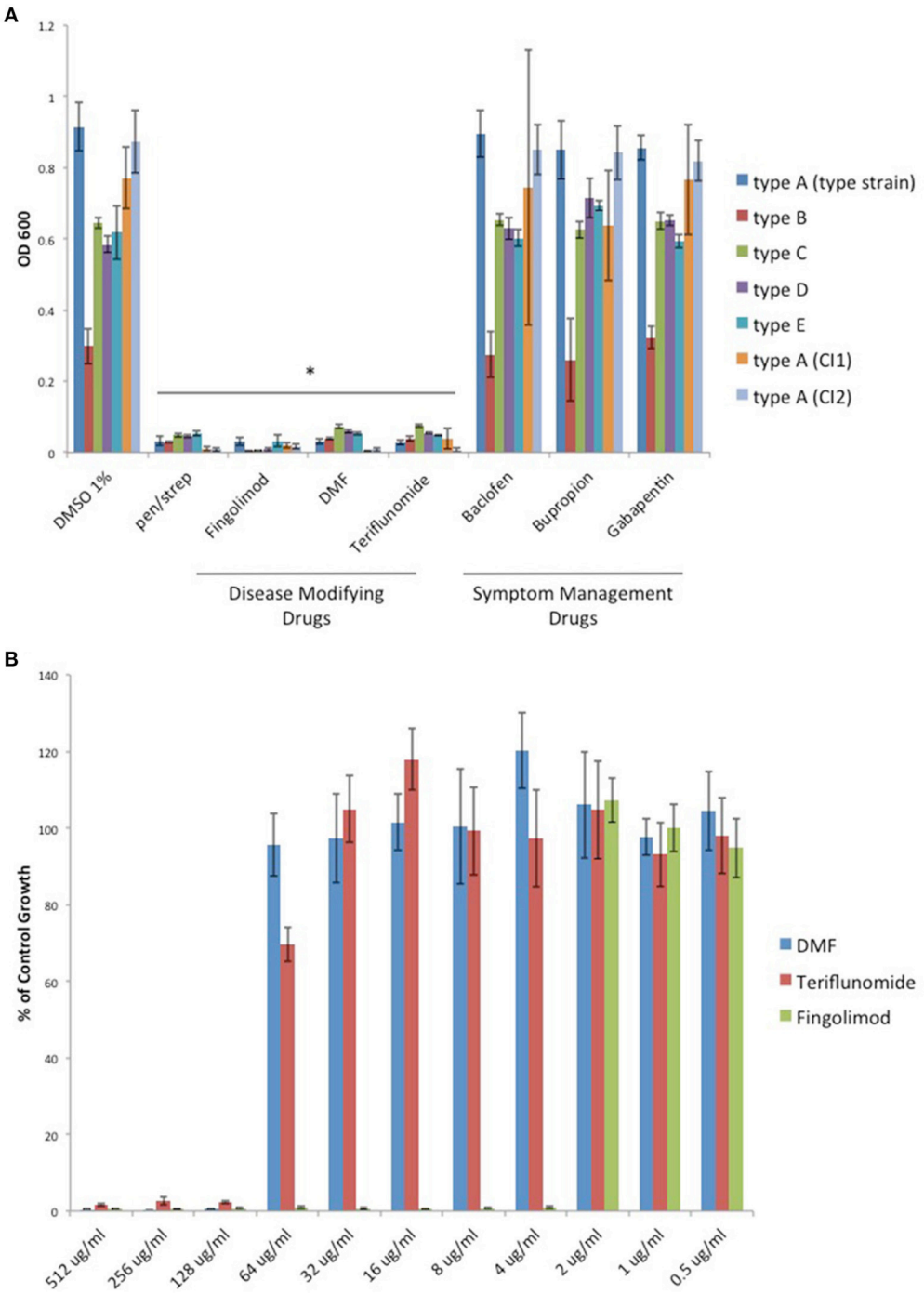

FIGURE 1 | Oral disease modifying MS drugs inhibit *C. perfringens* growth, while oral drugs used for MS symptom management do not. (A) *C. perfringens* toxinotypes A, B, C, D, E, and two type A clinical isolates (CI1 and CI2) were anaerobically cultured in the presence of 500 μg/ml of oral DMDs, Fingolimod, DMF, and Teriflunomide, each of which significantly inhibited bacterial growth for all strains tested, similar to what was observed when bacteria were cultured in the presence of known antibiotic mixture penicillin/streptomycin (pen/strep, 100 U/ml). In contrast, oral SMDs failed to inhibit *C. perfringens* growth, yielding OD_{600}-values similar to that of the DMSO vehicle control. Data are presented as means from three independent experiments. Error bars represent standard deviations, and asterisks indicate that results are statistically significant compared with the DMSO vehicle controls (Student's *t*-test, $^*P < 0.001$). **(B)** Serial dilutions of inhibitory oral DMDs were performed and the type strain, *C. perfringens* ATCC 13124 (type A), was cultured in each condition. OD_{600}-values for each concentration were divided by that of the corresponding dilution for the DMSO vehicle control. MIC-values were plotted for each oral DMD revealing that Fingolimod was the most potent compound with an MIC_{95} of 4 μg/ml, compared to 128 μg/ml for DMF and Teriflunomide.

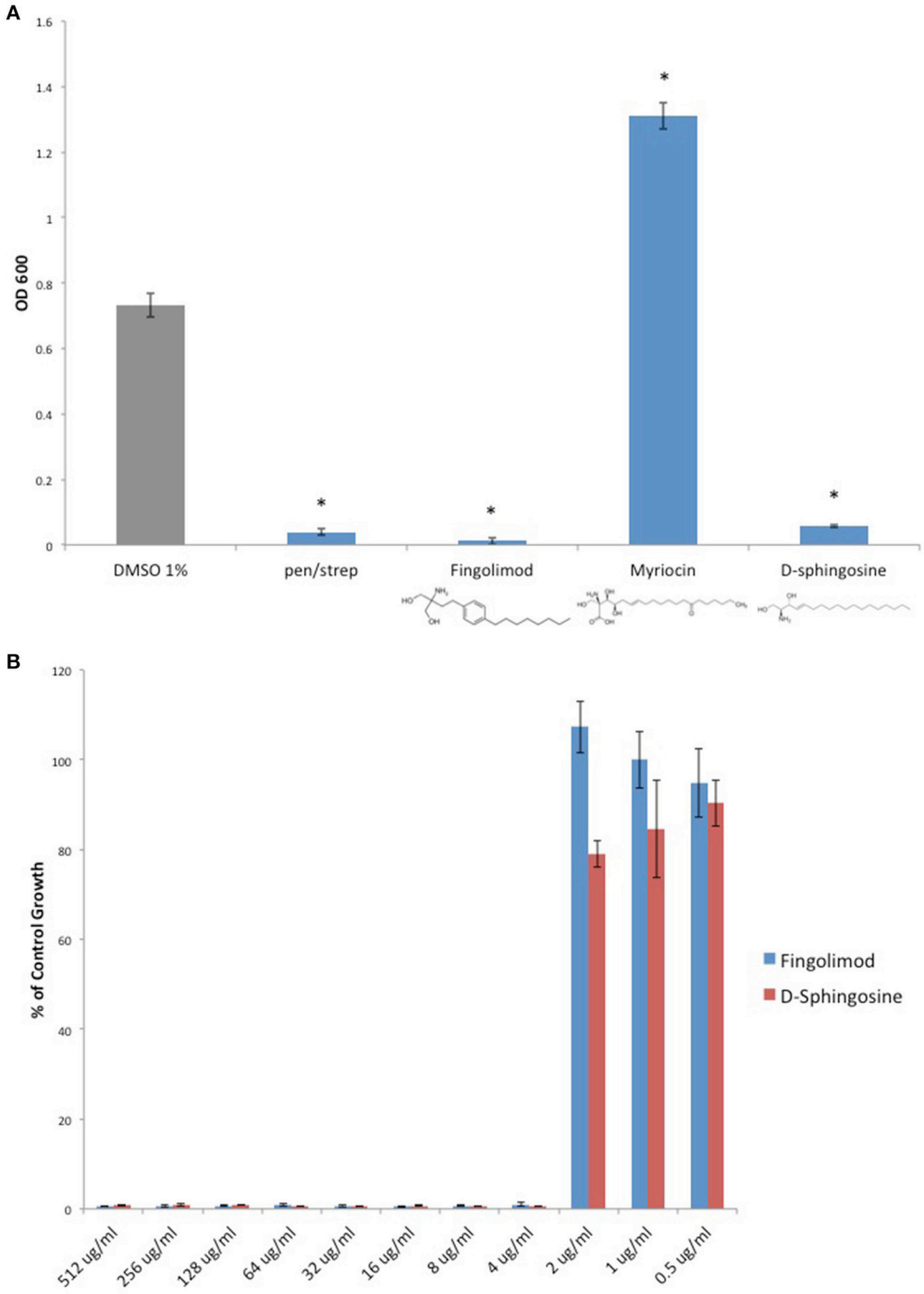

FIGURE 2 | D-sphingosine, a Fingolimod related compound, inhibits *C. perfringens* growth. (A) Type strain, *C. perfringens* ATCC 13124, was anaerobically cultured in the presence of 500 μg/ml Fingolimod and other sphingoid compounds, D-sphingosine and Myriocin. Like Fingolimod, D-sphingosine also inhibited *C. perfringens* growth. However, Myriocin failed to inhibit the bacterium. Instead, Myriocin enhanced *C. perfringens* growth above that of the DMSO vehicle control. Data are presented as means from three independent experiments. Error bars represent standard deviations, and asterisks indicate that results are statistically significant compared with the DMSO vehicle control (gray); Student's *t*-test, $^*P < 0.0001$. **(B)** Serial dilutions of inhibitory sphingoid molecules were performed and *C. perfringens* ATCC 13124 was cultured at each dilution. OD_{600}-values for each dilution were divided by that of the corresponding DMSO vehicle control dilution. MIC-values were plotted for each of the inhibitory sphingoid compounds revealing that D-sphingosine mimics Fingolimod's antibacterial potency with an MIC_{95}-value of 4 μg/ml.

We sought to determine if DMF's antimicrobial activity extended to *C. perfringens*. Furthermore, we examined DMF's Michael acceptor activity as pertaining to its antimicrobial properties. We screened DMF and its metabolites, monomethyl fumarate (MMF), and fumarate and found that each compound inhibited the growth of type strain, *C. perfringens* ATCC 13124. However, their saturated succinate counterparts dimethyl succinate (DMS), monomethyl succinate (MMS), and succinate, molecules devoid of Michael acceptor activity due to reduction of the α, β carbon double bond, failed to inhibit *C. perfringens* (**Figure 3A**). We plotted MIC-values for DMF, MMF, and fumarate and found that DMF was four times more potent than either MMF or fumarate (**Figure 3B**).

Given that Michael acceptor activity was necessary for *C. perfringens* inhibition by DMF and its fumarate metabolites, we sought to determine if unrelated molecules that share the α, β unsaturated carbonyl structure could also inhibit *C. perfringens*. We screened Michael acceptors from a diverse group of chemical families and found that natural product Michael acceptors Gambogic acid (a xanthonoid), Parthenolide (a sesquiterpenoid), and Curcumin (a curcuminoid) each inhibited *C. perfringens* (**Figure 4A**). Interestingly, we found that Gambogic acid was particularly inhibitory with an MIC_{95} of 1 μg/ml (**Figure 4B**).

To provide additional evidence that Michael acceptor activity is indeed critical to the antibacterial properties of α, β unsaturated carbonyls, we searched the literature to find compounds for which experimental values of Michael reaction potencies have been determined. Dinkova-Kostova et al. determined the potencies of several plant derived Michael acceptors for their ability to induce cellular quinone reductase activity; a cellular marker for a compound's reactivity with sulfhydryl containing molecules (Dinkova-Kostova et al., 2001). In our study, the antibacterial potencies of Cinnamic acid, trans-Chalcone, and Curcumin mirrored the Michael acceptor potencies described by Dinkova-Kostova and colleagues (**Figure 5**). Cinnamic acid was previously shown to be inactive as a Michael acceptor, and in our hands, this compound failed to inhibit *C. perfringens*. Furthermore, Curcumin was found to be approximately four times more potent than trans-Chalcone (ratio = 4.13; Dinkova-Kostova et al., 2001). Likewise, we found that Curcumin was four times more potent than trans-Chalcone as a *C. perfringens* inhibitor (ratio = 4).

Since Michael acceptors react with thiols and deplete cellular glutathione levels (Brennan et al., 2015), we surmised that Michael acceptor inhibition of *C. perfringens* might be abolished by the addition of exogenous glutathione. To test this, we compared *C. perfringens* growth in the presence of Michael acceptors with and without an equal quantity of exogenous glutathione. We also tested the effect of glutathione on the inhibitory activity of each of the oral MS DMDs. Glutathione completely abolished growth inhibition by the known Michael acceptors in our study, but failed to abolish the inhibitory effects of Fingolimod and Teriflunomide (**Figure 6A**). Because glutathione is an antioxidant, as are vitamins C and E, we sought to determine if the glutathione's abrogation of Michael acceptor antibacterial activity is based on its nucleophilic behavior or due, more generally, to its antioxidant properties. *C. perfringens* was challenged with DMF in the presence of vitamin C, vitamin E, or the Michael donor, glutathione. Of the antioxidant panel, only the Michael donor, glutathione, was able to neutralize DMF's inhibitory effect (**Figure 6B**).

DISCUSSION

In this study, we have shown that each of the oral DMDs approved for the treatment of MS, Fingolimod, Teriflunomide, and DMF, inhibits the *in vitro* growth of the epsilon toxin-secreting gut bacterium, *C. perfringens*. In contrast, oral therapies used specifically for symptomatic management fail to prevent *C. perfringens* growth. Of note, Fingolimod proved to be bactericidal, while Teriflunomide and DMF were bacteriostatic (**Supplemental Figure 1**). The antibacterial properties of oral DMDs raises the possibility that modulation of the intestinal microbiota may play a role in the clinical efficacy of these compounds. Preventing *C. perfringens* growth and toxin production may serve as a specific example of this. Furthermore, we have identified two distinct classes of molecules capable of inhibiting *C. perfringens*; namely sphingoid compounds such as Fingolimod and D-sphingosine, and Michael acceptors such as DMF, its fumarate metabolites, and various natural products that are α, β unsaturated carbonyls.

Important factors must be considered when attempting to extrapolate these *in vitro* findings to what may be occurring in the human gut. First, how do the *in vitro* inhibitory concentrations compare to concentrations found in the human gut? The resting volume of the human stomach is ∼0.08 L (Johnson, 1994), which yields a calculated gut concentration of 6.3 μg/ml for Fingolimod (MIC_{95} = 4 μg/ml), 87–175 μg/ml for Teriflunomide (MIC_{95} = 128 μg/ml), and 1500–3000 μg/ml for DMF (MIC_{95} = 128 μg/ml). Therefore, each compound's MIC_{95} is within the calculated range of the therapeutic concentration that will enter the small intestine. Furthermore, DMF is a delayed released capsule that dissolves in the more basic pH of the small intestine (Gold et al., 2016). Local release of DMF may increase its concentration in the small intestine where *C. perfringens* resides.

Second, our experimental growth conditions are likely to be more favorable to *C. perfringens* growth than the intestinal milieu. Anexic, *in vitro* growth protects *C. perfringens* from competition with other bacteria for nutrients. In addition, *C. perfringens* will not be exposed to toxic molecules secreted by competing bacteria such as bacteriocins or host derived antibacterial molecules such as defensins. Therefore, the MIC_{95} for each of the oral DMDs may be considerably less in an environment such as the human intestine where *C. perfringens* must contend with a multitude of external factors.

Conversely, each of the oral DMDs possesses a significant degree of hydrophobicity, and lipid-binding molecules within the gut lumen may sequester these compounds, preventing toxic interactions with gut bacteria. Specifically considering DMF, a Michael acceptor, extracellular nucleophiles present in the gut may react with its electrophilic β carbon before it can enter the bacterial cell, possibly diminishing its antibacterial activity within the gut.

DMF's Michael reaction-dependent inhibition of *C. perfringens* growth may be explained by its ability to deplete this bacterium of thiol containing compounds. It is

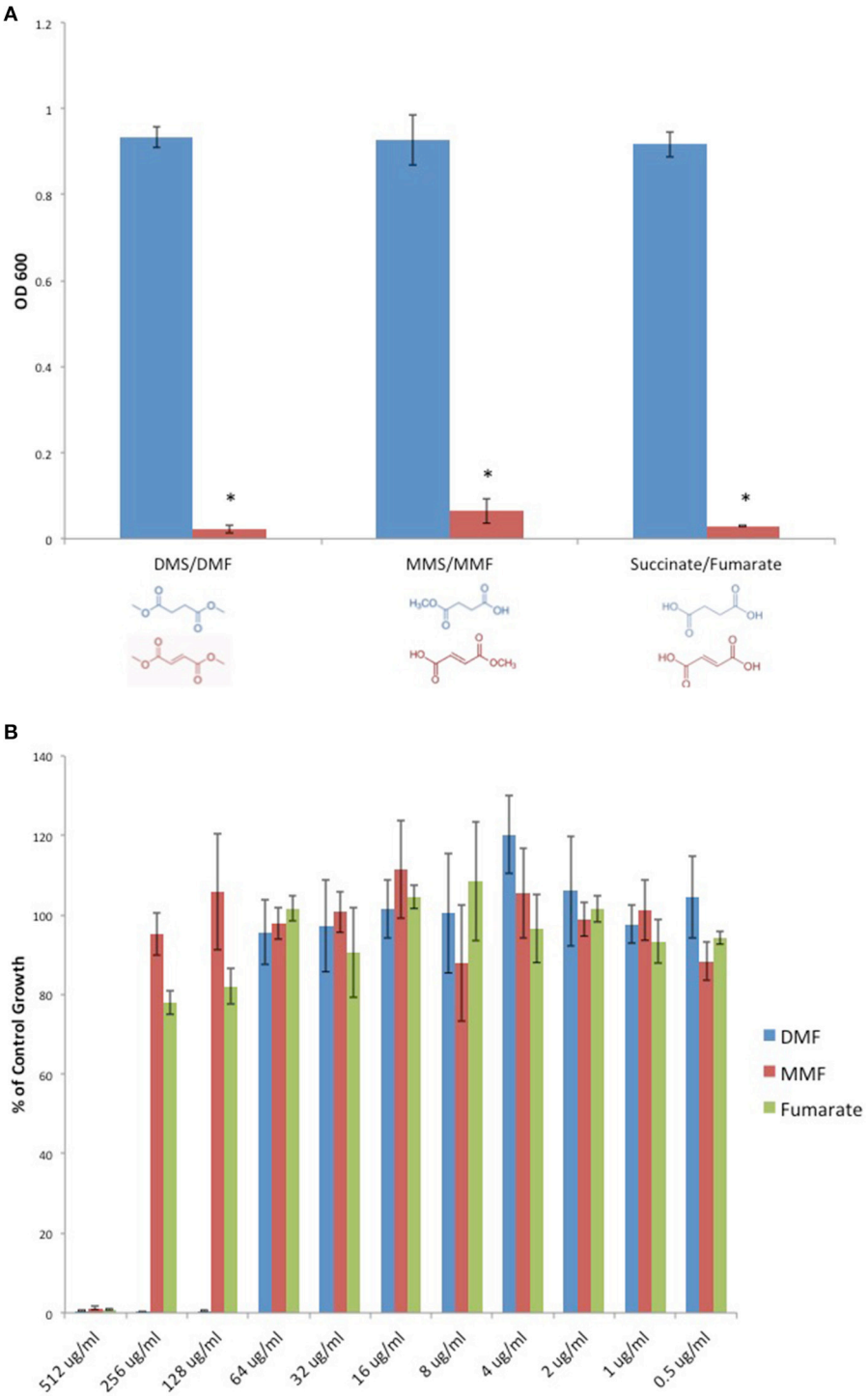

FIGURE 3 | Fumarates inhibit *C. perfringens* growth while their related saturated succinates do not. (A) The anaerobic growth of *C. perfringens* ATCC 13124 was compared for DMF and its corresponding succinate (DMS), MMF and its corresponding succinate MMS, fumarate, and succinate. In each case, the unsaturated fumarate compounds (red) displayed inhibitory activity, while the saturated succinates (blue) did not. Data are presented as means from three independent experiments. Error bars represent standard deviations, and asterisks indicate that the inhibition of bacterial growth observed in the presence of unsaturated fumarates is statistically significant when compared to the bacterial growth observed in the presence of corresponding saturated succinates; Student's *t*-test, $^*P < 0.0001$). **(B)** Serial dilutions of inhibitory fumarate compounds were performed and *C. perfringens* ATCC 13124 was cultured at each dilution. OD_{600}-values for each dilution were divided by that of the corresponding DMSO vehicle control dilution. MIC-values were plotted for each of the inhibitory fumarates revealing that DMF is approximately four times more potent that MMF and fumarate.

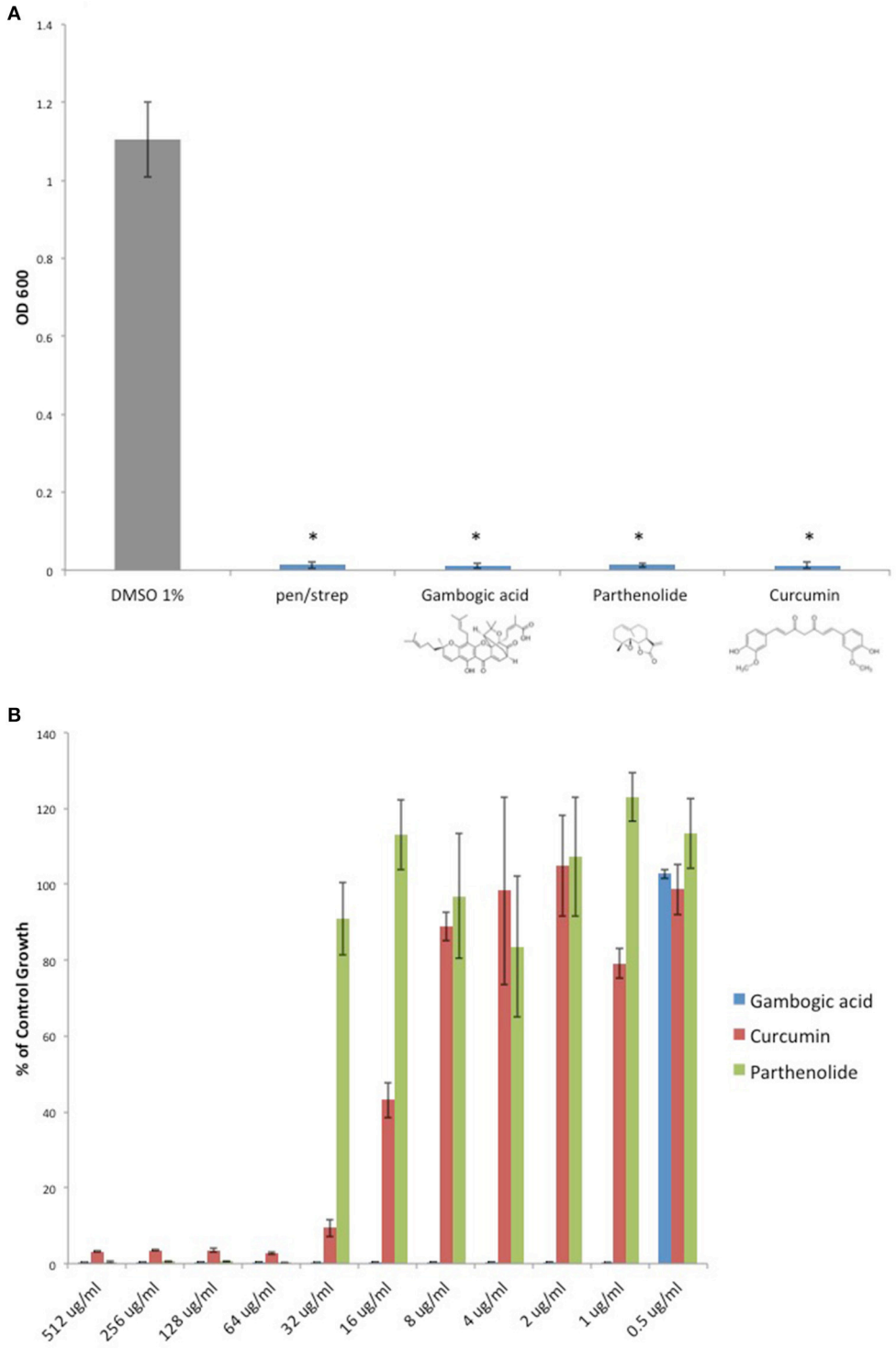

FIGURE 4 | Natural product Michael acceptors inhibit *C. perfringens* growth. (A) Plant derived Michael acceptors were tested for inhibitory activity against *C. perfringens* ATCC 13124. Bacteria were grown anaerobically in the presence of 500 μg/ml Gambogic acid, Parthenolide, and Curcumin. Each natural product Michael acceptor successfully inhibited *C. perfringens* growth, similar to what was observed when bacteria were cultured in the presence of known antibiotic penicillin/streptomycin (pen/strep, 100 U/ml). Data are presented as means from three independent experiments. Error bars represent standard deviations, and asterisks indicate that results are statistically significant compared with the DMSO vehicle control (gray); Student's *t*-test, $^*P < 0.0001$. **(B)** Serial dilutions of inhibitory natural product Michael acceptors were performed and *C. perfringens* ATCC 13124 was cultured at each dilution. OD_{600}-values for each dilution were divided by that of the corresponding DMSO vehicle control dilution. MIC-values were plotted for each compound revealing Gambogic acid as the most potent with an MIC_{95} of 1 μg/ml when compared to Parthenolide and Curcumin, which each inhibit *C. perfringens* at 64 μg/ml.

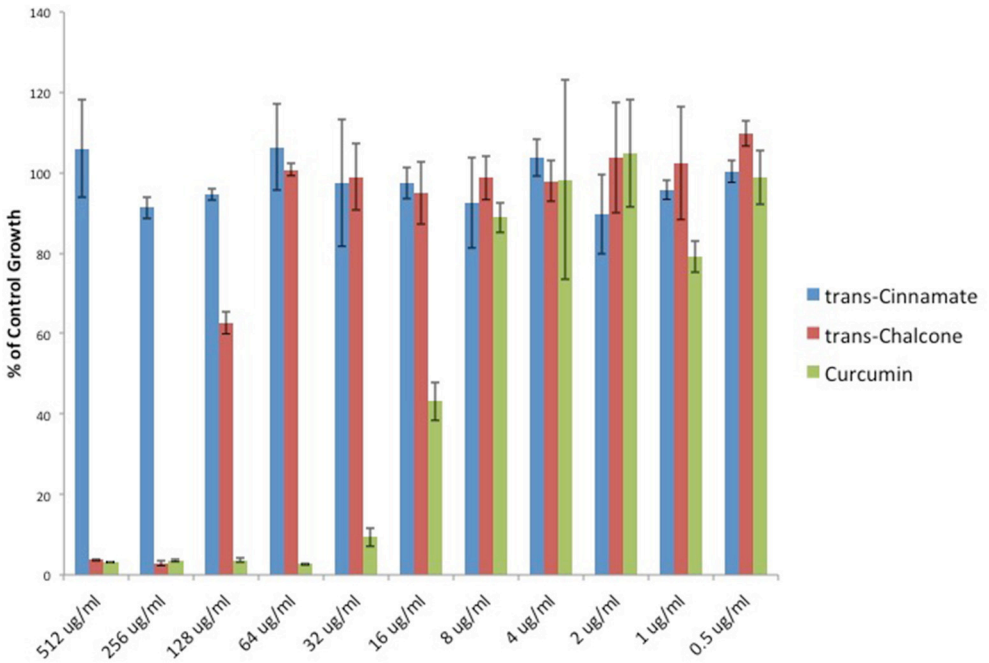

FIGURE 5 | Michael acceptor *C. perfringens* growth inhibition reflects known reactivity potencies. Serial dilutions of α, β unsaturated carbonyls were performed and *C. perfringens* ATCC 13124 was cultured at each dilution. OD_{600}-values for each dilution were divided by that of the corresponding DMSO vehicle control dilution. MIC-values were plotted for each compound revealing that Cinnamic acid displays no inhibitory activity, while Curcumin is four times more potent than trans-Chalcone. The relative inhibitory potencies of each compound corresponds almost exactly with the relative Michael acceptor potencies as demonstrated by Dinkova-Kostova et al. (2001).

striking that nucleophilic thiols not only play an important role in mammalian cell homeostasis, but are also necessary substrates for *C. perfringens* growth. This bacterium depends on an organic source of sulfur (thiols) and will not grow with strictly inorganic sources (SO_4^{2-}, SO_3^{2-}, $S_2O_3^{2-}$, and S_i; Fuchs and Bonde, 1957). Therefore, depleting *C. perfringens* of thiols may contribute to Michael acceptor mediated growth inhibition.

Although Teriflunomide is an α, β unsaturated carbonyl, we have shown that glutathione has no effect on its ability to inhibit *C. perfringens* growth. It is tempting to speculate that Teriflunomide inhibits *de novo* pyrimidine synthesis in rapidly dividing bacterial cells, as it does in mammalian cells, via inhibition of dihydroorotate dehydrogenase; a gene that has been annotated for *C. perfringens* in the Uniprot Knowledgebase. However, we have not examined the inhibitory mechanism of Teriflunomide in the present study.

That Michael acceptors such as DMF and its fumarate metabolites inhibit *C. perfringens* may open the door to development of new oral MS therapies derived from the Michael acceptor functional class. Gambogic acid has been used in Eastern medicine for centuries to treat intestinal ailments and parasites (Wu et al., 2004), and in our hands, it displays an impressive antibacterial potency ($MIC_{95} = 1\,\mu g/ml$).

We searched for Michael acceptors currently approved for human use that possess no known immunosuppressive properties. The naphthoquinone, Menadione (vitamin K3), is a synthetic precursor for vitamin K. It is commonly used as a dietary supplement for livestock and as a cost effective vitamin K replacement therapy in developing countries. Of note, Menadione has recently been shown to inhibit *S. aureus* and *B. anthracis* growth, and to suppress *S. aureus* secretion of toxic shock syndrome toxin 1 (TSST-1; Schlievert et al., 2013). Similarly, we find that Menadione inhibits *C. perfringens* growth, but related compounds with long aliphatic side chains, vitamin K1, vitamin K2, and ubiquinone do not (**Supplemental Figure 2A**). While Menadione's MIC_{95}-value was found to be 64 μg/ml (**Supplemental Figure 2B**), the inactivity of the Menadione related compounds, all of which are electron carriers in the electron transport chain, might be due to the fact that they are sequestered in the cell membrane by their aliphatic side chains. Membrane sequestration may protect cytosolic nucleophiles from undergoing Michael addition and subsequent depletion. Additionally, unlike Menadione but similar to Teriflunomide, these molecules possess a third σ bond at the β carbon position. This may prevent nucleophilic attack due to steric hindrance and abolish Michael acceptor activity (Schwöbel et al., 2010).

In light of the serious side effects associated with current oral DMDs, this study may be of immediate clinical importance. Some of these adverse effects are due to immunosuppression of the CNS, as evidenced by increased risk of JC virus infection and progressive multifocal leukoencephalopathy (PML, FDA Drug Safety Communication, 2014; Brooks, 2015). Perhaps new

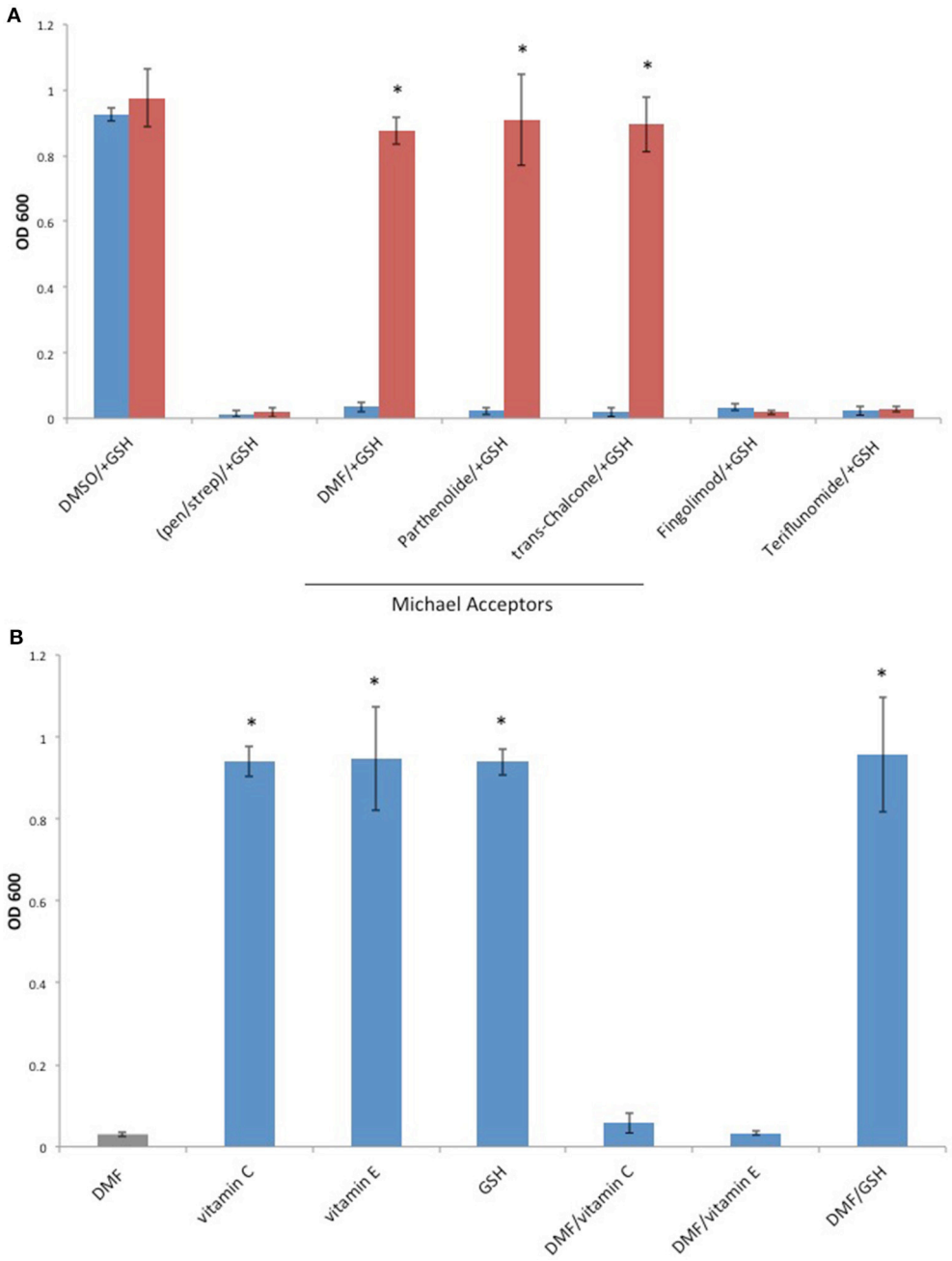

FIGURE 6 | The Michael donor, glutathione (GSH), abolishes Michael acceptor inhibition of *C. perfringens* growth. (A) *C. perfringens* ATCC 13124 was cultured anaerobically at a Michael acceptor (DMF, Parthenolide, and trans-Chalcone), and non-Michael acceptor (Fingolimod and Teriflunomide) concentration of 500 μg/ml, with (red) or without (blue) the addition of an equal quantity of exogenous Michael donor, GSH. Only Michael acceptor mediated growth inhibition could be abolished by the addition of exogenous GSH. The inhibitory activity Fingolimod and Teriflunomide remained unaffected by the presence of GSH, similar to what was observed when bacteria were cultured in the presence of pen/strep and GSH. Data are presented as means from three independent experiments. Error bars represent standard deviations, and asterisks indicate that GSH aided growth recovery is statistically significant when compared to the lack of growth recovery in the absence of GSH; Student's *t*-test, $^*P < 0.001$. **(B)** *C. perfringens* ATCC 13124 was cultured in the presence of DMF, vitamin C, vitamin E, and GSH each at concentration of 250 μg/ml. Only the Michael acceptor, DMF, inhibited bacterial growth. DMF was then paired with the antioxidants, vitamin C, vitamin E, and GSH at concentrations of 250 μg/ml for each compound. The Michael donor antioxidant, GSH, abolished DMF inhibition. However, the non-Michael donor antioxidants, vitamin C and vitamin E, were unable to abolish DMF's inhibitory effect on *C. perfringens* growth. Data are presented as means from three independent experiments. Error bars represent standard deviations, and asterisks indicate that results are statistically significant compared with the DMF control (gray); Student's *t*-test, $^*P < 0.001$.

TABLE 2 | Minimal Inhibitor Concentrations for all inhibitory compounds used in the study.

Compound	MIC_{95} (μg/ml)
Gambogic Acid	1
Fingolimod	4
D-sphingosine	4
Curcumin	64
Parthenolide	64
Menadione (vitamin K3)	64
Teriflunomide	128
Dimethyl fumarate (DMF)	128
Trans-Chalcone	256
Monomethyl fumarate (MMF)	512
Fumarate	512

antibacterial compounds based on these early oral DMDs, but lacking their immunosuppressive properties, may be of use in treating MS. For example, Fingolimod/D-sphingosine related compounds lacking hydroxyl head groups will not undergo phosphorylation and will not target lymphocyte S1PR1. Such compounds would not be immunosuppressive and may reduce the risk of JC virus infection and the development of PML. Along these lines, we have tabulated the MIC_{95}-values for each inhibitory compound used in this study (**Table 2**).

AUTHOR CONTRIBUTIONS

KR conceived the study. KR, VF, and TV designed the study. KR, VF, and TV performed the literature search. KR collected the data and wrote the paper. All authors analyzed the data.

FUNDING

This work was generously supported by the Rockefeller University's Robertson Therapeutic Development Fund (RTDF), the Center for Disorders of the Digestive System (CDDS), and the Weill Cornell Tisch Family Research Fund.

ACKNOWLEDGMENTS

We wish to thank Mr. Nick Lewis of Downing LLP for his valuable insights.

SUPPLEMENTARY MATERIAL

The Supplementary Material for this article can be found online at: http://journal.frontiersin.org/article/10.3389/fcimb.2017.00011/full#supplementary-material

Supplemental Figure 1 | Fingolimod is bactericidal, while DMF and Teriflunomide are bacteriostatic. *C. perfringens* ATCC 13124 was anaerobically cultured to stationary phase and exposed to Fingolimod (500 μg/ml), DMF (500 μg/ml), Teriflunomide (500 μg/ml), pen/strep (100 U/ml) or DMSO vehicle control for 4 h under anaerobic conditions. Treated cultures were diluted 1000 fold in fresh, pre-reduced Mueller Hinton broth and cultured anaerobically. Fingolimod inhibited *C. perfringens* growth in a bactericidal fashion, similar to what was observed with the known bactericidal antibiotic mixture pen/strep, as post-treatment dilution and repeat culture failed to restore bacterial growth. Conversely, DMF and Teriflunomide were shown to be bacteriostatic, as post-treatment dilution and culture successfully restored bacterial growth. Data are presented as means from three independent experiments. Error bars represent standard deviations, and asterisks indicate that results are statistically significant compared with the DMSO vehicle control (gray); Student's *t*-test, $^*P < 0.0001$.

Supplemental Figure 2 | Synthetic vitamin K3, Menadione, inhibits *C. perfringens* growth. (A) *C. perfringens* ATCC 13124 was anaerobically cultured in the presence of vitamin K homologs, vitamins K1, K2, K3, and ubiquinone. Only the synthetic vitamin K3 (Menadione) inhibited bacterial growth, similar to what was observed when bacteria were cultured in the presence known antibiotic penicillin/streptomycin (pen/strep, 100 U/ml). Conversely, bacteria derived vitamin K2 enhanced *C. perfringens* growth, while plant derived vitamin K1 and mammalian ubiquinone yielded OD_{600}-values similar to that of the DMSO vehicle control. Data are presented as means from three independent experiments. Error bars represent standard deviations, and asterisks indicate that results are statistically significant compared with the DMSO vehicle control (gray); Student's *t*-test, $^*P < 0.001$. **(B)** Serial dilutions of Menadione were performed and *C. perfringens* ATCC 13124 was cultured at each dilution. OD_{600}-values for each dilution were divided by that of the corresponding DMSO vehicle control dilution. MIC-values were plotted yielding an MIC_{95}-value of 64 μg/ml.

REFERENCES

Barnett, M. H., and Prineas, J. W. (2004). Relapsing and remitting multiple sclerosis: pathology of the newly forming lesion. *Ann. Neurol.* 55, 458–468. doi: 10.1002/ana.20016

Bar-Or, A., Pachner, A., Menguy-Vacheron, F., Kaplan, J., and Wiendl, H. (2014). Teriflunomide and its mechanism of action in multiple sclerosis. *Drugs* 74, 659–674. doi: 10.1007/s40265-014-0212-x

Bhargava, P., and Mowry, E. M. (2014). Gut microbiome and multiple sclerosis. *Curr. Neurol. Neurosci. Rep.* 14:492. doi: 10.1007/s11910-014-0492-2

Brennan, M. S., Matos, M. F., Li, B., Hronowski, X., Gao, B., Juhasz, P., et al. (2015). Dimethyl fumarate and monoethyl fumarate exhibit differential effects on KEAP1, NRF2 activation, and glutathione depletion *in vitro*. *PLoS ONE* 10:e0120254. doi: 10.1371/journal.pone.0120254

Brooks, M. (2015). Third case of PML with fingolimod (Gilenya) in MS. *Medscape.* Available online at: http://www.medscape.com/viewarticle/849677

Carman, R. J., Sayeed, S., Li, J., Genheimer, C. W., Hiltonsmith, M. F., Wilkins, T. D., et al. (2008). *Clostridium perfringens* toxin genotypes in the feces of healthy North Americans. *Anaerobe* 14, 102–108. doi: 10.1016/j.anaerobe.2008.01.003

Collins, S. M., Surette, M., and Bercik, P. (2012). The interplay between the intestinal microbiota and the brain. *Nat. Rev. Microbiol.* 10, 735–742. doi: 10.1038/nrmicro2876

Conway, D., and Cohen, J. A. (2010). Combination therapy in multiple sclerosis. *Lancet Neurol.* 9, 299–308. doi: 10.1016/S1474-4422(10)70007-7

Dinkova-Kostova, A. T., Massiah, M. A., Bozak, R. E., Hicks, R. J., and Talalay, P. (2001). Potency of Michael reaction acceptors as inducers of enzymes that protect against carcinogenesis depends on their reactivity with sulfhydryl groups. *Proc. Natl. Acad. Sci. U.S.A.* 98, 3404–3409. doi: 10.1073/pnas.051632198

Dorca-Arévalo, J., Soler-Jover, A., Gibert, M., Popoff, M. R., Martín-Satué, M., and Blasi, J. (2008). Binding of epsilon-toxin from *Clostridium perfringens* in the nervous system. *Vet. Microbiol.* 131, 14–25. doi: 10.1016/j.vetmic.2008.02.015

Dymicky, M., Bencivengo, M., Buchanan, R. L., and Smith, J. L. (1987). Inhibition of *Clostridium botulinum* 62A by fumarates and maleates and a relationship of activity to Inhibition of *Clostridium botulinum* 62A by fumarates and maleates and relationship of activity to some physicochemical constants. *Appl. Environ. Microbiol.* 53, 110–113.

FDA Drug Safety Communication (2014). *FDA Warns about Case of Rare Brain Infection PML with MS Drug TECFIDERA (Dimethyl Fumarate).* Available online at: http://www.fda.gov/Drugs/DrugSafety/ucm424625.htm, Retrieved 2 December 2014.

Fischer, C. L., Drake, D. R., Dawson, D. V., Blanchette, D. R., Brogden, K. A., and Wertz, P. W. (2012). Antibacterial activity of sphingoid bases and fatty acids against Gram-positive and Gram-negative bacteria. *Antimicrob Agents Chemother.* 56, 1157–1161. doi: 10.1128/AAC.05151-11

Frohman, E. M., Racke, M. K., and Raine, C. S. (2006). Multiple sclerosis–the plaque and its pathogenesis. *N. Engl. J. Med.* 354, 942–955. doi: 10.1056/NEJMra052130

Fuchs, A. R., and Bonde, G. J. (1957). The availability of sulphur for *Clostridium perfringens* and an examination of hydrogen sulphide production. *J. Gen. Microbiol.* 16, 330–340. doi: 10.1099/00221287-16-2-330

Gold, R., Arnold, D. L., Bar-Or, A., Hutchinson, M., Kappos, L., Havrdova, E., et al. (2016). Long-term effects of delayed-release dimethyl fumarate in multiple sclerosis: interim analysis of ENDORSE, a randomized extension study. *Mult. Scler.* doi: 10.1177/1352458516649037. [Epub ahead of print].

Johnson, G. B. (1994). *Holt Biology: Visualizing Life.* Orlando, FL: Holt, Rinehart and Winston, 769.

Linden, J. R., Ma, Y., Zhao, B., Harris, J. M., Rumah, K. R., Schaeren-Wiemers, N., et al. (2015). *Clostridium perfringens* epsilon toxin causes selective death of mature oligodendrocytes and central nervous system demyelination. *MBio* 6:e02513. doi: 10.1128/mBio.02513-14

Munier-Lehmann, H., Vidalain, P. O., Tangy, F., and Janin, Y. L. (2013). On dihydroorotate dehydrogenases and their inhibitors and uses. *J. Med. Chem.* 56, 3148–3167. doi: 10.1021/jm301848w

Pavadai, E., El Mazouni, F., Wittlin, S., de Kock, C., Phillips, M. A., and Chibale, K. (2016). Identification of new human malaria parasite *Plasmodium falciparum* dihydroorotate dehydrogenase inhibitors by pharmacophore and structure-based virtual screening. *J. Chem. Inf. Model.* 56, 548–562. doi: 10.1021/acs.jcim.5b00680

Pewzner-Jung, Y., Tavakoli Tabazavareh, S., Grassmé, H., Becker, K. A., Japtok, L., Steinmann, J., et al. (2014). Sphingoid long chain bases prevent lung infection by *Pseudomonas aeruginosa*. *EMBO Mol. Med.* 6, 1205–1214. doi: 10.15252/emmm.201404075

Phillips, J. T., and Fox, R. J. (2013). BG-12 in multiple sclerosis. *Semin. Neurol.* 33, 56–65. doi: 10.1055/s-0033-1343796

Popoff, M. R. (2011). Epsilon toxin: a fascinating pore-forming toxin. *FEBS J.* 278, 4602–4615. doi: 10.1111/j.1742-4658.2011.08145.x

Rumah, K. R., Linden, J., Fischetti, V. A., and Vartanian, T. (2013). Isolation of *Clostridium perfringens* type B in an individual at first clinical presentation of multiple sclerosis provides clues for environmental triggers of the disease. *PLoS ONE* 8:e76359. doi: 10.1371/journal.pone.0076359

Rumah, K. R., Ma, Y., Linden, J. R., Oo, M. L., Anrather, J., Schaeren-Wiemers, N., et al. (2015). The myelin and lymphocyte protein MAL is required for binding and activity of *Clostridium perfringens* ε-toxin. *PLoS Pathog.* 11:e1004896. doi: 10.1371/journal.ppat.1004896

Schlievert, P. M., Merriman, J. A., Salgado-Pabón, W., Mueller, E. A., Spaulding, A. R., Vu, B. G., et al. (2013). Menaquinone analogs inhibit growth of bacterial pathogens. *Antimicrob Agents Chemother.* 57, 5432–5437. doi: 10.1128/AAC.01279-13

Schwöbel, J. A., Wondrousch, D., Koleva, Y. K., Madden, J. C., Cronin, M. T., and Schüürmann, G. (2010). Prediction of michael-type acceptor reactivity toward glutathione. *Chem. Res. Toxicol.* 23, 1576–1585. doi: 10.1021/tx100172x,

Strader, C. R., Pearce, C. J., and Oberlies, N. H. (2011). Fingolimod (FTY720): a recently approved multiple sclerosis drug based on a fungal secondary metabolite. *J. Nat. Prod.* 74, 900–907. doi: 10.1021/np2000528

Wioland, L., Dupont, J. L., Doussau, F., Gaillard, S., Heid, F., Isope, P., et al. (2015). Epsilon toxin from *Clostridium perfringens* acts on oligodendrocytes without forming pores, and causes demyelination. *Cell. Microbiol.* 17, 369–388. doi: 10.1111/cmi.12373

Wu, Z. Q., Guo, Q. L., You, Q. D., Zhao, L., and Gu, H. Y. (2004). Gambogic acid inhibits proliferation of human lung carcinoma SPC-A1 cells *in vivo* and *in vitro* and represses telomerase activity and telomerase reverse transcriptase mRNA expression in the cells. *Biol. Pharm. Bull.* 27, 1769–1774. doi: 10.1248/bpb.27.1769

Conflict of Interest Statement: All authors are named as inventors on a pending patent entitled, "Methods to protect against and treat multiple sclerosis," (Publication number CA2899961 A1), which identifies *Clostridium perfringens* epsilon toxin as candidate trigger for multiple sclerosis.

Copyright © 2017 Rumah, Vartanian and Fischetti. This is an open-access article distributed under the terms of the Creative Commons Attribution License (CC BY). The use, distribution or reproduction in other forums is permitted, provided the original author(s) or licensor are credited and that the original publication in this journal is cited, in accordance with accepted academic practice. No use, distribution or reproduction is permitted which does not comply with these terms.

frontiers in Cellular and Infection Microbiology

ORIGINAL RESEARCH
published: 09 December 2016
doi: 10.3389/fcimb.2016.00179

Tissue-Associated Bacterial Alterations in Rectal Carcinoma Patients Revealed by 16S rRNA Community Profiling

*Andrew M. Thomas[1,2,3], Eliane C. Jesus[1,4], Ademar Lopes[4], Samuel Aguiar Jr.[4], Maria D. Begnami[5], Rafael M. Rocha[6], Paola Avelar Carpinetti[7], Anamaria A. Camargo[7], Christian Hoffmann[8], Helano C. Freitas[1,9], Israel T. Silva[10], Diana N. Nunes[1], João C. Setubal[2,11] and Emmanuel Dias-Neto[1,12]**

[1] Medical Genomics Laboratory, CIPE/A.C. Camargo Cancer Center, São Paulo, Brazil, [2] Departamento de Bioquímica, Instituto de Química, Universidade de São Paulo, São Paulo, Brazil, [3] Curso de Pós-Graduação em Bioinformática, Universidade de São Paulo, São Paulo, Brazil, [4] Department of Pelvic Surgery, A.C. Camargo Cancer Center, São Paulo, Brazil, [5] Department of Pathology, A.C. Camargo Cancer Center, São Paulo, Brazil, [6] Laboratory of Molecular Gynecology, Department of Gynecology, Medicine College, Federal University of São Paulo, São Paulo, Brazil, [7] Centro de Oncologia Molecular, Hospital Sirio-Libanês, São Paulo, Brazil, [8] Departamento de Alimentos e Nutrição Experimental, Faculdade de Ciências Farmacêuticas, Food Research Center (FoRC), Universidade de São Paulo, São Paulo, Brazil, [9] Department of Clinical Oncology, A.C. Camargo Cancer Center, São Paulo, Brazil, [10] Laboratory of Computational Biology and Bioinformatics, A.C. Camargo Cancer Center, São Paulo, Brazil, [11] Biocomplexity Institute, Virginia Tech, Blacksburg, VA, USA, [12] Laboratory of Neurosciences (LIM-27) Alzira Denise Hertzog Silva, Institute of Psychiatry, Faculdade de Medicina, Universidade de São Paulo, São Paulo, Brazil

OPEN ACCESS

Edited by:
Venkatakrishna Rao Jala, University of Louisville, USA

Reviewed by:
David Albert Scott, University of Louisville, USA
Daniel Raimunda, CONICET–UNC, Argentina

***Correspondence:**
Emmanuel Dias-Neto
emmanuel@cipe.accamargo.org.br

Received: *26 September 2016*
Accepted: *24 November 2016*
Published: *09 December 2016*

Citation:
Thomas AM, Jesus EC, Lopes A, Aguiar S Jr., Begnami MD, Rocha RM, Carpinetti PA, Camargo AA, Hoffmann C, Freitas HC, Silva IT, Nunes DN, Setubal JC and Dias-Neto E (2016) Tissue-Associated Bacterial Alterations in Rectal Carcinoma Patients Revealed by 16S rRNA Community Profiling. Front. Cell. Infect. Microbiol. 6:179. doi: 10.3389/fcimb.2016.00179

Sporadic and inflammatory forms of colorectal cancer (CRC) account for more than 80% of cases. Recent publications have shown mechanistic evidence for the involvement of gut bacteria in the development of both CRC-forms. Whereas, colon and rectal cancer have been routinely studied together as CRC, increasing evidence show these to be distinct diseases. Also, the common use of fecal samples to study microbial communities may reflect disease state but possibly not the tumor microenvironment. We performed this study to evaluate differences in bacterial communities found in tissue samples of 18 rectal-cancer subjects when compared to 18 non-cancer controls. Samples were collected during exploratory colonoscopy (non-cancer group) or during surgery for tumor excision (rectal-cancer group). High throughput 16S rRNA amplicon sequencing of the V4–V5 region was conducted on the Ion PGM platform, reads were filtered using *Qiime* and clustered using *UPARSE*. We observed significant increases in species richness and diversity in rectal cancer samples, evidenced by the total number of OTUs and the Shannon and Simpson indexes. Enterotyping analysis divided our cohort into two groups, with the majority of rectal cancer samples clustering into one enterotype, characterized by a greater abundance of *Bacteroides* and *Dorea*. At the phylum level, rectal-cancer samples had increased abundance of candidate phylum *OD1* (also known as *Parcubacteria*) whilst non-cancer samples had increased abundance of *Planctomycetes*. At the genera level, rectal-cancer samples had higher abundances of *Bacteroides*, *Phascolarctobacterium*, *Parabacteroides*, *Desulfovibrio,* and *Odoribacter* whereas non-cancer samples had higher abundances of *Pseudomonas*, *Escherichia*, *Acinetobacter*, *Lactobacillus,* and *Bacillus*. Two *Bacteroides fragilis* OTUs were more

abundant among rectal-cancer patients seen through 16S rRNA amplicon sequencing, whose presence was confirmed by immunohistochemistry and enrichment verified by digital droplet PCR. Our findings point to increased bacterial richness and diversity in rectal cancer, along with several differences in microbial community composition. Our work is the first to present evidence for a possible role of bacteria such as *B. fragilis* and the phylum *Parcubacteria* in rectal cancer, emphasizing the need to study tissue-associated bacteria and specific regions of the gastrointestinal tract in order to better understand the possible links between the microbiota and rectal cancer.

Keywords: mucosa-associated microbiota, rectal cancer, 16S rRNA gene sequencing, *Bacteroides fragilis*, Bacterial diversity and community composition

INTRODUCTION

The gut microbiota is a vast and diverse ensemble of bacteria and other microorganisms that work together to help digestion, produce vitamins, fatty acids, amino acids and other bioactive compounds, and participate in the regulation of our immune, metabolic, and neurological systems (Shapiro et al., 2014; Boulangé et al., 2016). The understanding of our microbiota, together with the determination of its composition when contrasting healthy vs. diseased states allows the identification of microorganism disturbances that are possibly related to disease development and, therefore, offers a new approach for diagnosis as well as preventive and therapeutic interventions.

Specific dietary components, tobacco and alcohol consumption, which have been linked to the development of a number of pathological states (such as obesity, allergy, diabetes, Crohn's disease, irritable colon syndrome, and cancer) are known to drive microbiome alterations and lead to dysbiosis (Turnbaugh et al., 2009; Leclercq et al., 2014; Allais et al., 2016). The direct action of these elements or of the dysbiosis they cause, appears to be instrumental in the pathogenesis of many diseases and, under certain circumstances, it is possible that dysbiosis may, *per se,* have a direct link with disease development (Duboc et al., 2013). In oncology, studies have been conducted in different neoplastic conditions, identifying roles for specific bacteria in carcinogenesis (Kostic et al., 2012; Riley et al., 2013; Rubinstein et al., 2013), immune evasion (Gur et al., 2015), modulation of the tumor microenvironment (Kostic et al., 2013), and interference with anti-cancer immune responses and immune-surveillance that facilitate chemotherapy activity (Zitvogel et al., 2013; Galluzzi et al., 2015; Vétizou et al., 2015). As a consequence, the emerging concept that cancer needs to be studied considering the complex tumor microenvironment, which includes components such as tumor cells, the surrounding microenviroment and the microbiome, may aid in the development and improvement of cancer treatment, including immunotherapy (Pitt et al., 2016).

Tumors of the lower digestive tract, which include colon and rectal cancer, are among the most prevalent neoplasias worldwide, as well as one of the most fatal. Colorectal cancer (CRC) is the third most commonly diagnosed cancer with 1.4 million people diagnosed annually (Torre et al., 2015). The World Health Organization estimates an increase of 77% in the number of newly diagnosed CRC cases and an increase of 80% in deaths from CRC by 2030 (Binefa et al., 2014). Whereas, colon and rectal cancers have been routinely studied together as CRC, evidences indicate these to be distinct nosological entities. Differences in embryological origin, anatomy, treatment, metastatic potential, and outcome between colon cancer and rectal cancer have led to discussions as to whether neoplastic lesions of these two anatomical sites should be considered as different diseases, with further dichotomization of colon cancers into distal and proximal (Tamas et al., 2015).

The mechanisms involved in sporadic CRC predisposition or development are still poorly understood and the long list of cancer risk factors is continuously expanding and includes age, tobacco, and alcohol consumption, lack of physical activity, increased body weight and, most importantly, diet (Moore and Moore, 1995; Bingham, 2000). Of particular importance is the fact that all these risk factors can directly or indirectly modify the microbiota, making the precise definition of their roles a very complex task. Fecal microbiota studies have contributed greatly in our understanding of the general gut microbiota composition and its dysbiosis in different scenarios (Wu et al., 2013; Sabino et al., 2016). However, possibly due to practical issues related to obtaining the required biopsy samples—from patients and controls—there are still very few available studies focused on the analysis of microbial community compositions of more specific regions of the lower digestive tract, such as the proximal and distal colon, and the rectal tissue. Furthermore, few studies contemplate the fact that fecal- and tissue-associated microbiota are significantly different (Durbán et al., 2011; Hong et al., 2011; Mira-Pascual et al., 2015; Flemer et al., 2016). This fact is particularly relevant for CRC as the intimate crosstalk between the host's epithelium layer and the gut microbial community is a key factor for cell proliferation and development, as well as the regulation of inflammation, a major driver of rectal carcinogenesis (Arthur et al., 2014). Such differences lead to a lack of representativeness with respect to the bacterial biofilm of the rectal mucosa (Durbán et al., 2011; Gevers et al., 2014) and may reflect the disease state but possibly not the tumor microenvironment, which is of great importance to study possible microbiota:disease links.

Here we have addressed such shortcomings by studying the tissue-associated microbiota of 36 subjects, 18 with and 18 without rectal adenocarcinoma. The use of 16S rDNA deep

sequencing allowed us to compare non-cancer x cancer mucosa, pointing to specific OTUs and bacterial genera potentially associated with rectal adenocarcinoma.

MATERIALS AND METHODS

Cohort

A total of 36 subjects were included after approval by AC Camargo Cancer Center's review board (ACCCC - 1614/11, January 30th, 2012). Tissue biopsies were collected from subjects belonging to one of the following groups:

Non-cancer Subjects

(Non-Cancer, NC, $n = 18$): All subjects had medical indication of exploratory colonoscopy due to complaints, such as bleeding, abdominal pain, constipation, and chronic diarrhea. No subjects had personal or familial history of colorectal cancer or colitis (either ulcerative, Crohn's, radiation or infectious colitis, chronic inflammatory illnesses), previous colonic or small bowel resection, nor previous colon adenomas or familial polyposis syndrome. Only individuals with complete colonoscopies that allowed the full visualization of the entire colon and showed no significant clinical alterations were included.

Colonoscopy and Biopsy Procedures for the NC Subjects

All patients received standard instructions for preparation for colonoscopy that included consumption of 500 ml of mannitol for bowel cleansing, luftal, and bisacodyl. Eligible subjects gave written informed consent to provide colorectal biopsies, had their anthropometric measures taken and answered questions about diet, consumption of alcohol, and tobacco. Colonoscopy was performed using a Pentax videoscope model FC38LX. During biopsy procurement, the rectum was inflated with air and care was taken not to use any suction during advancement of the scope to 7–8 cm from the anal verge. Sterile biopsy forceps were not taken out of the channel of the scope until an area that was completely clear of stool was seen with clear pink mucosa. Biopsies were taken with 2.2 mm sterile standard forceps.

Patients Diagnosed with Rectal Adenocarcinomas

(Rectal-Cancer, RC, $n = 18$): Tumor specimens, located in the higher ($N = 15$), mid ($N = 2$), and lower rectum ($N = 1$), were obtained from surgeries to remove the tumor mass. All subjects belonging to this group were recruited at AC Camargo Cancer Center's Pelvic Surgery Department, in São Paulo, Brazil. We included patients that were diagnosed with rectal adenocarcinoma (tumors of stage pT1 or pT2 low- or mid-straight, pT1 or pT2 or pT3 high-straight), that had not undergone any neoadjuvant therapy and had their tumors surgically resected at the Pelvic Surgery Department, AC Camargo Cancer Center, with diagnosis confirmed by the Pathology Department of the same institution. After the histopathologic confirmation of rectal adenocarcinoma diagnosis, surplus samples were macrodissected by an experienced pathologist and used for DNA extraction and bacterial community profiling. *Exclusion criteria* were: Patients subjected to neoadjuvant therapy prior to tissue collection; patients reporting inflammatory bowel diseases or with hereditary cancer syndromes. We also excluded all subjects (cases and controls) who reported the use of antibiotics for at least 4 weeks prior to sample-collection.

DNA Extraction

DNA extraction started after incubating the samples for 18 h in 600 µl of a lysis buffer (Qiagen) and 15 µl of proteinase K (20 µg/µl) at 55°C. After this period, DNA samples were extracted using a standard phenol chloroform protocol, followed by ethanol precipitation, quantification using a spectrophotometer (Nanodrop—Thermo Scientific), and visualized on 2% agarose gels to inspect DNA integrity.

PCR Amplification and Sequencing of the V4–V5 Region of 16S rRNA Gene

Oligonucleotide Primer Selection and Coverage Analysis

The V4–V5 region was amplified using a primer set designed to generate amplicons compatible with the chemistry available for the Ion Torrent PGM platform, that allowed ∼400 nt of high quality sequences (Ion PGM Sequencing 400 Kit). Coverage of the primer set was evaluated using the Ribosomal Database Project's (RDP—Release 11.2) ProbeMatch (Cole et al., 2014) and the ARB Silva's (Release 115) TestPrime (Klindworth et al., 2013). The forward primer (5′-AYTGGGYDTAAAGNG-3′) and reverse primer (5′-CCGTCAATTCNTTTRAGTTT-3′) corresponded to positions 562 and 906, respectively, of the *Escherichia coli* 16S rRNA gene.

PCR Amplification and Amplicon Sequencing

Three 50 µl amplification replicate reactions were performed per sample, each containing: 2.5 µM of each primer; 25 µl of Kapa Hotstart High Fidelity Master Mix (Kapa Technologies) and 25 ng of genomic DNA (gDNA). Thermocycling conditions were: 95°C, 3 min; 98°C, 15 s, and 40°C, 30 s for 35 cycles; followed by a last extension step at 72°C for 5 min. Amplicons of the three reactions from each subject were pooled and purified using a MinElute PCR Purification Kit (Qiagen). The purified products were run on 1.5% agarose gels and gel bands within the expected amplicon range were excised using sterile and disposable scalpels and purified using the Qiaquick gel extraction kit (Qiagen) to remove artifacts, primer-dimers and non-specific bands. Amplicons were end-repaired and Ion Torrent adaptors with barcodes were ligated. Equimolar amounts of amplicons from each sample were pooled, using the Ion Torrent qPCR quantitation kit (Thermo Scientific, Carlsbad, USA), and used for emulsion PCR. All samples were sequenced on the Ion torrent PGM platform (Thermo Scientific, Carlsbad, USA) using two 318 v2 chips. Samples from both groups were processed simultaneously, to avoid possible batch effects.

Sequence Analysis

Sequence Filtering

Sequences processed by the latest version of the Ion Torrent server (v3.6.2) were used as input into the *Qiime* (*Quantitative insights into microbial ecology*) software package (Version 1.6.0) (Caporaso et al., 2010a). We first removed sequences with an average quality score <20 using a 50 nt sliding window. Then, we identified barcodes used for subject-assignment, allowing a maximum of 2 mismatches, and discarded sequences with no barcodes, and <200 nt or >500 nt after barcode removal. PCR primers identified at the start or at the end of the reads, allowing a maximum of 4 nt mismatches, were trimmed and sequences with no identifiable primers were discarded. After primer trimming we removed all sequences below 200 nt and the remaining sequences were used as input for downstream analysis.

Sequence Clustering and OTU Filtering

Filtered sequences were clustered with 97% identity using UPARSE (implemented in USEARCH v7) (Edgar, 2013) and the seed sequence of each cluster was picked as a representative. Chimeric sequences (and clusters) were identified using UCHIME (Edgar et al., 2011) and the Broad Institute's chimera slayer database (version microbiomeutil-r20110519) and excluded from further analysis. The RDP classifier (Wang et al., 2007), as implemented within the *Qiime* interface (default parameters), was used to assign taxonomic ranks using a minimum confidence value of 80% and, subsequently, to each operational taxonomic unit (OTU). Unless otherwise stated, OTUs that occurred in less than 25% of all samples and with less than 3 reads were not considered.

Alpha and Beta Diversity Analysis

We rarefied the OTU table to 17,414 sequences per sample in order to calculate species diversity, using the Shannon-Weaver index (Shannon, 1948) and the Simpson index (Simpson, 1949), and richness (by using the observed species) implemented in the R Phyloseq package (McMurdie and Holmes, 2013).

For beta diversity analysis, OTU-representative sequences were aligned using PyNAST (Caporaso et al., 2010b) against the aligned green genes core set (DeSantis et al., 2006) with *Qiime* default parameters, and the alignments were lanemask-filtered (Lane, 1991). A phylogenetic tree was built using FastTree (Price et al., 2009), weighted and unweighted UniFrac (Lozupone and Knight, 2005) distances were calculated and a distance matrix was generated. Using the R phyloseq package, distance matrices were used to calculate coordinates for principal coordinate analysis (PCoA).

Enterotypes

Community types of each sample were analyzed by the Dirichlet multinomial mixture model-based method (Holmes et al., 2012) using rarefied genera level counts of 16S rRNA sequencing reads. Partioning around medoids (PAM) enterotyping was performed in R using genera level relative abundances and the "cluster" package (Maechler et al., 2015). We applied 4 distance metrics: Weighted UniFrac, Unweighted UniFrac, root Jensen-Shannon divergence, and Bray-Curtis and assessed the quality of the clusters using prediction strength (Tibshirani and Walther, 2005), silhouette index (Rousseeuw, 1987), and the Caliński-Harabasz statistic (Calinski and Harabasz, 1974) using the "fpc" R package (Hennig, 2015).

Differential Abundance Analysis

To investigate differences in OTU, phyla and genera abundances between both groups, raw counts were normalized then log transformed using the normalization method below, as performed by a previous study (Sanapareddy et al., 2012):

$$Normalized\ count = \log_{10}\left(\left(\frac{raw\ count}{number\ of\ sequences\ in\ that\ sample}\right) \times\ average\ number\ of\ sequences\ per\ sample + 1\right)$$

We also evaluated high-level phenotypical differences in microbial composition between both groups. Quality control passed sequences were closed-reference picked at 97% identity using UCLUST_Ref (Edgar, 2010) and the green genes core set (Version 13.5). The resulting OTU table was rarefied to 13,944 sequences and submitted to BugBase (http://github.com/danknights/bugbase) in order to calculate differences between both groups in terms of microbial phenotypes.

Data Validation

Digital Droplet PCR of Bacteroides Fragilis 16S rRNA

We detected and quantified the absolute number of 16S rRNA *B. fragilis* copies in our samples using the *QX200™ Droplet Digital™ PCR System* (Bio-Rad). The primers used to amplify the *B. fragilis* 16S rRNA gene were: BF-fwd 5′-TCRGGAAGAAAGCTTGCT-3′ and BF-rev 5′-CATCCTTTACCGGAATCCT-3′(Tong et al., 2011) and to ensure further specificity, a labeled probe BF-p 5′(FAM)-ACACGTATCCAACCTGCCCTTTACTCG-3′ (BHQ1) (Tong et al., 2011) was included in the reaction. We used a commercial RNAseP *Copy Number Reference Assay* (Thermo-Fisher) to detect and quantify human DNA. Microdroplets (≈20.000/reaction) were generated on the Bio-Rad *QX-100* following the manufacturer's instructions. RNAse P and *B. fragilis* ddPCR were performed in 96 well-plates, in a final volume of 20 μl, containing: 15 ng of total DNA, 10 ul of ddPCR supermix for probes (Bio-Rad), 8 pmol of each PCR BF-primer and 2 pmol of the BF-probe, or 1 μl of RNAse P assay. PCR conditions were: 50°C- 2 min; 95°C- 10 min; 95°C- 15 s and 60°C- 1 min for 40 cycles. After cycling, the 96-well plate was immediately transferred on a *QX200 Droplet Reader* (Bio-Rad), where flow cytometric analysis determined the fraction of PCR-positive droplets vs. the number of PCR-negative droplets in the original sample. Data acquisition and quantification was carried out using *QuantaSoft Software* (Bio-Rad). To ensure the accuracy of the results, a minimum of 10,000 acceptable droplets per reaction were required for quantification using the *QuantaSoft software*. Samples yielding a minimum of 3 positive droplets from 10–15,000 droplets analyzed were scored as positive.

Immunohistochemistry

Immunohistochemistry was performed in an automated Benchmark platform (Ventana Medical Systems, USA) for Anti-*B. fragilis* LPS antibody (mouse monoclonal—Abcam 1265/30) in whole slide tissues. Alkaline phosphatase conjugated to secondary polymeric system was used for IHC visualization. The selection of positive and negative samples was guided by the high-throughput sequencing (HTS) data and used to confirm the presence of *B. fragilis* in the sample set. The primary antibody was omitted to evaluate background staining.

Statistical Analysis

Wilcoxon tests were used to compare mean differences between tumor and biopsy samples for phyla, genera and OTU log-abundances. Considering t = total number of taxa tested, p = raw p-value and R = sorted rank of the taxon, P-values were corrected for multiple testing (Sanapareddy et al., 2012) using:

$$Adjusted\ p\ value\ =\ \frac{t\ \times\ p}{R}$$

Fold changes for each genera/OTU were calculated using:

$$Log2\,FC\ =\ \log_2(RC\ average\ +\ 1)\ -\ \log_2(NC\ average\ +\ 1)$$

Chi-Square tests were performed on subject's categorical data such as gender, alcohol and tobacco use and vital status. Student t-tests were performed to compare differences in the means between both groups for age, height, weight, BMI, and alpha diversity. We used ANOSIM and ADONIS (Oksanen et al., 2016) to compare differences in beta-diversity between groups using 3 distance metrics weighted UniFrac, unweighted UniFrac and Bray-Curtis for categorical, and numerical variables, respectively. Linear models were built using normalized counts at the genera and OTU level to investigate associations with clinical-pathological characteristics of rectal-cancer samples, such as lymph node and perineural neoplastic invasion status. Unless otherwise stated, values were reported as mean ± *SD* (standard deviation) and P-values <0.05 were considered statistically significant. All calculations were performed within the R statistical computing environment (R Foundation, 2011) unless otherwise stated.

RESULTS

Subjects and Tissue Sample Characteristics

We analyzed tissue-associated bacteria from mucosal biopsies of 18 non-cancer controls and 18 rectal adenocarcinoma tumors using 16S rRNA high throughput amplicon sequencing. We found no significant differences between rectal-cancer and non-cancer subjects regarding age and gender distribution, tobacco, and alcohol use and other risk factors (**Table 1**). All samples consisted of rectal-biopsies. The biopsies of individuals with no tumor lesions derived from the mid rectum and were distributed along the ∼12 cm-long human rectum, with most samples deriving from the higher-mid rectum (94%).

TABLE 1 | Subject and sample data.

Demographic	Non-cancer (n = 18)	Rectal-cancer (n = 18)	P-value
Age	55.2 ± 15.7	59.3 ± 8.8	0.348
GENDER (%)			
Female	9 (50)	8 (44)	1
Male	9 (50)	10 (56)	
Height	1.65 ± 0.08	1.70 ± 0.09	0.1
Weight	73 ± 14.1	73.8 ± 13.5	0.87
BMI	26.6 ± 3.7	25.3 ± 3.6	0.29
ALCOHOL USE (%)			
Yes	8 (44)	5 (28)	0.568
No	10 (56)	12 (67)	
Undetermined	0 (0)	1 (5)	
TOBACCO USE (%)			
Yes	12 (67)	6 (28)	0.129
No	6 (33)	11 (62)	
Undetermined	0 (0)	1 (5)	
Pathological tumor size staging (%)			
pT2	N.A.	5 (28)	N.A.
pT3		13 (72)	
Pathological lymph node metastasis staging (%)			
pN0	N.A.	11 (62)	N.A.
pN1		3 (16)	
pN2		4 (22)	
Distant metastasis staging (%)			
M0	N.A.	18 (100)	N.A.
Invasion (%)			
Perineural	N.A.	4 (22)	N.A.
Angiolymphatic		14 (78)	
Vital status (%)			
Alive	18 (100)	17 (95)	1
Deceased	0 (0)	1 (5)	

N.A., Not applicable.

Primer Coverage

Our analyses indicate that the PCR primers used here (V4–V5 region of the 16S rRNA gene) cover 84.4 and 52.1% of all eubacterial sequences present in the ARB SILVA database and the Ribosomal Database Project, respectively (Supplementary Table 1). Coverage rates were evenly distributed among most bacterial phyla, except for *Verrucomicrobia*, where coverage rates were 21 and 10.9%, dropping below the 75 and 48% averages of taxa present in the SILVA and RDP databases, respectively.

Sequence Analysis

Sequence Generation and Filtering

A total of 12,078,140 sequence reads were generated, with a mean sequence length of 304.5 ± 97.34 nt (standard deviation—std). After quality filtering and primer trimming,

5,593,020 (46.3%) sequences remained, with an average of 155,361 sequences/sample and a mean sequence length of 315 ± 30 nt.

Sequence Clustering and OTU Filtering

When all individuals were considered, a total of 3222 OTUs were obtained. Thirty-one (0.7%) OTUs were identified as chimeras by UCHIME and 209 (4.7%) could not be assigned to a taxonomic rank. After filtering OTUs with less than three sequences and not present in at least 25% of all samples (NC and RC combined), 1492 OTUs remained.

Alpha and Beta Diversity

Species Richness and Diversity

We observed significantly higher species richness and species diversity in rectal cancer samples compared to controls. This was observed for the number of OTUs, the Shannon index and the Simpson Index (P-values = 0.002, <0.001, and <0.001, respectively) (**Figures 1A,B**). When we stratified rectal-cancer samples into smaller (pT2) and larger tumors (pT3), we observed an increase in species richness, with an average of 280 and 366 OTUs, respectively, compared to 236 OTUs in NC; however this effect reached no statistical significance between pT2 and pT3, maybe because of the reduced number of pT2 samples ($N = 5$, compared to $N = 13$ for pT3) (**Figure 1B** and data not shown).

Beta Diversity

Using three distance metrics we observed consistent and statistically significant differences between the sample groups when considering cancer status (Bray-Curtis, Unweighted and Weighted UniFrac; p-value: 0.001; ANOSIM using 999 permutations), but not for any other categorical or numerical variable, which included amplicon library construction, age, gender, BMI, alcohol, and tobacco use (**Figure 1D**; Supplementary Table 2).

Enterotypes

Enterotyping analysis using a Dirichlet multinomial mixture model divided our cohort in two clusters (**Figures 2A–C**). Enterotype I was significantly enriched for rectal-cancer samples, whilst enterotype II was composed mostly of non-cancer samples (p-value: 0.0001, Fisher's exact test). Enterotype I had higher abundances of *Bacteroides, Clostridiales*, *Dorea,* and other genera, whilst enterotype II was characterized by elevated amounts of *Pseudomonas* and *Brevundimonas* (**Figure 2D**). When using the PAM based enterotyping method and criterion adopted by a meta-analysis of human enterotypes (Koren et al., 2013), we found two enterotypes with prediction strength above 0.9 (meaning that 90% of the data points fall within the cluster and 10% are outliers) using the Weighted UniFrac distance (Supplementary Figure 1).

Global Signatures of the Microbial Community

Phyla Log Abundances

We observed a significant difference in the log abundances of 6 out of 12 detected phyla between both groups (Supplementary Figure 2). The most abundant phyla identified were (in decreasing order) *Proteobacteria*, *Firmicutes*, *Bacteroidetes*, *Fusobacteria*, *Actinobacteria,* and *Verrucomicrobia*. In non-cancer samples, we observed higher log abundances of *Actinobacteria*, *Cyanobacteria, Proteobacteria,* and *Planctomycetes,* whose presence was detected in 9/18 NC samples, with an average log abundance of 0.54 and was absent from all RC individuals (p-value < 0.001). In rectal-cancer we found greater log abundances of *Bacteroidetes* and of the much less known candidate phylum *OD1* (also known as *Parcubacteria)*, whose presence was detected in 14/18 RC samples with an average log abundance of 0.71 vs. 1/19 NC samples and an average log abundance of 0.02 (p-value < 0.001).

Genera Log Abundances

At the genus level, 86 out of 260 genera (33%) showed significant differential log abundances between both groups (**Figure 3A** and Supplementary Table 3). The top five genera with differential log abundances between the groups were *Bacteroides*, *Phascolarctobacterium*, *Odoribacter*, *Parabacteroides, Desulfobrio* (more abundant in the cancer group), and *Lactobacillus, Pseudomonas*, *Bacillus, Escherichia*, *Acinetobacter* (more abundant in the non-cancer set) (**Figure 3B**).

OTU Log Abundances

Of the 1492 OTUs identified, 163 (10.9%) were found to have significant differential log abundances between both groups (**Figure 3C**). Three OTUs assigned to the genus *Bacteroides, two* belonging to *B. fragilis* and one to *B. uniformis,* as well as OTUs assigned to *Bilophila* sp. and *Fusobacterium* sp., were significantly more abundant in rectal-cancer samples (**Figure 3D**). In non-cancer samples, OTUs assigned to *Alcaligenes faecalis, Bacillus cereus*, *Lactobacillus delbruecki*, *Prevotella melaninogenica* and *Pseudomonas* ssp had higher log abundances compared to rectal-cancer samples. Four OTUs belonging to the *Bacilli* class were more abundant among non-cancer samples, including *L. delbrueckii* (**Figure 3D**).

When analyzing high-level phenotypical differences, the most striking differences included a higher abundance of anaerobic bacteria and a deficit in biofilm-forming bacteria in rectal-cancer samples (Supplementary Figure 3). In our searches for associations between rectal-cancer samples' clinical data and genera/OTU log abundances using linear regression, we found significant associations between genera/OTUs with regards to the presence of lymph node disease (Supplementary Table 4) and perineural invasion (data not shown). We found a significant increase of *Coprococcus*, *Dorea*, *Roseburia,* and *Mogibacterium* in lymph node positive rectal-cancer (Supplementary Figure 4).

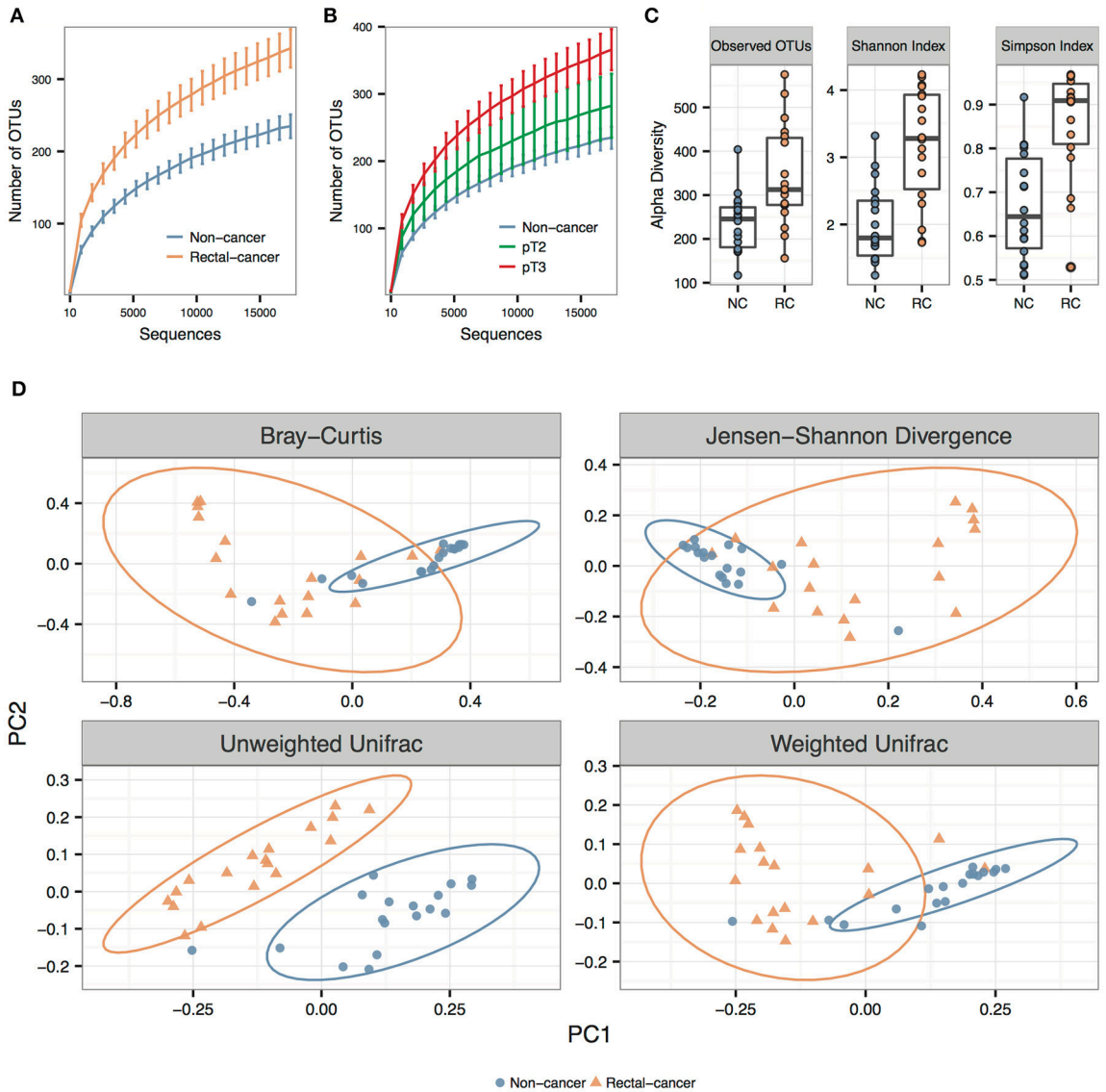

FIGURE 1 | Alpha and beta diversity for non-cancer and rectal-cancer samples. (A) Rarefaction curves showing the average number of observed OTUs for both groups. Error bars represent ± standard error of the mean. Blue: Non-cancer samples; red: Rectal-cancer samples. **(B)** Rarefaction curves showing the average number of observed OTUs for NC samples and for smaller (pT2) and larger rectal tumors (pT3). Error bars represent ± standard error of the mean. **(C)** Boxplots showing alpha diversity in rectal-cancer samples and non-cancer samples using different metrics (Observed OTUs, Shannon index and Simpson index). **(D)** Principal Coordinate Analysis (PCoA) ordination plots for four distance metrics (Bray-Curtis, Jensen-Shannon Divergence, Weighted and Unweighted UniFrac). Ellipses represent the 95% confidence level assuming a multivariate t-distribution.

ddPCR Confirms the Higher Counts of *B. fragilis* in Tumor Samples

As two OTUs classified as *B. fragilis* were among the smallest *p*-values found and with the highest fold change between the groups, we designed a specific ddPCR assay for *B. fragilis* in order to verify the validity of the results using an alternative approach. As can be seen in **Figures 4A,B**, we observed the expected correlation ($R^2 = 0.78$) between both methods and confirmed the higher ratio of *B. fragilis*/human DNA in rectal cancer samples, validating the results of our sequencing approach (P-value = 0.04, Wilcoxon Rank-Sum Test). To further evidence the presence of *B. fragilis* in tumor specimens, we performed an immunohistochemistry assay on 3 rectal-cancer samples using an anti-*B. fragilis* LPS antibody and found that this bacterium was present in rectal-cancer tissue (**Figures 4C,D**).

DISCUSSION

In face of the microbiota gradient found in the human digestive tract (Zhang et al., 2014; Gao et al., 2015; Flemer et al., 2016) and the possibility that tissue-associated microorganisms could play a more direct role in immunomodulation and cancer

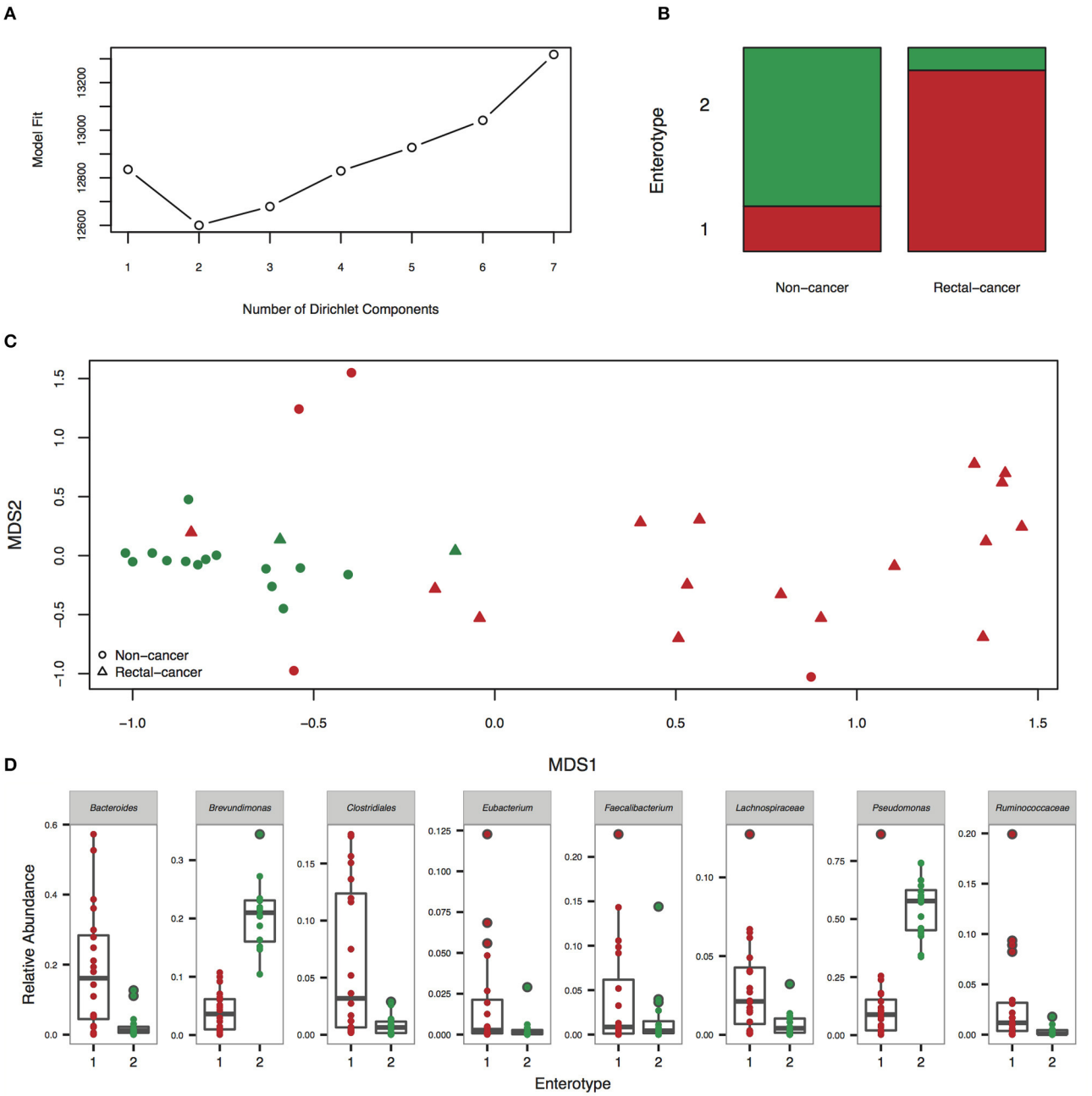

FIGURE 2 | Enterotyping analysis reveals the presence of two community types. (A) Fitting to the Dirichlet Multinomial Mixture model indicates optimal classification into two community types. **(B)** Distribution of rectal-cancer samples and non-cancer samples in both enterotypes ($P = 0.0001$, Fisher's exact test). **(C)** Non-metric dimensional scaling (NMDS) ordination plot of Jensen–Shannon divergence values between samples. Red, community type-1; green, community type-2. **(D)** Relative abundances of the top 8 most abundant genera in the two community types.

development, we investigated bacterial populations present in tissue biopsies, which may be relevant to pathological processes. Instead of studying colon and rectum samples together, our work is more specific as it is focused and contains only rectal tumors. Whereas, we achieved high 16S rRNA coverage from a large spectrum of bacteria from cancer samples, before any therapeutic intervention, we also see limitations, such as our relatively small sample size of 36 individuals. However, effect size analysis (Kelly et al., 2015) between both groups revealed an ω^2 ranging from 0.13 to 0.26, depending on the metric of pairwise distance, with PERMANOVA p-values <0.001 and power of 1 (data not shown), a finding that indicates

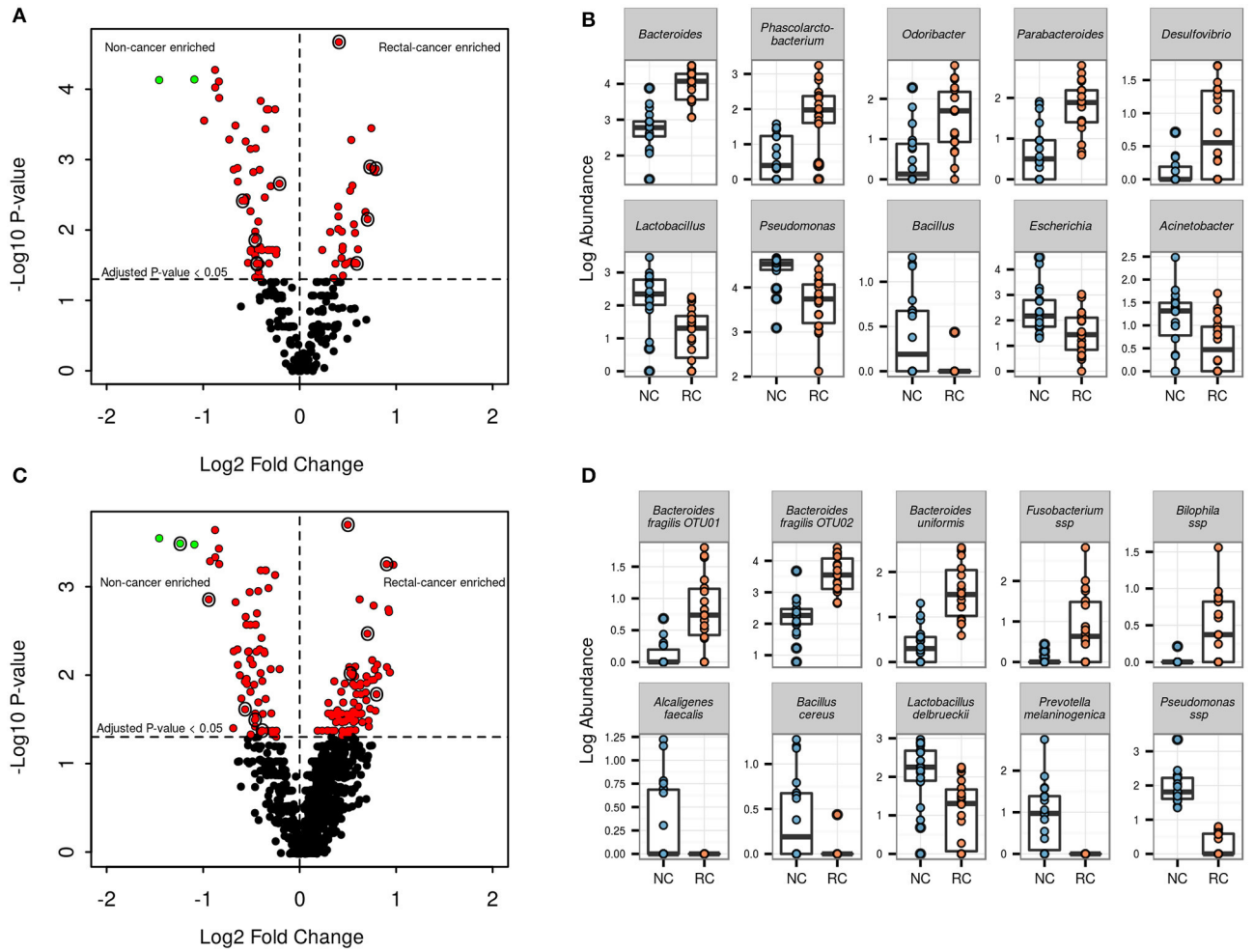

FIGURE 3 | Genera and OTU level differential abundance signatures. (A) Volcano plot for all 260 genera found in our samples. Red points indicate genera with an adjusted *p*-value <0.05; green points indicate genera with an adjusted *p*-value <0.05 and $\log_2$FC > 1. Points circled in black are genera shown in the adjacent boxplot. **(B)** Boxplots showing log abundances for 5 genera with significant increases (top) and 5 genera with significant decreases in rectal-cancer samples (bottom). **(C)** Volcano plot for 1492 OTUs found in our samples. Points color scheme is the same as in **(A). (D)** Boxplots showing log abundances for 5 OTUs with significant increases (top) and 5 OTUs with significant decreases in rectal-cancer samples (bottom).

that this sample size allows the observation of significant microbial differences between our two sample groups. We also need to point out that, whereas the primer pair used here gives a good coverage of most phyla, it has a poor coverage of the two closely related bacteria phyla *Lentisphaerae* and *Verrucomicrobia*.

In our study, we observed increased species-diversity and -richness among rectal-cancer samples. Higher species-diversity and -richness were seen in rectal tissue samples from adenomas compared to normal samples (Sanapareddy et al., 2012) and CRCs vs. adenomas (Nakatsu et al., 2015) and increased richness was found in CRCs compared to both adenomas and controls (Mira-Pascual et al., 2015). However, when looking at fecal samples, studies have had conflicting results. One study found increased diversity of both genes and genera along the adenoma-carcinoma transition (Feng et al., 2015), whereas another found a decrease in diversity when comparing carcinoma samples and normal controls (Ahn et al., 2013) and a third found no differences between controls, adenomas and carcinomas (Zeller et al., 2014). It is noteworthy to state that these fecal studies grouped proximal and distal colon cancers together with rectal cancers, which could have led to differences in their results. We should note that the five cases of early-stage lesions (pT2) showed, on average, intermediate microbial richness, when compared to non-cancer biopsies and a more advanced neoplastic stage (pT3). This suggests that increased species richness of cancer lesions could have an early role in rectal carcinogenesis.

Inter-individual microbial community heterogeneity of the human gut is influenced by spatial distribution, micro-heterogeneity, host genetics, dietary preferences,

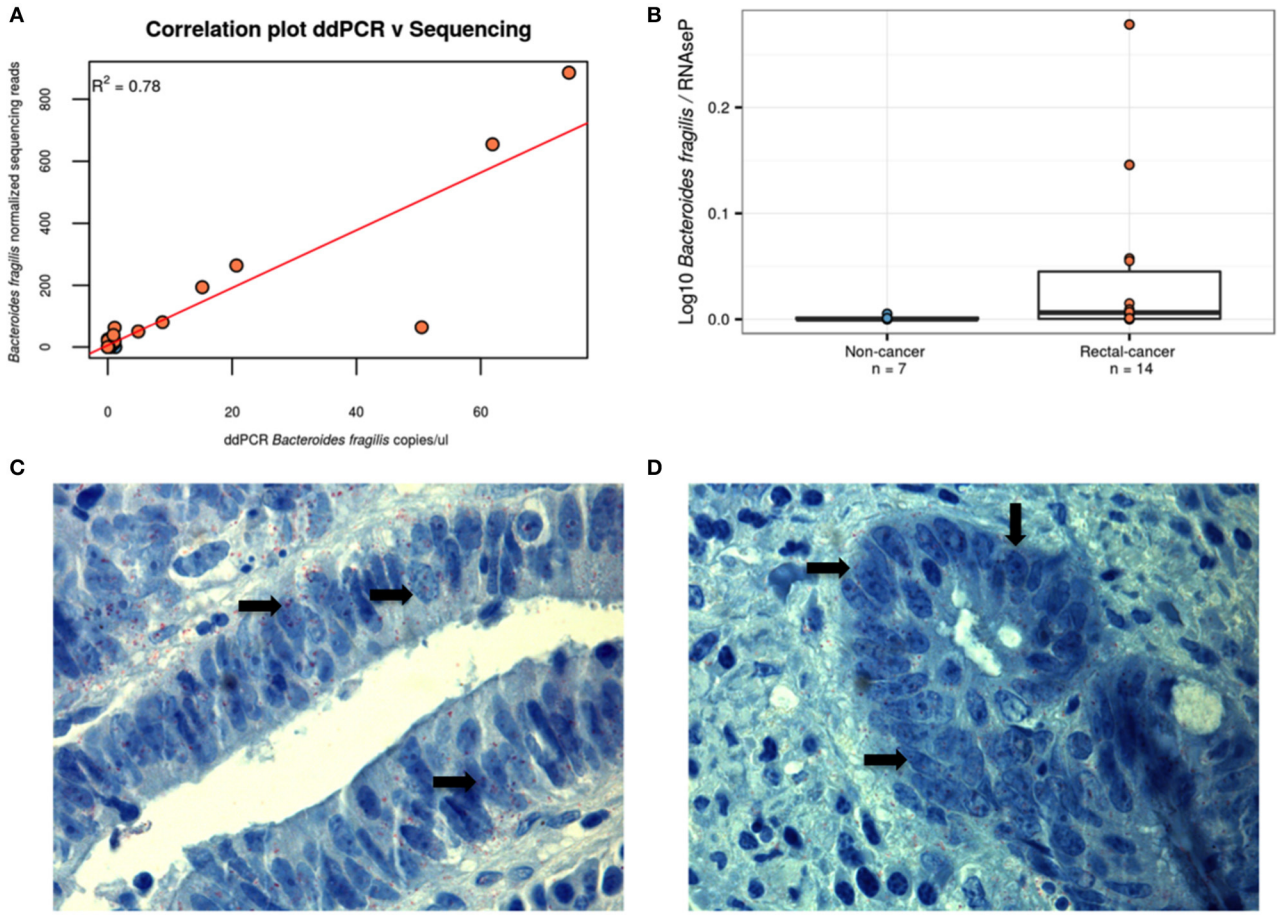

FIGURE 4 | Alternative approaches demonstrating the presence of *B. fragilis*. (A) *B. fragilis* ddPCR quantification correlates with HTS-derived data. Using linear regression we obtained a correlation of $R^2 = 0.78$, $P < 0.001$. Blue: Non-cancer samples; red: Rectal-cancer samples. **(B)** Boxplot showing log10 of the ddPCR ratio found for *B. fragilis* after normalizing for RNAseP values for both groups. Blue: Non-cancer samples; red: Rectal-cancer samples. **(C,D)** Immunohistochemisty analysis of two *B. fragilis*-positive rectal-cancer samples, demonstrating the presence of this microbe (antibodies are labeled in red and shown with arrows) using magnification of 1000X.

and mucin content (Eckburg et al., 2005; Hong et al., 2011; Zhang et al., 2014), and has posed a long-standing challenge when investigating microbial signatures implicated in CRC tumorigenesis. However, our results show that despite the high inter-individual differences, a common microbial community pattern appears to emerge, as shown in the PCoA analysis that clustered non-cancer and rectal-cancer groups separately (**Figure 1D**), suggesting a common dysbiotic setting related to this neoplasia.

We performed a global analysis of high-level phenotypical differences for bacteria identified in both groups. We highlight the higher abundance of anaerobic bacteria in the RC group in agreement with a previous study (Warren et al., 2013) and the reduction of biofilm-forming bacteria. The latter is a finding that may point to barrier breakage that would contribute to rectal colonization by relevant bacteria (Reid et al., 2001) (Supplementary Figure 3).

The alterations we found at the phylum level include higher levels of *Cyanobacteria* (possibly *Melainabacteria*) (Soo et al., 2014), *Actinobacteria*, *Bacteroidetes*, *OD1*, *Proteobacteria,* and *Planctomycetes* in the RC-group. We should note an important abundance difference for bacteria of the candidate phylum *OD1* (*Parcubacteria*). These highly adapted organisms have not been isolated *in vitro* yet; they have small genomes (<1 Mb) and reduced metabolic properties identified in a range of anoxic environments. The absence of biosynthetic capabilities and DNA repair enzymes, derived from the genomic analyses of some *OD1* bacteria, suggests a role as ectosymbionts (Nelson and Stegen, 2015). However, the putative role of these microbes in rectal cancer remains to be determined. A second phylum, *Planctomycetes*, which are atypical bacteria (Fuerst and Sagulenko, 2011) relatively close to *Verrucomicrobia* (Hou et al., 2008) and more frequently observed in aquatic environments (such as saltwater, fresh water, and acidic mud), also showed potential as a

biomarker for RC, with striking differences between the groups.

Interestingly, our study also indicated the differential abundance of more specific microbes after comparing NC and RC groups. *B. fragilis*, a symbiotic organism common to the human intestinal tract, was found to be more abundant in rectal-cancer samples seen by 16S rRNA HTS and confirmed by ddPCR. Other studies that investigated tissue-associated bacteria also found increased abundance of *B. fragilis* in tumor samples (Wang et al., 2012; Zeller et al., 2014; Nakatsu et al., 2015). *B. fragilis* has been identified as an important human intestinal symbiont and has been suggested to act as a "keystone pathogen" in the development of CRC (Hajishengallis et al., 2012). *B. fragilis* is an obligate anaerobe and is a minority member of the normal colonic microbiota with a propensity for mucosal adherence (Sears et al., 2014). Previous reports have linked enterotoxigenic *B. fragilis* (ETBF) to human diarrheal illnesses and increased tumorigenesis in an IL-23-dependent and STAT3-dependent manner (Wick et al., 2014). The toxin fragylisin, produced by ETBF, is a zinc-dependent metalloprotease that triggers NF-kB signaling and cleaves E-cadherin, and has been suggested to be oncogenic (Wu et al., 2009). Bacterial genera known for their role in butyrate production, such as *Ruminococcus*, *Roseburia,* and *Butyricimonas* were more abundant among rectal-cancers, differing from results reported so far. An explanation for this difference could involve the fact that most data has been derived from fecal samples and/or grouping different anatomical tumor sites (such as proximal, distal, and rectal). An OTU assigned to *Bilophila,* a bile-resistant, strictly anaerobic bacterial genus, was also more abundant among rectal-cancer samples, and evidence suggests that products of bacterial bile acid conjugation, secondary bile acids, are carcinogenic (McGarr et al., 2005; Ridlon et al., 2014). *Desulfovibrio*, a commensal sulfate-reducing bacterium, may contribute to mucosal inflammation through hydrogen sulfide production, a resulting by-product of sulfated mucin metabolism (Earley et al., 2015). *Phascolarctobacterium,* known to produce propionate via succinate fermentation, was also increased among cancer samples. On the other hand, we found that *L. delbrueckii* was more abundant in non-cancer samples. Probiotic *Lactobacilli* can modify the enteric flora and are thought to have a beneficial effect on enterocolitis. Treatment of IL-10-deficient mice with the probiotic *Lactobacillus salivarius* ssp. reduced the intensity of mucosal inflammation and the incidence of colon cancer from 50 to 10%. These effects were accompanied by significant reductions in fecal coliform, enterococci, and *Clostridium perfringens* levels (O'Mahony et al., 2001). This study exemplifies the effect of changes at the flora level on the development of inflammation, and supports the hypothesis that there are "protective" species and "harmful" species in the normal bacterial flora.

After identifying relevant cancer-related microorganisms, the next steps of microbiome studies will certainly involve microbial manipulations to reduce disease-associated agents, or increase the frequency of protective and health-associated microbes. This can be achieved through diet, exemplified by a previous study using animal models that showed taurine consumption lead to a reduction of *Proteobacteria* (especially *Helicobacter*), as well as an elevation in short-chain fatty acids (SCFA) and a reduction in fecal lipopolysaccharides (LPS) (Yu et al., 2016). Duque et al., recently demonstrated, using SHIME® (Simulator of the Human Microbial Ecosystem), that the consumption of non-pasteurized fresh orange juice was able to significantly increase levels of *Lactobacillus* spp., *Enterococcus* spp., *Bifidobacterium* spp., and *Clostridium* spp. and to reduce enterobacteria (Duque et al., 2016).

Long before associations between cancer and the microbial flora started to be uncovered, diet recommendations—including low consumption of red meat and fat, and high ingestion of fibers and vegetables—have been recognized as protective against the development of colorectal cancer. Current evidences suggest that diet recommendations may be effective, together with tissue environment and host-related factors, because they also help shape the gut microbiota (Sonnenburg and Bäckhed, 2016). Further research may show that treatment of rectal dysbiosis may contribute to the prevention of inflammation-induced rectal carcinoma development and aid in chemotherapy and overall treatment response (Yang and Pei, 2006).

AUTHOR CONTRIBUTIONS

Conceived and designed the experiments: AT, EJ, AL, SA, DN, ED; Performed the experiments: AT, EJ, RR, PC; Analyzed the data: AT, CH, DN, JS, ED; Contributed reagents/samples/analysis tools: MB, AL, SA, AC, HF, IS; Wrote or edited the manuscript: AT, HF, CH, JS, DN, ED. All authors read and approved the final manuscript.

FUNDING

AT was supported by a fellowship from FAPESP (2015/01507-7). CH was supported by CAPES grant (88887.062078/2014-00) and FAPESP grant (2013/07914-8). This project was supported by PRONON (SIPAR 25000.055.167/2015-23), by Associação Beneficiente Alzira Denise Hertzog Silva (ABADHS) and by CAPES grant 3385/2013.

ACKNOWLEDGMENTS

The authors are grateful to the institutional tumor bank of the AC Camargo Cancer Center. ED and JS are research fellows of the Conselho Nacional de Desenvolvimento Cientifico e Tecnologico (CNPq).

SUPPLEMENTARY MATERIAL

The Supplementary Material for this article can be found online at: http://journal.frontiersin.org/article/10.3389/fcimb.2016.00179/full#supplementary-material

Availability of Supporting Data

Nucleotide sequences used for this study have been deposited in the SRA under accession SRP077097.

REFERENCES

Ahn, J., Sinha, R., Pei, Z., Dominianni, C., Wu, J., Shi, J., et al. (2013). Human gut microbiome and risk for colorectal cancer. *JNCI J. Natl. Cancer Inst.* 105, 1907–1911. doi: 10.1093/jnci/djt300

Allais, L., Kerckhof, F.-M., Verschuere, S., Bracke, K. R., De Smet, R., Laukens, D., et al. (2016). Chronic cigarette smoke exposure induces microbial and inflammatory shifts and mucin changes in the murine gut. *Environ. Microbiol.* 18, 1352–1363. doi: 10.1111/1462-2920.12934

Arthur, J. C., Gharaibeh, R. Z., Mühlbauer, M., Perez-Chanona, E., Uronis, J. M., McCafferty, J., et al. (2014). Microbial genomic analysis reveals the essential role of inflammation in bacteria-induced colorectal cancer. *Nat. Commun.* 5, 4724. doi: 10.1038/ncomms5724

Binefa, G., Rodríguez-Moranta, F., Teule, À., and Medina-Hayas, M. (2014). Colorectal cancer: from prevention to personalized medicine. *World J. Gastroenterol.* 20, 6786. doi: 10.3748/wjg.v20.i22.6786

Bingham, S. A. (2000). Diet and colorectal cancer prevention. *Biochem. Soc. Trans.* 28, 12–16. doi: 10.1042/bst0280012

Boulangé, C. L., Neves, A. L., Chilloux, J., Nicholson, J. K., and Dumas, M.-E. (2016). Impact of the gut microbiota on inflammation, obesity, and metabolic disease. *Genome Med.* 8:42. doi: 10.1186/s13073-016-0303-2

Calinski, T., and Harabasz, J. A. (1974). Dendrite method for cluster analysis. *Commun Stat. Simul Comput* 3, 1–27. doi: 10.1080/03610917408548446

Caporaso, J. G., Bittinger, K., Bushman, F. D., DeSantis, T. Z., Andersen, G. L., and Knight, R. (2010b). PyNAST: a flexible tool for aligning sequences to a template alignment. *Bioinformatics* 26, 266–267. doi: 10.1093/bioinformatics/btp636

Caporaso, J. G., Kuczynski, J., Stombaugh, J., Bittinger, K., Bushman, F. D., Costello, E. K., et al. (2010a). QIIME allows analysis of high-throughput community sequencing data. *Nat. Methods* 2010, 335–336. doi: 10.1038/nmeth.f.303

Cole, J. R., Wang, Q., Fish, J. A., Chai, B., McGarrell, D. M., Sun, Y., et al. (2014). Ribosomal Database Project: data and tools for high throughput rRNA analysis. *Nucleic Acids Res.* 42, D633–D642. doi: 10.1093/nar/gkt1244

DeSantis, T. Z., Hugenholtz, P., Larsen, N., Rojas, M., Brodie, E. L., Keller, K., et al. (2006). Greengenes, a chimera-checked 16S rRNA gene database and workbench compatible with ARB. *Appl. Environ. Microbiol.* 72, 5069–5072. doi: 10.1128/AEM.03006-05

Duboc, H., Rajca, S., Rainteau, D., Benarous, D., Maubert, M.-A., Quervain, E., et al. (2013). Connecting dysbiosis, bile-acid dysmetabolism and gut inflammation in inflammatory bowel diseases. *Gut* 62, 531–539. doi: 10.1136/gutjnl-2012-302578

Duque, A. L. R. F., Monteiro, M., Adorno, M. A. T., Sakamoto, I. K., and Sivieri, K. (2016). An exploratory study on the influence of orange juice on gut microbiota using a dynamic colonic model. *Food Res. Int.* 84, 160–169. doi: 10.1016/j.foodres.2016.03.028

Durbán, A., Abellán, J. J., Jiménez-Hernández, N., Ponce, M., Ponce, J., Sala, T., et al. (2011). Assessing gut microbial diversity from feces and rectal mucosa. *Microb. Ecol.* 61, 123–133. doi: 10.1007/s00248-010-9738-y

Earley, H., Lennon, G., Balfe, A., Kilcoyne, M., Clyne, M., Joshi, L., et al. (2015). A Preliminary study examining the binding capacity of *Akkermansia muciniphila* and *Desulfovibrio* spp., to colonic mucin in health and ulcerative colitis. *PLoS ONE* 10:e0135280. doi: 10.1371/journal.pone.0135280

Eckburg, P. B., Bik, E. M., Bernstein, C. N., Purdom, E., Dethlefsen, L., Sargent, M., et al. (2005). Diversity of the human intestinal microbial flora. *Science* 308, 1635–1638. doi: 10.1126/science.1110591

Edgar, R. C. (2010). Search and clustering orders of magnitude faster than BLAST. *Bioinformatics* 26, 2460–2461. doi: 10.1093/bioinformatics/btq461

Edgar, R. C., Haas, B. J., Clemente, J. C., Quince, C., and Knight, R. (2011). UCHIME improves sensitivity and speed of chimera detection. *Bioinformatics* 27, 2194–2200. doi: 10.1093/bioinformatics/btr381

Edgar, R. C. (2013). UPARSE: highly accurate OTU sequences from microbial amplicon reads. *Nat. Methods* 10, 996–998. doi: 10.1038/nmeth.2604

Feng, Q., Liang, S., Jia, H., Stadlmayr, A., Tang, L., Lan, Z., et al. (2015). Gut microbiome development along the colorectal adenoma–carcinoma sequence. *Nat. Commun.* 6:6528. doi: 10.1038/ncomms7528

Flemer, B., Lynch, D. B., Brown, J. M., Jeffery, I. B., Ryan, F. J., Claesson, M. J., et al. (2016). Tumour-associated and non-tumour-associated microbiota in colorectal cancer. *Gut*. doi: 10.1136/gutjnl-2015-309595. [Epub ahead of print].

Fuerst, J. A., and Sagulenko, E. (2011). Beyond the bacterium: planctomycetes challenge our concepts of microbial structure and function. *Nat. Rev. Microbiol.* 9, 403–413. doi: 10.1038/nrmicro2578

Galluzzi, L., Buqué, A., Kepp, O., Zitvogel, L., and Kroemer, G. (2015). Immunological effects of conventional chemotherapy and targeted anticancer agents. *Cancer Cell* 28, 690–714. doi: 10.1016/j.ccell.2015.10.012

Gao, Z., Guo, B., Gao, R., Zhu, Q., and Qin, H. (2015). Microbiota disbiosis is associated with colorectal cancer. *Front. Microbiol.* 6:20. doi: 10.3389/fmicb.2015.00020

Gevers, D., Kugathasan, S., Denson, L. A., Vázquez-Baeza, Y., Van Treuren, W., Ren, B., et al. (2014). The treatment-naive microbiome in new-onset crohn's disease. *Cell Host Microbe* 15, 382–392. doi: 10.1016/j.chom.2014.02.005

Gur, C., Ibrahim, Y., Isaacson, B., Yamin, R., Abed, J., Gamliel, M., et al. (2015). Binding of the Fap2 Protein of *Fusobacterium nucleatum* to human inhibitory receptor TIGIT protects tumors from immune cell attack. *Immunity* 42, 344–355. doi: 10.1016/j.immuni.2015.01.010

Hajishengallis, G., Darveau, R. P., and Curtis, M. A. (2012). The keystone-pathogen hypothesis. *Nat. Rev. Microbiol.* 10, 717–725. doi: 10.1038/nrmicro2873

Hennig, C. (2015). *fpc: Flexible Procedures for Clustering:R Package Version 2.1–10.*

Holmes, I., Harris, K., and Quince, C. (2012). Dirichlet multinomial mixtures: generative models for microbial metagenomics. *PLoS ONE* 7:e30126. doi: 10.1371/journal.pone.0030126

Hong, P.-Y., Croix, J. A., Greenberg, E., Gaskins, H. R., and Mackie, R. I. (2011). Pyrosequencing-based analysis of the mucosal microbiota in healthy individuals reveals ubiquitous bacterial groups and micro-heterogeneity. *PLoS ONE* 6:e25042. doi: 10.1371/journal.pone.0025042

Hou, S., Makarova, K. S., Saw, J. H., Senin, P., Ly, B. V., Zhou, Z., et al. (2008). Complete genome sequence of the extremely acidophilic methanotroph isolate V4, Methylacidiphilum infernorum, a representative of the bacterial phylum Verrucomicrobia. *Biol. Direct* 3:26. doi: 10.1186/1745-6150-3-26

Kelly, B. J., Gross, R., Bittinger, K., Sherrill-Mix, S., Lewis, J. D., Collman, R. G., et al. (2015). Power and sample-size estimation for microbiome studies using pairwise distances and PERMANOVA. *Bioinformatics* 31, 2461–2468. doi: 10.1093/bioinformatics/btv183

Klindworth, A., Pruesse, E., Schweer, T., Peplies, J., Quast, C., Horn, M., et al. (2013). Evaluation of general 16S ribosomal RNA gene PCR primers for classical and next-generation sequencing-based diversity studies. *Nucleic Acids Res.* 41:e1. doi: 10.1093/nar/gks808

Koren, O., Knights, D., Gonzalez, A., Waldron, L., Segata, N., Knight, R., et al. (2013). A guide to enterotypes across the human body: meta-analysis of microbial community structures in human microbiome datasets. *PLoS Comput. Biol.* 9:e1002863. doi: 10.1371/journal.pcbi.1002863

Kostic, A. D., Chun, E., Robertson, L., Glickman, J. N., Gallini, C. A., Michaud, M., et al. (2013). *Fusobacterium nucleatum* potentiates intestinal tumorigenesis and modulates the tumor-immune microenvironment. *Cell Host Microbe* 14, 207–215. doi: 10.1016/j.chom.2013.07.007

Kostic, A. D., Gevers, D., Pedamallu, C. S., Michaud, M., Duke, F., Earl, A. M., et al. (2012). Genomic analysis identifies association of Fusobacterium with colorectal carcinoma. *Genome Res.* 22, 292–298. doi: 10.1101/gr.126573.111

Lane, D. J. (1991). "16S/23S rRNA sequencing," in *Nucleic Acid Techniques in Bacterial Systematics*. ed E. G. M. Stackebrandt (Chichester: John Wiley and Sons), 115–175.

Leclercq, S., Matamoros, S., Cani, P. D., Neyrinck, A. M., Jamar, F., Stärkel, P., et al. (2014). Intestinal permeability, gut-bacterial dysbiosis, and behavioral markers of alcohol-dependence severity. *Proc. Natl. Acad. Sci.U.S.A.* 111, E4485–E4493. doi: 10.1073/pnas.1415174111

Lozupone, C., and Knight, R. (2005). UniFrac: a new phylogenetic method for comparing microbial communities. *Appl. Environ. Microbiol.* 71, 8228–8235. doi: 10.1128/AEM.71.12.8228-8235.2005

Maechler, M., Rousseeuw, P., Struyf, A., Hubert, M., and Hornik, K. (2015). *Cluster Analysis Basics and Extensions. R package version 2.0.1. CRAN*. Available online at: https://cran.r-project.org/web/packages/cluster/citation.html

McGarr, S. E., Ridlon, J. M., and Hylemon, P. B. (2005). Diet, anaerobic bacterial metabolism, and colon cancer: a review of the literature. *J. Clin. Gastroenterol.* 39, 98–109.

McMurdie, P. J., and Holmes, S. (2013). phyloseq: an R package for reproducible interactive analysis and graphics of microbiome census data. *PLoS ONE* 8:e61217. doi: 10.1371/journal.pone.0061217

Mira-Pascual, L., Cabrera-Rubio, R., Ocon, S., Costales, P., Parra, A., Suarez, A., et al. (2015). Microbial mucosal colonic shifts associated with the development of colorectal cancer reveal the presence of different bacterial and archaeal biomarkers. *J. Gastroenterol.* 50, 167–179. doi: 10.1007/s00535-014-0963-x

Moore, W. E., and Moore, L. H. (1995). Intestinal floras of populations that have a high risk of colon cancer. *Appl. Environ. Microbiol.* 61, 3202–3207.

Nakatsu, G., Li, X., Zhou, H., Sheng, J., Wong, S. H., Wu, W. K., et al. (2015). Gut mucosal microbiome across stages of colorectal carcinogenesis. *Nat. Commun.* 6:8727. doi: 10.1038/ncomms9727

Nelson, W. C., and Stegen, J. C. (2015). The reduced genomes of Parcubacteria (OD1) contain signatures of a symbiotic lifestyle. *Front. Microbiol.* 6:173. doi: 10.3389/fmicb.2015.00713

Oksanen, J., Blanchet, F., Kindt, R., Legendre, P., and O'Hara, R. (2016). *Vegan: Community Ecology Package. R Package 23-3 2016*:Available online at: https://cran.r-project.org/web/packa

O'Mahony, L., Feeney, M., O'Halloran, S., Murphy, L., Kiely, B., Fitzgibbon, J., et al. (2001). Probiotic impact on microbial flora, inflammation and tumour development in IL-10 knockout mice. *Aliment. Pharmacol. Ther.* 15, 1219–1225. doi: 10.1046/j.1365-2036.2001.01027.x

Pitt, J. M., Marabelle, A., Eggermont, A., Soria, J.-C., Kroemer, G., and Zitvogel, L. (2016). Targeting the tumor microenvironment: removing obstruction to anticancer immune responses and immunotherapy. *Ann. Oncol.* 8, 1482–1492. doi: 10.1093/annonc/mdw168

Price, M. N., Dehal, P. S., and Arkin, A. P. (2009). FastTree: computing large minimum evolution trees with profiles instead of a distance matrix. *Mol. Biol. Evol.* 26, 1641–1650. doi: 10.1093/molbev/msp077

Reid, G., Howard, J., and Gan, B. S. (2001). Can bacterial interference prevent infection? *Trends Microbiol.* 9, 424–428. doi: 10.1016/S0966-842X(01)02132-1

R Foundation (2011). *R Foundation for Statistical Computing*. Vienna AI 3-900051-07-0: R Development Core Team.

Ridlon, J. M., Kang, D.-J., Hylemon, P. B., and Bajaj, J. S. (2014). Bile acids and the gut microbiome. *Curr. Opin. Gastroenterol.* 30, 332–338. doi: 10.1097/MOG.0000000000000057

Riley, D. R., Sieber, K. B., Robinson, K. M., White, J. R., Ganesan, A., Nourbakhsh, S., et al. (2013). Bacteria-human somatic cell lateral gene transfer is enriched in cancer samples. *PLoS Comput. Biol.* 9:e1003107. doi: 10.1371/journal.pcbi.1003107

Rousseeuw, P. J. (1987). Silhouettes: a graphical aid to the interpretation and validation of cluster analysis. *J. Comput. Appl. Math.* 20, 53–65.

Rubinstein, M. R., Wang, X., Liu, W., Hao, Y., Cai, G., Han, Y. W., et al. (2013). *Fusobacterium nucleatum* promotes colorectal carcinogenesis by modulating E-cadherin/β-catenin signaling via its FadA adhesin. *Cell Host Microbe* 14, 195–206. doi: 10.1016/j.chom.2013.07.012

Sabino, J., Vieira-Silva, S., Machiels, K., Joossens, M., Falony, G., Ballet, V., et al. (2016). Primary sclerosing cholangitis is characterised by intestinal dysbiosis independent from IBD. *Gut.* 10, 1681–1689. doi: 10.1136/gutjnl-2015-311004

Sanapareddy, N., Legge, R. M., Jovov, B., McCoy, A., Burcal, L., Araujo-Perez, F., et al. (2012). Increased rectal microbial richness is associated with the presence of colorectal adenomas in humans. *ISME J.* 6, 1858–1868. doi: 10.1038/ismej.2012.43

Sears, C. L., Geis, A. L., and Housseau, F. (2014). *Bacteroides fragilis* subverts mucosal biology: from symbiont to colon carcinogenesis. *J. Clin. Invest.* 124, 4166–4172. doi: 10.1172/JCI72334

Shannon, C. E. (1948). The mathematical theory of communication. 1963. *MD Comput.* 14, 306–317.

Shapiro, H., Thaiss, C. A., Levy, M., and Elinav, E. (2014). The cross talk between microbiota and the immune system: metabolites take center stage. *Curr. Opin. Immunol.* 30, 54–62. doi: 10.1016/j.coi.2014.07.003

Simpson, E. H. (1949). Measurement of diversity. *Nature* 163, 688–688. doi: 10.1038/163688a0

Sonnenburg, J. L., and Bäckhed, F. (2016). Diet-microbiota interactions as moderators of human metabolism. *Nature* 535, 56–64. doi: 10.1038/nature18846

Soo, R. M., Skennerton, C. T., Sekiguchi, Y., Imelfort, M., Paech, S. J., Dennis, P. G., et al. (2014). An expanded genomic representation of the phylum cyanobacteria. *Genome Biol. Evol.* 6, 1031–1045. doi: 10.1093/gbe/evu073

Tamas, K., Walenkamp, A. M. E., De Vries, E. G. E., Van Vugt, M. A. T. M., Beets-Tan, R. G., Van Etten, B., et al. (2015). Rectal and colon cancer: not just a different anatomic site. *Cancer Treat. Rev.* 41, 671–679. doi: 10.1016/j.ctrv.2015.06.007

Tibshirani, R., and Walther, G. (2005). Cluster validation by prediction strength. *J. Comput. Graph. Stat.* 14, 511–528. doi: 10.1198/106186005X59243

Tong, J., Liu, C., Summanen, P., Xu, H., and Finegold, S. M. (2011). Application of quantitative real-time PCR for rapid identification of *Bacteroides fragilis* group and related organisms in human wound samples. *Anaerobe* 17, 64–68. doi: 10.1016/j.anaerobe.2011.03.004

Torre, L. A., Bray, F., Siegel, R. L., Ferlay, J., Lortet-tieulent, J., and Jemal, A. (2015). Global cancer statistics, 2012. *CA Cancer J. Clin.* 65, 87–108. doi: 10.3322/caac.21262

Turnbaugh, P. J., Ridaura, V. K., Faith, J. J., Rey, F. E., Knight, R., and Gordon, J. I. (2009). The effect of diet on the human gut microbiome: a metagenomic analysis in humanized gnotobiotic mice. *Sci. Transl. Med.* 1, 6ra14. doi: 10.1126/scitranslmed.3000322

Vétizou, M., Pitt, J. M., Daillere, R., Lepage, P., Waldschmitt, N., Flament, C., et al. (2015). Anticancer immunotherapy by CTLA-4 blockade relies on the gut microbiota. *Science* 350, 1079–1084. doi: 10.1126/science.aad1329

Wang, Q., Garrity, G. M., Tiedje, J. M., and Cole, J. R. (2007). Naïve Bayesian classifier for rapid assignment of rRNA sequences into the new bacterial taxonomy. *Appl. Environ. Microbiol.* 73, 5261–5267. doi: 10.1128/AEM.00062-07

Wang, T., Cai, G., Qiu, Y., Fei, N., Zhang, M., Pang, X., et al. (2012). Structural segregation of gut microbiota between colorectal cancer patients and healthy volunteers. *ISME J.* 6, 320–329. doi: 10.1038/ismej.2011.109

Warren, R. L., Freeman, D. J., Pleasance, S., Watson, P., Moore, R. A., Cochrane, K., et al. (2013). Co-occurrence of anaerobic bacteria in colorectal carcinomas. *Microbiome* 1:16. doi: 10.1186/2049-2618-1-16

Wick, E. C., Rabizadeh, S., Albesiano, E., Wu, X., Wu, S., Chan, J., et al. (2014). Stat3 activation in murine colitis induced by enterotoxigenic *Bacteroides fragilis*. *Inflamm. Bowel Dis.* 20, 821–834. doi: 10.1097/MIB.0000000000000019

Wu, N., Yang, X., Zhang, R., Li, J., Xiao, X., Hu, Y., et al. (2013). Dysbiosis signature of fecal microbiota in colorectal cancer patients. *Microb. Ecol.* 66, 462–470. doi: 10.1007/s00248-013-0245-9

Wu, S., Rhee, K.-J., Albesiano, E., Rabizadeh, S., Wu, X., Yen, H.-R., et al. (2009). A human colonic commensal promotes colon tumorigenesis via activation of T helper type 17 T cell responses. *Nat. Med.* 15:1016–1022. doi: 10.1038/nm.2015

Yang, L., and Pei, Z. (2006). Bacteria, inflammation, and colon cancer. *World J. Gastroenterol.* 12, 6741–6746. doi: 10.3748/wjg.v12.i42.6741

Yu, H., Guo, Z., Shen, S., and Shan, W. (2016). Effects of taurine on gut microbiota and metabolism in mice. *Amino Acids* 48, 1601–1617. doi: 10.1007/s00726-016-2219-y

Zeller, G., Tap, J., Voigt, A. Y., Sunagawa, S., Kultima, J. R., Costea, P. I., et al. (2014). Potential of fecal microbiota for early-stage detection of colorectal cancer. *Mol. Syst. Biol.* 10, 766–766. doi: 10.15252/msb.20145645

Zhang, Z., Geng, J., Tang, X., Fan, H., Xu, J., Wen, X., et al. (2014). Spatial heterogeneity and co-occurrence patterns of human mucosal-associated intestinal microbiota. *ISME J.* 8, 881–893. doi: 10.1038/ismej.2013.185

Zitvogel, L., Galluzzi, L., Smyth, M. J., and Kroemer, G. (2013). Mechanism of action of conventional and targeted anticancer therapies: reinstating immunosurveillance. *Immunity* 39, 74–88. doi: 10.1016/j.immuni.2013.06.014

Conflict of Interest Statement: The authors declare that the research was conducted in the absence of any commercial or financial relationships that could be construed as a potential conflict of interest.

The reviewer DAS and handling Editor declared their shared affiliation and the handling Editor states that the process nevertheless met the standards of a fair and objective review.

Copyright © 2016 Thomas, Jesus, Lopes, Aguiar, Begnami, Rocha, Carpinetti, Camargo, Hoffmann, Freitas, Silva, Nunes, Setubal, and Dias-Neto. This is an open-access article distributed under the terms of the Creative Commons Attribution License (CC BY). The use, distribution or reproduction in other forums is permitted, provided the original author(s) or licensor are credited and that the original publication in this journal is cited, in accordance with accepted academic practice. No use, distribution or reproduction is permitted which does not comply with these terms.

Advantages of publishing in Frontiers

OPEN ACCESS
Articles are free to read for greatest visibility and readership

FAST PUBLICATION
Around 90 days from submission to decision

HIGH QUALITY PEER-REVIEW
Rigorous, collaborative, and constructive peer-review

TRANSPARENT PEER-REVIEW
Editors and reviewers acknowledged by name on published articles

Frontiers
Avenue du Tribunal-Fédéral 34
1005 Lausanne | Switzerland

Visit us: www.frontiersin.org
Contact us: info@frontiersin.org | +41 21 510 17 00

REPRODUCIBILITY OF RESEARCH
Support open data and methods to enhance research reproducibility

DIGITAL PUBLISHING
Articles designed for optimal readership across devices

FOLLOW US
@frontiersin

IMPACT METRICS
Advanced article metrics track visibility across digital media

EXTENSIVE PROMOTION
Marketing and promotion of impactful research

LOOP RESEARCH NETWORK
Our network increases your article's readership